

Controlled Radical Polymerization

Controlled Radical Polymerization

Krzysztof Matyjaszewski, EDITOR
Carnegie Mellon University

Developed from a symposium sponsored by the Division
of Polymer Chemistry, Inc., at the 213th National Meeting
of the American Chemical Society,
San Francisco, CA,
April 13–17, 1997



American Chemical Society
Library
1155 16th St., N.W.
Washington, D.C. 20036

In *Controlled Radical Polymerization*; Matyjaszewski, K.;
ACS Symposium Series; American Chemical Society: Washington, DC, 1998.



Controlled radical polymerization

Library of Congress Cataloging-in-Publication Data

Controlled radical polymerization / Krzysztof Matyjaszewski, editor.

p. cm.—(ACS symposium series, ISSN 0097-6156; 685)

“Developed from a symposium sponsored by the Division of Polymer Chemistry at the 213th National Meeting of the American Chemical Society, San Francisco, CA, April 6–11, 1997.”

Includes bibliographical references and indexes.

ISBN 0-8412-3545-7

1. Polymerization--Congresses. 2. Free radical reactions--Congresses

I. Matyjaszewski, K. (Krzysztof), 1950- . II. American Chemical Society. Division of Polymer Chemistry. III. American Chemical Society. Meeting (213th: 1997: San Francisco, Calif.) IV. Series.

QD281.P6C66 1998
547'.28—dc21

97-43731
CIP

This book is printed on acid-free, recycled paper.



Copyright © 1998 American Chemical Society

All Rights Reserved. Reprographic copying beyond that permitted by Sections 107 or 108 of the U.S. Copyright Act is allowed for internal use only, provided that a per-chapter fee of \$20.00 plus \$0.25 per page is paid to the Copyright Clearance Center, Inc., 222 Rosewood Drive, Danvers, MA 01923, USA. Republication or reproduction for sale of pages in this book is permitted only under license from ACS. Direct these and other permissions requests to ACS Copyright Office, Publications Division, 1155 16th Street, N.W., Washington, DC 20036.

The citation of trade names and/or names of manufacturers in this publication is not to be construed as an endorsement or as approval by ACS of the commercial products or services referenced herein; nor should the mere reference herein to any drawing, specification, chemical process, or other data be regarded as a license or as a conveyance of any right or permission to the holder, reader, or any other person or corporation, to manufacture, reproduce, use, or sell any patented invention or copyrighted work that may in any way be related thereto. Registered names, trademarks, etc., used in this publication, even without specific indication thereof, are not to be considered unprotected by law.

PRINTED IN THE UNITED STATES OF AMERICA

American Chemical Society
Library
1155 16th St., N.W.
Washington, D.C. 20036

In Controlled Radical Polymerization; Matyjaszewski, K.;
ACS Symposium Series; American Chemical Society: Washington, DC, 1998.

Advisory Board

ACS Symposium Series

Mary E. Castellion
ChemEdit Company

Arthur B. Ellis
University of Wisconsin at Madison

Jeffrey S. Gaffney
Argonne National Laboratory

Gunda I. Georg
University of Kansas

Lawrence P. Klemann
Nabisco Foods Group

Richard N. Loepky
University of Missouri

Cynthia A. Maryanoff
R. W. Johnson Pharmaceutical
Research Institute

Roger A. Minear
University of Illinois
at Urbana-Champaign

Omkaram Nalamasu
AT&T Bell Laboratories

Kinam Park
Purdue University

Katherine R. Porter
Duke University

Douglas A. Smith
The DAS Group, Inc.

Martin R. Tant
Eastman Chemical Co.

Michael D. Taylor
Parke-Davis Pharmaceutical
Research

Leroy B. Townsend
University of Michigan

William C. Walker
DuPont Company

Foreword

THE ACS SYMPOSIUM SERIES was first published in 1974 to provide a mechanism for publishing symposia quickly in book form. The purpose of this series is to publish comprehensive books developed from symposia, which are usually “snapshots in time” of the current research being done on a topic, plus some review material on the topic. For this reason, it is necessary that the papers be published as quickly as possible.

Before a symposium-based book is put under contract, the proposed table of contents is reviewed for appropriateness to the topic and for comprehensiveness of the collection. Some papers are excluded at this point, and others are added to round out the scope of the volume. In addition, a draft of each paper is peer-reviewed prior to final acceptance or rejection. This anonymous review process is supervised by the organizer(s) of the symposium, who become the editor(s) of the book. The authors then revise their papers according to the recommendations of both the reviewers and the editors, prepare camera-ready copy, and submit the final papers to the editors, who check that all necessary revisions have been made.

As a rule, only original research papers and original review papers are included in the volumes. Verbatim reproductions of previously published papers are not accepted.

ACS BOOKS DEPARTMENT

Preface

UNTIL RECENTLY, RADICAL POLYMERIZATION has been considered as one of the most mature areas of polymer synthesis. Many commercial polymers and copolymers are prepared by radical polymerization because of its undemanding conditions, the large number of available monomers, and the facileness of (co)polymerization. However, the main deficiency of conventional radical polymerization is a lack of macromolecular control and the difficulty of making well-defined (co)polymers.

After several years of relatively slow progress in controlled radical polymerization, the field began to undergo nearly exponential development in 1993, after the first disclosures of styrene radical polymerization mediated by nitroxide and several organometallic derivatives. Most recently, reports of metal-catalyzed or atom transfer radical polymerizations have further enhanced development of the field.

The recent emergence of controlled radical polymerization in both academic and industrial laboratories is expected to be converted to commercial practice in the near future. It is stimulating to be part of the current growth of this diverse field. This book comprises both the topical reviews and the contributions of specialists at a symposium presented at the 213th National Meeting of the American Chemical Society, titled "Advances in Free Radical Polymerization", sponsored by the Division of Polymer Chemistry, Inc., in San Francisco, California, April 13–17, 1997. The first five chapters provide a general introduction to radical reactions and controlled radical polymerization. The next four chapters are focused on recent advances in the kinetics of conventional radical (co)polymerization in homogeneous and heterogeneous media and on direct measurements of concentrations of growing species. Topics related to controlled radical polymerization are summarized in the remaining 18 chapters and are separated into four sections covering nitroxide-mediated polymerization, metal-mediated polymerization, and other systems, and the application of controlled radical polymerization to the synthesis of new well-defined materials.

The articles in this book give strong evidence that radical polymerization has entered a renaissance. Many new controlled radical systems have been discovered, and substantial progress has been achieved in understanding these

reactions and in quantitative measurement of the rates, equilibria, and concentrations of the species involved. It seems that a thorough understanding of the reactions involved in controlled radical polymerization, especially those carried out in the presence of organometallic derivatives, requires a concerted effort in various areas of chemistry, including theoretical and computational chemistry; kinetics; physical organic chemistry; organic and bioorganic synthesis; and organometallic and coordination chemistry.

This book is addressed to chemists interested in radical processes and especially in controlled/living radical polymerization. It provides an introduction to the field and summarizes the most recent accomplishments in controlled radical systems.

Acknowledgements

Financial support for the symposium from the following organizations is gratefully acknowledged: ACS Polymer Division, Inc., ACS Petroleum Research Fund, Amoco, Bayer, Aristech, BFGoodrich, Ciba-Geigy, Eastman Chemicals, Eastman Kodak, Elf Atochem, Exxon, Hoechst Celanese, ICI, Kaneka, Loctite, Mitsui Chemicals, National Starch, Procter & Gamble, Raychem, and S.C. Johnson.

KRZYSZTOF MATYJASZEWSKI
Department of Chemistry
Carnegie Mellon University
4400 Fifth Avenue
Pittsburgh, PA 15213

August 15, 1997

Chapter 1

Overview: Fundamentals of Controlled/Living Radical Polymerization

Krzysztof Matyjaszewski

Department of Chemistry, Carnegie Mellon University, 4400 Fifth Avenue,
Pittsburgh, PA 15213

The fundamentals of controlled/"living" polymerization are discussed and the effects of slow initiation, transfer, termination and slow exchange on rates, molecular weights, polydispersities and end-functionalities are described. Some special features of and requirements for controlled radical polymerization are presented. Historical evolution of concepts leading to controlled radical polymerization is reviewed. Developments of several basic concepts in this field are summarized. Potential prospects for controlled radical reactions are evaluated.

Radical polymerization is a very important commercial process for preparing high molecular weight polymers because it can be used for many vinyl monomers under mild reaction conditions, requiring the absence of oxygen but tolerant to water, and large temperature ranges (-20 to 200 °C).⁽¹⁾ In addition, many monomers can easily copolymerize radically leading to an infinite number of copolymers with properties dependent on the proportions of the comonomers. The only disadvantage to conventional radical polymerization is the poor control of macromolecular structures including degrees of polymerization, polydispersities, end functionalities, chain architectures and compositions. Thus, it is desirable to prepare, by radical polymerization, new well-defined block and graft copolymers, stars, combs and networks that have not been previously prepared using ionic

living polymerizations.(2) Therefore, controlled/"living" radical polymerizations allow for the synthesis of new well-defined and functional materials from a larger range of monomers under simpler reaction conditions than are appropriate for ionic processes.

This overview Chapter describes the fundamentals of controlled/"living" radical polymerization, discusses historical developments of several concepts in this field and attempts to show potential prospects for controlled radical reactions.

Requirements for Controlled /"Living" Polymerizations

Living polymerization was first defined by Szwarc (3) as a chain growth process without chain breaking reactions (transfer and termination). Such a polymerization provides end-group control and enables the synthesis of block copolymers by sequential monomer addition. However, it does not necessarily provide for molecular weight control and narrow molecular weight distributions (MWD). Additional prerequisites to achieve these goals are that the initiator should be consumed at early stages of polymerization and that exchange between species of various reactivities is fast in comparison with propagation.(4-8) If these additional criteria are met, a *controlled* polymerization results. Polymerization can also be defined as controlled if side reactions occur, but only to an extent which does not considerably disturb the control of the molecular structure of the polymer chain.

Recently, many new "living" polymerization systems, such as carbocationic, ring-opening metathesis, group transfer, and radical polymerizations, have been developed. The term "*living*" (with quotation marks) indicates synthesis of well-defined polymers under conditions in which chain breaking reactions undoubtedly occur, as in radical polymerization, but polymerization systems which lead to well-defined polymers but are not completely free of termination or transfer, as are radical polymerizations, should be named *controlled* rather than living. Since many researchers are used to the term living, the term *controlled/"living"* may also describe the essence of these systems.(9)

Ideally, controlled/"living" systems lead to polymers with degrees of polymerization predetermined by the ratio of the concentrations of consumed monomer to the introduced initiator $DP_n = \Delta[M]/[I]_0$, polydispersities close to Poisson distribution ($DP_w/DP_n \approx 1 + 1/DP_n$), and with all chains end-functionalized. Experimentally, the best way to evaluate such systems is to follow the kinetics of polymerization and the evolution of molecular weights, polydispersities and functionalities with conversion. Well-controlled systems should provide:

a) linear kinetic plots in semilogarithmic coordinates ($\ln([M]_0/[M])$ vs time), if the reaction is first order in monomer concentration; acceleration on such plots may indicate slow initiation whereas deceleration may indicate termination or deactivation of the catalyst,

b) linear evolution of molecular weights with conversion; molecular weights lower than predicted by $\Delta[M]/[I]_0$ ratios indicate transfer, molecular weights higher than predicted by $\Delta[M]/[I]_0$ indicate inefficient initiation or chain coupling (at most, twice higher than predicted molecular weights can be formed by bimolecular radical coupling),

c) polydispersities should decrease with conversion for systems with slow initiation and slow exchange; polydispersities increase with conversion when the contribution of chain breaking reactions becomes significant,

d) end functionalities are not affected by slow initiation and exchange but they are reduced when chain breaking reactions become important.

Typical dependencies for controlled/living systems and the corresponding deviations are illustrated schematically in Fig. 1.

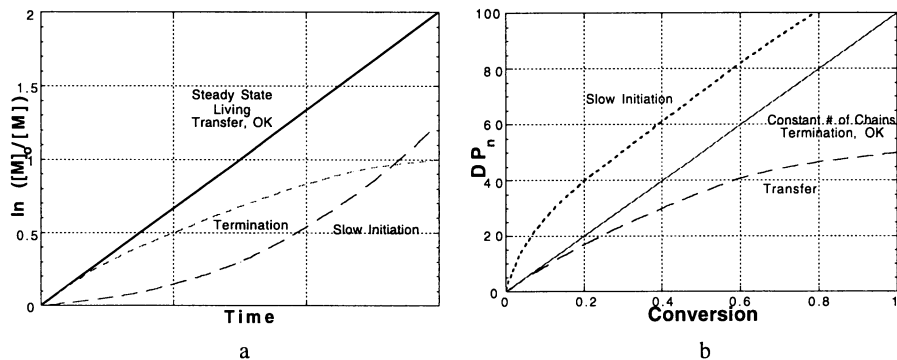


Fig. 1. Schematic effect of slow initiation, transfer, termination and exchange on: a) kinetics, b) molecular weights.

In the next sections, the effects of transfer, termination, slow exchange and slow initiation on polydispersities, molecular weights and functionalities are discussed more quantitatively.

Effect of chain transfer and termination. Figures 2a and 2b show the effects of transfer and termination on the proportion of active chains and polydispersities in systems with instantaneous initiation as a function of monomer conversion for ratios of $[M]_0/[I]_0 = 100$ and 1,000. The same ratios of $k_{tr}/k_p = 10^{-3}$ were chosen to illustrate how

(pseudo)unimolecular transfer (k_{tr}), transfer to monomer (k_{trm}) and (pseudo)unimolecular termination (k_t) affect the polymerization control for targeted DP = 100 and 1,000. Fig. 2a shows that for the arbitrarily chosen chemoselectivities (defined as the ratio of the rate constants of chain breaking to propagation) some chains lose their end-functionalities and polydispersities increase with the progress of the reaction. For example, if $k_{trm}/k_p=10^{-3}$, then 50% of the chains will have lost activity and the polydispersity will have reached $M_w/M_n=1.5$ at complete conversion. Nearly the same behavior is observed for (pseudo)unimolecular transfer, though the control at 80 to 90% conversion is much better than for transfer to monomer. The enhanced effect of unimolecular transfer at high conversions originates from the reduced rate of propagation and the constant rate of transfer. The effect of termination is even more surprising. At high conversions, chain termination has a minor influence on polydispersity, because chain growth is almost complete and only small redistributions of chain lengths can occur. In contrast, short chains formed by transfer at high conversions increase polydispersity significantly. Therefore, if transfer is the dominant chain breaking reaction, conversion should be limited to retain end functionality, an important consideration for the synthesis of end-functionalized polymers or block copolymers.

Fig. 2b shows that the synthesis of shorter chains with targeted DP=100 is much more successful. Although the conditions and chemoselectivities are exactly the same as for Fig. 2a, where only ill-defined polymers were formed, well-defined polymers with controlled functionalities and low polydispersities are obtained for shorter chains.

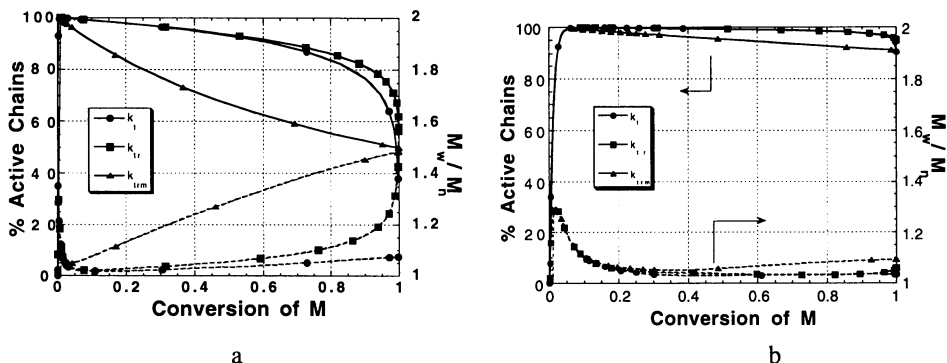
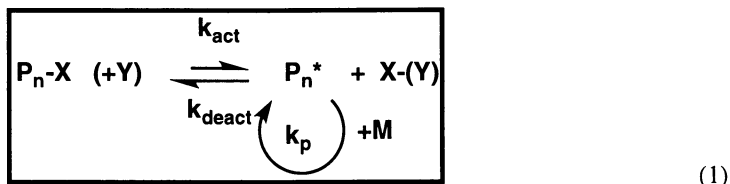


Fig. 2. Proportion of active chains and polydispersities as a function of monomer conversion for the ratios of $k_{t(tr)}/k_p=0.001$, $[M]_0=10$ mol/L, (a): $[I]_0=0.01$ mol/L and (b): $[I]_0=0.1$ mol/L.

Thus, in many new controlled/"living" polymerizations (radical systems included) it is possible to prepare well-defined polymers which are, however, limited to a certain molecular weight defined by contributions of side reactions.

Effect of exchange between species of different reactivities on polydispersities. Nearly all new controlled/"living" polymerizations (cationic, group transfer, and radical) are based on exchange between active and dormant species. The activation and deactivation process may take place uni- or bimolecularly:



The dormant species $\text{P}_n\text{-X}$ can be activated either spontaneously (thermally) or in the presence of a catalyst (Y), the rate constant of activation being k_a (or k_{act}) to form the active species P_n^* . This process is reversible and the active species are deactivated with the rate constant of deactivation being k_d (or k_{deact}) by the deactivator X (or XY). Only active species propagate with the rate constant of propagation (k_p). In such systems, the polydispersities and molecular weight control are defined by the relative ratios of the rates of deactivation and propagation (k_p). After all initiator ($[\text{I}]_0$) is converted to growing chains, the polydispersities for many systems with slow exchange are defined by a very simple equation (2):

$$M_w/M_n = 1 + ([\text{I}]_0 k_p) / ([\text{X}] k_d) (2/p - 1) \quad (2)$$

where $[\text{X}]$ is the concentration of deactivator (X or XY) and p is monomer conversion. If deactivation is unimolecular (ion pair, caged radicals), then $[\text{X}]$ is omitted in eq. 2. Eq. 2 is valid for systems in which the equilibrium is strongly shifted to dormant species, where sufficiently long chains are formed and polydispersities do not significantly exceed 2. For the degenerative transfer process (cf. equilibrium III in eq. 5) concentrations of deactivator and of chains are nearly identical and therefore eq. 2 simplifies to eq. 3:

$$M_w/M_n = 1 + k_p/k_{\text{exch}} (2/p - 1) \quad (3)$$

The evolutions of polydispersities and molecular weights with conversion for three systems with the ratios of $([\text{I}]_0 k_p) / ([\text{X}] k_d) = 0.01, 0.1$ and 1 are shown in Fig. 3. If the ratio is smaller than 1, then the rate of activation does not affect the polydispersities.

However, for ratios ≥ 1 , a small effect of the rate of activation can be noticed. The overall polydispersities were calculated without taking into account the residual initiator and therefore are smaller than those with the initiator taken into account.⁽⁵⁾

Figure 3a shows that the simulated polydispersities decrease with conversion (as observed in many "living" systems) and are lower for both smaller initiator concentrations (longer chains) and faster deactivation (higher $[X]$, higher k_d/k_p). Thus, polymers with lower polydispersities can be prepared for chains with the same length, provided that the deactivation process is faster. Deactivation rates can be increased by using either a higher concentration of deactivator or a more reactive deactivator (higher k_d). The effect of slow exchange, discussed above, is valid for systems when slow exchange is the only reason for elevated polydispersities. If an additional side reaction (transfer, termination, etc.) occurs then the polydispersity should increase with conversion, leading to a certain "window" of polymerization degree at which well-defined polymers can be prepared. This is probably the most realistic case. At a low range of molecular weights the polydispersities are higher than in ideal systems due to slow exchange but they increase at high DP due to progressively more noticeable side reactions.

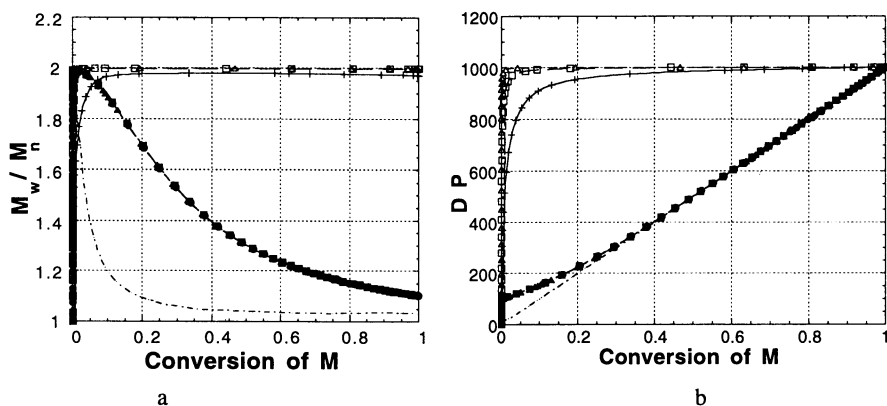


Fig. 3. Dependence of polydispersities (a) and degrees of polymerization (b) on conversion for systems with slow exchange and with the ratio of $([I]_0 k_p)/([X] k_d) = 0.01$ (---), 0.1 (variable k_d : \blacktriangle \bullet \blacksquare) and 1 (variable k_d : \triangle \square).

Figure 3b shows the effect of slow deactivation on evolution of DP with conversion. If deactivation is relatively fast, DP increases linearly with conversion. However, for slow deactivation $([I]_0 k_p)/([X] k_d) = 1$, DP is much higher than predicted. Control is better with faster deactivation or lower initiator concentration, meaning that longer chains are synthesized. This will be true until chain breaking reactions affect DP and polydispersities.

It must be noted that in some systems, slow exchange may lead to polymers with polydispersities $M_w/M_n > 2$. This can happen even in systems in which a contribution of chain breaking reactions is insignificant.

Initiation. Fast initiation is a prerequisite for the synthesis of polymers with degrees of polymerization predetermined by $\Delta[M]/[I]_0$ ratios. In systems without exchange and without chain breaking reactions, the upper polydispersity limit is due only to slow initiation, $M_w/M_n < 1.35$.⁽¹⁰⁾ When both initiator and growing chains exist in dormant and active forms then polydispersities originating from slow initiation may be significantly higher. Slow initiation leads to slower polymerization, usually accompanied by induction periods and to molecular weights higher than predicted by $\Delta[M]/[I]_0$. Slow initiation is especially dangerous when synthesizing low molar mass polymers.

Other factors. Control of molecular weights and polydispersities may be additionally affected by the reversibility of propagation and by inhomogeneity of the system, such as would result from slow dissolution of the initiating system. Heterogeneous catalytic systems may also sometimes lead to higher polydispersities. However, if the catalyst acts by the principle of activation/deactivation, then heterogeneity should not affect polydispersities unless exchange reactions are too slow (e.g. concentration of deactivator X or XY is too low).

Peculiarities of Controlled Radical Systems

The discussion in the previous section could lead to a pessimistic conclusion that conventional radical polymerizations can never be controlled, due to slow initiation and unavoidable termination. Fortunately, the concept of exchange between active and dormant species has been very helpful in converting ill-defined radical systems to controlled polymerizations.

Suppression of chain transfer and termination. Chain transfer is not the main obstacle for the synthesis of well-defined polymers by a radical mechanism. Monomer transfer coefficients are usually below $k_{trm}/k_p < 10^{-4}$. This means that half of the chains participate in transfer at the stage of $DP=10,000$ but less than 10% of chains at $DP=1,000$. Thus, transfer to monomer should not interfere with the synthesis of polymers with $DP_n < 1000$ ($M_n \approx 100,000$). Of course, transfer to solvent, polymer and transfer agents will

operate as usual, but the proper choice of reaction conditions should lead to well-defined polymers, especially at lower ranges of molecular weights.

In contrast, termination is impossible to avoid in homogeneous radical polymerization. Two radicals will recombine or disproportionate with nearly diffusion controlled rates. Fortunately, propagation is first order, whereas termination is second order with respect to the concentration of growing radicals. Thus, the contribution of termination decreases when the concentration of propagating radicals $[P^\bullet]$ is reduced. For example, in the bulk polymerization of styrene at $\approx 100^\circ\text{C}$, propagation is 1000 times faster than termination at $[P^\bullet] \approx 10^{-7}\text{ M}$:

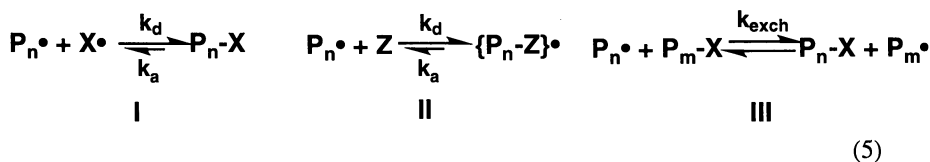
$$R_p/R_t = (k_p [P^\bullet] [M]) / (k_t [P^\bullet]^2) \quad (4)$$

$$R_p/R_t \approx (10^3 \text{ M}^{-1} \text{ s}^{-1} \cdot 10 \text{ M} \cdot 10^{-7} \text{ M}) / (10^7 \text{ M}^{-1} \text{ s}^{-1} \cdot 10^{-7} \text{ M} \cdot 10^{-7} \text{ M}) \approx 1000$$

This means that at $[P^\bullet] \approx 10^{-7}\text{ M}$, relatively well-defined polymers with $DP_n \approx 100$ would contain less than 10% of terminated chains. In order to prepare well-defined polystyrene with $DP \approx 1000$, concentration of growing radicals should be additionally a few times lower, e.g. $[P^\bullet] \approx 10^{-8}\text{ M}$. In acrylate polymerizations the concentrations of growing radicals could be higher because of the higher k_p/k_t ratios.

In conventional radical polymerization, a sufficiently low concentration of radicals is attained by slow initiation. However, as discussed above, slow initiation is incompatible with controlled polymerization. Thus, a low concentration of growing radicals must be achieved by other means.

Exchange between active and dormant species. Thus, a requirement for controlled radical systems is that initiation should be completed at low monomer conversions; the concentration of propagating radicals should be low ($[P^\bullet] \approx 10^{-8}\text{ M}$), but the total concentration of growing chains should be much higher, e.g. 10^{-2} M for bulk polymerization to obtain $DP \approx 1000$. These requirements can be met through dynamic equilibration of minute amounts (ppm) of propagating radicals with some form of dormant chains. Three general equilibrium systems are shown schematically below:



The first system is based on the deactivation of growing radicals with relatively stable (persistent) radicals, X^\bullet , which may also be inorganic or organometallic species. The reversible activation process may be spontaneous (thermal) or catalyzed as in atom transfer radical polymerization.

The deactivation in the second system involves species with even numbers of electrons forming stable (persistent) radicals. Z may be a nonpolymerizable vinyl monomer, or inorganic, or organometallic species, etc. In both systems, the equilibria are very strongly shifted towards the dormant species to reduce the concentration of growing radicals to $[P^\bullet] \approx 10^{-8 \pm 1}$ M.

The last system employs the so-called degenerative transfer process which has an equilibrium constant of $K=1$. In this case, the protected group is never spontaneously cleaved but rather transferred in a bimolecular process from the dominating dormant species carrying the protecting group X (usually iodine) to a minute amount of propagating radicals. If exchange is faster than propagation, well-defined polymers can be prepared. This system can employ conventional initiators such as AIBN, BPO, etc, provided that their concentration is smaller than that of the transfer agent ($R-X$).

In these systems, the prerequisite for the synthesis of controlled polymers is a sufficiently fast exchange process. As discussed in Section 1.2, polydispersities decrease with conversion and are lower for systems with higher concentrations of deactivator (X^\bullet for system I, Z for system II), lower k_p/k_d ratios (relatively faster deactivation) and lower concentration of chains ($[P_n-X]$ or $[P_n-Z]^\bullet$, respectively). In system III polydispersities depend only on conversion and k_p/k_{exch} .

The thermodynamics and the dynamics of exchange in these reactions are the most important parameters affecting the control of radical polymerizations. Therefore, structures and reactivities of persistent radicals and catalysts which may accelerate exchange are among the most important features of these systems.

Initiators. In systems I and II, the initiators can be either prepared in situ or synthesized in advance. Then, by either increasing temperature or adding catalyst/activator, initiation may start. As a rule of thumb, the structure of the initiator should resemble the dormant macromolecular species. For example, in the TEMPO-mediated polymerization of styrene, 1-phenylethyl alkoxyamine is very successful,⁽¹¹⁾ in atom transfer radical polymerization (ATRP) of acrylates 2-bromopropionates are good initiators,^(12,13) whereas 2-bromopropionitrile is an efficient initiator for acrylonitrile polymerization.⁽¹⁴⁾ If the initiator is more difficult to activate than the polymeric species, initiation is usually slower than propagation. If, however, the initiator is more easily activated than dormant chains, it

may dimerize, reduce the initiation efficiency and significantly increase the concentration of persistent radicals, X. There are some exceptions to this rule. For example, sulfonyl halides(15) and 2-bromo-2-methylmalonates can be successfully applied to ATRP of several monomers because radicals derived from them dimerize relatively slowly, even though they are formed in high concentrations.

Some initiation systems can be prepared in situ. For example, the TEMPO - mediated styrene polymerization can be thermally self-initiated in the presence of TEMPO(16) or by using BPO/TEMPO(17) or AIBN/TEMPO(18) mixtures. Reverse ATRP can be initiated using AIBN/CuX₂/bipy mixtures (bipy =2,2'bipyridine).(19)

Contribution of thermal self-initiation. In the controlled polymerization of styrene and substituted styrenes, the thermal self-initiated polymerization of styrene occurs simultaneously with the controlled process (systems I, II, or III). The contribution of thermal self-initiation to the overall rate and to the total number of polymer chains in the system should be carefully assessed.

The rate of thermal self-initiation has been studied and the rates of generation of new radicals are known at various temperatures.(20-22) The so-called Mayo dimer,(23,24) which is an intermediate in this process, is additionally responsible for the reduction of molecular weights since it has a very large transfer coefficient.(25) The overall rate of self-initiated polymerization, however, should not be confused with the rate of radical generation. For example, approximately 1 M/hour (about 15%/hour) of styrene is consumed at 130 °C in bulk thermal polymerization, but less than 10⁻³ M/hour of radicals are generated (which correlates to M_n≈200,000). Thus, in ten hours less than 10⁻² M radicals (equal to new chains) are generated. Usually this number may even be lower because the rate of self-initiation is second or third order in respect to monomer.(21,26)

It has been reported that in some TEMPO and other nitroxide-mediated styrene polymerizations, the overall rate is very close to the thermal self-initiated process.(27-29) At the same time, molecular weights correlate relatively well with the amount of TEMPO or alkoxyamine present in the system. This behavior was attributed to comparatively small contribution of radicals generated by activation (dissociation) of dormant alkoxyamines to the overall propagation rate.(29) At the same time, newly generated chains were continuously trapped by the small excess of TEMPO which was present in the system. Therefore, this system can be considered as self-regulating, because without self-initiation the overall polymerization rate would be much smaller, which is actually the case for polymerizations of acrylates. The overall polymerization rate is defined by the total concentration of radicals, those resulting from self-initiation and those from the reversible

activation process. Since the exchange between them is fast, they all grow simultaneously yielding well-defined polymers. Since the equilibrium constants (cf. equilibrium I in eq. 5) in TEMPO mediated styrene polymerization are low, e.g. $K=10^{-11}$ M, the contribution of radicals generated by dissociation of alkoxyamines is below 30% of the total concentration of radicals when $[P-X]_0=10^{-2}$ M, but this value increases to 50% when $[P-X]_0=10^{-1}$ M. Thus, potentially, at still higher concentration of alkoxyamines the rate of polymerization could start increasing, though this would lead to polymers with very low molecular weights. Another possibility to enhance the proportion of radicals formed from alkoxyamines is to increase the value of the equilibrium constant by either increasing temperature or using alkoxyamines which dissociate faster. Unfortunately, increasing temperature does not help because both dissociation and thermal self-initiation are accelerated. However, the second approach was quite successfully applied to polymerization of acrylates.(30)

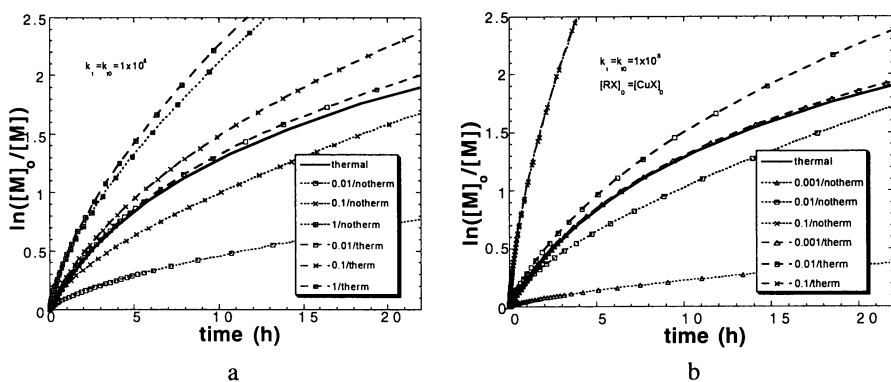


Fig. 4. Kinetics of (a) TEMPO-mediated and (b) ATRP bulk styrene polymerization at 130 °C. Simulations are based on $K=2.5 \cdot 10^{-11}$ M (a) and $K=3 \cdot 10^{-8}$ (b). In both systems parameters for the thermal self-initiation were taken from Ref. (29). For TEMPO-mediated systems, the concentration of alkoxyamines varied: 1, 0.1, 0.01 M. For ATRP, $[CuBr/2dNbipy]_0 = [RBr]_0 = 0.1, 0.01$ and 0.001 M.

Similar behavior can be found in ATRP. However, when the concentration of alkyl halides and $CuX/2bipy$ are high enough (both around 0.1 M), the polymerization rate is >10 times faster than the rate of thermal self-initiated polymerization. However, when the concentration of either catalyst or initiator is significantly reduced (ATRP is first order in respect to initiator and catalyst), the overall polymerization rate becomes comparable to that of a thermal process. A further decrease in the concentration of either reagent does not additionally reduce the polymerization rate which, under steady-state conditions, can not be smaller than that of a thermal self-initiation process! This minimum rate is not observed for (meth)acrylates which do not self-initiate.

Figure 4 shows rate of thermal styrene polymerization at 130 °C together with the

rates of several TEMPO-mediated and ATRP styrene polymerizations at various concentrations of initiators and catalysts. A hypothetical rate is shown for systems without thermal self initiation.

To summarize, self-initiation is important for the polymerization of styrene. It controls the polymerization rates for most TEMPO-mediated systems as well as some ATRP when low concentrations of either catalyst or initiator are used. Nevertheless, the exchange reactions provide for good control of molecular weights in both systems.

Evolution of Controlled/"Living" Radical Polymerization.

Table 1 illustrates development of fundamental concepts in organic radical processes, some concepts in living polymerization and advances in radical polymerizations which all have contributed to controlled/"living" radical polymerization and without which the present understanding and control of radical reactions would not be possible.

Radical addition reactions have for a long time been considered to be very difficult to control due to termination reactions which could not be avoided. Probably the first example of a successful addition of halogenated compounds to alkenes via radical intermediates (Atom transfer radical addition, ATRA) was provided by Kharash (31) under photochemical conditions. This atom transfer radical process was subsequently converted to metal catalyzed reactions by Minisci,(32) Vofsi (33) and others during the 1960s. At approximately the same time, various nitroxides were prepared as stable radicals but without any application to organic synthesis at that time.(34,35)

These reactions have found many synthetic applications as thoroughly summarized by Bellus in 1985.(36) At that time, it was not clear how these reactions occurred until Fischer (37) provided the explanation based on the persistent radical effect for the observed unexpectedly high chemoselectivities. Numerous systems based on atom transfer reactions were used for structure-reactivity comparisons (38) and for refined organic/bioorganic synthesis (39) with many organometallic catalysts.(40,41) Atom transfer radical reactions gained increasing importance in organic synthesis because of their high chemo-, regio-, and stereoselectivities and tolerance to many useful functional groups.(39,42-44) Future progress in this area requires additional developments of new catalysts which could increase the rates and selectivities of the addition, elimination and rearrangement reactions.

Radical addition reactions have for a long time been considered to be very difficult to control due to termination reactions which could not be avoided. Probably the first example of a successful addition of halogenated compounds to alkenes via radical intermediates (Atom transfer radical addition, ATRA) was provided by Kharash (31) under

photochemical conditions. This atom transfer radical process was subsequently converted to metal catalyzed reactions by Minisci,(32) Vofsi (33) and others during the 1960s. At approximately the same time, various nitroxides were prepared as stable radicals but without any application to organic synthesis at that time.(34,35)

Table 1
Evolution of Controlled/"Living" Radical Polymerization

Organic Synthesis	Living Polymerization	Controlled Radical Polymerization
1940's Kharash <i>First ATRA (hv)</i>	1950's Szwarc <i>Living Anionic, Block Copolymers</i>	≤1970's Borsig, Braun <i>Ar₂CH, Ar₃C</i> Minoura <i>Cr (II) Acetate/ MMA</i>
1960's Minisci, Vofsi <i>CuX/RX/olefin</i> Rosantsev <i>Nitroxides</i> Kochi <i>Free Radicals & OM</i>	1970's Penczek/Matyjaszewski <i>A* <=> D in CROP</i>	1980's Otsu <i>"1st" LRP, Iniferters</i> Rizzardo / Solomon <i>TEMPO</i> Rizzardo <i>Addn./Fragmentation</i>
1980's Fischer <i>Persistent Radical Effect</i> Curran, Giese, Newcome <i>RI, RSnH, RSeAr</i> Barton <i>Thiohydroxamate</i> Kochi, Halpern, Giese <i>Organocobalt</i>	1980's Kennedy <i>Inifers, "L" Carbocationic</i> Higashimura, Sawamoto, Sigwalt, Matyjaszewski <i>"Living" Carbocationic</i> DuPont, Müller, Quirk <i>GTP</i> Grubbs, Schrock, Novak <i>Living ROMP & OM</i>	1990's Georges <i>TEMPO / Styrene</i> Matyjaszewski <i>Degen. Transf., ATRP</i> Sawamoto <i>ATRP + AI (cocat.)</i> Various Groups <i>New nitroxides</i> <i>Various Mt/RX in ATRP</i>
1990's <i>Various Mt in ATRA</i> <i>Stereocontrol ...</i>	1990's Matyjaszewski, <i>Controlled & Ranking</i> Müller <i>Exchange Reactions</i>	

These reactions have found many synthetic applications as thoroughly summarized by Bellus in 1985.(36) At that time, it was not clear how these reactions occurred until Fischer (37) provided the explanation based on the persistent radical effect for the observed unexpectedly high chemoselectivities. Numerous systems based on atom transfer reactions

were used for structure-reactivity comparisons (38) and for refined organic/bioorganic synthesis (39) with many organometallic catalysts.(40,41) Atom transfer radical reactions gained increasing importance in organic synthesis because of their high chemo-, regio-, and stereoselectivities and tolerance to many useful functional groups.(39,42-44) Future progress in this area requires additional developments of new catalysts which could increase the rates and selectivities of the addition, elimination and rearrangement reactions.

Although radical polymerization has been known for a very long time, it was always difficult to control because of unavoidable termination between growing radicals. It was possible to control either rates or molecular weights or end groups but never all of these three parameters simultaneously. For example, several retarders or inhibitors were used to moderate polymerization rates, some of them can be used now as components of controlled/"living" radical systems; here both nitroxides or cupric halides can be cited.(45,46) Molecular weights were controlled by transfer agents and again some of them can be now used in controlled systems. End functionalities were controlled by using either functional initiators or functional transfer agents leading to telechelic polymers.(47,48) Special initiating systems were developed based on organometallic compounds employing redox systems.(49) Some of them are not very far from ATRP.

However, in none of these systems was it possible to prepare polymers with low polydispersities, to observe a linear increase of molecular weight with conversion or to convert the initiators to growing chains quantitatively. Thus, radical polymerization has always been very far from living systems.

Living polymerization as a chain growth process without chain breaking reactions was discovered and developed by Szwarc.(3) Living anionic polymerization of non-polar monomers was the first technique used to synthesize macromolecules with controlled topologies, with predetermined molecular weight and nearly Poisson distribution molecular weights and novel block copolymers with very high efficiency.(50) This system was based on entirely ionic species though differences in reactivities of ion pairs and free ions were very significant. The first system in which both dormant and active species were clearly spectroscopically observed and both kinetics and thermodynamics of exchange reactions determined was the cationic ring-opening polymerization of tetrahydrofuran.(51) A concept of equilibria between dormant and active species that arose from this work has subsequently been successfully used in carbocationic polymerization,(6) though initially pseudocationic mechanism,(52) invisible propagating species,(53) and stretched-covalent bonds (54). were postulated. Nearly simultaneously, group transfer polymerization (55) and other approaches based on exchange between active and dormant chains were used in anionic polymerization. Some new organometallic catalysts may also act in a similar way.

It was realized at that time that most of these new systems were much less controlled than the original living anionic polymerization and that chain breaking reactions did occur. Using many of these systems, it was possible to prepare well-defined polymers with $M_n=10,000$ but it was not possible to make polymers with $M_n=100,000$. It was considered useful to rank such "living" systems and to provide precise kinetic data on transfer and termination coefficients which would define limits for control of molecular weights under particular conditions.(56) An additional peculiarity of some of these systems was that polydispersities decreased with conversion in contrast to general expectation for contribution of chain breaking reactions.(7) The main reason for decreasing polydispersities was slow exchange between species of various reactivities. Kinetic treatment of such systems was very useful for better design of controlled/"living " radical polymerization systems.(57)

A more detailed and systematic discussion of controlled radical reactions will be covered in the next section. Here, only a chronological development of some concepts depicted in Table 1 is described. The first evidence of controlling radical polymerization was reported by Borsig (58) who used diaryl and triaryl protected groups in polymerizations of MMA and observed increase of molecular weights with conversion and also the formation of block copolymers. This system was later extensively studied by Braun.(59) However, polydispersities were always relatively high, initiation efficiencies low and the molecular weights did not evolve linearly with conversion. A possible reason for such big deviations from living characteristics was a slow but continuous initiation by the bulky organic radicals.

In the seventies, Minoura reported that MMA polymerization initiated by BPO in the presence of chromium (II) acetate led to a monotonous increase of molecular weight with conversion and also claimed the preparation of block copolymers.(60) He assigned these phenomena to propagation via radicals coordinated to chromium which were not able to terminate. Later, this system was criticized by Banderman (61) who clearly demonstrated that the system conforms to conventional radical polymerization, the apparent control being obtained by a combination of the dead-end and gel effects. Indeed, efficiency of initiation was very low, often well below 10%.

In 1982 Otsu, for the first time, used the term *living* radical polymerization to describe a polymerization in the presence of dithiocarbamates.(62) In analogy with the inifers used in carbocationic systems,(63) he proposed that dithiocarbamates act as iniferters, i.e. agents which initiate, transfer and terminate. Unfortunately, as in the previously discussed systems, polydispersities were always relatively high, molecular weights did not evolve linearly with conversion and initiation efficiency was low.

A new system for controlling radical polymerizations based on nitroxides as stable radicals appeared in the patent literature in 1985.(64) Unfortunately, the work of Rizzardo and Solomon was not sufficiently recognized at that time. Rizzardo has subsequently proposed another approach to controlled radical polymerization based on addition-fragmentation chemistry (65) which can be considered as a special case of degenerative transfer.

It was not until 1993 when Georges published his first paper on controlling the bulk radical polymerization of styrene in the presence of TEMPO, that interest in radical polymerization revitalized.(17) It now seems that TEMPO-mediated systems are among the most studied controlled radical polymerizations, but these systems have generally been limited to styrene and its copolymers. These limitations may be alleviated by the development of new nitroxides with higher equilibrium constants for the cleavage of the corresponding alkoxyamines.

Simultaneously, our group was working on various systems to control radical processes and reported in 1993 the formation of block copolymers using a $\text{AlR}_3/\text{bipy}/\text{TEMPO}$ system.(66) Subsequently, we used TEMPO in the thermal (16) as well as AIBN and BPO initiated polymerization of styrene.(67) used various substituted nitroxides, e.g. 4-phosphonoxy TEMPO derivative (18) and several nitronyl-nitroxides (68) to accelerate polymerization, and used various phosphites (69) and organometallic derivatives(70) to control the polymerization of several vinyl monomers. Another approach was based on degenerative transfer with alkyl iodides.(71) It should be stressed that although we estimated at that time what values of rate constants and equilibrium constants for exchange between active and dormant species were needed,(72) we were in a continuous search for better systems, hopefully catalytic, to control radical polymerization.

In 1995 two very promising systems for controlling radical polymerizations were reported. They were based on catalytic systems used for atom transfer radical additions and therefore were named atom transfer radical polymerization (ATRP). One of these systems was based on the $\text{RuCl}_2/(\text{PPh}_3)_2$ catalyst which was used for polymerization of MMA initiated by CCl_4 .(73) However, this system appeared to be inactive alone and required activation by aluminum alkoxides. The exact nature of this activation is not clear but probably involves exchange of ligands on ruthenium. Another system was based on the $\text{CuX}/2\text{bipy}$ catalyst used in many atom transfer radical addition reactions.(12) The Cu based ATRP system has proved to be very successful for styrene, (meth)acrylates, acrylonitrile and several other monomers (74) and comonomers. Many different alkyl halides and pseudohalides (75) as well as sulfonyl halides (15) have been used as initiators. Originally, the bipy ligands led to heterogenous systems and were later replaced by substituted bipy with alkyl groups such as dHbipy (4,4'-diheptyl-2,2'-bipyridine) and

dNbipy (4,4'-di(5-nonyl)-2,2'-bipyridine) (76) to homogenize the catalytic system. This considerably improved control and provided polystyrenes with polydispersities below $M_w/M_n < 1.05$, (76) polyacrylonitrile with $M_w/M_n < 1.03$, (14) poly(methyl methacrylate) with $M_w/M_n < 1.06$, (77) and poly(methyl acrylate) with $M_w/M_n < 1.08$. (13) This system has been used for many functional monomers and was successfully used for end-functional polymers and macromonomers. (78,79) In addition, not only homopolymers but also statistical, gradient, alternating, block and graft copolymers have been prepared. (80) It was also possible to prepare stars, combs, hyperbranched and branched (co)polymers. (81,82) An interesting possibility is offered by using polymers prepared by other mechanisms as macroinitiators for ATRP to prepare novel block and graft copolymers. (83-89)

It seems that ATRP can be used for the synthesis of many functional (co)polymers taking advantage of its catalytic nature. However, it uses approximately 1 to 0.1% of redox active transition metal which should be removed from the final polymers. There are many potential ligands for Cu based ATRP, for example Schiff bases (90) and simple alkyl amines or cyclams; (91) their role is discussed in Chapter 16. Not only can Cu and Ru based systems be used but also Fe, (92,93) Ni, (94,95) Rh (79) based systems and many others. The main requirement for a good catalyst is that it should be active in the atom transfer process with the appropriate equilibrium constant and fast exchange as well as high chemoselectivity. This field is expected to rapidly develop by combining many concepts from inorganic and coordination chemistry, as well as organic synthesis.

Approaches towards Controlled/"Living" Radical Polymerization

Table 2 presents main concepts and groups contributing to various areas of controlled/"living" radical polymerization. They can be divided into three subgroups based on three mechanistically different concepts as shown in eq. 5. The difference between the subgroups is related to the mechanism of exchange between active and dormant species:

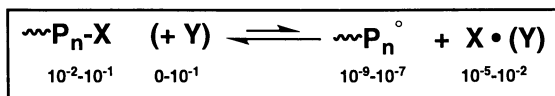
- reversible homolytic cleavage of covalent species
(systems 1-5)
- reversible formation of persistent hypervalent radicals
(systems 6)
- degenerative transfer
(systems 7-8)

All eight cases will be discussed in detail below.

Table 2
Major Concepts and Investigators of Controlled/"Living" Radical Polymerization

No	Concept	Investigators
1	Ar ₃ C / Ar ₂ CH	Borsig, Braun, Crivello, Otsu
2	R - Mt	Minoura, Wayland, Harwood, Matyjaszewski, ...
3	Iniferters	Otsu, Sigwalt, Turner, Smets, Clouet
4	Nitroxides	Rizzardo/Solomon/Moad, Georges, Hawker, Matyjaszewski, Frechet, Priddy, Sogah, Fukuda, Catala, Gnanou, Bon, Yamada,...
5	ATRP	Matyjaszewski, Sawamoto, Percec, Haddleton, Teyssie, Hawker, Frechet, Kops, Boutevin,...
6	Persistent Radical	Matyjaszewski, Harwood, Müllen, ...
7	Degenerative Transfer	Tatemoto, Matyjaszewski, ...
8	Addition / Fragmentation	Rizzardo, Moad, DuPont, Haddleton, Chaumont ...

Reversible Homolytic Cleavage of Covalent Species. The first five entries in Table 2 can be classified as belonging to group I in eq. 5. Thus, they all are based on the homolytic cleavage of covalent species. The first four entries rely on spontaneous thermal cleavage whereas ATRP is catalytic. It has to be, however, recognized that the concentration of the stable counter radical is much higher than that of the growing radical as a result of the persistent radical effect. This is the main reason why the polymerizations are controlled, since radicals do not react one with another but deactivate reversibly with a persistent radical present at a much higher (approximately 1000 times) concentration:



-X = -CAR₂L; -Cr^{III}L_n; -Co^{II}(TMP); -Co^{II}(DMG); -S-C(S)-NR₂; -O-NR₂

-X = -Cl; -Br; -I; -SCN Y = Cu^I•L_n; Ru^{II}•L_n; Fe^{II}•L_n; Ni^{II}•L_n (6)

System 1. Bulky arylalkyl radicals, though historically important, did not provide sufficient control to be considered as useful as some other systems. This system originally developed by Borsig (58) and Braun (59) was also later studied and partially improved by Otsu (96) and Crivello.(97) Research in this area has recently been relatively inactive.

System 2. The weak direct bond between a metalloradical and organic radical has been used successfully for Co-based systems to moderate radical polymerization of acrylates. High molecular weight polyacrylates with very low polydispersities were prepared.(98,99) In some cases photochemical activation was required. For high polymers it may be sometimes difficult to introduce useful functionalities to the chain ends. In addition, some metals may have a very high affinity towards H-atoms and can result in transfer by elimination of β -H atoms. Indeed, similar Co-based systems were successfully used as catalytic chain transfer agents in oligomerization of methacrylates.(100-102) Some other metals, such as Cr have also been used for the same purpose, but less successfully than Co based complexes.(103) In some cases, complexation of the growing radical with a metal rather than direct bonding was proposed. It is possible to imagine a large number of new organometallic species to mediate radical polymerization by this principle. A limitation might be that one organometallic center per chain is necessary.

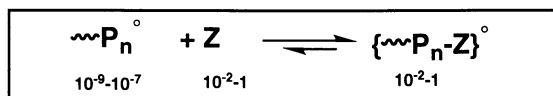
System 3. Dithiocarbamate iniferters have been used in many systems, both under thermal and photochemical conditions as relatively inexpensive and versatile initiators.(62,104) The main disadvantages of dithiocarbamates are that they decompose to CS_2 and aminyl radicals which irreversibly form the corresponding amines, and that they not only deactivate growing chains but also slowly self-initiate.(105) In addition, the exchange is not fast in comparison with propagation, resulting in polymers with higher polydispersities and poor control of molecular weights. It is also possible, that not only homolytic cleavage and degenerate transfer but also degradative transfer occurs in these systems.(106)

System 4. Nitroxides seem to be very efficient moderators for styrene (co)polymerization but especially designed structures are needed for polymerizations of acrylates and for methacrylates β -H abstraction is an important side reaction which is very difficult to avoid. Current research in this area includes design of new nitroxides,(30,107) kinetic studies to better describe the nature of the exchange reactions,(27,28) spectroscopic studies to determine concentrations of free nitroxides (108) and application of alkoxyamines to preparation of new controlled macromolecular structures.(109,110)

System 5. The current research in ATRP systems is focused on the development of new catalysts, and the preparation of new materials, including polymers with novel topologies, compositions and functionalities (80) as well as new block/graft copolymers by combining controlled radical polymerization with other controlled processes.(85-89) Model

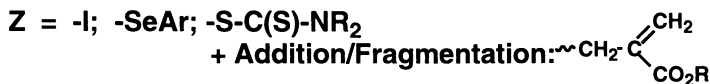
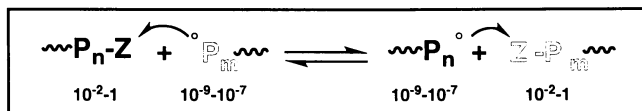
spectroscopic and kinetic studies to better understand quite complicated structures and reactivities of activators and deactivators are necessary. Correlations of structures of initiators with their efficiencies and correlations with macromolecular species is needed. However, the design and preparation of new, more efficient and more selective catalysts is probably the most challenging research direction.

Reversible Formation of Persistent Hypervalent Radicals. The second subgroup of systems employs persistent hypervalent radicals to control polymerization:



System 6. Based on kinetic evidence, however, without sufficient spectroscopic proof, it was originally proposed that such persistent radicals are formed in the presence of organoaluminum compounds complexed by several ligands.(111) However, it was later demonstrated that these systems are much more complex,(112) they are very sensitive to air and oxygen (113) and the formation of the hypervalent Al-based radicals is not very likely. Hypervalent phosphoranyl radicals are known in the literature (114) and can be used to partially control polymerization of vinyl acetate.(69) However, some phosphites are incorporated into polymer chains, reducing control. Cr(II) species interact with organic radicals to form paramagnetic Cr(III) species.(115) This system has not yet been applied in polymerization. Non-homopolymerizable stilbenes were used successfully to control polymerization of MMA presumably by reversible formation of stabilized but non-copolymerizable radicals.(116) Tetrathiafulvaline was also reported to control MMA polymerization, though the mechanism was not clear.(117) It is possible that a persistent radical mechanism was responsible for the polymerization control. Finally, many other species such as thiocarbonyl compounds or phosphoranimines may also provide similar persistent radicals. It is important that this species reacts reversibly to form persistent radicals with high equilibrium constants, high exchange rates and high chemoselectivities. Potential side reactions in the presence of phosphites as moderators include the copolymerization and fragmentation such as Arbuzov rearrangement.(69)

4.3. Degenerative Transfer. This last subgroup is based on degenerative transfer reactions:



Typical radical initiators (AIBN, BPO, etc.) but $\Delta[I] \ll [R\text{-Z}]_0$ (8)

System 7. In contrast to the previous two systems, equilibrium constant for the exchange reaction is $K=1$ and there is no thermodynamic driving force for the exchange process. Protecting group Z should not cleave spontaneously but only in a bimolecular displacement process. This is also the only system which is compatible with slow initiation and can employ AIBN, BPO and other peroxides at their typical temperature regimes. However, the initiator concentration affects here only the polymerization rate but does not affect the total concentration of chains which are defined by the transfer agent, R-Z. Thus, the concentration of the decomposed initiator should be much smaller than that of the transfer agent. In fact, the concentration of dead chains is equal to the concentration of the consumed initiator. If the latter is relatively small in comparison with that of the transfer agent, well-defined systems can be obtained, provided the rate constant of exchange is faster than that of propagation. This sets special requirements for the lability of the C-Z bond. So far, the best Z group is iodine,(71) but organoselenium derivatives also have some potential.(43) Various alkyl iodides were used as transfer agents in polymerization of fluorinated alkenes (118) as well as in polymerization of styrene and acrylates.(119) The structure of the transfer agent is very important and should, in principle, closely match that of the dormant chain. It has been previously proposed that degenerative transfer may also operate for dithiocarbamates,(72) however it is accompanied by degradative transfer.(106) It seems that the contribution of degenerative transfer in TEMPO-mediated systems is relatively low due to steric effects from the four 2,2,6,6-methyl groups.

System 8. A special case of the degenerative transfer is the addition-fragmentation process in the polymerization of methacrylates.(65,120) In this case, the growing radical (P_n^{\bullet}) adds to the unsaturated chain end (P_m^{\ominus}), forms an intermediate radical with both chains coupled (P_{n+m}^{\bullet}) and then fragments either back to the starting species or to P_m^{\bullet} and P_n^{\ominus} . The exchange between growing and unsaturated chains enables continuous growth of all chains, although the exchange is usually not faster than propagation.

Future Outlook

It seems that radical polymerization has entered a renaissance stage. After reaching a certain degree of maturity in the sixties, relatively slow progress was noted in this field during the last thirty years as major efforts were focused on cationic, anionic, ring opening and α -olefin polymerizations which allowed for better control of macromolecular structure and tacticity. However, recent discoveries of many controlled radical systems have refocused the interest of many synthetic chemists on radical polymerization. Indeed, substantial progress has been achieved in the preparation of new, previously unattainable materials, in the mechanistic understanding these reactions, and in the quantitative measurements of the rates and equilibria of the involved reactions and the concentrations of the species involved. It seems that thorough understanding of the reactions involved in controlled radical polymerization, especially those carried out in the presence of organometallic derivatives, requires concerted efforts in various areas of chemistry, starting from theoretical/computational chemistry, kinetics, physical organic chemistry, organic/bioorganic synthesis and organometallic/coordination chemistry. In addition, reliable kinetic measurements of conventional radical processes in homogeneous and heterogeneous media are extremely important for the determination of rate and equilibrium constants of controlled reactions (both for homopolymerization and copolymerizations). Direct observations of growing species and measurements of their concentrations are also very important.

Current research in controlled radical polymerization can be divided into the development of new initiating/catalytic systems, expansion of the range of monomers, and the synthesis of new well-defined materials with novel and controlled architecture, composition and functionality. It seems that currently the most successful methods to control radical polymerization are nitroxide-mediated (mostly TEMPO but other nitroxides are being progressively introduced) and ATRP which are briefly compared below.

The comparative advantage of ATRP is that it is catalytic, it can be used for a large number of monomers, it offers a nearly infinite number of initiators, not only those with low molar mass but also many macromolecular initiators containing activated (pseudo)halogen atoms. ATRP allows for the relatively easy replacement of terminal halogens by more useful functional groups using many many synthetic techniques such as nucleophilic or electrophilic displacement. On the other hand, it might be necessary to remove the redox active transition metal from the final polymer.

The main advantage of the TEMPO-mediated systems is that they are metal-free. However, one relatively expensive nitroxide molecule per chain is needed; it is difficult to

displace nitroxide from the chain end and introduce useful functional groups. At present TEMPO can be used only for preparation of polystyrene and copolymers, though substituted nitroxides can expand the range of monomers. Polymerization rates in TEMPO-mediated polymerization are usually quite low and there have been several reports describing the acceleration by destroying excess nitroxide with acids (121) and simple radical initiators.(122)

Controlled/"living" radical systems are not limited to TEMPO and ATRP and there are many other interesting systems, for example those based on degenerative transfer, on addition-fragmentation chemistry and metalloorganic species and several others.

It is expected that many new systems will be developed which may be transmitted from already successful or newly developed systems from organic/bioorganic synthesis. Three main parameters must be fulfilled for the initiating/catalytic system to be used in controlled radical polymerization.

1. The proportion of growing radicals should be relatively low to suppress bimolecular termination. This will depend on the targeted molecular weight and should be controlled by the corresponding equilibrium constant. Catalytic systems have a strong advantage because the position of equilibrium can be shifted by using more/less activator/deactivator.
2. Exchange between active and dormant species must be fast to prepare polymers with low polydispersities. Exchange can be accomplished by degenerative transfer, however, most often by the reaction with deactivator. Higher concentrations of deactivator will accelerate deactivation and reduce polydispersities but will also slow down the polymerization.
3. High chemoselectivities. Some initiating and catalytic systems may lead to side reactions such as β -H elimination or electron transfer and either oxidation or reduction of the radicals to carbocations or carbanions, respectively. Some other side reactions may take place with functional groups being a part of the monomer or end group. It must be noted that chemoselectivity of propagation should exceed 99.9%, meaning that propagation should occur 1000 times before such side reactions will happen. Thus, not all organic reactions can be transferred to polymer synthesis. Moreover, the polymer chemist can not separate the desired products from side product because both are incorporated to the same chain.

Concerning some other directions of expanding controlled radical polymerization, it is expected to expand the range of monomers, probably down to ethylene and α -olefins, to move towards heterogenous media like emulsions, dispersions and suspensions and to attempt to control polymer tacticity. The author of this overview is, however, skeptical about the possibility of significant control of stereochemistry of polymerization. First, due

to the nearly sp^2 hybridization of many organic radicals, and second due to the fact that in most systems monomer addition occurs to a free radical which is not in the solvent cage and it is probably not coordinated to a organometallic species.

Many spectators, but also some researchers active in the field of controlled radical polymerization, expect that this technique can be used for the synthesis of nearly any (co)polymer of even very high molecular weight. I am again more skeptical, feeling that new controlled radical systems may first find application in the synthesis of relatively low molar mass species ($M_n < 10,000$) with controlled topology, composition and functionalities. Such materials may find applications as additives, surfactants, lubricants, dispersants and may be components of adhesives, solventless coatings and other specialties. It is difficult to expect that polystyrene-polybutadiene-polystyrene triblock copolymers which are now very successfully made anionically can be prepared better and cheaper radically. However, similar triblock copolymers based on acrylates and other polar monomers, especially those containing hydroxy and other hydrophilic groups may be more economically prepared via controlled radical polymerization.

Thus, to summarize, controlled radical polymerization has a very bright future, a lot of new systems are expected to be developed soon but this also requires a lot of fundamental studies and the preparation of many new materials.

Acknowledgments. Support from ARO, NSF, ONR, PRF and ATRP Consortium is gratefully acknowledged.

References:

- (1) Moad, G.; Solomon, D. H. *The Chemistry of Free Radical Polymerization*; Pergamon: Oxford, 1995.
- (2) Webster, O. *Science* **1991**, *251*, 887.
- (3) Szwarc, M. *Nature* **1956**, *176*, 1168.
- (4) Quirk, R.; Lee, B. *Polym. Int.* **1992**, *27*, 359.
- (5) Matyjaszewski, K. *J. Phys. Org. Chem.* **1995**, *8*, 197.
- (6) Matyjaszewski, K., Ed. *Cationic Polymerizations: Mechanisms, Synthesis and Applications*; Marcel Dekker: New York, 1996.
- (7) Matyjaszewski, K.; Lin, C.-H. *Makromol. Chem. Macromol. Symp.* **1991**, *47*, 221.
- (8) Müller, A. H. E.; Zhuang, R.; Yan, D.; Litvinienko, G. *Macromolecules* **1995**, *28*, 4326.
- (9) Matyjaszewski, K.; Müller, A. H. E. *Polym. Prepr. (Am. Chem. Soc., Div. Polym. Chem.)* **1997**, *38(1)*, 6.
- (10) Gold, L. *J. Chem. Phys.* **1958**, *28*, 91.

- (11) Hawker, C. J. *J. Am. Chem. Soc.* **1994**, *116*, 11185.
- (12) Wang, J. S.; Matyjaszewski, K. *J. Am. Chem. Soc.* **1995**, *117*, 5614.
- (13) Paik, H.; Matyjaszewski, K. *Polym. Prepr. (Am. Chem. Soc., Div. Polym. Chem.)* **1996**, *37(2)*, 274.
- (14) Jo, S.; Paik, H.-J.; Matyjaszewski, K. *Polym. Prepr. (Am. Chem. Soc., Div. Polym. Chem.)* **1997**, *38(1)*, 697.
- (15) Percec, V.; Barboiu, B. *Macromolecules* **1995**, *28*, 7970.
- (16) Mardare, D.; Matyjaszewski, K. *Polym. Prepr. (Am. Chem. Soc., Div. Polym. Chem.)* **1994**, *35(1)*, 778.
- (17) Georges, M. K.; Veregin, R. P. N.; Kazmaier, P. M.; Hamer, G. K. *Macromolecules* **1993**, *26*, 2987.
- (18) Matyjaszewski, K.; Gaynor, S.; Greszta, D.; Mardare, D.; Shigemoto, T. *J. Phys. Org. Chem.* **1995**, *8*, 306.
- (19) Wang, J. S.; Matyjaszewski, K. *Macromolecules* **1995**, *8*, 7572.
- (20) Russell, K. E.; Tobolsky, A. V. *J. Am. Chem. Soc.* **1953**, *75*, 5052.
- (21) Hui, A. W.; Hamielec, A. E. *J. Appl. Polym. Sci.* **1972**, *16*, 749.
- (22) Barr, N. J.; Bengough, W. I.; Beveridge, G.; Park, G. B. *Europ. Polym. J.* **1978**, *14*, 245.
- (23) Chong, Y. K.; Rizzardo, E.; Solomon, D. H. *J. Am. Chem. Soc.* **1983**, *105*, 7761.
- (24) Mayo, F. R. *J. Am. Chem. Soc.* **1953**, *75*, 6133.
- (25) Olaj, O. F.; Kauffmann, H. F.; Breitenbach, J. W. *Makromol. Chem.* **1976**, *177*, 3065.
- (26) Fukuda, T.; Terauchi, T. *Chem. Lett.* **1996**, 293.
- (27) Catala, J. M.; Bubel, F.; Hammouch, S. O. *Macromolecules* **1995**, *28*, 8441.
- (28) Fukuda, T.; Terauchi, T.; Goto, A.; Ohno, K.; Tsujii, Y.; Miyamoto, T.; Kobatake, S.; Yamada, B. *Macromolecules* **1996**, *29*, 6393.
- (29) Greszta, D.; Matyjaszewski, K. *Macromolecules* **1996**, *29*, 7661.
- (30) Benoit, D.; Grimaldi, S.; Finet, J. P.; Tordo, P.; Fontanille, M.; Gnanou, Y. *Polym. Prepr. (Am. Chem. Soc., Div. Polym. Chem.)* **1997**, *38(1)*, 729.
- (31) Kharash, M. S.; Jensen, E. U.; Urry, W. H. *Science* **1945**, *102*, 128.
- (32) Minisci, F.; Pallini, U. *Gazz. Chim. Ital.* **1961**, *91*, 1030.
- (33) Asscher, M.; Vofsi, D. *J. Chem. Soc.* **1963**, *1963*, 1887.
- (34) Hoffman, A. K.; Hodgson, W. G.; Jura, W. H. *J. Am. Chem. Soc.* **1961**, *83*, 4675.
- (35) Rosantsev, E. G.; Sholle, V. D. *Synthesis* **1971**, 190.
- (36) Bellus, D. *Pure Appl. Chem.* **1985**, *57*, 1827.
- (37) Fischer, H. *J. Am. Chem. Soc.* **1986**, *108*, 3925.

- (38) Giese, B. *Angew. Chem. Int. Ed. Engl.* **1983**, *22*, 753.
- (39) Curran, D. P. In *Comprehensive Organic Synthesis*; Pergamon: Oxford, 1991; Vol. 4, pp. 715.
- (40) Kochi, J. K. *Organometallic Mechanisms and Catalysis*; Academic Press: New York, 1978.
- (41) Halpern, J.; Ng, F. T. T.; Rempel, G. L. *J. Am. Chem. Soc.* **1979**, *101*, 7124.
- (42) Curran, D. P. In *Free Radicals in Synthesis and Biology*; F. Minisci, Ed.; Kluwer: Dordrecht: 1989; pp p 37.
- (43) Curran, D. P.; Eichenberger, E.; Collis, M.; Roepel, M. G.; Thoma, G. *J. Am. Chem. Soc.* **1994**, *116*, 4279.
- (44) Iqbal, J.; Bhatia, B.; Nayyar, N. K. *Chem. Rev.* **1994**, *94*, 519.
- (45) Bamford, C. H. In *Comprehensive Polymer Science*; G. Allen, S. L. Aggarwal and S. Russo, Eds.; Pergamon: Oxford, 1991; Vol. First Supplement, pp 1.
- (46) Bengough, W. I.; Fairservice, W. H. *Trans. Faraday Soc.* **1971**, *67*, 414.
- (47) Goethals, E. J. *Telechelic Polymers: Synthesis and Applications*; CRC Press, Inc.: Boca Raton, 1989.
- (48) Mishra, M. *Macromolecular Design: Concept and Practice*; Polymer Frontiers International, Inc.: Hopewell, 1994.
- (49) Bamford, C. H. In *Comprehensive Polymer Science*; G. Allen, S. L. Aggarwal and S. Russo, Eds.; Pergamon: Oxford, 1989; Vol. 3; pp 123.
- (50) Szwarc, M. *Carbanions, Living Polymers and Electron Transfer Processes*; Interscience Publishers: New York, 1968.
- (51) Penczek, S.; Matyjaszewski, K. *J. Polym. Sci., Polym. Symp.* **1976**, *56*, 255.
- (52) Gandini, A.; Plesch, P. H. *J. Chem. Soc.* **1965**, *1965*, 4826.
- (53) Sawamoto, M.; Higashimura, T. *Macromolecules* **1978**, *11*, 501.
- (54) Kennedy, J. P.; Ivan, B. *Designed Polymers by Carbocationic Macromolecular Engineering. Theory and Practice*; Hanser: Munich, 1992.
- (55) Webster, O. W.; Hertler, W. R.; Sogah, D. Y.; Farnham, W. B.; RajanBabu, T. V. *J. Am. Chem. Soc.* **1983**, *105*, 5706.
- (56) Matyjaszewski, K. *Macromolecules* **1993**, *26*, 1787.
- (57) Litvinienko, G.; Müller, A. H. E. *Macromolecules* **1997**, *30*, 1253.
- (58) Borsig, E.; Lazar, M.; Capla, M.; Florian, S. *Angew. Makromol. Chem.* **1969**, *9*, 89.
- (59) Braun, D. *Macromol. Symp.* **1996**, *111*, 63.
- (60) Lee, M.; Minoura, Y. *J. Chem. Soc. Faraday Trans. 1* **1978**, *74*, 1726.
- (61) Hungenberg, K.-D.; Bandermann, F. *Makromol. Chem.* **1983**, *184*, 1423.
- (62) Otsu, T.; Yoshida, M. *Makromol. Chem. Rapid Commun.* **1982**, *3*, 127.

- (63) Kennedy, J. P.; Smith, R. A. *J. Polym. Sci., Polym. Chem. Ed.* **1980**, *18*, 1539.
- (64) Solomon, D. H.; Rizzardo, E.; Cacioli, P. *U. S. Pat.* **4, 581, 429**; 1986.
- (65) Rizzardo, E.; Meijs, G. F.; Tang, S. H. *Macromol. Symp.* **1995**, *98*, 101.
- (66) Mardare, D.; Matyjaszewski, K. *Polym. Prepr. (Am. Chem. Soc., Div. Polym. Chem.)* **1993**, *34(2)*, 566.
- (67) Matyjaszewski, K.; Gaynor, S.; Greszta, D.; Mardare, D.; Shigemoto, T. *Macromol. Symp.* **1995**, *98*, 73.
- (68) Shigemoto, T.; Matyjaszewski, K. *Macromol. Rapid Comm.* **1996**, *17*, 347.
- (69) Greszta, D.; Mardare, D.; Matyjaszewski, K. *Polym. Prepr. (Am. Chem. Soc., Div. Polym. Chem.)* **1994**, *35(1)*, 466.
- (70) Mardare, D.; Gaynor, S.; Matyjaszewski, K. *Polym. Prepr. (Am. Chem. Soc., Div. Polym. Chem.)* **1994**, *35(1)*, 700.
- (71) Matyjaszewski, K.; Gaynor, S.; Wang, J. S. *Macromolecules* **1995**, *28*, 2093.
- (72) Greszta, D.; Mardare, D.; Matyjaszewski, K. *Macromolecules* **1994**, *27*, 638.
- (73) Kato, M.; Kamigaito, M.; Sawamoto, M.; Higashimura, T. *Macromolecules* **1995**, *28*, 1721.
- (74) Wang, J. S.; Matyjaszewski, K. *Macromolecules* **1995**, *28*, 7901.
- (75) Matyjaszewski, K.; Wang, J. S. *WO 96/30421* **1996**,
- (76) Patten, T. E.; Xia, J.; Abernathy, T.; Matyjaszewski, K. *Science* **1996**, *272*, 866.
- (77) Grimaud, T.; Matyjaszewski, K. *Macromolecules* **1997**, *30*, 2216.
- (78) Matyjaszewski, K.; Coca, S.; Nakagawa, Y.; Xia, J. *Polym. Mat. Sci. Eng.* **1997**, *76*, 147.
- (79) Percec, V.; Barboiu, B.; Neumann, A.; Ronda, J. C.; Zhao, M. *Macromolecules* **1996**, *29*, 3665.
- (80) Gaynor, S. G.; Matyjaszewski, K. *Polym. Prepr. (Am. Chem. Soc., Div. Polym. Chem.)* **1997**, *38(1)*, 758.
- (81) Gaynor, S.; Balchandani, P.; Kulfan, A.; Podwika, M.; Matyjaszewski, K. *Polym. Prepr. (Am. Chem. Soc., Div. Polym. Chem.)* **1997**, *38(1)*, 496.
- (82) Matyjaszewski, K.; Gaynor, S. G. *Polym. Mat. Sci. Eng.* **1997**, *77*, 210.
- (83) Nakagawa, Y.; Matyjaszewski, K. *Polym. Prepr. (Am. Chem. Soc., Div. Polym. Chem.)* **1996**, *37(2)*, 270.
- (84) Nakagawa, Y.; Miller, P.; Pacis, C.; Matyjaszewski, K. *Polym. Prepr. (Am. Chem. Soc., Div. Polym. Chem.)* **1997**, *38*, 701.
- (85) Coca, S.; Matyjaszewski, K. *Macromolecules* **1997**, *30*, 2808.
- (86) Coca, S.; Matyjaszewski, K. *Polym. Prepr. (Am. Chem. Soc., Div. Polym. Chem.)* **1997**, *38(1)*, 693.

- (87) Chen, X.; Ivan, B.; Kops, J.; Batsberg, W. *Polym. Prepr. (Am. Chem. Soc., Div. Polym. Chem.)* **1997**, *38*(1), 715.
- (88) Gaynor, S. G.; Matyjaszewski, K. *Macromolecules* **1997**, *30*, 4241.
- (89) Hawker, C. J.; Mecerreyes, D.; Elce, E.; Dao, J. L.; Hedrick, J. L.; Barakat, I.; Dubois, P.; Jerome, R.; Volksen, W. *Macromol. Chem. Phys.* **1997**, *198*, 155.
- (90) Haddleton, D.; Jasieczek, C. B.; Hannon, M. J.; Schooter, A. J. *Macromolecules* **1997**, *30*, 2190.
- (91) Matyjaszewski, K. *unpublished results*
- (92) Wei, M.; Xia, J.; Matyjaszewski, K. *Polym. Prepr. (Am. Chem. Soc., Div. Polym. Chem.)* **1997**, *38*(2), 233.
- (93) Wei, M.; Xia, J.; McDermott, N. E.; Matyjaszewski, K. *Polym. Prepr. (Am. Chem. Soc., Div. Polym. Chem.)* **1997**, *38*(2), 231.
- (94) Granel, C.; Dubois, P.; Jerome, R.; Teyssie, P. *Macromolecules* **1996**, *29*, 8576.
- (95) Uegaki, H.; Kotani, Y.; Kamigaito, M.; Sawamoto, M. *Macromolecules* **1997**, *30*, 2249.
- (96) Yamada, B.; Tanaka, H.; Konishi, K.; Otsu, T. *J. Macromol. Sci.- Pure & Appl. Chem.* **1994**, *31*, 351.
- (97) Crivello, J. V.; Lee, J. L.; Conlon, D. A. *J. Polym. Sci., Polym. Chem.* **1986**, *24*, 1251.
- (98) Harwood, H. J.; Arvanitopoulos, L. D.; Greuel, M. P. *Polym. Prepr. (Am. Chem. Soc., Div. Polym. Chem.)* **1994**, *35*(2), 549.
- (99) Wayland, B. B.; Poszmik, G.; Mukerjee, S. L.; Fryd, M. *J. Am. Chem. Soc.* **1994**, *116*, 7943.
- (100) Davis, T. P.; Haddleton, D. M.; Richards, S. N. *J. Macromol. Sci., Rev. Macromol. Chem. Phys.* **1994**, *C34*, 243.
- (101) Melby, L. R.; Janowicz, A. H.; Ittel, S. D. *Eur. Pat. Appl. EP* **193**, 783
- (102) Burczyk, A. F.; O'Driscoll, K. F.; Rempel, G. L. *J. Polym. Sci., Polym. Chem. Ed.* **1984**, *22*, 3255.
- (103) Lee, M.; Utsumi, K.; Minoura, Y. *J. Chem. Soc., Farad. Trans. 1* **1979**, *75*, 1821.
- (104) Nair, C. P. R.; Clouet, G. *J. Macromol. Sci., Rev. Macromol. Chem. Phys.* **1991**, *C31*, 311.
- (105) Turner, R. S.; Blevins, R. W. *Macromolecules* **1990**, *23*, 1856.
- (106) Lambrinos, P.; Tardi, M.; Polton, A.; Sigwalt, P. *Eur. Polym. J.* **1990**, *26*, 1125.
- (107) Puts, R. D.; Sogah, D. Y. *Macromolecules* **1996**, *29*, 3323.
- (108) Veregin, R. P. N.; Georges, M. K.; Hamer, G. K.; Kazmaier, P. M. *Macromolecules* **1995**, *28*, 4391.
- (109) Hawker, C. *Trends Polym. Sci.* **1996**, *4*, 183.

- (110) Grubbs, R. B.; Hawker, C. J.; Dao, J.; Frechet, J. M. J. *Angew. Chem.* **1997**, *36*, 270.
- (111) Mardare, D.; Matyjaszewski, K. *Macromolecules* **1994**, *27*, 645.
- (112) Haddleton, D. M.; Hastings, J. J.; Howarth, O. W.; Tann, S. M. *Polym. Prepr. (Am. Chem. Soc., Div. Polym. Chem.)* **1994**, *35*(2), 566.
- (113) White, D.; Matyjaszewski, K. *J. Macromol. Sci., Pure & Appl. Chem.* **1997**, *34*, 221.
- (114) Davies, A. G.; Griller, D.; Roberts, B. P. *J. Chem. Soc. Perkin II* **1972**, 2224.
- (115) Espenson, J. H. *Acc. Chem. Res.* **1992**, *25*, 222.
- (116) Harwood, H. J.; Christov, L.; Guo, M.; Holland, T. V.; Huckstep, A. Y.; Jones, D. H.; Medsker, R. E.; Rinaldi, P. L.; Soito, T.; Tung, D. S. *Macromol. Symp.* **1996**, *111*, 25.
- (117) Steenbock, M.; Klapper, M.; Muellen, K.; Pinhal, N.; Hubrich, M. *Acta Polym.* **1996**, *47*, 276.
- (118) Yutani, Y.; Tatemoto, M. *European Patent 0 489 370*; **1991**.
- (119) Gaynor, S.; Wang, J. S.; Matyjaszewski, K. *Macromolecules* **1995**, *28*, 8051.
- (120) Moad, C. L.; Moad, G.; Rizzardo, E.; Tang, S. H. *Macromolecules* **1996**, *29*, 7717.
- (121) Veregin, R. P. N.; Odell, P. G.; Michalak, L. M.; Georges, M. K. *Macromolecules* **1996**, *29*, 4161.
- (122) Greszta, D.; Matyjaszewski, K. *J. Polym. Sci., Part A: Polym. Chem.* **1997**, *35*, 1857.

Chapter 2

Radical Addition to Alkenes: A Theoretical Perspective

Leo Radom¹, Ming Wah Wong², and Addy Pross³

¹Research School of Chemistry, Australian National University, Canberra,
Australian Capital Territory 0200, Australia

²Department of Chemistry, National University of Singapore, 10 Kent Ridge
Crescent Singapore, 119260

³Department of Chemistry, Ben Gurion University, Beer Sheva 84105, Israel

An account of the use of *ab initio* molecular orbital calculations to study the addition of free radicals to alkenes is presented. The studies involve three stages: (a) *assessment* of the various possible theoretical procedures, (b) *application* of a selected procedure to specific chemical problems, and (c) *qualitative rationalization* of the results. It is found that high levels of theory are required in order to obtain quantitatively useful results. Methyl radical addition to alkenes is found to be dominated by the reaction enthalpy while polar effects are also important for the additions of CH₂OH[•], CH₂CN[•] and *t*-butyl radicals.

The addition of radicals to alkenes



has received extensive attention (see references 1–4 for recent reviews). Such reactions are of fundamental interest as carbon-carbon bond-forming reactions and are also of practical relevance as prototypes for the propagation step in free-radical polymerizations (see references 5 and 6 for leading references).

The purpose of the present article is to briefly review our recent theoretical studies (7–12) in this area. Our approach is to use *ab initio* molecular orbital theory (13) to obtain quantitative information about the reactions under investigation. We then attempt to provide qualitative rationalizations within the framework of the curve-crossing model (14, 15).

There are three key stages in our theoretical approach. The first stage is assessment. Here we test out many levels of *ab initio* molecular orbital theory with a view to answering the question: what level of theory is required to obtain usefully reliable results? Having chosen a suitable level of theory, we are then in a position to apply this level of theory widely and obtain quantitative results for the addition of a

variety of radicals to a variety of alkenes. Our aim here is to find out what factors are important in determining the reactivities for radical additions. And finally, we attempt to rationalize the results using the curve-crossing model.

It is beyond the scope of this article to discuss the excellent contributions that have been made by other workers to the understanding of radical addition reactions. The reader should refer to the cited reviews (1–4) and to our original papers (5–12) for the appropriate references.

Theoretical Considerations

Quantitative information about radical addition reactions is provided by *ab initio* molecular orbital theory (13). The *ab initio* calculations enable us to obtain information of the type displayed in Figure 1. This shows a schematic potential energy profile corresponding to the reaction between a radical R^\bullet and an alkene $CH_2=CXY$, proceeding via a transition structure (TS) to produce the product radical RCH_2CXY^\bullet . The calculations allow us to obtain complete geometries, i.e. bond lengths, bond angles and torsional angles, of all species including the transition structure. We can also determine vibrational frequencies which rigorously characterize stationary points as minima or first-order (or higher) saddle points on the potential surface and which also are useful in thermochemical and kinetic analyses. Note that obtaining *experimental* geometries and vibrational frequencies is difficult for radicals and virtually impossible for transition structures so theory is playing a particularly useful role here. We can also determine thermochemical quantities such as the reaction barrier and exothermicity. And we can obtain information on the direction and extent of charge transfer (determined using a so-called Bader analysis, based on the theory of atoms in molecules (16)). The *ab initio* calculations allow us to answer questions such as: are enthalpy effects important in radical addition

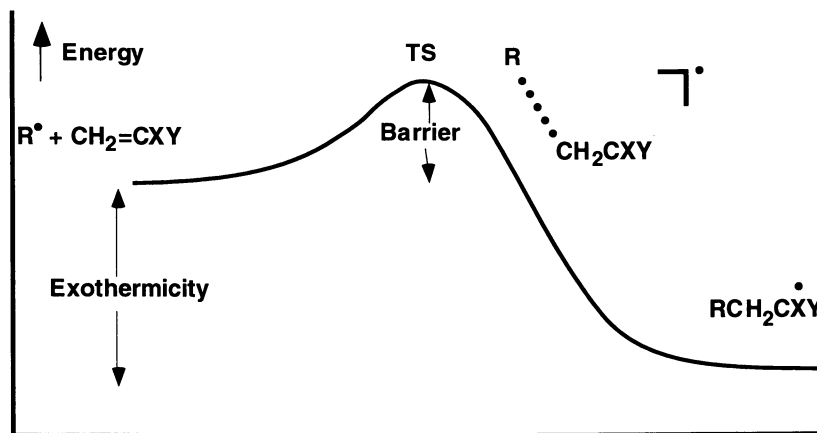


Figure 1. Schematic energy profile showing the reaction of a radical R^\bullet with the alkene $CH_2=CXY$.

reactions? Are polar effects important? The beauty of the *ab initio* calculations is that we can calculate these effects directly. We can calculate *explicitly* the barrier height and enthalpy change in the reaction. We can calculate *explicitly* the charge transfer in the transition structure.

It is important to note that there are a broad variety of *ab initio* calculations, ranging from cheap and (potentially) nasty to expensive and very accurate. The quality of an *ab initio* calculation depends on two things, namely the size of the basis set used in the calculation and the extent of incorporation of electron correlation. Better calculations are more expensive. In choosing the level of theory at which the calculations are to be performed, we need to strike a compromise between the accuracy that we require and the computational expense that we can afford. It is also important to note that the cost of an *ab initio* calculation goes up very rapidly with the size of the system that is being examined ... roughly between the 2nd and 7th power of the number of electrons (for a given basis set).

A more explicit illustration of the range of levels of *ab initio* theory is shown in the Pople diagram (17) displayed as Figure 2. In the left-hand column are representative basis sets in order of increasing size. Thus, STO-3G is a small basis set, 6-31G(d) is a medium-sized basis set, while large basis sets have names such as 6-311+G(3df,2p). Increasingly refined correlation procedures are shown in the top row. These include procedures such as Hartree-Fock (HF), Møller-Plesset perturbation theory truncated at second (MP2), third (MP3) or fourth (MP4) order,



		Improvement of Correlation Treatment 	
Improvement of Basis Set 		HF MP2 MP3 MP4 QCISD(T)	Full Configuration Interaction
	STO-3G 3-21G 6-31G(d) 6-311+G(2df,p) 6-311+G(3df,2p)		
	Infinite Basis Set		Exact Soln of Schrödinger Equation

Figure 2. Pople diagram showing the dependence on basis set and level of incorporation of electron correlation of *ab initio* calculations.

and quadratic configuration interaction including single, double and (perturbatively calculated) triple excitations (QCISD(T)). An *ab initio* calculation requires the specification of a correlation procedure and a basis set. If we choose HF/STO-3G, that represents a low level of theory. QCISD(T)/6-311+G(3df,2p) represents a high level of theory. In between are intermediate levels of theory. The ultimate level of theory corresponds to full electron correlation with an infinite basis set. This would yield the exact answer to the non-relativistic Schrödinger equation and hence the answers to all our questions. Unfortunately, this is not accessible in practice for normal systems so we have to be content with an appropriate compromise.

In order to approximate high levels of theory from lower-level calculations, we sometimes take advantage of additivity approximations. These are of the form shown as equations 2 and 3:

$$\begin{aligned} \Delta E[\text{QCISD(T)/6-311G(d,p)}] &\approx \Delta E[\text{QCISD(T)/6-31G(d)}] \\ &+ \Delta E[\text{RMP2/6-311G(d,p)}] - \Delta E[\text{RMP2/6-31G(d)}] \end{aligned} \quad (2)$$

$$\begin{aligned} \Delta E[\text{QCISD(T)/6-311+G(3df,2p)}] &\approx \Delta E[\text{QCISD(T)/6-31G(d)}] \\ &+ \Delta E[\text{RMP2/6-311+G(3df,2p)}] - \Delta E[\text{RMP2/6-31G(d)}] \end{aligned} \quad (3)$$

There is an additional degree of freedom for calculations on open-shell systems such as the radicals involved in radical addition reactions. Calculations may be carried out using either a restricted (RHF) or unrestricted (UHF) Hartree-Fock starting point. In the restricted (RHF) procedure, the α and β orbitals are constrained to be the same. This has the advantage that the resultant wave function is a pure doublet, characterized by the spin-squared expectation value $\langle S^2 \rangle$ being 0.75. On the other hand, if we allow the α and β orbitals to be different, leading to the unrestricted (UHF) procedure, the energy becomes lower. However, the wave function is no longer a pure doublet but is contaminated by states of higher spin multiplicity, as reflected in an $\langle S^2 \rangle$ value greater than 0.75. It is not clear beforehand which out of RHF or UHF is better.

When electron correlation is introduced, the procedures can be based on either UHF or RHF starting points. For example, Møller-Plesset perturbation theory can be based on UHF and is then denoted UMP. If there is severe spin contamination, there can be poor convergence in the Møller-Plesset expansion so that it may be inadvisable to use the UMP procedure (see, for example, references 18–20). There is generally a significant improvement with the use of restricted Møller-Plesset theory (RMP) (21) or projected Møller-Plesset theory (PMP) (22) in such circumstances. For more sophisticated procedures such as quadratic configuration interaction (QCI) (23), the difference between the unrestricted (UQCI) and restricted (RQCI) approaches is generally much smaller. Calculations using variants of density functional theory (see, for example, reference 24 and references therein), e.g. UB–LYP and UB3–LYP, should be carried out in the unrestricted form (25). The "U" denoting the unrestricted procedure is often dropped for simplicity in the present article.

Our qualitative approach is based on the curve-crossing model (14,15). A curve-crossing representation of the potential energy profile for the reaction of methyl

radical plus ethylene is shown in Figure 3. The methyl radical (denoted $C\uparrow$) reacts with ethylene (denoted $C\uparrow\downarrow C$) to produce the propyl radical (denoted $C\downarrow\uparrow C-\uparrow C$). In the curve-crossing approach, the barrier for the reaction is considered to arise as a result of an avoided crossing between the reactant configuration and the product configuration. There are also higher-energy charge-transfer configurations that may contribute to the description of the reaction profile. These correspond either to electron donation from the radical to the alkene (leading to radical⁺/alkene⁻) or to electron donation from the alkene to the radical (leading to radical⁻/alkene⁺). The energies of the charge-transfer configurations depend on the ionization energies and electron affinities of the radical and the alkene. For example, the lower-energy charge-transfer configuration shown in Figure 3 corresponds to methyl cation plus ethylene anion and has an energy relative to the ground-state reactants equal to the ionization energy of methyl radical minus the electron affinity of ethylene.

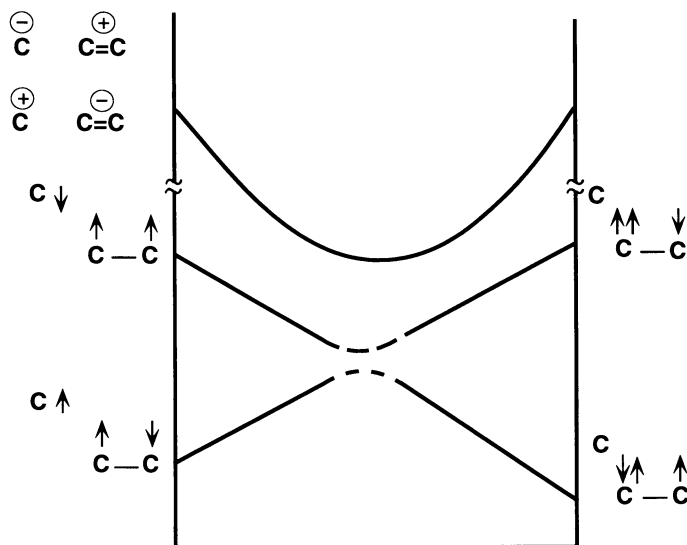


Figure 3. Curve-crossing diagram for the addition of methyl radical (represented by $C\uparrow$) to ethylene (represented by $C\uparrow\downarrow C$) to produce propyl radical (represented by $C\downarrow\uparrow C-\uparrow C$).

The curve-crossing model makes various predictions about radical addition reactions. Firstly, the barrier should decrease with increasing exothermicity. That is simply saying that the barrier decreases as the point corresponding to product (denoted $C\downarrow\uparrow C-\uparrow C$) moves down in energy; this is consistent with Bell-Evans-Polanyi. Secondly, the barrier should decrease as the charge-transfer states are lowered in energy, i.e. with decreasing difference between the ionization energy and electron affinity of the respective species. This follows because as one or other of the charge-transfer states comes down in energy, it will mix in to a greater extent and

hence stabilize the transition structure. And finally, the barrier should decrease with decreasing triplet-singlet gap in the alkene. This is the energy gap between the ground-state reactants and the point corresponding to methyl radical plus triplet ethylene (denoted $C\downarrow C\uparrow-\uparrow C$). As the triplet energy comes down, the barrier decreases. Normally the exothermicity and triplet-singlet gap go together because substituents that stabilize the triplet alkene will generally also stabilize the product radical. So the whole line corresponding to the product configuration is lowered and the barrier is lowered as a consequence.

Assessment of Theoretical Procedures

Previous studies have shown that radical addition reactions are not at all straightforward theoretically. An essential initial part of our investigation was therefore to assess which theoretical methods are suitable for studying radical addition reactions (11).

The type of results obtained is exemplified by the barriers for methyl radical addition to ethylene, calculated with a wide variety of theoretical procedures (Table I). The experimental gas-phase barrier with which we should be making comparison (26,27), back corrected for temperature, zero-point energy and basis set effects, is 28 kJ mol⁻¹. Our best level of theory, QCISD(T), gives a barrier of 31.7 kJ mol⁻¹, respectably close to the experimental value. However, the calculated barriers at the other levels show a massive dependence on level of theory. The values range from about 5 kJ mol⁻¹ using the UB-LYP density functional theory procedure and 7.1 kJ mol⁻¹ for the widely used AM1 semi-empirical procedure to nearly 90 kJ mol⁻¹ by RHF. The commonly used UMP2 procedure also gives a very high barrier.

These results are hinting that, of the procedures examined, only QCISD and QCISD(T) might be suitable for the prediction of quantitatively reliable *absolute* barriers. Often in chemistry, however, we don't need absolute quantities. It would often be sufficient if we could reliably predict trends. So we ask now: what about *relative* barriers? Do the trends come out well with simpler levels of theory?

Table I. Effect of Level of Theory on Calculated Barriers for the Addition of Methyl Radical (CH₃^{*}) to Ethylene (CH₂=CH₂)^{a,b}

Level	Barrier	Level	Barrier
AM1	7.1 ^c	RHF	89.7
UHF	39.4	RMP2	40.3
UMP2	60.1	RMP4	8.2
UMP4	53.7	UB-LYP	5.3
PMP2	20.1	UQCISD	35.5
PMP4	21.5	UQCISD(T)	31.7

^a 6-31G(d) basis set, kJ mol⁻¹, from ref. 11.

^b UHF/6-31G(d) geometries unless otherwise noted.

^c AM1 geometries.

A selection of the results that enable us to examine the performance of theory in predicting relative barriers is shown in Table II. Again we believe that the QCISD(T) level is the most reliable and the substituents are ordered in Table II so that the QCISD(T) barriers decrease monotonically. We can then examine results at the other levels to see how they compare. UMP2 is by far the worst. The trend, i.e. monotonically decreasing barriers, is not reproduced at all. If anything, it goes the other way. UHF is not particularly good but does much better than UMP2. AM1 is also very poor. The other procedures – UB-LYP, PMP2, RMP2 and QCISD – are very respectable in reproducing the trends, even though the absolute values are poor, particularly for UB-LYP. QCISD is the best of these, the absolute barrier always being about 4 kJ mol⁻¹ above the QCISD(T) value.

Table II. Effect of Level of Theory on Calculated Barriers for the Addition of Methyl Radical (CH₃•) to Alkenes (CH₂=CHX)^{a,b}

X	AM1 ^c	UHF	UB-LYP ^d	UMP2	PMP2	RMP2	QCISD	QCISD(T)
OH	3.3	50.3	13.1	62.8	24.7	40.4	36.5	32.2
F	0.3	43.6	13.2	62.4	22.2	40.8	35.8	31.8
H	7.1	39.4	13.2	60.1	20.1	40.3	35.5	31.7
CH ₃	5.5	42.2	13.4	60.6	21.0	38.3	34.8	30.7
NH ₂	0.3	48.2	9.9	59.4	21.9	37.1	33.7	29.2
SiH ₃	7.3	36.9	9.6	55.6	17.2	33.5	29.4	25.6
Cl	2.9	34.5	9.0	56.6	15.8	33.3	29.4	25.5
CHO	2.5	21.6	1.3	73.8	9.6	23.7	23.3	18.8
CN	2.1	19.9	1.1	68.6	6.8	21.3	20.6	16.7
NO ₂	-0.1	26.5	-2.7	43.7	5.6	22.3	19.1	15.4

^a 6-31G(d) basis set, kJ mol⁻¹, from ref. 11.

^b UHF/6-31G(d) geometries unless otherwise noted.

^c AM1 geometries.

^d UB-LYP/6-31G(d) geometries.

These observations are mirrored in calculated correlation coefficients (Table III). The R² values listed are for correlations of barriers calculated with the simpler methods against barriers calculated by QCISD(T). QCISD(T) itself, of course, correlates perfectly with QCISD(T) and so gives a value of 1.000. QCISD is nearly perfect with an R² value of 0.998, as we anticipated from Table II. RMP2, PMP2 and UB-LYP are all reasonably good while UMP2 is hopeless, with a correlation coefficient of 0.004. AM1 is also very bad.

As a result of the assessment work touched on here but described in detail elsewhere (11), we are able to select a standard level of theory to apply to specific problems. We have recommended in the first instance QCISD/6-311G(d,p) or QCISD(T)/6-311G(d,p) energy calculations on UHF/6-31G(d) geometries with (scaled) UHF/6-31G(d) zero-point vibrational energies.

Table III. Correlation Coefficients for Barriers for the Addition of Methyl Radical to Alkenes ($\text{CH}_2=\text{CHX}$) Computed at Various Levels of Theory Against UQCISD(T) Values^a

AM1	UHF	UB-LYP	UMP2	PMP2	RMP2	UQCISD	UQCISD(T)
0.123	0.838	0.966	0.004	0.967	0.989	0.998	1.000

^a 6-31G(d) basis set, UHF/6-31G(d) geometries, kJ mol^{-1} , from ref. 11.

The performance of the QCISD(T)/6-311G(d,p)//UHF/6-31G(d) level of theory (evaluated using equation 2) can be tested immediately against the results of recent extensive experimental measurements in solution from Fischer's laboratory in Zurich (see, for example, references 28–30). In particular, we can make comparisons between our theoretical results and experimental results obtained by Zytowski and Fischer (30) for methyl radical addition to a wide variety of alkenes.

Comparison of our calculated barriers with the experimental values determined in Zurich for the subset of 10 systems common to both investigations (Figure 4) gives a very respectable correlation coefficient of 0.856. The explicit results are displayed in Table IV and show that the experimental values are consistently smaller than the calculated values. It is not clear whether this difference is a solvent effect or a specific problem associated with theory or experiment. But the very encouraging feature is that the discrepancy is reasonably systematic and the differences between theory and experiment lie within a small range of about 3 to 11 kJ mol^{-1} .

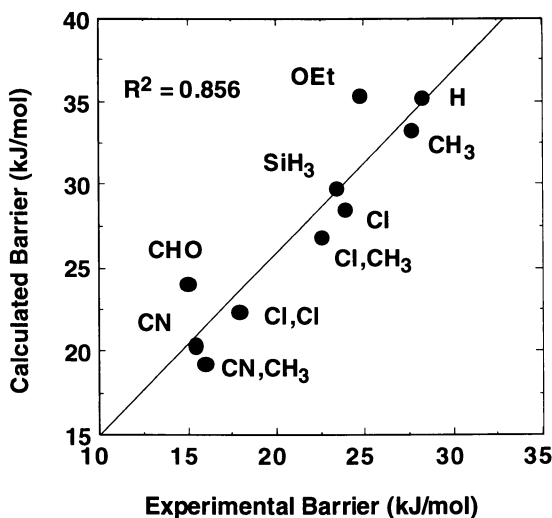


Figure 4. Comparison of calculated (QCISD(T)/6-311G(d,p)//UHF/6-31G(d), 0 K) (from refs 8,12) and experimental (298 K) (from ref. 30) barriers for methyl radical additions to alkenes ($\text{CH}_2=\text{CXY}$).

In order to examine the effect of moving to still higher levels of theory, we have very recently obtained higher level QCISD(T)/6-311+G(3df,2p)//QCISD/6-31G(d) energies (using equation 3) with ZPVEs determined at the B3-LYP/6-31G(d) level for a subset of our systems (12). The barriers are found to slightly increase (compared with the standard values above) by 1.1–5.5 kJ mol⁻¹. The discrepancy between theory and experiment actually becomes a little larger with differences ranging from 6 to 12 kJ mol⁻¹. However, the good correlation between theoretical and experimental barriers is maintained, with an R² value of 0.903 (Figure 5).

Zytowski and Fischer also estimated reaction enthalpies in their work using Benson-type additivity rules. The reliability of such procedures depends both on the accuracy of the primary data and on the extent to which bond energies are additive. Both of these aspects carry with them significant uncertainty and the comparisons with theoretical values should be viewed in that light. Indeed, the correlation between theoretical and estimated experimental values of reaction enthalpies (Figure 6) is much poorer than for barriers, with an R² value of 0.760.

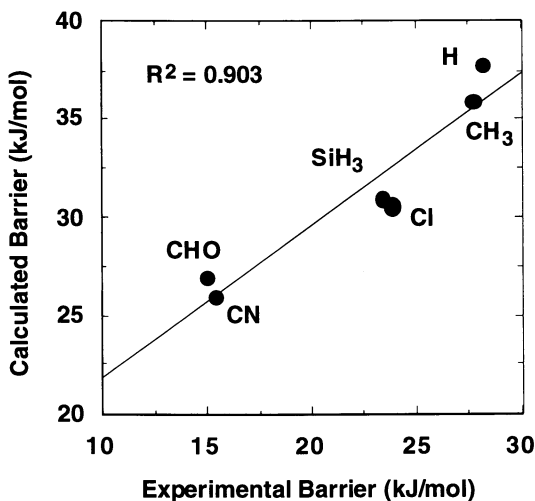


Figure 5. Comparison of calculated (QCISD(T)/6-311+G(3df,2p)//QCISD/6-31G(d), 0 K) (from ref. 12) and experimental (298 K) (from ref. 30) barriers for methyl radical additions to alkenes ($\text{CH}_2=\text{CHX}$).

Addition of Methyl Radical to Alkenes

We return now to the more chemical aspects of the addition of methyl radical to alkenes. Because the reaction is accelerated by electron-withdrawing groups X on the alkene substrate, it had been concluded previously (see, for example, references 1–3) that polar effects are important and, in particular, that the methyl radical is nucleophilic in such reactions. We wanted to critically assess such conclusions. The

Table IV. Comparison of Theoretical (QCISD(T)/6-311G(d,p)//UHF/6-31G(d), 0 K)^a and Experimental (298 K)^b Barriers (kJ mol⁻¹) for the Addition of Methyl Radical to Alkenes (CH₂=CXY)

X	Y	Theory	Expt	Difference
OCH ₂ CH ₃	H	35.4	24.8	10.6
H	H	35.2	28.2	7.0
CH ₃	H	33.3	27.7	5.6
SiH ₃	H	29.8	23.4 ^c	6.4
Cl	H	28.5	23.9	4.6
Cl	CH ₃	26.8	22.5	4.3
CHO	H	24.1	15.0	9.1
Cl	Cl	22.3	17.9	4.4
CN	H	20.4	15.4	5.0
CN	CH ₃	19.2	16.0	3.2

^a From refs 8 and 12.

^b From ref. 30.

^c Result for Si(CH₃)₃ substituent.

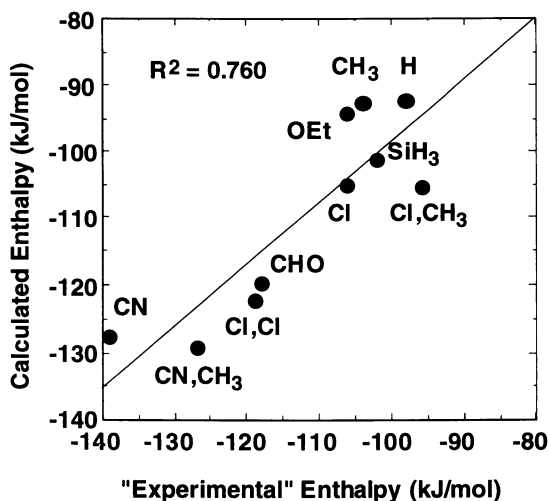


Figure 6. Comparison of calculated (QCISD(T)/6-311G(d,p)//UHF/6-31G(d), 0 K) (from refs 8,12) and "experimental" (298 K) (from ref. 30) reaction enthalpies for methyl radical additions to alkenes (CH₂=CXY).

questions we sought to answer include: are enthalpy effects important, is the methyl radical nucleophilic, and are polar effects important (7,8)?

We can tackle quite straightforwardly the first question, namely the possible influence of reaction enthalpy on the reactivity of methyl radical with alkenes, by plotting barrier height against exothermicity for a range of substituents X (Figure 7). We observe a nice straight line correlation with an R^2 value of 0.973. This excellent correlation suggests that reaction thermodynamics has a very strong, if not dominant, influence on the rate of methyl radical addition to alkenes, consistent with classical rate-equilibrium considerations.

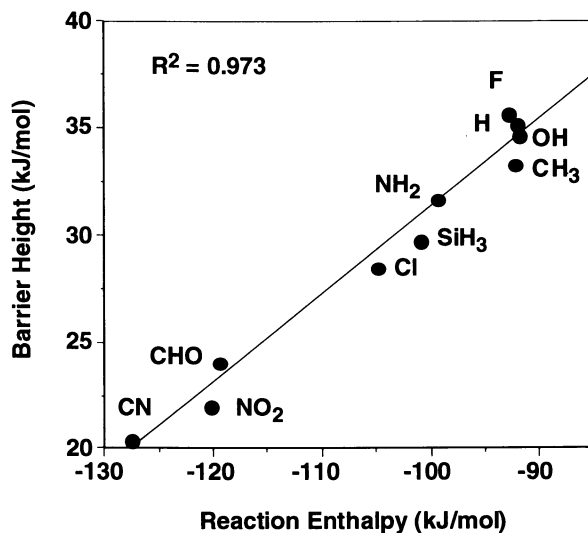


Figure 7. Influence of reaction enthalpy on barrier height for methyl radical additions to alkenes ($\text{CH}_2=\text{CHX}$) (QCISD(T)/6-311G(d,p)//UHF/6-31G(d), 0 K) (from ref. 8).

What about the question of whether the methyl group is nucleophilic, i.e. an electron donor? We have looked at two measures of the direction and extent of charge transfer in the transition structure (Table V). One measure comes from the calculated Bader charges in the transition structures, which predict that for most substituents (including H) methyl carries a negative charge; it is positive only for $\text{X}=\text{CHO}$, NO_2 and CN . The second measure is the relative energy of the charge-transfer states $\text{CH}_3^+/\text{CH}_2=\text{CHX}^-$ and $\text{CH}_3^-/\text{CH}_2=\text{CHX}^+$. We observe that in most cases, again including the unsubstituted case, the energy of the charge-transfer state $\text{CH}_3^-/\text{CH}_2=\text{CHX}^+$ is lower than the charge-transfer state $\text{CH}_3^+/\text{CH}_2=\text{CHX}^-$, i.e. again showing that methyl prefers to be an electron acceptor rather than an electron donor. It is an electron donor only when there are strong electron-withdrawing substituents on the alkene. So our calculations on two counts suggest that the answer

to the second question is that methyl radical does *not* display general nucleophilic behavior, in contrast to the current conventional wisdom. It is nucleophilic only with alkenes such as acrolein and acrylonitrile that bear strong π -electron-withdrawing substituents.

The remaining question we wished to address is whether polar effects have an important influence on reactivity in methyl radical addition reactions. The charges in Table V tell us that there is some charge transfer in the transition structure but they don't say anything about the energetic consequences. We want to know whether polar effects are important *energetically*. Do they influence barrier heights?

Table V. Examination of Polar Effects in the Reaction of Methyl Radical (CH_3^\bullet) with Alkenes ($\text{CH}_2=\text{CHX}$)^a

X	Energies (eV) of Charge-Transfer States ^b		Charge on CH_3 in TS ^c
	$\text{CH}_3^+/\text{CH}_2=\text{CHX}^-$	$\text{CH}_3^-/\text{CH}_2=\text{CHX}^+$	
F	11.4	10.3	-0.012
H	11.6	10.5	-0.017
OH	11.5	9.2	-0.029
CH_3	11.6	9.8	-0.024
NH_2	11.7	8.1	-0.039
SiH_3	10.7	10.1	-0.009
Cl	11.0	9.9	0.000
CHO	9.7	10.2	+0.006
NO_2	9.0	11.8	+0.030
CN	10.0	10.9	+0.012

^a From ref. 8.

^b G2(MP2) values.

^c Bader charges calculated at the UHF/6-31G(d) level.

Because the direction of charge transfer is generally from the alkene to the methyl radical, we might expect that if polar effects are important they would manifest themselves in a nice correlation of reaction barrier with the ionization energy of the alkene. However, when we plot our calculated barrier heights against the ionization energies of the alkenes (Figure 8) there is no correlation at all.

On the other hand, when we plot the reaction barrier against the electron affinities of the alkenes (Figure 9), there is a reasonable correlation. This would not have been anticipated on the basis of the charge-transfer results. Only the π -electron-withdrawing substituents CHO, CN and NO_2 might have been expected to show a correlation but in fact they don't correlate particularly well on their own, as can be seen in Figure 9. What is the significance then of this correlation, mirrored also in

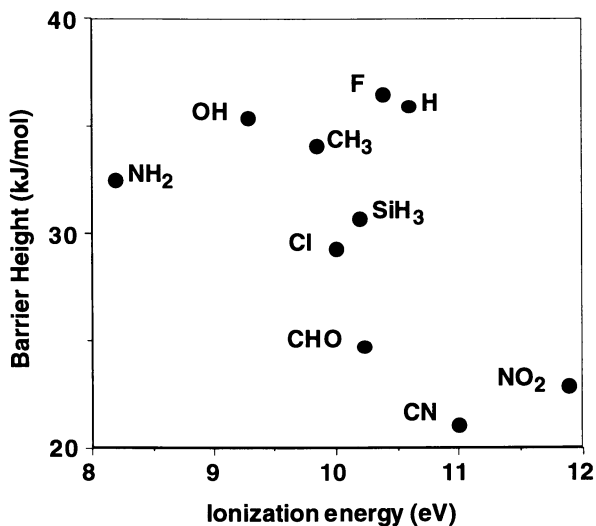


Figure 8. Influence of alkene ionization energy for methyl radical additions to alkenes ($\text{CH}_2=\text{CHX}$) (QCISD(T)/6-311G(d,p)//UHF/6-31G(d), 0 K) (from ref. 8).

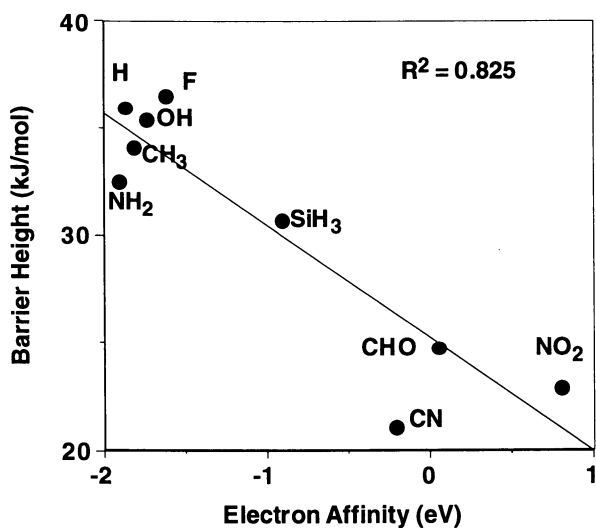


Figure 9. Influence of alkene electron affinity for methyl radical additions to alkenes ($\text{CH}_2=\text{CHX}$) (QCISD(T)/6-311G(d,p)//UHF/6-31G(d), 0 K) (from ref. 8).

the experimental observation noted above that electron-withdrawing substituents in the alkene generally lead to lower reaction barriers?

We believe that the answer, as also noted particularly in Fischer's work, is that π -electron-accepting groups such as CHO, NO₂, and CN can enhance reactivity not only through stabilization of a polar transition structure but also through increasing the reaction exothermicity. We think that the exothermicity effect is more important in the addition reactions of methyl radical. The π -electron-accepting groups tend to increase reaction exothermicity because they stabilise the product radical (CH₃CH₂CHX[•]) formed from the addition of methyl radical to the alkene.

In summary, we believe that polar contributions to the reactivity of methyl radical with alkenes are generally small, the methyl radical does not show general nucleophilic behaviour, and it is reaction exothermicity that is the main factor that dominates reactivity.

Addition of Other Radicals to Alkenes

If we believe that polar effects are not very important in the reactions of methyl radical with alkenes, a logical question to ask at this stage is: under what circumstances *do* polar effects become energetically important in radical addition reactions (9)? Well, according to the curve-crossing model, we require that one or other of the charge-transfer states must lie low in energy, i.e. either the difference between the ionization energy of the radical and the electron affinity of the alkene, or the difference between the ionization energy of the alkene and the electron affinity of the radical, must be relatively small. This may give rise to charge-transfer states of sufficiently low energy so as to contribute significantly to the total wave function. The CH₂OH[•] radical has a low IE – 7.43 eV vs 9.77 eV for methyl radical – and therefore, depending on the EA of the alkene, may satisfy the first of these requirements. Potentially it is a highly nucleophilic radical. The CH₂CN[•] radical, on the other hand, has a high EA – 1.59 eV vs 0.04 eV for methyl radical – and therefore, depending on the IE of the alkene, may satisfy the second of these requirements. Potentially it is a strongly electrophilic radical.

The calculated energies for the possible charge-transfer states formed from each of the CH₃[•], CH₂OH[•] and CH₂CN[•] radicals with the set of alkenes is shown in Table VI. We can see that the CH₂CN[•] radical is always electrophilic, the radical⁻/alkene⁺ (R⁻A⁺) state being low in energy in an absolute sense and always lying below the radical⁺/alkene⁻ (R⁺A⁻) state. On the other hand, CH₂OH[•] is generally nucleophilic, the charge-transfer radical⁺/alkene⁻ state being low in energy in an absolute sense and generally lying below the radical⁻/alkene⁺ state. As we have seen before, the charge-transfer states involving the methyl radical are considerably higher in energy. These results suggest that polar effects in the addition reactions of the CH₂OH[•] and CH₂CN[•] radicals should be considerably greater than for the methyl radical, where we concluded that they were generally energetically unimportant.

A comparison of the enthalpy dependence of the barriers for methyl and CH₂OH[•] addition to alkenes is presented in Figure 10. The key observation is that the CH₂OH[•] points lie below the methyl line, i.e. for a given enthalpy, the barrier for CH₂OH[•] addition is lower than the barrier for methyl addition. We attribute this

lowering to the polar effect. It amounts to about 5–15 kJ mol⁻¹ and increases as the acceptor ability of the alkene increases. The larger slope of the CH₂OH• line compared with the methyl line would conventionally be interpreted as indicating a later transition structure but we believe that it arises because of the growing contribution of transition structure stabilization from polar mixing for alkenes with more electron-withdrawing substituents (CHO and CN). This growing polar contribution fortuitously preserves the linearity of the barrier–enthalpy plot.

Table VI. Calculated Energies of Charge-Transfer States Related to CH₃•, CH₂OH• and CH₂CN• Addition Reactions to Alkenes (CH₂=CHX) (eV)^a

X	CH ₃ •		CH ₂ OH•		CH ₂ CN•	
	R ⁺ A ⁻	R ⁻ A ⁺	R ⁺ A ⁻	R ⁻ A ⁺	R ⁺ A ⁻	R ⁻ A ⁺
F	11.4	10.3	9.1	10.5	11.8	8.8
H	11.6	10.5	9.3	10.7	12.0	9.0
NH ₂	11.7	8.1	9.4	8.3	12.1	6.6
Cl	11.0	9.9	8.7	10.1	11.4	8.4
CHO	9.7	10.2	7.5	10.4	10.1	8.6
CN	10.0	10.9	7.7	11.1	10.4	9.4

^a G2(MP2) values from ref. 9.

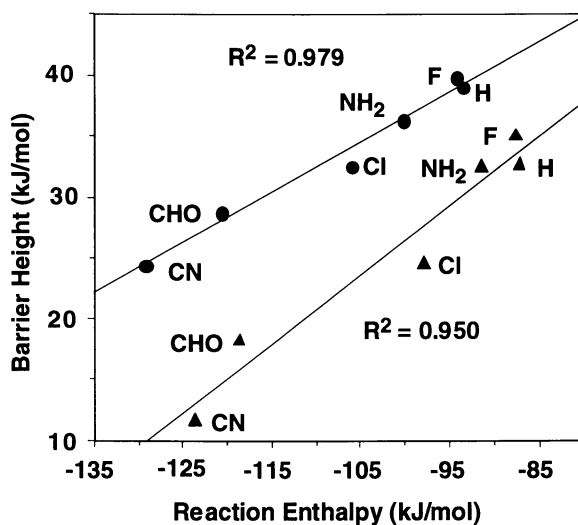


Figure 10. Comparison of enthalpy dependence of barrier heights for additions of CH₃• (●) and CH₂OH• (▲) to alkenes (CH₂=CHX) (QCISD/6-311G(d,p)//UHF/6-31G(d), 0 K) (from ref. 9).

A plot of barrier height vs enthalpy for CH_2CN^* addition (Figure 11) shows that the CH_2CN^* points also lie below the methyl line, indicating polar stabilization. This time, however, we have lost the barrier height–enthalpy correlation that was fortuitously preserved for CH_2OH^* addition. We interpret these results as indicating that the reactivity of CH_2CN^* is also influenced by a combination of enthalpy and polar effects and that strong polar effects can upset a possible linear correlation. For example, the barrier for addition to $\text{CH}_2=\text{CHNH}_2$ is lower by about 5 kJ mol^{-1} than the barrier for addition to $\text{CH}_2=\text{CHCl}$, despite the fact that the enthalpies of reaction are similar. This may be attributed to a particularly large polar contribution, arising because the IE for $\text{CH}_2=\text{CHNH}_2$ is particularly low (8.18 eV).

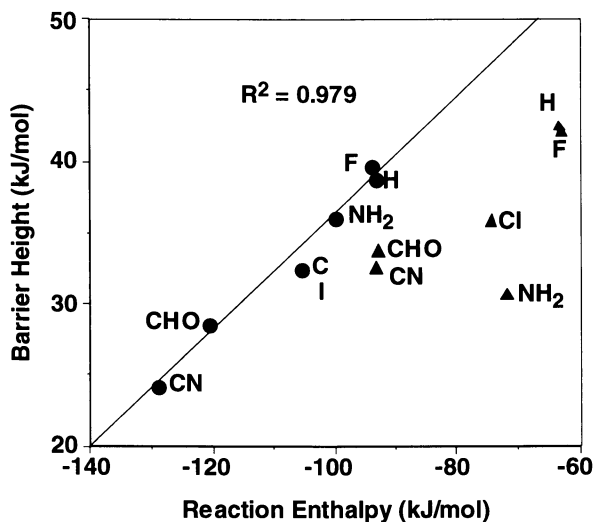


Figure 11. Comparison of enthalpy dependence of barrier heights for additions of CH_3^* (●) and CH_2CN^* (▲) to alkenes ($\text{CH}_2=\text{CHX}$) (QCISD/6-311G(d,p)//UHF/6-31G(d), 0 K) (from ref. 9).

The *t*-butyl radical is even more nucleophilic than CH_2OH^* : the ionization energies go from 9.77 eV for methyl to 7.43 eV for CH_2OH^* to 6.78 eV for *t*-butyl. We might expect *t*-butyl additions on this basis to have particularly low R^+A^- states and therefore even greater polar stabilizations and lower barriers. In fact, it has previously been claimed that the reactivity of *t*-butyl radical depends *only* on polar factors and that reaction enthalpy is not important. However, based on the barrier height–enthalpy correlation for *t*-butyl radical addition shown in Figure 12, we certainly don't agree with this last assertion. Enthalpy plays a major role, as with the other radicals that we have examined. However, if we compare the enthalpy dependence of the barrier heights for methyl, CH_2OH^* and *t*-butyl addition to alkenes (Figure 12), we can see that for a given enthalpy, the barrier indeed decreases as we

go from methyl to $\text{CH}_2\text{OH}^\bullet$ to *t*-butyl, indicating progressively stronger polar contributions (10).

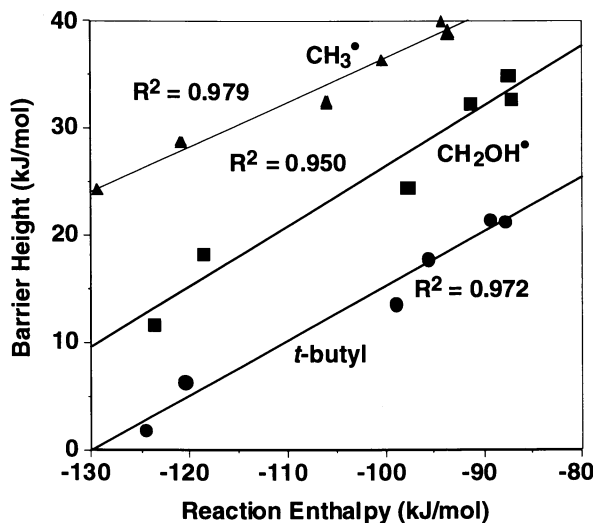


Figure 12. Comparison of enthalpy dependence of barrier heights for additions of CH_3^\bullet (▲), $\text{CH}_2\text{OH}^\bullet$ (■) and *t*-butyl radical (●) to alkenes ($\text{CH}_2=\text{CHX}$) (QCISD/6-311G(d,p)//UHF/6-31G(d), 0 K) (from ref. 10).

Concluding Remarks

Several important points emerge from the present study. Firstly, we have seen that obtaining quantitatively useful absolute barrier heights for radical addition reactions requires a high level of theory. Careful selection of the level of theory is also required for relative barrier heights. In particular, UMP can be very poor. The indications are that our calculated barriers at the present levels of theory may be slightly overestimated. We are continuing to work on doing better. Notwithstanding this result, there is a nice general correlation between theoretical and experimental barriers. Every now and then, there is a significant discrepancy but for the most part the difference between theory and experiment for a particular type of radical addition appears to be systematic. A point of difference between our position and that of some others in the field is that we believe that enthalpy effects are always important in radical addition reactions: other things being equal, more exothermic reactions will have lower barriers. Of course, other things are *not* always equal and in particular we have seen that polar effects are important in some cases, in which case they are superimposed on enthalpy effects. Finally, it needs to be borne in mind that part of the difference between the theoretical and experimental results and the conclusions that derive from them may be associated with the effect of solvent in the experimental

results, since the theoretical treatment refers to the gas phase. However, the other side of this coin is that the remarkably good match between theoretical and experimental results suggests that the overall importance of solvent effects in radical addition reactions is generally relatively minor.

Acknowledgments

We gratefully acknowledge a continuing dialogue with Professor Hanns Fischer and the support of the Australian National University Supercomputing Facility in the form of generous grants of computer time.

Literature Cited

1. Giese, B. *Angew. Chem., Int. Ed. Engl.* **1983**, *22*, 753.
2. Tedder, J. M. *Angew. Chem., Int. Ed. Engl.* **1982**, *21*, 401.
3. Tedder, J. M.; Walton, J. C. *Adv. Free Radical Chem.* **1980**, *6*, 155.
4. Fischer, H. In *Free Radicals in Biology and Environment*; Minisci, F., Ed.; Kluwer Academic Publishers: Dordrecht, 1997.
5. Heuts, J. P. A.; Gilbert, R. G.; Radom, L. *Macromolecules* **1995**, *28*, 8771.
6. Heuts, J. P. A.; Gilbert, R. G.; Radom, L. *J. Phys. Chem.* **1996**, *100*, 18997.
7. Wong, M.W.; Pross, A.; Radom, L. *J. Am. Chem. Soc.* **1993**, *115*, 11050.
8. Wong, M.W.; Pross, A.; Radom, L. *Isr. J. Chem.* **1993**, *33*, 415.
9. Wong, M.W.; Pross, A.; Radom, L. *J. Am. Chem. Soc.* **1994**, *116*, 6284.
10. Wong, M.W.; Pross, A.; Radom, L. *J. Am. Chem. Soc.* **1994**, *116*, 11938.
11. Wong, M. W.; Radom, L. *J. Phys. Chem.* **1995**, *99*, 8582.
12. Wong, M. W.; Radom, L. unpublished results.
13. Hehre, W. J.; Radom, L.; Schleyer, P. v. R.; Pople, J. A. *Ab Initio Molecular Orbital Theory*; Wiley: New York, 1986.
14. Shaik, S. S.; Schlegel, H. B.; Wolfe, S. *Theoretical Aspects of Physical Organic Chemistry, The S_N2 Transition State*, Wiley: New York, 1992.
15. Pross, A. *Theoretical and Physical Principles of Organic Reactivity*; Wiley: New York, 1995.
16. Bader, R. F. W. *Atoms in Molecules: A Quantum Theory*; Clarendon Press: Oxford, 1990.
17. Radom, L. *Org. Mass Spectrom.* **1991**, *26*, 359.
18. Knowles, P. J.; Somasundram, K.; Handy, N. C.; Hirao, K. *Chem. Phys. Lett.* **1985**, *113*, 8.
19. Gill, P. M. W.; Radom, L. *Chem. Phys. Lett.* **1986**, *132*, 16.
20. Nobes, R. H.; Moncrieff, D.; Wong, M. W.; Radom, L.; Gill, P. M. W.; Pople, J. A. *Chem. Phys. Lett.* **1991**, *182*, 216.
21. Knowles, P. J.; Andrews, J. S.; Amos, R. D.; Handy, N. C.; Pople, J. A. *Chem. Phys. Lett.* **1991**, *186*, 130.
22. Schlegel, H. B. *J. Chem. Phys.* **1986**, *84*, 4530.
23. Pople, J.A.; Head-Gordon, M.; Raghavachari, K. *J. Chem. Phys.* **1987**, *87*, 5968.

24. Kohn, W.; Becke, A. D.; Parr, R. G. *J. Phys. Chem.* **1996**, *100*, 12974.
25. Pople, J. A.; Gill, P. M. W.; Handy, N. C. *Int. J. Quantum Chem.* **1995**, *56*, 303.
26. Kerr, J. A. In *Free Radicals*; Kochi, J., Ed.; Wiley: New York, 1972; Vol. 1.
27. Baulch, D. L.; Cobos, C. J.; Cox, R. A.; Esser, C.; Frank, P.; Just, T.; Kerr, J. A.; Pilling, M. J.; Troe, J.; Walker, R. W.; Warnatz, J. *J. Phys. Chem. Ref. Data* **1992**, *21*, 411.
28. Wu, J. Q.; Beranek, I.; Fischer, H. *Helv. Chim. Acta* **1995**, *78*, 194.
29. Wu, J. Q.; Fischer, H. *Int. J. Chem. Kinet.*, **1995**, *27*, 167.
30. Zytowski, T.; Fischer, H. *J. Am. Chem. Soc.* **1996**, *118*, 437.

Chapter 3

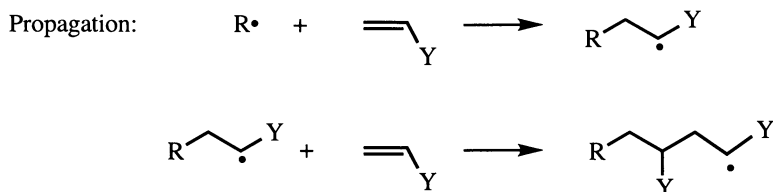
Factors Influencing the Addition of Radicals to Alkenes

Anne Ghosez-Giese and Bernd Giese

Department of Chemistry, University of Basel, St. Johannis-Ring 19,
CH-4056 Basel, Switzerland

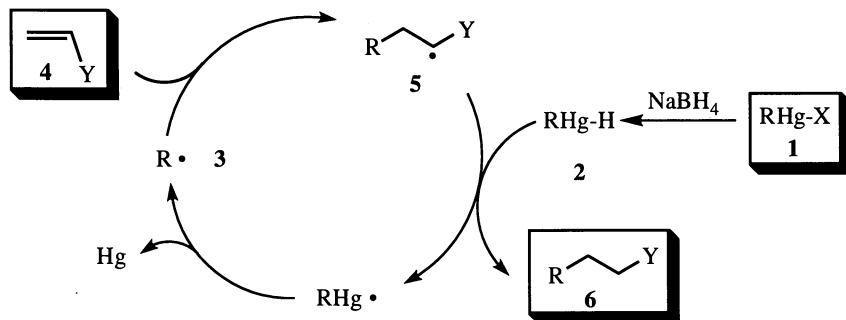
The addition of radicals to alkenes is largely governed by polar and steric effects as well as, in some cases, stability effects. These factors play also an important role on the regio- and the stereoselectivity of the additions and in radical polymerization reactions. An overview is presented on the basis of the data collected over the past 20 years.

The question of the factors influencing the radical addition to alkenes is a major one in polymer chemistry since it concerns the parameters governing the propagation step during radical polymerization. In this report, we have summarized the rules controlling the radical addition to alkenes using data that were obtained mostly in the seventies and eighties.



Method

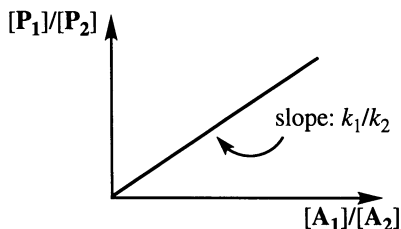
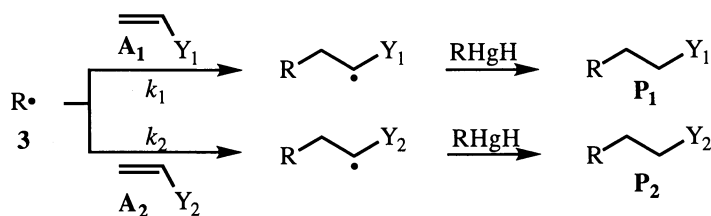
The measurements of the radical additions to alkenes were performed using the „mercury method“ (1) a chain reaction in which the radical precursor is an alkylmercury hydride 2 (2). Indeed, alkylmercury halides 1 react with NaBH_4 giving alkylmercury hydride 2 which, after loss of metallic mercury, yields alkyl radical 3. In the presence of an alkene 4, radical 3 adds to the double bond and forms radical adduct 5 which abstracts a H-atom from the alkylmetal hydride 2 to give the 1:1 addition product 6 and regenerates alkyl radical 3. The formation of polymers is observed only in special cases (3) because alkylmercury hydrides 1 trap alkyl radicals 3 with rate coefficients of at least $10^7 \text{ M}^{-1}\text{s}^{-1}$ at room temperature (4).



Scheme 1

This method is very useful in synthesis (5) as well as for kinetics studies (6) since the yields are high, the reaction conditions are mild (room temperature, no light) and the reaction times are short (in the order of minutes). Moreover, the separation of the products from metallic mercury is easy.

The relative rates of radical addition to alkenes were determined by pseudo-first order competition kinetics (6). The alkyl radicals **3** were treated with a pair of alkenes (A_1, A_2) and this led exclusively to the products P_1 and P_2 . Since dimerization, polymerization, disproportionation, or oxygen trapping reactions can be suppressed, the quantitative conversion of the adduct radicals into the products P_1, P_2 allows the measurement of the relative addition rates. The competition constants k_1/k_2 can be determined following a pseudo-first order kinetics if one works with a large excess of alkenes so that their relative concentration $[A_1]/[A_2]$ vary only negligibly during the reaction.



$$\frac{[P_1]}{[P_2]} = \frac{k_1 [A_1]}{k_2 [A_2]}$$

Scheme 2

The relative rates that we have measured are in accordance with the absolute rates obtained by H. Fischer in later work (7).

Polar and Stability Effects (8)

The stability of the adduct radical **5** plays only a modest role in the addition rate. Not stability effects but *polar* effects are dominant when nucleophilic or electrophilic radicals **3** are involved. This can be illustrated by the correlation of the relative reactivities of *monosubstituted* alkenes **4** (towards cyclohexyl radical **3a**) with the Hammett σ^- parameters of the substituent Y at the double bond (Figure 1)(8). This plot shows that the variation of Y has a strong effect on the rate of addition: the better the electron withdrawing group Y, the faster the addition. Thus, the rate of addition is increased by 8500 in going from the electron rich 1-hexene (Y = C₄H₉) to the electron poor acrolein (Y = CHO)(9).

However, substituents Y which stabilize radicals very strongly, *e.g.* a phenyl group, deviate from linearity (9). Thus, styrene (Y = Ph) reacts faster as would be expected from the σ^- values (Figure 1). However, it still reacts much more slowly than acrolein (Y = CHO), for instance, although radicals are better stabilized by a phenyl group than by a carbonyl substituent.

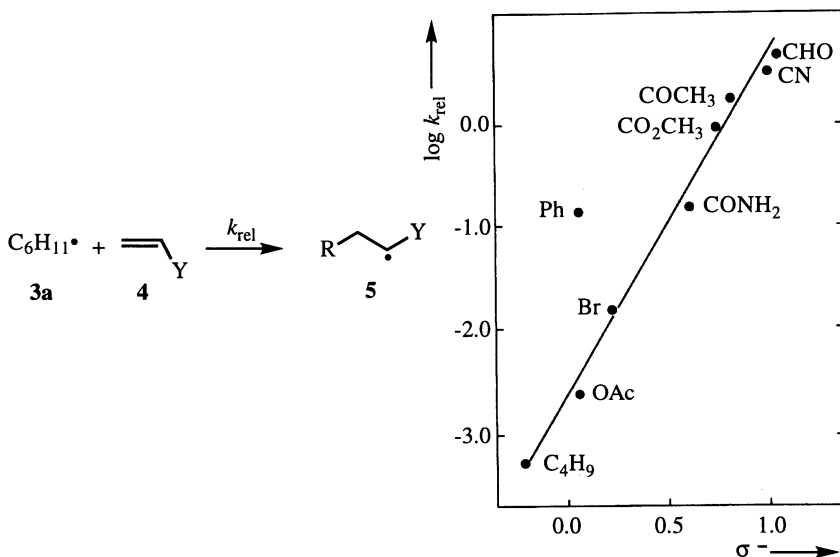


Figure 1. Correlation of the relative reactivities of cyclohexyl radical **3a** with the Hammett σ^- parameters of the substituents at the *monosubstituted* alkene **4** (20°C).

The variation of geminal substituents at 1,1-*disubstituted* alkenes **7** shows a good correlation of the relative reactivities with the Hammett parameters and no deviation is observed for stabilizing substituents like phenyl or capto-dative groups (Figure 2). This can be explained by a slight twisting of the substituent (especially the phenyl group) out of conjugation because of the presence of the geminal group. Thus, the stabilizing effect of the phenyl group is reduced and only the polar effects remain effective in these cases as well.

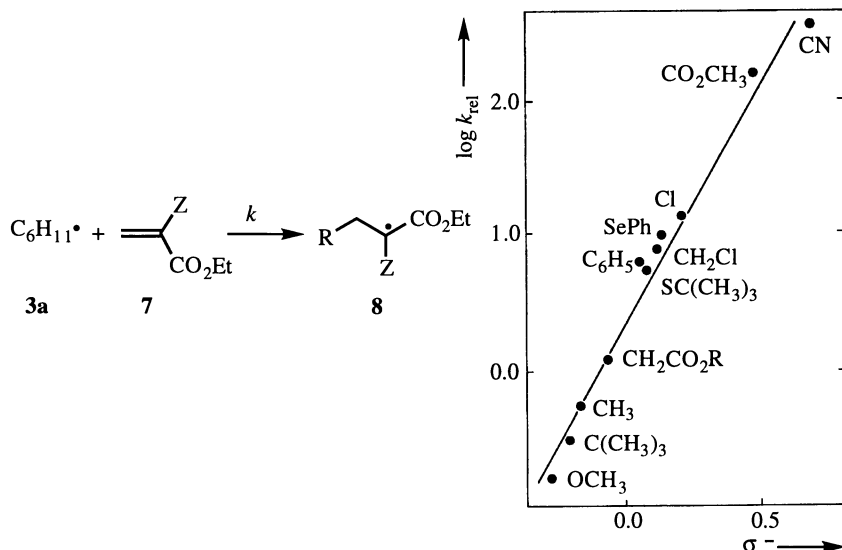


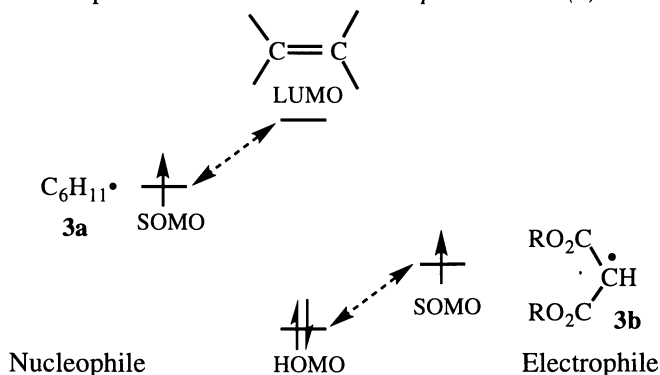
Figure 2. Correlation of the relative reactivities of cyclohexyl radical with the Hammett σ^- parameters of the substituent Z at the 1,1-disubstituted alkene 7 (20°C).

Substituents at the radical center also influence to a great extent the absolute (7) and the relative rates of the addition to alkenes. Radicals behave either as nucleophiles (4) (e.g. alkyl radicals) or as electrophiles (e.g. malonyl (4) radical 3b, malononitrile radical (10), perfluoroalkyl radicals (11)). Table I illustrates this phenomenon: the differences in relative rates for both nucleophilic (3a) and electrophilic (3b) radicals with alkenes of various polarities are very large and depend on the polarity of the alkene. Thus, cyclohexyl radical 3a react 5900 times faster with the electron deficient α -phenyl-acrylonitrile (X = CN) than with an electron rich enol ether (X = OEt). On the other hand, the relative rate of addition of malonyl radical 3b to a nucleophilic enamine (X = morpholino) is 34 times larger than to the electrophilic α -benzoyl styrene (X = COPh)(12).

Table I: Relative Rates of Addition of Radicals 3a-d to α -substituted Styrenes 9 (20°C)(12).

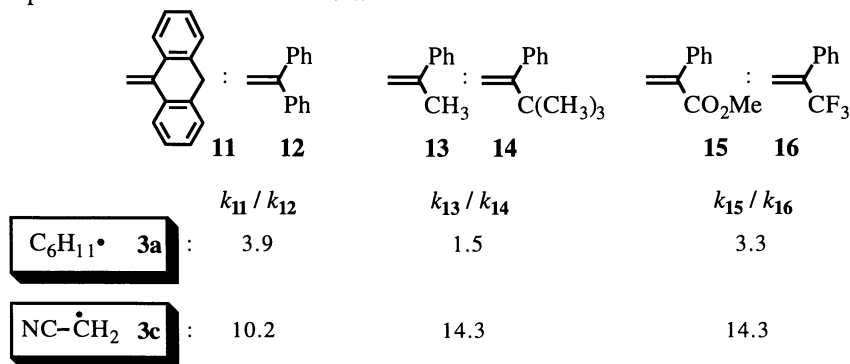
		$\text{R}\cdot + \text{C}(\text{Ph})=\text{C}(\text{X}) \longrightarrow \text{R}-\text{C}(\text{Ph})-\dot{\text{C}}(\text{X})$			
		3	9	10	
X		C ₆ H ₁₁ •	(R'O ₂ C) ₂ CH•	•CH ₂ CN	•CH ₂ CO ₂ Me
		3a	3b	3c	3d
			34	3.6	5.0
MeO		≡1.0	12	1.0	≡1.0
Me		12	5.5	≡1.0	1.1
Ph		45	6.7	1.6	
CO ₂ Et		570	1.5	1.5	1.8
COPh		680	≡1.0	1.3	1.5
CN		5900			

The predominance of the polar effects can be explained by the FMO theory which predicts two extreme cases for the addition of R^\bullet to olefins (8): 1) the interaction between the SOMO of the radical and the LUMO of the alkene is most important, or 2) the interaction between the SOMO of the radical and the HOMO of the alkene is decisive (Scheme 3). When the SOMO/LUMO interaction dominates, the rate of addition of **3** is increased by the presence of electron withdrawing groups at the olefin. These radicals are nucleophiles (e.g. $C_6H_{11}^\bullet$ **3a**). On the other hand, strong electron withdrawing substituents at the radical center turn the radicals electrophilic (e.g. malonyl radical **3b**). They react faster with electron rich olefins, and in this case the reaction is controlled by the SOMO/HOMO interaction. The role of polar effects can be described by plotting the reactivities *versus* the difference of the radical's ionization potential (IP) and the electron affinity of the alkene (EA) for *nucleophilic* radicals or *versus* the difference of the electron affinity of the radical and the ionization potential of the alkene for *electrophilic* radicals (7).



Scheme 3

When the energy difference between the SOMO of the radical and the LUMO or HOMO of the alkene is too large to allow a good interaction, then the stabilization of the adduct radicals start to play a significant role. This is observed for instance with the cyanomethyl and methoxycarbonylmethyl radicals **3c** and **d**. Table I shows that these radicals do not exhibit a strong variation in reactivity when going from electron rich to electron poor alkenes. They are on the borderline between electrophilic and nucleophilic radicals and their rates of addition depend mainly on the stabilization of the adduct radical (12,13). This becomes very clear in the experiments described in Scheme 4.



Scheme 4

The pairs of alkenes **11/12**, **13/14**, **15/16** have similar polarities but different abilities to stabilize radicals. Thus, cyclohexyl radical **3a** (nucleophilic) reacts with these olefins with similar rates. However, cyanomethyl radical **3c** reacts 10 times faster with **11** than with **12**, since in **11** a methylene group maintains both phenyl groups in the plane of conjugation allowing a better stabilization of the adduct radical. A similar effect is observed in the pair **13/14** in which the *tert*-butyl group forces the phenyl group to rotate out of the plane thus reducing its stabilizing effect on the radical. But this decreases only the rate of reaction with radical **3c**. In the pair of alkenes **15/16**, a radical *destabilizing* group CF_3 has been introduced. Again, this has a large effect only on the reaction rate of the enthalpic radical **3c**.

Steric Effects (8)

Substituents at the alkene exert not only polar effects but also steric effects on the reactivity of radicals. Our experiments demonstrated that a substituent **Z** at the attacked carbon has a major steric influence on the rate of addition whereas substituent **Y** at the remote carbon plays only a small role on the reactivity (Figure 3). Thus, increasing the steric bulk of **Z** in a β -substituted acrylate from **Z=H** to **Z=*tert*-butyl** causes a decrease of the addition rate of cyclohexyl radical of 20 000, whereas by changing **Y** in the same way the addition is only 4.2 times slower when **Y=*tert*-butyl**.

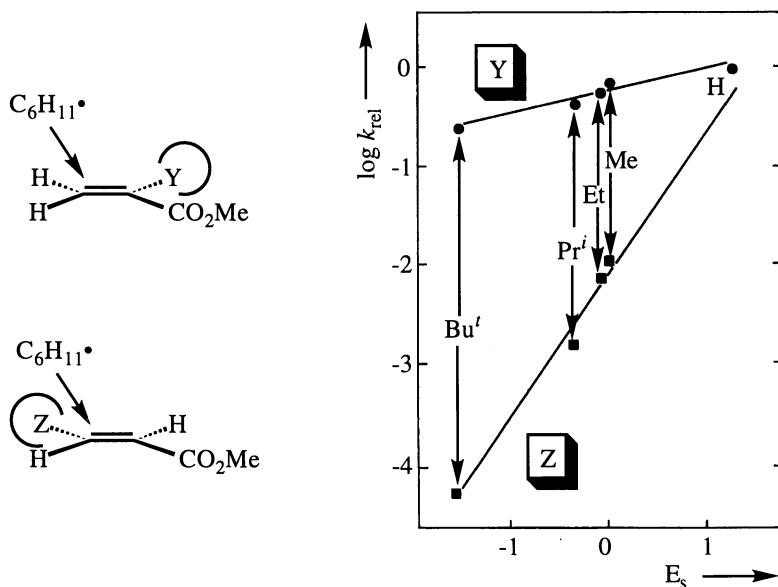
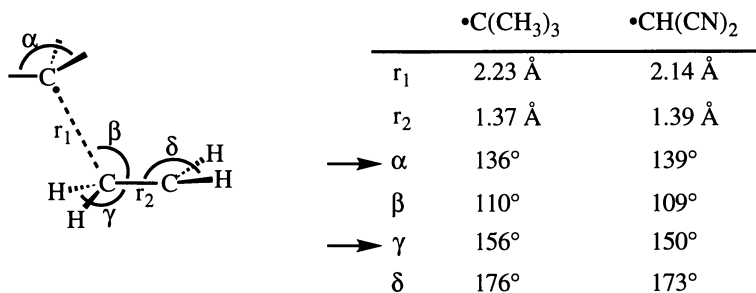


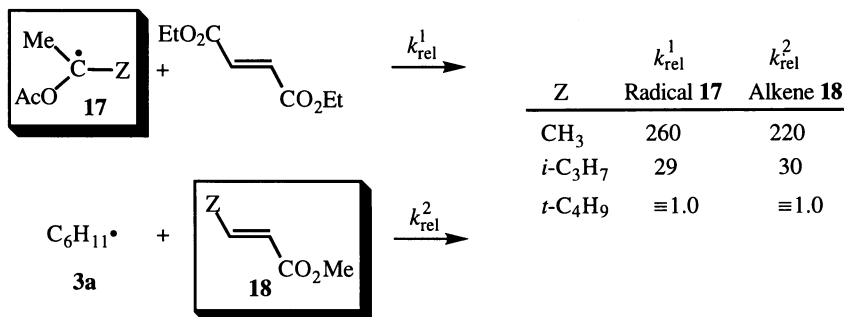
Figure 3. Correlation between the reactivities of cyclohexyl radical **3a** with the E_s parameters (Taft) for the alkene substituents **Y** (●) and **Z** (■).

This can be explained by the unsymmetrical geometry of the transition state of the radical addition (14). The radical attacks the alkene following a tetrahedral angle β . The angles α and γ at the radical and at the attacked carbon of the olefin are already bent whereas angle δ at the remote carbon remains close to 180° . It is remarkable that the transition state structures for the addition of nucleophilic and electrophilic radicals are very similar.



Scheme 5

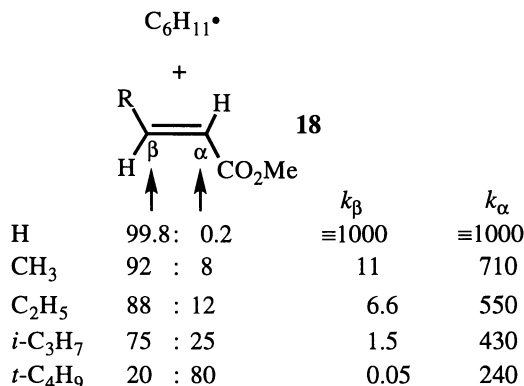
Substituents at the radical center **17** exert also strong steric effects on the rate of addition. Bulky groups decrease the reactivity towards alkenes in a similar extent as the group Z at the attacked carbon atom of the olefin **18** (Scheme 6)(15).



Scheme 6

Regioselectivity (8)

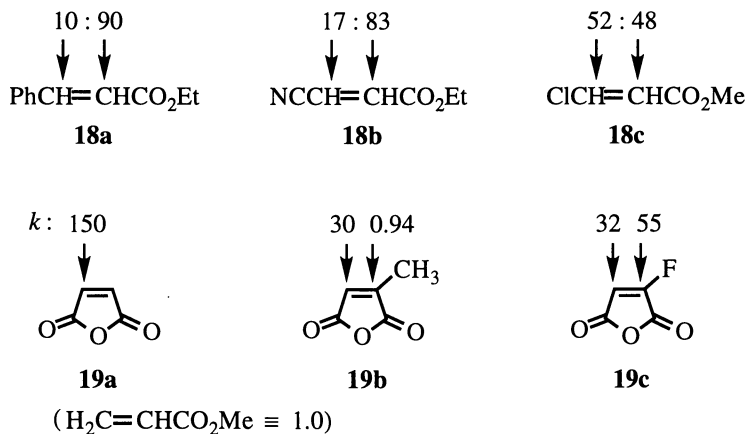
The regioselectivity of the radical addition to alkenes is strongly influenced by steric effects. This can be illustrated by the regioselectivity of the addition of cyclohexyl radical to β -substituted acrylates **18** (Scheme 7)(8,16).



Scheme 7

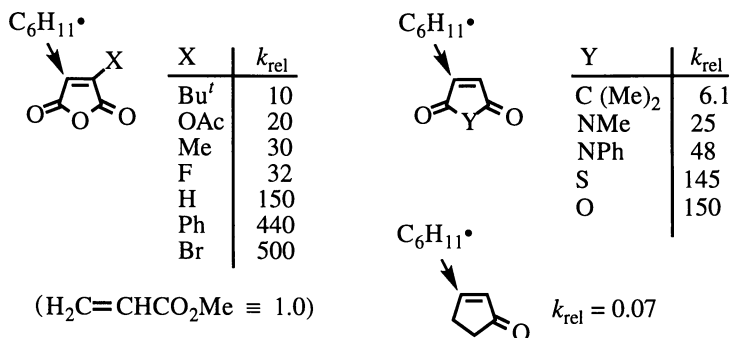
Methyl acrylate (R=H) reacts mainly at the β -position ($k_\alpha/k_\beta = 500$). However, while group R turns bulkier, the amount of α -attack increases and becomes predominant with very large groups like R=*tert*-butyl (Scheme 7). These steric effects are the main reason for the preferred attack at the less substituted (or less hindered) carbon of unsymmetrical alkenes. The influence of radical stabilizing effects is small. For example, if the preferred attack at the less substituted carbon of methyl maleic anhydride **19b** would result from the higher stability of a tertiary radical (compared to a secondary radical) then **19b** should react faster than **19a**. This is not the case (Scheme 8).

When the shielding substituents are very small (*e.g.* fluorine) or when the steric differences in 1,2-disubstituted olefins are minor, the orbital coefficients of the olefinic carbon atoms start to play a role in the regioselectivity (Scheme 8)(8,17). For instance, in fluoro maleic anhydride **19c** the radical attack occurs mainly α to the fluorine atom. Indeed, fluorine is not only small but it is also a mesomeric electron donating substituent which implies that the LUMO coefficient of the α -carbon atom is larger than β to the fluorine. Another case in which the regioselectivity of the addition is also controlled by the orbital coefficients of the alkene is illustrated by olefin **18b**. Although the ester group is bulkier than the nitrile, the radical attacks the alkene preferentially α to the ester because the nitrile group is a stronger electron withdrawing substituent and thus the LUMO coefficient α to the ester group is larger than α to the nitrile.



Scheme 8

Since maleic anhydride is an important monomer in polymer chemistry, some more data on the reactivity of derivatives or analogues of this alkene might be interesting. The examples of Scheme 9 illustrate the influence of the polarity effects on the reactivity of the radical addition. For example, maleic anhydride reacts 25 times faster than the corresponding 1,4-cyclopentendione and 2100 times faster than 2-cyclopentenone.

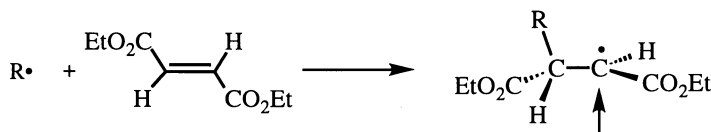


Scheme 9

Stereochemistry

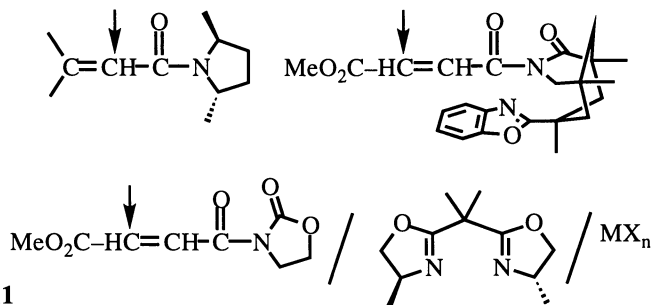
The control of stereochemistry in the radical addition to alkenes involving *cyclic* radicals is mainly influenced by steric effects (18). Since cyclic systems (radicals or alkenes) are relatively rigid, it is often easy to predict the stereoselectivity of their reactions on the basis of the different shielding of the two faces by the substituents. In five-membered ring radicals, for instance, addition mostly occurs at the face *anti* to the substituent neighboring the radical center. Steric effects are also responsible for high stereoselectivities in the addition of radicals to *cyclic* alkenes (18).

On the other hand, *acyclic* radicals are very flexible, nevertheless very high levels of stereoselectivity can also be achieved in these systems. The control of stereochemistry is made possible because the radicals can adopt preferred conformations on the basis of 1,3-allylic strain, for instance (Scheme 10)(19,20).



Scheme 10

Chiral auxiliaries have also been used to shield the two faces of the radicals or alkenes to a different extent so that the addition occurs preferentially at the less hindered side (Scheme 11)(19,20). Furthermore, metal complexation has proven to be an excellent way to control the stereochemistry of radical additions to alkenes. In this context, the first example of enantioselective radical addition under catalytic conditions was achieved recently (21).

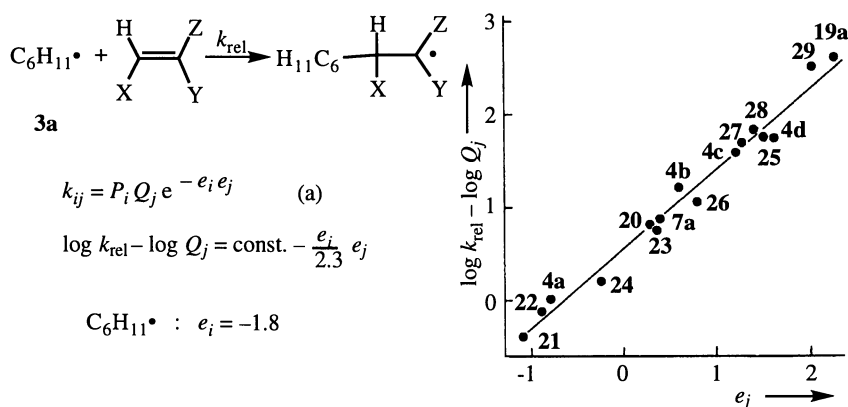


Scheme 11

Generally, one can say that the rules which control the stereochemistry in ionic chemistry in most cases also apply in radical chemistry. The concepts and guidelines to the problem of controlling the stereoselectivity of radical reactions have been collected recently in a book (20).

Radical Polymerization

The substituent effects which direct the addition of radicals to alkenes are very important for the radical polymerization. Indeed, the rates of addition of cyclohexyl radical to olefins correlate well with the parameters of the Alfrey-Price equation (a)(22,23).

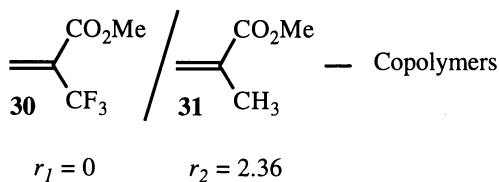


Alkene	X	Y	Z	k_{rel}
20	CH ₃	H	CO ₂ Me	0.067
21	H	H	<i>p</i> -MeOC ₆ H ₄	0.53
22	H	H	<i>p</i> -MeC ₆ H ₄	0.84
4a	H	H	Ph	≡1.00
23	H	Cl	Cl	1.2
24	H	H	<i>p</i> -ClC ₆ H ₄	1.6
25	CO ₂ Et	CO ₂ Et	H	3.3
7a	H	CH ₃	CO ₂ Me	5.0
4b	H	H	CO ₂ Me	6.7
26	H	CH ₃	CN	13
4c	H	H	CN	24
27	CO ₂ Et	H	CO ₂ Et	30
19a	methyl	maleic	anhydride	140
28	H	Cl	CN	200
4d	H	CO ₂ Et	CO ₂ Et	270
29	CN	H	CN	310

Figure 4. Correlation between the relative reactivities ($\log k_{\text{rel}}$) of cyclohexyl radical **3a** and the Q_j and e_j values of various alkenes.

It is also possible to measure the Q_i and e_i values of alkenes even if one r value approaches zero as in the case of the copolymerization of methyl α -trifluoromethylacrylate **30** with methyl methacrylate **31**. From the correlation between the reactivity of the cyclohexyl radical with polymerization parameters and

the value $r_2 = 2.36$, we could determine Q_j and e_j of **30** as being 0.74 and 0.4, respectively (24).



$$\text{radical addition} \longrightarrow \log k_{\text{rel}} - \log Q_j = 0.5 + 0.825 e_j$$

$$r_2 = Q_1/Q_2 e^{-e_2(e_2 - e_1)}$$

Scheme 12

$$Q_1 = 0.74 \quad e_1 = 0.40$$

References

- (1) B. Giese, *Angew. Chem. Int. Ed. Engl.* **1985**, *24*, 553.
- (2) N. Bellec, J. C. Guillemin, *Tetrahedron Lett.* **1995**, *36*, 6883. E. Nakamura, Y. Yu, S. Mori, S. Yamago, *Angew. Chem. Int. Ed. Engl.* **1997**, *36*, 374.
- (3) B. Giese, J. Meister, *Chem. Ber.* **1977**, *110*, 2588.
- (4) B. Giese, G. Kretzschmar, *Chem. Ber.* **1984**, *117*, 3160.
- (5) B. Giese, *Radicals in Organic Synthesis*, Pergamon Press, Oxford, 1986.
- (6) B. Giese, G. Kretzschmar, J. Meixner, *Chem. Ber.* **1980**, *113*, 2787.
- (7) H. Fischer in *Substituent Effects in Radical Chemistry*, H. G. Viehe, Z. Janousek, R. Merenyi Eds., D. Reidel, Dordrecht, 1986, p.123. H. Fischer, in *Free Radicals in Biology and Environment*, F. Minisci Ed., D. Reidel, Dordrecht, 1997, p. 63.
- (8) B. Giese, *Angew. Chem. Int. Ed. Engl.* **1983**, *22*, 753.
- (9) B. Giese, G. Kretzschmar, *Chem. Ber.* **1983**, *116*, 3267.
- (10) K. Riemenschneider, H. M. Bartels, R. Dornow, E. Drechsel-Grau, W. Eichel, H. Luthé, Y. M. Matter, W. Michaelis, P. Boldt, *J. Org. Chem.* **1987**, *52*, 205.
- (11) H. C. Low, J. M. Tedder, J. C. Walton, *Int. J. Chem. Kinet.* **1978**, *10*, 325. D. V. Avila, K. U. Ingold, J. Luszyk, W. R. Dolbier, jr., H. Q. Pan, M. Muir, *J. Am. Chem. Soc.* **1994**, *116*, 99.
- (12) B. Giese, J. He, W. Mehl, *Chem. Ber.* **1988**, *121*, 2063.
- (13) T. Zytowski, H. Fischer, *J. Am. Chem. Soc.* **1996**, *118*, 437. M. W. Wong, A. Pross, L. Radom, *J. Am. Chem. Soc.* **1993**, *115*, 11050. M. W. Wong, A. Pross, L. Radom, *J. Am. Chem. Soc.* **1994**, *116*, 6284.
- (14) H. Zipse, J. He, K. N. Houk, B. Giese, *J. Am. Chem. Soc.* **1991**, *113*, 4324. See also: K. N. Houk, M. N. Paddon-Row, D. C. Spellmeyer, N. G. Rondan, S. Nagase, *J. Org. Chem.* **1986**, *51*, 2874. C. Gonzalez, C. Sosa, H. B. Schlegel, *J. Phys. Chem.* **1989**, *93*, 2435. T. Fueno, M. Kamachi, *Macromolecules* **1988**, *21*, 908. R. Arnaud, S. Vidal, *New. J.*

- Chem.* **1992**, *16*, 471. D. J. Tozer, J. S. Andrews, R. D. Amos, N. C. Handy, *Chem. Phys. Lett.* **1992**, *199*, 229.
- (15) B. Giese, H. Harnisch, U. Lüning, *Chem. Ber.* **1985**, *118*, 1345.
- (16) B. Giese, S. Lachhein, *Angew. Chem. Int. Ed. Engl.* **1981**, *20*, 967.
- (17) B. Giese, G. Kretzschmar, *Chem. Ber.* **1984**, *117*, 3175.
- (18) B. Giese, *Angew. Chem. Int. Ed. Engl.* **1989**, *28*, 969.
- (19) N. A. Porter, B. Giese, D. P. Curran, *Acc. Chem. Res.* **1991**, *24*, 296.
- (20) D. P. Curran, N. A. Porter, B. Giese, „*Stereochemistry of Radical Reactions, Concepts, Guidelines, and Synthetic Applications*“, VCH, Weinheim, 1996.
- (21) M. P. Sibi, M. P. Sibi, J. Ji, J. H. Wu, S. Gürtler, N. A. Porter, *J. Am. Chem. Soc.* **1996**, *118*, 9200.
- (22) B. Giese, J. Meixner, *Angew. Chem. Int. Ed. Engl.* **1980**, *19*, 207.
- (23) B. Giese, J. Meixner, *Polymer Bull.* **1980**, *2*, 805.
- (24) H. Ito, R. Engelbrecht, B. Giese, *Macromolecules* **1984**, *17*, 2204.

Chapter 4

Cascade Radical Reactions in Organic Synthesis: An Overview

Dennis P. Curran

Department of Chemistry, University of Pittsburgh, Pittsburgh, PA 15260

Abstract: This lecture will provide an overview of the past decade of developments of cascade radical reactions in organic synthesis that is targeted towards a polymer audience. Many of the principles in play in today's small molecule cascades emerged from polymer chemistry and were modified accordingly. Indeed, the lecture might instead be titled "How to Start a Radical Polymerization and Then Stop It Before It Really Gets Going". The similarities between polymer chemistry and small molecule synthesis will be apparent. The key difference is that the goal of a radical polymerization is to get every radical to do the same thing while the goal of a cascade radical reaction is to get every radical to do a different thing. Prototypical sequences of inter- and intramolecular radical reactions will be discussed along with the methods that are used to conduct them.

I. Introduction

Cascade reactions are now commonly used by synthetic organic chemists to fashion complex molecules from simpler precursors in the fastest and most efficient way possible.¹ Cascade radical reactions (sometimes called sequential or tandem radical reactions) are an important subclass that has played a central role in the growth in popularity of cascade reactions. The key features that impact on the design of cascade radical reactions are now relatively well understood, and it has become possible to design and execute an astounding assortment of useful reactions. This lecture will provide an overview of the criteria for planning tandem radical reactions and show how these criteria are applied to the design and execution of large, important classes of cascade radical reactions. Given the increasing popularity of the field, comprehensive coverage is not possible. Instead, work from our laboratory will be used to highlight key lessons that have been learned over the past fifteen years or so. There is no recent comprehensive review of this fast moving field, but older overviews and more recent treatments of some aspects of the field are available.²

The introduction of radical reactions to the synthetic repertoire has provided significant new options that both supplement and complement synthetic methods based on ionic and pericyclic reactions.³ Radical-based methods to form carbon-carbon bonds have been especially useful because they occur under such mild conditions that high selectivity is often possible. Tributyltin hydride and tris(trimethylsilyl)silicon hydride⁴ are the most popular reagents that are currently available for mediating radical reactions, but a new fluorinated tin hydride is now providing new options as well (see

Figure 1).⁵ Although reactions based on tin hydride remain the most popular for synthetic applications, there are a number of other fundamentally different strategies that offer unique advantages for synthetic applications.³ One of the most useful of these is the atom transfer method, summarized in Figure 2.⁶

Figure 1. Radical Reactions with Tributyltin Hydride

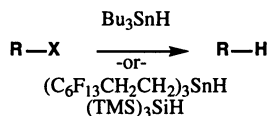
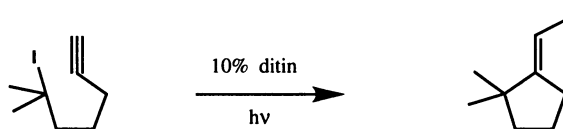


Figure 2. A Typical Atom Transfer Cyclization



In a very real sense, even the simplest radical reactions such as reductions of halides by tin hydrides are sequential reactions because they occur in multi-step chains. However, for synthetic purposes, radical reactions are generally only considered sequential if more than one bond forming or breaking process occurs between generation of the initial radical and removal of the final radical.⁷ Thus, the atom transfer cyclization shown in Figure 2 is not a tandem radical reaction; only one bond is formed between radical generation and trapping.

Radical reactions are ideal for sequencing for a very simple reason: the product of every radical–molecule reaction is a radical.⁷ This, the generation of a radical from an initial precursors by the tin hydride method, the atom transfer method, or any other method can set off a cascade of events. Controlling the cascade is the key to developing a successful tandem radical reaction. Each individual radical must react selectively, which is a special challenge because radicals are transient. This generally means that cascades cannot be conducted “one step at a time” by sequential addition of reagents. Instead, once started, they go from beginning to end. A whole collection of different radicals is present in the same reaction medium and exposed to the same reaction conditions at the same time. As the sequence becomes more and more complex, it becomes more and more difficult to control the selectivities of the individual intermediate radicals.

Perhaps the most important step in a radical cascade from a selectivity standpoint is the last one. It is this step which draws the line between a cascade to make a small molecule in general steps and a polymerization of many steps. Even if all the intermediate radicals react as planned to complete a cascade, the product is still not formed until the last radical in the cascade is removed to provide a closed shell product. When chain chemistry is used, this radical is removed by the chain transfer reaction. Controlling the chain transfer step is a crucial design element in any tandem reaction; ideally, only the last radical in the cascade should suffer chain transfer. Reaching this ideal situation can be more or less difficult depending on the types of radical reactions in the sequence and the method by which they are conducted.

II. Sequences of Intramolecular Reactions

Among the easiest kinds of radical sequences to conduct are those that contain only intramolecular reactions. In these kinds of sequences, the selectivities of the radicals are determined by the structures of the substrates. In general, each individual radical only has one reaction of reasonable rate that is can be expected to undergo. The large body of knowledge about rate constants of radical reactions and the many examples of individual intramolecular reactions serve as guides for planning successful intramolecular sequences. In general, the last radical in a sequence is not given a good intermolecular option, and therefore it suffers chain transfer by default. The only requirement is that this chain transfer must be faster than radical–radical or radical–solvent reactions. Given this, the sequence will succeed provided that the slowest reaction along the way is still faster than chain transfer.

In short, the requirements for designing sequences of intramolecular reactions are not that much more stringent than those for conducting a single intramolecular reaction. In both cases, selectivity is imposed by intramolecularity.

The three most popular types of intramolecular radical reactions are cyclization, ring opening (the reverse of cyclization) and 1,5-hydrogen transfer. These reactions are often combined under the tin hydride method, although many of the other methods can and have been used to conduct sequences containing only intramolecular reactions. Prototypical examples of three representative sequences selected from among many are shown in Figure 3. Figure 3a shows now classic examples of tandem cyclizations to form vicinal carbon–carbon double bonds.⁸ This is by far the most popular kind of tandem radical reaction, and many imaginative double, triple, and even tetracyclizations have been executed. In these types of tandem cyclizations, the number of new C–C bonds formed equals the number of steps between radical generation and chain transfer.

Figure 3a. Early Tandem Cyclizations

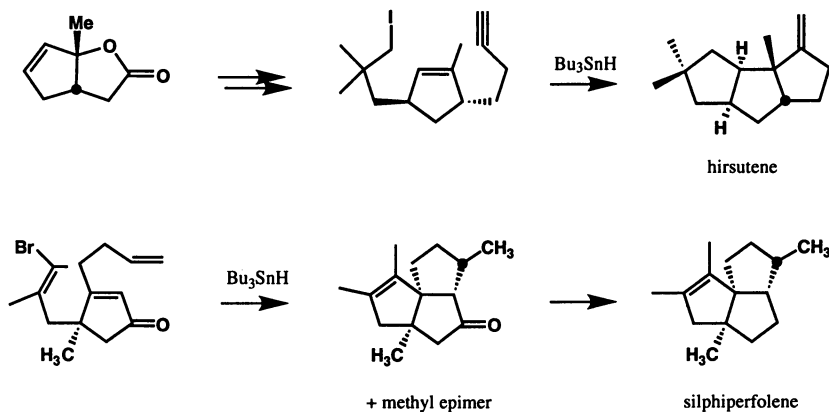


Figure 3b shows an example of a so-called Dowd-Beckwith ring expansion⁹ that is capped off with another cyclization.¹⁰ A sequence of cyclization–fragmentation–cyclization occurs between radical generation and chain transfer. In one sense, this type of sequence is less powerful than straight tandem cyclization: only one net C–C bond is

gained in this process (the other is “lost” in the fragmentation). However, as the example in Figure 3b clearly shows, the complexity of a tandem process cannot be measured simply by the number of bonds gained.

Sequences of radical reactions can also involve radical translocations. In these reactions, the first-formed radical is “translocated” from a site where it is easy to generate to one where it is not, and a reaction or series of reactions then follows.¹¹ The most popular types of radical translocations are hydrogen transfers, and these allow the indirect use of a C–H bond as a radical precursor. An example is shown in Figure 3c.

Figure 3b. A Cyclization–Fragmentation–Cyclization Sequence

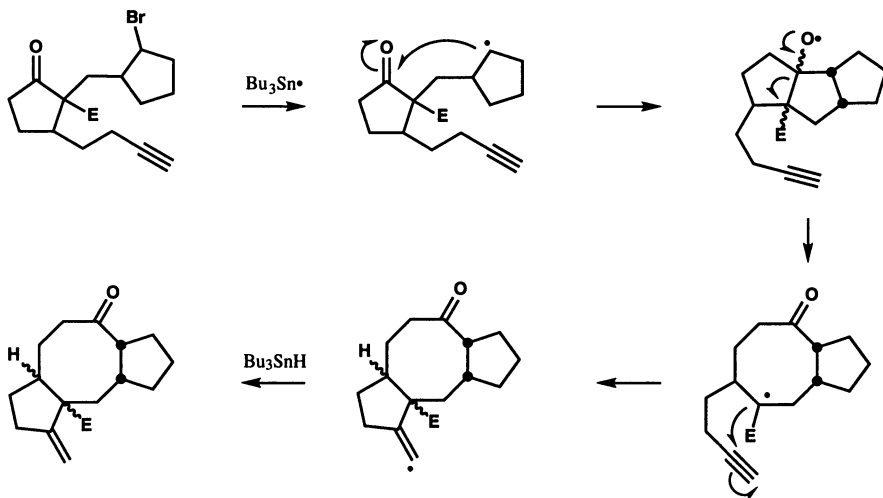
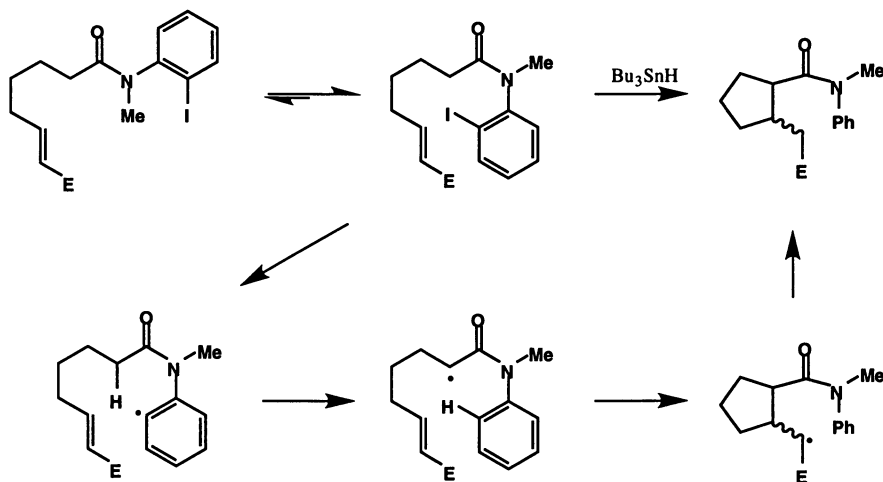


Figure 3c. A Radical Translocation–Cyclization Sequence



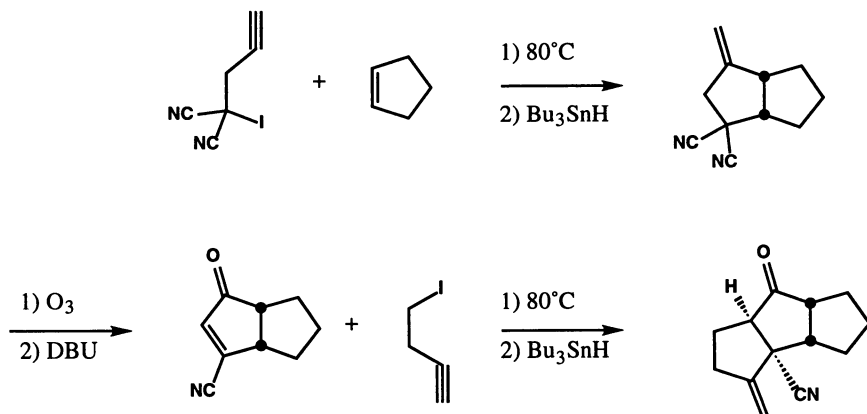
III. Radical Annulations

Sequences that combine inter- and intramolecular reactions become more difficult to conduct. In general, it is easier to conduct the intramolecular reaction first (because it is fast and can handily beat out a competing bimolecular reaction), and there are many examples of sequences of cyclization–addition. It is also relatively easy to conduct reactions in the reverse order (addition–cyclization) when radicals are added to dienes and related molecules.

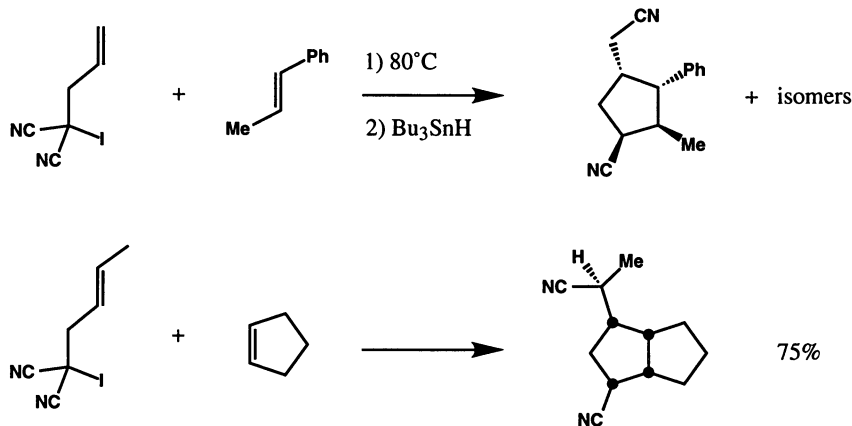
The most interesting type of sequence in the “inter/intra” class is a “radical annulation” because a new ring is formed from two acyclic precursors by a sequence of addition (brings the two pieces together) and cyclization (forms the ring). In this sequence, both pieces are integrated into the new ring. This is in contrast to the above sequences, where all of the atoms of the ring are present in the cyclization component, and the addition component is tacked on before or after cyclization.

A radical annulation also presents a unique selectivity problem: it is especially difficult to differentiate the initial radical from the final radical. Tin hydride is a relatively poor reagent for differentiating many kinds of radicals, and therefore the tin hydride method is not the most popular method for conducting radical annulations. Instead, these reactions are conducted either by atom transfer methods or by unimolecular chain transfer methods (see below). The iodine atom transfer method is especially useful. Almost all exothermic iodine atom transfer reaction are very fast, so the timing of iodine transfer can be controlled by the design of the intermediate radicals. In general, atom transfer can be timed to stop a sequence (and, because this is a chain transfer step, start the next one) whenever an intermediate radical is formed that: 1) is less stable than the starting radical, and 2) has no rapid unimolecular option. Several representative examples are shown in Figure 4a. In each case, the iodides were removed in the end by tin hydride. However, the annulations cannot be conducted with tin hydride directly.¹²

Figure 4a. Atom Transfer Annulations



The malononitrile class of reactions is especially interesting because the radical annulation can be followed by a nitrile transfer reaction, as shown by the examples in Figure 4b.¹³ Two simple molecules come together to selectively form complex, substituted rings in one operation by a sequence of addition–cyclization (to the alkene)–cyclization (to the nitrile) and fragmentation.

Figure 4b. Addition-Cyclization-Cyclization-Fragmentation

Alkenes serve as natural reagent equivalents⁷ for the “two atom” components of “n + 2” radical annulations. But by using carbon monoxide, isonitriles or a few other reagents, it is possible to conduct “n + 1” radical annulations.^{2g} For example, the sequence of addition–cyclization–cyclization shown in Figure 5 is a powerful way to make cyclopenta-fused quinolines,¹⁴ as has been shown by a recent synthesis of camptothecin and more than two dozen members of the camptothecin family of anti-tumor agents.¹⁵

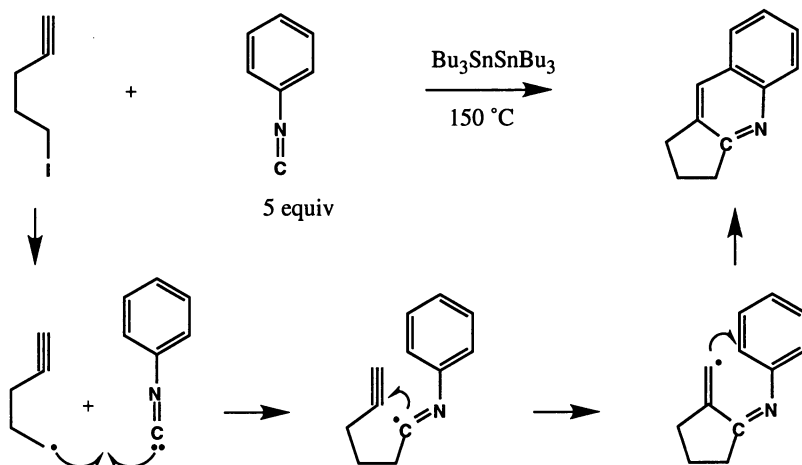
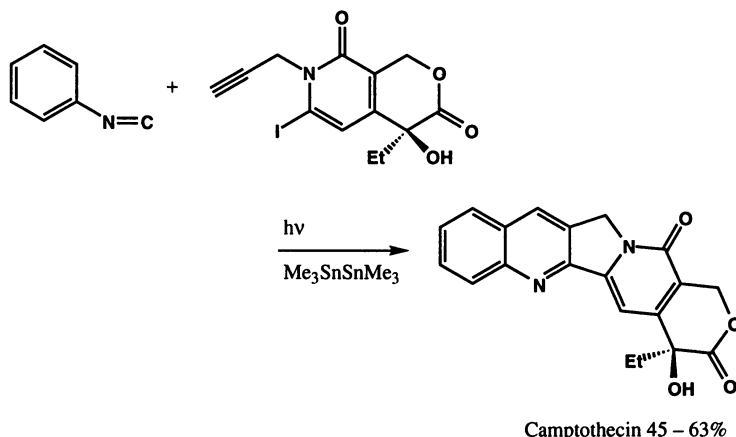
Figure 5a. An Addition-Cyclization-Cyclization

Figure 5b. Application to Camptothecin



IV. Sequences of Intermolecular Reactions Only

Sequences of intramolecular reactions are the most difficult to conduct because they come dangerously close to polymerizations. It is possible to use alternating electronic requirements to control selectivity in a double addition. For example, if a nucleophilic radical is generated in the presence of both an electron rich and an electron poor alkene, it will add to the electron poor alkene first. The resulting electrophilic radical will add to the electron rich alkene, so that the order of the double addition is controlled. But there now is a major problem because the last radical is also nucleophilic, and appears destined to repeat the fate of the first radical. The result is a well known alternating copolymerization. How can a chain transfer reaction rescue the double addition sequence from polymerization?

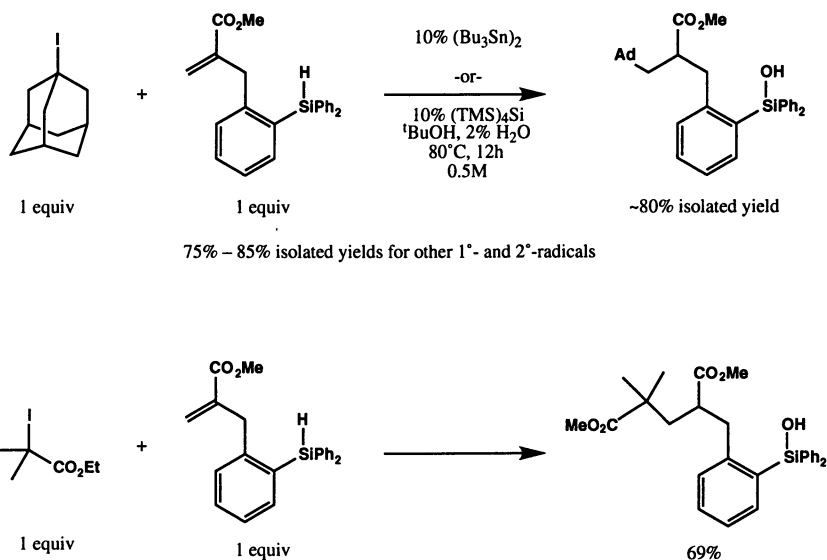
The general solution to this fundamental selectivity problem is simple—the *chain transfer reaction should be rendered unimolecular*.¹⁶ Indeed, this is the logical reversal of the popular synthetic mode of operation, which involves conducting intramolecular radical additions (radical cyclizations) by using bimolecular chain transfer reactions. The same kinds of selectivity benefits can be gained by using unimolecular chain transfer reactions (UMCT) to conduct intermolecular radical addition reactions or other types of radical sequences.

Previous work has focused on using allyl stannanes and related molecules as UMCT reagents. But hydrogen transfer is the most popular chain transfer reaction, so we have been developing silicon hydrides as UMCT reagents. Normal silicon hydrides have C–H bonds that are too strong to function as hydrogen donors in bimolecular reactions with radicals;¹⁷ however, intramolecular hydrogen transfer reactions will still occur. Thus, the problem of competing bimolecular reactions is solved by choosing a chain transfer reaction that will only work intramolecularly; chain transfer cannot occur until the radical with the UMCT option is produced.

An example of a UMCT reagent that has been synthesized and used in Giese reactions is shown in Figure 6.¹⁶ These reactions give high yields without the usual requirements for excess alkene (only 1 equiv is used) or high dilution (0.5–1.0 M are the typical reaction conditions). By using (TMS)₄Si as an initiator, tin-free reactions can be conducted. Beyond these practical improvements, the UMCT method can be used to

selectively conduct bimolecular reactions that would be considered impossible by standard methods. This is illustrated by the last example in Figure 6. In this case, both the initial radical and the adduct radical are tertiary ester-substituted radicals, and they could never undergo competing bimolecular reactions (addition/hydrogen transfer) at different rates—selectivity is impossible and ratios of adducts (reduced, mono, di, tri, etc.) would be statistical. However, by using UMCT methods, control is straightforward because only the adduct radical can undergo intermolecular hydrogen transfer.

Figure 6. Examples of Giese Reactions Conducted by the UMCT Method



V. Conclusions and Outlook

Over the past 15 years, many of the basic concepts of how to plan and conduct tandem radical reactions have been laid out. But the types of transformations that can be conducted by radical reactions continues to expand rapidly, and imaginative new combinations of reactions continue to be introduced regularly. Thus, the prospects for research in this area continue to be very bright.

Acknowledgments

I express my sincere gratitude to all the present and former coworkers in my group who have worked in the “tandem radical” area. Many of their names are listed in the references. I also thank the National Institutes of Health and the National Science Foundation for sustained funding of our program.

References

1. a) Wender, P. A. *Chem. Rev.* **1996**, *96*, 1. b) Ho, T.-L. *Tandem Organic Reactions*; Wiley-Interscience: NY, 1992, pp 398. c) Tietze, L. F.; Beifuss, U. *Angew. Chem. Int. Ed. Eng.* **1993**, *32*, 131.
2. a) Bertrand, M. P. *Org. Prep. Procedure Int.* **1994**, *26*, 257. b) Bunce, R. A. *Tetrahedron* **1995**, *51*, 13103. c) Little, R. D. *Chem. Rev.* **1996**, *96*, 93. d) Malacria, M. *Chem. Rev.* **1996**, *96*, 289. e) Molander, G. A.; Harris, C. R. *Chem. Rev.* **1996**, *96*, 307. f) Parsons, P. J.; Penkett, C. S.; Shell, A. J. *Chem. Rev.* **1996**, *96*, 195. g) Ryu, I.; Sonoda, N.; Curran, D. P. *Chem. Rev.* **1996**, *96*, 177. h) Snider, B. B. *Chem. Rev.* **1996**, *96*, 339. i) Tietze, L. F. *Chem. Rev.* **1996**, *96*, 115. j) Wang, K. K. *Chem. Rev.* **1996**, *96*, 207. k) Koert, U. *Angew. Chem. Int. Ed.* **1996**, *35*, 405.
3. a) Giese, B. "Radicals in Organic Synthesis", Pergamon: Oxford, 1986. b) Motherwell, W. B.; Crich, D. "Free Radical Chain Reactions in Organic Synthesis", Academic Press: London, 1991. c) Curran, D. P. "The Design and Application of Free Radical Chain Reactions in Organic Synthesis." *Synthesis* **1988**, 417-439 and 489-513. d) Curran, D. P. "Radical Addition Reactions", In *Comp. Org. Syn.* B. M. Trost and I. Fleming, Ed.; Pergamon: Oxford, 1991; Vol. 4; pp 715-778. e) Curran, D. P. "Radical Cyclizations and Sequential Radical Reactions", In *Ibid.* Vol. 4; pp 779-832.
4. Chatgililoglu, C. *Acc. Chem. Res.* **1992**, *25*, 188.
5. a) Curran, D. P.; Hadida, S. *J. Am. Chem. Soc.* **1996**, *118*, 2531. b) Studer, A.; Hadida, S.; Ferritto, R.; Kim, S. Y.; Jeger, P.; Wipf, P.; Curran, D. P. *Science* **1997**, *275*, 823.
6. Curran, D. P. In *Free Radicals in Synthesis and Biology*, 1989; Vol. Nato Asi Ser., Ser. C, 260; pp 27.
7. Curran, D. P. *Synlett* **1991**, 63.
8. a) Curran, D. P.; Kuo, S. C. *J. Am. Chem. Soc.* **1986**, *108*, 1106. b) Curran, D. P.; Rakiewicz, D. M. *Tetrahedron* **1985**, *41*, 3943. c) Curran, D. P.; Chen, M.-H. *Tetrahedron Lett* **1985**, *26*, 4991. d) Curran, D. P.; Chen, M.-H.; Leszczewski, D.; Elliott, R. L.; Rakiewicz, D. M. *J. Org. Chem.* **1986**, *51*, 1612. e) Curran, D. P.; Kuo, S. C. *Tetrahedron* **1987**, *43*, 5653. f) Fevig, T. L.; Elliott, R. L.; Curran, D. P. *J. Am. Chem. Soc.* **1988**, *110*, 5064. g) Curran, D. P. In *Adv. Free Radical Chem.*; D. D. Tanner, Ed.; JAI, Greenwich, CN: 1990; Vol. 1; pp 121. h) Curran, D. P.; Wang, S. *Tetrahedron* **1993**, *49*, 755.
9. Dowd, P.; Zhang, W. *Chem. Rev.* **1993**, *93*, 2091.
10. Dr. M. Yu and Mr. D. Christen, unpublished observations.
11. a) Curran, D. P.; Kim, D.; Liu, H. T.; Shen, W. *J. Am. Chem. Soc.* **1988**, *110*, 5900. b) Snieckus, V.; Cuevas, J. C.; Sloan, C. P.; Liu, H.; Curran, D. P. *J. Am. Chem. Soc.* **1990**, *112*, 896. c) Curran, D. P.; Abraham, A. C.; Liu, H. T. *J. Org. Chem.* **1991**, *56*, 4335. d) Curran, D. P.; Kim, D.; Ziegler, C. *Tetrahedron* **1991**, *47*, 6189. e) Curran, D. P.; Yu, H. S. *Synthesis* **1992**, 123. f) Curran, D. P.; Somayajula, K. V.; Yu, H. S. *Tetrahedron Lett.* **1992**, *33*, 2295. g) Curran, D. P.; Abraham, A. C. *Tetrahedron* **1993**, *49*, 4821. h) Curran, D. P.; Demello, N. C. *J. Chem. Soc., Chem. Commun.* **1993**, 1314. i) Curran, D. P.; Shen, W. *J. Am. Chem. Soc.* **1993**, *115*, 6051. j) Curran, D. P.; Liu, H. T. *J. Chem. Soc., Perkin Trans. 1* **1994**, 1377. k) Curran, D. P.; Yu, H. S.; Liu, H. T. *Tetrahedron* **1994**, *50*, 7343. l) Yamazaki, N.; Eichenberger, E.; Curran, D. P. *Tetrahedron Lett.* **1994**, *35*, 6623. m) Curran, D. P.; Xu, J. Y. *J. Am. Chem. Soc.* **1996**, *118*, 3142.

12. a) Curran, D. P.; Seong, C. M. *J. Am. Chem. Soc.* **1990**, *112*, 9401. b) Curran, D. P.; Chen, M.-H.; Spletzer, E.; Seong, C. M.; Chang, C.-T. *J. Am. Chem. Soc.* **1989**, *111*, 8872.
13. a) Curran, D. P.; Seong, C. M. *Tetrahedron* **1992**, *48*, 2157. b) Curran, D. P.; Seong, C. M. *Tetrahedron* **1992**, *48*, 2175.
14. Curran, D. P.; Liu, H. *J. Am. Chem. Soc.* **1991**, *113*, 2127.
15. a) Curran, D. P.; Liu, H. *J. Am. Chem. Soc.* **1992**, *114*, 5863. b) Curran, D. P. *J. Chin. Chem. Soc.* **1993**, *40*, 1. c) Curran, D. P.; Sisko, J.; Yeske, P. E.; Liu, H. *Pure Appl. Chem.* **1993**, *65*, 1153. d) Curran, D. P.; Ko, S. B.; Josien, H. *Angew. Chem. Int. Ed.* **1995**, *34*, 2683. e) Curran, D. P.; Liu, H.; Josien, H.; Ko, S. B. *Tetrahedron* **1996**, *52*, 11385.
16. a) Curran, D. P.; Xu, J. Y.; Lazzarini, E. *J. Am. Chem. Soc.* **1995**, *117*, 6603. b) Curran, D. P.; Xu, J. Y.; Lazzarini, E. *J. Chem. Soc., Perkin Trans. 1* **1995**, 3049. c) Curran, D. P.; Xu, J. Y. *J. Chem. Soc., Perkin Trans. 1* **1995**, 3061.
17. a) Chatgililoglu, C. in "Free Radicals in Synthesis and Biology", Minisci, F., Ed, Kluwer: Dordrecht: **1989**, 215-23. b) Walsh, R., *Acc. Chem. Res.* **1981**, *14*, 246-52.

Chapter 5

Selective Product Formation with Organometallic Radicals of Nickel and Zinc

Gerard van Koten, Robert A. Gossage, David M. Grove,
and Johann T. B. H. Jastzebski

Debye Institute, Department of Metal-Mediated Synthesis, Utrecht University,
Padualaan 8, 3584 CH Utrecht, Netherlands

A summary is presented of the mechanistic study of the 1 : 1 Kharasch addition reaction of polyhalogenated alkanes to olefins catalyzed by mononuclear or dendrimer-bound aryl-Ni complexes. These compounds contain the terdentate monoanionic aryldiamino ligand, $[C_6H_2(CH_2NMe_2)_2-2,6-R-4]^-$ or "(NCN)". The catalysis occurs *via* inner sphere single electron transfer (SET) with the formation of a Ni^{III} organometallic radical and a polyhalogenated alkane radical. This study is also relevant to the use of such compounds for the controlled radical polymerization of alkenes. A review is also given of the chemistry of α -diimine containing organozinc radicals that are also formed by a SET process. These metal-based radicals are useful for a variety of highly selective group transfer reactions in organic synthesis.

Moses Gomberg was the first to isolate an organic radical, the triphenylmethyl radical, almost 100 years ago (1). It is unlikely that he could have foreseen the important role that such organic and organometallic radicals play in modern synthetic chemistry. Radicals are key intermediates in many important chemical processes including addition, polymerization and group transfer reactions. Research in our group has been aimed at controlling these reactions by the use of isolable, paramagnetic (*i.e.* radical) organometallic complexes.

Homogeneous Catalysis with Organonickel Complexes; Reactions and Mechanism.

Catalysis. We have designed and synthesized a vast array of main-group and transition metal complexes of the general structure **1** (Figure 1) incorporating the monoanionic diaminoaryl ligand $[C_6H_2(CH_2NMe_2)_2-2,6-R-4]^-$, abbreviated as "(NCN)". (2, 3) This organic fragment generally enforces a rigid trans disposition of the N donor atoms in relation to the metal-aryl group, an arrangement which

generally constrains an overall meridonal geometry around the metal centre (2,3). $\text{NiX}_n(\text{NCN})$ complexes have been isolated for the formally Ni^{II} ($\text{X} = \text{halide}$; $n = 1$) and Ni^{III} ($\text{X} = \text{halide}$; $n = 2$) oxidation states (Figure 1). The trivalent compounds were the first organometallic Ni^{III} compounds to be isolated and structurally characterized (2-4). It has been shown that when $[\text{Ni}^{\text{II}}(\text{NCN})]$ complexes are used as pre-catalysts, that the active species (discussed below) is a highly active promoter not only for addition reactions but also in the controlled radical polymerization of alkenes. The mononuclear Ni complex **1a** is an excellent homogeneous catalyst for the 1 : 1 Kharasch addition reaction of halocarbons to olefins *via* an inner sphere electron transfer process (also referred to as "atom transfer", see Scheme 1), when a large excess of halocarbon is used. This reaction occurs readily at ambient temperature and pressure (5).

Kharasch addition is important in specialty chemical synthesis, as the trichloromethyl group can be readily converted into a variety of useful functional groups (6). We have carried out an extensive investigation of the factors that control this process (*i.e.* catalytic 1 : 1 Kharasch addition) and by so doing have identified that during catalysis a paramagnetic, d^7 , $\text{Ni}(\text{III})$ organometallic complex (*i.e.*, a radical) is formed.

Mechanistic Studies of Nickel-Catalyzed Kharasch Addition. We have carried out a detailed study of the catalytic mechanism using $[\text{NiX}(\text{NCN})]$ as catalyst. The systematic adjustment of the ligand environment and reaction conditions during catalysis was carried out by: (i) varying the ligand X bound to Ni (5), (ii) varying the R group on the para-position of the (NCN) ligand (Figure 1) (8), (iii) substitution of the methyl groups attached to nitrogen by bulkier and more electron rich fragments (5, 6, 9, 10) and (iv) adjustment of the reagents (catalyst, alkene and polyhalogenated alkane) used and their concentrations under controlled catalytic conditions.

Early Work. Early experiments had indicated that the type of the halide anion (Cl, Br or I) coordinated to Ni had little effect on the overall reaction profile for the catalytic Kharasch (*i.e.* 1 : 1) addition of CCl_4 to methyl methacrylate (MMA) or other alkenes (4). Replacement of this halide by a neutral donor ligand results in the formation of a Ni^{II} cation as the catalyst precursor, such as the complex $[\text{Ni}(\text{NCN})(\text{MeCN})]\text{BF}_4$ (4, 5). These cationic species are completely *inactive* as catalysts for the Kharasch addition reaction, a result which clearly demonstrates the necessity of a halide ligand in the catalytic cycle and *not* the availability of an open coordination site(s).

Ligand Modification. The effect of replacing the proton as the R group on the para position of the (NCN) ligand was also investigated. Catalytic reaction rates were found to increase with electron donating substituents while electron withdrawing groups have the opposite effect. A linear relationship was found between the Hammett (substituent) parameters of the R group and the reaction rate. This result indicates that there is an electron demand at or just before the rate determining step. It was also observed that this modification of the rate of catalysis could be directly related to the value of the $\text{Ni}^{\text{II}} / \text{Ni}^{\text{III}}$ redox couple. This suggests that oxidation of the metal is an essential part of the catalysis and that Ni^{III} complexes are probably formed (8,11).

The increase in the catalytic rate as a result of the introduction of electron donating R groups led us to investigate if this effect could be further enhanced by the replacement of the methyl groups attached to nitrogen. Modified (NCN) ligands incorporating electron-rich (*e.g.* isopropyl) groups were used to synthesize the corresponding Ni^{II} catalyst precursors. These complexes have greatly *reduced* (or no) catalytic behaviour. The effect seems to be steric in nature and indicates that the NMe₂ groups are a necessary component of this catalytic system. This also provides evidence that the initial process involves the formation of an inner sphere activated complex between [NiX(NCN)] and the polyhalogenated alkane. Increased steric congestion at the N donor atoms will interfere with the production of this complex and hence the reaction rate will be retarded.

Concentration Effects on Catalysis. Catalytic studies have also been performed using different concentrations of catalyst, alkene and halocarbon. The rate law is distinctly first order in relation to catalyst and alkene concentration. This indicates that the activated complex is a mononuclear one and that alkene activation is rate determining. Varying the concentration of the polyhalogenated alkane shows that the reaction rate has a dependence that is typical of *saturation kinetics*. The inference here is that the reaction of this alkane with the Ni complex is *reversible*. Furthermore, cross-over experiments with mixtures of CCl₄ and CBr₄ indicate that an equilibrium, such as that shown in Scheme 2, is probably operating (*i.e.* in step 1, k_1 and k_{-1} are reversible and "X" can be readily exchanged for a halide atom from CCl₄ or CBr₄).

Spectroscopic Studies During Catalysis. Spectroscopic studies (IR, NMR) of the catalytic and stoichiometric reaction of [NiBr(NCN)] with MMA revealed no evidence for η^2 -coordination of the olefinic C=C bond to the metal centre. Measurements by ESR spectroscopy taken during catalysis confirm the formation of a Ni^{III} complex of very similar structure to that of the previously isolated [NiX₂(NCN)] compounds (4, 11).

These data suggest the presence of radicals, similar to those that have been proposed in the mechanism of Kharasch addition mediated by inorganic halides and RuCl₂(PPh₃)₃ (12, 13). Two main factors also point to the production of radicals in the coordination sphere of the metal. First, none of the reaction products that have been detected are consistent with the bulk release of free radicals into the reaction medium under the conditions of study, *e.g.*, the formation of hexachloroethane from the addition reaction of two free •CCl₃ radicals. Secondly, the observation of Ni^{III} radical complexes indicates directly that inner sphere single electron transfer (SET) has occurred from the interaction of the Ni^{II} pre-catalyst and the polyhalogenated alkane.

Proposed Mechanism. Based on all of the above observations, we have proposed a catalytic cycle (see Scheme 2) based on a non-chain mechanism with a mononuclear Ni species. During or just prior to the rate determining step, oxidation of the Ni^{II} metal centre to a d⁷ Ni^{III} organometallic radical occurs *via* SET (complex C, Scheme 2; *c.f.*, B represents the possible case of oxidative addition of CCl₄ to the Ni center). This step leads to the generation of both a [NiX₂(NCN)] centre and a polyhalogenated organic radical in the coordination sphere of the metal atom where it reacts, in the rate determining step, with the alkene. Following this,

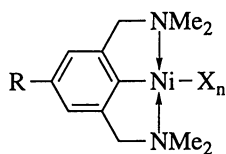
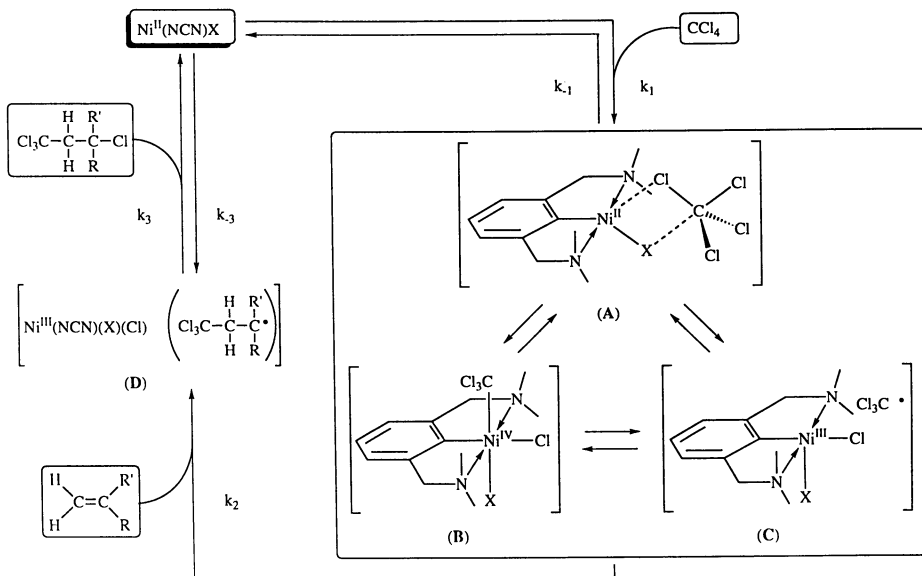
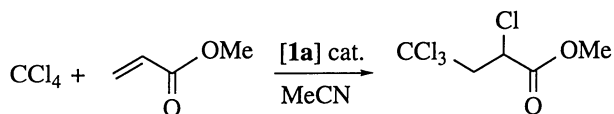


Figure 1.



rapid halide transfer (atom transfer) is mediated by the Ni^{III} halide moiety to the adduct radical. The 1 : 1 addition product is then eliminated from the vicinity of the metal with regeneration of the [NiX(NCN)] complex, see Scheme 2 (11). We believe that the organic radicals that are involved in this chemistry remain in the coordination sphere of the metal complex. This is suggested by the reaction profile and the products thus formed, *vide supra* (7, 11, 12). An interesting feature of this system is the role of the Ni-X fragment as an anchoring site for the formation of an innersphere activated complex A in the absence of a free coordination site. This is a previously unrecognized concept in homogeneous catalysis that could be of fundamental significance in systems that comprise elementary steps involving SET and metal species with an odd number of electrons (*i.e.* radicals).

Other Catalytic Applications (Controlled Radical Polymerization). A common feature of all metal-based Kharasch addition catalysts is a low inherent redox couple. For example the Ru^{II} / Ru^{III} and Cu^I / Cu^{II} redox couples are -0.08 and approximately +0.16 V respectively for RuCl₂(PPh₃)₃ and Cu halide systems (12, 13). Our [NiX(NCN)] complexes have an average redox couple of about +0.20 V (2, 8-10). Typical values for the Ni^{II} / Ni^{III} redox couple are on the order of +0.70 to +1.2 V (14). An interesting recent observation by Teyssié and coworkers is that complexes which possess this low oxidation potential can be tuned to perform polymerization reactions by adjusting the conditions. This switch of reactivity occurs at elevated temperatures in the presence of a large excess of alkene if the polyhalogenated alkane (*e.g.*, CCl₄) is used in *stoichiometric* amounts relative to the catalyst (15). Teyssié's group has shown that our [NiBr(NCN)] (R = H) complex combined with a slight excess of CCl₄ and a large (>1000 fold) excess of olefin is a highly active catalytic system for the controlled radical polymerization of MMA (15). This area has been the focus of pioneering studies by Matyjaszewski and collaborators who have produced polymers with very narrow polydispersities ($M_n < 1.05$) from a variety of olefins using a number of different catalysts (16, 17). An immediate consequence of Teyssié's work is the realization that controlled radical polymerization can be "switched" over to a 1 : 1 Kharasch polymer "capping" addition reaction. This could be performed *in situ* simply by quenching the living polymer with a large excess of polyhalogenated alkane with concurrent lowering of the reaction temperature. This implies that kinetic control of the reaction can be achieved by varying the reagent concentrations. In other words, the rate of polymerization (k_p) would have to be much less than the corresponding rate of Kharasch addition (k_K) in the presence of a large excess of halocarbon (*i.e.*, $k_p \ll k_K$ if [CCl₄] \gg [catalyst]). Teyssié's results clearly show that this reactivity is inverted if the concentration of catalyst and halocarbon are similar (*i.e.*, $k_p \gg k_K$ if [CCl₄] \approx [catalyst]) and the reaction is performed above ambient temperature. A recent example of this *in situ* adjustment of catalytic reactivity has been demonstrated by Coca and Matyjaszewski. In this case a Cu halide / amine catalyst system was used to mediate the formation of block copolymers of styrene and (methyl)acrylates *via* initially living carbocationic then later living radical polymerization (18).

Dendrimer Catalysts. Following our early success with the [NiX(NCN)] series as Kharasch addition catalysts (19), we also wished to expand this chemistry to include macromolecules incorporating the active Ni unit. This can lead to the

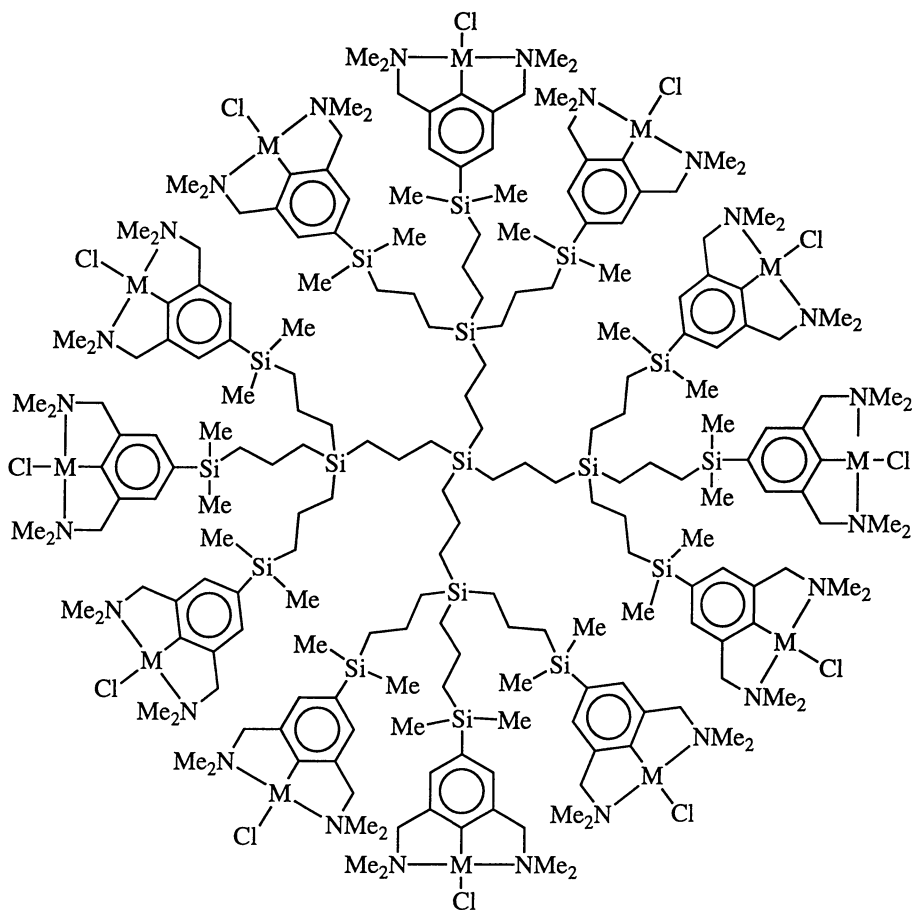


Figure 2. An example of a carborane dendrimer catalyst.

formation of soluble species that can be easily removed from the reaction stream by filtration or other techniques. In this regard, we designed and tested the first "dendrimer catalyst" (20). Dendrimers are large monodispersed molecules that are generally synthesized by a repetitive reaction sequence (21, 22). By using an appropriate R group attached to the (NCN) moiety (Figure 1), the grafting of the [NiX(NCN)] catalytic site on to the exterior of a carbosilane dendrimer (23, 24) has been achieved, see Figure 2. Catalytic activity per Ni site is maintained relative to the monomeric complex and the dendrimer unit is highly soluble in most solvents (20, 25). We are currently expanding these investigations to include the use of ultrafiltration technology to facilitate dendrimer (*i.e.*, catalyst) recovery from the reaction medium (25).

Heterogeneous Catalysts and New Materials. Our work on homogeneous and dendrimeric catalysis with the [NiX(NCN)] system has also been expanded to include heterogeneous catalysis. Using a similar methodology as has been shown in the dendrimer synthesis, the attachment of the Ni moiety to siloxane polymers has also been demonstrated (26). These polymeric materials containing the immobilized catalyst show good catalytic activity in the Kharasch addition reaction that is of the same order of magnitude as that observed with the homogeneous mononuclear complex (26).

Our involvement in the synthesis of new materials is not restricted to the design and use of dendrimers. We have also shown that the [NiX(NCN)] fragment is a useful starting material for the incorporation of paramagnetic (*i.e.*, radical) Ni ions into inorganic colloids (27). Thus, Ni(NCN) complexes have been used to produce magnetic silica particles and this presents an opportunity to study model colloidal materials that contain a covalently bound paramagnetic surface layer.

Organozinc Radicals.

Thus far we have described our work (and the work of others) in radical based catalysis (both homo- and heterogeneous) for selective addition and polymerization reactions. We have also shown that Ni complexes can be used to form stable paramagnetic materials. In separate studies we have also explored the use of selective group transfer reactions in organic synthesis. This chemistry involves the employment of organozinc complexes and substrates containing the α -diimine $-N=CH-CH=N-$ skeleton. These reactions occur *via* radical pathways involving persistent organozinc α -diimine radical species. Reports on this chemistry can be found in the literature in references 28-32. Although these reactions are extremely useful for the "one-pot" synthesis of rather complex organic molecules, it is particularly the mechanistic aspects and the intermediacy of organozinc α -diimine radicals that make this chemistry interesting.

Group Transfer Reactions. Selective group transfer reactions can be performed with dialkylzincs containing a coordinated α -diimine $R'N=CHCH=NR'$. If the α -diimine used has $R' = t\text{-Bu}$, this reagent reacts with ZnR_2 with high regioselectivity to form either the nitrogen-alkylated product, $ZnR(t\text{-Bu}N(R)CHCHNt\text{-Bu})$ ($R =$ primary alkyl group) or the carbon-alkylated product, $ZnR(t\text{-Bu}NCH(R)CHNt\text{-Bu})$ ($R =$ tertiary/benzylic alkyl group) (31). Two possible mechanisms for this alkylation reaction have been put forward, *i.e.* a

radical and a polar mechanism, see Scheme 3. Earlier studies have shown that in both mechanisms the initial step is the formation of a thermally unstable 1:1 coordination complex $\text{ZnR}_2(\text{t-BuNCHCHNt-Bu})$ (**2**), which undergoes an intramolecular single-electron transfer (SET) reaction to give radical pair, $[\text{R}\bullet / \text{ZnR}(\text{t-BuNCHCHNt-Bu})\bullet]$ (**3**), in a solvent cage. In the radical mechanism, **3** collapses in the solvent cage, resulting in the nitrogen- (**6**) and carbon-alkylated (**7**) products. In the polar mechanism, a steady state concentration of the free organozinc radical is formed. The latter transfers its unpaired electron to the initial 1:1 coordination complex $\text{ZnR}_2(\text{t-BuNCHCHNt-Bu})$ (**2**), to give a organozinc cation / diorganozinc radical-anion pair, $[\text{ZnR}(\text{t-BuNCHCHNt-Bu})^+][\text{ZnR}_2(\text{t-BuNCHCHNt-Bu})\bullet^-]$ (**8**). Nucleophilic attack of an alkyl group of the diorganozinc radical-anion $[\text{ZnR}_2(\text{t-BuNCHCHNt-Bu})\bullet]^-$ on the organozinc cation $[\text{ZnR}(\text{t-BuNCHCHNt-Bu})^+]$ gives the alkylation products and simultaneous regeneration of the free organozinc radical (**4**). In the polar mechanism **6** and **7** can be regarded as 1,2- and 1,4-addition products, respectively.

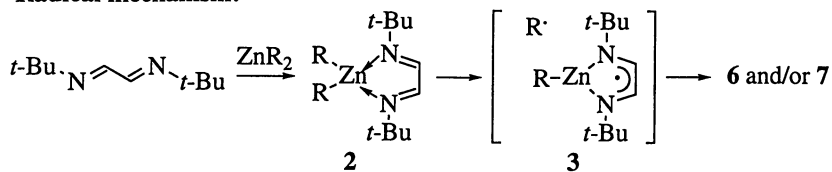
Radical Mechanisms in Group Transfer. Thus far, both mechanisms are supported by the isolation of the 1:1 coordination complex $\text{ZnMe}_2(\text{t-BuNCHCHNt-Bu})$ (**2a**) (*30*) and of $[\text{ZnR}(\text{t-BuNCHCHNt-Bu})]_2$ ($\text{R} = \text{Me}$ (**5a**), Et (**5b**)), which exist in solution in equilibrium with the corresponding neutral organozinc radicals $[\text{ZnR}(\text{t-BuNCHCHNt-Bu})]$ (**4**), see Scheme 4 (28-32). Although the radical mechanism has been used as a working hypothesis for the reaction of t-BuNCHCHNt-Bu with ZnR_2 , the proposal of an alternative, polar mechanism seemed justified by the EPR-detection of an unprecedented paramagnetic species during the alkylation reaction in THF solution (THF = tetrahydrofuran).

Recent results provide indirect evidence for a radical mechanism in the alkylation reactions of t-BuNCHCHNt-Bu with diorganozinc compounds. The paramagnetic species detected during this alkylation reaction in THF is tentatively assigned to be the solvated neutral organozinc radical complex $[\text{ZnR}(\text{t-BuNCHCHNt-Bu})(\text{THF})]$. This conclusion is further corroborated by the observed stability of the 1:1 coordination complex **2a** toward reduction by **4a**. We have also investigated the use of the stable dimeric zinc species **5a** (and its derivatives) to generate alkylzinc(α -diimine) radicals (*e.g.*, **4a**, see Scheme 4) in the radical polymerization of alkenes.

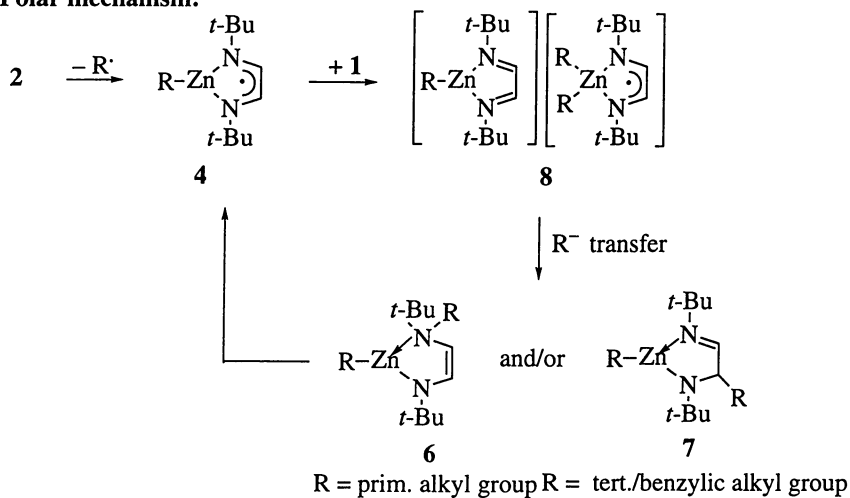
Conclusions.

So far we have been unable to initiate polymerization with these organozinc α -diimine radicals. It should be noted that Matyjaszewski *et al* have successfully polymerized MMA with $\text{Cu}^{\text{I}}\text{X}(\alpha\text{-diimine})$ compounds (α -diimine = 2,2'-bipyridine) *via* controlled living radical polymerization. The coordinated α -diimine ligand has a low lying π^* orbital that can readily accommodate a single electron. This is also the case with our organozinc complexes (28-32), whereas in the case of the $[\text{Ni}^{\text{III}}\text{X}_2(\text{NCN})]$ radical the single electron resides on the metal in a HOMO directed towards the apical halide atom (4, 9, 10). It is this latter property that makes the $[\text{Ni}^{\text{III}}\text{X}_2(\text{NCN})]$ species a highly efficient single electron acceptor and

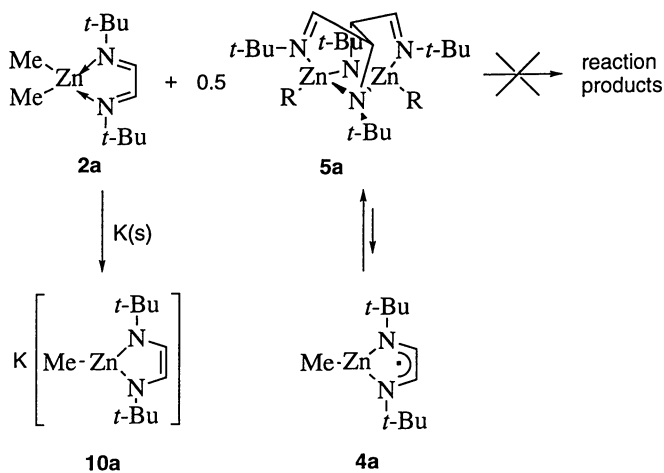
Radical mechanism:



Polar mechanism:



Scheme 3.



Scheme 4.

halide donor to a radical species. Thus, these characteristics make this compound both an excellent atom transfer (Kharasch addition) catalyst (5, 6, 20, 26) as well as an effective mediator of controlled radical polymerization (15).

Acknowledgments.

The organozinc / α -diimine chemistry is part of the Ph.D. theses of Dr. E. Rijnberg and Dr. E. Wissing. We thank Dr. J. Boersma for his interest and suggestions and Dr. A. L. Spek (Utrecht University) for the crystallographic support.

This work was supported by the Netherlands Foundation for Scientific Research (SON) with financial aid from the Netherlands Organization for Scientific Research (NWO).

Literature Cited.

- Gomberg, M. *Chem. Ber.* **1900**, *33*, 3150; *J. Am. Chem. Soc.* **1900**, *22*, 757.
- van Koten, G. *Pure & Appl. Chem.* **1989**, *61*, 1681.
- Rietveld, M. H. P.; Grove, D. M.; van Koten, G. *New. J. Chem.* **1997**, *21*, 751.
- Grove, D. M.; van Koten, G.; Zoet, R.; Murrall, N. W.; Welch, A. *J. Am. Chem. Soc.* **1983**, *105*, 1379.
- Grove, D. M.; van Koten, G.; Verschuuren, A. H. M. *J. Mol. Catal.* **1988**, *45*, 189.
- Grove, D. M.; Verschuuren, A. H. M.; van Koten, G.; van Beek, J. A. M. *J. Organomet. Chem.* **1989**, *372*, C1.
- Bellus, D. *Pure & Appl. Chem.* **1985**, *57*, 1827.
- van de Kuil, L. A.; Luitjes, H.; Grove, D. M.; Zwikker, J. W.; van der Linden, J. G. M.; Roelofsens, A. M.; Jenneskens, L. W.; Drenth, W.; van Koten, G. *Organometallics* **1994**, *13*, 468.
- van de Kuil, L. A.; Veldhuizen, Y. S. J.; Grove, D. M.; Zwikker, J. W.; Jenneskens, L. W.; Drenth, W.; Smeets, W. J. J.; Spek, A. L.; van Koten, G. *Recl. Trav. Chim. Pays-Bays* **1994**, *113*, 267.
- van de Kuil, L. A.; Veldhuizen, Y. S. J.; Grove, D. M.; Zwikker, J. W.; Jenneskens, L. W.; Drenth, W.; Smeets, W. J. J.; Spek, A. L.; van Koten, G. *J. Organomet. Chem.* **1995**, *488*, 191.
- van de Kuil, L. A.; Grove, D. M.; Gossage, R. A.; Zwikker, J. W.; Jenneskens, L. W.; Drenth, W.; van Koten, G. *Organometallics*, in press.
- Minisci, F. *Acc. Chem. Res.* **1975**, *8*, 165.
- Davis, R.; Furze, J. D.; Cole-Hamilton, D. J.; Pogorzelec, P. J. *Organomet. Chem.* **1992**, *440*, 191 and references therein.
- Haines, R. I.; McAuley, A. *Coord. Chem. Rev.* **1981**, *39*, 77.
- Granel, C.; Dubois, Ph.; Jérôme, R.; Teyssié, Ph. *Macromolecules* **1996**, *29*, 8576.
- Matyjaszewski, K.; Patten, T. E.; Xia, J. *J. Am. Chem. Soc.* **1997**, *119*, 674 and references therein.
- Patten, T. E.; Xia, J.; Abernathy, T.; Matyjaszewski, K. *Science* **1996**, *272*, 866.
- Coca, S.; Matyjaszewski, K. *Macromolecules* **1997**, *30*, 2808.
- van de Kuil, L. A.; Grove, D. M.; Zwikker, J. W.; Jenneskens, L. W.; Drenth, W.; van Koten, G. *6th IUPAC Symposium on Organometallic*

- Chemistry Directed Towards Organic Synthesis*, Utrecht, The Netherlands, **1991**.
20. Knapen, J. W. J.; van der Made, A. W.; de Wilde, J. C.; van Leeuwen, P. W. N. M.; Wijkens, P.; Grove, D. M.; van Koten, G. *Nature* **1994**, *372*, 659.
 21. Fréchet, J. M. J. *Science* **1994**, *263*, 1710.
 22. Tomalia, D. M. *Sci. American* **1995**, *272*, 62.
 23. Roovers, J.; Zhou, L. L. Toporowski, P. M.; van der Zwan, M.; Iatrou, H.; Hadjichristidis, N. *Macromolecules* **1993**, *26*, 4324 and references therein.
 24. van der Made, A. W.; van Leeuwen, P. W. N. M.; de Wilde, J. C.; Brandes, R. A. C. *Adv. Mater.* **1993**, *5*, 466 and references therein.
 25. Kleij, A. W.; Gossage, R. A.; Kleijn, H.; van Koten, G.; Kragl, U.; Brinkmann, N. *KNCV Katalyse Symposium*, May **1997**, Kerkrade, The Netherlands, Poster 37.
 26. van de Kuil, L. A.; Grove, D. M.; Zwikker, J. W.; Jenneskens, L. W.; Drenth, W.; van Koten, G. *Chem. Mater.* **1994**, *6*, 1675.
 27. Pathmamanoharan, C.; Wijkens, P.; Grove, D. M.; Philipse, A. P. *Langmuir* **1996**, *12*, 4372.
 28. Klerks, J. M.; Jastrzebski, J. T. B. H.; van Koten, G.; Vrieze, K. J. *Organomet. Chem.* **1982**, *244*, 107.
 29. van Koten, G.; de Meijere, K.; tom Dieck, H. in *Organometallics in Organic Synthesis*, Springer-Verlag, **1987**, 277.
 30. Kaupp, M.; Stoll, H.; Preuss, H.; Kaim, W.; Stahl, T.; van Koten, G.; Wissing, E.; Smeets, W. J. J.; Spek, A. L. *J. Am. Chem. Soc.* **1991**, *113*, 5606.
 31. Wissing, E.; Kaupp, M.; Boersma, J.; Spek, A. L.; van Koten, G. *Organometallics* **1994**, *13*, 2349.
 32. Wissing, E.; van der Linden, S.; Rijnberg, E.; Boersma, J.; Smeets, W. J. J.; Spek, A. L.; van Koten, G. *Organometallics* **1994**, *13*, 2602.

Chapter 6

Pulsed Laser Experiments Directed Toward the Detailed Study of Free-Radical Polymerizations

Sabine Beuermann and Michael Buback¹

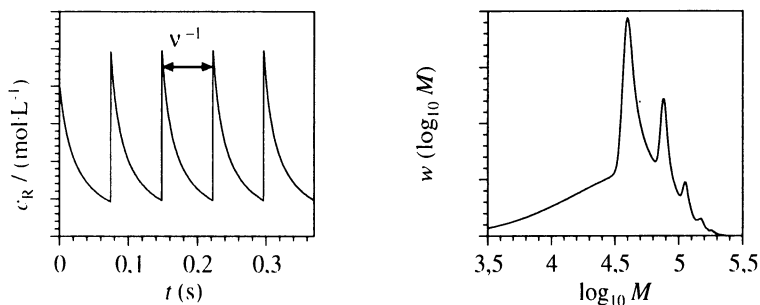
Institut für Physikalische Chemie der Georg-August-Universität,
Tammannstrasse 6, D-37077 Göttingen, Germany

Pulsed-laser polymerization (PLP) in conjunction with either molecular weight analysis of the polymeric product or time-resolved measurement of monomer conversion induced by a single pulse or by pulse sequences allows for the reliable determination of rate coefficients in free-radical polymerization. This article is primarily concerned with the application of PLP methods toward measuring propagation rate coefficients, k_p , and chain-length averaged termination rate coefficients, $\langle k_t \rangle$, as a function of temperature and partly up to high pressure. Termination rate coefficients may significantly vary during the course of a free-radical bulk polymerization. PLP experiments allow to study these changes. They also provide access to the investigation of a chain-length dependence of k_t . Moreover, chain transfer rates may be derived from PLP experiments.

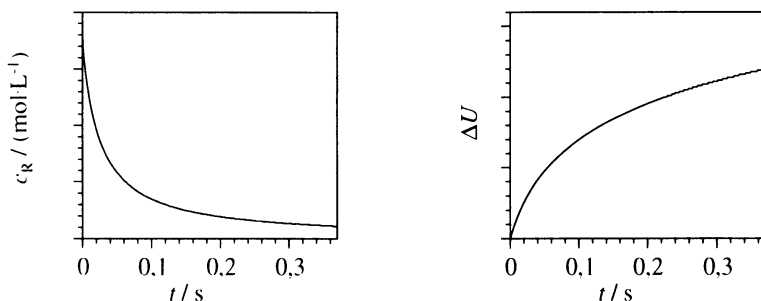
Over the past ten years, since the introduction of pulsed laser techniques into the detailed study of free-radical polymerization, a considerable amount of accurate rate coefficient data has become available. The principal types of pulsed laser polymerization (PLP) experiments are illustrated in Figure 1. Among them, the PLP-SEC (size exclusion chromatography) technique, pioneered by Olaj and coworkers (1,2), is of primary importance. An evenly spaced sequence of laser pulses is applied onto a monomer/photoinitiator system and a small initial monomer conversion, typically of one per cent, is reached. The almost instantaneous production of free radicals by each laser pulse causes an enhanced termination probability for radicals from the preceding pulse(s). This situation gives rise to a characteristic structure of the molecular weight distribution (MWD), as is illustrated by a simulated (see below) polymer size distribution in Figure 1a, where the weight fraction w is plotted vs. the logarithm of molecular weight, $\log_{10}M$. As will be shown in Section I, the propagation rate coefficient, k_p , may be directly obtained from the structured MWD.

¹Corresponding author.

a PLP - SEC experiment $\rightarrow k_p$ (Olaj, Bitai, Hinkelmann 1987)^{1,2}



b SP - PLP experiment $\rightarrow k_t/k_p$ (Buback, Hippler, Schweer, Vögele 1986)³



c PS - PLP experiment $\rightarrow k_t/k_p$ (Buback, Huckestein, Leinhos 1987)⁴

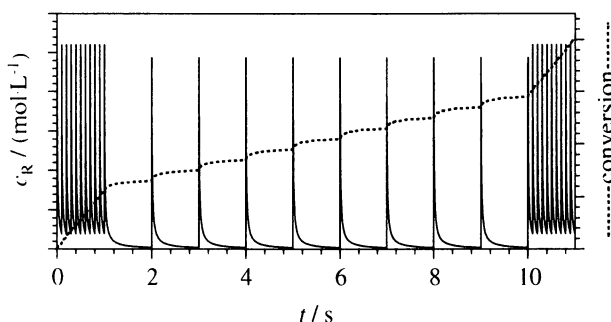


Figure 1: Pulsed laser methods used to evaluate rate coefficients for free-radical polymerization.

The application of the PLP-SEC technique is restricted to studies at low monomer conversions up to a few per cent. Information about kinetics during the course of a polymerization is available from the single pulse (SP)-PLP experiment (Figure 1b) which may be performed at any time during polymerization (3). The monomer conversion induced by the laser pulse, which usually has a width of about 20 ns, is

recorded by online vibrational spectroscopic analysis with time resolution in the micro- and millisecond range. From the measured conversion-time trace the ratio of rate coefficients, k_t/k_p , becomes available for the rather narrow conversion interval of the experiment, extending typically over no more than 0.1 to 0.5 per cent. With k_p from PLP-SEC analysis, the SP-PLP experiment thus provides direct access to a chain-length averaged termination rate coefficient, $\langle k_t \rangle$, for a well-defined narrow conversion region. The SP-PLP and PS-PLP experiments are carried out such that the entire sample is irradiated and that significant gradients in free-radical concentration are avoided (3-5).

The SP-PLP experiment may be performed at several stages during a polymerization in order to map out the conversion dependence of $\langle k_t \rangle$ over a wide range. An important point to note is that the SP-PLP experiment in addition to providing $\langle k_t \rangle$ (for each of the narrow conversion intervals where an experiment has been carried out) may also be used to investigate chain-length dependent $k_t(i,i)$ for a given conversion (interval). This is easily understood from the r.h.s. plot in Figure 1b. The measured change in conversion, ΔU , with the time t (after applying the laser pulse) is brought upon by small radicals at low t , by medium-sized free-radicals at intermediate t and by large radicals after extended times t . The size of the free radicals which are created by the laser pulse at $t = 0$ linearly increases with time t unless chain transfer events come into play. As a consequence, the SP-PLP experiment provides a unique access to measuring $k_t(i,i)$ where i characterizes chain-length. The sizes i for each pair of terminating radicals in an SP-PLP experiment are almost identical as both species are generated at the same time. $k_t(i,j)$ characterizing termination of two radicals differing in size is not easily accessible from this type of experiment. If not stated otherwise, the subsequent discussion addresses the chain-length averaged termination rate coefficient, $\langle k_t \rangle$, which will be referred to as k_t .

The SP-PLP experiment, in order to achieve a reasonable signal to noise of the ΔU vs. t trace (Figure 1b), requires a considerable propagation rate of the monomer under investigation. It is for this reason that SP-PLP studies until now have been restricted to high k_p monomers, such as acrylic esters and to ethene at high temperature. For the slowly propagating monomers, e.g. methacrylic esters and styrene, where conversion per pulse is small, the pulse sequence (PS)-PLP procedure has been derived (4,5). The monomer conversion induced by a precisely known number of laser pulses is measured. In order to introduce some kind of time resolution within the experiment, the technique is mostly applied with pulse repetition rate alternating between subsequent pulse packages. In situations where both k_p and k_t remain constant over extended initial ranges of monomer conversion, as found for the methacrylates and for styrene, k_p/k_t is directly obtained from such an alternating PS-PLP experiment as depicted in Figure 1c.

Within the subsequent text, applications of these three basic types of PLP experiments (Figs. 1a-c) will be demonstrated. Section I illustrates the potential of PLP-SEC procedures mainly for k_p analysis, but also for the measurement of chain transfer and of termination at low conversion and thus at low levels of polymer concentration. Section II primarily addresses the investigation of conversion dependent k_t via SP-PLP and PS-PLP techniques.

I. PLP-SEC Experiments

The principle underlying the measurement of k_p via PLP-SEC experiments has already been outlined in the previous section. The method has been extensively used during recent years and detailed discussions of the procedure are given in the literature (6,7) including publications by the IUPAC-Working Party "Modeling of Polymerization Kinetics and Processes" (8,9). The SEC trace shown on the r.h.s. of Figure 1a is a simulated curve which has been obtained by PREDICI simulation (10) for a styrene PLP at 70°C (7). The PREDICI program allows for a simulation of the full distribution of free-radical and polymer chain lengths (10). The structure of SEC traces from real experiments is less pronounced, in most cases only two maxima or one maximum with a shoulder are observed. This is a consequence of imperfections of the experiment, such as polymerization that is not induced by pulsed laser light, chain transfer activity, gradients of free-radical concentration in space and in time and, most importantly, axial broadening during gel permeation chromatography (GPC, SEC).

The propagation rate coefficient k_p is derived from a characteristic degree of polymerization, L_0 , which is directly available from the SEC trace, via eq 1:

$$L_0 = k_p \cdot c_M \cdot v^{-1}, \quad (1)$$

where c_M is the monomer concentration and v the laser pulse repetition rate. There has been quite some debate about whether to identify L_0 with the location of the point of inflection on the low molecular weight side of the maximum (according to the suggestion by Olaj et al. (1,2) or whether to read L_0 from the peak maximum position. This latter procedure has been advocated by Sarnecki and Schweer (11). A detailed study (7), on PLP-SEC curves, simulated (via PREDICI) for a wide range of PLP conditions, revealed that under conditions of c_R^0 , the free-radical concentration generated by a single laser pulse, being not too high, the determination of k_p from the inflection point position constitutes the far more reliable general procedure. In addition, at low and moderately high c_R^0 values, the internal consistency check of observing a second or even third point of inflection at degrees of polymerization around $2 L_0$ and $3 L_0$ may be performed.

Figure 2 shows an example of data from this study (7) of simulated styrene PLP-SEC curves. The pulse laser induced free-radical concentration c_R^0 has been significantly varied. The k_p value introduced into this particular PREDICI simulation is 499 L·mol⁻¹·s⁻¹. As can be seen, analysis (via eq 1) based on point of inflection positions yields this value back within ± 2 per cent. Moreover, the analysis is almost insensitive toward the type of MWD: number distribution, $f(M)$, weight distribution, $w(M)$, or logarithmic weight (or SEC) distribution, $w(\log_{10} M)$, from which the point of inflection is derived. At low levels of c_R^0 , the maximum position (from all these MWDs) significantly fails to reproduce the true k_p value (Figure 2). On the other hand, at fairly high values of c_R^0 , situations may be reached where the peak maximum position provides a better measure for L_0 (Figure 2).

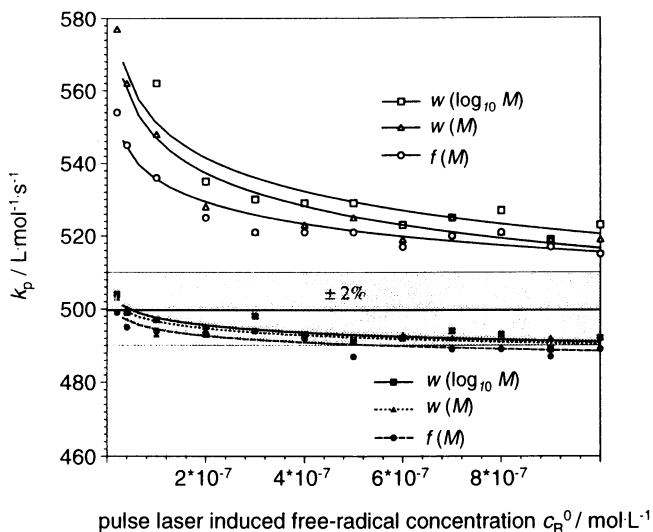


Figure 2: Influence of free-radical concentration c_R^0 on the accuracy of k_p determination by PLP-SEC; data obtained from simulation via PREDICI. (Reproduced with permission from ref. 7. Copyright 1996 from Hüthig & Wepf Publishers, Zug, Switzerland.)

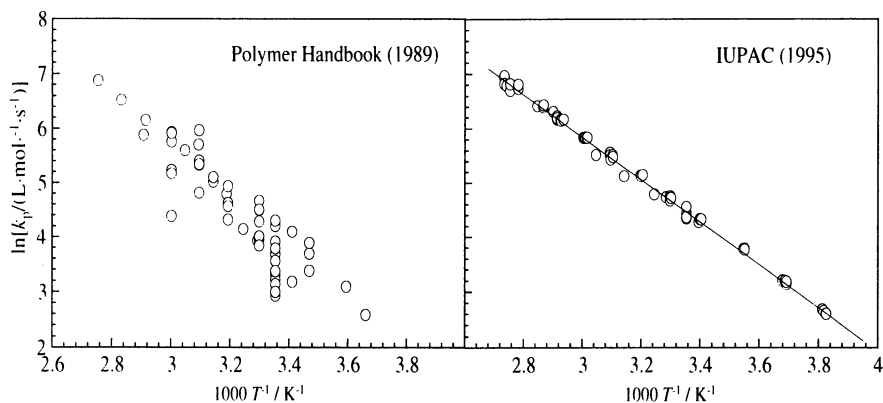


Figure 3: Variation of propagation rate coefficient k_p with temperature for styrene bulk polymerization at ambient pressure. (Partly reproduced from ref. 9 with permission. Copyright 1996 from Hüthig & Wepf Publishers, Zug, Switzerland.)

It is beyond the scope of the present paper to review in any detail the influence of several other experimental parameters, e.g. of gradients in free-radical concentration and of axial broadening in SEC analysis, on the quality of k_p measurement. The interested reader is referred to ref. 7. If the recommendations put forward by the

IUPAC Working Party (9) are considered and the internal consistency checks are performed, the PLP-SEC experiment turns out to be very robust. As the MWD of polymer material produced by PLP depends in a rather complex way on experimental parameters, it is certainly useful to accompany PLP studies by simulation.

Figure 3 demonstrates the enormous impact of PLP-SEC on the reliable estimate of k_p for styrene homopolymerization over a wide temperature range at ambient pressure. The data on the l.h.s. of Figure 3 are the entries from the Polymer Handbook (12). The data on the r.h.s. are the results from independent PLP-SEC experiments performed in eight laboratories.

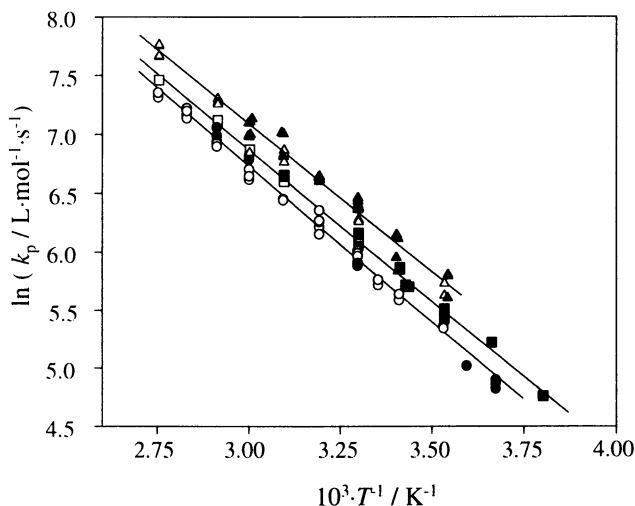


Figure 4: Temperature dependence of the propagation rate coefficient k_p at ambient pressure for methyl methacrylate (circles), butyl methacrylate (squares) and dodecyl methacrylate (triangles); open symbols are data from ref. 13 and full symbols from ref. 14.

Very satisfactory agreement is also obtained for k_p data of the methacrylate family with the experiments, however, coming from a smaller number of groups. Figure 4 shows ambient pressure k_p data reported by Hutchinson et al. (13) and by our group (14) for methyl methacrylate (MMA), butyl methacrylate (BMA), and dodecyl methacrylate (DMA). Due to the high quality of k_p data from PLP-SEC, finer details such as the slight increase of k_p with the size of the ester group are clearly detected from the data. The temperature dependence of k_p for these methacrylates (at ambient pressure) is given by the relations:

$$\text{MMA (15):} \quad \ln\left[k_p / (\text{L} \cdot \text{mol}^{-1} \cdot \text{s}^{-1})\right] = 14.79 - 2686(T / \text{K})^{-1}$$

$$\text{BMA (14):} \quad \ln\left[k_p / (\text{L} \cdot \text{mol}^{-1} \cdot \text{s}^{-1})\right] = 14.79 - 2638(T / \text{K})^{-1}$$

$$\text{DMA (14): } \ln\left[k_p / \left(\text{L} \cdot \text{mol}^{-1} \cdot \text{s}^{-1}\right)\right] = 14.71 - 2536(T / \text{K})^{-1}$$

$$\text{styrene (9): } \ln\left[k_p / \left(\text{L} \cdot \text{mol}^{-1} \cdot \text{s}^{-1}\right)\right] = 17.57 - 3910(T / \text{K})^{-1}$$

The Arrhenius relations for BMA and DMA are constructed from the combined data sets of Hutchinson et al. (13) and Buback et al. (14). In Table I k_p values of MMA, BMA, DMA, and styrene are listed for 30 °C and ambient pressure.

monomer	$k_p / (\text{L} \cdot \text{mol}^{-1} \cdot \text{s}^{-1})$
styrene	106
methyl methacrylate	373
butyl methacrylate	439
dodecyl methacrylate	567

Table I: Propagation rate coefficients k_p at 30 °C and ambient pressure as calculated from the Arrhenius relations given above.

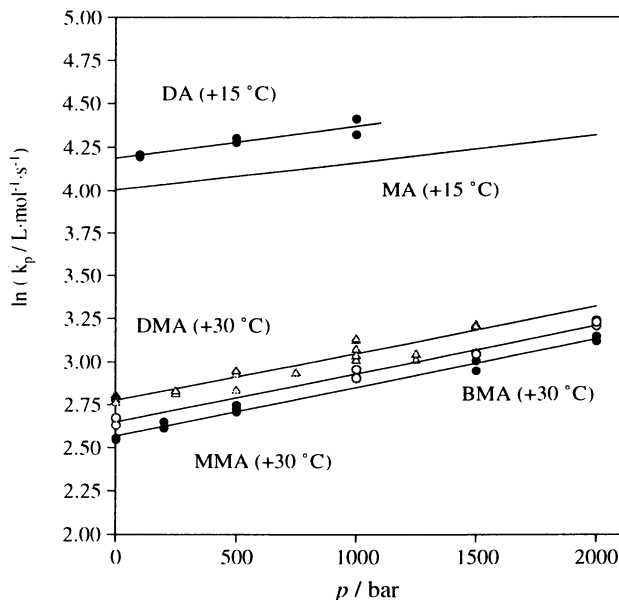


Figure 5: Pressure dependence of the propagation rate coefficient k_p for acrylates studied at 15 °C and for methacrylates at 30 °C. Monomers are as follows: methyl acrylate (MA), dodecyl acrylate (DA), methyl methacrylate (MMA), butyl methacrylate (BMA) and dodecyl methacrylate (DMA); methacrylate data from ref. 14; acrylate data from ref. 16.

In addition, PLP-SEC studies have been performed at high pressures. Such experiments are attractive, because only the PLP part of the experiment needs to be carried out under pressure. As an example of such investigations, the pressure dependence of k_p for MMA, BMA, and DMA is plotted together with data for methyl acrylate (MA) and dodecyl acrylate (DA) (16) in Figure 5.

As with the methacrylates, k_p is seen to increase with ester size for the acrylate family. The propagation rate of acrylates is significantly above k_p of the methacrylates. The clear difference in k_p suggests a “family-type“ behaviour for acrylic acid alkyl esters and methacrylic acid alkyl esters, respectively. Also significant differences are seen between the activation energies, 15 and 17 kJ·mol⁻¹ for the acrylates and 21 to 23 kJ·mol⁻¹ for the methacrylates, and between the activation volumes $\Delta V^\ddagger(k_p) = R \cdot T \cdot (\partial \ln k_p / \partial p)_T$, -10 and -12 cm³·mol⁻¹ for the acrylates and -16 to -17 cm³·mol⁻¹ for the methacrylates.

PLP-SEC investigations of acrylate k_p in extended ranges of temperature and pressure are less easily performed. As a consequence of the high propagation rates, molar masses may be controlled by chain transfer processes whereas k_p measurement via PLP-SEC requires that termination resulting from laser pulses is the major chain-stopping event. The associated problems may be partly circumvented by using high pulse repetition rates.

In situations where propagation is not too fast, by a special choice of the laser pulse pattern, k_p and chain transfer rate coefficients k_{tr} may be derived from a single experiment. Figure 6 illustrates a suitable pulse sequence.

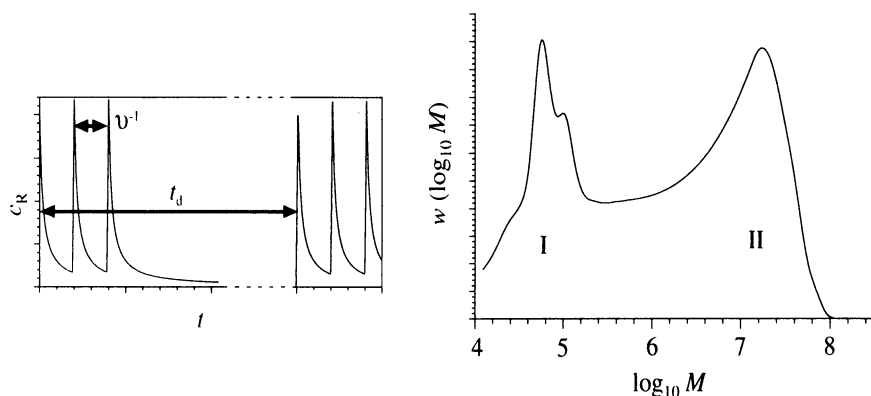


Figure 6: Laser pulse sequence as used for the determination of the propagation rate coefficient k_p and of the transfer rate coefficient k_{tr} from a single PLP-SEC experiment. For further details see text. (Reproduced with permission from ref. 18. Copyright 1996 from Hüthig & Wepf Publishers, Zug, Switzerland.)

Three laser pulses separated by a time interval of $t = v^{-1}$ are followed by an extended dark time t_d . The packages of three pulses are sufficient to create the PLP structure I, shown on the r.h.s. of Figure 6. Chain stopping during the dark time

period. t_d , is dominated by chain transfer and yields the molecular weight contour II. Analysis of the high molecular range of component II, e.g. by plotting the logarithm of the number distribution vs. molecular weight, according to the procedure introduced by Clay and Gilbert (17), yields the transfer rate coefficient. The feasibility of this procedure for simultaneous k_p and transfer rate measurement has been shown by simulations elsewhere (18).

Within the PLP-SEC experiments described so far, data analysis is restricted to measuring the positions of the first point of inflection, L_0 , on the low molecular weight side of the MWD peak maximum and of the higher order inflection points and to calculate k_p from this data via eq 1. Comprehensive kinetic analyses based on an inspection of the entire MWD for PLP samples are rare, although several groups (1,2,19) pointed out that e.g. termination rate coefficients may be accessible from an analysis of the MWD if additional information on overall polymerization rate (or on pulse induced free radical concentration) is available. Olaj and Schnöll-Bitai (2) were the first to illustrate such a procedure. They used the classical expression (20), eq 2,

$$k_t = \frac{k_p^2 \cdot c_M^2 \cdot (3 - \delta)}{L_w \cdot r_0} \quad (2)$$

for the k_t determination from a styrene PLP experiment, after having shown that this relation is valid for arbitrary pseudo-stationary polymerization (1) (in the absence of chain transfer and for k_t being independent of chain-length). δ is the relative contribution of disproportionation to overall termination, L_w is the weight average degree of polymerization, and r_0 is the overall polymerization rate (under pseudo-stationary conditions). The method is reliable and (when calculating L_w from a GPC trace) is almost insensitive toward axial broadening of SEC analysis, as was confirmed by PREDICI simulation (21,22). Difficulties in k_t analysis via eq 2 may, however, result from uncontrolled polymerization (20), from polymerization subsequent to PLP, and from chain transfer processes. These reactions may give rise to high molecular weight material which significantly influences the size of L_w . To partially circumvent such problems, the high molecular weight part of the MWD may be cut off or may be suitably modified. This procedure obviously introduces some arbitrariness into k_t analysis.

Alternative procedures of estimating k_t from PLP-SEC data have been introduced by Lämmel (22). He used the PREDICI program (10), based on an adequate kinetic scheme, to simulate both the entire MWD and the conversion for a PLP experiment. Termination rate coefficient k_t and laser induced free-radical concentration c_R^0 are obtained by fitting the measured MWD and the experimental conversion. This procedure may be rather time consuming. In addition, problems associated with non laser-induced polymerization (that gives rise to high molecular weight polymer) interfere also with this type of analysis. To avoid such difficulties, Lämmel suggested to consider the MWD trace only within the range of characteristic PLP structures. From the simulations, he recommended fitting the ratio of areas, RA , under the number MWD curve, e.g. the area between the second and third point of inflection divided by the area between the first and second point of inflection. Fitting of experimental RA

and conversion data via PREDICI or, with a significant reduction of the number of differential equations, by adopting a lumping scheme (21,22), yields k_t and c_R^0 . It should be noted that the application of this procedure requires δ , the contribution of disproportionation to overall termination, and the extent of GPC axial broadening to be (at least approximately) known. The fitting procedure according to the lumping scheme is easily and effectively performed.

In Figure 7 is illustrated a comparison of low conversion k_t values of styrene at 1000 bar and various temperatures deduced from three independent types of analysis. The full circles indicate data from fitting RA and conversion by the lumping scheme technique (22). The stars are derived from an analysis via eq 2 (23). The open triangles are results from PS-PLP work (23,24) (see Section II). These latter data are considered to be accurate. The rather close agreement of all three sets of k_t values (Figure 7) shows that the procedures via L_w (eq 2) and via RA are also capable of producing reasonable estimates of termination rate coefficients.

Further study is needed to see if these methods of deriving k_t from PLP-SEC traces are generally applicable. In situations where conversion data are not available, the RA method may also be used to derive, from a given value of k_t at ambient pressure and temperature, the variation of k_t with p and T (22). Irrespective of these promising aspects, it needs to be realized that the k_t determinations from PLP-SEC are restricted to situations of low monomer conversion. While k_p stays constant over extended conversion ranges, k_t is diffusion controlled and has to be measured as a function of monomer conversion. The PLP methods which enable this kind of analysis are illustrated in the subsequent section.

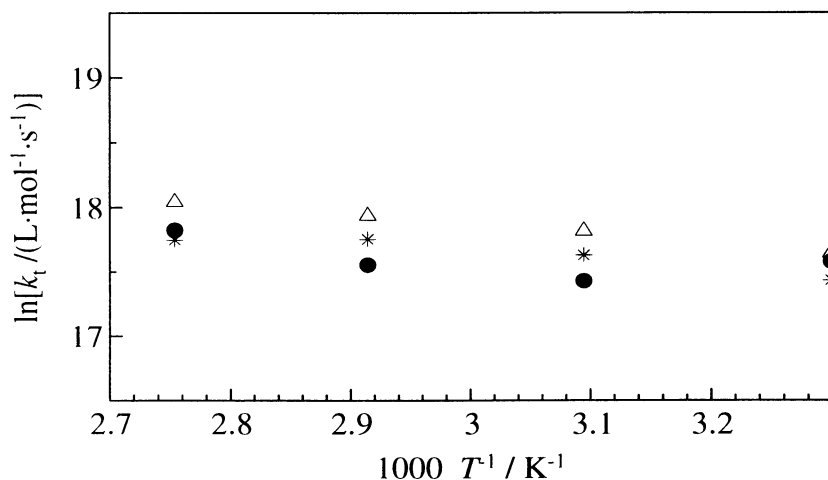


Figure 7: Temperature dependence of the termination rate coefficient k_t for styrene polymerization at 1000 bar as deduced from PLP experiments. Rate coefficients were determined by three alternative procedures: PS-PLP (Δ), PLP-SEC according to eq 2 ($*$), and fitting RA and conversion for PLP-SEC samples by the lumping scheme technique (\bullet). For further details see text.

II. Single-Pulse and Pulse-Sequence Experiments with Online Spectroscopic Analysis of Monomer Conversion

The basic features of SP-PLP and PS-PLP experiments have already been described in the introduction. The application of an excimer laser pulse to a polymerizable system leads to the almost instantaneous production of an initial concentration c_R^0 of photoinitiator-derived free radicals:

$$c_R^0 = 2 \cdot \Phi \cdot c_{\text{abs}} = \frac{2 \cdot \Phi \cdot E_{\text{puls}} (1 - 10^{-A(\lambda)})}{V \cdot E_\lambda} \quad (3)$$

c_{abs} is the amount of laser photons (in $\text{mol} \cdot \text{L}^{-1}$) absorbed by the photoinitiator, Φ denotes the fraction of these photons that yields polymerization-starting free-radicals. c_{abs} may be estimated from the measured laser pulse energy, E_{puls} , incident upon the reaction volume V for known photoinitiator absorbance $A(\lambda)$ at the laser wavelength λ . E_λ is the energy of one mole of photons.

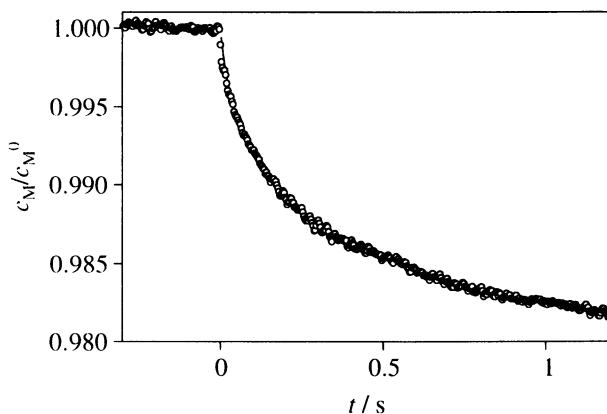


Figure 8: Variation of relative monomer concentration with time for a SP-PLP experiment of dodecyl acrylate performed at 40°C, 500 bar and a polyDA content of 40 per cent; c_M^0 : monomer concentration before the pulse arrives at $t = 0$.

Within the SP-PLP experiment, the monomer conversion induced by a single laser pulse and thus resulting from an instantaneously created c_R^0 is directly measured via infrared or near-infrared spectroscopy on the C-H stretching modes at olefinic or at saturated carbon atoms (3,25). The experimental set-up basically consists of an IR-NIR light source, a monochromator, and a rapid (MHz) detection unit, e.g. a liquid nitrogen cooled InAs detector. The time interval between successive data points may be adjusted to the time required for one propagation step. Thus the growth of a Poisson ensemble of free radicals created by the laser pulse at time $t = 0$ may be

directly monitored. Figure 8 shows the concentration - time SP-PLP profile measured for a dodecyl acrylate (DA) polymerization at 40 °C and 500 bar. The polyDA content of the sample prior to applying the laser pulse at $t = 0$ was 40 per cent. The monomer conversion induced by a single pulse is fairly large in the DA system. As a consequence, the noise on the SP-PLP signal is relatively low. Fitting of the experimental trace to eq 4 yields the coupled parameters k_p/k_t and $k_t \cdot c_R^0$:

$$\frac{c_M(t)}{c_M^0} = \left(2 \cdot k_t \cdot c_R^0 \cdot t + 1\right)^{\frac{-k_p}{2 \cdot k_t}} \quad (4)$$

where c_M^0 is the monomer concentration at $t = 0$. It should be noted that k_t in eq 4 and throughout this paper refers to the IUPAC preferred defining equation of termination rate: $dc_R/dt = -2 \cdot k_t \cdot c_R^2$. The k_t value in eq 4 holds for the termination rate coefficient being independent of chain length. Fitting procedures that take chain-length dependent $k_t(i,i)$ into account have also been used (26,27).

The intense single pulse signal in Figure 8 is essentially due to the appreciable propagation rate of DA ($k_p = 34000 \text{ L} \cdot \text{mol}^{-1} \cdot \text{s}^{-1}$ in this particular case (16)). For methacrylates at similar p and T , k_p is by about two orders of magnitude smaller (see Figure 5). This leads to an enormous decrease in signal to noise and makes quantitative SP-PLP analysis rather difficult. Under such conditions, a series of subsequently measured SP-PLP traces may be co-added, e.g. as many individual SP-PLP curves as are required to yield the same extent of monomer conversion as within the (true) single pulse experiment depicted in Figure 8.

The more common strategy for k_p/k_t analysis of slowly propagating monomers consists of the application of laser pulse packages at a constant pulse repetition rate. As has been shown in detail elsewhere (5), the change in monomer concentration per pulse, Δc_M , is given by eq 5:

$$\frac{\Delta c_M}{c_M} = \frac{k_p \cdot \Phi}{2 \cdot k_t \cdot \Phi} \cdot \ln\left(2 \cdot v^{-1} \cdot k_t \cdot c_{R,\max} + 1\right) \quad (5)$$

$c_{R,\max}$, which differs from c_R^0 in eq 4, denotes the maximum free-radical concentration that is reached immediately after the arrival of a laser pulse under pseudostationary conditions. $c_{R,\max}$ is directly available from v , c_{abs} , Φ and k_t (5). Usually between 100 and a few thousand laser pulses are applied per pulse package. The pseudo-stationary situation underlying eq 5 is reached after a very few, mostly after less than 10 pulses. The monomer conversion per pulse, Δc_M , in eq 5 is very small. Nevertheless this quantity may be accurately derived from the change in monomer conversion brought upon by the entire sequence consisting of a precisely known number of laser pulses. c_M in eq 5 refers to the arithmetic mean of the spectroscopically measured monomer conversions before and after applying a pulse sequence.

Even with c_{abs} and v being known, the experimentally accessible quantity $\Delta c_M/c_M$ (eq 5) depends on the three unknown parameters: k_p , k_t and Φ (or c_R^0). Under

conditions where k_p and k_t remain constant over a range of monomer conversion which is sufficiently large to apply (at least two) pulse sequences, with repetition rates ν_{low} and ν_{high} . $k_p \cdot \Phi$ and $k_t \cdot \Phi$ (or k_p/k_t) are available from $\Delta C_M/C_M$ values measured at these two pulse repetition rates (5). Another restriction toward PS-PLP experiments performed in this alternating pulse sequence mode comes from chain-length dependent k_t . Obviously in situations where k_t significantly varies with chain-length, (overall) termination rate will not be the same for pseudostationary polymerization at quite different "dark time" intervals, ν_{low}^{-1} and ν_{high}^{-1} . Thus prior to alternating PS-PLP experiments, pulse sequence measurements at constant laser repetition rate should be carried out. With k_p and Φ being obtained by separate experiments, k_t is found (via eq 5) for a particular dark time situation and thus for a certain range of chain lengths. From several such experiments for a different, but constant value of ν (during the course of a single polymerization) a chain-length dependence of k_t may be detected.

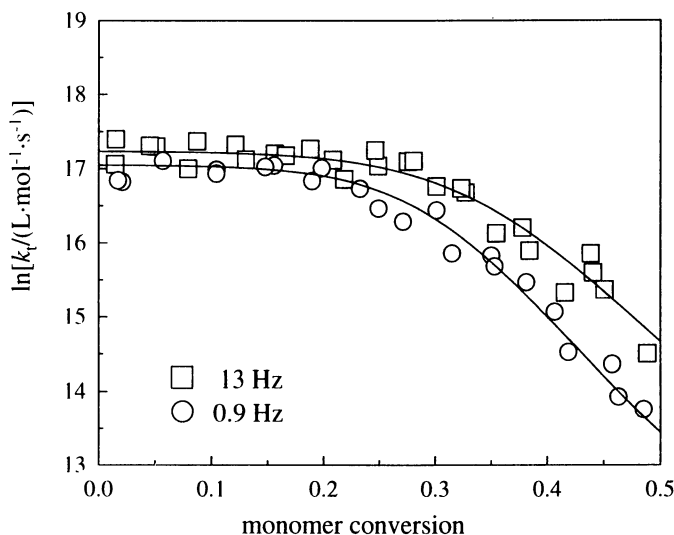


Figure 9: Variation of termination rate coefficient k_t with monomer conversion in laser-induced styrene bulk polymerizations at 50°C, 2000 bar carried out at different laser pulse repetition rates, $\nu = 0.9$ and 13 Hz; ν stays constant within each experiment. The lines are fitted according to eq 6. (Reproduced with permission from ref. 24. Copyright 1996 from Hüthig & Wepf Publishers, Zug, Switzerland.)

Figure 9 shows an example of such an analysis. The termination rate coefficient k_t for the bulk homopolymerization of styrene at 50°C and 2000 bar has been measured by PS-PLP experiments at two pulse repetition rates, 0.9 and 13 Hz (23,24) for monomer conversions up to 50 per cent. Actually, for each of the two repetition rates data from several independent measurements are contained in Figure 9. The k_p and Φ values required for k_p determination via eq 5 are separately measured (23). At conversions below 20 per cent, k_t data from experiments with $\nu = 0.9$ Hz and $\nu = 13$

Hz are rather close to each other which suggests that k_t does not or not significantly depend on chain length in this initial polymerization range. Above 20 per cent monomer conversion, k_t for the higher repetition rate (which corresponds to a lower chain length) is clearly above the k_t values found for $\nu = 0.9$ Hz. This observation is indicative of some chain-length dependence of termination rate coefficient. It must, however, be noted that the larger free-radical size (within the $\nu = 0.9$ Hz experiment) necessarily leads to the production of higher molecular weight polymer. Such material, at an identical degree of monomer conversion, is associated with a larger viscosity of the polymerizing medium. This may also affect the diffusion-controlled termination kinetics. The PS-PLP experiments at different pulse repetition rates (Figure 9) thus indicate an influence of both free-radical size and polymer size on the termination rate in styrene polymerization (50°C / 2000 bar) at monomer conversions between 20 and 50 per cent.

It is important to note from Figure 9, that pulse repetition rate (and thus chain length) may influence termination rate to quite different extents in different ranges of monomer conversion. During bulk polymerization, viscosity may increase by several orders of magnitude. These changes vary from monomer to monomer and they are strongly dependent on polymer molecular weight and architecture. An increase by a factor of 10 with 10 per cent monomer conversion is not untypical and different mechanisms of diffusion-controlled termination become operative with the enormous increase in viscosity during bulk free-radical polymerization to high conversion.

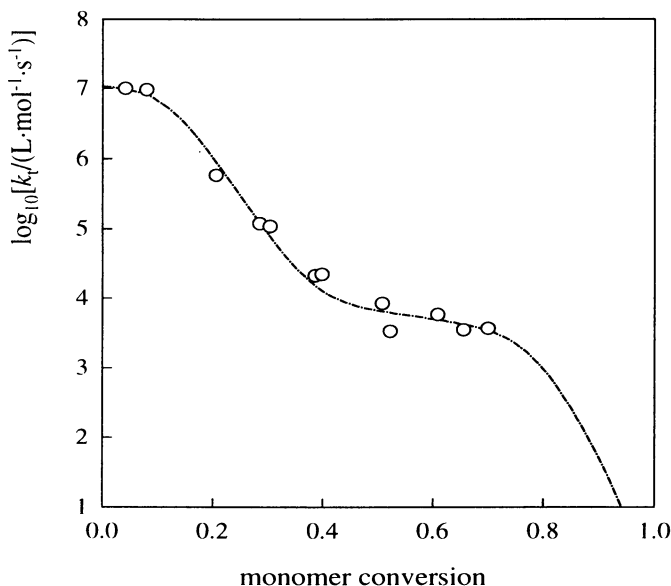


Figure 10: Conversion dependence of the termination rate coefficient k_t for polymerizations of methyl methacrylate at ambient pressure. Experimental data are from ref. 29. The line is fitted according to eq 6. (Reproduced with permission from ref. 31. Copyright 1996 from Hüthig & Wepf Publishers, Zug, Switzerland.)

The conversion dependence of k_t has been intensively studied for methyl methacrylate (MMA) by several groups (28-30). There is general agreement that the variation of k_t with conversion U is of the type illustrated in Figure 10. A plateau region of k_t at low conversion is followed by a steep decrease in k_t . Above 40 per cent monomer conversion, k_t is only slightly lowered upon further polymerization until, at around 75 per cent conversion, k_t strongly decreases again. The transitions from plateau-type behaviour to significant changes of k_t with conversion, and back again, indicate transitions in the type of diffusion control. The initial plateau range is assigned to segmental diffusion, followed by translational diffusion. The subsequent weak decrease of k_t is explained by reaction diffusion control with termination occurring via propagation. At the highest conversions even propagation may become diffusion-controlled and, as a consequence, also reaction-diffusion controlled k_t is significantly lowered with conversion. These variations of k_t with U are described and discussed in more detail elsewhere (31). Depending on the monomer under investigation and on the specific polymerization conditions, different types of $\ln k_t$ vs. U behaviour are measured. The observed conversion dependencies may be reasonably fitted by eq 6 (31):

$$k_t = \frac{1}{k_{SD}^{-1} + \eta_r / k_{TD}^0} + \frac{C_{RD} \cdot (1-U)}{k_{p,0}^{-1} + \eta_r / k_{p,D}^0} \quad (6)$$

k_{SD} , k_{TD}^0 and $k_{p,0}$ denote the rate coefficients of segmental diffusion, translational diffusion at zero conversion, and propagation at low conversion, respectively. $k_{p,D}^0$ refers to diffusion-controlled propagation at zero conversion and η_r is the relative bulk viscosity ($\eta_r = \eta / \eta_0$ with η_0 being the pure monomer viscosity). C_{RD} is an empirical constant which relates reaction-diffusion controlled termination rate, $k_{t,RD}$, to k_p and to the fraction of unreacted monomer, $1-U$, according to eq 7:

$$k_{t,RD} = C_{RD} \cdot k_p (1-U) \quad (7)$$

The second term on the r.h.s. of eq 6 represents the contribution of reaction diffusion, $k_{t,RD}$, to k_t . The only difference between this term and the expression for $k_{t,RD}$ in eq 7 consists in the replacement of k_p by $(k_{p,0}^{-1} + \eta_r / k_{p,D}^0)^{-1}$ which allows to take diffusion control of k_p explicitly into account. The first term on the r.h.s. of eq 6 considers diffusion control (31) of k_t by segmental diffusion and by translational diffusion ($k_{TD} = k_{TD}^0 / \eta_r$). Joining together the individual contributions to yield the simple relation for k_t (eq 6) is described in ref. 31.

The capability of eq 6 to represent experimental k_t vs. U behaviour is demonstrated by the curve plotted in Figure 10 which is a fit by eq 6 of experimental data from ref. 29. Eq 6 has also been used to model the conversion dependence of termination rate coefficient of the other methacrylates (33) and of styrene (23,24). Thus the fits to the data in Figure 9 are also made via eq 6. The monomers mentioned so far, methacrylic acid esters and styrene, seem to be within one class, where an initial plateau value of k_t is followed by a strong decrease of k_t from a certain monomer

conversion onwards. The subsequent weak decrease of k_t with conversion (e.g. above 50% in MMA polymerizations, see Figure 10) is also observed for styrene (Figure 11) and will probably also occur with some of the other methacrylates.

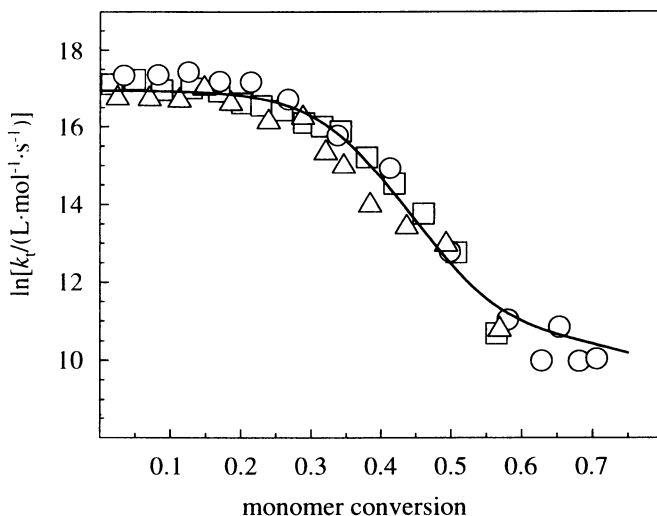


Figure 11: Variation of termination rate coefficient k_t with monomer conversion in laser-induced bulk polymerization of styrene at 50°C and 2800 bar; data from three independent experiments are shown. The line is fitted according to eq 6. (Reproduced with permission from ref. 24. Copyright 1996 from Hüthig & Wepf Publishers, Zug, Switzerland.)

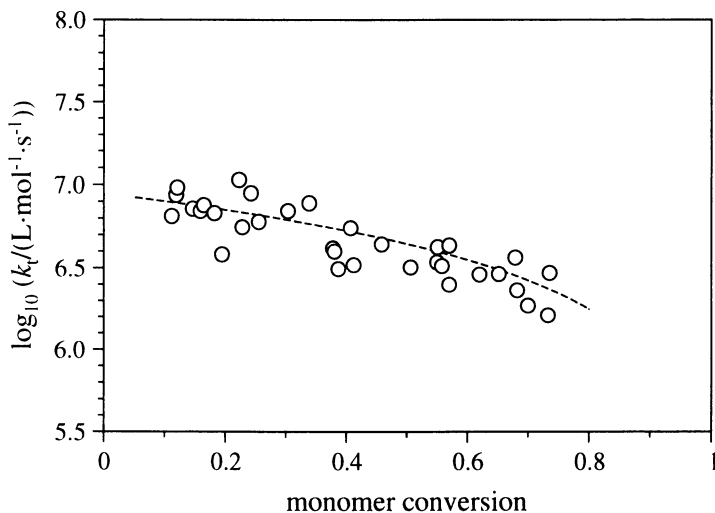


Figure 12: Conversion dependence of the termination rate coefficient k_t for butyl acrylate polymerization at 25°C and 2000 bar. The line is a fit according to eq 6.

With respect to their k_t behaviour acrylic acid esters and ethene seem to belong to another class. The measured k_t vs. U dependencies are, however, also adequately fitted by eq 6. Figure 12 shows k_t of butyl acrylate (BA) during the course of a BA bulk polymerization at 25°C and 2000 bar (34). k_t decreases from the very beginning of the polymerization. The change in k_t even up to 80% conversion is however small compared to what is seen with MMA (Figure 10) or with styrene (Figure 11). Because of the rather high propagation rate of acrylic ester monomers (see Figure 4) termination by reaction diffusion is a very efficient chain-stopping event. In order to see whether reaction diffusion, according to eq. 7, is capable of describing overall termination, it appears rewarding to plot experimental rate data as $\log(k_t/k_p \cdot (1-U))$ vs. conversion. A particular advantage of this type of presentation is that k_t/k_p (or k_p/k_t) is a primary experimental quantity from SP-PLP experiments. Subjecting k_p/k_t data for BA (35) to this treatment yields the plot shown in Figure 13. Over a very extended conversion range, reaction diffusion seems to be operative and a single value of $C_{RD} = k_t/k_p \cdot (1-U)$ is sufficient to fit the measured termination rate coefficient. The surprisingly large conversion range where eq 7 describes termination behaviour is characteristic of a second class of monomers. Common to these so-called type A monomers (35) is a rather high propagation rate coefficient and a lower hindrance to segmental mobility (which is associated with a low glass transition temperature of the resulting polymer). On the other hand, for type B monomers, such as methacrylics and styrene, low values of k_p and an appreciable restriction toward segmental motion are characteristic.

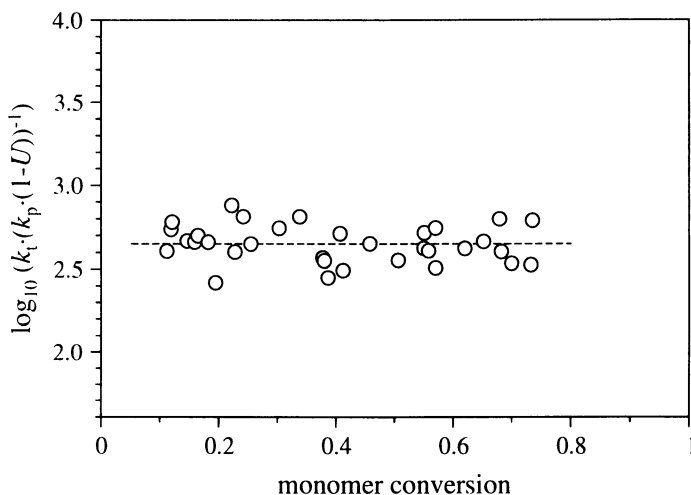


Figure 13: Variation of $k_t/k_p \cdot (1-U)$ with monomer conversion U for butyl acrylate polymerizations at 25°C and 2000 bar. The line is a fit according to eq 7. For details see text.

It goes without saying that eq 6 is capable of representing also k_t vs. conversion behaviour that is intermediate between the situations for MMA (Figure 10) and for BA (Figure 12). It is, however, beyond the scope of this article to comment in any detail

the potential of eq 7 toward modeling or even predicting termination kinetics for arbitrary polymerization conditions. As a matter of fact, the different types of diffusion mechanisms that control termination are associated with quite different dependencies on temperature, pressure, free-radical chain-length, and various other properties of the polymerizing medium. With respect to the important question concerning chain-length dependence several trends became clear from the preceding results and discussion: For type B monomers, k_t is not very sensitive toward chain length in the initial reaction period whereas the size of radicals and of polymer molecules strongly influences k_t in the translation diffusional range. In this regime, where k_t dramatically changes with conversion, the modeling of termination rate is particularly difficult as k_t is dependent on the history of the polymerization (31,32). Polymer size and architecture control the viscosity of the polymerizing medium and thus translational diffusion of k_t . Under conditions where reaction diffusion dominates k_t , no influence of free-radical size on termination rate is expected to occur as propagation rate is independent of chain length.

It is a matter of priority to investigate k_t for the more common monomers over extended ranges of temperature, pressure, and up to high conversion. The initiation mode should be significantly varied, by changing the type and the amount of initiator and by using both chemical and photochemical initiators. The impact of these changes on k_t should provide information about the extent of chain-length dependent termination.

Detailed studies of this type have primarily been performed for the initial range of styrene homopolymerization (23,24). The plateau value of k_t for monomer conversion up to about 20 per cent is found to vary with temperature and pressure in almost exactly the same way as does the inverse of styrene (monomer) viscosity. This observation is consistent with the idea of segmental diffusion controlling k_t in this early polymerization range. It needs to be studied whether alternative models for conversion dependent k_t , which e.g. have been reviewed by Kaminsky and Litvinenko (36), are capable of describing this type of behaviour.

In conclusion: The introduction of pulsed laser techniques into studying rate coefficients has enormously improved the situation with k_p . For an appreciable number of monomers accurate values for k_p are becoming available, partly within fairly extended ranges of temperature and pressure. These k_p values have been and will be critically reviewed and benchmark data will be published by the IUPAC Working Party "Modeling of Polymerization Kinetics and Processes". The beauty of such k_p data is that the propagation rate coefficient stays constant during the course of a polymerization up to fairly high degrees of monomer conversion even in bulk free-radical polymerization. For the termination rate coefficient, on the other hand, extended conversion ranges of a constant k_t are less typical. The sensitivity of free-radical termination toward the physical properties of the polymerizing medium poses problems toward establishing k_t values over wider ranges of p , T , and monomer conversion. Nevertheless, PLP methods turned out to be very important for identifying the major influences on k_t and for measuring accurate termination rate coefficients. Research into diffusion-controlled termination will be a matter of priority in the near future as will be studies into rate coefficients in free-radical copolymerization.

Acknowledgments

The authors are grateful to the *Volkswagen-Stiftung* and the *Fonds der Chemischen Industrie* for financial support of this work. This survey contains results from studies by C. H. Kurz, F.-D. Kuchta, and C. Schmaltz who prepared their dissertations under the auspices of the Graduiertenkolleg „Kinetik und Selektivität chemischer Prozesse in verdichteter fluider Phase“ funded by the *Deutsche Forschungsgemeinschaft*.

References

- (1) Olaj, O.F.; Bitai, I.; Hinkelmann, F. *Makromol. Chem.* **1987**, *188*, 1689
- (2) Olaj, O.F.; Schnöll-Bitai, I. *Eur. Polym. J.* **1989**, *25*, 635
- (3) Buback, M.; Hippler, H.; Schweer, J.; Vögele, H.-P. *Makromol. Chem., Rapid Commun.* **1986**, *7*, 261
- (4) Buback, M.; Huckestein, B.; Leinhos, U. *Makromol. Chem., Rapid Commun.* **1987**, *8*, 473
- (5) Beuermann, S.; Buback, M.; Russell, G.T. *Macromol. Chem. Phys.* **1995**, *196*, 2493
- (6) Hutchinson, R.A.; Aronson, M.T.; Richards, J.R. *Macromolecules* **1993**, *26*, 6410
- (7) Buback, M.; Busch, M.; Lämmel, R.A. *Macromol. Theory Simul.* **1996**, *5*, 845
- (8) Buback, M.; Gilbert, R.G.; Russell, G.T.; Hill, D.J.T.; Moad, G.; O'Driscoll, K.F.; Shen, J.; Winnik M.A. *J. Polym. Sci., Polym. Chem. Ed.* **1992**, *30*, 851
- (9) Buback, M.; Gilbert, R.G.; Hutchinson, R.A.; Klumperman, B.; Kuchta, F.-D.; Manders, B.G.; O'Driscoll, K. F.; Russell, G. T.; Schweer, J. *Macromol. Chem. Phys.* **1995**, *196*, 3267
- (10) Wulkow, M. *Macromol. Theory Simul.* **1996**, *5*, 393
- (11) Sarnecki, J.; Schweer, J. *Macromolecules* **1995**, *28*, 4080
- (12) Brandrup, A.; Immergut, E.H.; Eds., *Polymer Handbook*, 3rd edition, Wiley-Interscience, New York, 1989
- (13) Hutchinson, R.A.; Paquet, Jr., D.A.; McMinn, J.H.; Beuermann, S.; Fuller, R.; Jackson, C.: *5th International Workshop on Polymer Reaction Engineering (DECHEMA Monographs 131)*; VCH Publishers, 1995, 467
- (14) Buback, M.; Geers, U; Kurz, C.H.; Heyne, J. *Macromol. Chem. Phys.* **1997**, in press
- (15) Beuermann, S.; Buback, M.; Davis, T.P.; Gilbert, R.G.; Hutchinson, R.A.; Olaj, O.F.; Russell, G.T.; Schweer, J.; van Herk, A.M. *Macromol. Chem. Phys.* **1997**, *198*, 1545
- (16) Buback, M.; Kurz, C.H.; Schmaltz, C. *Macromol. Chem. Phys.* in preparation
- (17) Clay, P. A.; Gilbert, R. G.; *Macromolecules* **1995**, *28*, 552
- (18) Buback, M.; Laemmel, R.A. *Macromol. Theory Simul.* **1997**, *6*, 145
- (19) Deady, M.; Mau, A.W.H.; Moad, G.; Spurling, T.H. *Makromol. Chem.* **1993**, *194*, 1691
- (20) Henrici-Olivé, G.; Olivé, S. *Fortschr. Hochpolym.-Forsch.* **1961**, *2*, 496
- (21) Buback, M.; Lämmel, R.A. *Macromol. Theory Simul.* submitted

- (22) Lämmel, R. *Ph.D. Thesis*, Göttingen 1996
- (23) Kuchta, F.-D. *Ph.D. Thesis*, Cuvillier Verlag, Göttingen 1995
- (24) Buback, M.; Kuchta, F.-D. *Macromol. Chem. Phys.* **1997**, *198*, 1455
- (25) Buback, M.; Schweer, J. *Makromol. Chem., Rapid Commun.* **1988**, *9*, 699
- (26) Buback, M.; Schweer, J. *Z. Phys. Chem. N. F.* **1989**, *161*, 153
- (27) Kurz, C. H. *Ph.D. Thesis*, Graphikum Verlag, Göttingen, 1995
- (28) Cardenas, J.N.; O'Driscoll, K.F. *J. Polym. Sci., Polym. Chem. Ed.* **1976**, *14*, 883; Cardenas, J.N.; O'Driscoll, K.F. *ibid.* **1976**, *15*, 2097; Stickler, M.; Panke, D.; Hamielec, A.E. *J. Polym. Sci., Polym. Chem. Ed.* **1984**, *22*, 2243
- (29) Sack-Kouloumbri, R.; Meyerhoff, G. *Makromol. Chem.* **1989**, *190*, 1133
- (30) Ballard, M.J.; Napper, D.H.; Gilbert, R.G. *J. Polym. Sci., Polym. Chem. Ed.* **1984**, *22*, 3225
- (31) Buback, M. *Macromol. Chem. Phys.* **1990**, *191*, 1575
- (32) Buback, M.; Garcia-Rubio, L.H.; Gilbert, R.G.; Napper, D.H.; Guillot, J.; Hamielec, A.E.; Hill, D.; O'Driscoll, K.F.; Olaj, O.F.; Shen, J.; Solomon, D.; Moad, G.; Stickler, M.; Tirrell, M.; Winnik, M.A. *J. Polym. Sci., Polym. Lett.* **1988**, *26*, 293
- (33) Bergert, U. *Ph.D. Thesis*, Cuvillier Verlag, Göttingen 1994
- (34) Buback, M.; Degener, B. *Macromol. Chem. Phys.* **1993**, *194*, 2875
- (35) Buback, M.; Huckestein, B.; Russell, G.T. *Macromol. Chem. Phys.* **1994**, *195*, 539
- (36) Litvinenko, G. I.; Kaminsky, V.A. *Prog. Reaction Kinetics* **1994**, *19*, 139

Chapter 7

Termination Rate Coefficients from Molecular Weight Distributions

Paul A. Clay, David I. Christie, and Robert G. Gilbert

Chemistry School, Sydney University, New South Wales 2006, Australia

An extended Mayo method is deduced to obtain rate coefficients and mechanistic information from molecular weight distributions (MWDs), using the high molecular weight part of the full instantaneous number MWD, $P(M)$, together with rate data. $P(M)$ is readily obtained from the GPC MWD. The method can yield the following rate coefficients (a) termination, $\langle k_t \rangle$ (the average of chain-length dependent termination rate coefficients over the chain lengths of the radical population) (b) transfer, and, for emulsion polymerizations, (c) entry; all of these can be obtained over a wide range of conversion. The technique is applied in an extensive series of experiments on styrene seeded emulsion polymerizations (persulfate initiator, stabilized by anionic surfactant), wherein MWDs are obtained at successive conversions, from which instantaneous MWDs are obtained by successive subtraction. Values for $\langle k_t \rangle$ as a function of conversion are in moderate but imperfect accord with those obtained from data on relaxation kinetics; the difference, which is within experimental uncertainty but seems real, may arise from chain-length dependent termination, since the different radical fluxes in the two means of measuring $\langle k_t \rangle$ affect the radical populations over which the average is taken. Either set of $\langle k_t \rangle$ values can be reproduced by *a priori* theory based on diffusion control, with minor adjustment of parameters. Results for entry and transfer rate coefficients had large uncertainty but were consistent with the literature. An excess of low molecular weight species seen at high conversion is ascribed to surface-anchoring effects causing increased termination as entering radicals are confined to a shell.

The Mayo method for obtaining rate coefficients from rate and molecular weight distribution (MWD) in free-radical polymerizations suffers from certain disadvantages: e.g. it is often difficult (*1*) to obtain accurate number-average molecular weights, rendering the required extrapolation difficult. This paper derives and employs an extension of the Mayo method whereby MWD data in free-radical polymerizations can be treated in a way which separates radical creation, transfer and termination rate coefficients. An objective of this paper is to obtain values of the termination rate coefficient over a wide range of conversion, including at relatively high polymer fractions where many traditional methods are difficult to apply. The method is applied to data from seeded emulsion polymerizations, whereby one can have excellent temperature

control and can cover a wide range of conversion. The data for the dependence of the rate coefficients so deduced are then compared with models for these quantities, thus providing tests of theories for radical termination.

Theory for MWDs and for termination rate coefficients.

There is good reason to suppose that termination is diffusion-controlled, with the possible exception of some systems with very low polymer concentrations (say, below 10% (2)). Given diffusion control, it is likely that the termination rate coefficient, k_t , depends on the degrees of polymerization N and N' of the two terminating radicals (3). Any experimental measure of termination must therefore give an *average* $\langle k_t \rangle$, where this average is over the (possibly time-dependent) radical distribution in the particular system. We here give a brief summary of a theory (4-8) for diffusion-controlled $k_t(N, N')$ and MWDs. A novel extension to this approach is then deduced which provides means of treating MWDs so that one can separate the various chain-stopping and starting events. Although the treatment is general, we present it here in the form applicable to emulsion polymerization systems.

Zero-one and Pseudo-Bulk Kinetics. Subdividing emulsion polymerization into two classes provides a convenient means of categorizing kinetics in emulsion polymerizations (9). *Zero-one* kinetics are applicable when intra-particle termination is very rapid compared with other kinetic events (*e.g.* propagation, radical desorption, transfer). When termination is not rate-determining, two radicals cannot coexist in any given particle. Hence any given particle will contain either zero or one free radical (hence the name *zero-one*). As a result of these conditions, it can be seen that the maximum average number of radicals per particle, \bar{n} , will be $1/2$ for a zero-one polymerization. Moreover, in systems where zero-one kinetics apply, entry of a radical into a particle that already contains a radical will lead to mutual annihilation of both radicals. Thus radical entry into a particle, normally considered to a radical gain event, can lead to a subsequent loss of radical activity. The kinetics are highly compartmentalized (*i.e.*, show strongly the effect of the isolation of radicals into separate particles). *Pseudo-bulk* kinetics are applicable when compartmentalization has no effect, *e.g.*, when intra-particle termination is slow compared with other kinetic events. As a result of relatively slow termination, radicals may co-exist within a particle, and therefore \bar{n} may take any value. Pseudo-bulk kinetics always hold for systems where \bar{n} appreciably exceeds $1/2$ (Smith-Ewart Case 3). It also applies in low- \bar{n} systems where there is extensive exit (desorption) *and* the desorbed radicals always undergo re-entry and re-escape until eventually terminated (9).

Model for $k_t(N, N')$ With the possible exception of low conversion (2), it seems that termination in free-radical polymerizations is diffusion-controlled, and therefore the rate coefficient can be estimated from a Smoluchowski model, as follows (5-7):

$$k_t(N, N') = 2\pi p(N, N')(D(N) + D(N'))\sigma N_A \quad (1)$$

where $D(N)$ is the diffusion coefficient of an N -meric radical, σ is the encounter distance at which an N - and an N' -mer are assumed to always react (σ is taken as the van der Waals radius of a monomer unit, although that may not be the case at low conversion (2)). The quantity $p(N, N')$ is the probability of reaction upon encounter between these species; $p(N, N')$ may be less than unity because of spin multiplicity (the radicals must have opposite spin) and hindrance, and one expects $1/4 \leq p \leq 1$. The reason for the lower bound being $1/4$ and not $1/2$ is that two unpaired spins belong to a *triplet* surface, while two paired spins belong to a singlet; the upper bound is 1 to allow for spin flip while the radicals are in proximity, which becomes more likely at high weight-fraction polymer. In the present treatment, it is assumed that $p(N, N')$ is independent of the two degrees of polymerization, and its value may be adjusted

between 0.25 and 1. The diffusion coefficient is broken up into a center-of-mass and reaction-diffusion (D) term, the latter not depending on the degree of polymerization:

$$D(N) = D(N)^{\text{com}} + D^{\text{rd}} = \frac{D_{\text{mon}}(w_p)}{Nu(w_p)} + \frac{1}{6} k_p C_p a^2 \quad (2)$$

Here D_{mon} = diffusion coefficient of a monomeric radical, k_p = propagation rate coefficient, w_p = weight-fraction of polymer, u expresses how the diffusion coefficient scales with degree of polymerization, C_p = concentration of monomer in the polymerization locus (which for an emulsion polymerization is the interior of the particles) and a = root-mean-square end-to-end distance per square root of number of monomer units in a polymer chain. Reaction-diffusion only becomes significant at relatively high conversion (10,11). Simulations (discussed later) show that reaction-diffusion has no effect on calculated MWDs for the range of w_p used in the present systems.

Molecular weight distributions. These are expressed in terms of the *instantaneous number* MWD $P(M)$: the number of chains of molecular weight $M = NM_0$ (where M_0 is the molecular weight of monomer). The instantaneous MWD at time t is in turn the time derivative of the *cumulative* molecular weight distribution $\bar{P}(M, t)$. $\bar{P}(M, t)$ is related to the more familiar GPC trace $G(V)$, where V is elution volume, by (8,12):

$$\bar{P}(M(\mathcal{V})) = M^{-1} G(V) \frac{d\mathcal{V}}{dM} \quad (3)$$

where $\mathcal{V}(M)$ is the GPC calibration curve. If the calibration curve is linear in $\log M$, as is often the case, $\mathcal{V}(M) = a \log M + b$. In this case, one has simply:

$$\bar{P}(M) = G(V) / M^2 \quad (4)$$

where now $G(V)$ is also the "GPC distribution", often denoted $w(\log M)$. The number and weight average molecular weights $\langle M_n \rangle = \int M \bar{P}(M) dM / \int \bar{P}(M) dM$ and $\langle M_w \rangle = \int M^2 \bar{P}(M) dM / \int M \bar{P}(M) dM$ are respectively the first moment, and the ratio of the second to the first moment, of this distribution.

For zero-one systems without chain branching, $P(M)$ is (8,13):

$$P(M) = \exp\left\{-\left(\frac{k_{tr}}{k_p} + \frac{\rho}{k_p C_p}\right) \frac{M}{M_0}\right\} \quad (5)$$

where k_{tr} is the rate coefficient for transfer to monomer (for simplicity, we assume absence of chain-transfer agent, although its inclusion is straightforward) and ρ the total rate coefficient for entry of radicals into particles (which, by the definition of a zero-one system, results in chain stoppage through instantaneous termination).

For a pseudo-bulk system, the MWD is more complex (8). One starts by writing down the evolution equations for the concentration $R(N)$ of radicals of degree of polymerization N , taking into account all chain-length dependences (5). The corresponding equations for the kinetics of chain stoppage (including both $k_t(N, N')$ and transfer) then yield $P(M)$. While numerical solution of these equations poses no difficulties (at least for unbranched chains!), what is important is that *analytic* approximate solutions can be obtained for certain regions, provided that termination is diffusion-controlled. Diffusion-controlled termination in rubbery systems is predominantly between a long, entangled polymeric radical and a small, highly mobile radical (*short-long* termination) (5-7). Since the diffusion coefficients of small species are much larger than those of the large species, termination in rubbery systems is dominated by contributions to the diffusion coefficient from the small species. Moreover, short-long termination implies that, for longer chains, the molecular weight of the resulting *dead* chain is essentially that of the *long radical*. These results are indepen-

dent of the mode of termination (combination or disproportionation). One then obtains, for longer chains, the following analytic approximation:

$$\lim_{M \rightarrow \infty} P(M) = \exp \left\{ - \frac{k_{tr} C_P + (\langle k_t \rangle \bar{n} / N_A V_s) M}{k_p C_P} \frac{M}{M_0} \right\} \quad (6)$$

where N_A is Avogadro's constant, V_s is the swollen volume of a latex particle, and $\langle k_t \rangle$ is the *average* termination rate coefficient:

$$\langle k_t \rangle = \frac{\int_0^\infty \int_0^\infty k_t(N, N') R(N) R(N') dN dN'}{\left(\int_0^\infty R(N) dN \right)^2} \quad (7)$$

Equations 5 and 6 imply that the instantaneous number MWD, when plotted as $\ln P(M)$ against M , should be linear at higher molecular weights. Exact simulations of the MWDs support the accuracy of the approximations which lead to this result (8), assuming the correctness of the underlying models.

Means of obtaining rate coefficients from MWD data. We now derive a new method for using the high-molecular-weight part of the MWD to obtain kinetic information. We define (2) the slope of the linear region of a $\ln P(M)$ curve as Λ :

$$\lim_{M \rightarrow \infty} \left(\frac{\ln P(M)}{M} \right) = - \frac{\Lambda}{M_0} \quad (8)$$

Consider now an emulsion polymerization in Interval 3, i.e., in the absence of monomer droplets. Samples of MWDs taken at successive conversions (and hence different w_p) will therefore correspond to different monomer concentrations C_P and different polymerization rates R_p . Equation 5 then implies:

$$\text{zero-one system: } \Lambda = \frac{k_{tr}}{k_p} + \frac{\rho}{k_p C_P} \quad (9)$$

i.e., for a zero-one system, a plot of Λ against C_P^{-1} should have slope ρ/k_p and intercept k_{tr}/k_p , assuming that all these quantities are independent of conversion. This conversion independence will indeed be the case for k_{tr}/k_p , even in the glassy regime (14). Consider now the conversion independence of the entry rate coefficient. While the most accepted mechanism for entry (involving competing propagation and termination in the aqueous phase until a critical degree of polymerization for entry, z , is reached (15)) suggests that ρ might depend on conversion in Interval 3 (since the concentration of monomer in the aqueous phase is changing), simulations (16) suggest that the dependence will usually be weak until relatively high conversion.

A similar relationship for Λ can be obtained for a pseudo-bulk system as follows. The polymerization rate per particle, R_p , is

$$R_p = k_p C_P \bar{n} \quad (10)$$

One has also, for pseudo-bulk kinetics:

$$\frac{d\bar{n}}{dt} = \rho - \frac{2\langle k_t \rangle}{N_A V_s} \bar{n}^2 \quad (11)$$

Equations 6, 10 and 11 in the steady-state ($d\bar{n}/dt = 0$) then yield:

$$\lim_{M \rightarrow \infty} \ln P(M) = - \left(\frac{k_{tr}}{k_p} + \frac{\rho}{2R_p} \right) \frac{M}{M_0} \quad (12)$$

Analogous to the preceding result for a zero-one system, equation 12 then implies:

$$\text{pseudo-bulk system: } \Lambda = \frac{k_{tr}}{k_p} + \frac{\rho}{2R_p} \quad (= \frac{k_{tr}}{k_p} + \frac{\langle k_t \rangle \bar{n}^2}{N_A V_s R_p}) \quad (13)$$

i.e., for a pseudo-bulk system, a plot of Λ against $1/2R_p$ for successive samples in a given run should have slope ρ and intercept k_{tr}/k_p (again assuming that ρ is independent of conversion). Equation 13 is also valid for bulk or solution polymerizations (with R_p and ρ being replaced by the appropriate terms).

These simple slope-intercept relations for the high- M slope of $\ln P(M)$, equations 9 and 13, comprise the data reduction method of the present paper: they enable one (in principle) to obtain the transfer, entry (equivalent to initiator efficiency) and average termination rate coefficients from MWD and rate data obtained at successive conversions in a zero-one or pseudo-bulk system. These expressions are not novel in themselves, and indeed equation 13 and the resulting treatment is essentially the familiar Mayo method, and can be derived from chain statistics (1); however, such a treatment does not take complete account of the dependence of rate coefficients on chain length. What is novel in the present approach is that this is deduced rigorously from the full evolution equations for radical populations, taking into account dependence of all quantities on chain length. This treatment shows that it is by using the *high molecular weight part of the full MWD* that the complexities of this chain length dependence can be avoided and a simple Mayo-type treatment employed. This is especially important as it is often difficult to obtain an accurate value of $\langle M_n \rangle$ for use in the conventional Mayo method, and there can be extensive chain-length-dependent contributions to $\langle M_n \rangle$ at low M .

It has been pointed out (1,17) that a real problem with the application of equation 8 (and hence equations 9 and 13) is identifying the true linear region in an experimental $\ln P(M)$. $P(M)$ must be found by successive subtraction, i.e., one has really a pseudo-instantaneous distribution (18) which is subject to some uncertainty, particularly at very high molecular weights where not much polymer is formed. Uncertainties are apparent in the scatter in the resulting $P(M)$ curves. Moreover, the occurrence of effects such as very small amounts of branching could vitiate high- M data. As has been noted out elsewhere (17) and is also seen here, there may not even be an obvious high- M linear region in a $\ln P(M)$ plot, and under those circumstances there is some arbitrariness in the value of Λ . Where extensive nonlinear regions of $\ln P(M)$ are seen in the present work, we follow the recommendation of others (1,17) and take the value of Λ from the region where there is extensive polymer formed and a good GPC signal, namely around either the maximum in $w(\log M)$ (the "peak molecular weight") or at $\langle M_w \rangle$.

Experimental

In order to obtain suitable data to test the various hypotheses given here, MWD and rate data were obtained for seeded styrene emulsion polymerization, with the pseudo-instantaneous MWD being obtained by successive subtraction of appropriately normalized GPC traces. Styrene was chosen because many aspects of its free-radical polymerization are well understood, including the availability of highly accurate values for k_p (19), and because it is well established that termination is dominated by combination. Reactions were carried out at 50°C using potassium persulfate as initiator, with unswollen seed radii 44 and 130 nm, designed to go from zero-one (44 nm) to pseudo-bulk (130 nm) conditions. Particles were stabilized with sodium

dodecyl sulfate. Samples were taken at different conversions, from which rates were obtained using gravimetry and MWDs using GPC. Especial care was taken with GPC procedures (including duplicate runs) to avoid artifacts and uncertainties due to baseline subtraction, day-to-day variability of the GPC equipment and error inherent in the subtraction of MWDs. Full details of techniques have been given elsewhere (2) in a corresponding study on low-conversion bulk polymerization. Uncertainties in $P(M)$ are greatest for very low and very high values of M , especially the latter where there is little polymer.

Figure 1 shows some GPC distributions for the 130 nm particles. The GPC trace at the lowest polymer fraction shown is dominated by the MWD of the seed, whereas at higher conversion, the second-stage growth progressively dominates. Some of the resulting pseudo-instantaneous distributions are shown as $\ln P(M)$ in Figure 2. Figures 3 and 4 show corresponding results for the 44 nm particles.

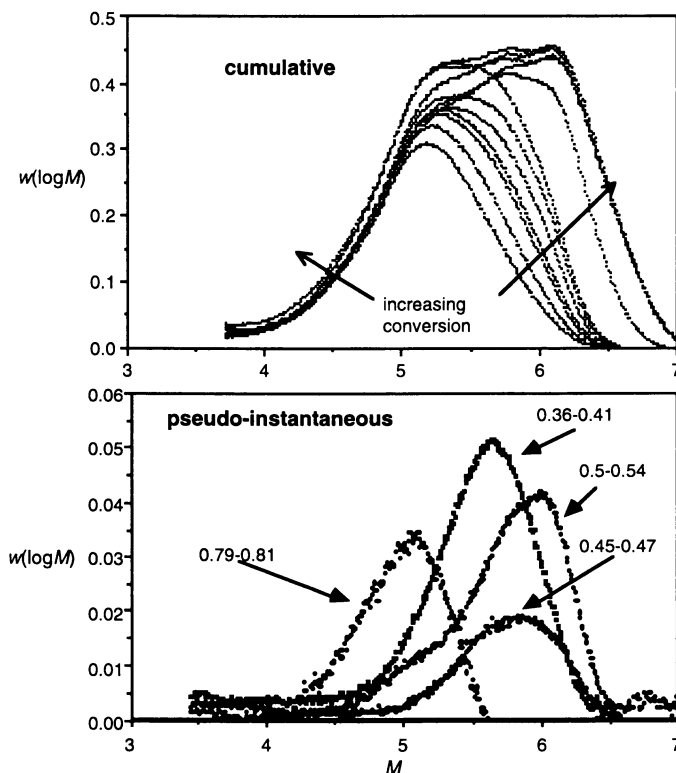


Figure 1. Cumulative and pseudo-instantaneous GPC distributions (with baseline subtracted), $w(\log M)$, for seeded styrene emulsion polymerization at 50°C, 10^{-3} mol dm^{-3} persulfate initiator. Particle concentration = 1×10^{15} dm^{-3} , unswollen particle radius = 130 nm. The maximum value of \bar{n} is about 15. Samples taken at the following w_p : 0.36 (which is the seed without any second-stage polymerization), 0.41, 0.45, 0.47, 0.50, 0.54, 0.61, 0.67, 0.75, 0.79, 0.81, 0.84; the pseudo-instantaneous $w(\log M)$ are for the indicated ranges of w_p .

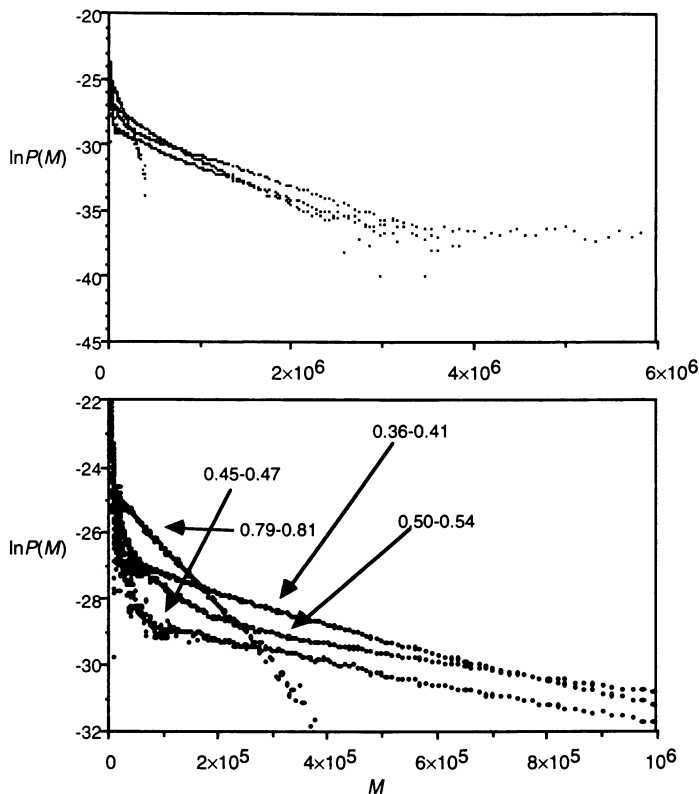


Figure 2. Some data of Figure 1 converted to instantaneous number distributions, for samples taken over the indicated ranges of w_p , showing the entire range of molecular weights, and the range near the peak molecular weight (see lower panel in Figure 1) from which the values of Λ were obtained.

Figure 2 shows that, for the 130 nm particles, the predicted linearity in $\ln P(M)$ at higher M is indeed observed (except occasionally for the highest range of w_p). Does the observed linearity in $\ln P(M)$ imply that termination must be chain-length dependent (since this was used to infer the existence of this linearity)? It is informative to plot the data as appropriate for chain-length *independent* termination by combination. The number MWD for this mechanism has the functional form $P(M) \propto M \exp(-2M / \langle M_n \rangle)$ — see, e.g., (20). Figure 5 shows a plot of $\ln(M^{-1}P(M))$ for the same data as in Figure 2; such a plot would be linear if termination were by combination with a size-independent k_t . It can be seen that linearity also holds for such a plot over about the same range as for a $\ln P$ plot. This is not surprising, since the difference between the two modes of displaying the data, which is $\ln M$, becomes unimportant at higher molecular weights. Hence one can only say that the number MWD data are consistent with either chain-length dependent or independent termination.

Rate data show that \bar{n} for the 44 nm seed systems are all below $1/2$, consistent with the expectation that this is a zero-one system. The $\ln P(M)$ for this system, exemplified in Figure 4, also show moderate linearity over the range of M near and

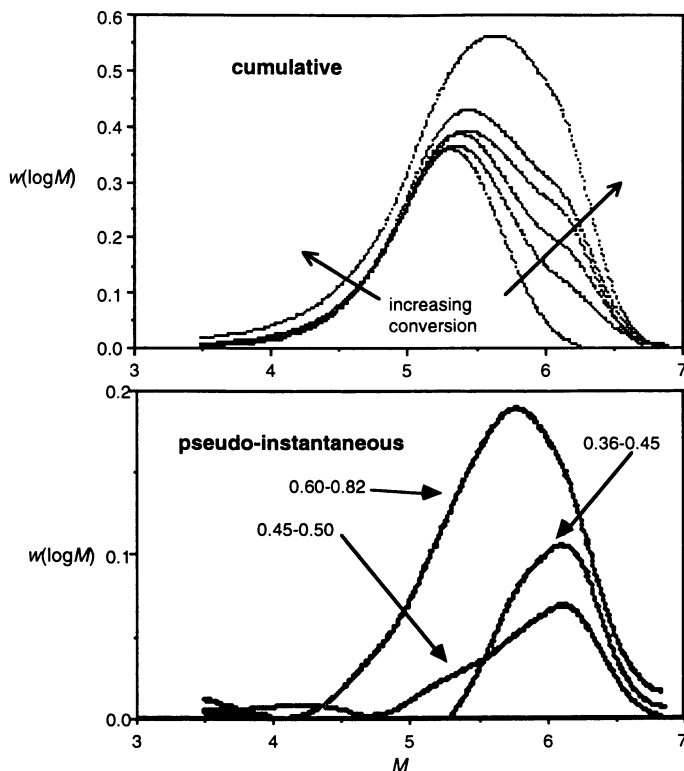


Figure 3. Cumulative and pseudo-instantaneous GPC distributions (with baseline subtracted) for zero-one seeded styrene emulsion polymerization at 50°C, 9.48×10^{-5} mol dm⁻³ persulfate initiator. Particle concentration = 2×10^{16} dm⁻³, unswollen particle radius = 44 nm. Samples taken at the following w_p : 0.36 (the seed without any second-stage polymerization), 0.45, 0.50, 0.55, 0.60, 0.82; the pseudo-instantaneous $w(\log M)$ are for the indicated ranges of w_p .

above the peak in the corresponding instantaneous $w(\log M)$, and an upturn at low molecular weights at higher conversion; this last point is discussed later.

Figure 6 shows the variation of the linear part of the $\ln P(M)$ data with C_p^{-1} or $1/2R_p$, as suggested by equations 9 and 13. Since equation 9 assumes a constant value of ρ , and since this quantity depends on C_w (the monomer concentration in the water phase), points for the zero-one values were confined to a range of w_p where there was only a slight change in C_w : particle-water phase partitioning relationships (15) for this system predict a change of ca. 40% in C_w over the range of C_p shown, which should not lead to a significant change in ρ . The intercepts and slopes of these plots should yield the transfer constant and entry rate coefficients, and the latter for the pseudo-bulk system then yield $\langle k_t \rangle$. The $\langle k_t \rangle$ values so obtained are shown in Figure 7. The entry rate coefficients obtained from these slopes are as follows: for the zero-one system, $(2.1 \pm 1.8) \times 10^{-2}$, $(8.7 \pm 5.6) \times 10^{-2}$ and $(1.9 \pm 1.6) \times 10^{-1}$ s⁻¹ for 0.02, 0.1 and 1 mM persulfate, and for the pseudo-bulk system, 0.15 ± 0.1 , 0.34 ± 0.31 and 0.90 ± 0.14 s⁻¹ for 0.013, 0.1 and 1 mM persulfate. The results for k_{tr} are $(2.6 \pm 2.0) \times 10^{-2}$ (from the zero-one data) and $(1.9 \pm 1.3) \times 10^{-2}$ s⁻¹ (from the pseudo-bulk data).

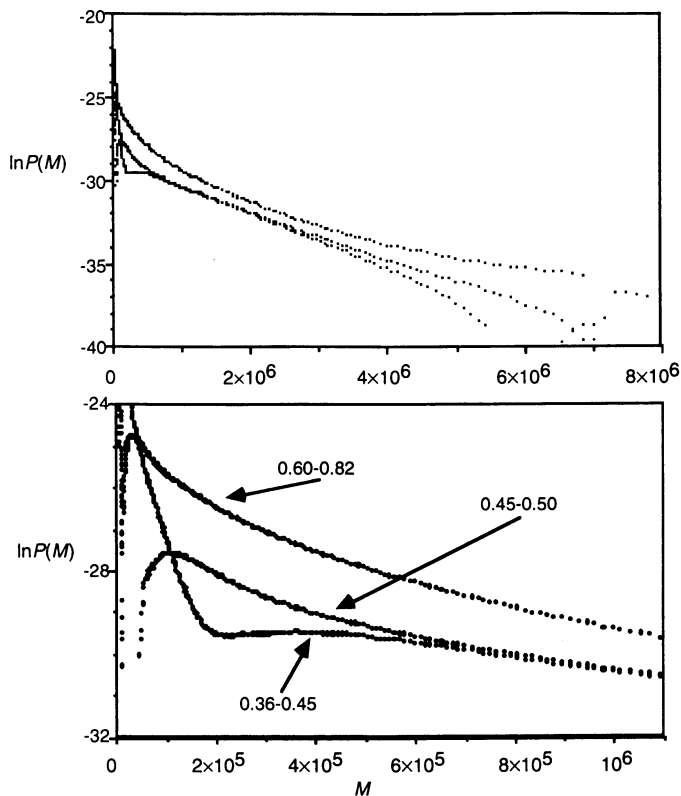


Figure 4. Some pseudo-instantaneous MWDs, $P(M)$, for 44 nm unswollen radius particles, from the data in Figure 3, for the indicated ranges of w_p , showing both the whole range of M and the range near the peak molecular weight (see lower panel in Fig. 3) from which the values of Λ were obtained.

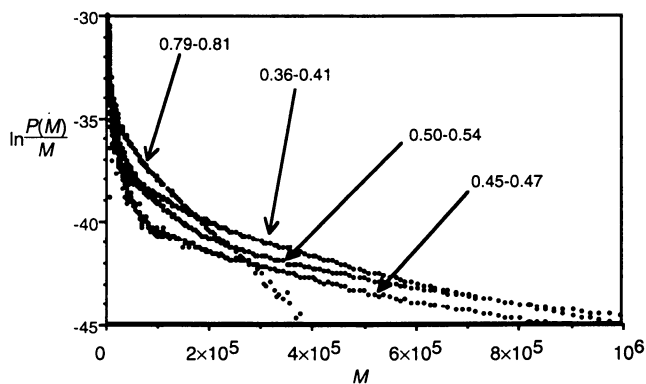


Figure 5. Data of Figure 2 re-plotted as $\ln(P(M)/M)$, which should be linear if all termination were by chain-length-independent combination.

Comparison with $\langle k_t \rangle$ values from relaxation experiments

An alternative method for obtaining $\langle k_t \rangle$ is from time-varying polymerization, particularly relaxation experiments where the source of radicals is switched off. For emulsion polymerization systems, the optimal method for this purpose is γ -radiolysis relaxation (21,22). However, caution must be used when comparing $\langle k_t \rangle$ values so obtained with values from the present technique: *radical fluxes are different in each case*, and (because $\langle k_t \rangle$ is an average over radical distributions $R(N)$, as in equation 7) hence the $\langle k_t \rangle$ values may differ even though the individual $k_t(N, N')$ are the same. However, as suggested by simulations (5,23), this effect is unlikely to be large. The largest variation one might expect in the non-stationary flux of a γ relaxation is the variation in $\langle k_t \rangle$ at the highest and lowest fluxes present during the experiment. The calculations of $\langle k_t \rangle$ for different radical fluxes discussed in a later section and presented in Figure 7 suggest an expected variation between the γ and steady-state MWD $\langle k_t \rangle$ of at worst a factor of 3 for the present system.

Given the time evolution of conversion, and hence \bar{n} , in a γ relaxation experiment, the value of $\langle k_t \rangle$ can be found by fitting to equation 11. This can be done in two ways: either the integrated form, i.e., fitting the observed $\bar{n}(t)$ to the explicit form for $\bar{n}(t)$ found by integrating equation 11, or the differential form, by numerical differentiation of the experimental $\bar{n}(t)$ to yield $d\bar{n}/dt$; the latter involves fitting to noisier data and is therefore subject to higher uncertainty (21). Some $\langle k_t \rangle$ values for styrene have been reported in the literature (21), for large particles (178 nm unswollen radius). For large particles, there is the possibility of invalidation of the assumption of a uniform particle implicit in all the kinetic treatment (through the surface anchoring effect discussed later in this paper), and hence we carried out similar experiments for the present paper but with particles of unswollen radius 130 nm. These new, and the earlier, γ -relaxation results for $\langle k_t \rangle$ are shown in Figure 7. The new data have been fitted by both the integral and differential method to give different values of $\langle k_t \rangle$ (except for lower values of w_p , where the uncertainty in differential $\langle k_t \rangle$ values was too large for the results to be meaningful).

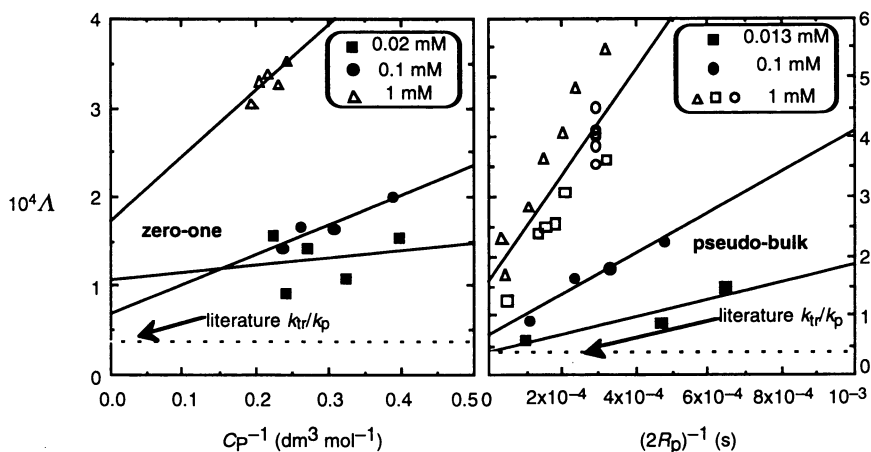


Figure 6. Dependence of high- M slope of $\ln P$ on C_p^{-1} (zero-one system) and $(2R_p)^{-1}$ (pseudo-bulk system) for different initiator concentrations for 44 (zero-one) and 130 nm latexes (pseudo-bulk; 1 mM data are triplicate runs); each point represents a sample taken at different conversion. Literature value of k_t/k_p (24) is also shown. Lines are least-squares fitted to appropriate data.

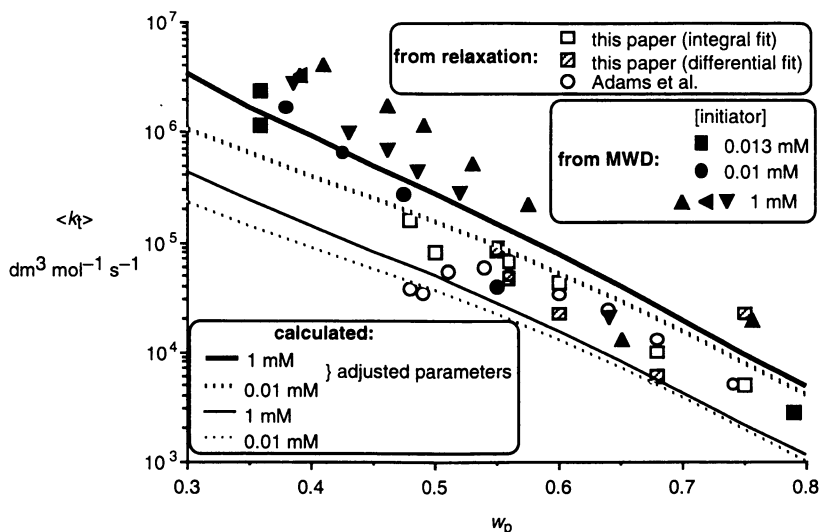


Figure 7. Points: $\langle k_t \rangle$ values as a function of w_p from the MWD data of Figure 6, for different initiator concentrations (those for 1 mM are from triplicate runs), and from γ relaxation data (both new results from the present work and earlier results of Adams *et al.* (21)). Lines: model predictions for 1 and 0.01 mM initiator, using the parameter values described in the text, both expected (lower pair of lines) and using slightly adjusted values for p and D_{mon} (upper pair of lines).

It can be seen that the values of $\langle k_t \rangle$ inferred from the γ -relaxation data for two different-sized latices are consistent, except at the lowest values of w_p . Moreover, the $\langle k_t \rangle$ values found from the relaxation and MWD data appear consistent within experimental uncertainty, except for the lower w_p values from Adams *et al.* The expected decrease in $\langle k_t \rangle$ with increasing w_p is seen (this decrease is of course ultimately responsible for the gel effect in free-radical polymerizations). However, the values from MWDs appear to be consistently larger than those from relaxation. This may or may not be significant. A similar anomaly between $\langle k_t \rangle$ values from kinetic and MWD measurements has also been reported by Tefera *et al.* (25). This difference, if it is real, may arise from the differences in radical flux between the γ and chemical initiation (MWD) measurements, since as is seen from Figure 7, calculations (to be discussed later) show that the high-to-low radical flux from the γ experiment should produce a lower value of $\langle k_t \rangle$.

The $\langle k_t \rangle$ values from the MWD data in Figure 7 seem to show a dependence on radical flux, with those at high initiator concentration being greater than those at lower; although this apparent trend is still within experimental uncertainty, it seems to be real. This is as expected from theory, and indeed the apparent initiator-concentration dependence seen in the data is in quantitative accord with that predicted from modelling (with minor parameter adjustment, as discussed in the next section), as shown by the upper pair of lines in Figure 7.

Comparing theory and experiment.

Model calculations of values of $\langle k_t \rangle$ were performed (a) to see what variation might be expected with radical flux, and (b) to compare with those inferred from experiment. The calculations used the following parameters. The value of the entry

rate coefficient ρ was calculated using the model put forward by Maxwell *et al.* (15,26), whereby a new initiator-fragment radical propagates with monomer in the aqueous phase until it reaches a critical degree of polymerization z , whereupon it enters irreversibly; this aqueous-phase propagation competes with aqueous-phase termination. The parameters used are those cited in (27). As now established to be the case for styrene, it was assumed that exited radicals undergo complete re-entry (26). The value of k_{tr} has been reported in the literature (24) as $9 \times 10^{-3} \text{ dm}^3 \text{ mol}^{-1} \text{ s}^{-1}$; however, this quantity is subject to some uncertainty and is also sensitive to the presence of trace impurities which can act as adventitious chain transfer agents; we here take $k_{tr} = 1.8 \times 10^{-2} \text{ dm}^3 \text{ mol}^{-1} \text{ s}^{-1}$ (see later). The value of p is taken as $1/4$. The value of k_p is taken from the IUPAC recommended Arrhenius parameters (19) as $2.4 \times 10^2 \text{ dm}^3 \text{ mol}^{-1} \text{ s}^{-1}$. Values of k_p for oligomers, which can have a significant effect on rate and MWDs (since short chains dominate termination) are taken as $k_p^1 = 4k_p$ and all other k_p^i being given by the long-chain value.

The diffusion coefficients of oligomeric species were taken to be given by equation 2, with the exponent u being that found from an extensive new study (28) of oligomeric MMA, BMA and styrene (29) species in various polymer matrices over a wide range of w_p and over the temperature range 25 – 40°C:

$$D(N, w_p) = \frac{D_{\text{mon}}}{N^{0.698 + 1.77w_p}} \quad (14)$$

Equation 14 is obtained from data with w_p above c^* and up to 40%; it is here taken as valid over the entire w_p range of interest (although it is essential to note that it cannot be valid when the system becomes glassy, which occurs for $w_p \geq 0.85$ for polystyrene/monomer systems at 50°C). Values of $D_{\text{mon}}(w_p)$ for styrene at 50°C are not available. Instead, literature data for similar penetrants were fitted to a polynomial, as shown in Figure 8, giving:

$$\log_{10}(D_{\text{mon}}/\text{cm}^2 \text{ s}^{-1}) = -4.5018 - 0.42414w_p - 8.5097w_p^2 + 29.624w_p^3 - 46.223w_p^4 + 22.889w_p^5 \quad (15)$$

Calculated values of $\langle k_t \rangle$ are given in Figure 7 for 1 and 0.01 mM persulfate at 50°C, covering the concentration range used in the present MWD experiments, and also the range of radical flux during a γ relaxation experiment.

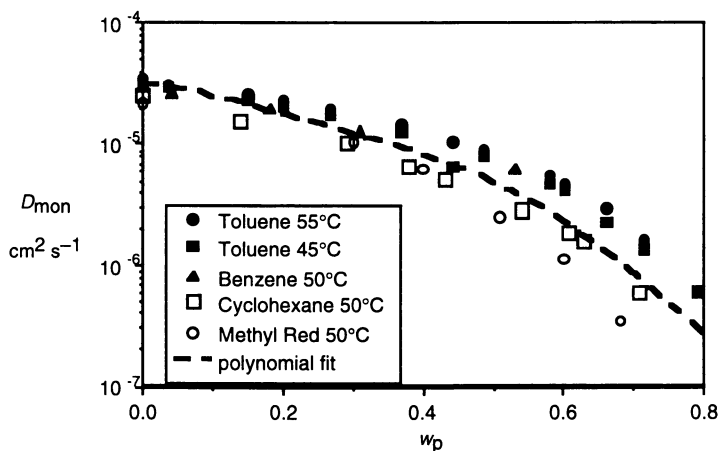


Figure 8. Measured diffusion coefficients of styrene-like penetrants in polystyrene, as shown: toluene at 45 and 55°C (30), benzene, cyclohexane and methyl red at 50°C (31-33). The polynomial fit of equation 15 is also shown.

(a) Using the “expected” values of the various rate parameters as just listed, the agreement between predicted and experimental $\langle k_t \rangle$ is poor. However, acceptable accord can be obtained by taking p (the spin factor) as 0.5 rather than 0.25 (recall the expected range is $1/4 \leq p \leq 1$), and increasing $D_{\text{mon}}(w_p)$ by a factor of 2 (it is apparent from Figure 8 that this is within the uncertainty of the data). Naturally, other parameters could also be varied within experimentally reasonable limits. Being able to obtain acceptable accord with experiment for $\langle k_t \rangle$ with quite acceptable parameter values is consistent with, but does not prove, the basic tenets of the Smoluchowski model used to predict these quantities.

(b) The variation of the calculated values of $\langle k_t \rangle$ with radical flux over the range used here (corresponding to $10^{-5} - 10^{-3}$ mol dm $^{-3}$ persulfate) is significant but within the scatter of the experimental $\langle k_t \rangle$ values.

(c) The “ Λ ” plots, Figure 6, show the linearity predicted by assuming short-long termination. One sees also that the data for duplicate experiments are consistent, and the scatter among these results indicates the experimental uncertainty. The values of ρ from these results are given above, and can be compared with those predicted from the above-cited *a priori* model for this quantity (15), which performs adequately for many anionically stabilized systems such as the present, although *not* for electrosterically stabilized latexes (34). Using parameters obtained by fitting extensive data for ρ for styrene (27) and literature data for other parameters, this model predicts $\rho = 0.2$ and 0.08 s $^{-1}$ for [persulfate] = 1 and 0.1 mM respectively, for the 130 nm latex system, compared with the values inferred from the MWD data of Figure 6 of 0.90 ± 0.14 and 0.34 ± 0.31 s $^{-1}$: a large discrepancy. The reason for this is not apparent. It can be postulated that this might be due to induced initiator decomposition, but such speculation could only be confirmed by further experiment.

(d) The literature value of k_{tr}/k_p (24) is consistent with the value of this quantity inferred from the intercepts of the data in Figure 6, although these intercepts are subject to high uncertainty and hence an acceptable estimate of k_{tr} cannot be obtained from them. Despite the high uncertainty, the apparent values of k_{tr} seem consistently higher than the literature value: the Λ plots give apparent values of $k_{tr} = (2.6 \pm 2.0) \times 10^{-2}$ (from the zero-one data) and $(1.9 \pm 1.3) \times 10^{-2}$ s $^{-1}$ (from the pseudo-bulk data) compared to 0.9×10^{-2} dm 3 mol $^{-1}$ s $^{-1}$ inferred from the literature (24). The reason for this is not apparent, although one can postulate the presence of adventitious transfer agents. Because of this possibility, it was decided to use in simulations a value of k_{tr} that is twice the literature value.

MWD at higher conversions: surface anchoring

Figures 1–4 show that the MWD data at higher conversions all show unexpected behavior: an excess of low molecular weight species. MWD simulations with values of the input parameters that reproduce the experimental $\langle k_t \rangle$ do not predict this effect: all predicted $\ln P(M)$ are linear down to quite low molecular weights (typically, the model predicts a slight maximum at $M \approx 10^4$) and the calculated slope of this linear region *decreases* with increasing w_p . Since the experimental data show instead an *increase* at the very highest w_p (while also showing the expected decrease with increasing w_p for lower conversion), the disagreement is qualitative, not quantitative. Moreover, this excess of low- M species is clearly not an artifact of the way the GPC data are treated to yield the pseudo-instantaneous $P(M)$, since it can also be distinguished (although not as obviously) in the GPC distributions such as shown in Figures 1 and 3. A similar effect has been reported in MMA emulsion polymerization (35). Furthermore, both the MMA work (35) and recent studies on butyl methacrylate

emulsion polymerization at relatively high conversion (16) suggest that this effect may also be associated with a drop in \bar{n} with increasing conversion (which goes against the trend expected from the gel effect).

It has been suggested (9,36,37) that this phenomenon may be due to a spatial inhomogeneity arising from *surface anchoring*. When an oligomeric radical enters a latex particle, it is likely that the initiator-derived sulfate end group is anchored on the surface due to its hydrophilicity. At intermediate conversions, where monomer concentration is relatively high, the radical end can grow rapidly by propagation away from the surface of the particle. Any transfer will increase this spatial randomization, by the rapid diffusion of the short species derived from transfer, prior to its propagation. However, at relatively high conversion, C_p is much lower, and so the radical cannot grow as quickly away from the surface; the transfer rate will also be reduced. This causes a larger radical concentration in the outer portion of the particle compared to that deep within the particle. This would lead to an increased rate of termination by an entering radical in the shell of the particle, causing an overall drop in \bar{n} and an increase in the amount of low molecular weight species. This effect has also been suggested by simulations of the spatial distribution of radicals in particles (38).

Conclusions

The method of simultaneously treating both MWD and rate data encapsulated in equations 9 and 13 is an extension of the traditional Mayo method, by using more information in the MWD than just the average molecular weight. Effectively, the method finds the kinetic chain length required in the Mayo method from the high molecular weight part of the full MWD (or more explicitly, from that part of the MWD near $\langle M_w \rangle$), and is a useful alternative to other procedures (e.g., (39)) which make use of more than just the value of $\langle M_n \rangle$. The new method looks at that part of the distribution where the molecular weight of the dead chain depends only upon that of the parent *long radical*, irrespective of whether the dead chain is formed by a combination, disproportionation or transfer reaction. In addition, the utility of displaying MWD data as the logarithm of the number distribution is apparent from the present method, as it can reveal hitherto unsuspected mechanisms.

In these styrene emulsion polymerization systems, the weight fraction of polymer always exceeds *ca.* 35%. Experimental data, in the form of the observed linearity of plots of the slope of $\ln P(M)$ with $(\text{rate})^{-1}$ at higher molecular weights, support the supposition that termination in this region is chain-length dependent, being dominated by combination between short and long radicals (at least for chains formed at higher molecular weights). The variation of $\langle k_t \rangle$ with polymer fraction (i.e., conversion) clearly shows the decrease with increasing polymer fraction which is ultimately responsible for the gel effect. There seems to be a significant dependence of $\langle k_t \rangle$ on radical flux (although this is still within experimental uncertainty), in accord with predictions from modelling the full chain-length dependence of individual $k_t(N, N')$. The chain-length dependence of $\langle k_t \rangle$ in these systems (well above c^*) contrasts to information gleaned from corresponding studies at low conversion (2), which suggest a large chain-length-independent component. The values of the average termination rate coefficients are consistent with those obtained by γ -radiolysis relaxation studies, although the relaxation values (where radical flux decreases in time) may be slightly but significantly smaller than those from the chemically-initiated MWD data (with steady radical flux). The explanation for this apparent discrepancy, if it is real, may arise from the chain-length dependence of the termination rate coefficient.

The apparent value for the rate coefficient for transfer to monomer obtained from these studies is significantly greater than that reported in the literature. This suggests that an adventitious chain transfer agent may be present in these emulsion polymerization systems.

An important inference from the present studies is that surface anchoring effects at relatively high conversion cause an excess of relatively low molecular weight (*ca.* 10^5) species to be formed in the outer region of the latex particle. This could influence film-forming and water-resistance properties of the latex, especially since these species have sulfate end-groups.

Acknowledgments

The financial support of the Australian Research Council, and of an Australian Post-graduate Research Award for PAC, are gratefully acknowledged, as are constructive discussions with Dr Hans Heuts, Professor Tom Davis and Dr Greg Russell. DIC and RGG especially acknowledge the support of E I DuPont de Nemours.

Literature Cited

- (1) Moad, G.; Moad, C. L. *Macromolecules* **1996**, *29*, 7727.
- (2) Clay, P. A.; Gilbert, R. G.; Russell, G. T. *Macromolecules* **1997**, *30*, 1935.
- (3) Benson, S. W.; North, A. M. *J. Am. Chem. Soc.* **1962**, *84*, 935.
- (4) Rubens, L. C.; Skochdopole, R. E. In *Encyclopedia of Polymer Science and Technology*; H. F. Mark, N. G. Gaylord and N. M. Bikales, Eds.; 1966; Vol. 5.
- (5) Russell, G. T.; Gilbert, R. G.; Napper, D. H. *Macromolecules* **1992**, *25*, 2459.
- (6) Russell, G. T.; Gilbert, R. G.; Napper, D. H. *Macromolecules* **1993**, *26*, 3538.
- (7) Scheren, P. A. G. M.; Russell, G. T.; Sangster, D. F.; Gilbert, R. G.; German, A. L. *Macromolecules* **1995**, *28*, 3637.
- (8) Clay, P. A.; Gilbert, R. G. *Macromolecules* **1995**, *28*, 552.
- (9) Gilbert, R. G. *Emulsion Polymerization: A Mechanistic Approach*; Academic: London, 1995.
- (10) Schulz, G. V. *Z. Phys. Chem. (Frankfurt am Main)* **1956**, *8*, 290.
- (11) Russell, G. T.; Napper, D. H.; Gilbert, R. G. *Macromolecules* **1988**, *21*, 2133.
- (12) Shortt, D. W. *J. Liquid Chromat.* **1993**, *16*, 3371.
- (13) Lichti, G.; Gilbert, R. G.; Napper, D. H. *J. Polym. Sci. A* **1980**, *18*, 1297.
- (14) Casey, B. S.; Mills, M. F.; Sangster, D. F.; Gilbert, R. G.; Napper, D. H. *Macromolecules* **1992**, *25*, 7063.
- (15) Maxwell, I. A.; Morrison, B. R.; Napper, D. H.; Gilbert, R. G. *Macromolecules* **1991**, *24*, 1629.
- (16) Kukulj, D.; Gilbert, R. G. In *Polymeric Dispersions. Principles and Applications*; J. M. Asua, Ed.; Kluwer Academic: Dordrecht, 1997 (NATO Advanced Studies Institute); p 97.
- (17) Suddaby, K. G.; Maloney, D. R.; Haddleton, D. M. *Macromolecules* **1997**, *30*, 702.
- (18) Cunningham, B. F.; Mahabadi, H. K. *Macromolecules* **1996**, *29*, 835.
- (19) Buback, M.; Gilbert, R. G.; Hutchinson, R. A.; Klumperman, B.; Kuchta, F.-D.; Manders, B. G.; O'Driscoll, K. F.; Russell, G. T.; Schweer, J. *Macromol. Chem. Phys.* **1995**, *196*, 3267.
- (20) Elias, H. G. *Macromolecules: Structure and Properties*; Plenum: New York, 1977.
- (21) Adams, M. E.; Russell, G. T.; Casey, B. S.; Gilbert, R. G.; Napper, D. H.; Sangster, D. F. *Macromolecules* **1990**, *23*, 4624.
- (22) Ballard, M. J.; Napper, D. H.; Gilbert, R. G.; Sangster, D. F. *J. Polym. Sci. Polym. Chem. Edn.* **1986**, *24*, 1027.

- (23) Tobita, H. *Macromolecules* **1996**, *29*, 3073.
- (24) Tobolsky, A. V.; Offenbach, J. J. *Polym. Sci.* **1955**, *16*, 311.
- (25) Tefera, N.; Weickert, G.; Bloodworth, R.; Schweer, J. *Macromol. Chem. Phys.* **1994**, *195*, 3067.
- (26) Casey, B. S.; Morrison, B. R.; Gilbert, R. G. *Prog. Polym. Sci.* **1993**, *18*, 1041.
- (27) Gilbert, R. G. In *Emulsion Polymerization and Emulsion Polymers*; P. A. Lovell and M. S. El-Aasser, Eds.; Wiley: London, 1997; p 165.
- (28) Griffiths, M. C.; Gilbert, R. G. in preparation.
- (29) Piton, M. C.; Gilbert, R. G.; Chapman, B. E.; Kuchel, P. W. *Macromolecules* **1993**, *26*, 4472.
- (30) Pickup, S.; Blum, F. D. *Macromolecules* **1989**, *22*, 3961.
- (31) Kosfeld, R.; Goffloo, K. *Kolloid-Z. u. Z. Polym.* **1971**, *247*, 801.
- (32) Goffloo, K.; Kosfeld, R. *Angew. Makromol. Chem.* **1974**, *37*, 105.
- (33) Landry, M. R.; Gu, Q. *Macromolecules* **1988**, *21*, 1158.
- (34) Coen, E.; Lyons, R. A.; Gilbert, R. G. *Macromolecules* **1996**, *29*, 5128.
- (35) Parker, H.-Y.; Westmoreland, D. G.; Chang, H.-R. *Macromolecules* **1996**, *29*, 5119.
- (36) Gilbert, R. G. *Trends in Polym. Sci.* **1995**, *3*, 222.
- (37) Miller, C. M.; Clay, P. A.; Gilbert, R. G.; El-Aasser, M. A. *J. Polym. Sci., Polym. Chem. Edn.* **1997**, *35*, 989.
- (38) Mills, M. F.; Gilbert, R. G.; Napper, D. H.; Croxton, C. A. *Macromolecules* **1993**, *26*, 3563.
- (39) Olaj, O. F.; Schnöll-Bitai, I. *Eur. Polym. J.* **1989**, *25*, 635.

Chapter 8

The Measurement and Meaning of Radical Reactivity Ratios

Johan P. A. Heuts, Michelle L. Coote, Thomas P. Davis¹,
and Lloyd P. M. Johnston

School of Chemical Engineering and Industrial Chemistry, University
of New South Wales, Sydney, New South Wales 2052, Australia

Problems in the current experimental determination of radical reactivity ratios (i.e., 's values') in free-radical copolymerization and the resulting limited physical meaning of these reactivity ratios are highlighted in the present work. It is exemplified that the radical reactivity ratios obtained via fitting of average propagation rate coefficients are very sensitive to small uncertainties in monomer reactivity ratios and homopropagation rate coefficients. Furthermore, the failure to select an appropriate modelling method, and to design experiments so as to satisfy its assumptions, may lead to incorrect parameter estimates. These problems result in large uncertainties in the measured values of the radical reactivity ratios, which in turn lead to large uncertainties in calculated ratios of propagating radical concentrations. This suggests that experimental determinations of the relative radical concentrations may lead to complimentary means for obtaining information on radical reactivity ratios, and possible ways of obtaining this information through catalytic chain transfer experiments are discussed.

¹Corresponding author

1. Introduction

It has been established for more than a decade that, although copolymer composition and sequence distribution are well described by the terminal model, its predictions of average propagation rate coefficients are generally incorrect¹ and several models have been proposed as possible alternatives.² All these alternative models accept the terminal model as a basis and then invoke factors, such as preferential solvation,³ complex formation⁴ or penultimate unit effects^{1,5} in order to account for the deviations of the terminal model predictions. These models all contain more adjustable parameters than the terminal model and hence will provide better fits to the experimental data, as was previously discussed in detail by Maxwell et al.⁶

It has been shown in several studies that it is very likely that penultimate unit effects are operative in free-radical copolymerization^{5,7,8} and therefore we adopt the penultimate model⁹ as promoted by Fukuda and co-workers¹ as a physically realistic model for the description of free-radical copolymerization kinetics. Within the penultimate model, the reactivity of a radical is assumed to be affected by both the terminal and penultimate monomer units, which leads to 8 distinct propagation steps to be considered: 4 different radicals (i.e., $\sim M_1M_1^\bullet$, $\sim M_2M_1^\bullet$, $\sim M_2M_2^\bullet$, and $\sim M_1M_2^\bullet$) react with 2 different monomers (i.e., M_1 and M_2).

In this paper we will use the implicit penultimate model, as proposed by Fukuda and co-workers,¹ in which it assumed that the magnitude of the penultimate unit effect is independent of the monomer (i.e., there is no penultimate unit effect in the monomer reactivity ratios) and hence it affects the average propagation rate coefficient, $\langle k_p \rangle$, but not copolymer composition and sequence distributions. The equations for describing the fraction of monomer 1 in the copolymer, F_1 , and $\langle k_p \rangle$ as a function of the fraction of monomer 1 in the monomer feed, f_1 are as follows.

$$F_1 = \frac{r_1 f_1^2 + f_1 f_2}{r_1 f_1^2 + 2f_1 f_2 + r_2 f_2^2} \quad (1)$$

$$\langle k_p \rangle = \frac{r_1 f_1^2 + 2f_1 f_2 + r_2 f_2^2}{\frac{r_1 f_1}{\bar{k}_{11}} + \frac{r_2 f_2}{\bar{k}_{22}}} \quad (2)$$

$$\bar{k}_{ii} = \frac{k_{iii}(r_i f_i + f_j)}{r_i f_i + \frac{f_j}{s_i}} \quad (i, j = 1 \text{ or } 2, i \neq j) \quad (3)$$

In this model there are six characteristic constants: the homopropagation rate coefficient (k_{111} and k_{222}), the monomer reactivity ratios (r_1 and r_2); and the radical reactivity ratios (s_1 and s_2). These latter four reactivity ratios are defined as follows:

$$r_i = \frac{k_{ii}}{k_{ij}} \quad (i, j = 1 \text{ or } 2, i \neq j) \quad (4)$$

$$s_i = \frac{k_{jii}}{k_{iii}} \quad (i, j = 1 \text{ or } 2, i \neq j) \quad (5)$$

In Eqs 3-5, $k_{(x)yz}$ denotes the rate coefficient for the addition of a monomer z to a propagating radical with terminal unit y and penultimate unit x .

The better performance of the implicit penultimate model as compared with the terminal model lies in the introduction of the two radical reactivity ratios which appear in the expression for $\langle k_p \rangle$. These radical reactivity ratios are commonly determined by fitting the implicit penultimate model to $\langle k_p \rangle$ data, but previous (simplistic) statistical analyses indicate that large uncertainties are associated with the radical reactivity ratios obtained by this procedure.^{2,10} Furthermore, the general absence of radical reactivity ratios with values greater than unity is very remarkable and no convincing chemical reason has been found to explain this observation.⁸ Overall, we may conclude that, although there are enough chemical and physical reasons to assume that penultimate unit effects exist, the physical meaning of the point estimates of radical reactivity ratios measured to date is very limited.

The main aim of this work is to investigate this problem in a statistically more rigorous manner and to investigate how the use of (possibly incorrect) values of the radical reactivity ratios affects the ratio of radical concentrations, $[M_1^*]/[M_2^*]$, which in principle determines most of the kinetics.

2. Problems with the Current Determination of Radical Reactivity Ratios

Values of the radical reactivity ratios (s_1 and s_2) are typically measured by fitting the implicit penultimate model to a set of kinetic data that consists of measured overall propagation rate coefficients $\langle k_p \rangle$ (of a given copolymerization system at a given temperature) as a function of the molar fraction of one of the comonomers in the feed (f_1). The implicit penultimate model predicts values of $\langle k_p \rangle$ as a function of f_1 and a set

of six characteristic constants: the monomer reactivity ratios (r_1 and r_2), the homopropagation rate coefficients (k_{111} and k_{222}) and the two radical reactivity ratios. To obtain estimates of these six parameters, their values are varied so as to maximise the agreement between the measured and predicted $\langle k_p \rangle$ data. However, since fitting a model with six parameters to relatively small data sets generally leads to indeterminate results, a two parameter analysis procedure has been favoured by most workers.^{1,2,6,10,11} In this approach, the monomer reactivity ratios are separately determined from composition or sequence distribution data and the homopropagation rate coefficients are also measured separately. These four coefficients are then fixed at their measured values, and only the two radical reactivity ratios are varied as the implicit penultimate model is fitted to the $\langle k_p \rangle$ data using a statistical modelling procedure, such as non-linear least squares analysis. At the optimum parameter estimates, the difference between the predicted and measured $\langle k_p \rangle$ values (generally measured as the sum of squares of residuals) is used as an indication of the uncertainty in the s values. This is often reported as a two-dimensional 95% joint confidence interval—an elliptically shaped plot of s_2 vs s_1 that encloses a region in which there is a 95% probability of finding the two values.

There are three main problems associated with this method of measuring radical reactivity ratios, and these are as follows:

- (i) Since radical reactivity ratios are measured indirectly (that is, by fitting a model to $\langle k_p \rangle$ data), their accuracy is dependent on the validity of this model (the implicit penultimate model) as a physical description of copolymerization kinetics. Until this validity is independently verified, these model based assumptions will remain as a source of uncertainty in s values that are measured in this way.
- (ii) Implicit in any statistical modelling procedure are assumptions about the error structure in the data. Failure to select an appropriate modelling method, and to design experiments so as to satisfy its assumptions, leads to incorrect parameter estimates. This can be seen in many of the previously published studies of radical reactivity ratios.
- (iii) The technique of fixing four of the parameters and regressing for only two of them is valid only if there is no uncertainty in the fixed parameters. However, the fixed parameters in the implicit penultimate model do contain significant uncertainty of their own. This therefore invalidates the '95% joint confidence intervals' for s_1 and s_2 that are obtained from this modelling procedure. When the uncertainty in the fixed parameters is taken into account, the true uncertainty

in the radical reactivity ratios that are measured in this way is so large as to preclude the attachment of any physical significance to their point estimates. Clearly some direct means of measuring radical reactivity ratios would avoid these problems, and perhaps facilitate accurate and precise estimation of these physically meaningful parameters. We examine possible alternative measurements of radical reactivity ratios in section 3 of this article. For the remainder of this section, we will assume the validity of the implicit penultimate model for common copolymerization systems such as styrene (1) with methyl methacrylate (2) (STY-MMA). We will thus be ignoring problem (i), and instead we will explore problems (ii) and (iii), suggest possible means of dealing with them, and discuss their implications.

Assumptions in the Statistical Analysis. When parameter estimates are obtained by fitting a model to experimental data, a statistical modelling procedure is used. These procedures are typically based on the principle that the optimum set of parameters are those for which the agreement between the measured values and those predicted by the model is maximised. However, the way in which this 'agreement' is quantified may vary from one method to another, according to the different assumptions that may be made about the error structure in the data used. Now, the method used will affect the optimum parameter estimates obtained. Hence the validity of the parameter estimates is contingent upon the validity of the assumptions inherent in the method used. In what follows we will firstly outline a typical modelling method (weighted non-linear least squares analysis) and then briefly explore some of its assumptions and their implications for the accurate and precise measurement of radical reactivity ratios.

Weighted Non-Linear Least Squares. The procedure used in this work is weighted non-linear least squares.¹² In this method, the optimum parameters are those which minimise the weighted sum of squares of residuals (SS), as given by:

$$SS = \sum_{i=1}^n \left(\frac{y_i - y(x_i)}{\sigma_i} \right)^2 \quad (6)$$

In Eq 6, n is the number of data points and σ_i is the standard deviation of the error distribution in each measured value y_i . Provided the measurement error is independently random and normally distributed about the true model, the minimum of SS is equivalent to the maximum likelihood estimation of the parameters. The

approximate $(1-\alpha)100\%$ joint confidence interval for the parameters obtained is defined by the following formula¹²

$$SS(\theta) \leq SS(\theta_0) \left(1 - \frac{p}{n-p} \right) F_{(p, n-p, 1-\alpha)} \quad (7)$$

In this formula θ is a vector of p parameters, θ_0 is the vector of the p parameters that minimise SS , and the F function is defined from statistical tables. Parameter combinations θ that satisfy this formula lie inside the joint confidence interval, and those that do not lie outside. It should be noted that Eq 7 defines only an approximate joint confidence interval for the parameters because it implicitly assumes that the model provides a good fit to the data and hence that the true error variance may be approximated as $SS(\theta_0)/(n-p)$.

Implicit in this modelling method are the following assumptions: (1) the error in the independent variable is negligible compared to that in the dependent variable and (2) the error is independently random and normally distributed about the true model. Furthermore, in order to implement this method a further assumption is often made. Namely, (3) that the error variance of each data point (σ_i) can be approximated by some (known) function of the dependent variable (y_i). The validity of each of these assumptions for the measurement of radical reactivity ratios from k_p data are examined below.

(1) Error in the Independent Variable. In selecting the above modelling method, the error in the independent variables is ignored. Now, in any real experimental data there will always be some error in the independent variable, and so, ideally, methods that take this error into account should be used. Such procedures are known as ‘error-in-variables’ methods (EVM).¹³ However, provided it can be shown that the sizes of the errors in the independent variables are vanishingly small relative to those in the dependent variables, EVMs are not necessary and an ordinary non-linear regression procedure, such as that outlined above, may be used. If an EVM is to be used, it is necessary to estimate both the error structure of the independent and dependent variables, and also their relative sizes. These are then used to weight the contribution of each error to the overall sum of squares of residuals. Failure to weight these errors correctly (through, for example, the use of arbitrary values for the relative sizes) may lead to incorrect parameter estimates. Hence it may be seen that, whether or not an EVM is used to model data, a realistic estimate of the relative sizes of the errors in the

independent and dependent variables is required in order either to (a) demonstrate that the error in the independent variable is negligible compared to that in the dependent variable and therefore show that an EVM is not necessary, or (b) weight the residuals in the EVM correctly. Hence, the correct estimation of this relative error size is important for the determination of accurate radical reactivity ratios from $\langle k_p \rangle$ data.

Unfortunately, measurement of the error in the independent variable is often difficult because, unlike the measurement of the error in the dependent variable, the study of replicate samples does not provide an accurate estimate of the error in the independent variable. For, in measuring the difference between two replicate samples a secondary measurement error is automatically introduced. Hence, in practice, the expected size of the error in the independent variable is not usually measured, but instead is merely estimated on the basis of some prior knowledge of the experimental procedure. As the estimated errors will affect the values of the parameters obtained from the selected modelling procedure, the uncertainty in these estimated errors should be taken into account when estimating the true uncertainty in the parameters obtained from a model fitting procedure.

An EVM has not been selected for the analysis presented in this article. This is because typical low conversion copolymerization data (consisting of $\langle k_p \rangle$ or copolymer composition data, measured as a function of f_1), such as that data analysed in this work, might reasonably be expected to satisfy the assumption that the errors in the independent variables are negligible compared to the errors in the dependent variables. The measurement error in dependent variables such as copolymer composition or $\langle k_p \rangle$ is typically of the order of 5-20%, while, provided the comonomers are carefully weighed, the error in the independent variable, f_1 , is likely to be less than 1%. Naturally, more specific knowledge of how the experiments were performed would be required to fully justify this assumption, and we recommend that, in future, more attention is given to this issue when estimates of radical reactivity ratios are published.

(2) *Independent Normally Distributed Error Variance.* The non-linear least squares method is based upon the assumption that the measurement error in the data is independent and normally distributed about the true model. This assumption may be invalidated by the presence of systematic error in the data (as such error often varies as some function of one of the variables), and by carelessly performed experiments (since data with normally distributed measurement errors will *not* contain 'outliers'). When values of the radical reactivity ratios are measured by fitting the implicit penultimate model to the measured $\langle k_p \rangle$ data, these assumptions are often invalidated. Now,

previous measures of radical reactivity ratios have utilised values of $\langle k_p \rangle$ measured by one of two techniques: rotating sector (RS)—or its flow analogue, spatially intermittent polymerization (SIP)— and pulsed laser polymerization (PLP). Both of these techniques are susceptible to sources of systematic error. In this section we will first discuss some of the sources of systematic error in the previously measured $\langle k_p \rangle$ data, and then we will compare previously measured radical reactivity ratios for the same system (STY-MMA) in order to show that these sources of error may result in widely differing estimates of radical reactivity ratios for the same system.

In the technique of RS (or SIP), values of k_p and the average termination rate coefficient, $\langle k_t \rangle$, are determined by combining separate measurements of $k_p/\langle k_t \rangle$ and $k_p^2/\langle k_t \rangle$, respectively obtained from a series of non-steady and steady state experiments. The validity of this procedure depends on the constancy of k_p and $\langle k_t \rangle$ throughout the set of experiments. Unfortunately, the chain-length dependence of the diffusion-controlled $\langle k_t \rangle$ renders it difficult, if not impossible, to maintain a constant $\langle k_t \rangle$ between the non-steady and steady state experiments. Errors arising from this technique are often systematic, since the quantities affecting $\langle k_t \rangle$ tend to vary systematically across a range of monomer feed ratios. It should also be noted that the technique of RS is no longer recommended by IUPAC for the low conversion measurement of k_p .¹⁴

In the technique of PLP, as introduced by Olaj et al.,¹⁵ k_p is determined from the molecular weight distribution of the polymer produced in a single non-steady state experiment. While this procedure is potentially very accurate, in practice its accuracy is limited by the accuracy of the molecular weight analysis, which is usually performed using size exclusion chromatography (SEC). Two calibration steps are required in order to analyse an unknown polymer for which narrow standards are not available. Firstly, a universal calibration curve—which relates elution volume of a polymer sample to its hydrodynamic volume—is constructed for a given piece of equipment by eluting narrow standards of known hydrodynamic volume. Secondly, some calibration equation is required to convert the measured hydrodynamic volume of the unknown polymer to its molecular weight. This second calibration step can be a major source of systematic error in the analysis of copolymers since information on the solution properties of copolymers as a function of their compositions is rarely available, and thus unverified assumptions are often made. For instance, previous PLP¹⁰ (or 'PLP-like'¹¹) studies of STY-MMA made the assumption that the calibration curves for different compositions of STY-MMA copolymers were a weighted average of those for their respective homopolymers. Such an assumption is yet to be verified and thus

remains as a possible source of systematic error in the radical reactivity ratios measured from this data.

These systematic errors are likely to be a cause of the discrepancy between previously published estimates of the radical reactivity ratios for the most widely studied system, STY-MMA. These previous studies comprise four data sets: [1] a 40°C RS study by Fukuda et al.,¹ [2] a 25°C PLP study by Davis et al.¹⁰ and [3] 25°C and [4] 40°C studies by Olaj et al.¹¹ in which PLP analysis was applied to RS data. To illustrate the difference between the radical reactivity ratios obtained from the different data sets, we reanalysed each of these data sets for s_1 and s_2 using the method of weighted non-linear least squares analysis. For each data set, we used the same monomer reactivity ratios (those published by Fukuda et al.,¹ $r_1=0.523$ and $r_2=0.460$) and the same assumption for weighting the residuals (constant relative error). In this way, differences between the estimates arising from these variables in the analysis were eliminated, enabling the differences in the data sets to be compared more clearly. The four 95% joint confidence intervals for s_1 and s_2 that were obtained from this analysis are illustrated in Figure 1, and in examining this figure large differences between the different estimates are evident. The possible temperature effect on the s values cannot account for the differences between these alternative estimates — as estimates at the same temperature are as different to each other as to those at different temperatures. Hence we may conclude that there is such inaccuracy in the $\langle k_p \rangle$ data obtained in the previous studies of STY-MMA as to render the uncertainty in estimates of the radical reactivity ratios based on these data too large to attach any physical significance to their values.

In a forthcoming publication¹⁶ we will address this problem of uncertainty in the measured $\langle k_p \rangle$ data of STY-MMA by combining the technique of PLP with direct molecular weight analysis. The advantage of these molecular weight sensitive detectors is that the need to invoke a calibration assumption for converting hydrodynamic volume into molecular weight is avoided —thus eliminating this source of systematic error.

(3) *Weighting of Residuals.* In the method of weighted non-linear least squares, the sum of squares of residuals is weighted by the inverse of the variance of the error in each data point, so that samples with a large error variance do not unfairly bias the analysis. This uncertainty should be measured by replicating all samples. Unfortunately this has rarely been done in previous studies: often no replicates are included at all or, at best, only a selection of the samples are replicated. Unless *every*

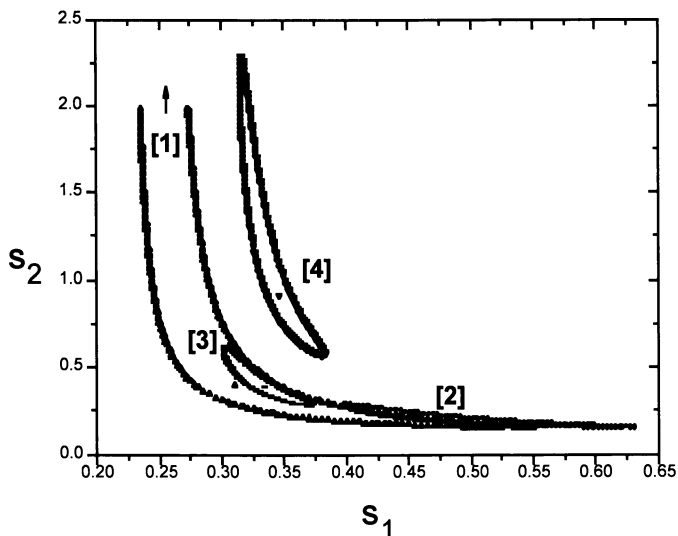


Figure 1. 95% Joint Confidence Intervals for values of s_1 and s_2 for STY-MMA, obtained from the reanalysis of the data of [1] (40°C Fukuda et al.,¹ [2] (25°C Davis et al.¹⁰ and [3] (25°C) and [4] (40°C) Olaj et al.¹¹ All data sets were analysed using the same monomer reactivity ratios¹ ($r_1=0.523$ and $r_2=0.460$), but using homopropagation rate coefficients determined in the respective studies. Constant relative error was assumed for all data sets.

sample is replicated, it is not possible to individually weight each term in the sum of squares of residuals and it is thus necessary to make an assumption about the error structure in the data. Typically it is assumed either that the *absolute* error is constant (in which case all residuals are equally weighted, and $\sigma_i=1$ in Eq 6) or that the *relative* error is constant (in which case the residuals are weighted according to the size of y , and $\sigma_i=y_i$ in Eq 6). Although some prior knowledge of the experimental technique, or the comparison of a selection of replicates, is sometimes used to justify such an assumption, frequently these assumptions are made without any justification at all. In what follows, we will show that the radical reactivity ratios that are obtained from a given set of data depend heavily upon which of these two assumptions is made. Hence we will show that it is necessary to fully justify any assumption made about the error structure in experimental data, as failure to do so will contribute to the uncertainty in measured radical reactivity ratios.

To illustrate the effect of the weighting method on the radical reactivity ratios obtained from a given set of data, we reanalysed the 25°C data of Olaj et al.¹⁰ twice, in order to obtain two different estimates for the ratios. In the analysis we held the values of the fixed parameters and the $\langle k_p \rangle$ data constant, and varied only the weighting method: assuming in case [1] that the absolute error was constant and in case [2] that the relative error was constant. A plot of the 95% joint confidence intervals for these two analyses are given in Figure 2, in which it is evident that the s values obtained from the two analyses are different.

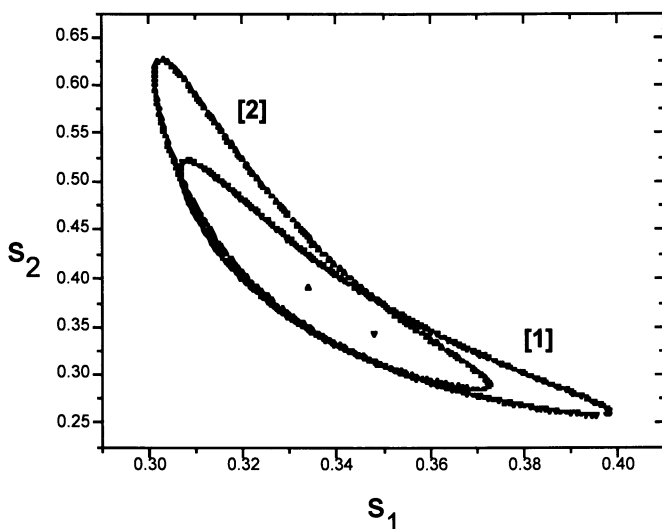


Figure 2. 95% Joint Confidence Intervals for values of s_1 and s_2 for STY-MMA, obtained from reanalysis of the 25°C data of Olaj et al.¹¹ All data sets were analysed using the same reactivity ratios¹ ($r_1=0.523$ and $r_2=0.460$) and the same k_{iii} values ($k_{111}=89.1 \text{ dm}^3\text{mol}^{-1}\text{s}^{-1}$ and $k_{222}=299.2 \text{ dm}^3\text{mol}^{-1}\text{s}^{-1}$). In case [1] constant absolute error was assumed and in case [2] constant relative error was assumed.

It might also be noted here that in the case of this PLP data set, neither assumption is likely to be correct. In a forthcoming publication¹⁶ we will show that the error in PLP-measured k_p values is best approximated as being proportional to the laser repetition rate. This quantity is typically varied throughout a copolymerization study, but not in some regular manner according to the size of f_1 , thus rendering the error variance neither constant nor proportional to the size of $\langle k_p \rangle$. Hence, it is apparent that

a further uncertainty in measured radical reactivity ratios is introduced when it is necessary to make an unverified assumption about the error structure in the data. To eliminate this source of error it is necessary to thoroughly study the error structure of a data set by means of several replicates of every data point measured.

Uncertainty in the Fixed Parameters. One very important source of error in the measured s values is the uncertainty in the fixed parameters (the monomer reactivity ratios and homopropagation rate coefficients) that are used when analysing $\langle k_p \rangle$ data for s values. Strictly speaking, the uncertainty in the s values obtained from fitting the implicit penultimate model to $\langle k_p \rangle$ data would be better represented as a six-dimensional 95% joint confidence interval, obtained from a simultaneous regression for all of the six parameters. However, as was noted above, this is impractical and a two-parameter analysis for the s values is favoured. However, it is still necessary to take into account the uncertainty in the fixed parameters when measuring the true uncertainty in the s values. In what follows, we will illustrate, using sensitivity analysis, the generally overlooked effect of small uncertainties in these fixed parameters on the estimated values of the radical reactivity ratios. A thorough analysis of this kind would involve simultaneous variation of each of the four parameters; however, for the sake of clarity we will demonstrate the effects of the homopropagation rate coefficients and monomer reactivity ratios separately.

(1) *Effect of Homopropagation Rate Coefficients.* Taking the 25°C data of Olaj et al.¹¹ for STY-MMA, we regressed for values of the radical reactivity ratios using the monomer reactivity ratios of Fukuda et al.¹ ($r_1=0.523$ and $r_2=0.460$), making the assumption of constant relative error. The analysis was performed five times: once for each of five possible different combinations of k_{111} and k_{222} values. Ranges of k_{iii} were taken from a publication by Olaj et al.¹⁷ in which values of the 25°C homopropagation rate coefficient of styrene were given in the range 84–95 $\text{dm}^3\text{mol}^{-1}\text{s}^{-1}$, and a single value of 299.2 $\text{dm}^3\text{mol}^{-1}\text{s}^{-1}$ was given for MMA at 25°C. For MMA, a range of $\pm 5\%$ was taken (284–314 $\text{dm}^3\text{mol}^{-1}\text{s}^{-1}$). Combinations of these homopropagation rate coefficients were then selected as follows:

- [1] $k_{111}=89 \text{ dm}^3\text{mol}^{-1}\text{s}^{-1}$ and $k_{222}=299 \text{ dm}^3\text{mol}^{-1}\text{s}^{-1}$ (the average of each value)
- [2] $k_{111}=84 \text{ dm}^3\text{mol}^{-1}\text{s}^{-1}$ and $k_{222}=284 \text{ dm}^3\text{mol}^{-1}\text{s}^{-1}$ (the two lowest values)
- [3] $k_{111}=95 \text{ dm}^3\text{mol}^{-1}\text{s}^{-1}$ and $k_{222}=314 \text{ dm}^3\text{mol}^{-1}\text{s}^{-1}$ (the two highest values)
- [4] $k_{111}=84 \text{ dm}^3\text{mol}^{-1}\text{s}^{-1}$ and $k_{222}=314 \text{ dm}^3\text{mol}^{-1}\text{s}^{-1}$ (the lowest k_{111} and highest k_{222})
- [5] $k_{111}=95 \text{ dm}^3\text{mol}^{-1}\text{s}^{-1}$ and $k_{222}=284 \text{ dm}^3\text{mol}^{-1}\text{s}^{-1}$ (the highest k_{111} and lowest k_{222})

The five 95% joint confidence intervals obtained (corresponding to the five different analyses) are plotted in Figure 3.

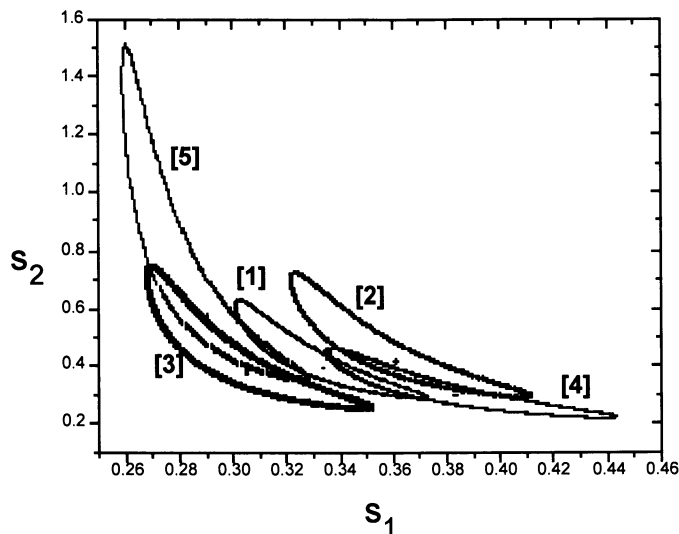


Figure 3. 95% Joint Confidence Intervals for values of s_1 and s_2 for STY-MMA, obtained from reanalysis of the 25°C data of Olaj et al.¹¹ All data sets were analysed using the same monomer reactivity ratios¹ ($r_1=0.523$ and $r_2=0.460$), and constant relative error was assumed for all. Five different combinations of k_{iii} values were used (see text above).

These show clearly that the effect of the homopropagation rate coefficients on the measured values of s_1 and s_2 is quite large. Hence, if the uncertainty in the homopropagation rate coefficients were to be properly taken into account, the observed size of the 95% joint confidence intervals for s_1 and s_2 would be much larger than the size of those usually published.

(2) *Effect of Monomer Reactivity Ratios.* Before examining the effect of the monomer reactivity ratios on measured values of the radical reactivity ratios, an estimate of the uncertainty in the monomer reactivity ratios is required. Estimating the true uncertainty in monomer reactivity ratios is a problem in itself, owing to the widely differing values that can be found in the literature for a given system. However, as a

more detailed analysis of these reactivity ratio data will be included in a forthcoming publication,¹⁸ for the purpose of this article, the composition data of Fukuda et al.¹ will be used to estimate the monomer reactivity ratios of STY-MMA and their uncertainty. Using the same non-linear regression method as used for the estimation of radical reactivity ratios, we fitted the implicit penultimate model to the composition vs f_1 data, assuming that the relative error in this data was constant (since in Fukuda's paper¹ it is stated that the composition data is subject to a relative error of 1.5%). A plot of the 95% joint confidence interval for the monomer reactivity ratios is given in Figure 4.

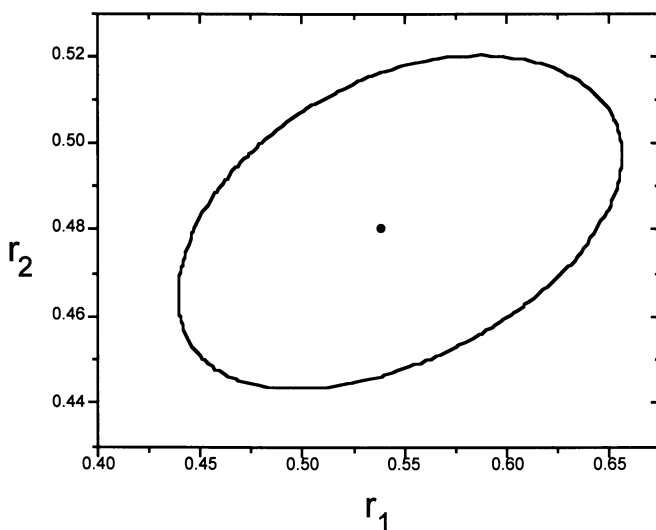


Figure 4. 95% Joint Confidence Intervals for values of r_1 and r_2 for STY-MMA at 40°C, obtained from reanalysis of the composition data of Fukuda et al.¹

In order to illustrate the effect of this uncertainty in the measured r values on measured s values, we again reanalysed the 25°C data of Olaj et al.¹¹ — this time holding the k_{111} and k_{222} values constant at their optimum values, using the same weighting method (assuming constant relative error) but allowing the monomer reactivity ratios to vary. Five pairs of reactivity ratios were chosen for the analysis: the optimum pair ([1]: $r_1=0.523$ and $r_2=0.460$) and four other pairs, each selected from within the 95% joint confidence interval for the data. These latter four pairs were:[2] $r_1=0.45$ and $r_2=0.45$;[3] $r_1=0.46$ and $r_2=0.49$; [4] $r_1=0.60$ and $r_2=0.45$; [5] $r_1=0.65$ and $r_2=0.50$. The 95% joint confidence intervals for the five estimates of the radical

reactivity ratios are plotted in Figure 5, in which it is again evident that the values of the fixed parameters (in this case the monomer reactivity ratios) have a large effect on measured values of s_1 and s_2 . In particular, the s_2 value becomes indeterminate when the full uncertainty in the monomer reactivity ratios is taken into account. Hence, as in the case of the homopropagation rate coefficients, if the uncertainty in the monomer reactivity ratios was properly taken into account, the observed size of the 95% joint confidence intervals for s_1 and s_2 would be much larger than those usually published.

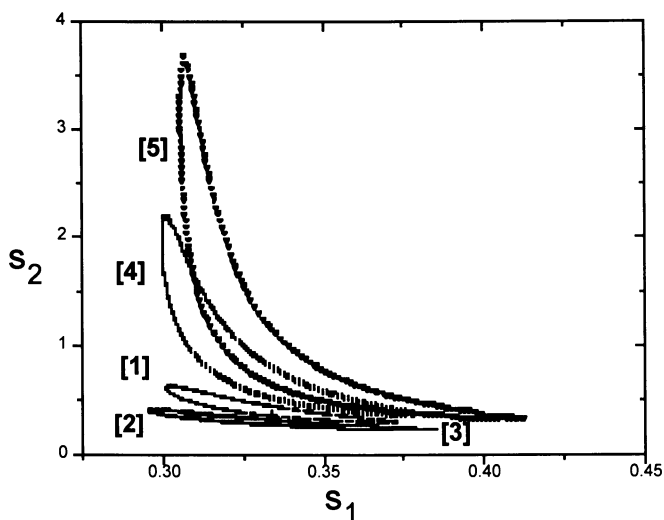


Figure 5. 95% Joint Confidence Intervals for values of s_1 and s_2 for STY-MMA, obtained from reanalysis of the 25°C data of Olaj et al.¹¹ All data sets were analysed using the same k_{iii} values ($k_{111}=89.1 \text{ dm}^3\text{mol}^{-1}\text{s}^{-1}$ and $k_{222}=299.2 \text{ dm}^3\text{mol}^{-1}\text{s}^{-1}$), and constant relative error was assumed for all data sets. Five different combinations of r_i values were used (see text above).

Implications of these Problems. Based on the studies above, it is apparent that the true 95% joint confidence interval for the radical reactivity ratios — as measured by fitting the implicit penultimate model to $\langle k_p \rangle$ data — is much larger than the 95% joint confidence intervals obtained from a two parameter analysis. When the uncertainty in the fixed parameters, in the assumptions inherent in the modelling

method used, and in the measured $\langle k_p \rangle$ data itself is taken into account, it is clear that the true uncertainty in published s values is so large as to preclude attaching any physical significance to their point estimates. To some extent these problems may be addressed by improving the accuracy of both the experimental data and the fixed parameters used in estimating these s values, and by designing experiments so as to satisfy the assumptions inherent in the modelling procedure selected. However, given the extreme sensitivity of s values to small changes in any of these variables, it is unlikely that the two parameter analysis of $\langle k_p \rangle$ data will enable accurate and precise estimation of s values. Furthermore, the possibility of systematic error in s values measured in this way can never be ruled out unless the implicit penultimate model can be independently verified as a true and complete description of copolymerization kinetics. For these reasons, it is necessary to look for complementary means of measuring radical reactivity ratios.

3. Relative Propagating Radical Concentrations

Background. In order to find alternatives for measuring radical reactivity ratios one needs to identify a different parameter that depends on the radical reactivity ratios. A parameter which is relatively sensitive to the values of the radical reactivity ratios, is the ratio of the two propagating radicals, A_{12} , which can be expressed as follows for the terminal and penultimate models:¹⁹

$$A_{12} = \frac{[\sim M_1^*]}{[\sim M_2^*]} = \frac{\bar{k}_{22}\bar{r}_2f_1}{k_{11}\bar{r}_1f_2} \quad (8)$$

This expression is derived from the steady-state assumption in the radical concentrations and directly results from the notion that the formation of $\sim M_1^*$ radicals through cross-propagation of $\sim M_2^*$ radicals equals the formation of $\sim M_2^*$ radicals through cross-propagation of $\sim M_1^*$ radicals.¹⁹ This is shown in Eq 9.

$$k_{12}[\sim M_1^*][M_2] = k_{21}[\sim M_2^*][M_1] \quad (9)$$

It can be seen that the expression for A_{12} contains the average homopropagation rate coefficients \bar{k}_{11} and \bar{k}_{22} which in turn depend on s_1 and s_2 (see Eq 3). Hence, the calculated value for A_{12} may vary for different sets of radical reactivity ratios which fit the average propagation rate coefficient data equally well. A good example of this effect is found in the copolymerization of styrene and methyl acrylate,²⁰ where equally good fits to the experimental $\langle k_p \rangle$ are obtained with the penultimate unit model using $\{s_s = 0.59, s_{MA} = 0.02\}$ and $\{s_s = s_{MA} = 0.41\}$. However, the values for A_{SMA} obtained with the former set of s values are approximately 40 times smaller than those obtained with the latter set (which are similar to those obtained with the terminal model). This observation is important, because it implies that values for the radical reactivity ratios can possibly be obtained from the relative propagating radical concentrations, which has also been suggested previously by Schoonbrood.²⁰ However, direct measurements of A_{12} (in principle obtainable from ESR experiments) have never been performed and will be very difficult.

Chain Transfer in Copolymerization. It is obvious from the example given above that modelling results for any process that involves the ratio of propagating radical concentrations will heavily depend on the values used for the radical reactivity ratios. This is very important in cases where kinetic analyses depend on the fractions of the respective propagating radicals, such as in the determination of cross-transfer to monomer rate coefficients.^{21,22} The experimentally accessible transfer rate coefficient will be a (weighted) average of the rate coefficients of all possible transfer reactions, and these, naturally, depend on the nature of the reacting radicals.^{7,23} In the case of transfer reactions with a chain transfer agent, the situation is simplified compared to the transfer to monomer situation as the radicals will predominantly react with only one substrate. Thus measurements of average chain transfer constants (i.e., $\langle C_s \rangle = \langle k_{tr,s} \rangle / \langle k_p \rangle$) should reveal information about A_{12} . A simple expression for the average transfer rate coefficient to chain transfer agent S, $\langle k_{tr,s} \rangle$, can be derived in the absence of penultimate unit effects in the transfer reaction (Eq 10).

$$\langle k_{tr,s} \rangle = \phi_1 k_{tr,1s} + (1 - \phi_1) k_{tr,2s} \quad (10)$$

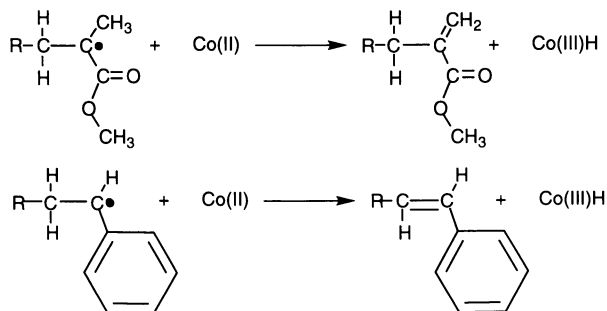
In this equation, $k_{tr,1s}$ and $k_{tr,2s}$ are the transfer rate coefficients of the two homopolymers with chain transfer agent S and ϕ_1 is the fraction of $\sim M_1^\bullet$ radicals simply related to A_{12} (Eq 11).

$$\phi_1 = \frac{A_{12}}{1 + A_{12}} \quad (11)$$

Hence, measurements of the average transfer constant as a function of monomer feed composition, should lead to values for ϕ_1 as a function of monomer feed composition. However, as stated before, such measurements may be complicated by possible penultimate unit effects in the transfer reaction. Evidence of such effects were observed by Bamford and Basahel in their moderated copolymerization studies,⁷ where they found that the transfer constants to CBr_4 of styryl radicals with a styrene or a methyl acrylate penultimate unit were about 5 times larger than the one obtained with methyl methacrylate as penultimate unit. This appearance of a penultimate unit effect in the transfer constant need not necessarily imply that penultimate unit effects are present in the transfer reaction, but strongly suggests this is the case. A stronger indication is found in the case of the transfer reaction of these three radicals with butane thiol, where no penultimate unit effect in the transfer constants is found.⁷ This result may be caused by two different effects: (1) penultimate unit effects do not exist for both the propagation and the transfer reaction or (2) the penultimate unit effect on transfer is of similar magnitude as that on the propagation reaction. Concerning the second point there have been some interesting discussions in the literature, where Bamford²⁴ strongly disagrees with this explanation on the basis of differences in transition states for the two reactions. This argument has been disputed by Fukuda and co-workers, who argued that having similar penultimate unit effects in transfer and propagation is the only way to explain the experimental results.²⁵ In contrast to Bamford's earlier assumptions about the nature of the transition structures, recent theoretical investigations of propagation and transfer reactions in free-radical polymerization,²⁶ indicate that the transition structures for propagation and (hydrogen) transfer are very similar in nature, suggesting that possible penultimate unit effects may affect the propagation and (hydrogen) transfer rate coefficients to a similar extent. Taking this into consideration, transfer agents which have different transition structures or react via a different mechanism may be useful, because these may cause the penultimate unit effects in transfer to become negligible.

Catalytic Chain Transfer. An interesting system in which the transfer reaction may proceed via a different transition state is a copolymerization in the presence of low-spin Co(II) complexes, which are known to act as catalytic chain transfer agents.²⁷ These complexes abstract a hydrogen atom from the growing radical

chain and then this hydrogen atom is transferred to a monomer. In the case of a methyl methacrylate radical, a hydrogen is abstracted from the α -methyl group, whereas in the case of styrene a β -hydrogen will be abstracted from the polymer backbone (see Scheme 1).



Scheme 1

Although the available experimental data suggest the existence of a Co(III)-H intermediate,^{27,28} no experimental evidence exists concerning the mechanism by which the hydrogen abstraction takes place. There is a large body of experimental data that suggests that the radical and the Co complex can (reversibly) form a bond, which may imply that the abstraction reaction is not a pure free-radical one, as is the case with ordinary chain transfer agents. If this is indeed the case, then it is very likely that the penultimate unit effect will be operative in a different quantitative way than in the case of ordinary propagation and transfer reactions. However it is not possible at this stage to make an a priori prediction of the magnitude of a possible penultimate unit effect. However, considering the different hydrogen atoms that are abstracted from the two different radicals, it is likely that, no matter how the actual abstraction reaction proceeds, the penultimate unit effect on the abstraction from the styryl radicals will be greater than the penultimate unit effect in the methyl methacrylate radical. Furthermore, transfer constants for the homopolymerizations of styrene and methyl methacrylate with cobaloxime boron fluoride at 60°C are 1,500 and 36,000, respectively, which corresponds to a factor of 60 difference between transfer rate coefficients. Since the penultimate unit effects in methyl methacrylate are likely to be much smaller than in styrene, and the transfer rate coefficient for methyl methacrylate is about 60 times larger than that for styrene, it is clear that the second term in Eq 10 will dominate at small

fractions of styrene in the monomer feed. Hence ignoring penultimate unit effects in the catalytic chain transfer reaction need not lead to significant errors. Making this assumption, the effect of radical reactivity ratios on the calculated average transfer constant and the fraction of unsaturated styrene end-groups (both experimentally accessible) will be investigated in the remainder of this section.

Effect of Radical Reactivity Ratios. In Figure 6, the effect of an increasing s_{MMA} ($s_{\text{MMA}}=0.6, 0.7, 0.8, 0.9, 1.0$ and 2.0) is investigated, keeping all other parameters constant.

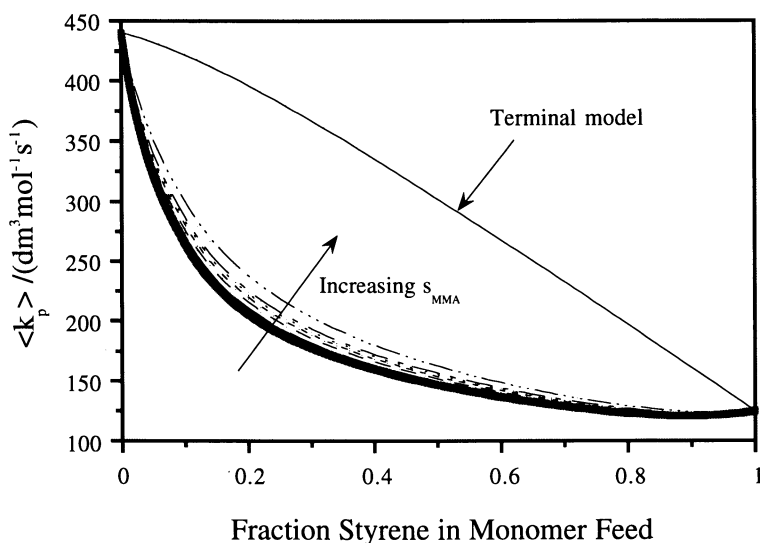


Figure 6. Effect of increasing s_{MMA} on the calculated average propagation rate coefficient of a copolymerization of styrene and methyl methacrylate at 40°C . (—) calculated using $k_{\text{SSS}} = 125 \text{ dm}^3 \text{ mol}^{-1} \text{ s}^{-1}$, $k_{\text{MMM}} = 440 \text{ dm}^3 \text{ mol}^{-1} \text{ s}^{-1}$, $r_{\text{S}} = 0.48$, $r_{\text{MMA}} = 0.42$, $s_{\text{S}} = 0.367$, $s_{\text{MMA}} = 0.524$.^{6,16} Curves indicate penultimate model predictions with increasing s_{MMA} values, where $s_{\text{MMA}} = 2$ (— · — · —) is the largest value used (see text).

It can be seen that even a large value of 2 gives a reasonable agreement with the prediction which is based upon using the point estimates obtained from fitting the average propagation rate coefficients at 40°C .¹⁶ Furthermore, this figure clearly illustrates the point made in the previous section concerning the large uncertainties in radical reactivity ratios. Although the value of 2 for s_{MMA} does not neatly fit the data, its

predictions are not too far out from those obtained with $s_{\text{MMA}} = 0.524$. However, the value of 2 suggests that a styrene penultimate unit increases the reactivity of a $\sim\text{MMA}^\bullet$ radical by a factor of two, whereas a value 0.524 suggests it is decreased by a factor of two. It is obvious from this example that one cannot attach any physical meaning to these values for the radical reactivity ratios.

Average Chain Transfer Constants. Let us now have a look at how similar changes in s_{MMA} to those shown in Figure 6 affect other measurable parameters. Firstly we will investigate the effect on the predicted average chain transfer constant, $\langle C_{\text{Co}} \rangle$ of the tetra phenyl derivate of cobaloxime boron fluoride (COPhBF) in the free-radical copolymerization of styrene and methyl methacrylate at 40°C, which is given by Eq 12.

$$\langle C_{\text{Co}} \rangle = \frac{\langle k_{\text{tr,Co}} \rangle}{\langle k_{\text{p}} \rangle} \quad (12)$$

In this equation, $\langle k_{\text{tr,Co}} \rangle$ is the average transfer rate coefficient with COPhBF given by Eq 10 (assuming negligible penultimate unit effects in the transfer reactions). The calculated average transfer constants with different values used for s_{MMA} (the same as those in Figure 6) are shown in Figure 7, and it is immediately clear from this figure that the average transfer constant, $\langle C_{\text{Co}} \rangle$, is much more sensitive to the value of s_{MMA} than is the average propagation rate coefficient.

Given the results shown in Figure 7, measurements of average transfer constants may be used in further studies to tighten the physically meaningful confidence intervals in which the true values of the radical reactivity ratios may lie (provided that penultimate unit effects in transfer may be neglected).

Fractions of Unsaturated End-Groups. A further parameter that is experimentally accessible is the fraction of unsaturated styrene end-groups in the same copolymerization. As shown in Scheme 1, both the styrene and methyl methacrylate terminated propagating radicals will form a terminal double bond after reaction with COPhBF, which may be measurable with nuclear magnetic spectroscopy.

The fraction of unsaturated styrene end-groups firstly depends on the fraction of styryl radicals (as given by Eq 11). Furthermore, it depends upon the probability, $P(\text{SiCo})$, that these radicals react with the catalytic chain transfer agent. This probability is straightforwardly given as the ratio of the rate of transfer and the total rate involving these radicals. The fraction of unsaturated styrene end-groups is then given as the product of the fraction of styryl radicals and the probability that these react with

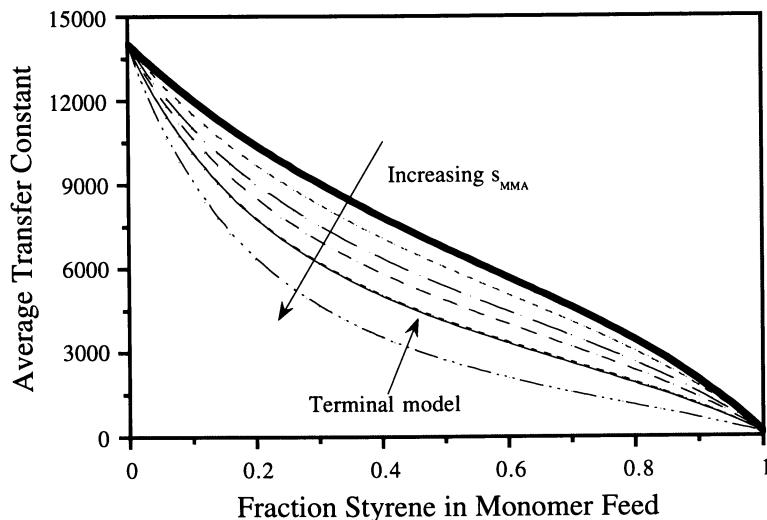


Figure 7. Effect of increasing s_{MMA} on the calculated average transfer constant of a copolymerization of styrene and methyl methacrylate in the presence of the catalytic chain transfer agent CPhBF at 40°C. (—) calculated using the same copolymerization parameters as used in Figure 6,¹⁶ and using transfer constants of 130 and 14,000 for styrene and methyl methacrylate, respectively.³⁰ Curves indicate penultimate model predictions with increasing s_{MMA} values, where $s_{\text{MMA}} = 2$ (— · — · —) is the largest value used.

the catalytic chain transfer agent, normalized by the overall probability of creating an end-group (Eq 13).

$$\Phi_s = \frac{\phi_s P(\text{S} | \text{Co})}{\phi_s P(\text{S} | \text{Co}) + (1 - \phi_s) P(\text{MMA} | \text{Co})} \quad (13)$$

Again, assuming that no penultimate unit effects are important in the catalytic chain transfer step, the results are shown in Figure 8.

This figure again clearly depicts the very large effect of the value used for s_{MMA} . The terminal and penultimate models based upon all the point estimates both predict a relatively small fraction of unsaturated styrene end-groups over the whole range of monomer feed compositions, whereas using a value of 2 for s_{MMA} predicts that the fraction of unsaturated styrene end-groups is approximately equal to the fraction of styrene in the monomer feed. This latter result was found experimentally by Greuel

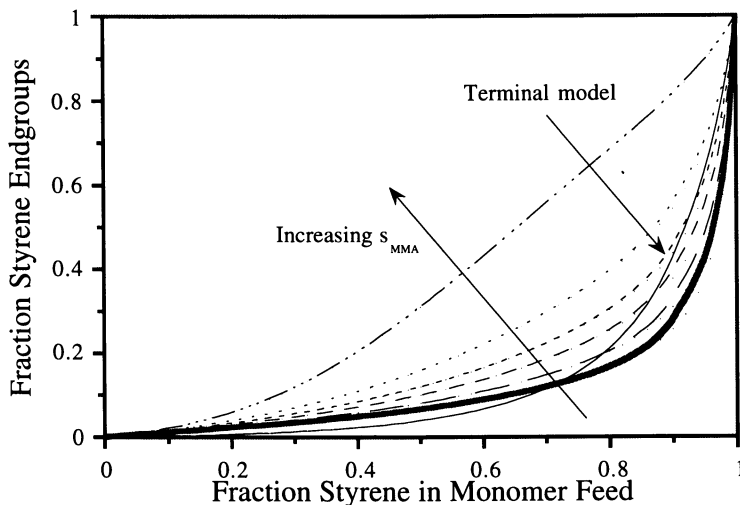


Figure 8. Effect of increasing s_{MMA} on the calculated fraction of styrene endgroups in a copolymerization of styrene and methyl methacrylate in the presence of the catalytic chain transfer agent CPhBF at 40°C. (—) calculated using the same parameters as used in Figure 7,^{16,30} Curves indicate penultimate model predictions with increasing s_{MMA} values, where $s_{\text{MMA}} = 2$ (---) is the largest value used.

and Harwood³¹ for a copolymerization of styrene and methyl methacrylate at 70°C using cobaloxime/pyridine as the catalytic chain transfer agent. This result suggests that this larger value for s_{MMA} may indeed be closer to the "true" physical value.

4. Concluding Remarks

In this article, we have highlighted some of the problems in the current experimental determination of radical reactivity ratios (i.e., s values), which increase the uncertainty in their measured values and thus limit their physical meaning. This limited physical meaning was illustrated by studies of two parameters that are also determined by the radical reactivity ratios — the average transfer constant and the fractions of unsaturated end-groups in catalytic chain transfer experiments. It was shown that (provided penultimate unit effects are negligible in the transfer reaction), these two parameters are more sensitive to the actual s values and may thus provide a

complimentary method to propagation rate coefficient measurements for obtaining physically realistic radical reactivity ratios.

Acknowledgment. Useful discussions relating to this work with Takeshi Fukuda, Bob Gilbert, Alex van Herk, Dax Kukulj, Ken O'Driscoll and Harold Schoonbrood, the award of an Australian Postgraduate Award to MLC, and financial support by the Australian Research Council and ICI are all gratefully acknowledged.

References and Notes

- (1) Fukuda, T.; Ma, Y.-D.; Inagaki, H. *Macromolecules* **1985**, *18*, 17.
- (2) Fukuda, T.; Kubo, K.; Ma, Y.-D. *Prog. Polym. Sci.* **1992**, *17*, 875.
- (3) Harwood, H.J. *Makromol. Chem., Macromol. Symp.* **1987**, *10/11*, 331.
- (4) Kamachi, M. *Adv. Polym. Sci.* **1981**, *38*, 56.
- (5) Fukuda, T.; Ma, Y.-D.; Inagaki, H. *Makromol. Chem., Rapid Commun.* **1987**, *8*, 495.
- (6) Maxwell, I.A.; Aerdt, A.M.; German, A.L. *Macromolecules* **1993**, *26*, 1956.
- (7) (a) Bamford, C.H.; Basahel, S.N. *J. Chem. Soc., Faraday Trans. I* **1978**, *74*, 1020. (b) Bamford, C.H.; Basahel, S.N. *J. Chem. Soc., Faraday Trans. I* **1980**, *76*, 112.
- (8) Heuts, J.P.A.; Gilbert, R.G.; Maxwell, I.A. *Macromolecules* **1997**, *30*, 726.
- (9) Merz, E.; Alfrey, T.; Goldfinger, G. *J. Polym. Sci.* **1946**, *1*, 75.
- (10) Davis, T.P.; O'Driscoll, K.F.; Piton, M.C.; Winnik, M.A. *J. Polym. Sci., Polym. Lett.* **1989**, *27*, 181.
- (11) Olaj, O.F.; Schnöll-Bitai, I.; Kremminger, P. *Eur. Polym. J.* **1989**, *25*, 535.
- (12) See, for example: (a) Draper, N.R.; Smith, H. *Applied Regression Analysis*; John Wiley & Sons: New York, 1981. (b) Van Herk, A.M. *J. Chem. Educ.* **1995**, *72*, 138.
- (13) Britt, H.L.; Luecke, R.H. *Technometrics* **1973**, *15*, 223.
- (14) Buback, M.; Gilbert, R.G.; Russell, G.T.; Hill, D.J.T.; Moad, G.; O'Driscoll, K.F.; Shen, J.; Winnik, M.A. *J. Polym. Sci., Polym. Chem.* **1992**, *30*, 851.
- (15) Olaj, O.F.; Bitai, I.; Hinkelmann, F. *Makromol. Chem.* **1987**, *188*, 1687.
- (16) Coote, M.L.; Zammit, M.D.; Davis, T.P.; Willett, G.D. *submitted to Macromolecules*.
- (17) Olaj, O.F.; Kremminger, P.; Schnöll-Bitai, I. *Makromol. Chem., Rapid Commun.* **1988**, *9*, 771.
- (18) Coote, M.L.; Johnston, L.P.M.; Davis, T.P. *submitted to Macromolecules*.

- (19) See, for example, Odian, G. *Principles of Polymerization*; 2nd Ed; Wiley: New York: 1981.
- (20) Schoonbrood, H.A.S. *Emulsion Co- and Terpolymerization*, PhD Thesis, Eindhoven University of Technology, The Netherlands, 1994.
- (21) Schoonbrood, H.A.S.; German, A.L.; Gilbert, R.G. *Macromolecules* **1995**, *28*, 34.
- (22) Schoonbrood, H.A.S.; Pierik, S.C.J.; Van den Reijen, B.; Heuts, J.P.A.; German, A.L. *Macromolecules* **1996**, *29*, 6717.
- (23) Tsuchida, E.; Kitamura, K.; Shinohara, I. *J. Polym. Sci., Polym. Chem. Edn.* **1972**, *10*, 3639.
- (24) Bamford, C.H. *Polymer Commun.* **1989**, *30*, 36.
- (25) Fukuda, T.; Ma, Y.-D.; Kubo, K.; Inagaki, H. *Macromolecules* **1991**, *24*, 370.
- (26) (a) Heuts, J.P.A.; Gilbert, R.G.; Radom, L. *Macromolecules* **1995**, *28*, 8771. (b) Heuts, J.P.A.; Sudarko; Gilbert, R. G. *Macromol. Symp.* **1996**, *111*, 147. (c) Heuts, J.P.A.; Pross, A.; Radom, L. *J. Phys. Chem.* **1996**, *100*, 17087. (d) Heuts, J.P.A.; Gilbert, R.G.; Radom, L. *J. Phys. Chem.* **1996**, *100*, 18997.
- (27) Davis, T.P.; Kukulj, D.; Haddleton, D.M.; Maloney, D.R. *Trends Polym. Sci.* **1995**, *3*, 365.
- (28) Gridnev, A.A.; Ittel, S.D.; Wayland, B.B.; Fryd, M. *Organometallics* **1996**, *15*, 5116.
- (29) Davis, T.P.; Haddleton, D.M.; Richards, S.N. *J. Macromol. Sci., Rev. Macromol. Chem. Phys.* **1994**, *C34*, 243.
- (30) Heuts, J.P.A.; Kukulj, D.; Forster, D.J.; Davis, T.P. *to be submitted*.
- (31) Greuel, M.P.; Harwood, H.J. *Polym. Prepr. (Am. Chem. Soc., Div. Polym. Chem.)* **1990**, *32(1)*, 545.

Chapter 9

Electron Spin Resonance Studies of Radical Polymerization

Mikiharu Kamachi

Department of Macromolecular Science, Graduate School of Science,
Osaka University, Toyonaka, Osaka 560, Japan

Well-resolved ESR spectra assigned to the propagating radicals for several vinyl and diene monomers were observed in a single scan without the aid of the computer accumulation and a special cavity. Accordingly, direct information on the structure, properties, and concentration of propagating radicals could be obtained. Furthermore, the ESR measurements were found to be possible in the steady state of the concentration of the propagating radicals if the optimum conditions are chosen in the initiator concentration and irradiation light intensity. Accordingly, apparent propagation rate constants (k_p) for vinyl and diene compounds were directly determined by the ESR spectroscopy. In the course of the determination of k_p for styrene, we found a difference in k_p between photo- and thermally-initiated polymerizations of styrene, although the origin of the difference still remains unsolved. Moreover, application of the time-resolved ESR spectroscopy to the elucidation of the mechanism of initiation process in the radical polymerization will be described. In this review, I will mention recent advance in ESR study on radical polymerization. Highly resolved ESR spectra of propagating radicals were observed in the radical polymerization of vinyl and diene compounds by choosing the optimum experimental condition. The structure of the propagating radicals was investigated from hyperfine splitting constants. The propagation rate constants for vinyl and diene compounds were determined on the basis of the time-dependence of the radical concentration, especially the confirmation of the steady state on the radical concentration, although there remain unsolved problems for the accurate determination of the k_p values. The stereoregular chain effect or hydrophobic chain effect on the k_p values was clearly shown in the macromonomers. Radical/cation transformation polymerization was performed for the preparation of the block polymer on the basis of the ESR study on the electron transfer reaction from model radicals of propagating radical end to electron acceptor. In addition, application of time-resolved ESR spectroscopy to initiation process will be described.

Much attention has been paid to electron spin resonance (ESR) studies on the radical polymerization of vinyl or diene compounds, because ESR spectroscopy can, in principle, provide direct information on the structure, properties, and concentration of free radicals (1,2). Accordingly, application of ESR spectroscopy to radical polymerization began in the early 1950s. Unfortunately, the radical concentration of the propagating radicals was too low to be detected in practical conditions (in liquid states) of the radical polymerization by conventional CW-ESR spectrometry. Since no signal could be detected in usual radical polymerizations in the liquid state, ESR detection of the propagating radical in usual radical polymerization of vinyl and diene compounds had been limited to such special conditions as the frozen or crystalline states, or had employed such special techniques as the flow method. The signals observed in the frozen state were usually too broad for a clear understanding of the structure and the electronic state of the propagating radicals on the basis of hyperfine splitting constants. In order to detect the propagating radicals, specially designed cavities and flow technique have been necessary for the detection of the propagating radicals in the liquid state. Several groups succeeded in the detection of the propagating radicals by the flow technique (3). However, the conditions for the measurement are very different from those in practical radical polymerization. Although Bresler et al. (4) observed ESR spectra of propagating radicals of styrene and MMA by a specially designed cavity, the resolution of the spectra was insufficient for an understanding of the structure and the electronic state of the propagating radicals due to their hyperfine splitting constants. More than ten years ago, Kamachi et al. (2) also observed well-resolved spectra of the propagating radicals in the photopolymerization of several vinyl monomers such as methacrylates and vinyl esters by means of a specially designed TM-mode cavity, and showed that more detailed information of their propagating radicals by their hyperfine splitting constants and the line shapes of the spectra. However, well-resolved ESR spectra of the propagating radicals of styrene and diene compounds could not be observed even by the TM-mode cavity. In 1992, Yamada et al. (5) found that an application of a computer to the ESR measurements led to higher sensitivity on ESR observation, and that well-resolved ESR spectra of propagating radicals of styrene and substituted styrenes were observed at room temperature.

Recently, we found that the well-resolved ESR spectra of the propagating radicals of vinyl and diene compounds could be observed even in a single scan without the aid of computer accumulation and that the ESR measurements were possible in the steady state of the concentration of the propagating radicals if the optimum conditions are chosen in the initiator concentration and irradiation light intensity (6-8). Accordingly, we determined propagation rate constants of vinyl and diene compounds by an ESR method. In order to get information on the reliability of the resulting k_p values, the rate constants for styrene were compared with ones determined by PLP methods (9). In the course of the determination of k_p for styrene, we came across the finding that there was an apparent difference in k_p between photo- and thermally-initiated polymerizations of styrene (8). Difference in reactivity between excited and ground-state radicals in the electron transfer reactions has been found and reported (10).

Furthermore, we applied, for the first time, time-resolved ESR spectroscopy to the elucidation of the mechanism of initiation process in the radical polymerization (11,12). In this review, I will mention results obtained in my laboratory over the last ten years

ESR Detection of Propagating Radicals

Highly Resolved ESR Spectra. We recently found that well-resolved spectra can be observed even with a single scan at room temperature by control of the measurement conditions: concentrations of monomer and initiator, amount of

solvents, intensity of Hg-light, and diameter of sample tube (6). Figure 1 shows well-resolved ESR spectra in the photo-initiated radical polymerization of several vinyl and diene compounds with *t*BPO. Higher initiator concentrations than those in usual radical polymerizations were necessary to obtain highly resolved spectra enough to investigate the behavior of the propagating radical.

ESR measurements of photo-initiated polymerization systems of styrene were performed in the temperature region between -20 and 70 °C, although an ESR spectrum of propagating radical of styrene initiated with *t*BPO (0.2 M) under UV-irradiation at 5 °C are shown in Figure 1. Similarly, ESR spectra were detected in other temperatures. ESR spectra of the propagating radicals of various vinyl compounds were also observed by similar methods. The ESR spectra observed in the radical polymerization of vinyl acetate and vinyl chloride are shown in Figures 2 and 3. To our knowledge, there has been no paper on ESR observations of the propagating radical in the polymerization of vinyl chloride.

ESR spectra taken during UV irradiation on neat diene compounds such as 1,3-butadiene, 2-methyl-1,3-pentadiene, and isoprene are shown in Figure 4. These spectra were satisfactorily simulated by using proper hyperfine splitting constants (*hfc*), as shown in Table I. The characteristic point of this simulation is the same coupling constant due to two protons attached to both sides of the allyl structure. From the coupling constants, we can conclude that the propagating radical is a delocalized allyl type radical. In 1967, Yoshida and Rånby (13) observed short-lived free radicals formed by addition of HO• to 1,3-butadiene in aqueous solution by means of a rapid flow method (3). Although the pattern of the spectrum is very similar to that of our spectrum, *hfc*'s due to non-allyl protons of butadiene of our signal are larger than those reported by Yoshida and Rånby (13). Usually, *hfc*'s of the polymeric radicals have been found to be different from those of the monomeric radicals (3), indicating that our data is due to higher molecular weight radicals.

Table I. Hyperfine Splitting Constants (mT)

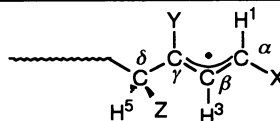
Diene	a_H^1	a_X	a_H^3	a_Y	a_H^5	a_Z
1,3-butadiene	1.605	1.461	0.412	1.605	1.350	1.353
2,4-hexadiene	1.30	0.95	0.30	1.30	1.10	0.95
2-methyl-1,3-pentadiene	1.50	1.25	0.31	1.25	1.60	1.50
isoprene	1.31	1.29	0.43	1.29	1.42	1.17
allyl radical	1.48	1.38	0.41	1.48		

1,3-Butadiene: X=H; Y=H; Z=H.

2,4-Hexadiene: X=CH₃; Y=H; Z=CH₃.

2-Methyl-1,3-pentadiene: X=CH₃; Y=CH₃; Z=H.

Isoprene: X=H; Y=CH₃; Z=H.



Addition Modes in Unsymmetrical Diene Compounds. Usually, the attack of a radical to vinyl compounds is controlled by the steric effect of the substituent of monomer and the stabilization of the resultant radical by the substituent. Accordingly, head to tail addition is quite usual in the polymerization of vinyl compounds. However, the two possibilities (a and b attacks in the following scheme) are considered in attack of a radical to unsymmetrical diene compounds such as isoprene (6).

In the case of isoprene, a doublet of 0.43 mT shows the presence of allylic β -proton. Since the presence of allylic β -proton is not considered in B-type structure shown in Scheme 1, we can conclude that the propagating radical is mainly composed of the A-type structure in Scheme 1. This finding shows that radical attack to isoprene mainly took place at the 1-position of isoprene. The reason why attack at the 1-position of isoprene is more predominant than at the 4-position is probably

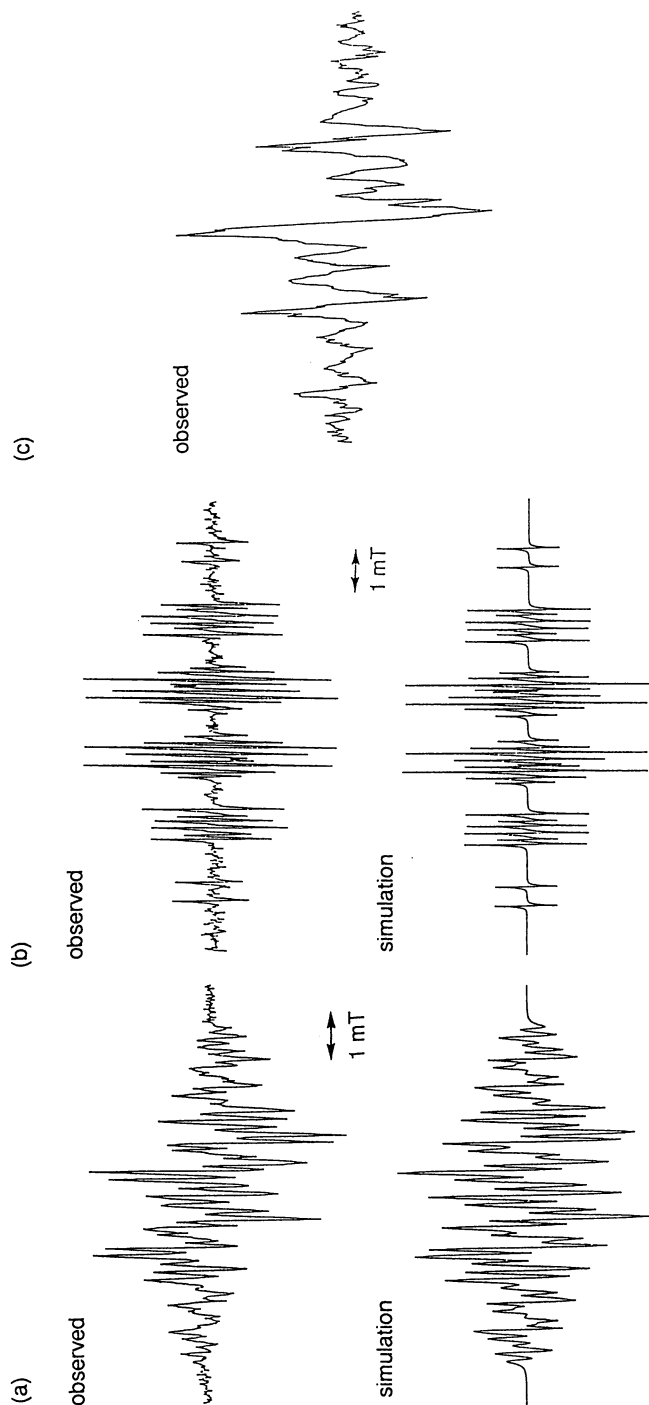


Figure 1. ESR spectra of the propagating radicals of styrene (a), butadiene (b), and MMA (c) observed at 5 °C; Spectra observed at 0.1 mT modulation and 1 scan.

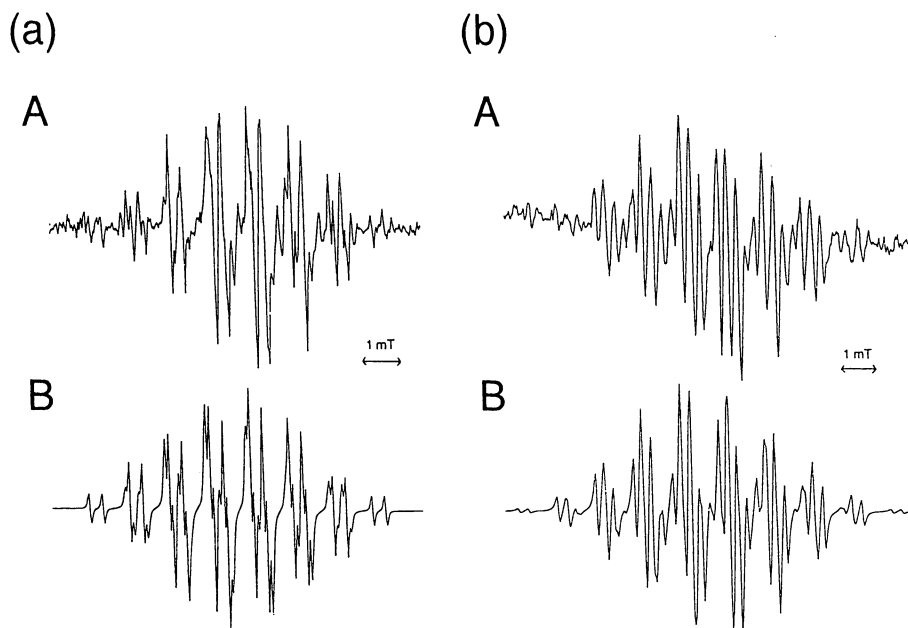
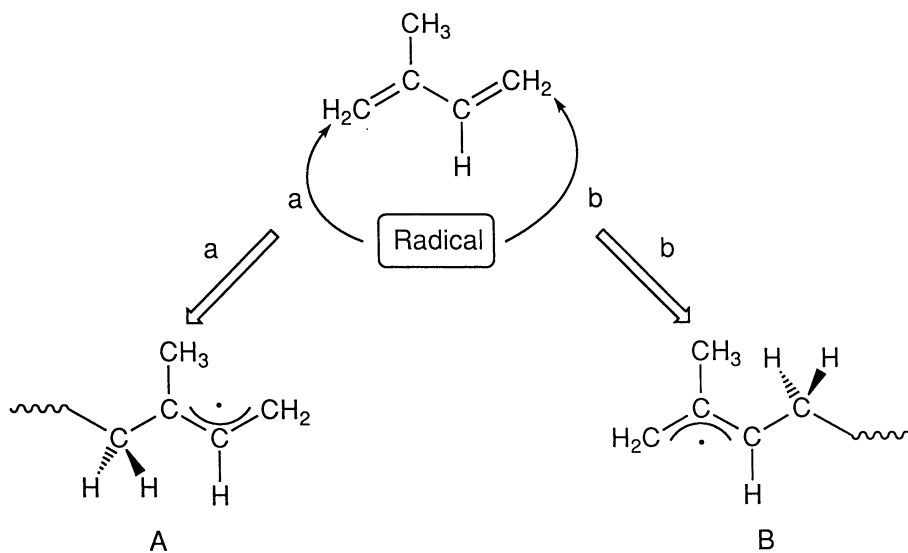


Figure 4. ESR spectra of the propagation radicals of isoprene (a) and 2-methyl-1,3-butadiene (b) observed at 20 °C: (A) observed spectrum at 0.125 mT modulation and 1 scan (32 min) (neat); (B) computer-simulated spectrum.



Scheme 1.

ascribable to the stabilization of the propagating radical with hyperconjugation of the methyl group. The values of hfc's of 2-methyl-1,3-pentadiene show that an unpaired electron in the propagating radical is delocalized in an allylic form, because the hfc due to the α -methyl protons is in agreement with that due to γ -methyl protons and, in addition, the hyperfine structure due to β -proton of allyl-type radical is observed in the ESR spectrum. If the attack at the 4-position is predominant, the hfc due to β -proton (0.3-0.4 mT) is not observed in the ESR spectrum. These findings show that radical attack is more predominant in the 1-position of diene bond than in the 4-position. The reason why the attack in 1-position of 2-methyl-1,3-pentadiene is more predominant is also ascribable to the steric effect of the methyl group bound to its 4-position.

Determination of Rate Constants. In the previous section, we showed that well-resolved spectra of the propagating radical of several vinyl and diene monomers could be observed with a single scan by the control of the measurement conditions.

Accordingly, if the steady state could be confirmed, the k_p value would be determined directly from

$$R_p (= -d[M]/dt) = k_p[P_n^*][M] \quad (1)$$

where R_p and $[P_n^*]$ are the rate of polymerization and the concentration of the propagating radical, respectively.

In order to confirm a steady state, the time dependence of signal intensity was investigated during irradiation in all cases. Examples are shown in Figure 5. The steady state radical concentrations were estimated by the double integration of this spectrum and calibrated with that of TEMPOL-radical in the same media. The rate of polymerization was estimated as a rate of consumption of monomer by gas-chromatography. Examples of first-order plot of rate of consumption of monomer are shown in Figure 6. The apparent values of k_p for photopolymerizations of various kinds of monomers were determined by equation 1 using the slope and the radical concentration estimated. The obtained k_p values are shown in Table II. An activation energy of the radical polymerization of several monomers was also able to be estimated from the k_p values at different temperatures.

Table II. Apparent Propagation Rate Constants of Radical Polymerization of Monomers

Monomers	Initiation	Temp., °C	k_p , M ⁻¹ s ⁻¹
Styrene	Thermal	70	190
Styrene	Photo	70	420
Styrene	Photo	5	180
MMA	Thermal	60	370
MMA	Photo	60	500
Vinyl Chloride	Photo	25	5800
Vinyl Acetate	Photo	5	4500
1,3-Butadiene	Photo	5	150
Isoprene	Photo	5	125
2-Methyl-1,3-pentadiene	Photo	5	35

The k_p values for styrene have been internationally estimated by pulsed-laser polymerization (PLP) method (14). Although the apparent k_p value for styrene at 70 °C (481 M⁻¹s⁻¹) agreed with that (479 M⁻¹s⁻¹) obtained by PLP method, there were some deviations in the k_p values estimated in other temperatures, because the activation energy (18 kJ/mol) determined by ESR method is smaller than that (29.5 kJ/mol) estimated by pulsed-laser polymerization (PLP) method (14). The reason

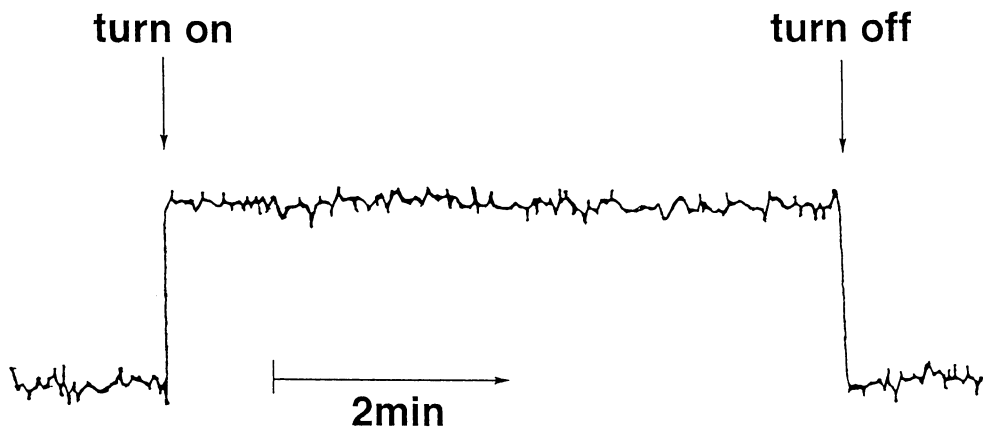


Figure 5. Time-dependence of signal intensity of ESR spectrum of butadiene at constant field.

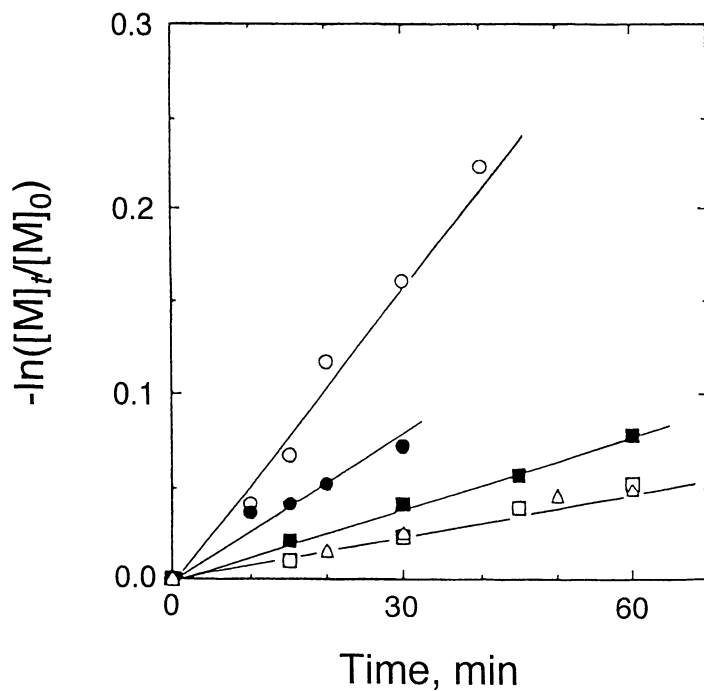


Figure 6. First-order plot of decrease in monomer concentration of dienes during radical polymerizations: 1,3-butadiene (●), isoprene (○), 2-methyl-1,3-pentadiene (■), 1,3-hexadiene (□), and 2,4-hexadiene (△).

why the activation energies are different is a problem to be solved in future. The chain length dependence of the k_p value might be a factor of the origin of the difference. The k_p values are generally considered to be due to the reactivity of the propagating radical and monomer. However, k_p values for vinyl and diene monomers can be usually correlated with the Q-values which reflect the resonance stabilization of the substituents (15), suggesting that the k_p value of monomer, whose propagating radical is more stable, is smaller. The order of the Q-values among isoprene (1.99), 1,3-butadiene (1.70) and styrene (1.00) was in agreement with the decreasing order of apparent k_p values for these monomers as shown in Table II. Accordingly, the propagating radicals of these dienes are more delocalized than that of styrene. This suggestion is in agreement with the conclusion from the hfc's that the propagating radicals of butadiene and isoprene are delocalized allyl type radicals.

Comparison of Apparent Propagation Rate Constants between Thermally- and Photo-Initiated Radical Polymerizations. The ESR spectrum of the propagating radical of styrene has been observed with a single scan in thermally-initiated polymerization at 70 °C under almost the same as that in photo-initiated polymerization. Accordingly, apparent propagation rate constants (k_p) for thermally- and photo-initiated radical polymerizations of styrene were determined by ESR spectroscopy. Apparent values of k_p for styrene at 70 °C were $(420 \pm 30) \text{ M}^{-1}\text{s}^{-1}$ under UV-irradiation and $(180 \pm 10) \text{ M}^{-1}\text{s}^{-1}$ in the dark. The apparent k_p value for the former at 70 °C was about three times as larger as that for the latter. For an understanding of the origin of the difference in the apparent k_p values between photo- and thermally-initiated polymerization, we paid attention to the absorption spectrum of the propagating radical, the influence of wavelength of the irradiation light on k_p values, and activation energy of k_p . The absorption spectrum of the propagating radical of styrene was investigated by the laser photolysis of azo compound, bis[1-methyl-2-(4-methylphenyl)ethyl]-diazene, which produces a model radical of the propagating end of styrene. The spectrum of the radical is shown in Figure 7, where an absorption maximum was clearly observed at 320 nm. The influence of wavelength of the irradiation light on k_p values was investigated by using two kinds of UV-filters, UV-31 and UV-37, which cut off the light below 310 and 370 nm, respectively. The apparent k_p values obtained are shown in Table III. The apparent k_p values were dependent on the wavelength of irradiation light. The apparent k_p values were 290 and 200 in irradiation through UV-31 and UV-37, respectively. The latter was in agreement with the apparent k_p value for thermally-initiated radical polymerization. These results suggest, as one reason, the change in the reactivity of the propagating radical might be due to its photoactivation (photoinduced excitation).

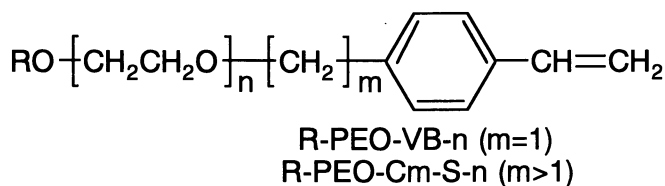
In order to confirm a wavelength dependence of photoexcitation of the k_p values for styrene, diene compound (1,3-hexadiene) was chosen, because allylic radicals obtained from diene compound have no absorption band higher than 300 nm. Accordingly, it is expected to show a weak photoexcitation effect. An ESR spectrum of the propagating radical of 1,3-hexadiene was clearly observed (6). Apparent values of k_p for photo- and thermally-initiated polymerizations at 60°C were determined to be (85 ± 10) and $(75 \pm 15) \text{ M}^{-1}\text{s}^{-1}$, respectively. The difference in these values is very small in comparison with that of styrene. The apparent k_p value for 1,3-hexadiene is considered to support the assumption of photoexcitation of propagating radical in the case of styrene. However, this still remains as an unsolved problem.

Table III. Apparent Propagation Rate Constants of Radical Polymerization of Styrene and 1,3-Hexadiene under Various Conditions

Monomer	Initiation (Filter)	Temp., °C	k_p , M ⁻¹ s ⁻¹
Styrene	Photo	-20	(55 ± 10)
	Photo	0	(120 ± 10)
	Photo	5	(180 ± 10)
	Photo	20	(190 ± 10)
	Photo	40	(290 ± 30)
	Photo	70	(420 ± 30)
	Photo (UV-31) ^a	70	(290 ± 30)
	Photo (UV-37) ^a	70	(200 ± 20)
	Thermal	70	(190 ± 10)
1,3-Hexadiene	Photo	5	(20 ± 10)
	Photo	60	(85 ± 10)
	Thermal	60	(75 ± 15)

^a UV-cutoff filter (in parentheses) was used for polymerization

Polymer Effect on the Determination of Propagation Rate Constants (k_p). Ito et al. (16,17) have been reported unusually rapid radical polymerization in water of poly(ethylene oxide) macromonomers of a general structure



where R stands for an alkyl group as an ω -end, PEO for poly(ethylene oxide), VB for *p*-vinylbenzyl, Cm-S for *p*-styrylbutyl ($m = 4$) or -heptyl ($m = 7$) as an α -end, and n for number average degree of polymerization of PEO.

Because of their amphiphilic constitution, PEO-chains are soluble while polystyrylalkyl groups are insoluble in water, and then they organize into micelles with the polymerizing end groups locally concentrated in the cores, to apparently enhance their polymerization rate. Their aggregation has in fact been confirmed by means of static light scattering and fluorescence probe methods. For an understanding of the origin of an unusually rapid radical polymerization, propagation rate constants and termination rate constants have been estimated in water and benzene, respectively, by ESR measurements (17).

ESR spectra of the propagating radicals in the radical polymerization of C1-PEO-VB-48 in benzene and water, respectively, are shown in Figure 8 (a) and (b). The ESR spectrum in benzene is similar to that of polystyryl radical in benzene, being reasonably assigned to the propagating radical of C1-PEO-VB-48. Although no hyperfine structure was observed in the ESR spectrum in water, the reason why highly resolved ESR spectrum was not observed is ascribable to micellar organization in water. Similar phenomena were also observed in ESR measurements of the radical polymerizations of C1-PEO-C4-S-48 ($R = \text{CH}_3$, $m = 4$, $n = 48$). The steady state was observed in all cases, and the apparent k_p values were easily estimated by the concentration of the propagating radical, and apparent k_t values evaluated by the decay of the ESR spectra upon turning off the irradiation, according to the following equation

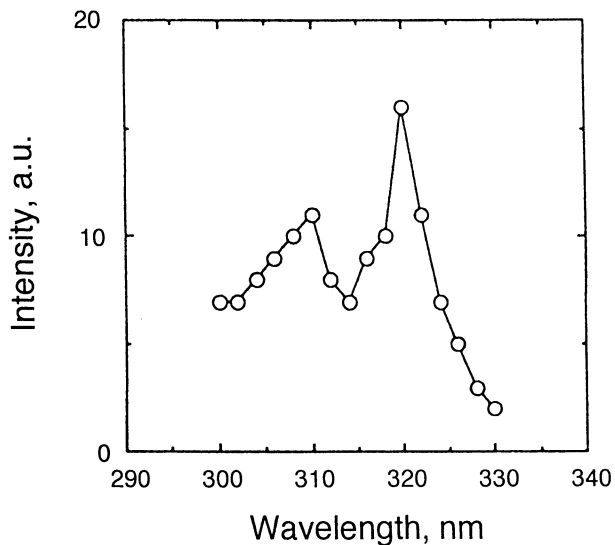


Figure 7. Transient absorption spectrum of cymenyl radical generated by photo decomposition of the corresponding azo compound bis[1-methyl-2-(4-methylphenyl)ethyl]diazene in cyclohexane at 25 °C.

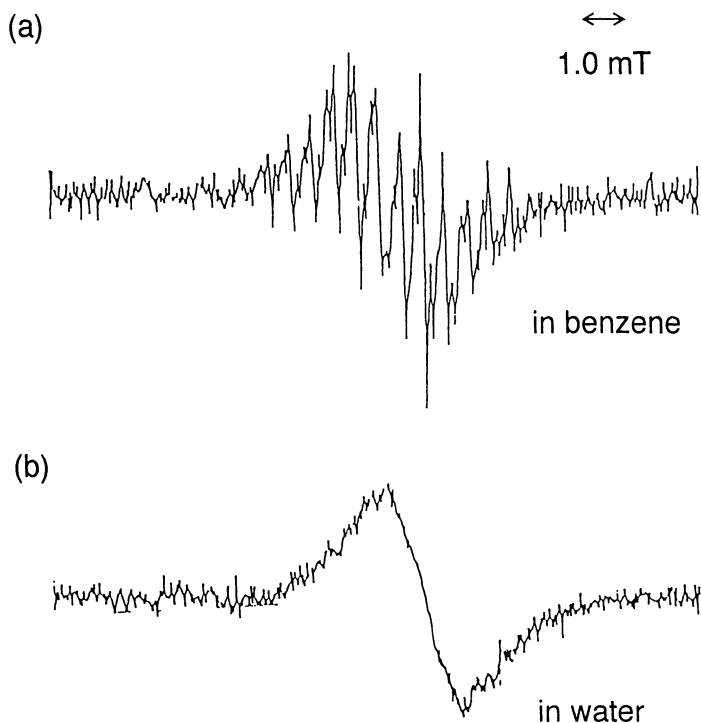


Figure 8. ESR spectra of Poly(C1-PEO-VB-48) in benzene (a) and water (b) at 20 °C.

$$([P^\bullet] - [P^\bullet]_t)/[P^\bullet]_t = k_t[P^\bullet]t \quad (2)$$

where $[P^\bullet]_t$ is the concentration of the polymer radicals at time, t , after the irradiation is turned off and $[P^\bullet]$ is now that at $t = 0$ or stationary concentration under the irradiation. Results are shown in Table IV.

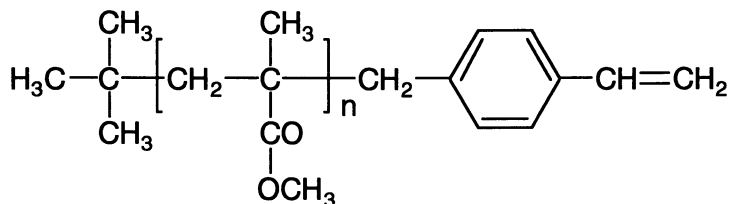
Table IV. Kinetic Parameters of Radical Polymerization under Irradiation at 20 °C^a

monomer/solvent	initiator	$R_p \times 10^6$ Ms ⁻¹	$[P^\bullet] \times 10^6$ M	k_p M ⁻¹ s ⁻¹	k_t M ⁻¹ s ⁻¹
C1-PEO-VB-48/ benzene	<i>t</i> BPO ^b	3.9	2	40	1800
C1-PEO-VB-48/ water	AVA ^c	210	4	1100	5400
C1-PEO-C4-S-48/ benzene	<i>t</i> BPO	15	5	45	4500
C1-PEO-C4-S-48/ water	AVA	510	5	2100	9000

^a $[M] = 50 \times 10^{-3}$ M, $[I] = 2.5 \times 10^{-3}$ M for the macromonomers, and $[I] = 0.2$ M for styrene. Values of R_p , $[P^\bullet]$, k_p , and k_t of the macromonomers in this work may include errors of 10-30 %. ^b Di-*t*-butyl peroxide. ^c 4,4'-Azobis-(4-cyanovaleric acid).

The apparent k_p values for the macromonomers in benzene seem to be a little smaller than that of styrene (Table III and ref. (18)), which can be reasonably explained by steric effect due to long side chains of macromonomers. Surprisingly, the apparent values of k_p in water are about 30 to 50 times higher as compared to those in benzene. This means that preexponential factor in water is much larger than in benzene, because the activation energies of the addition reaction should be almost the same in both solvents. Thus, it indicates that a rather easy access of the macromonomer double bond to the polymacromonomer radical is possible to perform an abnormally controlled propagation. The apparent k_t values for the macromonomers in benzene are about a half to one third of those in water, although the values for macromonomers are much smaller by a factor of 10^{-3} to 10^{-4} than that of styrene (19), indicating a severely hindered bimolecular termination between the highly branched polymacromonomer radicals.

Hatada et al. (20) have prepared stereoregular macromonomers as follows:



The elementary rate constants were measured by ESR methods. Results are shown in Table V. The apparent k_p value for isotactic macromonomer in toluene is 10 times larger than that for syndiotactic macromonomer, and the apparent k_t value for the former is 10^2 times larger than that for the latter. These results show that the mobility in the polymer chains is much higher in isotactic polymer than in syndiotactic polymer.

Table V. Kinetic Parameters for the Polymerization of PMMA Macromonomers or Styrene in Toluene at 60 °C with AIBN^a

Macromonomer <i>M_n</i>	<i>f</i> ^b	<i>R_p</i> , Ms ⁻¹	<i>k_t</i> , M ⁻¹ s ⁻¹	<i>k_p</i> , M ⁻¹ s ⁻¹
iso-2900	0.28	7.4 × 10 ⁻⁷	70000	50
syn-2720	0.18	6.6 × 10 ⁻⁷	670	5.2
syn-5380	0.18	5.3 × 10 ⁻⁷	590	3.9
styrene	0.7 ^c	1.9 × 10 ^{-7d}	3.6 × 10 ^{-7e}	176 ^e

^a [M]₀ = 0.05 M, [M]₀/[I]₀ = 20. ^b Initiator efficiency. ^c Data from ref. (5).

^d Calculated from the literature data. ^e Data from ref. (4).

Electron Transfer Reaction of Free Radicals and their extension to new polymer Formation

The Influence of Ph₂I⁺PF₆⁻ on ESR Spectra of Primary Radicals.

In the course of an ESR study of primary radicals obtained from azo-initiators, we found that some of the radicals transform to the corresponding cations in the presence of Ph₂I⁺PF₆⁻, which is an electron acceptor. The influence of Ph₂I⁺PF₆⁻ on the ESR spectra of primary radicals obtained by thermal decomposition of AIBN, ABMPE, and ABPOP are shown in Figure 9 (21). On the addition of Ph₂I⁺PF₆⁻ the ESR spectrum of the primary radical obtained from AIBN did not change while those of primary radicals produced from ABMPE and ABPOP almost disappeared. This result suggests that (CH₃)₂CCN having an electron-accepting substituent did not perform an electron-transfer reaction to Ph₂I⁺PF₆⁻, and that (CH₃)₂C(C₆H₄OCH₃) and (CH₃)₂C(OC₆H₅) having an electron-donating substituent undergo the electron-transfer reaction to form the corresponding carbocation. The ESR spectrum of the propagating radical was clearly detected in the radical polymerization of *p*-methoxystyrene (MOST), while no ESR spectrum was detected in the presence of Ph₂I⁺PF₆⁻. These ESR spectra were shown in Figure 10. The disappearance of the ESR spectra of the primary radicals from ABMPE and ABPOP, and the formation of carbocation were confirmed by the polymer formation from vinyl ethers which cannot be polymerized to high molecular weight polymer by radical initiators, as shown in the next section.

Radical/cation Transformation Polymerization. Polymerizations of *p*-methoxystyrene (MOST), *n*-butylvinylether (BVE), or cyclohexene oxide (CHO) were performed with AIBN, ABMPE and ABPOP, respectively. Polymer was obtained from MOST, and no polymer was obtained by the radical polymerization of vinyl ether and cyclohexene oxide with AIBN, ABMPE, and ABPOP (21). In the presence of Ph₂I⁺PF₆⁻, however, high molecular weight polymer was obtained in much higher yield from MOST and BVE by the polymerization with AIBN, ABPOP and ABMPE. High molecular weight polymer was also obtained from CHO by polymerization with ABMPE and ABPOP in the presence of Ph₂I⁺PF₆⁻, and was not allowed to polymerize with AIBN even in the presence of Ph₂I⁺PF₆⁻. Polymerizations of MOST, BVE, and CHO with Ph₂I⁺PF₆⁻ were performed as control experiments, which indicate that only a few polymers were obtained by the polymerizations. Results are shown in Table VI. Since BVE and CHO are not allowed to polymerize to high molecular weight polymer by radical initiators, the polymer formation from these monomers shows that cationic polymerization was performed with ABMPE in the presence of Ph₂I⁺PF₆⁻. ESR study showed that electron transfer reaction took place from the primary radical (CH₃)₂CC₆H₄(OCH₃), which is obtained by decomposition of ABMPE, to Ph₂I⁺PF₆⁻.

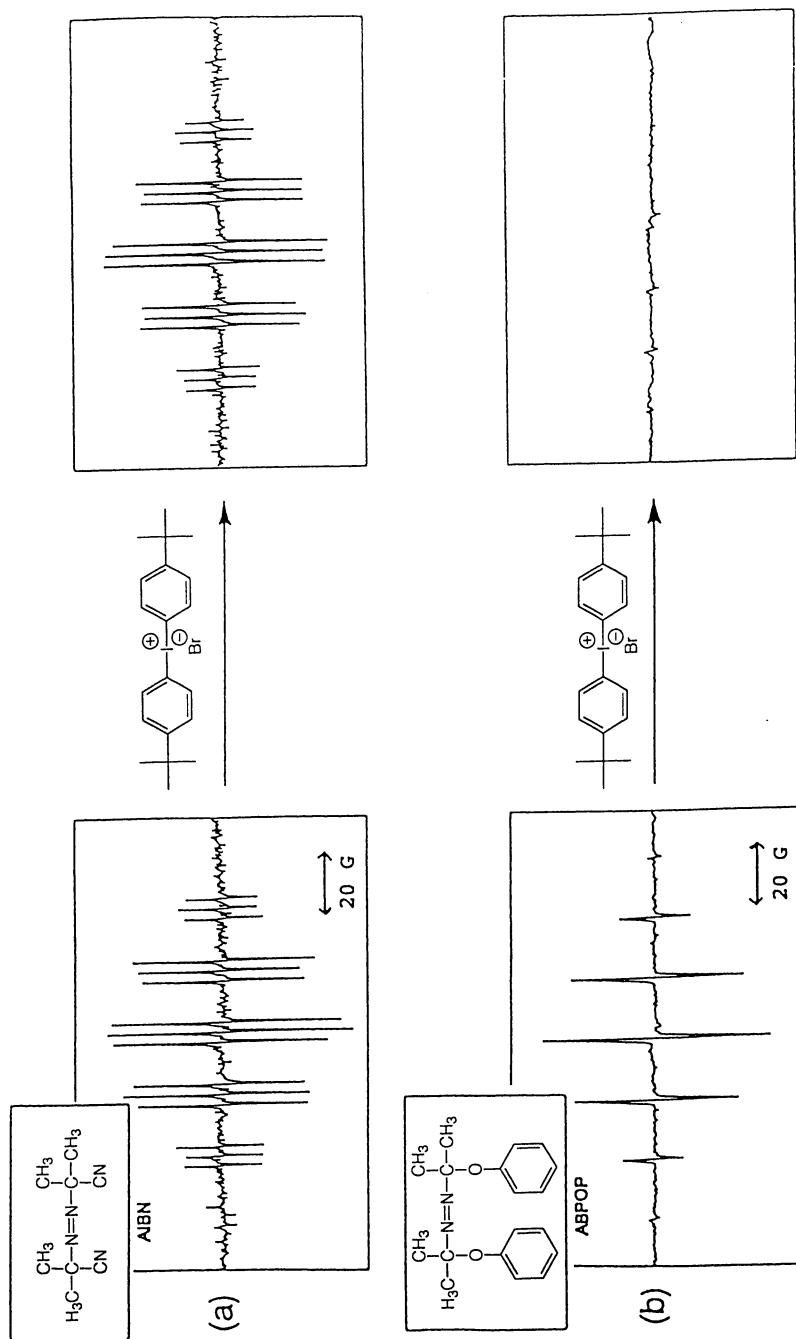


Figure 9. ESR spectra of primary radicals obtained by decomposition of AIBN (a) and ABPOP (b) in the absence and presence of an acceptor under irradiation of an ultra-high-pressure mercury lamp at 20 °C.

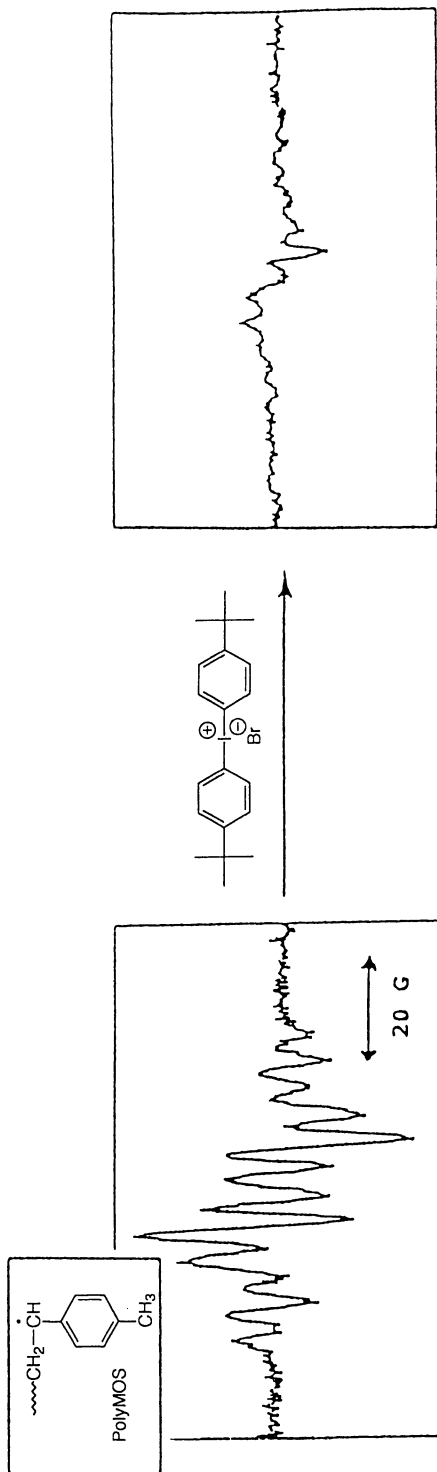


Figure 10. ESR spectra of propagating radical of *p*-methoxystyrene, in the absence and presence of an acceptor under irradiation of an ultra-high pressure mercury lamp at 20 °C.

Table VI. Cationic Polymerization of BVE, MOST, and CHO Promoted by Free Radical Initiators^a

monomer	radical initiator	conc., M	Ph ₂ I ⁺ PF ₆ ⁻ , M	temp, ^b °C	time, min	conv., %	M _w × 10 ⁻⁴
BVE	none	0	6 × 10 ⁻³	80	80	5	1.08
	AIBN	6 × 10 ⁻³	0	80	80	0	
	AIBN	6 × 10 ⁻³	6 × 10 ⁻³	80	80	62	0.85
	ABMPE	6 × 10 ⁻³	0	80	80	0	
	ABMPE	6 × 10 ⁻³	6 × 10 ⁻³	80	80	68	0.95
	ABPOP	6 × 10 ⁻³	0	80	80	0	
	ABPOP	6 × 10 ⁻³	6 × 10 ⁻³	80	80	63	1.11
MOST	none	0	1.2 × 10 ⁻²	80	120	4	3.40
	AIBN	6 × 10 ⁻³	0	80	120	10	2.26
	AIBN	6 × 10 ⁻³	1.2 × 10 ⁻²	80	120	74	4.23
	ABMPE	6 × 10 ⁻³	0	80	120	4	4.81
	ABMPE	6 × 10 ⁻³	1.2 × 10 ⁻²	80	120	34	3.24
	ABPOP	6 × 10 ⁻³	0	80	120	2	6.01
	ABPOP	6 × 10 ⁻³	1.2 × 10 ⁻²	80	120	64	4.46
CHO	none	0	1.2 × 10 ⁻²	80	120	~1	
	AIBN	6 × 10 ⁻³		80	120	0	
	AIBN	6 × 10 ⁻³	1.2 × 10 ⁻²	80	120	~1	
	ABMPE	1.2 × 10 ⁻²	0	100	24 (h)	0	
	ABMPE	1.2 × 10 ⁻²	2.4 × 10 ⁻²	100	24 (h)	30	1.74
	none	0	2.4 × 10 ⁻²	100	24 (h)	6	2.52
	none	0	2.4 × 10 ⁻²	100	24 (h)	6	2.52

^a Solvent, (CH₂)₂Cl₂; monomer:(CH₂)₂Cl₂ = 1:3 (vol). ^b Oil bath temperature.

The polymer formation can be reasonably explained by polymerization with carbocation formed by the electron transfer reaction from primary radicals having electron-donating substituents to Ph₂I⁺PF₆⁻. The fact that CHO did not polymerize with AIBN even in the presence of Ph₂I⁺PF₆⁻ is in agreement with the ESR observation in which no electron transfer reaction took place from (CH₃)₂CCN to Ph₂I⁺PF₆⁻. However, the finding that BVE was polymerized in a high yield by AIBN in the presence of Ph₂I⁺PF₆⁻ is inconsistent with this explanation, because it does not polymerize with radical initiators. The formation of cationic initiating species in the presence of BVE is explained by the electron transfer reaction of an initiating radical formed by the addition reaction of (CH₃)₂CCN to BVE (2I). MOST was initiated to form high molecular weight polymer by AIBN, and not by Ph₂I⁺PF₆⁻.

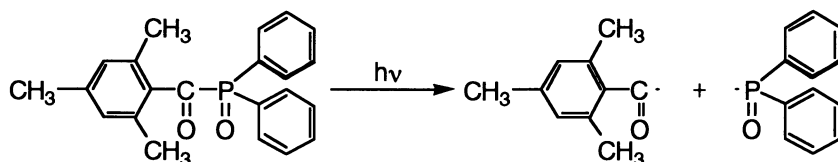
When the polymerization of MOST was performed with AIBN in the presence of Ph₂I⁺PF₆⁻, polymer formation from MOST was remarkably promoted, which indicates that polyMOST radicals initiated by AIBN were transformed into polyMOST cations by Ph₂I⁺PF₆⁻ before they disappeared by bimolecular termination such as the coupling reaction. The transformation of the propagating species from radical to cation is consistent with the change in the ESR spectrum as shown in Figure 10. This is also explained by the radical/cation transformation of the initiating radical and/or propagating radical in the propagation process.

Block Polymer of MOST and CHO. We note that MOST is polymerized with an AIBN/Ph₂I⁺PF₆⁻ initiating system, and that CHO is not polymerized with the initiating system. Since it is already known that the propagating cation of MOST initiates the polymerization of CHO and that the propagating oxonium ion of CHO does not initiate the polymerization of MOST, the formation of block polymers is

expected by the polymerization of a mixture of CHO and MOST with AIBN in the presence of $\text{Ph}_2\text{I}^+\text{PF}_6^-$ as shown in the Scheme 2. The formation of the block copolymer formation was confirmed by solvent extraction, NMR spectroscopy, turbidimetric titration and thin layer chromatography (TLC).

Time-Resolved Electron Spin Resonance Study

Acylphosphine oxides and acylphosphonates have been exploited by BASF researchers as new types of photoinitiators for photocuring of polymer resins (22). Schnabel et al. (23,24) performed laser photolysis of these compounds in the absence and presence of vinyl monomers, and suggested that phosphorus-centered radicals formed by the photolysis of these compounds were much more reactive with vinyl monomers than carbon-centered radicals which were obtained by photolysis of benzoin, benzoin methyl ether, or 1-phenyl-2-hydroxy-2-methylpropanone-1. However, they had no direct evidence on the phosphorus-centered radicals. About ten years ago, Kamachi et al. (11) started cooperative research on an understanding of the photolysis of 2,4,6-trimethylbenzoyl diphenylphosphine oxide (TMDPO). Unfortunately, diphenylphosphonyl and 2,4,6-trimethylbenzoyl radicals, which had been considered to be produced by the photolysis of TMDPO (Scheme 5), could not be detected by ESR measurements under continuous irradiation with a high pressure mercury lamp.



In order to get more information on the highly reactive radical, we carried out the time-resolved ESR spectroscopy combined with laser pulse irradiation. A block diagram of the time-resolved ESR measurements is shown in Figure 11. An example of the results of time-resolved ESR spectroscopy is shown three-dimensionally in Figure 12. Three absorptions due to transient species were clearly observed. The two absorptions at magnetic fields of 315.0 and 350.2 mT at both ends can be reasonably assigned to diphenylphosphonyl radicals generated by the laser pulse irradiation, because the separation between these absorptions corresponded to the hyperfine splitting constant of the diphenylphosphonyl radical with a phosphorus nucleus. In addition, the absorption at $g = 2.0008$ can be reasonably assigned to 2,4,6-trimethylbenzoyl radical. These results show that the transient species proposed by Schnabel et al. have been confirmed by time-resolved ESR spectroscopy with laser pulse irradiation.

Time-resolved ESR studies on the photolysis of TMDPO shows that the lifetime of the diphenylphosphonyl radical decreased with increasing concentration of vinyl and diene monomers, while that of the 2,4,6-trimethylbenzoyl radical did not change in both the presence and absence of vinyl monomers in the time region of 4 μs after irradiation of 355-nm laser light (12). This result shows that the diphenylphosphonyl radical is more reactive with vinyl and diene monomers than the 2,4,6-trimethylbenzoyl radical, and allows us to estimate rate constants for the addition of the diphenylphosphonyl radical to vinyl monomers.

Decays of ESR signals due to the diphenylphosphonyl radicals in the laser photolysis of TMDPO are shown in the presence of varying concentrations of phenyl vinyl ether (PVE) as an example in Figure 13. The decays became faster with increasing concentration of PVE. The first-order plots for the signal intensities gave

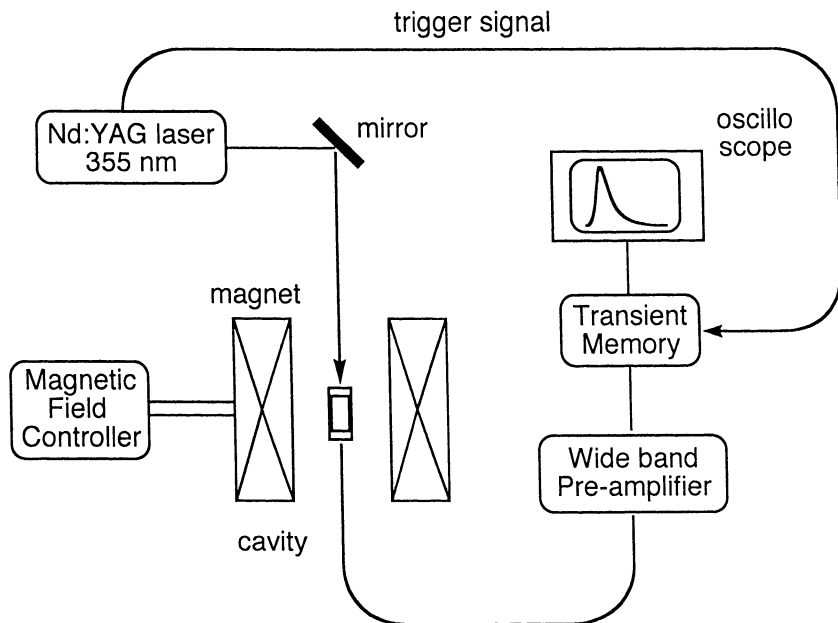


Figure 11. Schematic diagram of the system for time-resolved ESR spectroscopy.

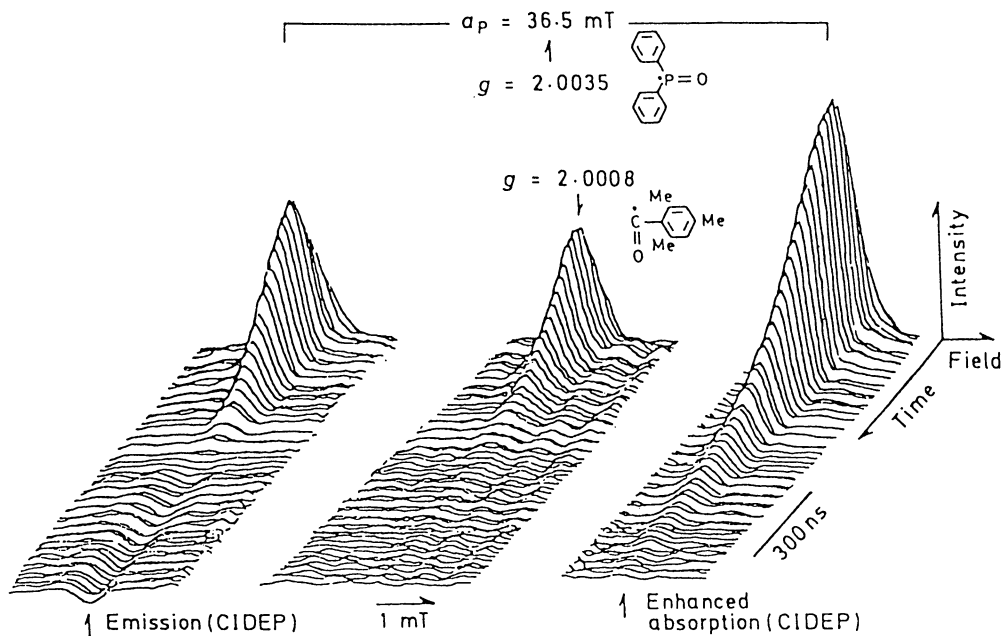


Figure 12. Time dependence of the transient ESR spectrum recorded after irradiation of a solution of TMDPO in benzene (0.1 M) with a 20 ns flash of 337.1 nm light.

linear relationships both in the absence and presence of the monomers (Figure 14). The apparent first-order rate constant (k') increased with increasing monomer concentration. The plots of the k' value against the monomer concentration yielded linear relationships as shown in Figure 15. Accordingly, k' follows

$$k' = k_1 + k_2 [M]$$

where k_1 is the first order decay constant in the absence of the monomer, and k_2 is the bimolecular rate constant for the reaction of a diphenylphosphonyl radical with the monomer. Similar results were observed in the time-resolved ESR measurements in the presence of vinyl or diene monomers (8,12). Their k_2 values are summarized in Table VII.

Table VII. Initiation Rate Constants for Monomers (TR-ESR)

Monomer	$k_2, M^{-1}s^{-1}$
1,1-diphenyl ethylene	$(2.4 \pm 0.1) \times 10^7$
di- <i>n</i> -butyl itaconate	$(1.9 \pm 0.4) \times 10^7$
1-acetoxy butadiene	$(1.5 \pm 0.3) \times 10^7$
α -methyl styrene	$(1.0 \pm 0.1) \times 10^7$
styrene	$(1.1 \pm 0.1) \times 10^7$
ethyl vinyl ether	$(1.5 \pm 0.5) \times 10^6$
<i>n</i> -butyl vinyl ether	$(4.4 \pm 0.4) \times 10^6$
<i>i</i> -butyl vinyl ether	$(2.5 \pm 0.3) \times 10^6$
<i>n</i> -decyl vinyl ether	$(3.1 \pm 0.3) \times 10^6$
phenyl vinyl ether	$(2.6 \pm 0.3) \times 10^6$
vinyl acetate	$(2.7 \pm 0.3) \times 10^6$
vinyl pivalate	$(2.5 \pm 0.3) \times 10^6$
acrylamide-TPP ^a	$(1.6 \pm 0.3) \times 10^6$

^a 5-(4-Acrylamidephenyl)-10,15,20-triphenylporphine).

The diphenylphosphonyl radicals decayed in the time region of 2 μ s after irradiation, and new ESR signals appeared around that of the 2,4,6-trimethyl benzoyl radical at about 200 ns after irradiation. The signals were assigned by computer simulation to a radical produced by the addition of the diphenylphosphonyl radical to methyl methacrylate (MMA) and α -methylstyrene. Therefore, k_2 is concluded to be the rate constant for the addition reaction of the diphenylphosphonyl radical to a vinyl monomer, which corresponds to the initiation rate constant in the radical polymerization of a vinyl monomer with TMDPO. These rate constants are on the order of 10^6 - $10^7 M^{-1}s^{-1}$, which are one or two orders of magnitudes larger than those of carbon-centered radicals, whose rate constants have been determined to be on the order of 10^4 - $10^5 M^{-1}s^{-1}$ (25). The decays of the signals due to the 2,4,6-trimethylbenzoyl radicals, which were formed along with the diphenylphosphonyl radical by the photolysis of TMDPO, were identical over a period of 40 μ s after irradiation in both the absence and presence of monomers, indicating that the 2,4,6-trimethylbenzoyl radicals did not attack vinyl monomers within this time region. This result shows that the 2,4,6-trimethylbenzoyl radical is less reactive with vinyl and diene monomers than is the diphenylphosphonyl radical.

In conclusion, rate constants for addition of the diphenylphosphonyl radical to vinyl monomers were directly estimated by time-resolved ESR spectroscopy with laser pulse irradiation, and were found to be one or two orders of magnitude larger than those of carbon-centered radicals.

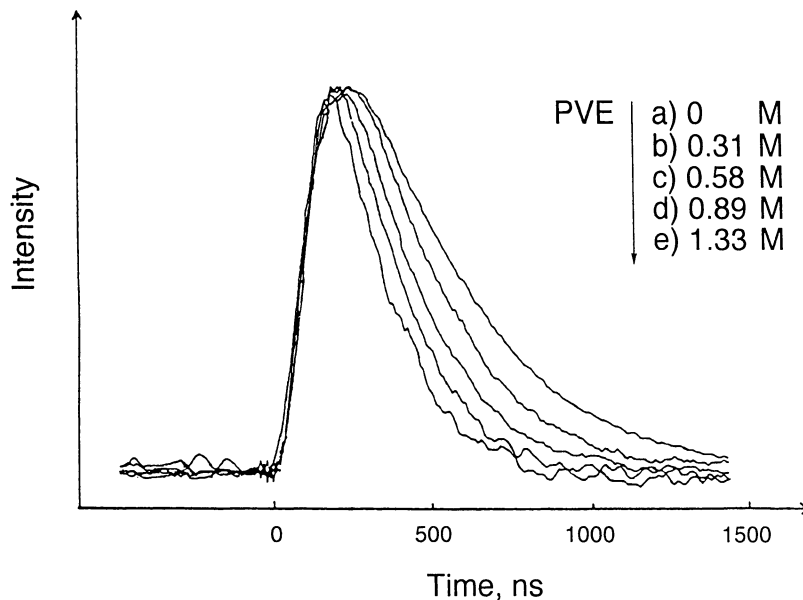


Figure 13. Time profiles of ESR signal intensities due to the diphenylphosphonyl radicals in the presence of varying concentrations of phenyl vinyl ether (PVE): (a) 0, (b) 0.31, (c) 0.58, (d) 0.89, and (e) 1.33 M.

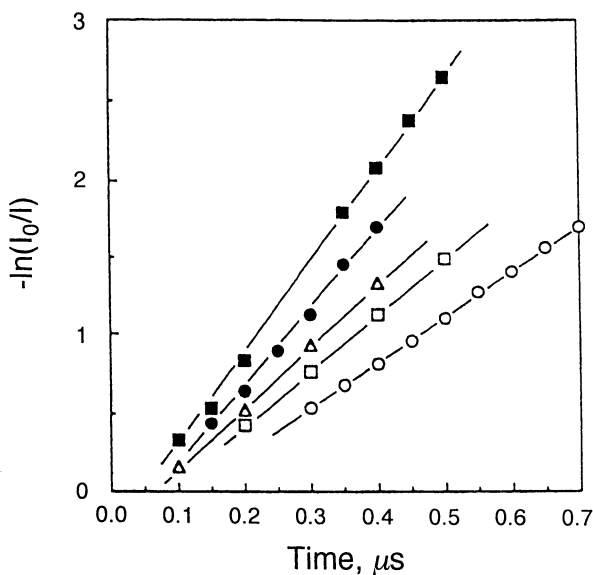


Figure 14. First-order plots for the decays of the diphenylphosphonyl radicals in the presence of varying concentrations of phenyl vinyl ether (PVE): (a) 0 (○), 0.31 (□), 0.58 (△), 0.89 (●), and 1.33 M (■).

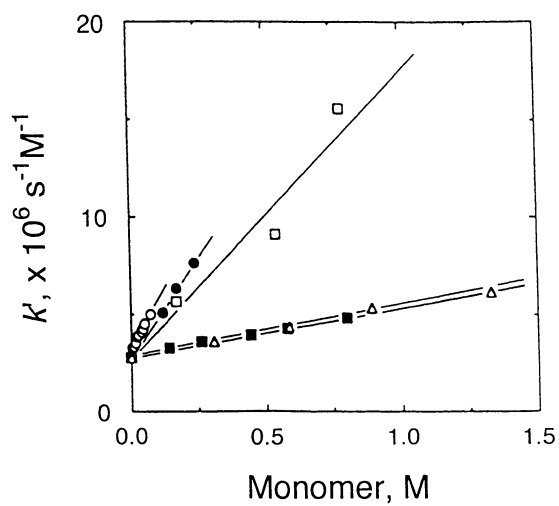


Figure 15. Plots of k' vs the concentration of added monomers: 1,1-diphenylethylene (○), di-n-butyl itaconate (●), 1-acetoxybutadiene (□), phenyl vinyl ether (△), and vinyl pivalate (■).

Acknowledgment

The author wishes to thank Drs.Kajiwara and Guo for carrying out many of the measurements and experiments reported in this manuscript, and Dr. Hashidzume for his reading of this manuscript.

References

- 1) Rånby, B.; Rabek, J. F. *ESR Spectroscopy in Polymer Research*; Springer-Verlag: Berlin, 1977.
- 2) Kamachi, M. *Adv. Polym. Sci.* **1987**, *82*, 209.
- 3) Fischer, H. Z. *Naturforsch.* **1964**, *19*, 267.
- 4) Bresler, S. D.; Kazbekov, E. N.; Saminskii, E. M. *J.Polym.Sci.* **1961**, *52*, 119.
- 5) Yamada, B.; Kageoka, M.; Otsu, T. *Macromolecules* **1992**, *25*, 4828.
- 6) Kamachi, M.; Kajiwara, A. *Macromolecules* **1996**, *29*, 2378.
- 7) Kamachi, M.; Kajiwara, A. *Makromol. Chem.* **1997**, *198*, 787
- 8) Kamachi, M.; Kajiwara, A.; Saegusa, K.; Morishima, Y. *Macromolecules* **1993**, *26*, 7369.
- 9) Buback, M.; Garcia-Rubio, L. H.; Gilbert, R. G.; Napper, D. H.; Guillot, J.; Hamielec, A. E.; Hill, D.; O'Driscoll, K. F.; Olaj, O. F.; Shen, J.-C.; Solomon, D.; Moad, G.; Stickler, M.; Tirrell, M.; Winnik, M. A. *J. Polym. Sci., Part C: Polym. Lett.* **1988**, *26*, 293.
- 10) Kavarnos, G. J. *Fundamentals of Photoinduced Electron Transfer*; VCH Publishers: New York, 1993.
- 11) Kamachi, M.; Kuwata, K.; Sumiyoshi, T.; Schnabel, W. *J. Chem. Soc., Perkin Trans. 2* **1988**, 961.
- 12) Kajiwara, A.; Konishi, Y.; Morishima, Y.; Schnabel, W.; Kuwata, K.; Kamachi, M. *Macromolecules* **1993**, *26*, 1656.
- 13) Yoshida H.; Rånby, B. *J. Polym. Sci., C16* **1967**, 1333.
- 14) Buback, M.; Gilbert, R. G.; Hutchinson, R. A.; Klumperman, B.; Kucta, F.-D.; Manders, B. G.; O'Driscoll, K. F.; Russell, G. T.; Schweer, J. *Macromol. Chem. Phys.* **1995**, *196*, 3267.
- 15) **Addition Rate Constants of Various Radicals to Monomers^a**

radicals	monomers						Q
	VAc	MA	AN	MMA	St	Bd	
VAc	2390 ^b	5901	59750	79667	239000	-	0.026
MA	810	2090 ^b	2459	5225	12440	29857	0.45
AN	484	1496	1960 ^b	14203	65333	42609	0.48
MMA	20	240	390	515 ^b	954	2060	0.78
St	4	335	672	429	242 ^b	288	1.00
Bd	-	92	279	133	69	100 ^b	1.70

^a r_1 and r_2 are referd from *Polymer Handbook*: 3rd ed.; Brandrup, J; Immergut, E. H., Ed.; John Wiley & Sons: New York, 1989, pp. II/153-II/266. ^b Data are from G. Odian *Principles of Polymerization*; 3rd ed.; John Wiley & Sons: New York, 1991; Chapter 3, p. 275.

- 16) Ito, K.; Tanaka, K.; Tanaka, H.; Imai, G.; Kawaguchi, S.; Itsuno, S. *Macromolecules* **1991**, *24*, 2348.
- 17) Ito, K.; Hashimura, K.; Itsuno, S.; Yamada, E. *Macromolecules* **1991**, *24*, 3997.
- 18) Nomura, E.; Ito, K.; Kajiwara, A.; Kamachi, M. *Macromolecules*, in Press.
- 19) Burnett, B. M.; Cameron, G. G.; Joiner, S. N. *Trans. Faraday Soc. I* **1973**, *69*, 322.
- 20) Hatada, K.; Kitayama, T.; Masuda, E.; Kamachi, M. *Macromol. Chem. Rapid Commun.* **1990**, *11*, 101.

- 21) Guo, H.; Kajiwara, A.; Morishima, Y.; Kamachi, M. *Macromolecules* **1996**, *29*, 2354.
- 22) a) Lechtken, P.; Buethe, I.; Henne, A. DOS 2 804 927; b) Lechtken, P.; Buethe, I.; Jacobi, M.; Trimborn, W. DOS 2 909 994; c) Nikolaus, W.; Henne, A.; Scholz, D. *Plastverarbeiter*, **1980**, *31*, 723; d) Jacobi, A.; Henne, A. *Radiat. Curing*, **1983**, *10*, 16.
- 23) Sumiyoshi, T.; Henne, A.; Lechtken, P.; Schnabel, W. *Z. Naturforsch.*, **1984**, *A39*, 434.
- 24) Sumiyoshi, T.; Schnabel, W. *Polymer*, **1985**, *26*, 141.
- 25) *Free Radicals*; Kochi, J. K., Ed.; John Wiley & Sons: New York, 1973; Vol. I, Chapter 1, p. 26.

Chapter 10

The Stable Free-Radical Polymerization Process: Role of Excess Nitroxide

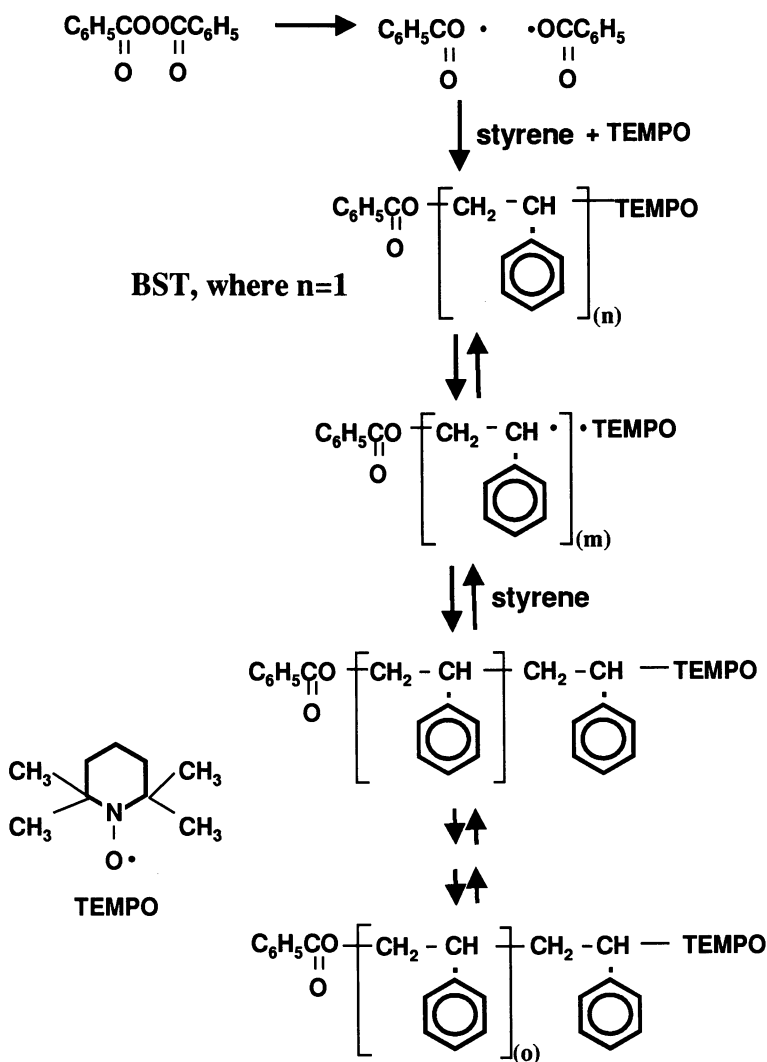
M. K. Georges, R. P. N. Veregin, and K. Daimon

The Xerox Research Centre of Canada, 2660 Speakman Drive,
Mississauga, Ontario L5K 2L1, Canada

The rate of polymerization of styrene in the stable free radical polymerization (SFRP) process is shown to be dependent on the excess of free nitroxide in the reaction mixture. Monomer conversion is independent of the amount of initiator and, instead, dependent on the concentration of excess nitroxide. While the excess nitroxide in styrene polymerizations is controlled by a combination of auto-initiation and termination, the actual amount of free nitroxide is proportional to the amount of initiator-adduct used.

The ability to synthesize narrow polydispersity polystyrene by a living free radical polymerization process was first reported in 1993 (1) leading to renewed interest in the free radical polymerization process. Living free radical polymerization has gained in popularity as a result of the continued expansion of the stable free radical polymerization (SFRP) process (2) and the development of the atom transfer radical polymerization process (3). Complex architectures, once thought impossible by free radical polymerization are now a reality (4) and new structures, previously not thought possible by a free radical polymerization process continue to be reported (5).

The SFRP process (1), typically performed at 125°C, is illustrated in Scheme 1 for the polymerization of styrene initiated by benzoyl peroxide. Initiation begins with the rapid formation of the benzoyloxy primary radical, which can undergo a series of reactions (6). The most important of these reactions is the addition of styrene, the products of which immediately react with TEMPO to form a unimer ($n=1$), referred to in Scheme 1 as BST, or a TEMPO terminated oligomer ($n>1$). The success of the SFRP process relies on the ease of homolytic dissociation of the C-O bond between the styryl end group and TEMPO at 125°C. The resulting styryl radical can either recombine with TEMPO to regenerate the original molecule or it can add monomer

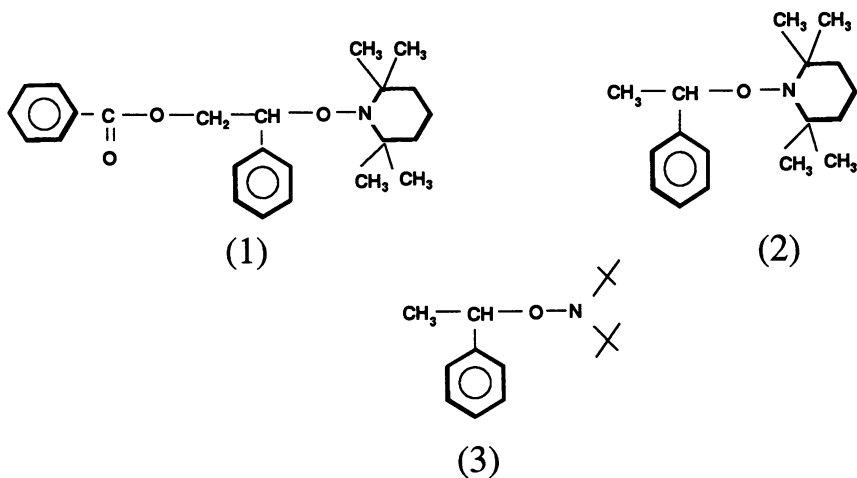


Scheme 1. Polymerization of styrene initiated with benzoyl peroxide in the presence of TEMPO.

before the now growing chain is terminated with TEMPO. This latter sequence repeats itself to produce a polymer. Since at any given time the majority of polymer chains are capped with nitroxide, the number of reactive propagating chains at any one time is very small (10^{-8} to 10^{-9} M) limiting the probability of termination by coupling (7). The quick initiation of all the chains, the fast exchange between the uncapped and capped polymer chains and the lack of premature termination all combine to enable narrow polydispersity polystyrene. Since at the end of the polymerization the polystyrene chains are terminated with TEMPO, further reaction can occur if these chains are heated in the presence of more of the same or another monomer.

The rate of polymerization was subsequently shown to be related to the amount of free nitroxide remaining in the reaction mixture after initiation (8). Initial successful polymerization employed a molar ratio of TEMPO to initiator of 1.3 to 1. A slight excess of nitroxide was required to ensure that all the newly generated polymer chains were terminated by nitroxide and that none escaped and grew out of control (9). Runaway polymer chains would not only would broaden the polydispersity but also result in dead chains (10) which become a problem if further reaction of the living chains is contemplated. Some nitroxide is also lost as a result of the promoted dissociation of BPO by TEMPO (11). After initiation, the excess nitroxide becomes a problem because it shifts the equilibrium from the uncapped to the capped form of the polymer chain resulting in a decrease in monomer addition and the polymerization rate. Reducing the excess nitroxide levels, and thereby, increasing the rate of polymerization, can be accomplished in a number of ways. The initiation can be performed with a molar ratio of TEMPO to BPO of less than 1.3. However, this causes a broadening in the polydispersity and the formation of dead polymer chains (10). Additives, such as camphorsulfonic acid (2a, 12) or 2-fluoro-1-methylpyridinium *p*-toluenesulfonate (13), have been shown to be effective at increasing the rate of polymerization by reducing the level of free nitroxide without adversely affecting the livingness of the system. And finally, the use of initiator-nitroxide adducts, such as (1) (14), (2) (15), (3) (16), enables the polymerization to proceed, ostensibly, with an equal ratio of initiating and nitroxide radicals, although in fact, there is always an excess of free nitroxide even in these materials. These initiator-adducts are also ideal molecules for studying the kinetics and mechanism of the SFRP process.

In 1996, Catala et al. (16) studied the kinetics of the SFRP process with (3) at temperatures below 100°C to avoid auto-initiation and showed that the molecular weight of the polystyrene varied according to the amount of initiator (3) used. That is, if the amount of initiator was doubled relative to a control polymerization, the number average molecular weight of the polymer was halved. This is not unexpected. However, what was interesting was that regardless of the amount of initiator used, the conversions, for a given set of reaction conditions, remained the same. To explain these results, Catala et al. proposed a high association of polymer chains. Matyjaszewski et al. (17) proposed the rate of polymerization was not affected by the



amount of initiator (adduct) because the majority or all the polymer propagating radicals in the SFRP process are produced by auto-initiation. The role of the adduct, it was suggested, is to control the molecular weights and polydispersities by bimolecular and/or unimolecular exchange. Fukuda et al. (18) explained the independence of conversion on the concentration of initiator by invoking a stationary state between the active propagating chains and free nitroxide. This enabled a polymerization rate expression to be derived that is the same as that of a conventional free radical polymerization and independent of the adduct-initiator concentration.

In a series of papers on the kinetics of the nitroxide-mediated free radical polymerization, initiated by BPO, we proposed that the rate of polymerization, and therefore, conversion, is related to the excess nitroxide in the polymerization mixture (5,19). Initial polymerizations, in which a 1.3 to 1 molar ratio of nitroxide to initiator was used, were slow as a result of the excess nitroxide, readily measured and monitored by electron spin resonance, ESR. Reducing the amount of excess nitroxide, by adding CSA, for example, resulted in an increase in the rate of polymerization and an increase in conversion with time. Catala, however, used (3) as the initiator to study the SFRP process assuming that there would be no excess nitroxide in the polymerization reaction mixture. This paper describes our results and the kinetic analysis of the SFRP process at both very low and high levels of excess nitroxide. In the process, the extent of the role of auto-initiation in these polymerizations is elucidated. The rate of monomer conversion in the SFRP polymerization is shown to be controlled by the excess of nitroxide in the polymerization reaction mixture.

Experimental

Polystyrene was distilled over calcium hydride and used immediately. BST was prepared by heating BPO and TEMPO in the presence of styrene for 10 minutes under argon in a preheated oil bath maintained at 135°C. The excess solvent was removed, the reaction mixture was diluted with ethyl acetate and washed with a dilute solution of sodium hydroxide to remove benzoic acid. The ethyl acetate solution was washed once with water, dried over sodium sulfate and concentrated under vacuum. The resulting material was passed through a column of silica gel using methylene chloride as the eluant. Yields of 25-30% of BST were typically obtained. The BST was recrystallized from either hexanes or isopropanol. Polymerizations were performed in sealed tubes after the samples were frozen and thawed twice under vacuum to remove air. The sealed tubes were completely submerged in an oil bath preheated to 130°C. Molecular weights were estimated using gel permeation chromatography (GPC) using a Waters/Millipore liquid chromatograph equipped with a Waters model 510 pump, Ultrastayragel columns of pore size 10^4 Å, 10^3 Å, 500 Å, and 100 Å and a flow rate of 0.8 mL/min. Samples were detected with a Waters differential refractometer. Molecular weights were determined on samples without any prior purification. Polydispersity was determined by the ratio of the weight average molecular weight (M_w) to the number average molecular weight (M_n).

Results and Discussion

Three polymerizations of styrene were performed with BST at concentrations of 6.6×10^{-3} , 13.2×10^{-3} , and 26.4×10^{-3} M, over a period of three hours with samples removed at each hour. The molecular weights, polydispersities and conversions of the samples from the polymerizations are shown in Table 1. In spite of the fact that we initiated our polymerizations with a different initiator-adduct and performed the polymerizations at higher temperature, both conditions chosen to mimic a typically SFRP process, our results are similar to those of Catala et al. (16). A dependence of molecular weight on the amount of initiator was evident. Conversions, however, were the same for each polymerization for a given time and independent of the amount of initiator.

While there is a dependence of molecular weight on the amount of initiator used, it is clear by looking at the 3 hour samples in Table 1, for example, that the number average molecular weights did not vary as expected with the change in concentration of the initiator. Ideally, the molecular weights of the 13.2×10^{-3} M and 26.4×10^{-3} M samples should have been one-half and one-quarter, respectively, that of the 6.6×10^{-3} M sample. If one compares the theoretical molecular weights with the actual number average molecular weights it can be seen that the lower the concentration of BST the larger the deviation between actual and theoretical molecular weights. These differences are likely dominated by auto-initiation (20) and the contribution it makes to the number of polymer chains in the reaction mixture. Clearly, at low

concentrations of initiator, auto-initiation makes a significant contribution to the total number of polymer chains, but not to the extent that it completely controls the number of propagating chains. However, for a given amount of styrene, the number of auto-initiated chains is more or less constant. Therefore, as the concentration of initiator is increased, producing more polymer chains, the contribution of the auto-initiated chains to the total number of polymer chains becomes less important. Thus, for the case where a 26.4×10^{-3} M concentration of BST is used, there is only a very small deviation between actual and theoretical molecular weight. However, these results do suggest that to make very high, predictable molecular weights by the SFRP process at 125°C or higher, the suppression of auto-initiation will be necessary. Furthermore, in spite of the fact that in some of these polymerizations auto-initiation is an important contributor and in others it is not significant, the conversions of these polymerizations are still the same for a given time. Therefore, the reason the conversions are the same from polymerization to polymerization cannot be attributed to auto-initiation.

Table 1. Physical parameters of polystyrene samples prepared with BST as the initiator at a reaction temperature 130°C.

Sample	BST/T (molar)	Mn	PD	Conversion
1	10	35,420	1.20	34
2	5	29,176	1.21	30
3	4	22,121	1.20	25
4	3.3	14,311	1.20	19

Oil bath temperature, 130°C; reaction time 2.5h

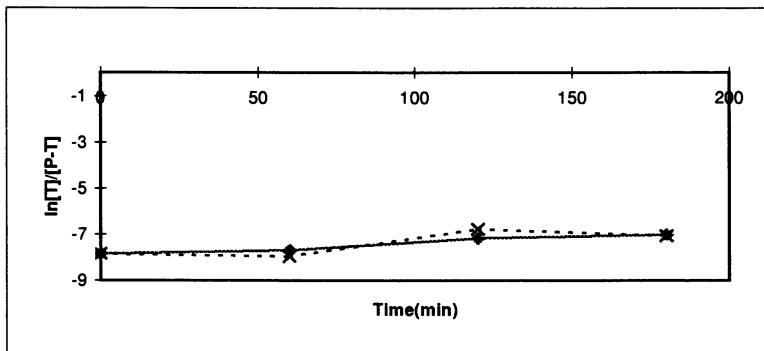
Another series of polymerizations with BST were performed for 2.5 hours in an oil bath maintained at 130°C but with added TEMPO, as summarized in Table 2. What is immediately evident is that as the concentration of TEMPO is increased the conversion is decreased, as is the molecular weight. Under these polymerization conditions, excess nitroxide affects the rate of polymerization by affecting the equilibrium between the capped and uncapped forms of the polymer chain, with excess nitroxide favoring the capped form. The question still remains, how do we tie these results in with those that are obtained with the initiator-nitroxide adducts such as (3) or BST, reagents which are assumed not to contain any excess nitroxide. To answer this question, we went back and looked more closely at the purity of the BST adduct. The amount of free nitroxide in a BST sample, crystallized from hexane and allowed to sit at room temperature for two weeks, was measured in xylene (2.7×10^{-3} M) and found to be 1.5×10^{-6} M. When the same sample was freshly recrystallized from isopropanol, crushed and dried under vacuum for 6 hours, the concentration of free nitroxide of a 3.4×10^{-3} M solution was found to be 5.80×10^{-7} M (16). So,

while the amount of free nitroxide was reduced, some was still present. As the second sample was allowed to sit in solution at room temperature for 6 hours, the free nitroxide level increased 250%. If the BST is purified to a very low level of free nitroxide, the free nitroxide level quickly equilibrates, at room temperature, to within a range of 10^{-6} M. When the BST is heated in xylene to 125°C , the temperature at which the polymerization of styrene is typically polymerized by the SFRP process, within minutes, the level of free nitroxide increases even further. Thus, it appears that regardless of how well the BST is purified, there will always be some residual nitroxide in the polymerization mixture. The total amount of nitroxide in the polymerization can be defined as follows:

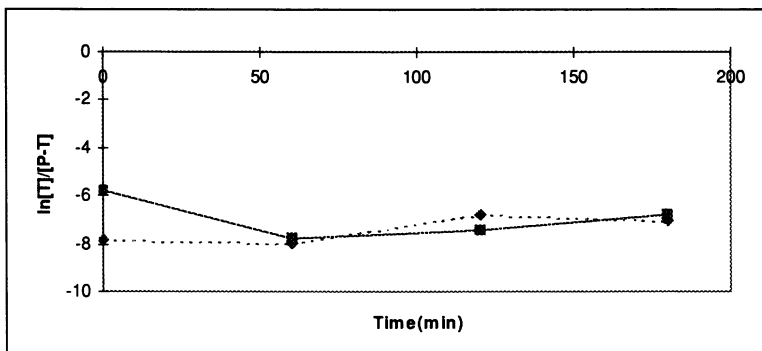
$$[\text{T}]_t = [\text{T}]_{\text{eq}} + [\text{T}]_{\text{ex}}$$

where $[\text{T}]_t$ is the total amount of free nitroxide in the polymerization mixture under a given set of polymerization conditions at any given time, $[\text{T}]_{\text{eq}}$ is the equilibrium amount of nitroxide resulting from homolytic dissociation of nitroxide from the polymer chain ends and is in the order of approximately 10^{-8} to 10^{-9} M (7,8), and $[\text{T}]_{\text{ex}}$ is the excess nitroxide level discussed above and is in the range of 10^{-6} M. $[\text{T}]_t$ is primarily determined by $[\text{T}]_{\text{ex}}$. Doubling the amount of BST will generate twice the amount of polymer chains which should lead to twice the conversion for a given amount of time. However, doubling the amount of BST will also double the amount of excess nitroxide, which will reduce the actual number of propagating radical chains at any one time by a half. Thus, although there are twice as many polymer chains in the reaction mixture only half as many propagating radical chains are present as compared to the reaction with half the amount of initiator. The net result is that both polymerizations contain the same number of propagating radical chains resulting in the same rate of polymerization for the polymerizations with different amounts of initiator adducts.

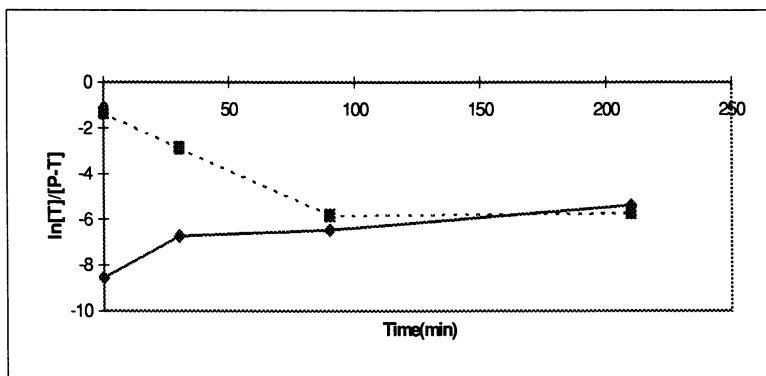
To demonstrate this experimentally, two polymerizations were performed under the same conditions with the exception that in one polymerization, 1.3×10^{-3} M BST was used and in the second 2.6×10^{-3} M BST was used. The level of free nitroxide in the reaction mixtures were monitored over time and plotted as a function of $\ln [\text{T}]/[\text{P-T}]$ versus time, where $[\text{T}]$ is the concentration of free nitroxide in the reaction mixture at any given time and $[\text{P-T}]$ is the concentration of BST added. What was interesting was that the ratio of $[\text{T}]/[\text{P-T}]$ remained more or less constant throughout the polymerizations, Plot 1. After three hours, the measured amount of free nitroxide in the polymerization with 13.2×10^{-3} M BST was 1.32×10^{-6} whereas, in the second polymerization in which 26.4×10^{-3} M BST was used, the free nitroxide level was 2.58×10^{-6} , or approximately twice the amount. The same trend has been found with substituted styrene polymerizations (21). If the polymerizations were repeated with added nitroxide, the $[\text{T}]/[\text{P-T}]$ ratio decreased with time until it reached the same ratio as the polymerization without the added TEMPO and then remained constant (Plot 2). The free nitroxide levels, after 3 hours, were 1.51×10^{-6} and 3.48×10^{-6} for the polymerizations with 13.2×10^{-3} M and 26.4×10^{-3} M BST, respectively, similar to the amounts found above for the system with no added nitroxide. In another case,



Plot 1. Change of TEMPO concentration as a function of time for the polymerization of styrene initiated with 13.2×10^{-3} (---) and 26.3×10^{-3} (—) M BST.



Plot 2. Change of TEMPO concentration as a function of time for the polymerization of styrene initiated with 13.2×10^{-3} M BST, with (—) and without (---) added TEMPO.



Plot 3. Change of TEMPO concentration as a function of time for the polymerization of styrene initiated with a BST sample with very little free nitroxide (—) and with added TEMPO (---).

where the amount of excess nitroxide was very low, the concentration increased and then remained constant, Plot 3 (22). The $[T]/[P-T]$ ratio corrects itself to attain an equilibrium value defined by reaction parameters such as temperature and $[P-T]$.

Table 2. Effect of molecular weight and conversion on the polymerization of styrene as a function of added TEMPO to BST.

Rxn. Time (h)	BST($10^{-3}M$)	Mn	% Mn Deviation	PD Conversion	%
1	6.6	27,396	14	1.26	23
2	6.6	41,054	22	1.20	38
3	6.6	51,385	23	1.23	48
1	13.2	14,364	6	1.24	22
2	13.2	24,053	11	1.19	39
3	13.2	30,231	13	1.17	50
3	26.4	16,627	3	1.16	50

Oil bath temperature, 130°C

In conclusion, it has been demonstrated that conversion in the nitroxide-mediated living free radical polymerization process is controlled by excess free nitroxide in the polymerization mixture. The excess free nitroxide is, in turn, determined by the amount of initiator (P-T). It has also been demonstrated that in the cases where only a small amount of initiator is required in order to achieve very high molecular weights, the contribution of auto-initiation to the number of living polymer chains must be considered. However, even under these conditions, the number of polymer chains is still predominantly determined by the amount of initiator used.

References

- (1) Georges, M. K.; Veregin, R. P.N.; Kazmaier, P. M.; Hamer, G. K. *Macromolecules*, **1993**, *26*, 2987
- (2) a) Georges, M. K.; Veregin, R. P. N.; Hamer, G. K.; Kazmaier, P. M.; Saban, M. *Macromolecules* **1994**, *27*, 7228. (b) Georges, M. K.; Veregin, R. P. N.; Kazmaier, P. M.; Hamer, G. K. *Macromol. Symp.* **1994**, *88*, 89. (c) Keoshkerian, B.; Georges, M. K.; Boils-Boissier, D. *Macromolecules* **1995**, *28*, 6381. (d) Saban, M.; Georges, M. K.; Veregin, R. P. N.; Hamer, G. K.; Kazmaier, P. M. *Macromolecules* **1995**, *28*, 7032. (e) Listigovers, N. A.; Georges, M. K.; Odell, P. G.; Keoshkerian, B. *Macromolecules* **1966**, *29*, 8992

- (3) Kato, M.; Kamigaito, M.; Sawamoto, M.; Higashimura, T. *Macromolecules*, **1995**, *28*, 1721. Wang, J.; Matyjaszewski, K. *J. Am. Chem. Soc.* **1995**, *117*, 5614.
- (4) Georges, M. K.; Veregin, R. P. N.; Hamer, G. K.; Kazmaier, P. M. *Polym. Prepr* **1994**, *35*(2), 582. Georges, M. K.; Veregin, R. P. N.; Hamer, G. K.; Kazmaier, P. M. *Macromol. Symp.* **1994**, *88*, 89. Yoshida, E.; Ishizone, T.; Hirano, A.; Nakahama, S. Takata, T.; Endo, T. *Macromolecules*, **1994**, *27*, 3119. Hawker, C. J. *J. Am. Chem. Soc.* **1994**, *116*, 11185. Fukuda, T.; Terauchi, T.; Goto, A.; Tsujii, Y.; Miyamoto, T. Shimizu, T. *Macromolecules*, **1996**, *29*, 3050
- (5) Hawker, C. J. *Angew. Chem., Int. Ed. Engl.* **1995**, *34*, 1456. Hawker, C. J.; Frechet, J. M. J.; Grubbs, R. B.; Dao, J. *J. Am. Chem. Soc.* **1995**, *117*, 10763
- (6) Moad, G.; Rizzardo, E.; Solomon, D. H. *Macromolecules*, **1982**, *15*, 909
- (7) Veregin, R.P.N.; Georges, M. K.; Hamer, G.K.; Kazmaier, P. M. *Macromolecules*: **1995**, *28*, 4391
- (8) Veregin, R. P. N.; Odell, P. G.; Michalak, L. M.; Georges, M. K. *Macromolecules*: **1996**, *29*, 2746
- (9) Veregin, R.P.N.; Georges, M. K.; Kazmaier, P. M.; Hamer, G. K. *Macromolecules*: **1993**, *26*, 5316
- (10) MacLeod, P. J.; Veregin, R. P. N.; Odell, P. G.; Georges, M. K. *Macromolecules* **1997**, *30*, 2207
- (11) Moad, G.; Rizzardo, E.; Solomon, D. H. *Tetrahedron Lett.* **1981**, 1165
- (12) Veregin, R. P. N.; Odell, P.G.; Michalak, L. M.; Georges, M. K. *Macromolecules* **1996**, *29*, 4161
- (13) Odell, P.G.; Veregin, R. P. N.; Michalak, L. M.; Brousmiche, D.; Georges, M. K. *Macromolecules*, **1995**, *28*, 8453
- (14) Veregin, R. P. N.; Georges, M. K.; Kazmaier, P. M.; Hamer, G. K. *Polym. Prepr (Am. Chem. Soc., Div. Polym. Chem.)*, **1994**, *35*(2), 582. Hawker, C. J. *J. Am. Chem. Soc.*, **1994**, *116*, 11185
- (15) Howell, B. A.; Priddy, D. B.; Li, I.Q.; Smith, P. B.; Kastl, P. E. *Polymer Bulletin* **1996**, *37*, 451
- (16) Catala, J. M.; Bubel, F.; Oulad Hammouch, S. *Macromolecules*, **1995**, *28*, 8441
- (17) Matyjaszewski, K.; Greszta, D. *Macromolecules*, **1996**, *29*, 5239
- (18) Fukuda, T.; Terauchi, T. *Chem. Letters*, **1996**, 293.
- (19) Veregin, R. P. N.; Odell, P. G.; Kazmaier, P. M.; Georges, M. K.; (Accepted for publication in *Chem. Letters*)
- (20) Moad, G.; Rizzardo, E.; Solomon, D. H. *Polymer Bulletin*, **1982**, *6*, 589. Georges M. K.; Kee, R. A.; Veregin, R. P. N.; Hamer, G. K.; Kazmaier, P. M.; *J. Phy. Org Chem.* **1995**, *8*, 301. Devonport, W; Michalak, L.; Malmstrom, E.; Mate, M.; Kurdi B.; Hawker, C. J.; Barclay, G. G.; Sinta, R. *Macromolecules*, **1997**, *30*, 1929
- (21) Daimon, K.; Kazmaier, P. M.; Veregin, R. P. N.; Hamer, G. K.; Georges, M. K. (Manuscript in preparation)
- (22) Baldovi, M. V.; Mohtat, N.; Scaiano, J. C. *Macromolecules*, **1996**, *29*, 549

Chapter 11

Mechanism and Kinetics of Nitroxide-Controlled Free-Radical Polymerization

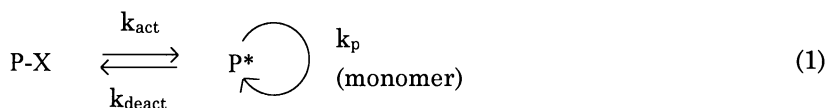
Takeshi Fukuda, Atsushi Goto, Kohji Ohno, and Yoshinobu Tsujii

Institute for Chemical Research, Kyoto University, Uji, Kyoto 611, Japan

The mechanism and kinetics of the polymerization of styrene in the presence of alkoxyamine (P-X) were discussed on the basis of experimental and computer-simulated data for a styrene/TEMPO system, where TEMPO is 2,2,6,6-tetramethylpiperidiny-1-oxy. It was confirmed that the stationary-state kinetics holds accurately except for an initial short time. Namely, in this state the radical concentration $[P^*]$ and hence the rate of polymerization are determined solely by the balance of the initiation and termination reactions, just like in a nitroxyl-free system. ESR studies showed the existence of the reversible dissociation of P-X. Two mutually related but basically different methods to determine the activation rate constant k_{act} were described. It was shown that the spontaneous dissociation of P-X is the only main mechanism of activation in the styrene/TEMPO system. The polydispersity of the product is thus determined by the rate constant of dissociation k_d ($= k_{act}$) and polymerization time, and the chain length is determined by the number of P-X adducts and $[P^*]$. Hence $[X^*]$ and the rate constant of combination (association) play no role (in the stationary state) but to maintain the stationary state. Other reactions such as initiation, termination and the thermal decomposition of P-X produce deviations from the behavior of an ideal living system. Since all these rate constants are available, details of the polymerization process and product characteristics can now be predicted.

The recent development of “living” radical polymerization is opening up a new and versatile route to well-defined, narrow-polydispersity polymers (*I-7*). This method has several different branches, but all of them are based on a common basic concept

of the alternating activation-deactivation process. Namely, a potentially reactive polymer species in such a system is supposed to go through an activated and a deactivated state alternately. In the activated state (P^*), it may be added by the monomer, while in the deactivated state ($P-X$), the reactive chain end is blocked with no polymerization allowed. Examples of blocking agents (X) include sulfur compounds (8), stable nitroxyls (9-11), halogens (12-14), and transition metal compounds (15, 16). The blocked chain remains dormant until it is reversibly deblocked by, e.g., thermal (9-11, 15), photochemical (8, 16) or chemical (12-14) activation:



Here k_p is the propagation rate constant, and k_{act} and k_{deact} are the rate constants of activation (deblocking) and deactivation (blocking) reactions, respectively, with a reaction order dependent on mechanistic details. A number of such activation-deactivation cycles and a low concentration of P^* allow all the chains to grow slowly and simultaneously, suppressing irreversible bimolecular termination to a minor level. This seems to be the current, most common understanding of the basic mechanism by which well-defined polymers are produced in such systems (17).

However, much remains to be studied of the mechanistic and kinetic details of the individual systems. This work concerns the nitroxyl-mediated polymerization of styrene, one of the most extensively studied systems (see reviews 1-7). Important progress in understanding the mechanistic and kinetic aspects of this system can be found in recent publications (18-34; literature 29 includes a recent review on this topic). However, there still is a great deal of confusion regarding the mechanism and the exact roles of the individual elementary reactions involved in this polymerization. The purpose of this work is to summarize published and unpublished studies mostly by ourselves, hopefully establishing some unified views of this important branch of "living" radical polymerization. We also hope that the particular experimental approaches adopted to the nitroxyl system will also be useful to study other systems.

Elementary Reactions in Alkoxyamine-Mediated Polymerization of Styrene

We confine ourselves to a styrene system containing a purified alkoxyamine and, if necessary, a radical initiator but with no extra nitroxyl added. In this condition, the system will quickly reach a stationary state that can be treated most simply, providing the clearest picture of what is happening in such a system. In this work, initiators will mean usual initiating compounds like benzoyl peroxide and azobisisobutyronitrile but not mediating compounds like alkoxyamines, and the term initiation will be used according to this definition, unless otherwise stated.

Generally, the alkoxyamine-containing styrene system at a high temperature may involve the eight elementary reactions given in Figure 1. The rate and rate constant of each reaction are defined in the figure. The thermal (spontaneous) initiation is assumed to be third order in the monomer concentration $[M]$ with a rate constant k_i (36). In the presence of a radical initiator I (overall initiation rate constant k_i'), the two initiations are assumed to be additive. The rate constants of propagation and termination are also available in the literature (36, 37). The chain transfer to the monomer (styrene) is known to be unimportant compared with that to the Diels-Alder adduct or the Mayo dimer (29, 36).

Li et al. (26) reported that 2,2,6,6-tetramethyl-1-(1-phenylethyl)piperidine (S-TEMPO; Figure 2) decomposes at high temperatures through the abstraction of the β -proton by the TEMPO radical, producing an alkene (styrene) and a hydroxyamine. We made NMR studies with the two model compounds BS-TEMPO and PS-TEMPO (Figure 2; $n \approx 10$) and confirmed that the decomposition is a first-order reaction with rate constants given by $k_{\text{dec}}/\text{s}^{-1} = 4.7 \times 10^{14} \exp(-157\text{kJ}/\text{RT})$ for BS-TEMPO and $5.7 \times 10^{14} \exp(-153\text{kJ}/\text{RT})$ for PS-TEMPO, in toluene (38). These results indicate that in the TEMPO-mediated polymerization of styrene, the decomposition of the active chain-ends would occur at an important level especially at high temperatures.

The remaining reactions, i.e., dissociation, combination, and degenerative transfer (4, 17) are supposed to form the "heart" of this "living" radical polymerization. To shed light on these reactions, in situ ESR studies (19, 20, 33) and computer-assisted analyses of the evolution of product polydispersities (21, 29) were carried out besides the most common time-conversion studies. Those approaches provided a lot of important information but were not necessarily powerful enough to reach the center of the "heart". For example, it has been suggested for some time that degenerative transfer may participate in the activation process of the styrene/TEMPO system (17, 25), but no clear answer has been provided by these approaches. We recently devised two mutually related but basically different methods that enable us to closely study activation processes, as will be described later.

Polymerization Rate

The rate (R_p) of nitroxyl-mediated polymerization of styrene had not been well understood until recently, when Catala et al. (23) reported the experimental data showing that R_p is independent of the concentration of the model adduct S-DBN (Figure 2) used as a mediator. Even though these authors attempted to interpret their result differently, we pointed out that it can be most simply interpreted in terms of the stationary-state kinetics (32). Of the eight reactions in Figure 1, only reactions 1, 2, 4, and 5 are relevant to changes in radical concentrations, and $[P^*]$ and $[X^*]$ should follow the differential equations

$$d[X^*]/dt = k_d[P-X] - k_c[P^*][X^*] \quad (2)$$

$$d[P^*]/dt = k_d[P-X] - k_c[P^*][X^*] + R_i - k_t[P^*]^2 \quad (3)$$

Reaction	Rate
(1) Dissociation $P-X \rightarrow P^* + X^*$	$k_d[P-X]$
(2) Combination $P^* + X^* \rightarrow P-X$	$k_c[P^*][X^*]$
(3) Propagation $P^* + M \rightarrow P^*$	$k_p[P^*][M]$
(4) Initiation	$k_i[M]^3 + k_i'[I]$
(5) Termination $P^* + P^* \rightarrow \text{dead polym.}$	$k_t[P^*]^2$
(6) Decomposition of P-X $P-X \rightarrow \text{dead polym.} + XH$	$k_{dec}[P-X]$
(7) Chain transfer $P^* + RH \rightarrow PH + R^*$	$k_{ct}[P^*][RH]$
(8) Degenerative transfer $P^* + P'-X \rightarrow P'^* + P-X$	$k_{ex}[P^*][P-X]$

Figure 1. Possible elementary reactions in a nitroxyl mediated polymerization of styrene.

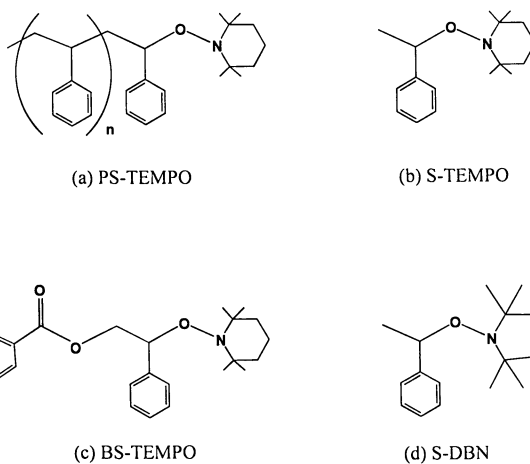


Figure 2. Structures of model compounds.

where R_i is the rate of initiation. If R_i is non-zero, the system will sooner or later reach the stationary state in which $d[P^*]/dt = d[X^*]/dt = 0$, and we have

$$[P^*] = (R_i / k_t)^{1/2} \quad (4)$$

$$[X^*] = (k_d / k_c) [P-X] / [P^*] \quad (5)$$

Namely, the stationary concentration of P^* is determined by the balance of the initiation and termination rates (equation 4), while that of X^* depends not only on this stationary value of $[P^*]$ but also on $[P-X]$ and the k_d/k_c ratio (equation 5). Hence R_p reads

$$\begin{aligned} R_p &= k_p [P^*] [M] \\ &= (k_p / k_t^{1/2}) R_i^{1/2} [M] \end{aligned} \quad (6)$$

which is independent of $[P-X]$, as experimentally observed (23).

We made further tests of equation 6. In one way, we followed the time-conversion relation by dilatometry (33). Figure 3 compares the first-order plots for the styrene polymerizations with and without a PS-TEMPO or a BS-TEMPO adduct. Clearly, the R_p s of the nitroxide systems are the same with each other, and when the conversion is small (< 30 %), they are equal to that of the thermal (nitroxide-free) system. Equation 6 was thus evidenced by this experiment. The deviations at higher conversions are due to changes in k_t arising from differences in chain length and viscosity. In fact, the dotted curve, which was calculated with $[M]^3$ -dependent R_i and constant k_t , gives the smallest R_p at high conversions.

In an alternative way to test equation 6, we added the radical initiator *t*-butylhydroperoxide (BHP) to PS-TEMPO containing styrene (35). As in a nitroxide-free system, R_p was observed to increase with increasing concentration of BHP. For example, the addition of 4×10^{-3} mol L⁻¹ of BHP increased R_p by a factor about 3. Nevertheless, the chain length and its distribution were well controlled at least in this range of R_p . This is demonstrated in Figure 4, in which the number-average molecular weight M_n and the M_w/M_n ratio are plotted against the conversion. The fact that all M_n values fall on a single straight line indicates constancy or approximate constancy of the number of polymers throughout the course of polymerization. For a given conversion, M_w/M_n increases with increasing [BHP], which, at a first sight, may appear to indicate that the control of the polydispersity becomes more difficult as [BHP] or R_p increases. However, this is not true. Main reasons for this are the difference in polymerization time and the chain length of the product polymer relative to that of the "initiator" adduct, as will be discussed in the *Computer Simulation* section.

All these results show the validity of the stationary-state arguments. The R_p of a nitroxide system is determined by the balance of the initiation and termination rates, as in a conventional system. In this regard, the thermal initiation and a radical initiator play essentially the same role. The reversible dissociation of $P-X$ plays the role of controlling the chain length distribution but not the stationary value of R_p .

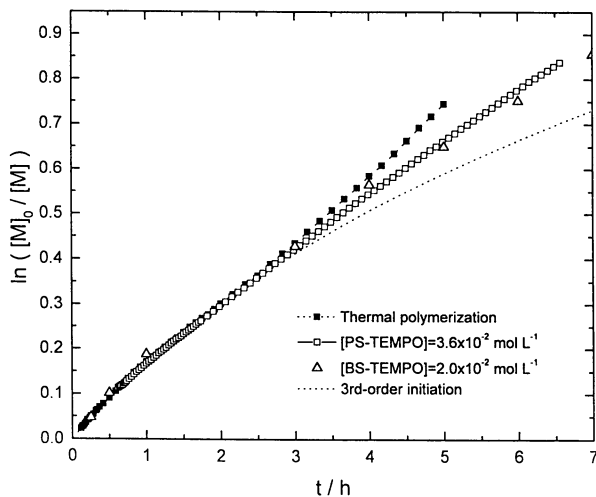


Figure 3. First-order plot for the polymerization of styrene at 125 °C: [PS-TEMPO]₀ = 36 mmol L⁻¹ (□); [BS-TEMPO]₀ = 20 mmol L⁻¹ (△); no nitroxide (■); the dotted line shows the [M]³-dependent initiation with constant k_i (no nitroxide): cited from literature 33.

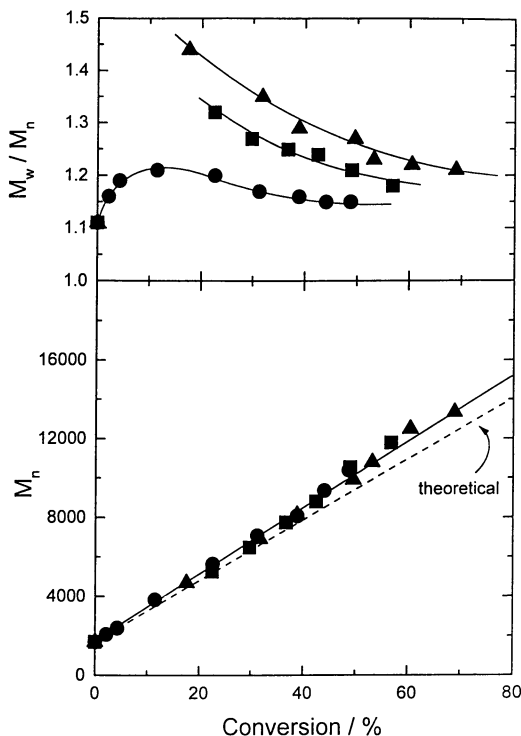


Figure 4. Plot of M_w/M_n and M_n vs. monomer conversion for the polymerization of styrene at 114 °C with [PS-TEMPO]₀ = 48 mmol L⁻¹: [BHP]₀ = 0 (●), 2.0 mmol L⁻¹ (■), and 4.0 mmol L⁻¹ (▲).

In Controlled Radical Polymerization; Matyjaszewski, K.;

ACS Symposium Series; American Chemical Society: Washington, DC, 1998.

Insofar as the cumulative number of the chains produced thermally or by means of a radical initiator is small compared with the number of P-X molecules as in the above-cited systems, the initiation (and termination) reactions have only a minor effect on the chain length distribution. This suggests a useful means to control the R_p (and hence M_n) of the nitroxide-mediated system by means of initiators. Moreover, there possibly can be systems in which the reversible dissociation of P-X does occur but a thermal initiation does not, and for this reason, controlled polymerization does not proceed successfully. Those dormant systems may possibly be “awaken” by using a radical initiator (32-35). Nearly the same conclusions regarding the roles of initiation and initiator in a nitroxide system have been reached by Greszta and Matyjaszewski independently (29; *J. Polym. Sci., Polym. Chem. Ed.*, in press).

Equilibrium Constant

The existence of the reversible dissociation of P-X adduct will be evidenced by showing the existence of the equilibrium constant K

$$K = k_d / k_c \quad (7)$$

$$= [P^*][X^*] / [P-X] \quad (\text{at equilibrium}) \quad (8)$$

Since the time scale of “living” radical polymerization is generally much larger than that of chemical equilibration, the validity of equation 8 should not be limited to the stationary state discussed above (cf. the *Computer Simulation* section).

In situ ESR measurements were made for the same PS-TEMPO/styrene/125°C system as in Figure 3 (33). Figure 5a shows the TEMPO concentration $[X^*]$ as a function of polymerization time, in which $[X^*]$ is on the order of 10^{-5} mol L⁻¹ and gradually *increases* with time. Figure 5b shows the PS radical concentration $[P^*]$ of the same system, which was estimated from Figure 3 by use of the known k_p value of 2300 L mol⁻¹ s⁻¹ (37). The figure shows that $[P^*]$ is on the order of 10^{-8} mol L⁻¹, and gradually *decreases* with time. Since the initial concentration of the adduct ($[P-X]_0 = 3.6 \times 10^{-2}$ mol L⁻¹) is much larger than both $[X^*]$ and $[P^*]$, $[P-X]$ can be equated to $[P-X]_0$. The value of K thus estimated is 2.1×10^{-11} mol L⁻¹, independent of time (Figure 5c). The time dependence of $[P^*]$ and $[X^*]$ is ascribed to the time dependence of R_i and k_t , as already mentioned.

A body of experimental data indicating the constancy of K have been reported also by Veregin et al. (20). The value of K at 125 °C estimated from their data (Figure 11 in literature 20) is about twice as large as the above-noted value. The reason for this discrepancy is unclear.

Activation-Rate Constant – Direct Evaluation

Method and Activation Mechanism of a Styrene/Nitroxyl System. The existence of the dissociation-combination equilibrium alone does not guarantee narrow polydispersity polymers. An essential parameter that controls the polydispersity is the dissociation rate constant k_d , or more generally, the activation

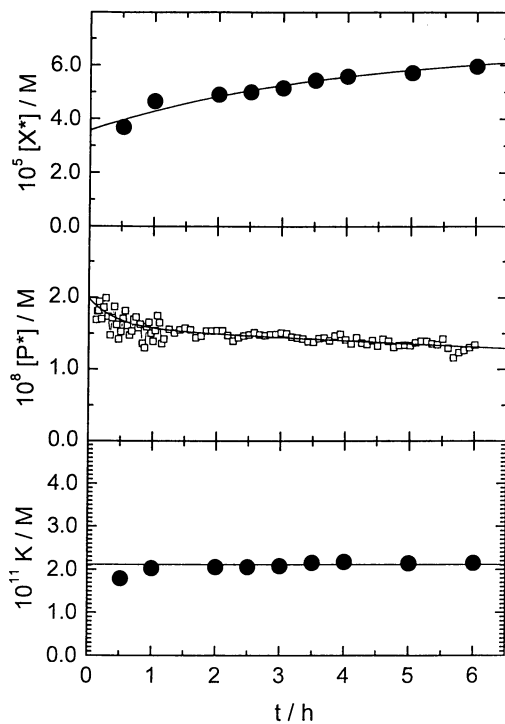


Figure 5. Plots of $[X^*]$, $[P^*]$ and K vs. t for the polymerization of styrene at 125 °C with $[PS\text{-}TEMPO]_0 = 36 \text{ mmol L}^{-1}$: cited from literature 33.

rate constant k_{act} . In the stationary state, the combination rate constant k_c controls the stationary concentration of X^* so that $k_c[X^*]$ is constant, but it has no effect on the polymer structure. (The process to reach the stationary state depends on k_c , however.) This is because the stationary concentration of P^* or R_p is independent of k_c (and k_d) in styrene/alkoxyamine systems (see above).

We have proposed a direct method to determine k_{act} (34, 39). It is based on the gel permeation chromatographic (GPC) observation of an early stage of the polymerization containing a probe adduct $P_0\text{-X}$. When $P_0\text{-X}$ is brought to a sufficiently high temperature, some $P_0\text{-X}$ molecules will undergo a cleavage of the C-ON bond during a given time interval t , and the dissociated P_0^* radicals will be added by the monomer until they are deactivated again by X^* to give new adducts $P_1\text{-X}$. Hence $P_0\text{-X}$ may be distinguishable from $P_1\text{-X}$ (or any other species possibly produced in the system) by GPC, owing to the difference in molecular weight and its distribution. Then k_{act} may be determined according to the first-order plot

$$\ln(S_0/S) = k_{\text{act}} t \quad (9)$$

where S_0/S is the ratio of the $P_0\text{-X}$ concentrations at time zero and t .

Technically, however, it is not always easy to resolve such a GPC curve quantitatively for the fraction of undissociated (or dissociated) $P_0\text{-X}$. To improve the resolution, the use of a radical initiator like BHP should be effective, as we have seen above. A styrene solution of a *constant* amount of PS-TEMPO ($[P\text{-X}]_0 = 23 \text{ mmol L}^{-1}$; $M_n = 1700$ and $M_w/M_n = 1.11$) and a variable amount of BHP was heated at $110 \text{ }^\circ\text{C}$ for time t , quenched to room temperature, and directly analyzed by GPC with a *constant* amount of the reaction mixture injected to the column system. Figure 6 shows the GPC curves of the mixtures for $t = 0$ and $t = 10$ min with various concentrations of BHP. Evident changes can be seen in the figure before and after the heat treatment. When $[\text{BHP}] = 0$, the curve becomes somewhat broader with the peak position slightly shifted to the higher-molecular weight side, but it is not easy to resolve such a curve into different components. When $[\text{BHP}]_0 \geq 5 \text{ mmol L}^{-1}$, the curves become bimodal. Clearly, they are composed of two components, i.e., the first component comprising the undissociated $P_0\text{-X}$ and the second component comprising $P_1\text{-X}$ and other minor species possibly originating from a further dissociation of $P_1\text{-X}$, the decomposition of BHP, etc. An analysis of these GPC curves show that the marked increase of the second component with increasing BHP is due predominantly to the dissociation of $P_0\text{-X}$ and the subsequent polymerization initiated with P_0^* that is prolonged by the effect of BHP. Such details, however, are not required in the present analysis.

The bimodal curves can be accurately resolved into the two components. The evolution of the $P_0\text{-X}$ concentration is shown in Figure 7 in a first-order plot. Since $P_0\text{-X}$ originally contains 5 % of potentially inactive species (without a TEMPO moiety), it has been corrected by subtracting $0.05S_0$ from both S_0 and S in equation 9. (The % inactive species was estimated by a chain-extension test. These species are presumed to be produced mainly by the thermal decomposition of the active chain ends and partly by bimolecular termination; literature 41.) Figure 7 shows that all

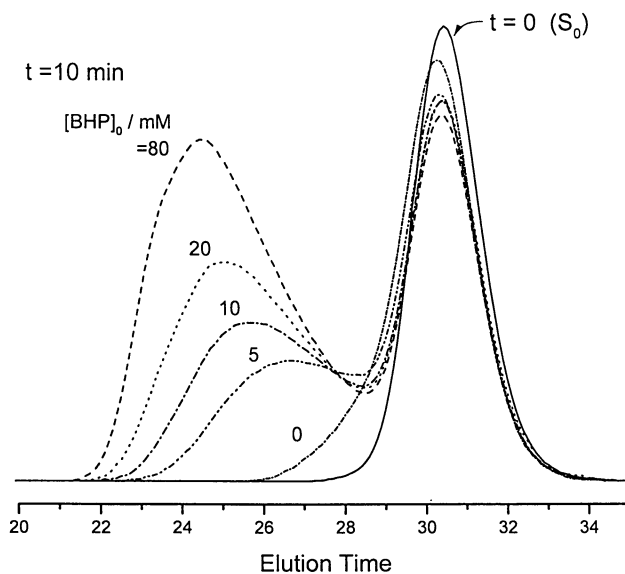


Figure 6. Polymeric regions of the GPC charts of the styrene/PS-TEMPO(P_0 -X)/BHP mixtures heated at 110 °C for 10 min: $[P_0\text{-X}]_0 = 23 \text{ mmol L}^{-1}$. The number attached on each curve indicates $[BHP]_0$ in mmol L^{-1} . The solid curve is for the original ($t = 0$) solution containing only P_0 -X as polymer species.

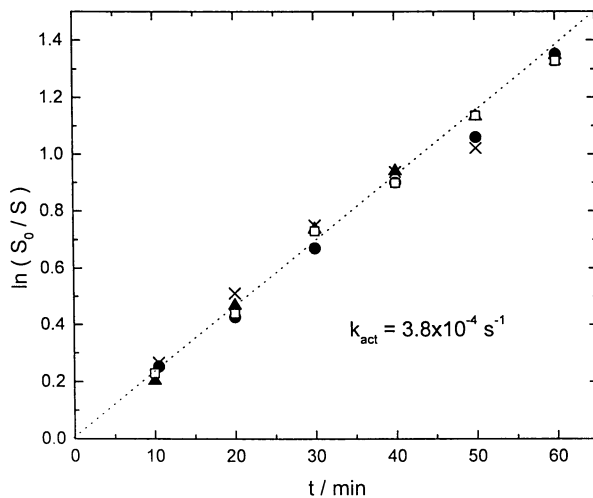


Figure 7. Plot of $\ln(S_0/S)$ vs. t : $[P_0\text{-X}]_0 = 23 \text{ mmol L}^{-1}$; $[BHP]_0 = 5$ (●), 10 (□), 20 (▲) and 80 (×) mmol L^{-1} .

the experimental points fall on a straight line passing through the origin with a slope of $3.8 \times 10^{-4} \text{ s}^{-1}$, showing no obvious trend with [BHP]. Thus this method allows us to determine the activation rate constant in a direct fashion with no regard to the kinetic details of the polymerization.

Another important implication of the mentioned experiment concerns the mechanism(s) of activation of this system. When degenerative transfer (17, 25) as well as spontaneous dissociation are operative in the system, the apparent rate constant of the activation reactions viewed as a first-order process will take the form (cf. Figure 1)

$$k_{\text{act}} = k_{\text{d}} + k_{\text{ex}} [\text{P}^*] \quad (10)$$

The above observation that k_{act} is independent of [BHP] hence R_p shows that the term $k_{\text{ex}}[\text{P}^*]$ is unimportant compared to k_{d} , and k_{act} may be identified with k_{d} , at least in the studied range of $R_p/[M] \leq 1 \times 10^{-4} \text{ s}^{-1}$ or $[\text{P}^*] \leq 1 \times 10^{-7} \text{ mol L}^{-1}$ (40). This conclusion should be valid at other temperatures, at least when the system contains no or a limited amount of a radical initiator.

Temperature Dependence of k_{d} . The above-mentioned method was used to determine k_{act} (actually k_{d}) of a PS-TEMPO adduct as a function of temperature (41). The result is given in an Arrhenius plot in Figure 8, which reads

$$k_{\text{d}} / \text{s}^{-1} = 3.0 \times 10^{13} \exp(-124 \text{ kJ} / \text{RT}) \quad (11)$$

(The equation for k_{d} given in our preliminary reports (34, 39, 43) is less accurate and should be replaced by equation 11.)

The k_{d} value of $1.6 \times 10^{-3} \text{ s}^{-1}$ at 125°C combined with the above-noted K value of $2.1 \times 10^{-11} \text{ mol L}^{-1}$ gives a k_{c} value of $7.6 \times 10^7 \text{ L mol}^{-1} \text{ s}^{-1}$. This value for the PS-TEMPO combination is reasonably compared to those between TEMPO and low-mass model radicals such as 1-phenylethyl (16×10^7) and 2-naphthyl-methyl (5.7×10^7) radicals (44).

By analyzing the evolution of polydispersities of a S-TEMPO containing system, Greszta and Matyjaszewski (29) estimated k_{c} to be $8 \times 10^7 \text{ L mol}^{-1} \text{ s}^{-1}$, in close agreement to the above value. By a similar analysis, Veregin et al. (21) reported a value of k_{c} of $1.5 \times 10^7 \text{ L mol}^{-1} \text{ s}^{-1}$ at 115°C . Since k_{c} should not largely depend on temperature, the difference in k_{c} cannot be ascribed to temperature. Possible causes for the difference were pointed out (29). Since the value of K estimated by Greszta and Matyjaszewski is crude, the mentioned agreement of the two k_{c} values may be accidental to some extent. A better parameter to make comparison of is k_{d} , which is essentially independent of the estimation of K (once the stationary state is reached). Their value of k_{d} of $8 \times 10^{-4} \text{ s}^{-1}$ is again in good agreement with the value $1.00 \times 10^{-3} \text{ s}^{-1}$ given by equation 11 (at 120°C). Since the polydispersities at later stages of polymerization are seriously affected by side reactions (29; see also below), k_{d} would be best estimated from the evolution of polydispersities at an early stage of

polymerization. The k_d value obtained by these authors seems to be based primarily on the early-stage data (28, 29). We will discuss this matter in detail in the next section.

Regarding the activation energy E of the PS-TEMPO dissociation reaction, Veregin et al. (20) made an ESR study and indirectly estimated E to be about 82 kJ mol^{-1} . This value is much lower than the value $130 \pm 4 \text{ kJ mol}^{-1}$ estimated by the same group (19) for the release of TEMPO from the low-mass model adduct BS-TEMPO. These authors suggested that the release of TEMPO is easier as the polymer chain becomes longer. This discussion is open to question, since the E value in equation 11 is rather close to their unimer value, indicating less significant dependence of k_d on chain length.

Activation-Rate Constant – Analysis of Polydispersities

The method for determining k_{act} described in the last section is free from any kinetic details, other than the existence of activation and propagation reactions, and it may be termed a “direct” method. The alternative approach described here is based on the use of GPC to follow the evolution of polydispersities. Unlike previous studies of this kind (21, 29), here we focus on a very initial stage of the polymerization started with a model adduct $P_0\text{-X}$, and analyze the differential polydispersities on the basis of the simple relations (35):

$$Y = w_A^2 Y_A + w_B^2 Y_B \quad (12)$$

$$2 [Y_B - (1 / x_{n,B})]^{-1} = k_{\text{act}} t \quad (13)$$

Here the product polymer is viewed as an A-B block copolymer with the subchains A and B referring to $P_0\text{-X}$ and the incremental part of the molecule, respectively; $Y = (x_w/x_n) - 1$, $Y_K = (x_{w,K}/x_{n,K}) - 1$, $w_A = 1 - w_B = x_{n,A}/x_n$, $x_n = x_{n,A} + x_{n,B}$, and x_n and x_w are the number- and weight-average degrees of polymerization ($K = A$ or B). Thus measurements of x_n and x_w of the product as a function of polymerization time t along with the known values of $x_{n,A}$ and $x_{w,A}$ (of $P_0\text{-X}$) allow one to calculate Y_B according to equation 12 and determine k_{act} according to the linear plot indicated by equation 13. This method is valid when side reactions are negligible and R_p is constant. This is an “indirect” method, since it depends totally on the accuracy of the theory and GPC and other kinetic details. However, unlike the direct method, it requires no particular resolution of GPC peaks (hence no addition of a radical initiator). We derived equation 13 by a probabilistic approach. An equivalent equation had been derived by Müller et al. (45, 46) by a kinetic approach, but the linearization based on the combination of equations 12 and 13 had never been embodied before us.

For example, Figure 9 shows the GPC traces of the polymers obtained by the polymerization of styrene at 110°C containing a fixed concentration (23 mmol L^{-1}) of PS-TEMPO ($x_{n,A} = 16.3$ and $x_{w,A} = 18.1$). The area under each curve minus that of the $t = 0$ curve gives the amount of monomer converted to polymer, which together with the x_n value estimated with the same curve gives the number of

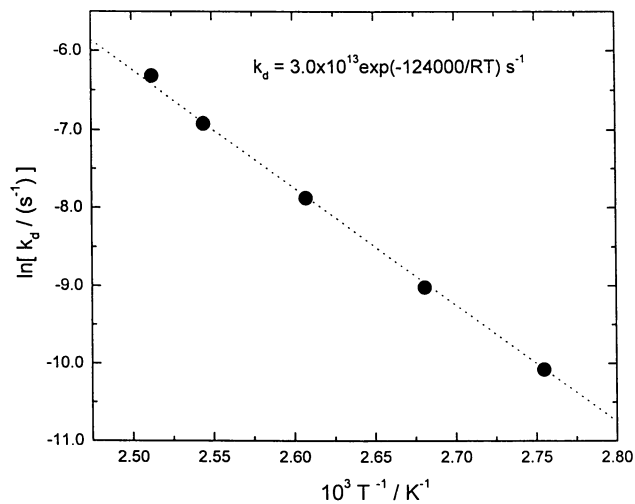


Figure 8. Plot of $\ln(k_d)$ vs. T^{-1} for the PS-TEMPO dissociation.

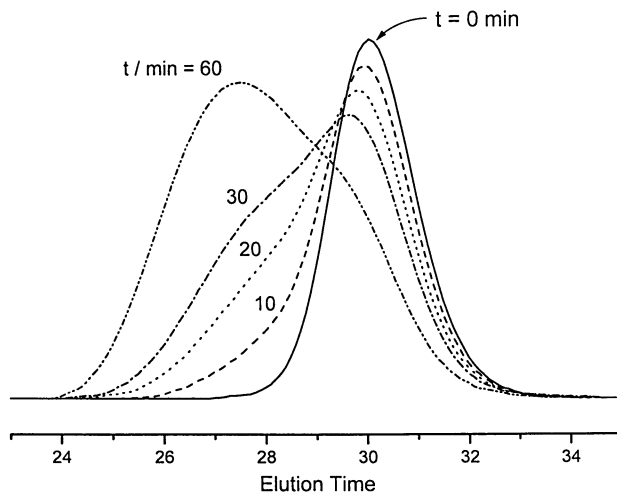


Figure 9. Polymeric regions of the GPC charts of the styrene/ PS-TEMPO (P_0-X) mixture heated at 110 °C for the time indicated in the figure: $[P_0-X]_0 = 23 \text{ mmol L}^{-1}$.

polymers $[N_p]$ per unit volume. The plot of $\ln([M]_0/[M])$ vs. t thus obtained was linear and justified the assumption of stationarity of R_p or $[P^*]$. The independence of $[N_p]$ on t indicated that side reactions are negligible in this range of t . With the GPC values of x_n , x_w , $x_{n,A}$, and $x_{w,A}$, we computed Y_B from equation 12 and made the plot indicated by equation 13. Appropriate correction was made for the inactive species included in P_0 -X in about 5 %. As Figure 10 shows, the plot is almost strictly linear.

The slope of the straight line gives a value of k_{act} (actually k_d) of $4.1 \times 10^{-4} \text{ s}^{-1}$. This value well agrees with the one determined by the direct method (see above). We have made a similar analysis of experimental data obtained at different temperatures with or without a radical initiator. In all cases, the rate constant values obtained by this and the direct methods agreed within $\pm 10 \%$. Thus, despite its indirect nature, this method provides sufficiently accurate values of k_{act} at least when the mentioned conditions are met (42).

Computer Simulation

We have seen that the stationary-state assumption provides simple descriptions of important aspects of nitroxide-mediated polymerization of styrene. The validity of the assumption was experimentally verified. More rigorous tests can be made by computer simulation (43). In this simulation, the transfer reactions (reactions 7 and 8 in Figure 1) and the termination by *disproportionation* were neglected, as they are of minor importance in the styrene/TEMPO system to be simulated here. The rate constants of all the remaining six reactions in Figure 1 are known. (Since the temperature dependence of k_c should be small, we assume $k_c = k_c(125 \text{ }^\circ\text{C}) = 7.6 \times 10^7 \text{ L mol}^{-1} \text{ s}^{-1}$.) Hence this simulation includes no adjustable parameters. The computation method of Yan et al. (47) was adopted.

In the simulated styrene polymerization at $110 \text{ }^\circ\text{C}$ with 23 mmol L^{-1} of PS-TEMPO (Figure 11), for example, it was observed that just after the onset of polymerization, $[P^*]$ steeply increases to a high value, much higher than the stationary-state value. This is because the dissociation of P-X predominates at this stage. As $[P^*]$ becomes higher, the combination between P*s occurs more and more frequently, leading to a rapid accumulation of X^* . Namely X^* increases more rapidly than P^* because of the bimolecular termination. When $[P^*]$ and $[X^*]$ reach a certain level, the combination between P^* and X^* and that among P*s dominate over the (constant rate of) dissociation, so that $[P^*]$ goes through a maximum, approaching the stationary value from above. On the other hand, $[X^*]$ steadily increases approaching the stationary value from below. These stationary values of $[P^*]$ and $[X^*]$ accurately agree with the values given by equations 4 and 5, respectively (the broken lines in the figure). The maximum in $[P^*]$ occurs at about 30 ms, and $[P^*]$ and $[X^*]$ reach within $\pm 10 \%$ of the stationary values in about a few minutes after the onset of polymerization. Thus, the stationary-state approximation is accurate enough to describe the polymerizations for $t > 10 \text{ min}$. The figure also shows that the constancy of $[P^*][X^*]/[P-X]$ or the equilibration holds from much earlier time ($< 1 \text{ min}$).

To demonstrate some other important implications given by the simulation, we

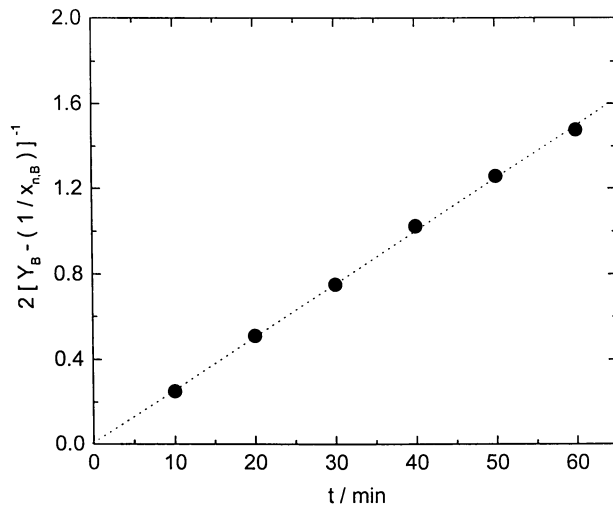


Figure 10. Plot of $2[Y_B - x_{n,B}^{-1}]^{-1}$ vs. t : data from Figure 9.

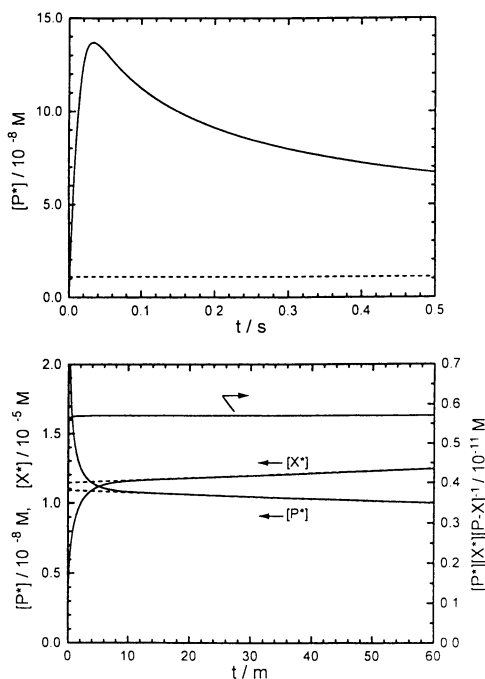


Figure 11. Plots of $[P^*]$, $[X^*]$, and $[P^*][X^*]/[P-X]$ vs. t : computer-simulated for the system in Figures 9 and 10 (110°C): $k_d = 4.4 \times 10^{-4} \text{ s}^{-1}$, $k_c = 7.6 \times 10^7 \text{ L mol}^{-1} \text{ s}^{-1}$, and other rate constants cited from the literature (see text). The broken lines show the stationary-state values (equations 4 and 5).

go back to Figure 4. Figure 12a shows the polydispersities of the polymers in Figure 4 with the contribution of the initiating $P_0\text{-X}$ (A subchain) subtracted by means of equation 12. All the data points fall approximately on the same curve, indicating that the polydispersity is determined essentially by polymerization time. The increase of R_p seems to affect the polydispersities very little in this plot. A more critical evaluation of this "living" radical polymerization is made by the plot of equation 13 (Figure 12b). The t axis was corrected for the inconstant monomer concentration in the batch polymerization, according to

$$t_{\text{corr}} = 2 C t [(C-2) \ln(1-C)]^{-1} \quad (14)$$

where C is the conversion (42; the factor -2 appearing in equation 4 in literature 42 is a misprint for $C-2$). The initial slope of the plot is equal to k_{act} , as before. If the system is an ideal living one with constant $[P^*]$ and no side reactions, it should follow the dotted straight line. Any deviations from the linearity indicate non-ideality, i.e., side reaction(s). In this plot, the data points clearly exhibit non-ideality above about 1 or 2 h, and the small differences observed in Figure 12a are more clearly visible: as the initiator concentration increases, the system shows larger deviations from the ideality. The three curves in Figure 12b were computer-simulated, which, with no adjustable parameter included, reproduce the experimental results satisfactorily.

Another implication of this simulation concerns the initial stage of the polymerization. In the region of $t < 1$ h, all the curves agree with each other, forming a single straight line and indicating that side reactions are unimportant in this region. Strictly speaking, the simulated line in a small t region ($t < 5$ min) had a curvature arising from the non-stationarity of $[P^*]$. However, this curvature was so small that the whole curve in the region of $10 \text{ min} < t < 60 \text{ min}$ could be well approximated by a straight line passing through the origin. The error in the evaluation of k_{act} arising from this source is estimated to be never larger than 10 %, if the experiments are made in the region $10 \text{ min} < t < 60 \text{ min}$. (The experiment given in Figure 10 was in fact conducted in this t range.) This magnitude of error is comparable with that of experimental one. The optimum range of t for the measurements can be different for different systems, but it can be predicted by computer simulation, as was illustrated here. Full details of the computer simulation will be described elsewhere (Tsuji, Y. et al., to be published).

Conclusions

(1) Except for a short time (typically a few minutes) after the onset of polymerization, the alkoxyamine-mediated polymerization of styrene can be accurately described by the stationary-state kinetics with $[P^*]$, $[X^*]$ and R_p given by equations 4, 5, and 6, respectively. Like in a nitroxyl-free system, R_i may include the contributions from the thermal initiation and radical initiators (if there is any in the system).

(2) In the absence of any other reactions (the "ideal" system), the polydispersity is determined by the number of activation-deactivation "cycles" that a

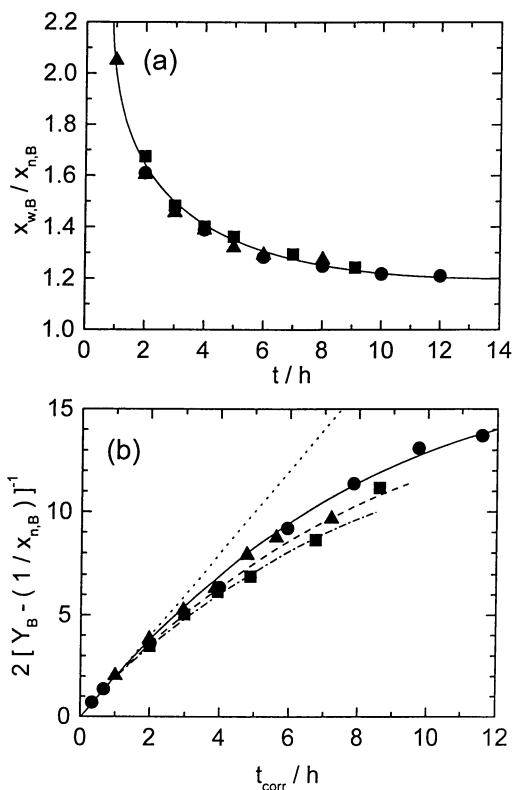


Figure 12. Plots of (a) $x_{w,B}/x_{n,B}$ vs. t and (b) $2[Y_B - (1/x_{n,B})]^{-1}$ vs. t_{corr} for the system in Figure 4; $t_{corr} = 2Ct[(C-2)\ln(1-C)]^{-1}$. In (b), the dotted straight line is for the "ideal" system, and the other three curves were computer-simulated

P-X adduct experiences during the polymerization time t . This number is given by $k_{\text{act}}t$ (which, in turn, defines the parameter k_{act}). The molecular weight M_n and hence the degree of polymerization per cycle are determined by $[P-X]$ and $[P^*]$. Therefore k_c and X^* play no role but to maintain the stationary state. The polydispersity of the ideal system is given by equations 12 and 13 (with equation 14 for a batch system).

(3) Other reactions such as initiation, termination and decomposition lower the M_n and broaden the polydispersity. Since all the relevant rate constants for the styrene/TEMPO system are known, details of polymerization process and product characteristics can be predicted by computer simulation.

(4) On the other hand, the plot such as given in Figure 12b may be useful to quickly evaluate the system with respect to both the “main” and “side” reactions.

(5) The rate constant k_{act} can be accurately determined by the GPC observations of an early stage of the polymerization including a probe adduct P_0-X . Both the direct method, which is based on the curve resolution, and the indirect one, which is based on equations 12 and 13, provide sufficiently accurate values of k_{act} for the styrene/TEMPO system.

(6) By these methods, it was confirmed that the degenerative transfer plays no detectable role, i.e., $k_{\text{act}} = k_d$, in the styrene/TEMPO system.

Acknowledgments

This work was supported by a Grant-in-Aid for Scientific Research, the Ministry of Education, Science, Sports, and Culture, Japan (Grant-in-Aid 09450351).

Literature Cited

- Georges, M. K.; Veregin, R. P. N.; Kazmaier, P. M.; Hamer, G. K. *Trends Polym. Sci.* **1994**, 2, 66.
- Moad, G.; Solomon, D. H. *The Chemistry of Free Radical Polymerization*; Pergamon: Oxford, U. K., **1995**; p 335.
- Davis, T. P.; Haddleton, D. M. In *New Methods of Polymer synthesis*; Ebdon, J. R.; Eastmond, G. C., Eds.; Blackie: Glasgow, U. K., **1995**, Vol. 2; p 1.
- Matyjaszewski, K.; Gaynor, S.; Greszta, D.; Mardare, D.; Shigemoto, T. *J. Phys. Org. Chem.* **1995**, 8, 306.
- Davis, T. P.; Kukulj, D.; Haddleton, D. M.; Maloney, D. R. *Trends Polym. Sci.* **1995**, 3, 365.
- Hawker, C. J. *Trends Polym. Sci.* **1996**, 4, 183.
- Sawamoto, M.; Kamigaito, M. *Trends Polym. Sci.* **1996**, 4, 371.
- Otsu, T.; Yoshida, M. *Makromol. Chem., Rapid Commun.* **1982**, 3, 127.
- Solomon, D. H.; Rizzardo, E.; Cacioli, P. *Eur. Pat. Appl. EP135280* (Chem. Abstr. **1985**, 102, 221335q).
- Rizzardo, E. *Chem. Aust.* **1987**, 54, 32.
- Georges, M. K.; Veregin, R. P. N.; Kazmaier, P. M.; Hamer, G. K. *Macromolecules* **1993**, 26, 2987.
- Kato, M.; Kamigaito, M.; Sawamoto, M.; Higashimura, T. *Macromolecules* **1995**, 28, 1721.

13. Wang, J.-S.; Matyjaszewski, K. *J. Am. Chem. Soc.* **1995**, *117*, 5614.
14. Matyjaszewski, K.; Gaynor, S.; Wang, J.-S. *Macromolecules* **1995**, *28*, 2093.
15. Wayland, B. B.; Poszmik, G.; Mukerjee, S. L.; Fryd, M. *J. Am. Chem. Soc.* **1994**, *116*, 7943.
16. Arvanitopoulos, L. D.; Grenel, M. P.; Harwood, H. J. *Polym. Prepr. (Am. Chem. Soc., Div. Polym. Chem.)* **1994**, *35(2)*, 549.
17. Greszta, D.; Mardare, D.; Matyjaszewski, K. *Macromolecules* **1994**, *27*, 638.
18. Johnson, C. H. J.; Moad, G.; Solomon, D. H.; Spurling, T. H.; Vearing, D. J. *Aust. J. Chem.* **1990**, *43*, 1215.
19. Veregin, R. P. N.; Georges, M. K.; Hamer, G. K.; Kazmaier, P. M. *Macromolecules* **1995**, *28*, 4391.
20. Veregin, R. P. N.; Odell, P. G.; Michalak, L. M.; Georges, M. K. *Macromolecules* **1996**, *29*, 2746.
21. Veregin, R. P. N.; Odell, P. G.; Michalak, L. M.; Georges, M. K. *Macromolecules* **1996**, *29*, 3346.
22. Veregin, R. P. N.; Odell, P. G.; Michalak, L. M.; Georges, M. K. *Macromolecules* **1996**, *29*, 4161.
23. Catala, J. M.; Bubel, F.; Hammouch, S. O. *Macromolecules* **1995**, *28*, 8441.
24. Hammouch, S. O.; Catala, J. M. *Macromol. Rapid Commun.* **1996**, *17*, 683.
25. Mardare, D.; Matyjaszewski, K. *Polym. Prepr. (Am. Chem. Soc., Div. Polym. Chem.)* **1994**, *35(1)*, 778.
26. Li, I.; Howell, B. A.; Matyjaszewski, K.; Shigemoto, T.; Smith, P. B.; Priddy, D. B. *Macromolecules* **1995**, *28*, 6692.
27. Greszta, D.; Matyjaszewski, K. *Macromolecules* **1996**, *29*, 5239.
28. Matyjaszewski, K. *Macromol. Symp.* **1996**, *111*, 47.
29. Greszta, D.; Matyjaszewski, K. *Macromolecules* **1996**, *29*, 7661.
30. Puts, R. D.; Sogah, D. Y. *Macromolecules* **1996**, *29*, 3323.
31. Hawker, C. J.; Barclay, G. G.; Orellana, A.; Dao, J.; Devonport, W. *Macromolecules* **1996**, *29*, 5245.
32. Fukuda, T.; Terauchi, T. *Chem. Lett. (Tokyo)* **1996**, 293.
33. Fukuda, T.; Terauchi, T.; Goto, A.; Ohno, K.; Tsujii, Y.; Miyamoto, T.; Kobatake, S.; Yamada, B. *Macromolecules*, **1996**, *29*, 6393.
34. Goto, A.; Terauchi, T.; Fukuda, T.; Miyamoto, T. *Polym. Prepr., Jpn.* **1996**, *45*, 1261.
35. Goto, A.; Fukuda, T. *Macromolecules*, **1997**, *30 (No. 15)*.
36. Hui, A. W.; Hamielec, A. E. *J. Appl. Polym. Sci.* **1972**, *16*, 749.
37. Buback, M.; Gilbert, R. G.; Hutchinson, R. A.; Klumperman, B.; Kuchta, F.-D.; Manders, B. G.; O'Driscoll, K. F.; Russell, G.; Schweer, J. *Macromol. Chem. Phys.* **1995**, *196*, 3267.
38. Ohno, K.; Tsujii, Y.; Fukuda, T. *Macromolecules*, **1997**, *30*, 2503.
39. Fukuda, T.; Tsujii, Y.; Miyamoto, T. *Polym. Prepr. (Am. Chem. Soc., Div. Polym. Chem.)* **1997**, *38(1)*, 723.
40. Goto, A.; Fukuda, T. *Macromolecules*, **1997**, *30 (No. 17)*.
41. Goto, A.; Terauchi, T.; Fukuda, T.; Miyamoto, T. *Macromol. Rapid Commun.* **1997**, *18 (No. 8/9)*.

42. Fukuda, T.; Goto, A. *Macromol. Rapid Commun.* **1997**, *18* (No. 8/9).
43. Tsujii, Y.; Fukuda, T.; Miyamoto, T. *Polym. Prepr. (Am. Chem. Soc., Div. Polym. Chem.)* **1997**, *38*(1), 657.
44. Bowry, V. W.; Ingold, K. U. *J. Am. Chem. Soc.* **1992**, *114*, 4992.
45. Müller, A. H. E.; Zhuang, R.; Yan, D.; Litvinenko, G. *Macromolecules* **1995**, *28*, 4326.
46. Müller, A. H. E.; Yan, D.; Litvinenko, G.; Zhuang, R.; Dong, H. *Macromolecules* **1995**, *28*, 7335.
47. Yan, D.; Jiang, H.; Fan, X. *Macromol. Theory Simul.* **1996**, *5*, 333.

Styrene Polymerization Mediated by Five-Membered Cyclic Nitroxides

B. Yamada¹, Y. Miura, Y. Nobukane, and M. Aota

Material Chemistry Laboratory, Faculty of Engineering, Osaka City University,
3-3-138 Sugimoto, Sumiyoshi-ku, Osaka 558, Japan

To evaluate the structural effect of nitroxides on the living free radical polymerization of styrene, substituted pyrrolidinyloxy and oxazolidinyloxy were synthesized and employed as mediators at 110 °C. All the cyclic nitroxides, except oxazolidinyloxy were found to control to different extents the molecular weight (\bar{M}_n) and polydispersity (\bar{M}_w/\bar{M}_n) of the polystyrene samples obtained. Among the nitroxides synthesized, 2,2,3,3,5-pentamethyl-5-phenylpyrrolidinyloxy and 2,3,3,5-tetramethyl-2,5-diphenylpyrrolidinyloxy, are of particular interest because polystyrene samples with $\bar{M}_n > 100000$ and $\bar{M}_w/\bar{M}_n < 1.5$ were obtained whereas 2,2,6,6-tetramethylpiperidinyloxy yielded polymers with considerably lower \bar{M}_n and slightly lower \bar{M}_w/\bar{M}_n under similar conditions. The polymerization in the presence of oxazolidinyloxy radical was found to proceed almost without any influence of the nitroxide.

The living free radical polymerization (LFRP) of styrene (St) mediated by 2,2,6,6-tetramethylpiperidinyloxy (TEMPO) has drawn much attention, because LFRP enables to control molecular weight and molecular weight distribution of the polymer by preservation of the activity of propagating radical through the reversible deactivation by TEMPO (1-7). Indeed, the propagating species rapidly reacts with TEMPO to form an alkoxyamine as dormant species that can regenerate the propagating radical and TEMPO upon thermally activated dissociation. The formation of the reversible bond from the propagating radical and TEMPO reduces the steady state concentration of the active radicals and leads to the diminution of the probability of uncontrolled bimolecular termination.

Overview of TEMPO Mediated Polymerization

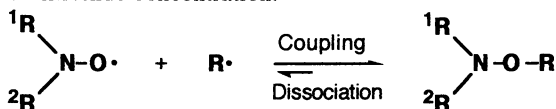
Recently, it has been revealed that thermal initiation of St, bimolecular termination, chain transfer to the reactive dimer produced by thermal initiation of St, and degradation of the alkoxyamine into an unsaturated group at polymer chain end and a hydroxyamine occur concurrently in the LFRP system (5-8). Furthermore, the

¹Corresponding author

role of thermal initiation as radical supplying process has been disclosed by Matyjaszewski *et al.* (4,6) and Fukuda *et al.* (5).

LFRP is conducted using a mixture of nitroxide and peroxide such as benzoyl peroxide (BPO) or a unimolecular initiator consisting of an alkoxyamine of the structure similar to that of the growing dormant species. Unimolecular initiators can be obtained by coupling of TEMPO with the carbon radicals prepared by addition of benzyloxy radical to St (2) or hydrogen abstraction from ethylbenzene (3).

The overall rate of LFRP is governed by the balance of the rates of thermal initiation and termination, which explains that the polymerization rate remains constant regardless of the concentrations of TEMPO and unimolecular initiator used (3,5,6). A much greater rate constant for the coupling than that for the dissociation is considered to bring about an almost constant concentration of the active species irrespective of the nitroxide concentration.



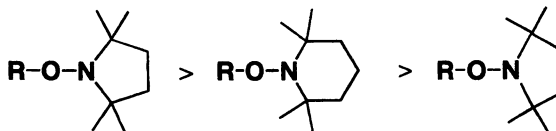
The chain transfer to the St dimer and the degradation of the alkoxyamine as chain stopping processes, which increase polydispersity (M_w/M_n), are considered to compete with propagation. Furthermore, changes in polymerization conditions and in the rates of elementary reactions with the increase of conversion also influence the relative rate of propagation with respect to chain transfer, bimolecular termination, and degradation of the dormant species. Actually, LFRP involves all kinds of elementary reactions of radical polymerization, besides the reactions in which TEMPO and alkoxyamine participate. As a result of the balance between the rates of these reactions, M_w/M_n is kept well below 1.5 which is the theoretical limit of conventional radical polymerization.

TEMPO functions exclusively as inhibitor of radical polymerization at lower temperature such as 60 °C, and the radical polymerization in the presence of a small amount of TEMPO may eventually start after an induction period at the same rate as that of the polymerization carried out in absence of TEMPO (9). To induce LFRP, the alkoxyamine has to dissociate into the active propagating species at a proper rate and the polymerization temperature has to be raised to 100 °C or above. The coupling of the nitroxide with propagating radical is quite a fast process irrespective of temperature (10), and the dissociation of the C-O bond seems to be one of the key steps of LFRP at 100 °C or above nevertheless thermal polymerization also occurs at this temperature range.

Hawker *et al.* (11) have explicitly shown that the alkoxyamines yielding carbon centered radicals that are less stabilized than poly(St) or phenethyl radicals are not adequate as initiator for LFRP, because their dissociation is too slow for LFRP. When a nitroxide is inert toward the poly(St) radical, no influence on the polymerization rate and M_n of the polymer is observed.

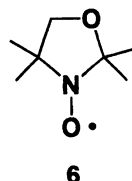
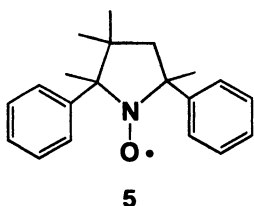
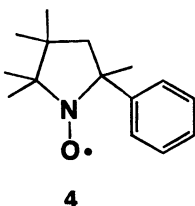
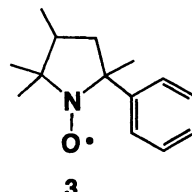
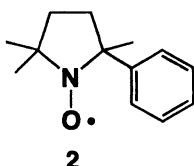
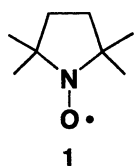
A decrease in the polymerization temperature is preferable to suppress both thermal initiation and degradation of the alkoxyamine, although such a decrease may bring about a slower cleavage of the C-O bond. For LFRP of St at lower temperatures, nitroxides that give rise to alkoxyamines of sufficiently labile C-O bond have to be chosen and the structural effects of the nitroxides on LFRP have to be studied. However, the polymerization in the presence of substituted nitroxides other than TEMPO has not been studied in detail (12-14). Concerning the cleavage of the C-O bonds in alkoxyamines, Moad and Rizzardo (15) have established the following increasing order of bond strength for the C-O bonds from the measurement of the dissociation rates of various alkoxyamines obtained from cyclic and acyclic nitroxides. They have shown that the alkoxyamines obtained from 2,2,5,5-

tetramethylpyrrolidinyl-1-oxyl (1) and TEMPO in one hand and 2-cyano-2-propyl radical in the other have half-life times of 280 and 65 min at 60 °C, respectively, in accordance with the order of the C-O bond strength. They have also deduced that the increase of the rate of dissociation of the C-O bond that is due to steric congestion depends on the structure of carbon centered radicals and of the nitroxides.



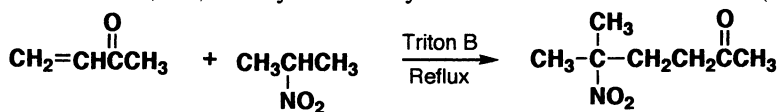
In the present study, our effort has been turned toward elucidating the effect of the structures of nitroxides on LFRP, our aim being to bring about LFRP with a minimum amount of the thermally produced polymer. We have chosen five-membered cyclic nitroxides, pyrrolidinyloxy, in which substituents have been introduced. Particularly, the substituents introduced in cyclic nitroxides are of interest because steric influences may hinder the coupling of the nitroxide with propagating radical and facilitate the dissociation of the alkoxyamine from the nitroxide. Rationalization of the steric effect due to the substituents introduced in the cyclic nitroxide is not an easy task because of the interposition of the oxygen atom between the moiety of the incipient radical and the five-membered cyclic moiety of the nitroxide.

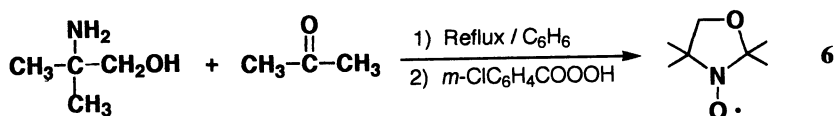
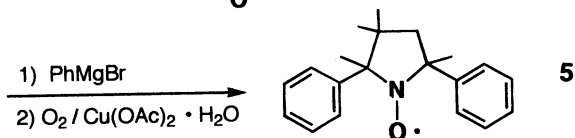
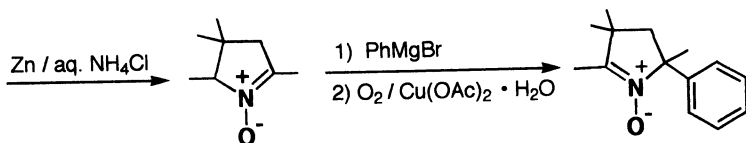
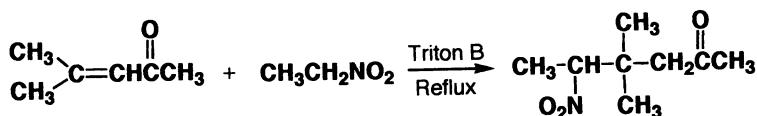
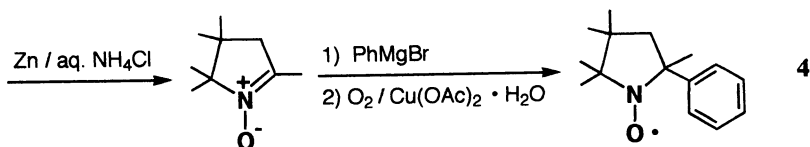
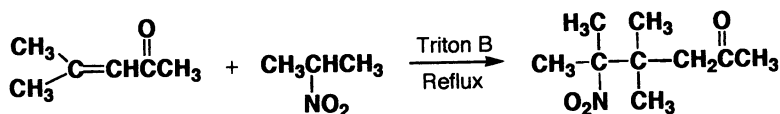
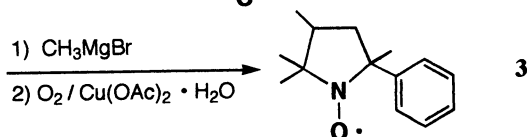
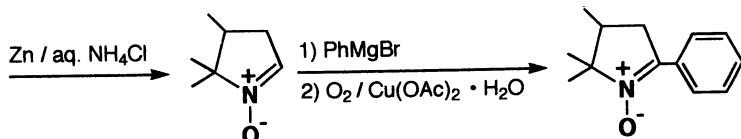
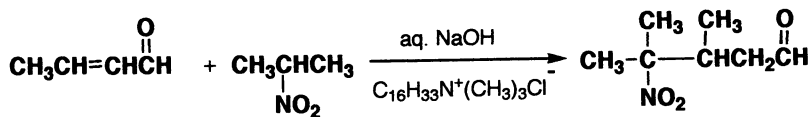
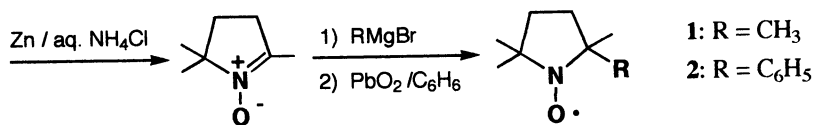
As five-membered cyclic nitroxides bearing various substituents at the 2-, 3-, and 5-positions, 1, 2,2,5-trimethyl-5-phenylpyrrolidinyloxy (2), 2,2,3,5-tetramethyl-5-phenylpyrrolidinyloxy (3), 2,2,3,3,5-pentamethyl-5-phenylpyrrolidinyloxy (4), 2,3,3,5-tetramethyl-2,5-diphenylpyrrolidinyloxy (5), and 2,2,4,4-tetramethyl-1-oxazolidinyl-3-oxyl (6), have been chosen as the mediators.



Experimental

The nitroxides, 1-6, were synthesized by the reactions outlined as follows (16-21).





Nitroxides 1-4 were isolated from the respective reaction mixtures by silica gel column chromatography using ethyl acetate/benzene (1/3) as eluant. After evaporation of the solvent, 1-4 were obtained as yellow to yellowish brown liquids. 5 was chromatographed on silica gel with diethyl ether/hexane (1/2) eluant to give yellow crystals; mp, 96-97 °C. Oxidation of the oxazoline prepared by the reaction of the amino alcohol with acetone yielded 6 as an orange liquid. The structures of 1-6 were verified by IR spectroscopy and ¹H-NMR spectra of the hydroxyamines formed on treatment with phenylhydrazine.

Commercial TEMPO was used as supplied. Commercially available BPO containing 20% water was purified by reprecipitation using chloroform and methanol as solvent and precipitant. *tert*-Butyl peroxide (TBP) was used as supplied. *p,p'*-Dimethoxybenzoyl peroxide (dimethoxy-BPO) was prepared by the reaction of *p*-methoxybenzoyl chloride with sodium peroxide and purified by the reprecipitation. The polymerizations of St in the presence of the nitroxides or TEMPO were run in glass ampoules sealed under vacuum at 110 °C. After the polymerization, the contents of the ampoule were poured into a large amount of methanol to precipitate the poly(St) formed. Conversion was calculated from the weight of the dried polymer. \bar{M}_n and \bar{M}_w/\bar{M}_n were measured by a TOSOH 8000 series high-performance liquid chromatograph equipped with GPC columns. ¹H-NMR and ESR spectra were taken by JEOL α -400 and Bruker ESP300 spectrometers, respectively. IR spectra were recorded on a JASCO FT IR-230 spectrometer.

Polymerization by BPO/TEMPO under the Present Conditions. The St polymerizations mediated by the five-membered cyclic nitroxides 1-6 were compared with that mediated by TEMPO with a view of evaluating the capability as mediator. Calculation of the theoretical molecular weight of the polymer, which is usually obtained as the ratio of the mass of polymerized St to that of unimolecular initiator, cannot be made for the polymerization with a mixture of BPO/nitroxide because the quantitative formation of the unimolecular initiator from the binary system could not be expected. However, it has been shown that there is no large difference between the polymerizations with the unimolecular initiator and with the BPO/TEMPO initiating system; polymerization rate is similar to each other and \bar{M}_w/\bar{M}_n is sufficiently low in both cases (22). Therefore, we can safely anticipate that the polymerization of St by the *in situ* formation of the adduct under the present conditions would proceed via LFRP mechanism as well as the polymerization by the unimolecular initiator.

To confirm this point, the efficiency of LFRP under the present conditions was estimated from the content of the benzoyloxy end group. Considering the convenience of quantification by ¹H-NMR spectroscopy, we employed dimethoxy-BPO instead of BPO in combination with TEMPO. The *p*-methoxybenzoyloxy group was expected to bind to the polymer chain at the α -end, and these peroxides in combination with TEMPO were confirmed to give quite similar results for conversion, \bar{M}_n , and \bar{M}_w/\bar{M}_n in LFRP of St at 110 °C. Although the conversion appears to depend on the TEMPO concentration, the polymerization rate after the induction period was quite similar to those of all the polymerizations including the case of the highest concentration of TEMPO.

The content of the methoxy group was determined from intensity ratio of the resonances due to the methoxy and aromatic protons in the ¹H-NMR spectra of the polymers. It was found that ca. 70% of the polymer bears the methoxy group almost irrespective of conversion and the concentration of TEMPO as summarized in Table I. Hawker *et al.* (11) have shown that the efficiency for the polymerization using the adduct obtained from TEMPO, St, and substituted BPO as the

unimolecular initiator is as high as 95% or above. Even though the lower efficiency was confirmed, the ability of the various nitroxides synthesized to control the free radical polymerization of St that involves the *in situ* formation of the adduct could be evaluated.

Table I. Polymerization of St by dimethoxy-BPO/TEMPO for 16 hours at 110 °C

[TEMPO] (mmol/L)	Convsn. (%)	\bar{M}_n	\bar{M}_w/\bar{M}_n	No. of CH ₃ O per chain	
				Before reprecipitation	After reprecipitation
6.5	60.1	49300	1.22	0.64	0.69
13	56.1	29300	1.19	0.76	0.77
26	38.5	12500	1.20	0.73	0.70

Polymerization Rate. The conversion-time plots in Figure 1A show that the nitroxides synthesized and TEMPO mediate the polymerization at a similar rate except for 1. All the polymerizations followed first order kinetics with respect to monomer. Although the polymerizations mediated by 2, 3, 4, and 5 seem to be faster than that controlled by TEMPO, the difference in the polymerization rates is too small to indicate any trend in the order of polymerization rates for a concen-

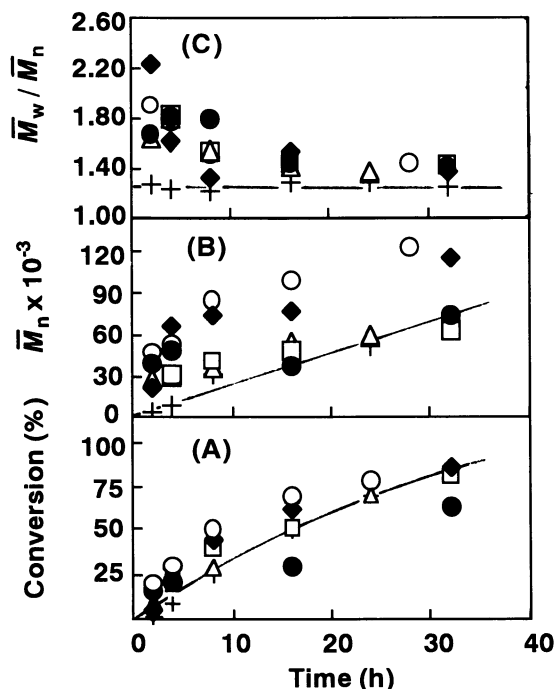


Figure 1. Polymerizations of St mediated by pyrrolidinyloxy 1-5 and TEMPO using BPO as initiator at 110 °C: [nitroxide] = 6.5 mmol/L, [BPO] = 5.0 mmol/L. ● : 1, □ : 2, △ : 3, ○ : 4, ◆ : 5, + : TEMPO. Curvatures for the TEMPO mediated polymerization are served as visual guides.

tration of the initiating system of 5.0 mmol/L for BPO and 6.5 mmol/L for nitroxide.

The effect of the nitroxide structure on polymerization rate is more significant for the higher concentration of the initiating system (10 mmol/L of BPO and 13 mmol/L of nitroxide) as shown in Figure 2A. The faster polymerizations in the presence of **2** and **5** are apparent from conversion-time plots. The slower polymerization in the presence of **1** irrespective of conversion shown by Figures 1A and 2A seems to be due to slower dissociation of the corresponding alkoxyamine as predicted by Moad and Rizzardo (15) whereas the effects of the 2- and 5-phenyl substituents of **2** and **5** on the dissociation rate have not been known yet.

An increase of the concentration of TEMPO in LFRP of St through the *in situ* formation of the adduct has been known to exhibit almost no effect on the polymerization rate (6). However, an increase in the concentrations of the initiating system from 5 to 10 mmol/L for BPO and from 6.5 to 13 mmol/L for **2** and **5** brought about 1.6 times faster polymerization. The faster and slower polymerizations in the presence of **2** or **5** and **1**, respectively, than that mediated by TEMPO indicate that the steady state concentration of the propagating radical changes with the nitroxide used, and accordingly the propagation rate. The steady state concentration of the propagating radical seems to be higher for the system of BPO/**2** or BPO/**5** than the system of BPO/TEMPO, and the initiation by the binary system and thermal initiation is considerably faster than the pure thermal initiation.

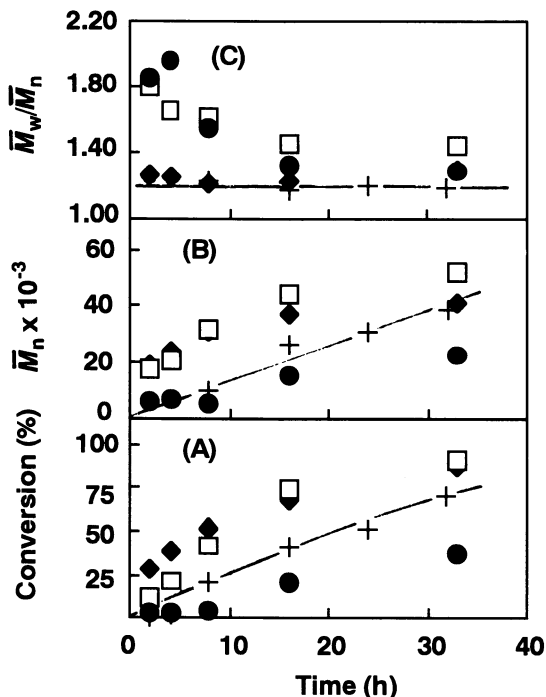
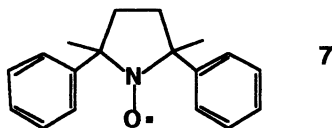


Figure 2. Polymerizations of St mediated by pyrrolidinyloxylys and TEMPO using BPO as initiator at 110 °C: [nitroxide] = 13 mmol/L, [BPO] = 10 mmol/L. ● : **1**, □ : **2**, ◆ : **5**, + : TEMPO. Curvatures for the TEMPO mediated polymerization are served as visual guides.

Puts and Sogah (13) have reported that the polymerization mediated by **7** using BPO as initiator at 137 °C is faster than that mediated by TEMPO by a factor of 1.9 for a concentration of 53 mmol/L of the nitroxide, and a higher concentration of the propagating radical was estimated. Similarly, the C-O bonds of the dormant species formed in the polymerizations using **2-5** are anticipated to be weaker than that of the dormant species from **1** and TEMPO. However, an enhanced concentration of the propagating radical might increase the rate of bimolecular termination.



\bar{M}_n of Polystyrene. The variation of the \bar{M}_n of the resulting poly(St) with time gives an indication of the influence of the structure of the nitroxides on the course of the polymerization (Figure 1B). Comparison of the \bar{M}_n 's of the poly(St) obtained after heating for 32 hours shows that the polymerizations with **1**, **2**, **3**, and TEMPO yield similar \bar{M}_n of 60000-70000. However, the polymerizations mediated by **4** and **5** which are the 3,3-dimethyl substituted pyrrolidinyls produced polymers with considerably higher \bar{M}_n of 116000-123000. The presence of two methyl groups at the 3-position of **4** and **5** seems not to modify the rate of polymerization which is essentially the same (the concentration of the initiating system is 5.0 mmol/L for BPO and 6.5 mmol/L for nitroxide) as that mediated by TEMPO, but it markedly affect the \bar{M}_n 's of the samples obtained.

Although Figure 3A suggest that a lower efficiencies of the initiation by BPO/**4** and BPO/**5** than those by the other initiating systems, **4** and **5** mediated the polymerization at similar rates to the polymerization mediated by TEMPO and other pyrrolidinyls except for **1**. The polymerization initiated by BPO/**5** at 10 mmol/L for BPO and 13 mmol/L for **5** proceeded faster than the polymerization initiated by 10 and 13 mmol/L of BPO and TEMPO, respectively, and attained \bar{M}_n which was not so high as 110000-120000.

These findings imply lower efficiencies of the initiation yielding the smaller amount of the polymer chain at the lower concentrations of BPO/**4** and BPO/**5**, and compensation of the slower initiation by the faster propagation because of the dissociation of the C-O bond to a higher extent. The increase of the concentration of the initiating system, which brought about the faster polymerization, improved the initiating efficiencies of BPO/**5** as high as those of the other initiating systems as confirmed by the single relationship in Figure 3B. Consequently, the 3,3-dimethyl substitutions are expected to suppress and facilitate the reaction of β -benzoyl-oxyphenethyl radical with **4** or **5** and the dissociation of the C-O bond of the dormant species, respectively.

As the dimethyl groups at the 3-position cannot be responsible for polar and resonance effects, the steric factor could be expected to favor or disadvantage the dissociation of the C-O bond or the coupling with the active polymer radical, respectively. No direct interaction between the 3,3-dimethyl groups and the approaching propagating radical can be anticipated. A change in the C-N-C bond angle arising from the introduction of two methyl groups is considered to be one of the most probable rationalizations (15).

As shown in Figure 2B, an increase of the concentration of the initiating system BPO/**5** resulted in a decrease in \bar{M}_n which is still higher than \bar{M}_n of the polymer obtained by TEMPO. In contrast, Puts and Sogah (13) have reported a faster poly-

merization of St in the presence of **7** than that mediated by TEMPO by a factor of 1.9 at 53 mmol/L of the nitroxide, and consistently quite similar \bar{M}_n -conversion plots for the polymerization mediated by **7** and TEMPO.

The 3-monomethyl substitution of **3** does not bring about appreciable changes in \bar{M}_n as well as polymerization rate. The polymerization mediated by **2** and **3** gave polymers whose \bar{M}_n increased with conversion from ca. 20000 to ca. 70000. The higher \bar{M}_n at low conversions is ascribed to the conventional radical polymerization involving bimolecular termination in competition with the coupling of **2** and **3** with the poly(St) radical. In LFRP, the active propagating species help to increase \bar{M}_n by reaction with St molecules at each dissociation of the C-O bond. It has been known that the nitroxide concentration is reduced to minimum at low conversions followed by a gradual increase to the almost constant concentration (23), and the decrease of the nitroxide concentration could increase the contribution of the conventional radical polymerization.

The polymerization mediated by the 2-methyl and 2-phenyl derivatives such as **2** and **3** showed profiles of the \bar{M}_n -time plot that are quite similar to that mediated by TEMPO as shown in Figure 1B. Furthermore, the \bar{M}_n -conversion plot in Figure 3A exhibits the same linear relationship for the polymerizations mediated by TEMPO, **1**, **2**, and **3**. Consequently, the 2- or 5-phenyl substituted nitroxides without the

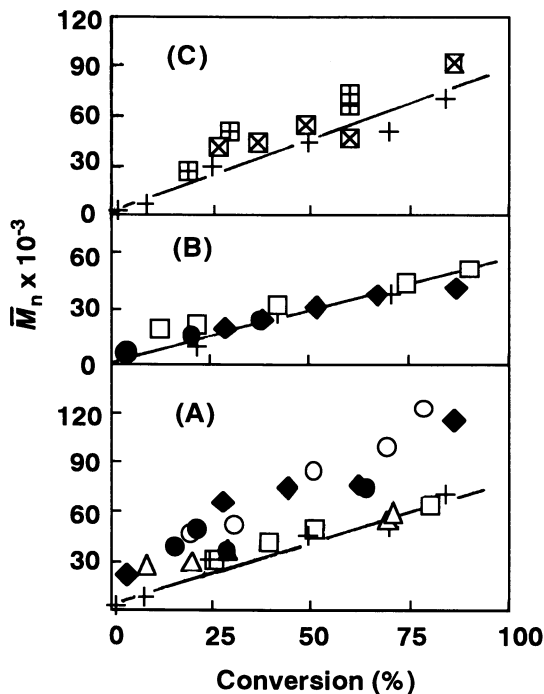


Figure 3. Dependence of \bar{M}_n on conversion of polymerizations by BPO (5.0 mmol/L) and nitroxide (6.5 mmol/L)(A), BPO (10 mmol/L) and nitroxide (13 mmol/L)(B), and BPO (10 mmol/L), nitroxide (6.5 mmol/L), and TBP (1.89 mmol/L) (C) at 110 °C. ● : BPO/**1**, □ : BPO/**2**, △ : BPO/**3**, ○ : BPO/**4**, ◆ : BPO/**5**, + : BPO/TEMPO, ⊠ : BPO/**4**/TBP, ⊞ : BPO/**5**/TBP. Linear relationships for the TEMPO mediated polymerization are served as visual guides.

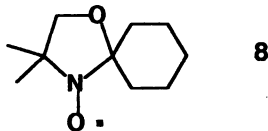
3,3-dimethyl substitutions seems not to reduce the initiation efficiency. In the case of **1**, \bar{M}_n increased with the conversion from 38000 at 16% conversion to 75000 at 64% conversion but certainly not linearly and contribution of bimolecular termination cannot be ruled out. It should be noted that the constant \bar{M}_n throughout the polymerization is one of the characteristics of conventional radical polymerization. An increase in the nitroxide concentration resulted in a decrease in \bar{M}_n as shown in Figure 2B. If the dissociation of the alkoxyamine is too slow, the polymerization may be initiated mainly by the thermal process allowing fast and uncontrolled bimolecular termination leading a constant \bar{M}_n and $\bar{M}_w/\bar{M}_n > 1.5$ irrespective of conversion.

\bar{M}_w/\bar{M}_n of Polystyrene. Figure 1C depicts changes in \bar{M}_w/\bar{M}_n with the structure of the nitroxide and polymerization time. All polymerizations yielded polymers with $\bar{M}_w/\bar{M}_n < 1.5$ after sufficiently long polymerization time. Among the nitroxides examined, TEMPO was found to control \bar{M}_w/\bar{M}_n most effectively throughout the polymerization. \bar{M}_w/\bar{M}_n higher than 1.5 can be noticed for conversions below 60% in the polymerizations mediated by pyrrolidinyloxylys.

The rapid decrease of \bar{M}_w/\bar{M}_n with increasing time or conversion that is observed in Figure 2C can be explained as in any controlled living process by the fact that the difference between the longest and shortest chains tend to be less perceptible as \bar{M}_n increases. Furthermore, at a higher concentration of **5**, $\bar{M}_w/\bar{M}_n < 1.5$ was attained in the initial stage of the polymerization, and the higher steady state concentration of the propagating radical presumably offers more chances of propagation and exchange among the dormant species resulting in a shorter time for averaging the chain length.

Polymerization by **6.** Figure 4 shows the results of the polymerization in the presence of **6** at 13.0 mmol/L in 1.3 molar ratio relative to BPO. Although a higher concentration of **6** was used, all polymers isolated exhibited $\bar{M}_w/\bar{M}_n > 1.5$ in the whole range of conversion. When the polymerization mixture containing **6** in an ESR tube was heated in the cavity, a three-line spectrum assigned to **6** was observed at 60 °C or above. The lower limits for the polymerizations in the presence of **7** and TEMPO were estimated to be 75 and 90 °C, respectively (13). The detection of an ESR signal at a lower temperature supports the inference in favor of the thermally more labile C-O bond in the alkoxyamine obtained from **6** than those obtained from TEMPO or **7**.

It can be concluded that **6** is unable to control the polymerization of St. The slow coupling relative to the bimolecular termination is considered to result in $\bar{M}_w/\bar{M}_n > 1.5$. The faster polymerization and the almost constant \bar{M}_n are also consistent with this aspect. Georges *et al.* (24) have predicted by means of energy calculation that the C-O bond of the alkoxyamine originating from 3,3-dimethyl-1-oxa-4-azaspiro[4,5]dec-4-yloxy (**8**) is stronger than that from TEMPO. Although the slow coupling of **6** with the growing radicals anticipated by Figure 4 is difficult to rationalize at this point, a change in the C-N-C bond angle (15) may be responsible for weakening for the C-O bond.



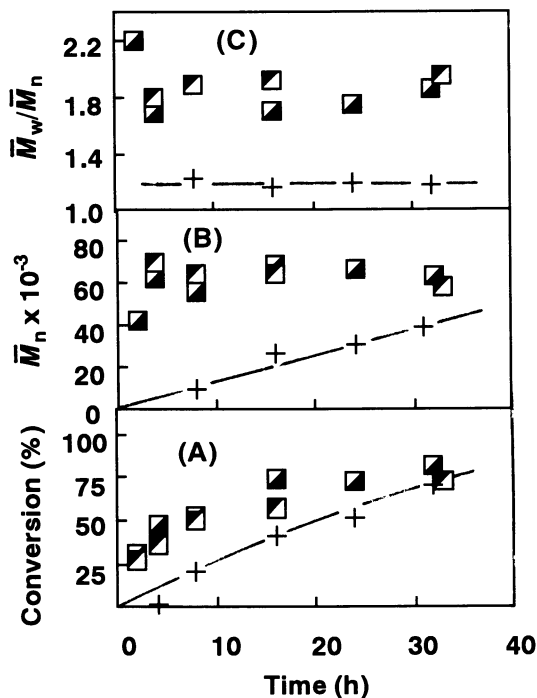


Figure 4. Polymerizations mediated by **6** using BPO and BPO/TBP as initiators at 110 °C: [**6**] = 6.5 mmol/L, [BPO] = 5.0 mmol/L, [TBP] = 1.89 mmol/L. ◼: BPO/**6**, ◻: BPO/**6**/TBP, +: BPO/TEMPO. Curvatures shown for the TEMPO mediated polymerization are served as visual guides.

Characteristics of Polymerization Mediated by Cyclic Nitroxide. Figure 1 and its three plots show that 3,3-dimethyl substitution on pyrrolidinyloxy effectively induced substantial change as to the ability of these stable radicals to control the free radical polymerization of St. Steric hindrance caused by these substituents seems to weaken the C-O bond of the dormant species and the effect is more perceptible on \bar{M}_n 's than the rate of polymerization. The polymerizations mediated by **1**, **2**, and **3** yield the polymers with slightly higher \bar{M}_n and higher \bar{M}_w/\bar{M}_n at low conversions.

The plots of \bar{M}_n vs. conversion for the individual polymerizations shown in Figure 3A reveal that the polymers obtained in the presence of 6.5 mmol/L of **1**, **4**, and **5** exhibit higher \bar{M}_n 's than those obtained by the TEMPO mediated polymerization. Considering the polymerizations by BPO/**4** and BPO/**5** as fast as that by BPO/TEMPO at 6.5 mmol/L for the nitroxide and 5 mmol/L for BPO, we can conclude that a lower efficiency of the initiation and a faster propagation in the polymerization mediated by **4** and **5** attained the \bar{M}_n as high as 116000-123000.

It has been reported that the overall rate of polymerization remains constant irrespective of the nitroxide or unimolecular initiator concentration (3,5,6). When a higher concentration of **1** (13.0 mmol/L) was employed at the same molar ratio relative to BPO, slightly slower polymerization than that at 6.5 mmol/L was observed. The slower dissociation of this alkoxyamine reduced the polymerization rate leading to a lower concentration of the propagating radical as one of the

structural effects of the nitroxide. In contrast, the increase in the concentration of the initiating system from 5.0 to 10 mmol/L for BPO and from 6.5 to 13 mmol/L for **2** and **5** brought about the faster polymerization than that controlled by TEMPO. The steady state concentration of the propagating species is expected to be higher in the polymerizations mediated by **2** and **5** than the TEMPO mediated polymerization in which the steady state concentration of the propagating species could be determined by the balance of the thermal initiation rate of St and the bimolecular termination rate (3,5,6).

Samples obtained in the presence of **5** at 6.5 mmol/L exhibited \bar{M}_n of 115900 at 86% conversion (Figure 1B), and \bar{M}_n of 41400 at 87% conversion for the BPO concentration of 10 mmol/L and the nitroxide concentration of 13 mmol/L (Figure 2B). However, the increase in the concentration of the initiating system comprised of BPO and **2** from 10 to 13 mmol/L reduced \bar{M}_n only slightly from 64500 at 80% conversion to 51600 at 90% conversion. The polymerizations mediated by **2** and **5** at 13 mmol/L also fit to the relationship for the BPO/TEMPO system in Figure 3B.

The higher \bar{M}_n of the polymer at the similar polymerization rate irrespective of the structure of the nitroxide could be interpreted by a lower efficiency of the initiation and a faster propagation which could compensate a smaller amount of polymer chain resulting from the lower efficiency of the initiation. As a result of the improvement of the initiation efficiency at the higher concentrations of BPO/**4** and BPO/**5**, the \bar{M}_n as high as 110000-120000 arising from the smaller amount of polymer chain is not expected any more. Alternatively, the faster polymerization initiated by BPO/**2** and BPO/**5** than that by BPO/TEMPO at the higher concentration of the propagating species was observed.

Effect of TBP. Fukuda *et al.* (25) have used *tert*-butyl hydroperoxide to augment the rate of LFRP and shown that the overall rate of the polymerization is proportional to the square root of the total of the initiation rates. Greszta and Matyjaszewski (26) have found the rate enhancement of the TEMPO mediated St polymerization in the presence of a variable amount of dicumyl peroxide at 120 °C to prepare the polymer retaining polydispersity below 1.5. An increase in the concentration ratio of the monomer to the active chain end is considered to contribute to a faster polymerization.

To accelerate the polymerization mediated **5**, BPO and TBP were employed as initiators: [TBP] = 1.89 mmol/L. Although BPO disappears within a short period, the half lifetime of TBP is 65 hours at 110 °C (27). According to the unimolecular decomposition rate constant of TBP in the literature, the total initiation rate would be greater than thermal initiation rate by a factor of 2.3. The results of the polymerization are illustrated in Figure 5.

We expected that TBP would supply the active species at almost a constant rate so as to facilitate the polymerizations by the systems of BPO/**4** and BPO/**5**. However, TBP did not affect the polymerization rate and \bar{M}_w/\bar{M}_n even though reduced \bar{M}_n was obtained; they were still higher than those of the TEMPO mediated polymerizations in the absence of TBP. These findings suggest that the concentration and lifetime of the active species did not change substantially by addition of TBP. The polymerization mediated by **4** in the presence of TBP yielded the polymer with broader \bar{M}_w/\bar{M}_n and GPC elution curve consisted of two components. TBP was also added to the polymerization effected in the presence of **6**, and the results are shown in Figure 4. However, the polymerization rate, \bar{M}_n of the polymer, and \bar{M}_w/\bar{M}_n were not changed by TBP. The \bar{M}_n vs. conversion plot in Figure 3C indicates that TBP contributes to the shift toward higher \bar{M}_n 's.

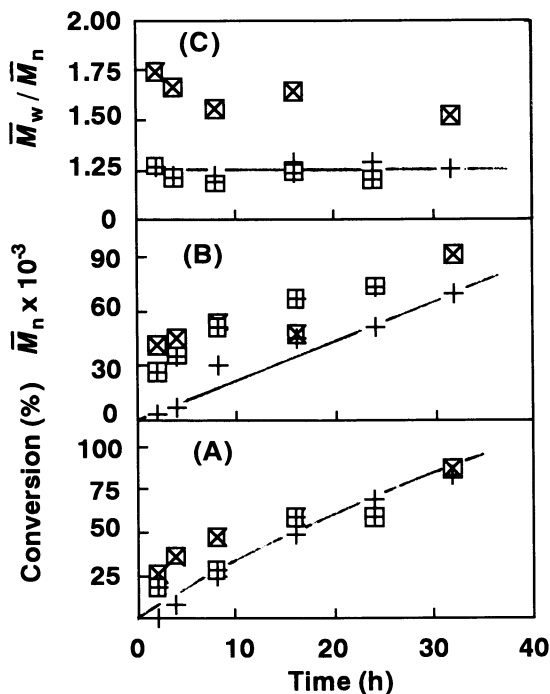


Figure 5. Polymerizations mediated by nitroxide using BPO and BPO/TBP as initiators at 110 °C: [nitroxide] = 6.5 mmol/L, [BPO] = 5.0 mmol/L, [TBP] = 1.89 mmol/L. \boxtimes : BPO/4/TBP, \boxplus : BPO/5/TBP, +: BPO/TEMPO. Curvatures are drawn for the TEMPO mediated polymerization as visual guides.

Conclusion

- 1) The polymerization mediated by the pyrrolidinyloxy's except for **1** took place at a similar rate to the polymerization mediated by TEMPO when 6.5 mmol/L of the nitroxide was used. At a higher concentration of the initiating system comprised of BPO faster polymerizations were observed than in the TEMPO case. The polymerization mediated by **1** was slower irrespective of concentration.
- 2) The \bar{M}_n of the poly(St) was found to exceed 100000 when the pyrrolidinyloxy's bearing the 3,3-dimethyl groups were chosen as mediators for 6.5 mol/L. An increase in the nitroxide concentration of the initiating system resulted in a decrease of \bar{M}_n , and the difference between the cases of **2** or **5** and TEMPO became smaller.
- 3) For concentrations of initiating system of 5.0 mmol/L for BPO and 6.5 mmol/L for the nitroxide, \bar{M}_w/\bar{M}_n of the polymer gradually approached \bar{M}_w/\bar{M}_n as low as those by TEMPO at high conversions. The use of the higher concentration of **5** effectively reduced \bar{M}_w/\bar{M}_n in low conversion range.

Acknowledgments

The authors are grateful to the Dow Chemical Company for support of this research and to Dr. D. B. Priddy for invaluable discussion.

References

1. Georges, M. K.; Veregin, R. P. N.; Kazmaier, P. K.; Hamer, G. K. *Macromolecules* **1993**, *26*, 2987.
2. Hawker, C. J. *J. Am. Chem. Soc.* **1994**, *116*, 11185.
3. Li, I.; Howell, B. A.; Matyjaszewski, K.; Shigemoto, T.; Smith, P. B.; Priddy, D. B. *Macromolecules* **1995**, *28*, 6692.
4. Greszta, D.; Matyjaszewski, K. *Macromolecules* **1996**, *29*, 5239.
5. Fukuda, T.; Terauchi, T.; Goto, A.; Ohno, K.; Tsujii, Y.; Miyamoto, T.; Kobatake, S.; Yamada, B. *Macromolecules* **1996**, *29*, 6393.
6. Greszta, G.; Matyjaszewski, K. *Macromolecules* **1996**, *29*, 7661.
7. Howell, B. A.; Priddy, D. B.; Li, I.; Smith, P. B.; Kastl, P. E. *Polym. Bull.* **1996**, *37*, 451.
8. Yoshida, E.; Okada, Y. *Bull. Chem. Soc. Jpn* **1997**, *70*, 275.
9. Miura, Y.; Masuda, S.; Kinoshita, M. *Makromol. Chem.* **1972**, *160*, 243.
10. Beckwith, A. L. J.; Bowry, V. W.; Ingold, K. U. *J. Am. Chem. Soc.* **1992**, *114*, 4893.
11. Hawker, C. J.; Elce, E.; Dao, J.; Volksen, W.; Russell, T. P.; Barclay, G. G. *Macromolecules* **1996**, *29*, 2686.
12. Klapper, M.; Benfaremo, N.; Steenbock, M.; Wunderlich, W.; Müllen, K., *Preprints*, 2nd International Symposium on Free Radical Polymerization, Santa Margherita, Italy, May, 1996.
13. Puts, R. D.; Sogah, D. Y. *Macromolecules* **1996**, *29*, 3323.
14. Veregin, R. P. N.; Georges, M. K.; Hamer, G. K.; Kazmaier, P. M. *Macromolecules* **1995**, *28*, 4391.
15. Moad, G.; Rizzardo, E. *Macromolecules* **1995**, *28*, 8722.
16. Bonnett, R.; Brown, R. F. C.; Clark, V. M.; Sutherland, I. O.; Todd, S. A. *J. Chem. Soc.* **1959**, 2094.
17. Hankovszky, H. O.; Hideg, K.; Lovas, M. J. *Can. J. Chem.* **1989**, *67*, 1392.
18. Ballini, R.; Bosica, G. *Tetrahedron Lett.* **1996**, *37*, 8027.
19. Hideg, K.; Lex, L. *J. Chem. Soc. Perkin Trans. 1* **1986**, 1431.
20. Chou, S.; Nelson, J. A.; Spencer, T. A. *J. Org. Chem.* **1974**, *39*, 2356.
21. Bapat, J. B.; Black, D. S. C. *Aust. J. Chem.* **1968**, *21*, 2483.
22. Hawker, C. J.; Barclay, G. C.; Orelana, A.; Dao, J.; Devonport, W. *Macromolecules* **1996**, *29*, 5245.
23. Veregin, R. P. N.; Odell, P. G.; Michalak, L. M.; Georges, M. K. *Macromolecules* **1996**, *29*, 2747.
24. Kazmaier, P. M.; Moffat, K. A.; Georges, M. K.; Veregin, R. P. N.; Hamer, G. K. *Macromolecules* **1995**, *28*, 1841.
25. Goto, J.; Terauchi, T.; Fukuda, T.; Miyamoto, T. *Polym. Preprints, Jpn.* **1996**, *45*, 1261.
26. Greszta, D.; Matyjaszewski, K. *J. Polym. Sci., Polym. Chem. Ed.* in press.
27. Masson, J. C. *Polymer Handbook*; 3rd ed.; Brandrup, J.; Immergut, E. H., Ed.; Wiley, New York, 1989; p II-1.

Chapter 13

Nitroxide-Mediated Radical Polymerization: End-Group Analysis

Yucheng Zhu¹, I. Q. Li¹, B. A. Howell¹, and D. B. Priddy²

¹Center for Applications in Polymer Science, Central Michigan University,
Mount Pleasant, MI 48859

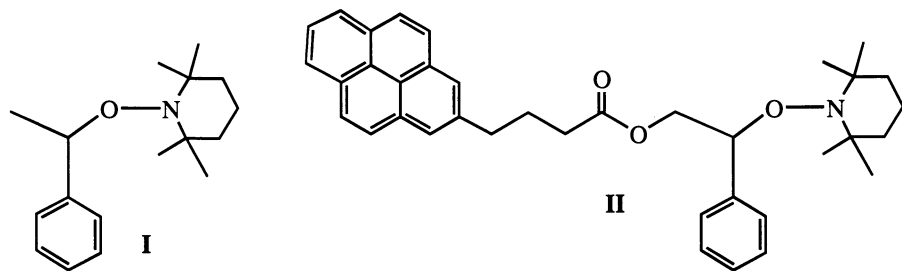
²Dow Polystyrene Research and Development, 438 Building, Midland, MI 48667

This paper is devoted to understanding the limitations of nitroxide mediated polymerization (NMP) for making highly end-functional polystyrene. It is believed that NMP virtually eliminates chain transfer and termination resulting in excellent control (>95%) of chain-end architecture. To further study the mechanism of NMP, we synthesized NMP initiator/mediators having a UV/vis chromophore attached to either the initiating or terminating fragments. This allowed us to both qualitatively and quantitatively analyze the chain-ends using a GPC-UV/vis technique. This technique showed that: 1) the chromophores are attached to the chain-ends, 2) initiating fragments give higher chain-end functionalization than the terminating nitroxyl fragment, 3) chain-end purity diminishes with both conversion and MW, 4) chain-end purity of >90% is only achieved when making low MW (i.e., <10,000) polystyrene.

Recently much attention has been devoted to developing an understanding of nitroxide mediated radical polymerization (NMRP). Early on, most of the work focused on obtaining narrow polydispersity polystyrene. However, recently most of the effort has been aimed at using this technology for the preparation of block copolymers; especially styrene-(meth)acrylate block copolymers.¹⁻⁴ The successful application of NMRP to the synthesis of pure block copolymers requires that the termination processes which typically take place during free radical polymerization (i.e., radical coupling, chain transfer, and disproportionation) be virtually eliminated.⁵ A key challenge for the use of NMRP for the preparation of block copolymers is that it only appears to work well for vinylaromatic monomers.^{6,7}

There have been two approaches to the study of the NMRP of styrene: 1) *in situ* formation of the NMRP initiator⁸⁻¹¹ and 2) presynthesis of the initiator.¹²⁻¹⁸ Most groups believe that presynthesis is best because the *in situ* approach leads to the formation of multiple nitroxide initiating species and there is not perfect stoichiometry between the initiating and mediating species.¹⁹ With the presynthesis approach, a pure compound can be used to initiate polymerization which should lead to “cleaner chemistry”. However, Georges *et al* take issue with this conclusion and believe that excess nitroxyl radicals is important to achieve narrow polydispersity and good end-group purity.¹¹

There has been debate over the extent that NMRP eliminates termination processes. Priddy *et al* were the first to synthesize and study the thermal stability of a small molecule (**I**) that models the propagating chain-end of NMP of styrene.^{20,21} They prepared **I** by H-atom abstraction from ethylbenzene and trapping the resultant radical with TEMPO. Thermolysis of **I** in an ESR spectrophotometer showed continuous formation of TEMPO. Further analysis of the decomposition products revealed the formation of primarily styrene. They went on to study the kinetics of the decomposition and found that **I** decomposes in the temperature range utilized for NMRP of styrene at a rate comparable to styrene conversion rate. Based on this observation they concluded that end-group purity achieved by NMRP of styrene should decrease with both M_n and monomer conversion. They further concluded that this termination process would likely seriously limit the ability of NMRP for the preparation of high molecular weight (>100,000) polystyrene having a narrow polydispersity. These conclusions have been disputed by other research groups who have attempted to prove that NMRP chemistry virtually eliminates all termination processes. These claims are supported by measuring the amount of nitroxyl moiety on the terminal chain-end. Both NMR²²⁻²⁴ and nitrogen analyses¹⁸ have been utilized to determine the nitroxyl content of polystyrene made using NMRP. However, these techniques are not very sensitive and provides only an approximation of the level of nitroxide groups in the polymer. Further, they cannot establish that the nitroxide is at the chain terminus. Furthermore, due to the insensitivity of these analytical techniques, TEMPO-end capped polystyrene samples to be analyzed have always had molecular weights <10,000. Most researchers have reported levels of nitroxide on the terminal chain-end at >90%. Hawker is the only researcher to date to quantify the initiated end of a polystyrene chain using NMRP. He synthesized a NMRP initiator having a pyrene chromophore attached to the initiating fragment (**II**). Both NMR and UV analyses were used to quantify the amount of initiator fragment attached to the chain-end and Hawker reported >95% incorporation.^{25,26} However, again the molecular weight of the chromophore tagged polystyrene was again below 10,000. To date, no one has reported the evolution of chain-end purity with styrene conversion and increasing molecular weight.



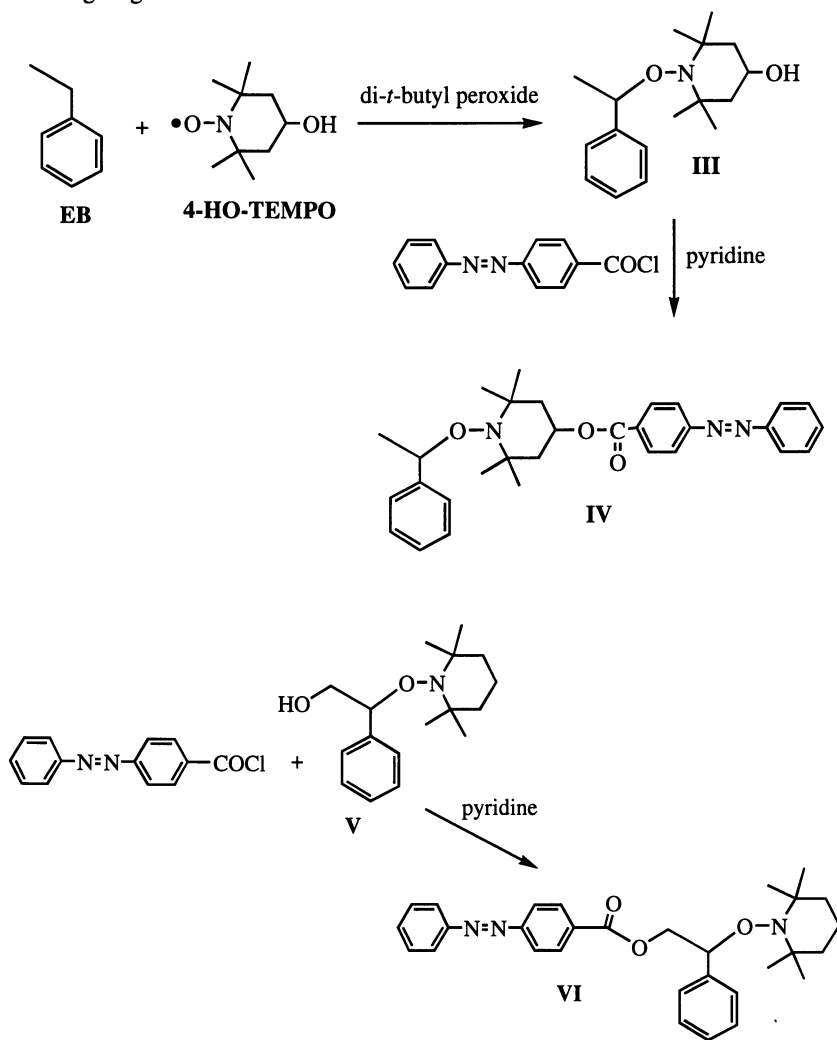
Recently Priddy developed a GPC-UV technique to precisely quantitate the level of chromophore attached to polymers.²⁷ The technique also determines the location of a chromophore; i.e., pendant vs chain-end. In this paper we report the results of GPC-UV analyses for polystyrenes made using NMRP. We have compared the end-group purity of polystyrene made by the *in situ* and presynthesis of initiator approaches, as well as demonstrating the impact of excess nitroxide on nitroxide end-group yield.

Results and Discussion

The GPC-UV technique for polymer end-group analysis requires that the initiator/mediator be tagged with a chromophore having a unique absorbance; i.e., absorb at a wavelength at which polystyrene is totally transparent (>280 nm). The chromophore chosen for study was the phenylazophenyl chromophore due to its intense absorption at >300 nm. Scheme 1 shows the synthetic route used to generate nitroxide initiators; one having a chromophore attached to the mediating fragment (IV) and another having the same chromophore attached to the nitroxide initiating fragment (VI). These two tagged initiators/mediators (IV and VI) are orange-red crystalline solids and their structures were confirmed using mass spectrometry and NMR spectroscopy.

The UV spectra of IV and VI are almost identical (Figure 1). Furthermore, the relative molar absorptivities of IV and VI were measured at 320 nm and also were found to be identical. This allows direct quantitative comparison of both the initiating and terminal ends of polystyrene initiated/mediated using these materials. To compare the relative performance of the *in situ* (Scheme 2) vs initiator presynthesis approaches for making polystyrene chains having chain-end functionality, we also made TEMPO having the same phenylazophenyl chromophore in the 4-position (VII) for use in conjunction with benzoyl peroxide (BPO). Polystyrene initiated using BPO and mediated using VII will place the same fragment on the terminal chain-end as if the polymer was initiated/mediated using IV. Since the terminal fragment attached to the end of the PS chain would be the same regardless of whether the presynthesis or *in situ* initiator process was used, direct comparison of the relative end-group purity can be determined. Also, VII was added to polymerizations initiated/mediated using IV to see if the presence of excess nitroxyl indeed enhanced the number of nitroxide functional chain-ends.

Scheme 1 Synthesis of initiators for NMP bearing a chromophore on either the initiating or mediating fragment



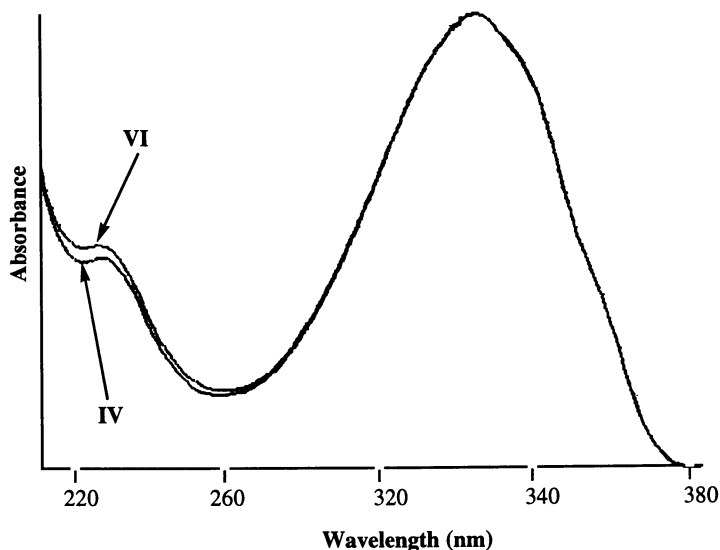
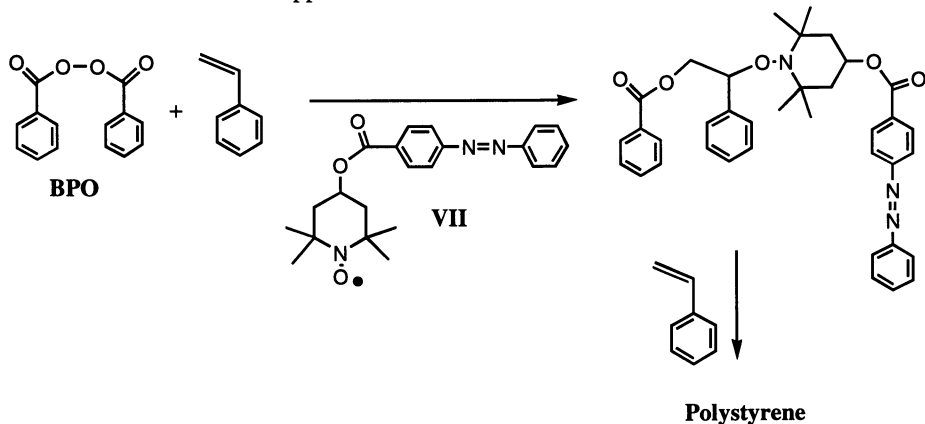


Figure 1 Comparison of the UV spectrum of **IV** and **VI**.

Scheme 2 *In situ* initiator approach for NMSP



Polymerizations were carried out in glass ampoules at two temperatures (i.e., 120 and 140 °C) and at a concentration of 27 mmolar in nitroxide. Polymerizations initiated/mediated using the *in situ* approach utilized a mixture of 27 mmolar benzoyl peroxide (BPO) and 34 mmolar **VII**. To see if excess nitroxide resulted in higher nitroxide chain end-group purity, a polymerization was conducted by adding 7 mmolar **VII** to a polymerization initiated/mediated using 27 mmolar **IV**. Polymers were isolated by multiple precipitation

to remove all non-polymeric components. The purified polymers were analyzed using both UV and GPC-UV analyses. The results obtained from the two techniques generally were in good agreement (Figure 2). Both techniques were calibrated using **IV** to determine the molar absorptivity at 320 nm for the phenylazophenyl chromophore. The GPC-UV technique is expected to be more precise because it excludes small molecules and only measures the absorbance of polymer bound chromophores.²⁷

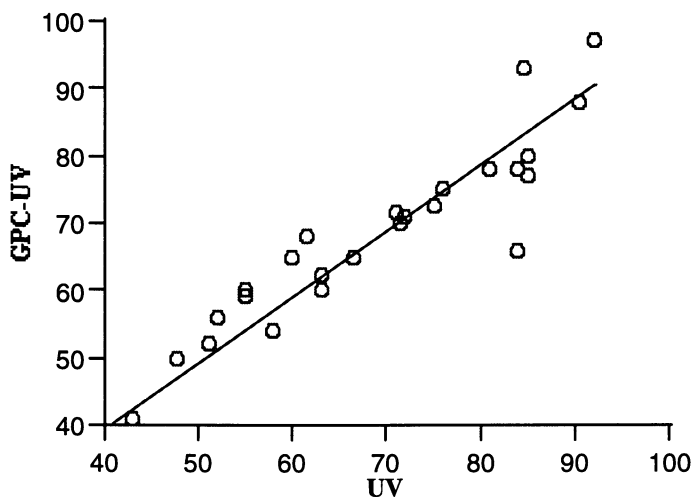


Figure 2 Correlation of measurement of percent chains having a phenylazophenyl chromophore using direct UV vs. GPC-UV analyses.

Another advantage of GPC-UV is that it also demonstrates the point of attachment of the chromophore to the chain (i.e., pendant vs chain-end).²⁷ If the chromophore is pendant, its concentration is independent of chain length. However, if the chromophore is attached to chain-ends, its concentration decreases as chain length increases. An overlay (Figure 3) of the GPC-UV curve collected at 260 nm (pendant phenyl absorbance) with the signal collected 320 nm (chromophore absorbance) shows an offset with the 320 nm absorbing species eluting at a later time (lower MW). In other words, the chromophore is more concentrated in shorter chains confirming that the chromophores are on the chain-ends rather than pendant to the chain.

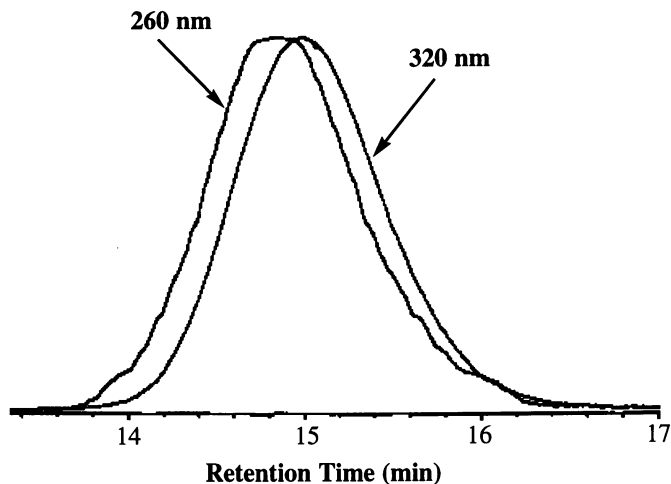


Figure 3 Comparison of the GPC-UV curves collected at 260 and 320 nm

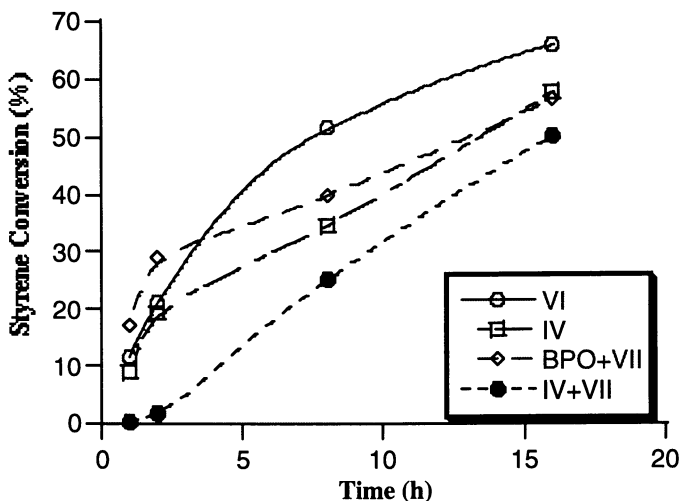


Figure 4 Monomer conversion rates for four initiator/mediator systems (functional group on nitroxyl (IV), functional group on initiating radical (VI), *in situ* initiator with functional group on nitroxyl (BPO+VII), and functional group on nitroxyl + excess functionalized nitroxyl (IV+VII)) at 120 °C

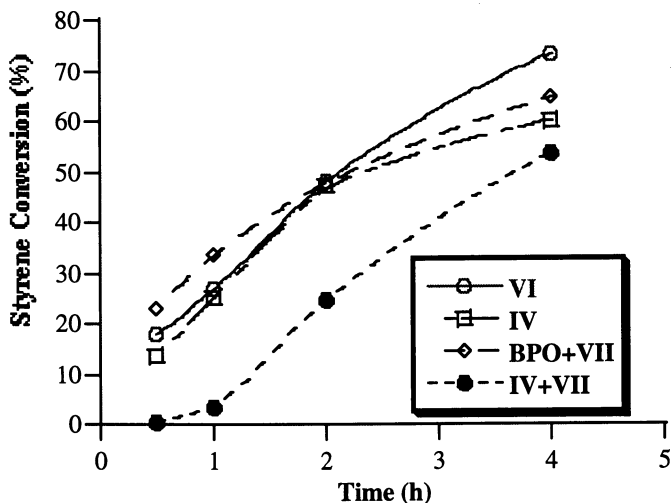


Figure 5 Styrene conversion vs. time at 140 °C

The polymerization temperatures (120 and 140 °C) were chosen because most of the published NMRP work is carried out in the 110 - 140 °C range. At 120 °C the rate of polymerization is quite slow and it takes many hours to achieve high (>60%) monomer conversion (Figure 4). Polymerizations conducted at 140 °C led to high conversion within a few hours (Figure 5). The presence of excess nitroxide results in an induction period at both temperatures. The presence of an induction period when using excess nitroxide has been previously observed.¹¹

The change in number average molecular weight with conversion is quite linear for all four initiator systems (Figure 6). Since industrial polymerization processes normally require the achievement of high conversion within a few hours for economic viability, we have performed most of our previous NMSP studies at temperatures >130 °C.^{1,16,28}

The data consistently show (at both 120 and 140 °C) that the number of polymer chains having chromophores attached to a chain-end decreases as number average molecular weight (M_n) (Figures 7 and 8). This trend is not as dramatic if the chromophore is attached to the initiating radical. Since M_n and styrene conversion are directly proportional (Figures 3 and 4), it follows that chain-end purity also decreases rapidly with monomer conversion. This was predicted from our earlier work in which we studied the thermal decomposition of a small molecule which models the dormant end during NMSP.¹⁶ During the course of this investigation we never obtained a polystyrene sample that had both a $M_n > 10,000$ and at the same time >90% of one of its chain-ends having a chromophore.

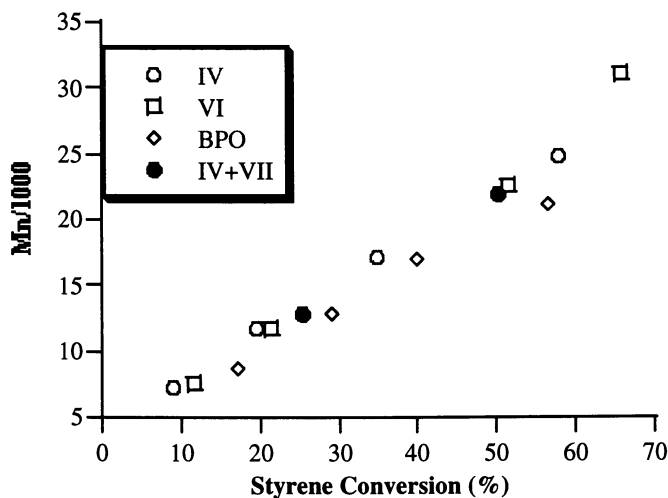


Figure 6 Linear increase of M_n with styrene conversion at 120 °C for four polymerization systems.

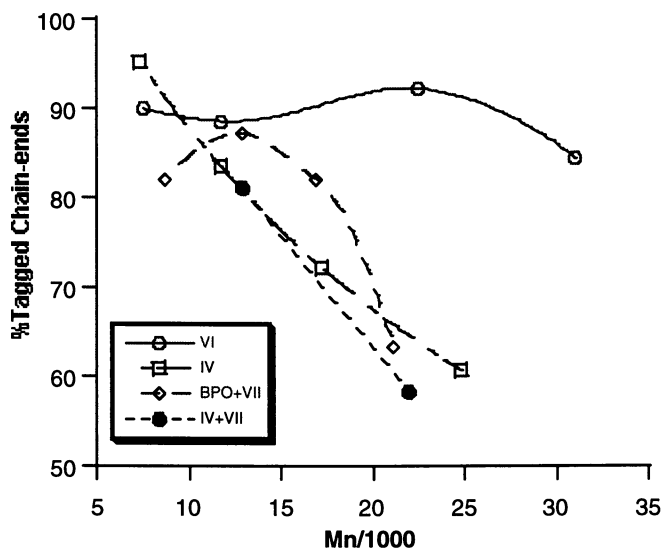


Figure 7 Percent of Chains functionalized vs. M_n at 120 °C.

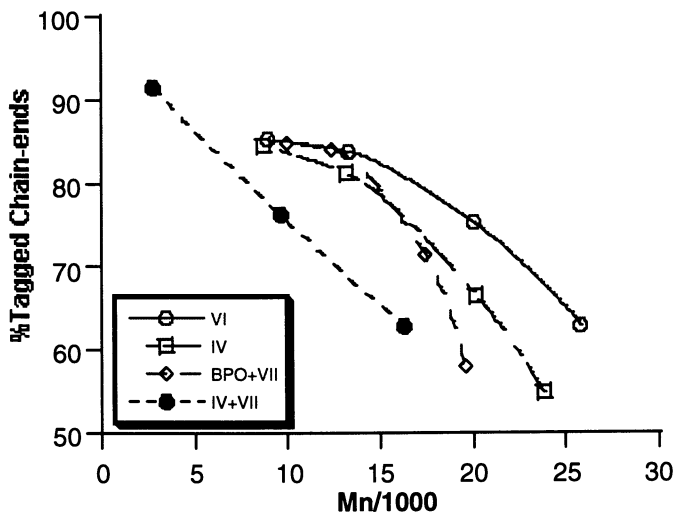


Figure 8 Percent of Chains functionalized vs. M_n at 140 °C

Conclusions

It has been suggested that >90% of the chain-ends of polystyrene prepared using NMRP contain nitroxyl fragments. However, to maximize analytical sensitivity, low M_n chains have generally been prepared. Our data shows high chain-end purity is only achieved during NMSP when making short chains ($M_n < 10000$). Terminal chain-end purity falls off more rapidly as chain length (and monomer conversion) increases than does initiated chain-ends. We believe this conclusion is consistent with our earlier work suggesting that the nitroxide functional chain-ends thermally decompose by elimination as the polymerization progresses.¹⁶ At 140 °C, again the chain-end purity falls rapidly with increasing M_n , even for the initiated end. This is likely due to an increased contribution of autoinitiation at the higher temperature.

The *in situ* initiator approach results in about the same number of terminal nitroxide functionalized chain-ends as the presynthesized initiator approach. The addition of excess nitroxide does not appear to offer a significant improvement of chain-end purity. The only significant change that takes place when excess nitroxide is added is the introduction of an induction period.

Our work indicates that if one wishes to prepare polystyrene having greater than 90% of one of its chain-ends functionalized by nitroxyl, conditions must be utilized (i.e., either high nitroxyl loading or very low monomer conversion) which leads to a low molecular weight polymer (i.e., <10,000 amu).

Bibliography

- 1) Li, I. Q.; Howell, B. A.; Dineen, M. T.; Kastl, P. E.; Lyons, J. W.; Meunier, D. M.; Smith, P. B.; Priddy, D. B. *Macromolecules* **1997**, to appear.
- 2) Benoit, D.; Grimaldi, S.; Finet, J.; Tordo, P.; Fontanille, M.; Gnanou, Y. *Polym. Prepr.* **1997**, *38*, 729.
- 3) DeLeon, M.; Gnanou, Y.; Guerrero, R. *Polym. Prepr.* **1997**, *38*, 667.
- 4) Grande, D.; Gnanou, Y.; Guerrero, R. *Polym. Prepr.* **1997**, *38*, 665.
- 5) Webster, O. W. *Science (Washington, D. C., 1883-)* **1991**, *251*, 887-93.
- 6) Steenbock, M.; Klapper, M.; Muellen, K.; Pinhal, N.; Hubrich, M. *Acta Polym.* **1996**, *47*, 276-279.
- 7) Matyjaszewski, K.; Gaynor, S.; Greszta, D.; Mardare, D.; Shigemoto, T. *J. Phys. Org. Chem.* **1995**, *8*, 306.
- 8) Georges, M. K.; Veregin, R. P. N.; Hamer, G. K.; Kazmaier, P. M. *Macromol. Symp.* **1994**, *88*, 89-103.
- 9) Saban, M. D.; Georges, M. K.; Veregin, R. P. N.; Hamer, G. K.; Kazmaier, P. M. *Macromolecules* **1995**, *28*, 7032-4.
- 10) Veregin, R. P. N.; Georges, M. K.; Hamer, G. K.; Kazmaier, P. M. *Macromolecules* **1995**, *28*, 4391-8.
- 11) Veregin, R. P. N.; Odell, P. G.; Michalak, L. M.; Georges, M. K. *Macromolecules* **1996**, *29*, 2746-54.
- 12) Hawker, C. J. *J. Am. Chem. Soc.* **1994**, *116*, 11185-6.
- 13) Hawker, C. J.; Hedrick, J. L. *Macromolecules* **1995**, *28*, 2993-5.
- 14) Hawker, C. J.; Barclay, G. G.; Orellana, A.; Dao, J.; Devonport, W. *Macromolecules* **1996**, *29*, 5245-5254.
- 15) Howell, B. A.; Priddy, D. B.; Li, I. Q.; Smith, P. B.; Kastl, P. E. *Polym. Bull. (Berlin)* **1996**, *37*, 451-456.
- 16) Li, I.; Howell, B. A.; Matyjaszewski, K.; Shigemoto, T.; Smith, P. B.; Priddy, D. B. *Macromolecules* **1995**, *28*, 6692-3.
- 17) Catala, J. M.; Bubel, F.; Hammouch, S. O. *Macromolecules* **1995**, *28*, 8441-8443.
- 18) Hammouch, S. O.; Catala, J.-M. *Macromol. Rapid Commun.* **1996**, *17*, 149-154.
- 19) Moad, G.; Rizzardo, E.; Solomon, D. H. *J. Macromol. Sci., Chem.* **1982**, *A17*, 51.
- 20) Li, I.; Howell, B.; Ellaboudy, A.; Kastl, P.; Priddy, D. *Polym. Prepr.* **1995**, *36*, 469.
- 21) Ellaboudy, A.; Jewett, G.; Kastl, P.; Priddy, D. *Polym. Prepr.* **1994**, *35*, 725.
- 22) Fukuda, T.; Terauchi, T.; Goto, A.; Ohno, K.; Tsujii, Y.; Miyamoto, T.; Kobatake, S.; Yamada, B. *Macromolecules* **1996**, *29*, 6393-6398.
- 23) Yoshida, E. *J. Polym. Sci., Polym. Chem. Ed.* **1996**, *34*, 2937-2943.
- 24) Yoshida, E.; Sugita, A. *Macromolecules* **1996**, *29*, 6422-6426.
- 25) Hawker, C. J. *Trends Polym. Sci. (Cambridge, U. K.)* **1996**, *4*, 183-188.
- 26) Hawker, C. J.; Elce, E.; Dao, J.; Volksen, W.; Russell, T. P.; Barclay, G. G. *Macromolecules* **1996**, *29*, 2686-8.
- 27) Priddy, D. B. *Mater. Eng. (N. Y.)* **1995**, *9*, 629-48.
- 28) Li, I. Q.; Howell, B. A.; Kastl, P. E.; Smith, P. B.; Priddy, D. B. *Macromolecules* **1996**, *29*, 8554.

Chapter 14

Controlled/Living Free-Radical Polymerization of Styrene and *n*-Butyl Acrylate in the Presence of a Novel Asymmetric Nitroxyl Radical

D. Benoit¹, S. Grimaldi², J. P. Finet², P. Tordo², M. Fontanille¹, and Y. Gnanou^{1,3}

¹Laboratoire de Chimie des Polymères Organiques UMR Centre National de la Recherche Scientifique, Ecole Nationale Supérieure de Chimie et de Physique de Bordeaux, Université Bordeaux I, Av. Pey-Berland, B.P. 108, 33402 Talence Cedex, France

²Laboratoire de Structure et Réactivité des Espèces Paramagnétiques UMR Centre National de la Recherche Scientifique, Université de Provence, Case 521, Av. Esc. Normandie Niemen, 13397 Marseille Cedex 20, France

A novel nitroxyl radical containing a diethyl phosphonate group in the β -position to the nitrogen atom has been used as radical scavenger in free radical polymerization. In the presence of this stable free-radical, styrene and *n*-butyl acrylate undergo controlled / « living » polymerization. The samples of polystyrene (PS) and poly (*n*-butyl acrylate) (PBuA) obtained in this way exhibit a narrow Poisson-type distribution of molar masses.

Free-radical polymerization remains the most convenient method to synthesize polymers. In contrast to ionic polymerizations, free radical processes do not require stringent experimental conditions (absence of moisture, expensive solvents) and can serve to polymerize a whole host of monomers. However, samples obtained through a free radical mechanism do not exhibit the same characteristics as those obtained by living ionic polymerizations in terms of controlled molar mass and well-defined chain end structure. Indeed, the radical active center cannot sustain indefinite growth because it can be deactivated at any time in competing termination reactions. Bimolecular termination being unavoidable, the chemoselectivity of the chain growth is poor in free-radical polymerization and therefore these processes cannot be termed as « living » or even controlled.

Despite this very challenging obstacle, many attempts to minimize the effects due to termination have been made over the last 15 years. The concept that is underlying in all these attempts rests on the same premises as those put forward in controlled cationic polymerization (1) :

³Corresponding author

- reversible deactivation of the vast majority of active centers
- induction of a fast equilibrium between the dormant species formed and the remaining minute amount of active species.

The literature proposes two major approaches to momentarily trap growing radicals and ensure the lowest possible concentration of active sites : one is based on the use of appropriate radical scavengers (2-4) and second is actually an extension of the metal-catalyzed Kharasch reaction to polymerization (5-9).

The first example of controlled free-radical polymerization emanates from the Xerox research group who used nitroxyl stable radicals to reversibly trap growing polymeric radicals (3), (4). Thermally labile alkoxyamines in dynamic equilibrium with growing styryl radicals were suggested to form in the presence of 2,2,6,6-tetramethyl-1-piperidinyloxy (TEMPO). This ideal picture, which implies the reversible combination of stable free radicals with styryl radicals and chain growth during the lifetime of the polymeric radical, was questioned by Catala *et al.* (10), Fukuda *et al.* (11), (12) and Greszta *et al.* (13), (14). These authors indeed found a zero order dependence of the rate of polymerization with respect to the concentration of dormant alkoxyamine, a result contradicting the model presented by the Xerox group (16). More recently, Fukuda *et al.* (11), (12) and Greszta *et al.* (13), (14) demonstrated that the rate of nitroxyl-mediated polymerizations of styrene coincides exactly with that of the thermal autopolymerization ; he also disclosed that the constant supply of radicals formed by the thermal process is essential for chain growth in such systems. In addition to the competing thermal initiation that simply mirrors the too slow rate of decomposition of the dormant adduct, another major limitation of this system is its inability to satisfactorily function with monomers other than styrene.

The second approach is based on the addition of plurihaloalkanes to alkenes via a radical mechanism and proceeds through successive transfer of the halogen atom : the so-called "atom transfer radical polymerization" (ATRP) is more versatile than TEMPO-mediated systems as it functions not only for styrene but also for (meth) acrylates. In the system described by Matyjaszewski (5-7), a copper complex containing bipyridyl reversibly activates the ω -halide function of a dormant chain and acts as a halide carrier in a redox process. Even though ATRP is a robust and inexpensive method , it is unfortunate that this mechanism requires rather large amounts of transition metal compounds.

As mentioned above, the crucial point in traditional nitroxyl mediated radical polymerization is the slow decomposition of the dormant adduct. Therefore, we sought to weaken the $-C-ON$ bond in the alkoxyamine that is formed upon combination of nitroxyl radicals with growing radicals. Analogues of classical nitroxyl compounds that carry a substituent purposely introduced to impart strong electronic and steric effects should give rise to better controlled free-radical polymerizations. This reasoning led us to design a novel nitroxyl radical, carrying in the β -position to the nitrogen atom a bulky and electron-withdrawing phosphonate group. Our interest in phosphonate containing stable radicals was also induced by the

work of Matyjaszewski *et al.* (15) who showed that styrene polymerizes quite fast in the presence of 4-phosphonoxy-TEMPO used as radical scavengers.

The ability of the newly synthesized nitroxyl radical, *N-tert*-butyl-1-diethylphosphono-2,2-dimethylpropyl nitroxyl (DEPN) (Figure 1) to effect faster and well controlled polymerization has been investigated. The controlled / « living » character of the free-radical polymerization of styrene and *n*-butyl acrylate in the presence of DEPN is also thoroughly discussed.

Experimental section

Materials. DEPN was obtained by oxidation of 2,2-dimethyl-1-(1,1-dimethylethylamino)propyl diethylphosphonate with *meta*-chloroperbenzoic acid. This aminoalkyl phosphonic ester was prepared by reaction between pivalaldehyde, *tert*-butylamine and dialkyl phosphite (17). TEMPO and di-*tert*-butylnitroxyl (DTBN) were purchased from Aldrich and used without further purification.

Styrene and *n*-butyl acrylate (Aldrich) were distilled over CaH₂ under reduced pressure just prior to polymerization. Azo-bis-isobutyronitrile (AIBN) (Aldrich) was recrystallized from diethyl ether solution, dried and kept at low temperature under a dry nitrogen atmosphere until use. Benzoyl peroxyde (BPO) (Aldrich) was recrystallized from methanol-dichloromethane solution and stored at low temperature until use.

Polymerizations. Into a dry Schlenk tube were introduced DEPN, the monomer and the required amount of initiator under an inert atmosphere. The solution was then thoroughly degassed before heating to the desired temperature.

Characterizations. All molar masses were determined using size exclusion chromatography. The latter characterization was performed using a JASCO HPLC pump type 880-PU, a RI-3 refractive index detector and a JASCO 875 UV /vis detector with THF as eluent. For the determination of the molar masses of PS samples, use was made of the calibration curve established with PS standards. The molar masses of PBuA samples were obtained from a SEC instrument equipped with a light scattering detector (Wyatt).

Results and discussion

Polymerization of Styrene in the presence of DEPN

Choice of the appropriate initiator. *N-tert*-butyl-1-diethylphosphono-2,2-dimethyl propyl nitroxyl (DEPN) (Figure 1) was first used as radical scavenger in the free-radical polymerization of styrene.

As the actual ability of the latter radical to control the polymerization of styrene was totally unknown to us, we decided to carry out the first experiment with the same ratio of stable free radical to initiator as the 1.2 ratio used by Georges *et al.* in their study of the TEMPO/BPO/styrene system (3). The polymerization of styrene

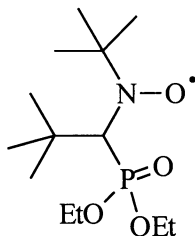


Figure 1. structure of DEPBN

was thus effected in bulk and at 110°C, with 5×10^{-3} mol/L of BPO and 6×10^{-3} mol/L of DEPBN. The increase of molar masses with time was followed by SEC by characterization of the aliquots removed from the reaction medium at the times indicated in Table I.

When comparing the results shown in Table I with those reported in reference (3), it appears that styrene obviously polymerizes faster in the presence of DEPBN than it does with TEMPO as moderator, even though the temperature in our case is 10°C lower than that used by Georges *et al.* (*see reference*). Molar masses were found to increase with conversion. The rather large polydispersity indexes that were obtained encouraged us to increase the proportion of DEPBN and examine the effect of the excess used on the course of the reaction. With 2.5 ratio of DEPBN to BPO, the distribution of molar masses becomes narrower and the rate of polymerization slows moderately.

The effect of temperature on the behavior of the system consisting of DEPBN / BPO / styrene was also examined and a series of two experiments were carried out at 123°C. Samples of 10^5 g/mol can be obtained within reasonable reaction periods and with acceptable polydispersity indices using DEPBN as radical scavenger.

These preliminary results that sharply contrast with those observed in the presence of TEMPO indicate that reaction between DEPBN and growing styryl radicals gives rise to weaker alkoxyamine bonds than in the case of TEMPO. However, the molar masses of the samples prepared appear not to correspond to the ratio of the monomer consumed to the initial BPO concentration. The experimental values of molar masses were found to be systematically higher than the targeted ones, indicating that the efficiency of the initiation step is lower than 1. This is in accord with the observations made by the Xerox group who also noticed a poor efficiency of BPO in the presence of TEMPO and invoked the induced decomposition of BPO by TEMPO to account for this result (18). To avoid possible degradation of BPO into benzoate by electron transfer from DEPBN, AIBN was substituted for BPO and a third series of experiments was carried out with AIBN as initiator. As shown in Table II, the system constituted of AIBN and DEPBN not only gives rise to samples of narrow molar mass distribution (MMD), but it also secures almost perfect control of the sample molar masses. The targeted molar masses and those experimentally measured indeed fall in close agreement.

Table I. Polymerization of Styrene as a function of DEPN/BPO ratio

$[DEPN]/[BPO]$	$[BPO]$ (mol/L)	a_T (°C)	b_{time}	c_p (%)	$\bar{M}_{n,th}$ (g/mol)	$\bar{M}_{n,exp}$ (g/mol)	$dPDI$
1.2	3.7×10^{-3}	110	1.66	30	36000	49600	1.42
			3.50	45	54000	66000	1.56
			7.00	62	74400	80300	1.76
2.5	3.7×10^{-3}	110	1.66	17.5	21000	30600	1.15
			3.50	30	36000	47600	1.18
			7.00	51	61200	70000	1.36
2.5	2.2×10^{-2}	123	1.66	35	7000	9700	1.13
			3.50	53	10600	15000	1.18
			7.00	95	14000	20000	1.17
2.5	3.7×10^{-3}	123	1.66	34	41000	53000	1.35
			3.50	51	61200	69000	1.53
			7.00	>95	96000	120000	1.47

a : Temperature of reaction ; b : reaction time in hours ; c : conversion ; d : polydispersity index (\bar{M}_w/\bar{M}_n).

Table II. Polymerization of Styrene initiated by the AIBN/DEPN system.

$[DEPN]/[AIBN]$	$[AIBN]$ (mol/L)	a_T (°C)	b_{time}	c_p (%)	$\bar{M}_{n,th}$ (g/mol)	$\bar{M}_{n,exp}$ (g/mol)	$dPDI$
2.5	2.2×10^{-2}	95	3.50	5.4	1090	1100	1.17
			7.00	9.5	1900	2000	1.16
2.5	1.1×10^{-3}	95	3.50	20	8100	9300	1.22
			7.00	30	12000	12800	1.25
			21.50	55	22200	23300	1.12
2.5	2.2×10^{-2}	123	1.66	40	8000	8500	1.12
			3.50	61	12200	12500	1.11
			7.00	80	16000	16000	1.12
2.5	3.6×10^{-3}	123	3.50	58	69600	70000	1.30
			7.00	80	96000	92000	1.32
			22.00	>95	114000	105000	1.40

a : Temperature of reaction ; b : reaction time in hours ; c : conversion ; d : polydispersity index (\bar{M}_w/\bar{M}_n).

The same observations about the control and the distribution of molar masses can be made for the polymerization carried out at 95°C ; the rate of polymerization appears to be logically slower than that measured at 123°C.

Controlled / Living nature of the DEPN-mediated polymerization of styrene. Two criteria must be concomitantly satisfied to qualify a chain polymerization as « living » or controlled :

- linear dependence of $\ln ([M]_0/[M])$ with time.
- linear variation of \bar{M}_n with conversion.

As shown in Figure 2, the system constituted of AIBN and 2.5 molar excess of DEPN is characterized by a linear variation of $\ln ([M]_0/[M])$ with time. The bimolecular termination that certainly occurs to a very moderate extent is not detected.

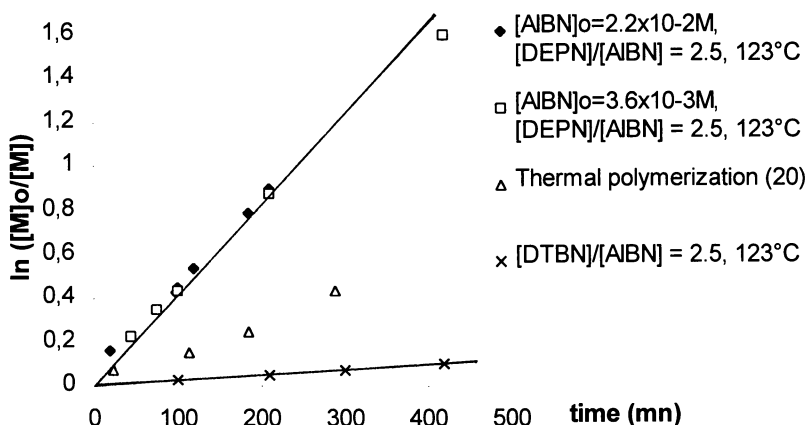


Figure 2. $\ln([M]_0/[M])$ versus time for Styrene free-radical polymerization at 123°C.

Under similar conditions, that is with 2.5 excess of radical scavenger, the AIBN/TEMPO (or DTBN) system exhibits quite a different pattern ; polymerization begins only after a long period of induction, a feature that has also been noticed by Matyjaszewski (19).

Another striking feature which deserves comment is the large difference between the processes respectively mediated by DEPN and more classical nitroxyls such as TEMPO or DTBN. In the latter cases, Fukuda *et al.* (11) and Greszta *et al.* (13), (14) established that the rate of polymerization is equal to the rate of the thermal process, independent of the initiator concentration and the type of nitroxyl used. The fact that the rate of DEPN-mediated polymerization strongly differs from

that of the thermal process contrasts with Fukuda's observation and can therefore be viewed as a major addition to the field of nitroxyl-mediated free-radical polymerizations. As DEPN-moderated processes are little affected by the monomer autopolymerization, they have no reason to obey the same kinetics and overall mechanisms as those described by Fukuda for the PS-TEMPO system (11). The determination of the kinetic orders with respect to initiator and monomer for DEPN-mediated polymerization and also the evaluation of the rate constants of dissociation (k_d) and formation (k_{rec}) of the dormant species will be the subject of a subsequent article. Such measurements indeed require that specific experiments be carried out, wherein stoichiometric amounts of initiator and radical scavenger will be used.

A close examination of the results plotted in Figure 2 reveals an apparent and intriguing zero order dependence of the rate of polymerization with respect to the initial concentration of AIBN ; regardless of the amount of AIBN used and the molar mass targeted, the conversion proceeds at the same pace. This result can be rationalized using the following arguments :

as $[P^\circ]$ (concentration of growing radicals) remains essentially constant throughout polymerization and is obviously supplied by the sole decomposition of [PS-DEPN] adduct, the formalism that serves to describe the persistent radical effect (21) can also be used here :

$$d[\text{DEPN}] / dt = k_d[\text{PS-DEPN}]_t - k_{rec}[\text{DEPN}]_t [P^\circ]_t = 0$$

As [PS-DEPN] can be identified to $2 \times [\text{AIBN}]_0$ -the efficiency of AIBN is indeed close to 1- and $[\text{DEPN}]_t$ to $0.5 \times [\text{AIBN}]_0$ - $[\text{DEPN}]_t$ is indeed equal to $[\text{DEPN}]_0 - 2 \times [\text{AIBN}]_0$ - , $[P^\circ]$ can be written as :

$$[P^\circ] = 4 k_d / k_{rec}$$

This expression shows that $[P^\circ]$ is effectively independent of the concentration of chains and is essentially controlled by k_d / k_{rec} when DEPN is used in excess with respect to the initiator as was done in this study.

The second criterion to be met before a chain polymerization qualifies as « living » or controlled, is the linear variation of \bar{M}_n with conversion. As shown in Figure 3, \bar{M}_n evolves linearly with monomer consumption for the AIBN/ DEPN system and coincides ideally with the targeted values.

Styrene therefore appears to undergo a truly controlled polymerization when DEPN is used as radical scavenger and in 2.5 molar excess with respect to AIBN.

Controlled Polymerization of n-Butyl Acrylate in the presence of DEPN

The experience gained in the control of the polymerization of styrene helped us to define the best suited conditions for n-butyl acrylate. In the first series of experiments, the same conditions as those successfully used with styrene were adopted.

In the presence of 2.5 molar excess of DEPN with respect to AIBN, samples of narrow MMD are generated but the control of molar masses turns out to be rather poor. The efficiency of the initiator is indeed found to revolve around 60-70 %

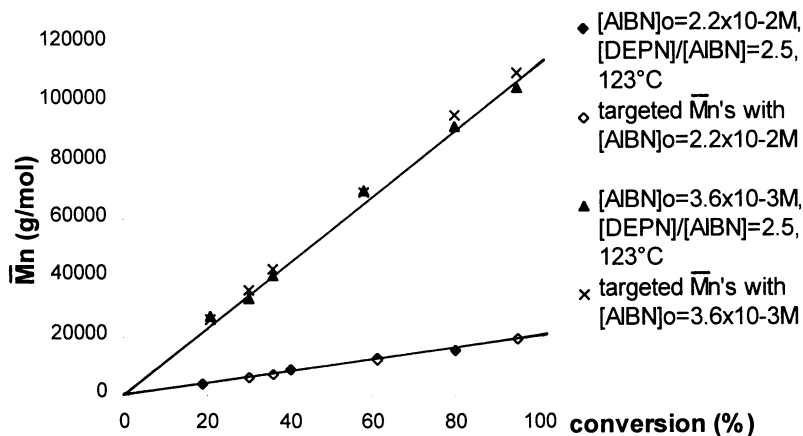


Figure 3. \bar{M}_n versus conversion for DEPn mediated Styrene polymerization at 123°C.

denoting that a good proportion of the initiator radicals is lost in unproductive reactions. Far better results are obtained upon increasing the molar excess of DEPn to 5 fold with respect to AIBN. Experimentally measured number average molar masses and targeted values are in excellent agreement whereas polydispersity indices never exceed 1.2 (Table III).

Table III. Polymerization of n-Butyl Acrylate as a function of [DEPN]/[AIBN] ratio

$\frac{[DEPN]}{[AIBN]}$	$\frac{[AIBN]}{(\text{mol/L})}$	aT (°C)	b time	$c\rho$ (%)	$\bar{M}_{n,th}$ (g/mol)	$\bar{M}_{n,exp}$ (g/mol)	$dPDI$
2.5	1.8×10^{-2}	120	2.33	12	2900	3800	1.12
			24.00	67	16000	24000	1.08
			42.00	95	23500	37000	1.20*
5	1.8×10^{-2}	120	2.50	5	1000	1100	1.12
			24.00	55	13000	13500	1.08
			42.00	72	17500	17000	1.09

a: temperature of reaction ; b : reaction time in hours ; c: conversion ; d : polydispersity index (\bar{M}_w/\bar{M}_n) ; * shoulder.

This remarkable control of molar mass is, however, obtained at the expense of a slower rate of polymerization, a feature which was expected.

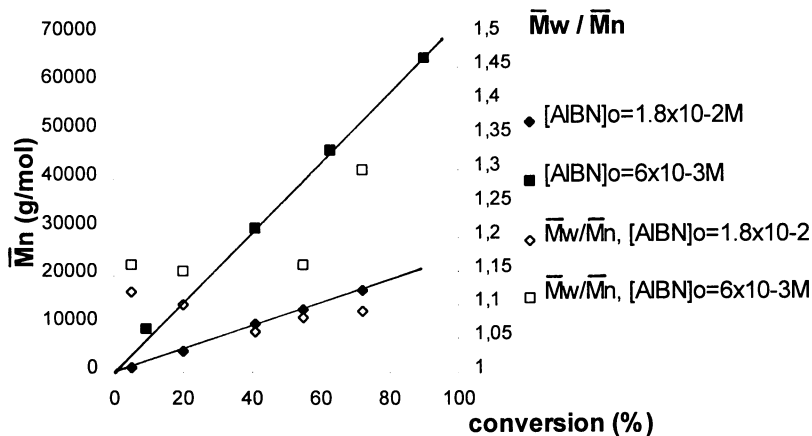


Figure 4. \bar{M}_n versus conversion for various concentrations of AIBN at 120°C using 5 : 1 excess of [DEPN] to [AIBN].

A second series of experiments was carried out with the aim of studying the effect of the initiator concentration. Concentrations of AIBN corresponding to targeted \bar{M}_n 's of 25000 and 75000 g/mol were used, the ratio of [DEPN] to [AIBN] being kept constant at 5 (Figure 4).

In these two cases, the samples obtained exhibited a narrow distribution of molar masses and the efficiency of the initiator falls close to 1 as shown by the excellent agreement between $\bar{M}_{n,exp}$ and $\bar{M}_{n,th}$.

As to the increase of the molar masses with conversion, it denotes the absence of any transfer; \bar{M}_n indeed increases linearly with conversion and comes close to agreement with targeted values whenever a 5 fold excess of DEPN with respect to AIBN is used.

The last parameter that was examined is the temperature of polymerization, all other factors being kept invariant. Not surprisingly, it was noticed that the rate of polymerization markedly decreases when the temperature drops to 100°C; it took five days to complete 58% conversion whereas one day was enough to achieve the same conversion at 123°C. The $\ln([M]_o/[M])$ vs time plot for the AIBN / DEPN (1 : 5) system exhibits a perfectly linear relationship, regardless of the temperature considered or the concentration of initiator used (Figure 5). The absence of any downward curvature in this plot indicates that the concentration of growing radicals remains essentially constant throughout polymerization.

Similar to the case of styrene, the rate of polymerization is independent of the concentration of initiator, being essentially governed by the excess of radical scavengers used; for n-butyl acrylate also, the value taken by $[P^\circ]$, that is obtained from the rate versus time plot is controlled by $K = k_d/k_{rec}$.

This is to our knowledge the first report disclosing that acrylic monomers can also be polymerized under truly « living »/controlled conditions by a free radical mechanism, provided appropriate nitroxyl radicals are used as radical scavengers.

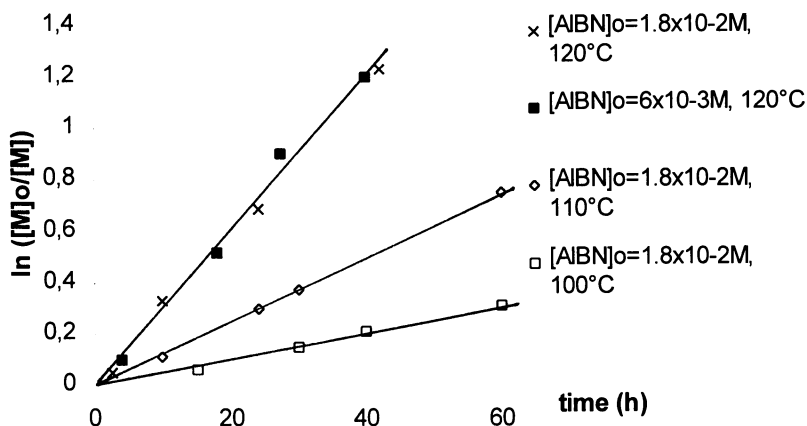


Figure 5. $\ln([M]_0/[M])$ versus time for DEPN-mediated polymerization of n-butyl acrylate at various temperatures (with 5 : 1 excess of [DEPN] vs. [AIBN]).

Conclusions

DEPN is a newly synthesized nitroxyl radical that has been successfully used to control the free-radical polymerization of styrene and n-butyl acrylate. The systems consisting of AIBN and DEPN yield well-defined polymers ($\overline{M}_w/\overline{M}_n \approx 1.1$ to 1.4) within a large range of molar masses. In sharp contrast to the processes mediated by TEMPO or DTBN, the polymerization of styrene, carried out in the presence of DEPN, is not affected by the thermal autopolymerization of the monomer. Indeed, DEPN couples to growing styryl radicals and forms alkoxyamine bonds that are weak enough to allow fast and yet controlled polymerization of styrene.

DEPN is even more interesting for acrylic monomers. In contrast to previous observations that stressed the inability of nitroxyl radicals to mediate controlled chain growth in the case of acrylates, the polymerization of n-butyl acrylate is found to fulfill all the criteria of a « living » system.

The « living »/controlled character that is observed for the two types of monomers paves the way for the synthesis of PS-b-PBuA di- and triblock copolymers; this aspect will be the subject of a subsequent article.

Extension of the AIBN/DEPN systems to methacrylic monomers is also currently investigated.

Acknowledgments

The authors gratefully acknowledge ELF-ATOCHEM and CNRS for joint financial support.

Literature Cited

- (1) Matyjaszewski, K. *J. Phys. Org. Chem.* **1995**, *8*, 197.
- (2) Solomon, D. H.; Rizzardo, E.; Cacioli, P. U.S. Patent **1986** 4, 581, 429.
- (3) Georges, M. K.; Veregin, R. P. N.; Kazmaier, P. M.; Hamer, G. K. *Macromolecules* **1993**, *26*, 2987.
- (4) Kazmaier, P. M.; Moffat, K. A.; Georges, M. K.; Veregin, R. P. N.; Hamer, G. K. *Macromolecules* **1995**, *28*, 1841.
- (5) Wang, J. S.; Matyjaszewski, K. *J. Am. Chem. Soc.* **1995**, *117*, 5614.
- (6) Wang, J. S.; Matyjaszewski, K. *Macromolecules* **1995**, *28*, 7901.
- (7) Matyjaszewski, K.; Patten, T.; Xia, J. *J. Am. Chem. Soc.* **1997**, *119*, 674.
- (8) (a) Sawamoto, M.; Kato, M.; Kamigaito, M.; Higashimura, T. *Polym. Prepr., ACS Polym. Div.* **1995**, *36*(1), 539, (b) Kato, M.; Kamigaito, M.; Sawamoto, M.; Higashimura, T. *Macromolecules* **1995**, *28*, 1721, (c) Ando, T.; Kato, M.; Kamigaito, M.; Sawamoto, M. *Macromolecules* **1996**, *29*, 1070, (d) Kotani, Y.; Kato, M.; Kamigaito, M.; Sawamoto, M. *Macromolecules* **1996**, *29*, 6979.
- (9) Granel, C.; Dubois, Ph.; Jérôme, R.; Teyssié, Ph. *Macromolecules* **1996**, *29*, 8576.
- (10) Catala, J. M.; Bubel, F.; Hammouch, S. O. *Macromolecules* **1995**, *28*, 8441.
- (11) Fukuda, T.; Terauchi, T.; Goto, A.; Ohno, K.; Tsuji, Y.; Miyamoto, M.; Kobatake, S.; Yamada, B. *Macromolecules* **1996**, *29*, 6396.
- (12) Fukuda, T.; Terauchi, T. *Chemistry Lett. (Tokyo)* **1996**, 293.
- (13) Greszta, D.; Matyjaszewski, K. *Macromolecules* **1996**, *26*, 5239.
- (14) Greszta, D.; Matyjaszewski, K. *Macromolecules* **1996**, *26*, 7661.
- (15) Matyjaszewski, K.; Gaynor, S.; Greszta, D.; Mardare, D.; Shigemoto, T. *J. Phys. Org. Chem.* **1995**, *8*, 306.
- (16) Veregin, R. P. N.; Georges, M. K.; Hamer, G. H.; Kazmaier, P. M. *Macromolecules* **1995**, *28*, 4391.
- (17) Grimaldi, S.; Finet, J. P.; Zeghdaoui, A.; Tordo, P.; Benoit, D.; Fontanille, M.; Gnanou, Y.; Nicol, P. *Polym. Prepr., ACS Polym. Div.* **1997**, *38*(1), 651.
- (18) Veregin, R. P. N.; Georges, M. K.; Kazmaier, P. M.; Hamer, G. H. *Macromolecules* **1993**, *26*, 5316.
- (19) Mardare, D.; Shigemoto, T.; Matyjaszewski, K. *Polym. Prepr., ACS Polym. Div.* **1994**, *35*(2), 557.
- (20) Wui, A.; Hamielec, A. *J. Applied Polym. Sci.* **1972**, *16*, 749.
- (21) Fischer, H. *J. Am. Chem. Soc.* **1986**, *108*, 3925.

Chapter 15

Nitroxide-Mediated Controlled Radical Polymerization: Toward Control of Molar Mass

Stefan A. F. Bon, Frank A. C. Bergman, J. J. G. Steven van Es,
Bert Klumperman, and Anton L. German

Eindhoven Polymer Laboratories, Eindhoven University of Technology,
Laboratory of Polymer Chemistry, P.O. Box 513, 5600 MB Eindhoven,
Netherlands

The mechanism of the TEMPO-mediated controlled radical polymerization of styrene in bulk is discussed. It is shown that the isotropic correlation time (τ_c) of a nitroxide can be used as a measure of the diffusive rate coefficient of trapping (k_{et}^D). A general empirical relationship for the density of polystyrene as a function of molar mass and temperature is established to correct concentration data obtained from CRP experiments for volume contraction. It is demonstrated that the overall rates of polymerization of styrene in bulk do not show a dependence upon alkoxyamine concentration. Broadening of the molar mass distribution in a CRP experiment is ascribed to a low rate of alkoxyamine C-O bond homolysis and permanent chain-stopping reactions, e.g. bimolecular termination.

The quest for a polymerization technique that can be applied to a wide variety of vinyl monomers and affords the possibility to design and synthesize a polymer material with control of the molar mass distribution as well as of the configurational and compositional monomer sequences may be a mirage. Fact is that numerous efforts are being undertaken to develop novel polymerization systems, for which one or preferably more of the above criteria are met.

One of the systems that presumably has the ability to fulfill all these expectations and has therefore received great attention lately, is the nitroxide-mediated controlled radical polymerization (CRP)(*I*). The concept of this novel technique is essentially an elementary living radical polymerization system, consisting of a constant number of dormant species that can be reversibly activated, at a rate fast compared to the overall rate of polymerization. In the activated form it undergoes

The rate coefficient for trapping (k_{et}) therefore has to be described as:

$$\frac{1}{k_{\text{et}}} = \frac{1}{k_{\text{et}}^{\text{D}}} + \frac{1}{k_{\text{et}}^{\text{chem}}} \quad (1)$$

Diffusion of T• and R•. The diffusive rate coefficient for trapping (k_{et}^{D}) is a function of the diffusion coefficient of the two species involved, i.e. R• and T•. Since the nitroxide usually is a compound of small size, its diffusion coefficient (D) can be described by the Stokes-Einstein equation, with $k_{\text{B}}/ \text{J}\cdot\text{K}^{-1}$ as the Boltzmann constant, T/ K as the absolute temperature, $\eta/ \text{Pa}\cdot\text{s}$ as the microviscosity, r/ m as the hydrodynamic radius (6, 7) and a constant $\beta = 4$ for stick boundary conditions or $\beta = 6$ for slip boundary conditions (8):

$$D = \frac{k_{\text{B}} T}{\beta \pi \eta r} \quad (2)$$

Data obtained in various solvents for the diffusion coefficient of 1-oxy-2,2,6,6-tetramethylpiperidine (TEMPO) reveal that the activation energy for diffusion merely coincides with the activation energy for viscosity changes of the solvent, indicating that no specific interactions between solvent and nitroxide could be observed (6).

However, a complication arises in finding a correct value for the microscopic viscosity that is perceived by the nitroxide in a polymer solution. It is plausible that the viscosity of a medium experienced by a diffusing molecule depends on its size and shape. Instead of the macroscopic viscosity, a value for viscosity should be used that fits the geometric scale of the solute.

Rotational Correlation Time (τ_{c}). As a measure of the microscopic viscosity of the nitroxide during a controlled radical polymerization, the rotational correlation time (τ_{c}) can be used. Its value can be calculated from ESR spectra, e.g. the spectra obtained when monitoring the nitroxide concentration vs. time during a CRP experiment. During the first stages of polymerization the rotational motion of the nitroxide will be rapid, which allows a simple analysis for τ_{c} , with $\Delta H_{(m=+1)}/ \text{G}$ as the peak-to-peak distance of the low-field absorption line, $I_{(m=+1)}/ \text{a.u.}$ as the peak-to-peak height of the low-field absorption line, $I_{(m=-1)}/ \text{a.u.}$ as the peak-to-peak height of the high-field absorption line (9):

$$\tau_{\text{c}} = 6.6 \times 10^{-10} \Delta H_{(m=+1)} \left[\sqrt{\frac{I_{(m=+1)}}{I_{(m=-1)}}} - 1 \right] \quad (3)$$

The isotropic rotational diffusion can be described by the Stokes-Einstein-Debye equation, which yields a value for the microscopic viscosity:

$$\tau_{\text{c}} = \frac{4 \pi r^3 \eta}{3 k_{\text{B}} T} \quad (4)$$

If the viscosity of the system becomes high, the rotational motion of the nitroxide is restricted. This induces anisotropy implying that severe deformations of the ESR spectrum will occur, and, therefore, a more complex analysis to describe the microscopic viscosity and, consequently, the diffusion coefficient, is required (10).

The other species involved in the trapping reaction is the carbon-centered radical $R\cdot$. Due to the presence of monomer, these radicals will be able to propagate to yield species of variable chain length. The chain length distribution of these carbon-centered radicals depends on the kinetic events that occur throughout the polymerization. Together with the solute specificity of the microscopic viscosity, this results in an intricate task to describe the diffusive rate coefficient for trapping.

An approximation that can be made is to consider only a chain length dependence for the diffusive rate coefficient of trapping (k_{et}^D) of oligomeric species (11). In addition it is assumed that the dimensions for the microscopic viscosity are identical for these small species (In general, however, the diffusion coefficient for $R\cdot$ will have a minor influence on the mutual diffusion coefficient, $D = D_R + D_T$). Thus, it can be assumed that the diffusive rate coefficient of trapping (k_{et}^D) is solely determined by D_T .

If k_{et}^D is expressed as a Smoluchowski equation and the isotropic correlation time τ_c is used as a measure of the microviscosity, with σ_r/m as the non-reversible distance of interaction, N_A/mol^{-1} as Avogadro's number, p as the spin factor, its combination with Equations 2 and 4 yields (with $\sigma_r = r$, $\beta = 4$ and $p = 1/4$):

$$k_{et}^D = 4\pi\sigma_r N_A p (D_R + D_T) \cong \frac{\pi N_A r^3}{3\tau_c} \quad (5)$$

From this equation it can be observed that τ_c can be used as a measure of the diffusive rate coefficient (k_{et}^D) of trapping. The monitoring of the nitroxide concentration by quantitative ESR measurements during a CRP experiment could therefore be used to investigate a decrease in k_{et}^D .

Intrinsic Chemical Reaction between $R\cdot$ and $T\cdot$. The overall rate of trapping (k_{et}) also depends on the intrinsic chemical reaction between $R\cdot$ and $T\cdot$ (12). Therefore, to study the corresponding intrinsic chemical rate of trapping (k_{et}^{chem}) both species, i.e. $R\cdot$ and $T\cdot$, have to be considered.

One of the relevant aspects that has to be taken into account is the two canonical forms of the nitroxide bond (see Figure 1). Polar solvents will stabilize the dipolar form, thereby increasing the spin density on nitrogen. This effect decreases the reactivity of the nitroxide for the trapping reaction, as has been confirmed by Beckwith *et al.* (13) for the trapping of benzyl radicals with TEMPO.

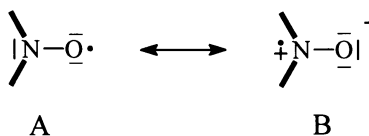


Figure 1. Canonical structures of a nitroxide.

Rate of Alkoxyamine C-O Bond Homolysis

The rate coefficient of homolytic dissociation (k_{ed}) of the alkoxyamine C-O bond is one of the fundamental aspects that has to be considered in a controlled radical polymerization (4). We have developed a method to obtain data for k_{ed} , inspired by

the half-life measurements of Rizzardo *et al.*(5). These so-called nitroxide-exchange experiments are based upon a system that obeys pseudo-first order kinetics.

In a typical experiment an alkoxyamine (L_1) is dissociated into radical species $R\bullet$ and the corresponding nitroxide $T_1\bullet$. An excess of a different nitroxide ($T_2\bullet$) present in the reaction mixture assures that the only fate for $R\bullet$ is to be trapped with this nitroxide $T_2\bullet$ to yield the alkoxyamine L_2 . In this study the dissociation of compound (1) in toluene with 4-benzoyloxy-1-oxy-2,2,6,6-tetramethylpiperidine as $T_2\bullet$ was investigated by following its consumption and the corresponding production of L_2 by reversed phase HPLC analysis, leading to k_{ed} (4).

The following Arrhenius equation for the rate coefficient of homolytic dissociation (k_{ed}) of compound (1) in toluene was obtained ($333\text{ K} \leq T \leq 373\text{ K}$):

$$k_{ed} = 9.1_2 \times 10^{14} \exp\left(\frac{-138.8 \times 10^3}{RT}\right) \quad (6)$$

Noteworthy is that a hydrogen atom abstraction by 4-benzoyloxy-1-oxy-2,2,6,6-tetramethylpiperidine from toluene to yield a benzyl radical and the corresponding hydroxyl amine, has been observed as a non-intervening side-reaction.

Relative Inertness of Nitroxides. It is known that nitroxides are able to abstract hydrogen atoms readily under photochemical conditions. The hydrogen atom is abstracted by the photoexcited nitroxyl group in the $n \rightarrow \pi^*$ excited state (14). Thermal hydrogen atom abstraction, as has been observed, is possible at elevated temperatures for conventional nitroxides, such as TEMPO and derivatives thereof (15, 16). (Nitroxides with electron-withdrawing substituents are much more reactive towards hydrogen atom abstraction and addition reactions to vinyl groups, e.g. 1-oxy-1,1-bis(trifluoromethyl)amine (17)). This confirms that nitroxides are not completely inert and capable of hydrogen atom abstraction.

The hydrogen atom abstraction from the styrene Diels-Alder dimer, observed by Moad *et al.*(18) for TEMPO and TMIO would influence the initiation process markedly. However, it is likely to assume that the hydrogen atom abstraction of the Diels-Alder dimer is a side reaction of minor importance in a CRP experiment, since the overall concentration of $T\bullet$ is low in comparison with the systems for which the hydrogen atom abstraction was observed.

However, the capability of nitroxides to abstract hydrogen atoms may lead to trapping by disproportionation, that is hydrogen atom abstraction from $R\bullet$ to yield an unsaturated end-functionalized dead polymeric chain and the corresponding hydroxyl amine. This indeed is observed clearly for systems having an α -methyl group as substituent next to the alkoxyamine bond (5, 19).

Since absolute inertness of the nitroxide species is ruled out, any possible addition of a nitroxide to a monomer to yield a carbon centered radical species also has to be considered. Whether this occurs at all, and if so as a simple addition or via a concerted mechanism induced by polarization of the vinyl group by the nitroxide is still unsolved (16-18, 20).

Impact of Reversible Homolysis of Alkoxyamine C-O Bond on Fundamental Free-Radical Polymerization Kinetics

The occurrence of permanent chain stopping reactions, i.e. bimolecular termination and transfer, cannot be excluded in a free-radical polymerization. If no specific interaction between T^\bullet and R^\bullet occurs, the alkoxyamine C-O bond homolysis and trapping can be incorporated as additional reactions in the events occurring during a free-radical polymerization.

Imagine a system composed of an alkoxyamine dissolved in an inert solvent. The three fundamental reactions that can occur in this system are the homolytic dissociation of the alkoxyamine, trapping of R^\bullet by T^\bullet and permanent bimolecular termination of two R^\bullet . It is easy to understand that the occurrence of permanent bimolecular termination leads to a continuous production of T^\bullet , resulting in $[T^\bullet]$ being considerably higher than $[R^\bullet]$. It can be inferred that, due to a continuous decrease in the probability of bimolecular termination, a quasi-equilibrium will be reached when time goes to infinity (4):

$$\lim_{t \rightarrow \infty} \frac{[R^\bullet][T^\bullet]}{[L]} = \lim_{t \rightarrow \infty} K = \frac{k_{ed}}{k_{et}} = K_{eq} \quad (7)$$

The continuous decrease in $[R^\bullet]$ results in a decreasing overall rate of polymerization, eventually leading to long reaction times and incomplete conversion.

To suppress the production of $[T^\bullet]$, as a direct result of bimolecular termination, and to simultaneously increase the overall rate of polymerization, an additional radical flux, i.e. the production of radicals by a source other than the homolytic dissociation of the alkoxyamine, can be added. In Figure 2, $[T^\bullet]$ and $[R^\bullet]$ vs. time are plotted for an imaginary system discussed above, having an additional radical flux of $\sigma = 1.0 \times 10^{-8} \text{ mol}\cdot\text{L}^{-1}\cdot\text{s}^{-1}$ with $k_{ed} = 1.0 \times 10^{-5} \text{ s}^{-1}$, $k_{et} = 5.0 \times 10^8 \text{ L}\cdot\text{mol}^{-1}\cdot\text{s}^{-1}$, $k_t = 2.5 \times 10^9 \text{ L}\cdot\text{mol}^{-1}\cdot\text{s}^{-1}$ and $[L]_0 = 0.01 \text{ mol}\cdot\text{L}^{-1}$, $[R^\bullet]_0 = [T^\bullet]_0 = 0 \text{ mol}\cdot\text{L}^{-1}$.

It can be observed from this picture that the current system reaches a steady-state after a certain period of time with a value of the overall radical concentration corresponding to:

$$R_{s.s.} = \sqrt{\frac{\sigma}{2 k_t}} \quad (8)$$

The process eventually leading to steady-state conditions is also referred to as the "persistent radical effect" (21, 22). Furthermore, the steady-state implies:

$$K_{s.s.} = \frac{[R^\bullet]_{s.s.} [T^\bullet]_{s.s.}}{[L]_{s.s.}} = K_{eq} \quad (9)$$

These simulations indicate that the overall radical concentration in a CRP experiment with a properly adjusted additional radical flux is independent of the radical production by homolytic dissociation of the alkoxyamines present.

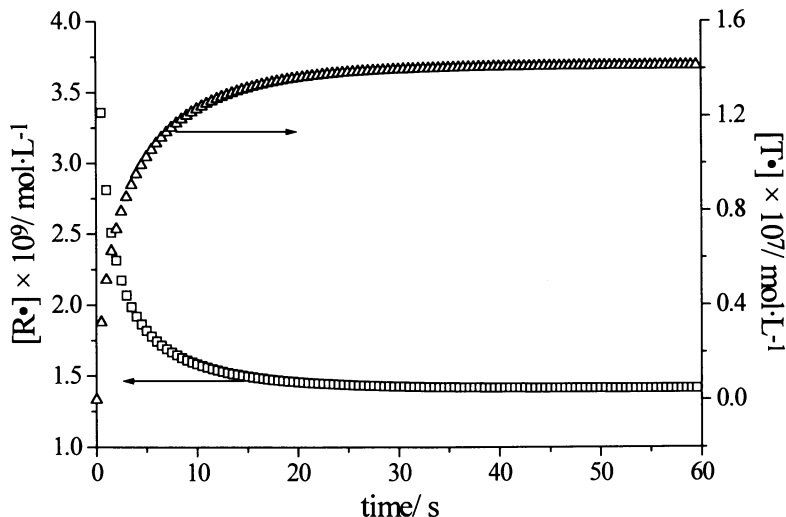


Figure 2. Imaginative system of an alkoxyamine dissolved in an inert solvent, in which the three fundamental reactions that can occur are the homolytic dissociation of the alkoxyamine, trapping of $R\cdot$ by $T\cdot$ and permanent bimolecular termination of two $R\cdot$. Simulated $[T\cdot]$ and $[R\cdot]$ vs. time (Δ and \square , resp.) with $k_{ed} = 1.0 \times 10^{-5} \text{ s}^{-1}$, $k_{et} = 5.0 \times 10^8 \text{ L}\cdot\text{mol}^{-1}\cdot\text{s}^{-1}$, $k_t = 2.5 \times 10^9 \text{ L}\cdot\text{mol}^{-1}\cdot\text{s}^{-1}$, $\sigma = 1.0 \times 10^{-8} \text{ mol}\cdot\text{L}^{-1}\cdot\text{s}^{-1}$ and $[L]_0 = 0.01 \text{ mol}\cdot\text{L}^{-1}$, $[R\cdot]_0 = [T\cdot]_0 = 0 \text{ mol}\cdot\text{L}^{-1}$.

It can be calculated that for chain length-independent values for k_{et} and k_t , the ratio of radicals derived from the additional radical flux over radicals derived from alkoxyamine homolysis (r_σ) equals:

$$r_\sigma = \frac{\sigma}{k_{ed} [L]} \quad (10)$$

As r_σ is small, the major part of the radicals propagating are derived from an alkoxyamine. This results in a controlled chain-growth of the constant number of alkoxyamines leading, under ideal conditions, to a linear relation between average molar mass vs. conversion (X_w) and narrow molar mass distributions.

Volume Contraction

To investigate the kinetics of a TEMPO-mediated controlled radical polymerization of styrene in bulk, e.g. by monitoring the overall gravimetrically determined conversion, X_w , vs. time or the concentration of TEMPO, $[T\cdot]$, it is important to mention that the data obtained need to be corrected for volume contraction, as a direct result of polymerization.

It is assumed that a negligible volume contraction occurs upon mixing of polymer and monomer (23). Ideal behavior of mixing leads to the following expression for the average density of the system:

$$\rho = \frac{\rho_M \rho_P}{(1 - X_w)\rho_P + X_w \rho_M} \quad (11)$$

The molar mass distribution (MMD) of a controlled radical polymerization is a function of conversion, as can be observed in ,e.g., Figures 9a and 9b. Consequently, the molar mass dependence of the density of the polymer has to be taken into account. As a measure of the molar mass, the theoretical weight average molar mass can be taken:

$$\frac{1}{\rho} = \frac{(1 - X_w)}{\rho_M} + \frac{X_w}{\rho_P \langle M_w^{\text{theor}} \rangle} \quad (12)$$

However, a more accurate description representing the polymer solution is obtained, when using the normalized weight MMD determined from SEC analysis, yielding:

$$\frac{1}{\rho} = \frac{(1 - X_w)}{\rho_M} + w(M) \frac{X_w}{\rho_P(M)} \quad (13)$$

To correct the data of the polymerization reactions of styrene for volume contraction, an empirical relationship for the density of polystyrene as a function of molar mass and temperature has been established (24):

$$\rho(M, T) = A - B \times 10^{-4} T \quad (14)$$

with:

$$\begin{aligned} A &= a_A + b_A \xi + c_A \xi^2 + d_A \xi^3 \\ B &= a_B + b_B \xi^{-1} + c_B \xi^{-2} + d_B \xi^{-3} \end{aligned} \quad (15)$$

$$\xi = \ln(\log(M))$$

The values for the constants a_A, \dots, d_B are given in Table I. Figure 3 represents the density of polystyrene, ρ , vs. $\log(M)$ at 393.15 K. As can be observed, a large dependence of ρ on molar mass is observed for low molar mass material up to about $5.0 \times 10^4 \text{ g}\cdot\text{mol}^{-1}$.

Table I. Constants of $\rho(M, T)$ for Polystyrene

Index:	a_i	b_i	c_i	d_i
A	0.96402817	0.42456027	-0.23245121	0.045159034
B	6.289622	-1.6441887	0.16572399	1.5493251

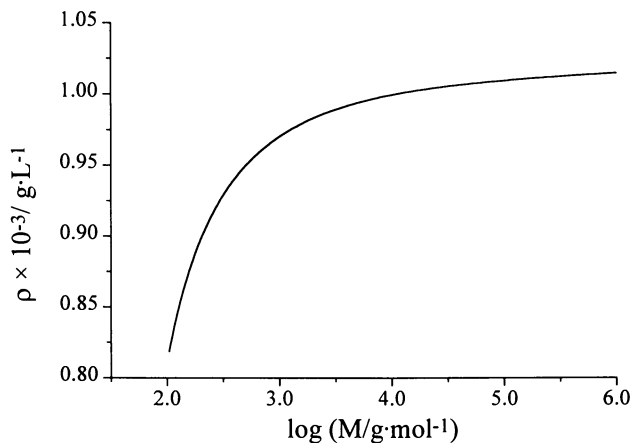


Figure 3. Density ($\rho \times 10^{-3} / \text{g}\cdot\text{L}^{-1}$) vs. log molar mass ($M / \text{g}\cdot\text{mol}^{-1}$) of polystyrene at 393.15 K.

These results indicate that a constant value for the density of polystyrene cannot be assumed implying that molar mass dependent volume contraction has to be taken into account when analyzing concentration data.

Controlled Radical Polymerization of Styrene in Bulk

Initial Overall Rate of Polymerization. In Figure 4 the concentration of monomer, $[M]$, vs. time for both a thermally initiated spontaneous polymerization of styrene and CRPs at 393 K with $[L]_0 = 9.63 \times 10^{-4} \text{ mol}\cdot\text{L}^{-1}$, $9.02 \times 10^{-3} \text{ mol}\cdot\text{L}^{-1}$ and $4.51 \times 10^{-2} \text{ mol}\cdot\text{L}^{-1}$ are given. The initial overall rates of polymerization are presented in Table II. The data were corrected for volume contraction on the basis of their theoretical molar mass assuming an ideal “living” polymerization system, using Equations 12, 14 and 15.

Table II. Initial Overall Rates of CRPs of Styrene in Bulk at 393 K

$[L]_0 / \text{mol}\cdot\text{L}^{-1}$	$R_{p, t=0} \times 10^4 / \text{mol}\cdot\text{L}^{-1}\cdot\text{s}^{-1}$
0.0	1.1
9.63×10^{-4}	1.0
9.02×10^{-3}	1.0
4.51×10^{-2}	1.2
4.51×10^{-2}	1.2
4.51×10^{-2}	1.1

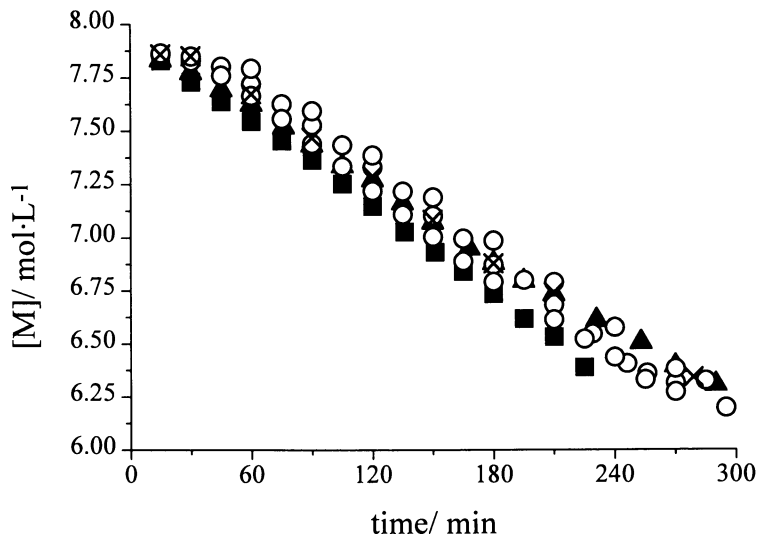


Figure 4. $[M]$ vs. time for both a thermally initiated spontaneous polymerization of styrene (■) and CRPs in bulk at 393 K with $[L]_0 = 9.63 \times 10^{-4} \text{ mol}\cdot\text{L}^{-1}$ (×), $9.02 \times 10^{-3} \text{ mol}\cdot\text{L}^{-1}$ (▲) and $4.51 \times 10^{-2} \text{ mol}\cdot\text{L}^{-1}$ (○).

From these results it can be seen that the initial rates of polymerization merely coincide for all cases within experimental error and, therefore, do not show a significant dependence upon alkoxyamine concentration. This behavior is properly described by the imaginative system represented previously (see also Equation 8). The steady-state overall radical concentration depends on the spontaneous thermal self-initiation of styrene (25) and the average rate coefficient of bimolecular termination.

Since the overall rates of polymerization of the experiments carried out merely coincide and the additional radical flux is presumed not to be influenced markedly by the presence of the alkoxyamines and nitroxides (see section on alkoxyamine C-O bond homolysis) the average rate coefficients for bimolecular termination have to be identical within experimental error. However, the chain length distribution of R^\bullet is different in each case and strongly depends on the amount of alkoxyamines present. Therefore, it can be concluded that for the initial stages of polymerization the chain length dependence of the average rate coefficient of bimolecular termination is leveled out.

ESR Measurements: $[T^\bullet]$ vs. time and τ_c . In Figure 5 the $[T^\bullet]$ vs. time is plotted for a CRP of styrene in bulk at 393 K with $[L_0] = 9.0 \times 10^{-3} \text{ mol}\cdot\text{L}^{-1}$. The ESR spectra measured consisted only of a conventional signal for TEMPO, indicating that a large excess of T^\bullet , in comparison with R^\bullet , is present and no specific interactions occur throughout the controlled radical polymerization. The slight increase in $[T^\bullet]$ vs. time can be ascribed to a decrease in the rate of thermal self-initiation of styrene (25) and to the volume contraction of the system, for which the data acquired have not been corrected.

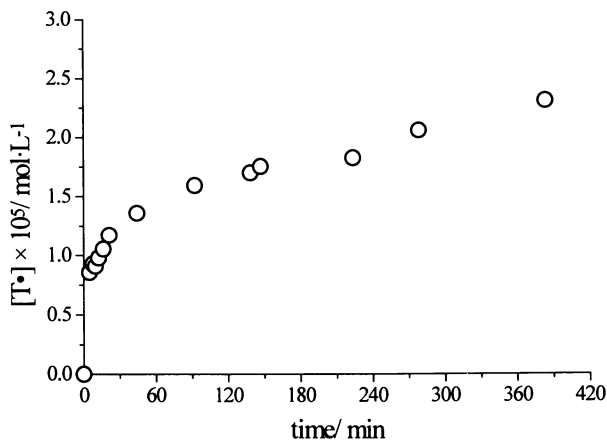


Figure 5. TEMPO concentration ($[T\bullet]$) vs. time for a CRP of styrene in bulk at 393 K with $[L_0] = 9.0 \times 10^{-3} \text{ mol}\cdot\text{L}^{-1}$.

No distinct differences between the intensities of the high-field and low-field absorption lines of the ESR spectra could be detected during polymerization up to high conversion. Therefore, a value of the rotational correlation time needed to calculate a value for k_{et}^D (see Equations 3 and 5) cannot be obtained from these spectra at these elevated temperatures. This indicates that no severe changes in the diffusion coefficient of TEMPO occur, in other words the microscopic viscosity for TEMPO does not show a pronounced change when conversion increases. This can partly be ascribed to the relatively low molar mass material and to the strongly reduced thermal self-initiation of styrene at high conversion levels. (As comparison the diffusion coefficient of toluene in different solutions of polystyrene (26) and the diffusion of styrene-analog penetrants in different solutions of polystyrene can be given (27). A sharp decrease of the diffusion coefficient at moderate temperatures is observed for toluene and styrene at high weight fractions of polystyrene.) Consequently, the k_{et}^D can be considered as a constant under the present experimental conditions.

Trommsdorff Effect. In Figure 6 the concentration of monomer, $[M]$, vs. time for both a thermal spontaneous polymerization of styrene and a CRP with $[L]_0 = 4.40 \times 10^{-2} \text{ mol}\cdot\text{L}^{-1}$ at 413 K are given. The data were corrected for volume contraction on the basis of their theoretical molar mass assuming an ideal “living” polymerization system, using Equations 12, 14 and 15.

The average molar mass produced in a CRP is much lower than in a spontaneous thermal polymerization, as a result of the monomer distribution over the relatively large number of alkoxyamines (see e.g. Figures 7a, 7b and 7c). This difference is also reflected in the chain length distribution (CLD) of the propagating radicals ($R\bullet$). Together with a lower microviscosity for a specific $R_i\bullet$ in the CRP experiment in

comparison with the thermal polymerization at the same X_w , the Trommsdorff effect is less pronounced in the CRP experiment. (Noteworthy is that when all radical species are considered to be identical, the process of reversible homolytic dissociation could be described as randomly removing a radical from the system by trapping with T^\bullet , and reintroducing it at a new position of a randomly chosen alkoxyamine. Whether or not this process contributes to the suppression of the Trommsdorff effect in a highly microviscous system, by enhancing the probability for two radicals to terminate at a specific time scale, is uncertain and needs to be investigated.)

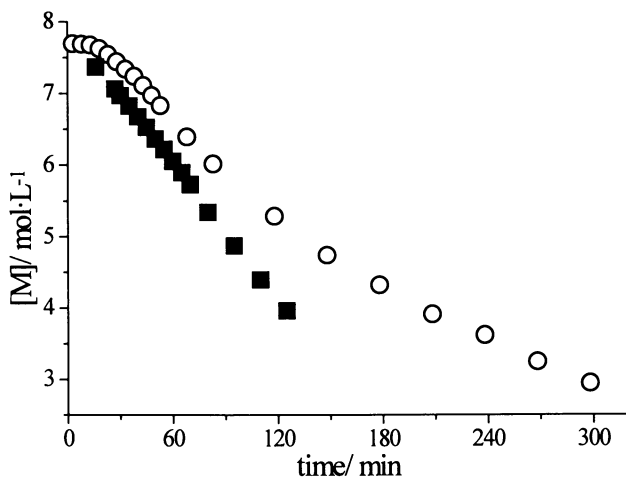


Figure 6. $[M]$ vs. time for both a thermal spontaneous polymerization of styrene (■) and a CRP with $[L]_0 = 4.40 \times 10^{-2} \text{ mol}\cdot\text{L}^{-1}$ (○) in bulk at 413 K.

Fundamental CRP Kinetics. From the data on the overall rate of polymerization and the $[T^\bullet]$ determined for a CRP of styrene at 393 K, with $[L]_0 = 9.0 \times 10^{-3} \text{ mol}\cdot\text{L}^{-1}$, a value of $1.33 \times 10^{-11} \text{ mol}\cdot\text{L}^{-1}$ for K_{eq} can be calculated ($k_p = 2045 \text{ L}\cdot\text{mol}^{-1}\cdot\text{s}^{-1}$, $[M]_0 = 7.86 \text{ mol}\cdot\text{L}^{-1}$, $R_p = 1.1 \times 10^{-4} \text{ mol}\cdot\text{L}^{-1}\cdot\text{s}^{-1}$ and $[T^\bullet] = 1.75 \times 10^{-5} \text{ mol}\cdot\text{L}^{-1}$). (Since a specific interaction between TEMPO and the carbon-centered radical or monomer is not observed it is assumed that the benchmark values of the Arrhenius parameters for the k_p of the bulk polymerization of styrene can be applied (28).) The k_{ed} of compound (1) at 393 K calculated with Equation 11 is $3.3 \times 10^4 \text{ s}^{-1}$. This results in $k_{\text{et}} = 2.5 \times 10^7 \text{ L}\cdot\text{mol}^{-1}\cdot\text{s}^{-1}$. In comparison with literature values of k_{et} for analogous systems (2, 12, 13), the obtained value is an underestimate. This, however, was to be expected, because the rate coefficient of alkoxyamine C-O bond homolysis (k_{ed}) is markedly larger for longer chain lengths, implying that a higher value of the rate coefficient of alkoxyamine homolysis during a CRP experiment must be used.

A large enhancement in k_{ed} is expected and ascribed to the disappearance of the stabilizing electrostatic effect of the electrophilic *tert*-butoxy group on the C-O bond. Moreover, the entropic effects for a higher chain length presumably result in a

small increase in the pre-exponential factor of the Arrhenius equation describing k_{ed} (29). Both effects will result in a higher calculated value for the rate coefficient of homolytic dissociation (k_{ed}).

“Stepwise” Growth. An important requirement to synthesize a uniform polymer material by CRP with proper control of both the molar mass distribution and the chemical composition distribution, is that the average number of monomeric units polymerized per event of chain activation (ν) needs to be smaller than 1 to assure "stepwise" growth of the propagating radicals.

$$\nu = \frac{k_p [M][R\cdot]}{k_{et} [R\cdot][T\cdot] + 2 k_t [R\cdot]^2} \quad (16)$$

A value of 37 for ν can be calculated for the system given above (assuming: $k_t = 1.0 \times 10^7 \text{ L}\cdot\text{mol}^{-1}\cdot\text{s}^{-1}$), which would rule out control of the MMD. Figures 7a, 7b and 7c represent the number and weight average molar masses, $\langle M_n \rangle$ and $\langle M_w \rangle$, together with theoretical molar mass of an ideal living polymerization system ($\langle M_n^{\text{theor.}} \rangle = \langle M_w^{\text{theor.}} \rangle$, $\gamma = 1$) for both a thermally initiated spontaneous polymerization of styrene and CRPs at 393 K with $[L]_0 = 9.63 \times 10^{-4} \text{ mol}\cdot\text{L}^{-1}$ and $4.51 \times 10^{-2} \text{ mol}\cdot\text{L}^{-1}$. In Figures 7b and 7c the polydispersity of the MMD (γ) is included. From these plots it can be concluded that a reasonable control of the MMD is still possible. This confirms the earlier statement that a higher k_{ed} is to be expected for polymeric alkoxyamines.

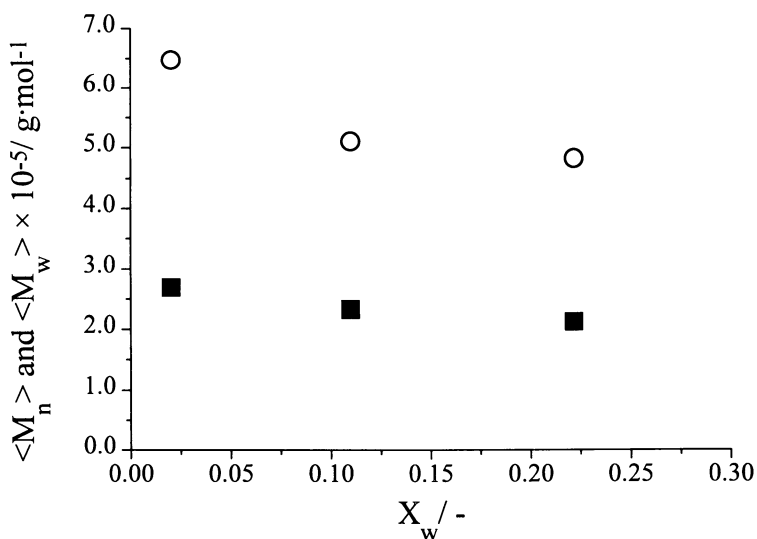


Figure 7a. $\langle M_n \rangle$ (■) and $\langle M_w \rangle$ (○) vs. X_w for a thermally initiated spontaneous polymerization of styrene in bulk at 393 K.

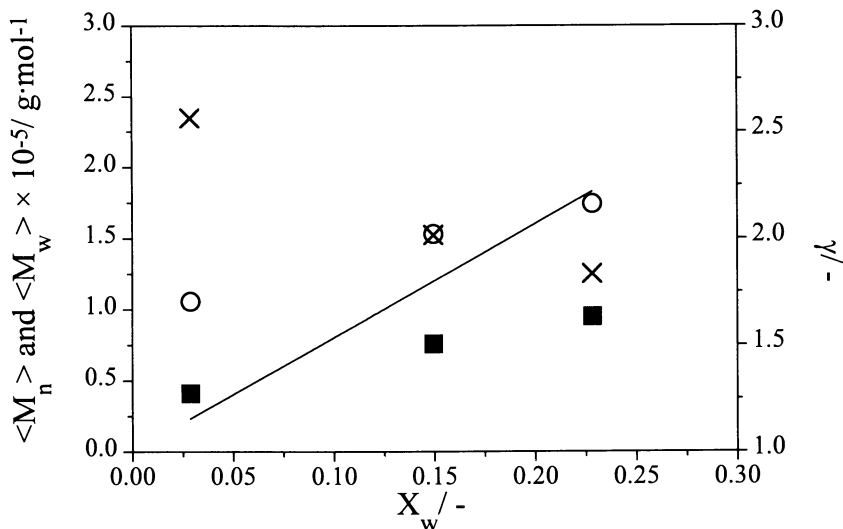


Figure 7b. $\langle M_n \rangle$ (■), $\langle M_w \rangle$ (○) and γ (×), together with theoretical molar mass of an ideal living polymerization system (—) ($\langle M_n^{\text{theor.}} \rangle = \langle M_w^{\text{theor.}} \rangle$, $\gamma = 1$) vs. X_w for a CRP of styrene in bulk at 393 K with $[L]_0 = 9.63 \times 10^{-4} \text{ mol}\cdot\text{L}^{-1}$.

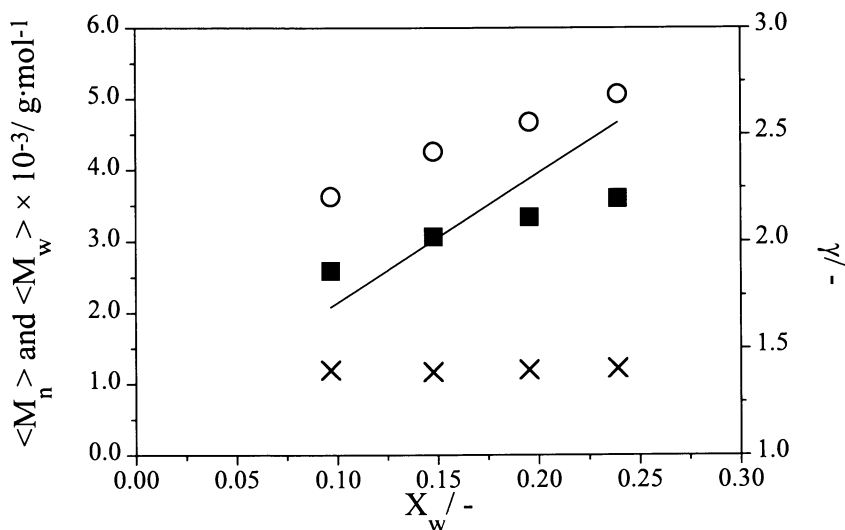


Figure 7c. $\langle M_n \rangle$ (■), $\langle M_w \rangle$ (○) and γ (×), together with theoretical molar mass of an ideal living polymerization system (—) ($\langle M_n^{\text{theor.}} \rangle = \langle M_w^{\text{theor.}} \rangle$, $\gamma = 1$) vs. X_w for a CRP of styrene in bulk at 393 K with $[L]_0 = 4.51 \times 10^{-2} \text{ mol}\cdot\text{L}^{-1}$.

However, the control of the MMD is inadequate and a low polydispersity (γ) is not obtained, in terms of what could be expected from a proper CRP experiment. This could be ascribed to both the slow rate of homolytic dissociation and to the occurrence of permanent chain-stopping reactions.

The k_{ed} of compound (1) at 393 K calculated from Equation 11 is $3.3 \times 10^{-4} \text{ s}^{-1}$ and, therefore, (1) has a corresponding half-life of about 35 min. Since the overall rate of polymerization and, therefore, the monomer consumption rate is fixed, this slow activation leads to broadening of the MMD as a result of the non-instantaneous rate of activation. The molar mass of the polymer material produced during the initial stages of polymerization will be higher than the theoretical value calculated for an ideal "living" radical polymerization system. This effect is clearly seen in Figures 7b and 7c. From Figure 8 the slow dissociation of the initial alkoxyamine, monitored as the outer right peak in the SEC plots, is clearly observed for a CRP of styrene at 393 K, with $[L]_0 = 4.51 \times 10^{-2} \text{ mol}\cdot\text{L}^{-1}$.

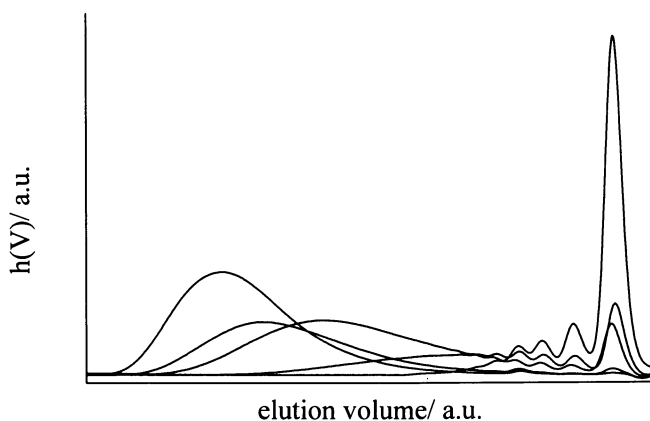


Figure 8. Dissociation of compound (1) monitored as the outer right peak for a CRP of styrene in bulk at 393 K, with $[L]_0 = 4.51 \times 10^{-2} \text{ mol}\cdot\text{L}^{-1}$ ($X_w = 1.4 \times 10^{-3}$, 9.7×10^{-3} , 4.0×10^{-2} , 0.10 and 0.21).

Permanent chain-stopping events restrict the molar mass that can be achieved and broaden the MMD. The production of dead polymer material can largely be ascribed to the additional radical flux. The cumulative fraction of the dead polymer chains has to be kept low to yield a uniform polymer material that is able to undergo further polymerization (e.g. to synthesize a blockcopolymer). Since the overall rates of polymerizations are similar up to moderate conversion, the total number of radicals produced by thermal self-initiation is equal in all cases, implying a similar number of dead polymer chains in each system. Consequently, the fraction of dead polymer material is higher in CRP systems with a lower amount of alkoxyamines. This will be reflected in a broader MMD for these systems. This is confirmed by the polydispersity

(γ) of the MMD from the CRP experiments with $[L]_0 = 9.63 \times 10^{-4} \text{ mol}\cdot\text{L}^{-1}$ and $4.51 \times 10^{-2} \text{ mol}\cdot\text{L}^{-1}$ plotted in Figures 7b and 7c.

To reduce the effect of the low rate of alkoxyamine bond homolysis on the MMD, experiments were carried out at higher temperatures. In Figure 9a the $x(M)$ vs. $\log(M)$ at different stages of conversion for a CRP of styrene with $[L]_0 = 4.40 \times 10^{-2} \text{ mol}\cdot\text{L}^{-1}$ and $[T\cdot]_0 = 1.0 \times 10^{-4} \text{ mol}\cdot\text{L}^{-1}$ is presented. A small amount of TEMPO is added to prevent the average number of monomeric units polymerized per chain activated (ν) to exceed unity at the initial stages of polymerization. In Figure 9b the number and weight average molar masses, $\langle M_n \rangle$ and $\langle M_w \rangle$, together with the corresponding polydispersity γ are given. The line represents the theoretical molar mass for an ideal living polymerization system ($\langle M_n^{\text{theor}} \rangle = \langle M_w^{\text{theor}} \rangle$, $\gamma = 1$).

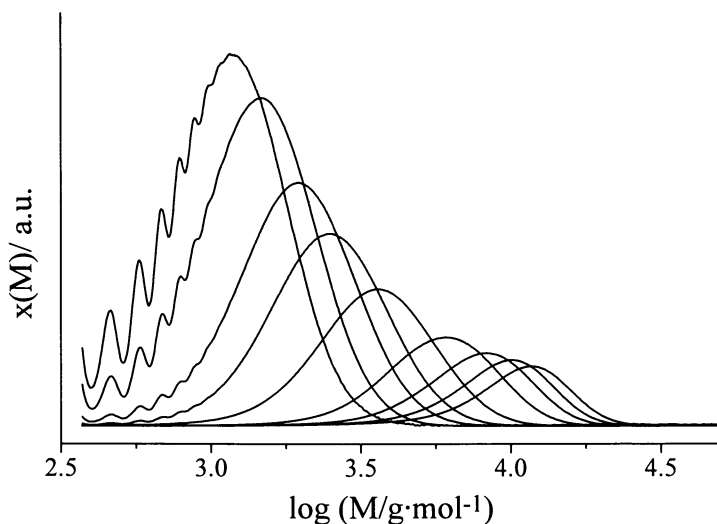


Figure 9a. $x(M)$ vs. $\log(M)$ at different stages of conversion for a CRP of styrene in bulk at 413 K, with $[L]_0 = 4.40 \times 10^{-2} \text{ mol}\cdot\text{L}^{-1}$ and $[T\cdot]_0 = 1.0 \times 10^{-4} \text{ mol}\cdot\text{L}^{-1}$.

At this temperature the measured values for $\langle M_n \rangle$ and $\langle M_w \rangle$ at the initial stages of polymerization are comparable to the theoretical values for an ideal “living” polymerization system. Therefore, the k_{ed} for compound (1) at 413 K calculated from Equation 6, being $2.6 \times 10^{-3} \text{ s}^{-1}$, which corresponds to a half life of about 4.5 min, is sufficiently fast. The comparable average molar masses also indicate that the average number of monomeric units polymerized per event of chain activation (ν) is small. If $R_p/(k_{ed}[L]_0)$ is taken as an estimate for ν ($R_p, t=0 = 4.3 \times 10^{-4} \text{ mol}\cdot\text{L}^{-1}\cdot\text{s}^{-1}$), a value of 3.8 would be obtained. Since the k_{ed} value for compound (1) is an underestimate for its value for a polymeric alkoxyamine, it can be presumed that “stepwise” insertion of monomer takes place. This is confirmed by the SEC results shown in Figure 9a.

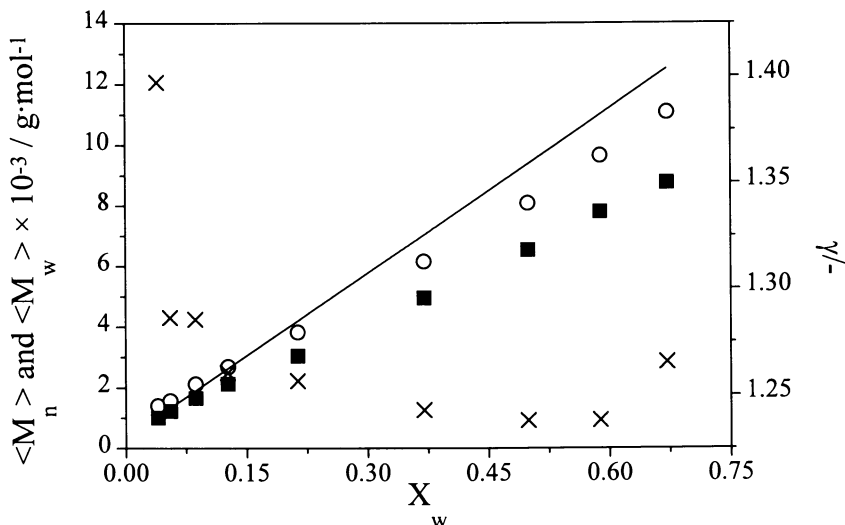


Figure 9b. $\langle M_n \rangle$ (■), $\langle M_w \rangle$ (○) and γ (×), together with theoretical molar mass of an ideal living polymerization system (—) ($\langle M_n^{\text{theor.}} \rangle = \langle M_w^{\text{theor.}} \rangle$, $\gamma = 1$) vs. X_w for a CRP of styrene in bulk at 413 K with $[L]_0 = 4.40 \times 10^{-2} \text{ mol}\cdot\text{L}^{-1}$.

The occurrence of permanent chain stopping reactions is reflected in negative deviation for $\langle M_n \rangle$ and $\langle M_w \rangle$ vs. conversion (X_w), from the dependence of the average molar masses on conversion for the ideal “living” polymerization system. Due to the thermal self-initiation of styrene (25), short-short and short-long bimolecular termination (3, 11) are in direct competition with the trapping of $R\cdot$ by $T\cdot$ (2, 12, 13). This results in the production of dead polymer material and the formation of novel alkoxyamines of, relatively, low molar mass. Consequently, a broadening of the MMD will occur, acting as a cumulative effect throughout the polymerization. This effect is more pronounced in the number MMD. This, indeed, is observed in Figures 9a and 9b.

Conclusions

Further progress in molar mass control of nitroxide-mediated controlled radical polymerization requires detailed insight in the impact on the kinetics and mechanism upon addition of the alkoxyamine and nitroxide. Several aspects to investigate these influences were presented in a study on the TEMPO-mediated radical polymerization of styrene in bulk. It has been shown that the isotropic correlation time (τ_c) of a nitroxide can be used as a measure of the diffusive rate coefficient of trapping (k_{et}^{D}) and that under the conditions of the CRP experiments performed a constant value of k_{et} can be assumed. The Arrhenius parameters obtained for model compound (1), accurately determined by the nitroxide-exchange experiments, give an underestimated value of the

k_{ed} of polymeric alkoxyamines. A general empirical relationship for the density of polystyrene as a function of molar mass and temperature has been established to correct concentration data obtained from CRP experiments for volume contraction.

Finally, it has been found that the overall rates of polymerization of styrene in bulk do not show a dependence upon alkoxyamine concentration. Broadening of the molar mass distribution in a CRP experiment has been ascribed to a low rate of alkoxyamine C-O bond homolysis and permanent chain-stopping reactions, e.g. bimolecular termination.

Experimental

Syntheses. The syntheses of the nitroxides and alkoxyamines have been described elsewhere (4).

Simulations. The differential equations were solved using a Gear algorithm for solving a set of stiff differential equations, modified from the NAG library subroutine D02AEF. All calculations were performed on a Silicon Graphics Challenge XL Supercomputer (30).

Quantitative ESR (31). All measurements were carried out on a Bruker ER200D SRC spectrometer, operating with an X-band standard cavity and interfaced to a Bruker Aspect 3000 data system. Temperature was controlled by a Bruker ER4111 variable temperature unit. The TEMPO concentrations were determined by double integration of the ESR spectra and the data were calibrated with stock solutions of TEMPO measured in *tert*-butylbenzene under identical conditions.

Procedure. Prior to use *tert*-butylbenzene was distilled and stored over molsieves (4Å). Styrene was distilled and passed over a column of inhibitor remover (Aldrich) before use. A $1 \cdot 10^{-2}$ M solution of compound (1) in styrene was prepared (0.0333 g in 10 mL). Approximately 1 mL was put in an NMR tube and deoxygenated by purging helium through the solution in the NMR tube for several minutes. Next, the tube was placed under an argon atmosphere and sealed. Time-resolved measurements were performed at 393 K.

Controlled Radical Polymerizations of Styrene in Bulk. Styrene was distilled and passed over a column of inhibitor remover (Aldrich) before use. Compound (1) was purified by recrystallization from methanol.

Procedure. Styrene, compound (1) and TEMPO were charged into a three-necked 100 mL round-bottomed flask equipped with a Teflon-coated magnetic stirrer. The reaction mixture was deaerated by three freeze-pump-thaw cycles in order to place the reaction mixture under an argon atmosphere. The flask was placed in a thermostated oil bath at the required temperature. Conversion was determined gravimetrically.

SEC Analysis. The molar mass distributions (MMD) of the polymers produced were determined by SEC. 0.1 w/v % Solutions in tetrahydrofuran (THF, stabilized, Biosolve,

AR) were prepared of each sample which was isolated by freeze drying. The solutions were filtrated through 0.2 μm syringe filters. The SEC analyses were carried out with two Shodex KF-80M (linear) columns or two PL gel 10^3 and 500, at 40 °C. The eluent was THF at a flow rate of 1 mL·min⁻¹. A Waters 410 differential refractometer and a Waters 440 UV detector (254 nm) were used for the detection. Narrow-distribution polystyrene standards (Polymer Labs) with molar masses (M) ranging from 370 to 6.5×10^6 g·mol⁻¹ were used for calibration of the columns. After a baseline correction, the SEC chromatograms were converted to the differential log molar mass distributions (x(M) vs log(M)), weight MMD (w(M) vs. M) and number MMD (n(M) vs. M) according to the procedure described by Shortt (32).

Literature Cited

- ¹ Georges, M. K.; Veregin, R. P. N.; Kazmaier, P. M.; Hamer, G. K. *Macromolecules* **1993**, *26*, 2987. Hawker, C. J. *J. Am. Chem. Soc.* **1994**, *116*, 11185. Fukuda, T.; Terauchi, T.; Goto, A.; Tsujii, Y.; Miyamoto, T.; Shimizu, Y. *Macromolecules* **1996**, *29*, 3050. Greszta, D.; Matyjaszewski, K. *Macromolecules* **1996**, *29*, 7661. Bon, S. A. F.; Bosveld, M.; Klumperman, B.; German, A.L. *Macromolecules* **1997**, *30*, 324.
- ² Beckwith, A. L. J.; Bowry, V. W.; O'Leary, M.; Moad, G.; Rizzardo, E.; Solomon, D. H. *J. Chem. Soc., Chem. Commun.* **1986**, 1003. Beckwith, A. L. J.; Bowry, V. W.; Moad, G. *J. Org. Chem.* **1988**, *53*, 1632.
- ³ Benson, S. W.; North, A. M. *J. Am. Chem. Soc.* **1962**, *84*, 935. Schuh, H.; Fischer, H. *Int. J. Chem. Kinet.* **1976**, *8*, 341. Schuch, H.-H.; Fischer H. *Helv. Chim. Acta* **1978**, *61*, 2130. Walling, C. *Tetrahedron* **1985**, *41*, 3887. Ruegge, D.; Fischer, H. *J. Chem. Soc., Faraday Trans 1*, **1988**, *84*, 3187.
- ⁴ Bon, S. A. F.; Chambard, G.; Klumperman, B.; German, A. L., in press.
- ⁵ Solomon, D. H.; Rizzardo, E.; Caciolo, P. Eur. Pat. Appl. 135280, 1985; *Chem. Abstr.* **1985**, *102*, 221335q.
- ⁶ Masahide, T.; Shoji, T.; Hiroshi, W.; Toshihiro, T. *J. Chem. Soc., Faraday Trans.* **1996**, *92*, 3057.
- ⁷ Edward, J. T. *J. Chem. Educ.* **1970**, *47*, 261.
- ⁸ Cussler, E. I. *Diffusion*, Cambridge University Press, New York, 1984. Tyrrel, H. J. V.; Harris, K. R. *Diffusion in Liquids*, Butterworths, London, 1984.
- ⁹ Sueishi, Y.; Takeuchi, T. *J. Phys. Org. Chem.* **1996**, *9(4)*, 234.
- ¹⁰ Schneider, D. J.; Freed, J. H. In *Spin Labeling: Theory and Applications*; Berliner, L. J.; Reuben, J. (Eds.); Biological Magnetic Resonance; Plenum Press: New York, N.Y., 1989, Vol. 8; pp 1-76.
- ¹¹ For example: Piton, M. C.; Gilbert, R. G.; Chapman, B. E.; Kuchel, P. W. *Macromolecules* **1993**, *26*, 4472.
- ¹² Bowry, V. W.; Ingold, K. U. *J. Am. Chem. Soc.* **1992**, *114*, 4992. Chateaufneuf, J.; Luszyk, J.; Ingold, K. U. *J. Org. Chem.* **1988**, *53*, 1629.
- ¹³ Beckwith, A. L. J.; Bowry, V. W.; Ingold, K. U. *J. Am. Chem. Soc.* **1992**, *114*, 4983.
- ¹⁴ Keana, J. F. W.; Dinerstein, R. J.; Baitis, F. *J. Org. Chem.* **1971**, *36*, 209. Call, L.; Ullman, E. *Tetrahedron Lett.* **1973**, 961.

- ¹⁵ Wasserman, A. M.; Buchachenko, A. L. *Izv. Akad. Nauk SSSR, Ser. Khim.* **1967**, 1947. Hill, D. J. T.; O'Donnel, J. H.; O'Sullivan, P. W. *Prog. Polym. Sci.* **1982**, *8*, 215.
- ¹⁶ Connolly, T. J.; Scaiano, J. C. *Tetrahedron Lett.* **1997**, *38*, 1133.
- ¹⁷ Banks, R. E.; Haszeldine, R. N.; Stevenson, M. J. *J. Chem. Soc. (C)* **1966**, 901. Banks, R. E.; Choudhury, D. R.; Haszeldine, R. N. *J. Chem. Soc., Perkin I* **1973**, 1092. Banks, R. E.; Birchall, J. M.; Brown, A. K.; Haszeldine, R. N.; Moss, F. *J. Chem. Soc., Perkin I* **1975**, 2033. Malatesta, V.; Ingold, K. U. *J. Am. Chem. Soc.* **1981**, *103*, 3094. Doba, T.; Ingold, K. U. *J. Am. Chem. Soc.* **1984**, *106*, 3958.
- ¹⁸ Moad, G.; Rizzardo, E.; Solomon, D. H. *Polym. Bull. (Berlin)* **1982**, *6*, 589.
- ¹⁹ Li, I.; Howell, B. A.; Matyjaszewski, K.; Shigemoto, T.; Smith, P. B.; Priddy, D. B. *Macromolecules* **1995**, *28*, 6692.
- ²⁰ Nakatsuji, S.; Takai, A.; Nishikawa, K.; Morimoto, Y.; Yasuoka, N.; Suzuki, K.; Enoki, T.; Anzai, H. *J. Chem. Soc., Chem. Commun.* **1997**, 275.
- ²¹ Fisher, H. *J. Am. Chem. Soc.* **1986**, *108*, 3925.
- ²² Matyjaszewski, K.; Patten, T. E.; Xia, J. *J. Am. Chem. Soc.* **1997**, *119*, 674.
- ²³ Xie, H.; Nies, E.; Stoeks, A.; Simha, R. *Polym. Eng. Sci.* **1992**, *32*, 1654.
- ²⁴ PVT-data were obtained from: Zoller, P.; Walsh, D. *Standard Pressure-volume-temperature Data for Polymers*, Technomic Publishing Company, Inc., Basel, 1995. Smith, B. D.; Srivastava, R. *Thermodynamic Data for Pure Compounds, Part A: hydrocarbons and ketones*, Elsevier Science Publishers BV., Amsterdam, 1986.
- ²⁵ Mayo, F. R. *J. Am. Chem. Soc.* **1968**, *90*, 1289. Buzanowski, W. C.; Graham, J. D.; Priddy, D. B.; Shero, E. *Polymer* **1992**, *33*, 3055.
- ²⁶ Pickup, S.; Blum, F. D. *Macromolecules* **1989**, *22*, 3961.
- ²⁷ Scheren, P. A. G. M.; Russell, G. T.; Sangster, D. F.; Gilbert, R. G.; German A. L. *Macromolecules* **1995**, *28*, 3637.
- ²⁸ Buback, M.; Gilbert, R. G.; Hutchinson, R. A.; Klumperman, B.; Kuchta, F.-D.; Manders, B. G.; O'Driscoll, K. F.; Russel, G. T.; Schweer, J. *Macromol. Chem. Phys.*, **1995**, *196*, 3267.
- ²⁹ Heuts, J. P. A.; Gilbert, R. G.; Radom, L. *Macromolecules* **1995**, *28*, 8771.
- ³⁰ NAG Library Mark 5, Numerical Algorithms Group, Oxford.
- ³¹ Czoch, R. *Appl. Magn. Reson.* **1996**, *10*, 293.
- ³² Shortt, D. W. *J. Liquid Chromatogr.* **1993**, *16*, 3371.

Chapter 16

Mechanistic Aspects of Atom Transfer Radical Polymerization

Krzysztof Matyjaszewski

Department of Chemistry, Carnegie Mellon University, 4400 Fifth Avenue,
Pittsburgh, PA 15213

Typical conditions and experimental results of Atom Transfer Radical Polymerization (ATRP) of styrene, (meth)acrylates, acrylonitrile and other monomers are reviewed which include polymerization rates, evolution of molecular weights and polydispersities with conversion. The role of all major components of ATRP is discussed which comprises the structure of various alkyl halides, metals, ligands, solvents, additives as well as reaction times and temperatures. Enhancement of the initiation efficiency by some special procedures such as slow addition of initiator or catalyst is described. Origins and contributions of side reactions such as bimolecular termination, electron transfer and β -H elimination are discussed.

This paper is focused on the mechanistic aspects of Atom Transfer Radical Polymerization (ATRP) and will attempt to explain the role of various components and reaction conditions on ATRP. Synthetic aspects as well as a general introduction to controlled radical polymerization are reviewed in Chapters 15 and 1, respectively

Atom Transfer Radical Addition (ATRA) and ATRP

Until recently, radical reactions had found limited application in organic synthesis due to the low yields of desired addition and substitution products caused by radical termination reactions. The importance of radical reactions increased dramatically after the discovery that persistent radicals could be used to reduce the stationary concentration of

reacting radicals and minimize the contribution of termination.(1-6) One of the most efficient methods developed using this concept is atom transfer radical addition (ATRA). ATRA employs atom transfer from an organic halide to a transition-metal complex to generate the substrate radical, followed by the addition to an alkene and the back-transfer from the transition metal to the product radical, resulting in the final product (cf. top left corner of Scheme 1).

In ATRA a metal catalyst, usually a complex of a copper(I) halide and 2,2'-bipyridyl (5,7,8) (although Ni,(9,10) Pd,(11) Ru,(12) Fe(4) and other metals (6) have been used as well), undergoes a one-electron oxidation with simultaneous abstraction of a halogen atom from a substrate. This inner-sphere electron transfer process reversibly generates an organic radical and a copper(II) complex. The experimental evidence is not conclusive whether the intermediate radicals are free-radicals, in a solvent cage, or coordinated to the metal center, but the most plausible mechanism based upon experimental evidence involves free-radicals. After the back-transfer, the copper(I) complex is reformed, completing the catalytic cycle. The substrates are typically chosen such that if addition occurs, then the newly formed radical is much less stabilized relative to the initial radical and will essentially react irreversibly with the copper(II) complex to form an inactive alkyl halide product. Therefore, in ATRA, only one addition step should occur.

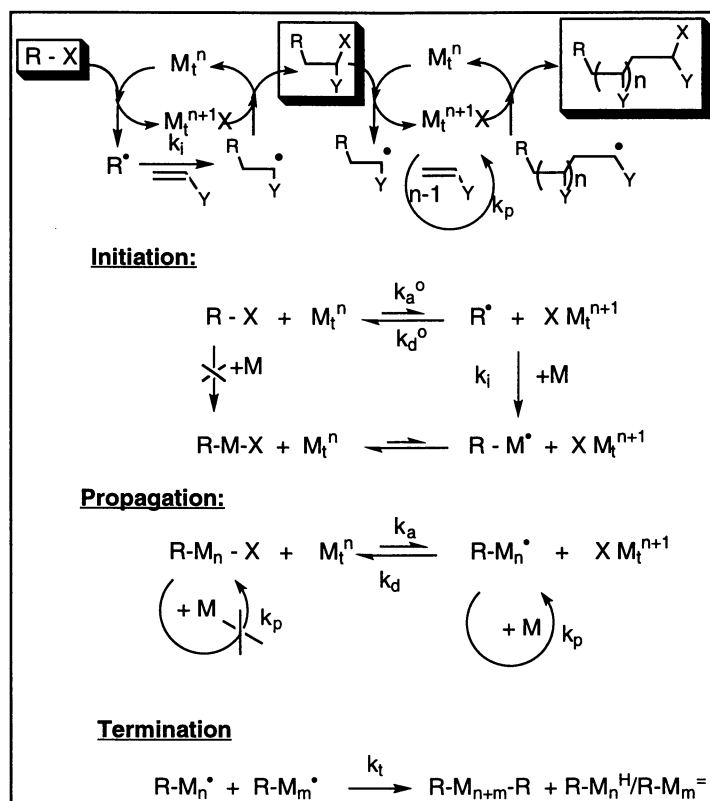
Atom transfer radical addition can be extended to atom transfer radical polymerization (ATRP) if the conditions can be modified such that more than one addition step is possible. Thus, if the radical species, before and after addition of the unsaturated substrate, possess comparable stabilization, then the activation-addition-deactivation cycle will repeat until all of the unsaturated substrate is consumed. This process results in a chain-growth polymerization.

Scheme 1 shows the mechanism of ATRP adapted from ATRA. The mechanism consists of phenomenologically related initiation and propagation processes. These sequences are comprised of an atom-transfer equilibrium along with radical addition to the monomer. Termination by radical coupling and disproportionation are included in the mechanism because of the magnitude of the associated rate constants; however, only a few percent of the polymer chains in ATRP undergo bimolecular termination. Additionally some other side reactions may limit attainable molecular weights.(13) The presence of radical intermediates in the mechanism is consistent with experimental results from trapping experiments,(14,15) copolymerization reactivity ratios,(16,17) and the regio- and stereochemistry of the polymerization.(14) Thus, the net propagation sequence can be considered an "insertion" process proceeding via radical intermediates. A "reverse ATRP" experiment demonstrated that the proposed copper(II) complex formed after atom transfer

is also an intermediate in ATRP. In reverse ATRP, the polymerization is entered from the right-hand side of the atom transfer by generating radicals from AIBN or BPO in the presence of $\text{CuBr}_2 / 2$ bipy and monomer.(18)

The proper choice of the initiator, RX , is very important for efficient ATRP. As will be discussed later, important parameters include correct values of the rate constants of activation, deactivation and addition at the initiation stage in comparison with those at the propagation stage (k_a° , k_d° , k_i versus k_a , k_d , k_p).

Scheme 1
General Mechanism of ATRP

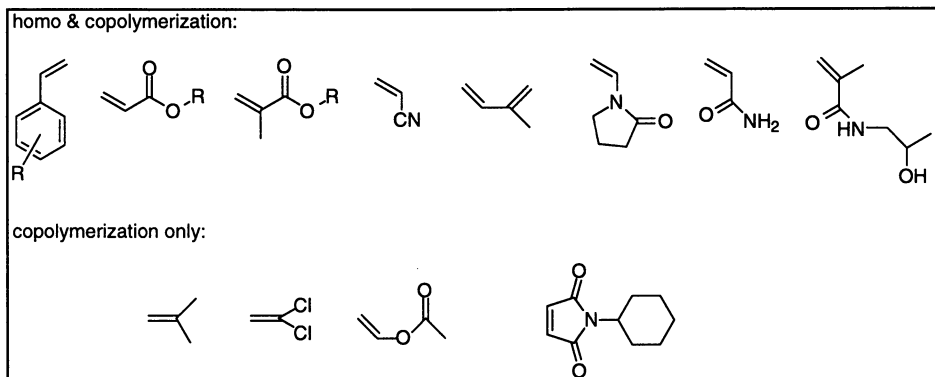


Polymerization systems utilizing this concept have been developed using Cu(I) ,(14,19-22) Ni(II) ,(23,24) Ru(II) / Al(OR)_3 ,(25) and Fe(II) ,(26-28) complexes to catalyze the radical-forming equilibrium; however, this Chapter is primarily focused on developments in copper-based ATRP.

Kinetics and Mechanism of ATRP

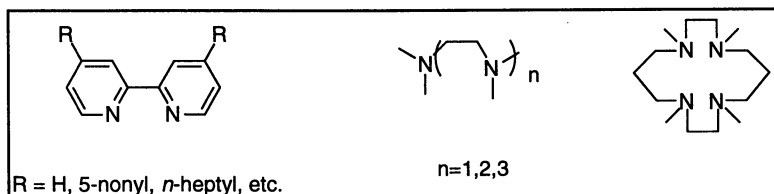
A typical ATRP system consists of an initiator, a copper(I) halide complexed with some ligand(s), and of course, monomer. Thus far, the copper-based ATRP system has been used successfully for the controlled/"living" (co)polymerization of styrenes, acrylates, methacrylates, acrylonitrile, isoprene, acrylamide and some other monomers:

Scheme 2 Monomers Polymerized and Copolymerized by ATRP



The choice of monomer to be polymerized dictates the types of other components that can be used. The initiator usually, but not always, should have a structure homologous to the corresponding polymer endgroup. The halogen atom in both the initiator and copper(I) halide is usually, but not necessarily the same. Typically, two equivalents of a bidentate ligand are added per copper center. The most effective ligands for ATRP are derivatives of 2,2'-bipyridine (19,20) or other π -accepting, chelating nitrogen-based ligands such as 2-iminopyridines.(22) Aliphatic polyamines are also successful.(29)

Scheme 3 Typical Ligands for Cu-based ATRP



Long alkyl chain substituents at the 4,4'-positions of the bipyridine ligand are necessary to solubilize the copper complex in the nonpolar media of bulk polymerizations, as the complexes from the parent 2,2'-bipyridine with copper(I) halides are largely insoluble under such conditions.(20,30)

The rate law for ATRP can be derived from Scheme 1 by neglecting contribution of termination, assuming that initiation is complete and using the fast equilibrium approximation - a necessary condition for observing low polydispersities.(31) Under these conditions the concentration of propagating radicals, $[P^\bullet]$, is equal to $(k_a/k_d) [R-M_n-X] ([Cu^I]/[XCu^{II}]$):

$$R_p = k_{app}[M] = k_p [P^\bullet] [M] = k_p \cdot k_a / k_d \cdot [M] [RX]_0 ([Cu^I] / [XCu^{II}])$$

(1)

In eq. 1 $[RX]_0$ refers to the initial concentration of the initiator which corresponds to the concentration of dormant chains ($[R-M_n-X]$). Results from kinetic studies of the polymerizations using soluble catalyst systems indicate that the rate of polymerization is first order with respect to monomer, alkyl halide (initiator), and copper(I) complex concentrations.(31) These observations are all consistent with eq. 1. However, in the polymerization of styrene, even at low concentration of both initiator and catalyst, the rate of polymerization can not be smaller than the rate of self-initiated polymerization.(32,33) Thus, under such conditions, kinetics may change from external first order to zero order in both initiator and catalyst. This observation is limited only to styrene derivatives which can thermally autopolymerize.

It is recognized that in ATRP and in all other controlled radical polymerizations termination is not entirely eliminated. Therefore, chains will continuously terminate resulting in the increase of the persistent radical concentration and the progressive decrease of the growing radical concentration which may lead to some deviation from the first order kinetics in respect to monomer. However, contribution of the termination process under appropriate conditions is small and the concentration of radicals is reduced less than 10% during consumption of nearly all monomer and, therefore, deviation from the first order kinetics may not be detectable.

The polymerization rate is usually inverse first order with respect to the copper(II) complex concentration; however, determining the precise kinetic order with respect to the deactivator concentration is rather complex due to the generation of copper(II) via the persistent radical effect. In the atom transfer step, a reactive organic radical is generated along with a stable copper(II) species regarded as a persistent metallo-radical. If the initial concentration of copper(II) in the polymerization is not sufficiently large to ensure that the rate of deactivation is fast, then coupling of the organic radicals will occur leading to an

increase in the deactivating copper(II) concentration. This process has been observed experimentally using ESR, ^1H NMR, UV-Vis and GC-MS techniques. More radicals and deactivator will be formed and more radical combination will occur until the radical concentration decreases approximately to 10^{-7} M and the deactivator concentration increases approximately to 10^{-3} M. At these concentrations the rate at which radicals combine ($k_{\text{term}} [\text{R}\cdot]^2$) will be significantly slower than the rate at which radicals will react with the copper(II) complex ($k_{\text{deact}} [\text{R}\cdot] [\text{Cu(II)}]$) in a deactivation process, and a controlled / "living" polymerization will ensue. Under the aforementioned conditions, less than 10% of the polymer chains are terminated during this initial, short nonstationary process, but the majority of the chains (>90 %) continue the polymerization successfully. If a small amount of a deactivator (≈ 10 %) is added initially to the polymerization, then the proportion of terminated chains is greatly reduced.(31)

In styrene polymerization, radicals are additionally generated by self-initiation with the rate approximately 10^{-3} M/hour at 130 °C.(32) Thus, a small excess of CuX_2 is rapidly consumed by newly generated radicals and should have no effect on polymerization. However, the addition of 10^{-2} M CuX_2 at the beginning of the reaction leads to approximately twice lower rate, indicating that the concentration of CuX_2 under normal ATRP conditions is twice less than was the added amount ($5 \cdot 10^{-2}$ M, i.e. 5% of CuX).

In a polymerization based upon the ATRP catalytic cycle, the control of the polymerization and of the resulting polymers will depend upon the stationary concentration of the growing radicals and the relative rates of propagation and deactivation. During one activation step any number of monomer units can be added to the polymer chain with varying effects upon the polydispersities of the polymers formed.

$$M_w/M_n = 1 + \left(\frac{k_p [\text{RX}]_0}{k_d [\text{XCu}^{\text{II}}]} \right) \left(\frac{2}{p} - 1 \right) \quad (2)$$

Equation 2 explains how the polydispersities in polymerization systems with relatively fast exchange decrease with conversion, where p is the polymerization conversion, $[\text{RX}]_0$ corresponds to the concentration of dormant polymer chains, and $[\text{XCu}^{\text{II}}]$ is the concentration of deactivator.(34,35) Polydispersities are higher for shorter chains (higher $[\text{RX}]_0$) due to the fact that, relative to longer chains, the growth of smaller chains involves fewer activation-deactivation steps and therefore fewer opportunities for exchange and controlled growth. Second, the final polydispersities should be higher for higher values of the ratio, k_p/k_d . Thus, under similar conditions, the polymerization of acrylates yields higher polydispersities than that of styrene, because k_p for acrylates is much larger than that for styrene.

At the limit in which the deactivation process is very slow or does not occur ($k_p \gg k_d$), ATRP simply becomes a conventional redox-initiated radical polymerization,(36) and high polydispersities are observed. At the limit in which an average of one or a few monomer molecules are added per activation step, the polymerization is well-controlled and the polydispersities can approach a Poisson distribution.(20)

Finally, ATRP is a catalytic process in which rates depend on concentrations of Cu(I) and Cu(II) species but molecular weights do not. Polymerization degree is exclusively defined by the ratio of concentrations of the reacted monomer to the introduced initiator (provided that initiation is complete) as shown in eq. 3:

$$DP_n = \Delta[M]_o / [RX]_o \neq f ([Cu^{I/II}]_o) \quad (3)$$

The Role of Components and Reaction Conditions in ATRP

Although all ATRP processes utilize similar initiators and catalysts, one set of conditions cannot be applied to every set of monomers because of the specific values of propagation and exchange rate constants. For each particular ATRP, a specific initiator, metal, ligands, deactivator, temperature, reaction time, and solvent should be selected. Therefore, understanding the role of each component of ATRP is crucial for obtaining well-defined polymers as well as for potentially expanding the scope of ATRP to new monomers.

1. Monomers: ATRP can be used for many vinyl monomers including styrenes,(19,21) acrylates,(14) methacrylates,(14,22,23,25) acrylonitrile,(37) and dienes.(26) The currently used catalyst systems are not sufficient to polymerize less reactive monomers that produce non-stabilized, reactive radicals such as ethylene, α -olefins, vinyl chloride and vinyl acetate, though copolymerization is sometimes successful. This may be due to inherently small values of the propagation rate constants even though the cross-propagation rate is much faster. Unfortunately, there are a limited number of reliable kinetic data on propagation and nearly no data on crosspropagation rate constants. A few reliable k_p values (in $10^3 M^{-1} s^{-1}$, at 20 °C and extrapolated to 100 °C) include: 0.070 and 1.2 (styrene),(38) 0.28 and 2.0 (methyl methacrylate),(39) 2.9 and 33 (vinyl acetate),(40) 14 and 65 (butyl acrylate).(41)

Fortunately, more data are available from model addition studies.(42) Table 1 illustrates some examples of the rate constants of the addition of carbon centered radicals to alkenes and shows that addition of t-butyl radicals to isobutene is 1000 times slower than to (meth)acrylates.

Table 1(42)
Rate constants of room temperature addition of model radicals
to substituted alkenes CH₂=CXY

X/Y	Rad	*CMe ₃	*CH ₂ OH	*CH ₂ CO ₂ R	*CH ₂ CN	*CH ₂ Ph	Me ₂ C*CN
H/OEt		390	180	1.5.10 ³	4.3.10 ⁴	14	108
Me/Me		740	240	1.8.10 ⁵	1.1.10 ⁴	-	-
H/Et		1100	300	5.4.10 ⁴	1.1.10 ⁴		
H/H		1250	410	1.1.10 ⁴	3.3.10 ³		
H/OAc		4200	590	6.5.10 ⁴	1.3.10 ⁴	15	41
H/Cl		1.6.10 ⁴	5000	7.1.10 ⁴	1.2.10 ⁴		
H/Ph		1.3.10 ⁵	2.3.10 ⁴	1.9.10 ⁶	3.8.10 ⁵	1100	2410
Me/CO ₂ Me		6.6.10 ⁵	6.10 ⁵	1.3.10 ⁶	2.4.10 ⁵	2100	1590
Ph/Ph		1.0.10 ⁶	1.4.10 ⁵	~10 ⁷	2.4.10 ⁶	4100	7010
H/CO ₂ Me		1.1.10 ⁶	7.1.10 ⁵	4.9.10 ⁵	1.1.10 ⁵	430	370
H/CN		5.2.10 ⁶	1.1.10 ⁶	5.4.10 ⁵	1.1.10 ⁵	2200	1590

A similar difference can be noted for the hydroxymethyl radical which can be considered as a model of the vinyl acetate species. Thus, nucleophilic radicals exhibit higher selectivities than electrophilic radicals. The second conclusion from Table 1 is that the rate constants of addition of model compounds are significantly larger than the homopropagation rate constants. Thus, a benzyl radical reacts with styrene at 20 °C with $k=1100 \text{ M}^{-1}\text{s}^{-1}$, whereas $k_p=70 \text{ M}^{-1}\text{s}^{-1}$ (approximately the same values were found for cumyl radical and can be assumed for 1-phenylethyl radical) (43) This difference is assigned primarily to the entropic factor. Similar differences may be expected for the activation and deactivation processes in ATRP. Such kinetic studies are very important and urgently needed.

Some peculiarities of ATRP for each class of monomers are discussed below.

A. Styrenes: Styrene ATRP is usually conducted at 110 °C for bromide-mediated polymerization and 130 °C for the chloride-mediated polymerization.(14,21,31) The corresponding 1-phenylethyl halide is commonly used as the initiator; however, a wide variety of compounds have been used successfully as initiators for styrene ATRP, such as benzylic halides,(19) allylic halides,(44) α -bromoesters,(14) polyhalogenated alkanes,(14) and arenesulfonyl chlorides.(21) Solvents may be used for styrene ATRP, but the stability of the halide endgroup displays a pronounced solvent dependence as

evidenced by model studies using 1-phenylethyl bromide.(13) Therefore, nonpolar solvents are recommended for styrene ATRP.

Well-defined polystyrenes can be prepared within the molecular weight range of 1,000 to 90,000. In the region from 1,000 to 30,000, polydispersities (M_w / M_n) are less than 1.10,(20) and above 30,000, polydispersities increase to within the range of 1.10 to 1.50 due to some side reactions, predominantly HX elimination.(13) These side reactions can be reduced at lower polymerization temperatures. For example, the bulk ATRP of styrene at 110 °C allows synthesis of a polymer with a predetermined molecular weight, $M_n = 40,000$ and $M_w/M_n = 1.18$; however when the synthesis of polystyrene of $M_n = 80,000$ is attempted, a polymer with $M_n = 70,000$ and $M_w/M_n = 1.5$ is obtained. At 100 °C the molecular weight control is slightly better. For example, polystyrene with a predetermined molecular weight $M_n = 55,300$ can be prepared with $M_w/M_n = 1.15$; however when the synthesis of polystyrene with $M_n = 180,000$ is attempted, a polymer with $M_n = 150,000$ and $M_w/M_n = 1.7$ is obtained.

A wide range of styrene derivatives have been polymerized in a controlled fashion using ATRP; however, there are some limitations in monomer structure. For example, the polymerization of *p*-methoxystyrene is accompanied by side reactions, and the structure of the oligomers formed suggests the involvement of cationic intermediates.(45) The growing radical for this polymerization is very electron rich and might be oxidized to the corresponding cation. Generally, styrenes with electron withdrawing substituents polymerize faster. The Hammett correlation provides an overall value of $\rho \approx 1.5$ which is significantly larger than the correlation for the propagation rate constants, $\rho \approx 0.5$.(45) This indicates that the equilibrium is shifted more towards the radical species for styrenes with the electron donating substituents. It seems that the observed dependence, for styrene derivatives, is caused by lower stability of the corresponding dormant alkyl halides because reactivities of radicals are very similar. Nearly identical conclusions come from model studies of benzyl halides and benzyl radicals.(46,47)

For a typical bromine-mediated bulk styrene ATRP at 110 °C the observed rate constant is $k_{obs} = 1.6 \times 10^4 \text{ s}^{-1}$ ($[\text{CuBr}]_0 = [\text{dNbipy}]_0/2 = [\text{1-PEBr}]_0 = 0.087 \text{ M}$). Using the known rate constant of propagation ($k_p = 1.6 \times 10^3 \text{ M}^{-1} \text{ s}^{-1}$ at 110°C), one can calculate the steady state radical concentration: $[\text{P}\cdot] = 1.0 \times 10^{-7} \text{ M}$. If the polymerization is conducted with an initial 10 mol % excess of the copper(II) complex, relative to Cu(I), in order to keep the deactivator concentration relatively constant, then the atom transfer equilibrium constants can be estimated: $K_{eq} = k_a/k_d = 4 \times 10^{-8}$.(31)

B. Methyl Methacrylate: The standard conditions for methyl methacrylate (MMA) ATRP are similar to those of styrene ATRP except that less copper(I) catalyst is

needed and the polymerizations are conducted in 50% solution in diphenyl ether or dimethoxybenzene at 90 °C. The use of copper bromide instead of copper chloride leads to more rapidly decreasing polydispersities (*p*-TsCl/CuCl, conversion = 25 %, $M_n = 8500$, $M_w/M_n = 2$, while for *p*-TsCl/CuBr for the same conversion, $M_n = 7800$, $M_w/M_n = 1.18$).⁽⁴⁸⁾ This is due to the better efficiency of bromine in the deactivation step. The polymerization also is less controlled when bipy is used instead of dNbipy due to the correspondingly smaller concentration of deactivator (as discussed later). The best initiators for MMA ATRP are *p*-toluenesulfonyl chloride (*p*-TsCl), 2-bromo-2-methyl malonate and benzhydryl chloride. With these initiators the apparent rate constant of initiation is larger than that of propagation.

Well-defined poly(methyl methacrylate) has been prepared within the molecular weight range of 1,000 to 180,000. In the region from 1,000 to 90,000 the polydispersities are less than 1.10, and above 90,000 the polydispersities fall within the range of 1.10 to 1.50.⁽⁴⁸⁾ For a typical bromine-mediated solution MMA ATRP, the observed rate constant is $k_{\text{obs}} = 8.3 \times 10^{-5} \text{ s}^{-1}$ ($[\text{MMA}]_0 = 4.7 \text{ M}$; $[\text{CuBr}]_0 = [\text{dNbipy}]_0/2 = 0.0105 \text{ M}$; $[\text{p-TsCl}]_0 = 0.021 \text{ M}$). The steady-state radical concentration of $5.1 \times 10^{-8} \text{ M}$ can be calculated using the aforementioned propagation rate constant. The estimated equilibrium constant, $K_{\text{eq}} = 2 \times 10^{-7}$, is larger than in the styrene polymerization in spite of the lower temperature used. This must be due to the structure of the tertiary radical which does not react fast enough with XCu(II) species to form the more sterically hindered tertiary alkyl halide. Earlier inhibition studies indicate that inhibition coefficients for FeCl₃ and CuCl₂ in DMF in the polymerization of styrene are significantly higher than in MMA polymerization.⁽⁴⁹⁾

C. Methyl Acrylate: The standard conditions for methyl acrylate (MA) ATRP are similar to those of styrene ATRP except that the polymerizations are conducted at 90 °C. Typically, an alkyl bromopropionate is used as the initiator, because its structure is homologous to that of the polymer endgroup, however, 1-phenylethyl and isobutyryl derivatives are also very efficient initiators. Well-defined poly(methyl acrylate) with polydispersities of less than 1.10 can be prepared within the molecular weight range of 1,000 to 80,000.⁽⁵⁰⁾ Above 90,000 the polydispersities increase to >1.3. The estimated equilibrium constant for MA is $K_{\text{eq}} = 3 \times 10^{-9}$ at 90 °C which is nearly 100 times smaller than for MMA which can be mainly attributed to the difference between secondary and tertiary structure of the growing radicals.

Because the monomer is an ester, a wide range of polyacrylates with differing side chains were prepared using ATRP. Thus far, acrylates with primary, secondary and tertiary alkyl groups⁽⁵¹⁾ have been polymerized successfully, as well as those with alcohol, epoxide and vinyl groups.⁽⁵²⁾ Acrylic acid polymerization has not yet been

successful. Some polymerizations such as 2-hydroxyethyl acrylate were carried out in 50% aqueous solution showing low sensitivity of catalyst and growing species to water and alcohols.

D. Acrylonitrile: The ATRP of acrylonitrile is necessarily conducted using a solvent, because polyacrylonitrile is not soluble in acrylonitrile. The polymerizations are conducted at 45 to 65 °C using a 33 % solution in ethylene carbonate, 0.1 mole percent 2-bromopropionitrile initiator, and 0.01 to 0.05 mole percent copper(I) catalyst.(37) Again, α -halopropionitriles are good initiators for these polymerizations, since they are homologous to the structure of the dormant polymer endgroup. Well-defined polyacrylonitrile with polydispersities of less than 1.05 can be prepared within the molecular weight range of 1,000 to 10,000.(53) Acrylonitrile can be copolymerized with styrene in a well-controlled fashion to yield gradient copolymers with molecular weights ranging from 1,000 to 15,000.(54)

E. Other monomers: Some other monomers require additional adjustments to the reaction conditions. For example, the polymerization of N-vinylpyrrolidinone and 2-hydroxypropyl methacrylamide requires the use of a tetradentate ligand such as cyclam. Otherwise, the Cu/bipy complex dissociates and the nature and activity of the catalyst is altered by complexation of the amide functionalities of the polymer and/or monomer.

2. Initiators: The main role of the alkyl halide (RX) species is to dictate the number of initiated chains. The polymerization rates in ATRP are first order with respect to the concentration of RX, and the molecular weights scale reciprocally with the initial concentration of initiator. The (pseudo)halide group, X, must rapidly and selectively migrate between the growing chain and the transition-metal complex. Thus far, bromine and chlorine are the halogens that afford the best molecular weight control. With alkyl fluorides, the fluorine-carbon bond strength is apparently too strong for atom transfer to occur. Iodine works well for acrylate polymerizations; however, in styrene polymerizations the heterolytic elimination of hydrogen iodide is too fast at high temperatures.(55) As for other groups, X, some pseudohalogens, specifically thiocyanates, have been used successfully in polymerization of acrylates and styrenes.(55) To choose a good initiator, the ratio of the apparent initiation rate constant ($k_i \cdot K_o$, where k_i and K_o refer to the absolute rate constant of addition of the initiating radical to the alkene and the atom transfer equilibrium constant for the initiating species, respectively) to the apparent propagation rate constant ($k_p \cdot K_{eq}$, where k_p and K_{eq} refer to the absolute rate constant of propagation and the atom transfer equilibrium constant for the dormant chain, respectively) must be considered. If $k_i \cdot K_o$ is much less than $k_p \cdot K_{eq}$, then initiation will be

incomplete during the polymerization, and the molecular weights and polydispersities will be too high.

To a first approximation, the structure of the alkyl group, R, of the initiator should be similar to the structure of the dormant polymer species. For example, 1-phenylethyl derivatives resemble dormant polystyrene chain ends, α -halopropionates approximate dormant acrylate end groups, etc. This is true for secondary radicals but not necessarily for tertiary radicals. For example, isobutyrate is not the best initiator for MMA. This is probably due to the so called B-strain effect.⁽⁵⁶⁾ For initiators that are not structurally related to the dormant polymer chain end, it is better to use organic (pseudo)halides that form less reactive radicals and that have relatively higher efficiency than the dormant chain ends. For example, alkyl 2-chloroisobutyrate and arenesulfonyl chlorides are good initiators for styrene and alkyl (meth)acrylate ATRP, but chloroacetates, 2-chloropropionates and 1-phenylethyl chloride are poor initiators for the polymerization of methyl methacrylate. In general, any alkyl halide with activated substituents on the α -carbon, such as aryl, carbonyl, or allyl groups, potentially can be used as ATRP initiators. Polyhalogenated compounds (CCl_4 and CHCl_3) and compounds with a weak R-X bond, such as N-X, S-X, and O-X, also can be used as ATRP initiators.^(14,21) This list includes not only small molecules, but also macromolecular species which can be used to synthesize block / graft copolymers. There is an upper limit to the stability of the initiating radicals beyond which it becomes an inefficient initiator. Trityl halides, for example, are poor initiators for ATRP.

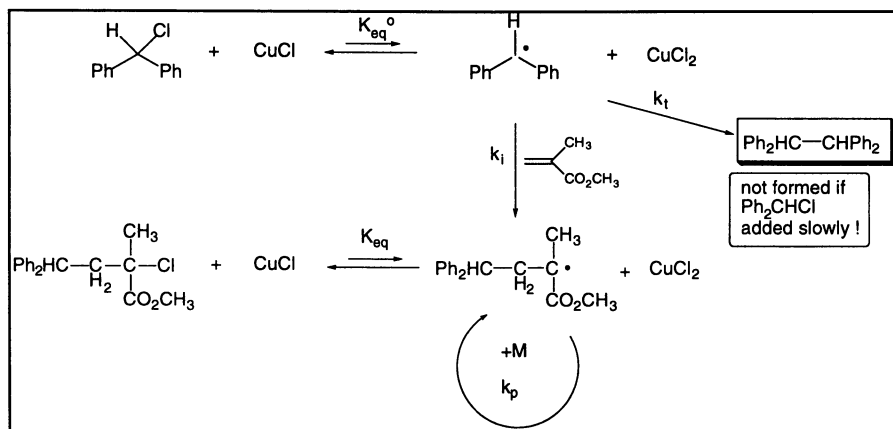
A final important factor to consider in choosing an ATRP initiator is that R-X bonds can be cleaved heterolytically, as well as homolytically, depending on the substituents on R, the nucleophilicity of X, the Lewis acidity of the transition-metal complex, the solvent, and the polymerization temperature. Hence, some initiators work well when R possesses electron-withdrawing substituents but fail when R possesses electron-donating substituents. For example, alkyl iodides are useful initiators for acrylate polymerizations but not for styrene polymerizations. Other initiators that possess multiple strong electron-withdrawing groups, such as malonate derivatives, exhibit a noticeable side reaction which is presumably the reduction of the radical to the corresponding carbanion.

It is possible to improve the efficiency of initiation in several ways. The first approach involves the exchange of ligands. When MMA polymerization was initiated by benzyl chloride with $\text{CuBr}/2$ dNbipy as the catalyst, molecular weight of the obtained polymer was >10 times higher than predicted and the polydispersity was $M_w/M_n=3.2$. On the other hand, when benzyl bromide was used as the initiator and $\text{CuCl}/2$ dNbipy as the

catalyst, final molecular weight was in good agreement with the predicted value and the polydispersity was much lower, $M_w/M_n=1.3$. This is due to the fact that alkyl bromides are easier to activate than alkyl chlorides and, at the initiation stage, alkyl bromides were exclusively present whereas at the propagation stage predominantly alkyl chlorides were formed. NMR studies indicate that when equimolar amounts of either RCl/CuBr or RBr/CuCl are mixed, the same equilibrium state is rapidly reached at which 83% of RCl/CuBr and 17% of RBr/CuCl are formed by rapid ligand exchange.

The second way to improve initiator efficiency is to add the initiator slowly to the reaction mixture. When benzhydryl chloride is added rapidly at the beginning of MMA polymerization, slow polymerization is observed and molecular weights are significantly higher than predicted although they increase linearly with conversion and polydispersities are low ($M_w/M_n < 1.1$). This is due to the fact that the equilibrium constant at the initiation stage is very large ($K_{eq}^o \gg K_{eq}$) and benzhydryl radicals react with one another (k_t) rather than initiating polymerization (k_i). Approximately 40% of 1,1,2,2-tetraphenylethane is formed in less than 5 minutes. This system, however, can be converted to a well controlled polymerization when a solution of RCl is added slowly over a 10 minute period. The instantaneous concentration of radicals is significantly reduced, allowing monomer addition to compete successfully, and dominate over termination. As a consequence, less CuX_2 is formed, reactions are faster and molecular weights agree well with theoretical values (Scheme 4).

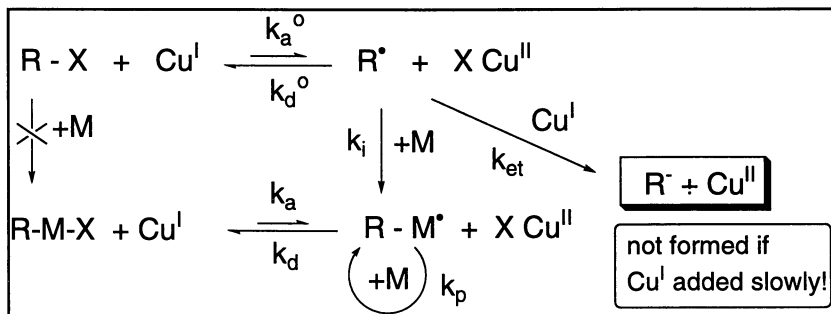
Scheme 4 Increasing Initiation Efficiency by Slow RX Addition



The third way of improving initiator efficiency is by slow addition of catalyst. This is related to electron transfer reactions which may occur between Cu(I) species and

organic radicals with strong electron withdrawing groups, such as malonate radicals or trichloromethyl radicals (Scheme 5).

Scheme 5
Increasing Initiation Efficiency by Slow Catalyst Addition



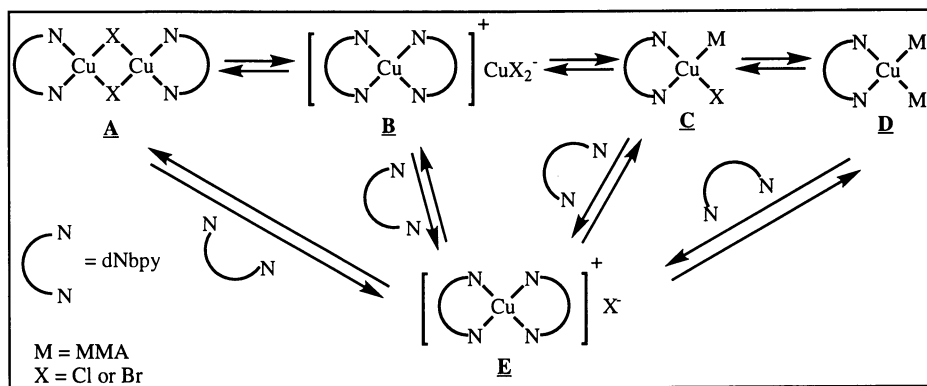
When the Cu(I) species is present in large amounts, the malonate radicals or CCl_3 radicals are easily reduced to the corresponding anions. In the polymerization of styrene with dNbipy as a ligand, a nearly instantaneous change in color from brown-red to dark-green indicates the formation of a Cu(II) species. No monomer is consumed in this case. However, when a solution of the catalyst is added slowly (over 10 minutes at room temperature) to the reaction mixture containing monomer and initiator, polymerization occurs with a typical rate and well defined polystyrenes are formed. Thus, the small amount of Cu(I) in the system is sufficient for the formation of radicals which add to styrene and are converted to less active R-M-X species but there is not enough Cu(I) species available for the electron transfer process and this side reaction is suppressed.

3. Catalysts: In the case of copper-catalyzed ATRP, the most active catalyst system contains two equivalents of a bidentate ligand, such as dNbipy, per copper(I) halide (CuX). The rate of polymerization is first-order with respect to the concentration of CuX / 2 dNbipy, and the molecular weights *do not* depend upon the concentration of CuX / 2 dNbipy. The role of the copper(I) complex is to generate radicals via atom transfer, and it was demonstrated that the copper(I) complex does not react reversibly with the growing radicals in any manner that results in polymerization control.⁽³¹⁾ This experiment involved adding CuX / 2 dNbipy to dicumyl peroxide-initiated free-radical polymerizations of styrene and monitoring the kinetics, molecular weights and polydispersities of the polymerizations.

The kinetically optimum ratio of dNbipy to copper depends on the monomer and counterion. For the polymerization of styrene and acrylates it was determined to be two-

to-one. Below this ratio the polymerization rate was usually much slower, and above this ratio the polymerization rate remained unchanged. The same behavior was observed in polymerization of MMA catalyzed by CuPF_6 . However, in ATRP of methyl methacrylate catalyzed by CuBr , the maximum rate was found at a one-to-one ratio. This may be explained by the presence of different structure with different reactivities of the CuX species with different counterions. For example, dimeric structure **A** or structure **B** with a linear Cu(I)X_2^- anion shown in Scheme 6 have an average ratio $\text{dNbipy}/\text{Cu} = 1$:

Scheme 6
Some Possible Structures of Complexes of Copper(I)
with Bidentate Ligands (e.g. bipy)

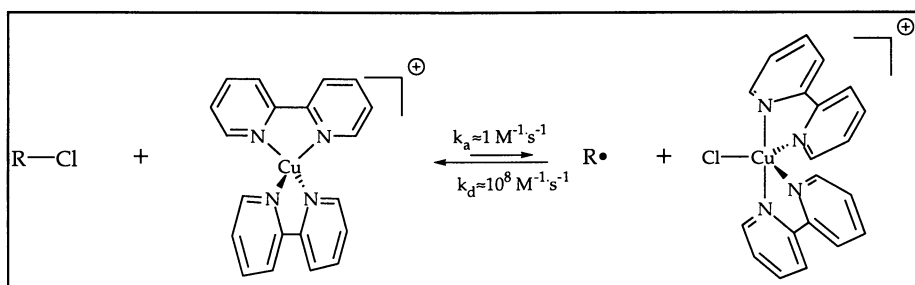


For CuPF_6 , bridging is unlikely and presumably structure **E** is responsible for the atom transfer process. It has been independently determined that CuX_2^- (as a counterion of tetra-*n*-butyl ammonium salt) is not an efficient catalyst. However, it should be remembered that according to eq. 1, the rate depends on the ratio $[\text{Cu(I)}]/[\text{XCu(II)}]$. Thus, it may happen that at less than a two-to-one ratio, less Cu(II) species is soluble and the rate is comparatively faster. A similar set of equilibria can be considered for the XCu(II) species.

Preliminary EPR and UV studies indicate the formation of mixed-valency dimers ($\text{Cu}^{\text{I}}\text{-X-Cu}^{\text{II}}$). The exact structure of Cu(I) and Cu(II) species is not clear and it perhaps changes with temperature, concentration, solvent, monomer or small amounts of additives. It is most likely that several species coexist together in a dynamic equilibrium. Bipyridyl ligands are quite labile and when four equivalents of 4,4'-(di-*tert*-butyl)-2,2'-bipyridine to CuBr are used, only one set of ^1H NMR signals corresponding to the rapidly exchanging complexed and free ligands is observed down to -50 °C. Only at lower temperatures is the ligand exchange slow on the NMR time scale, resulting in two separate

sets of signals. Therefore, the simplified picture that the Cu(I)/bipy₂ species is in a tetrahedral coordination (57) and XCu(II)/(bipy)₂ is a trigonal bipyramid,(58) adopted from the X-ray structures of the corresponding isolated solid, may not be fully correct in solution, especially in non-polar solvents. (Scheme 7)

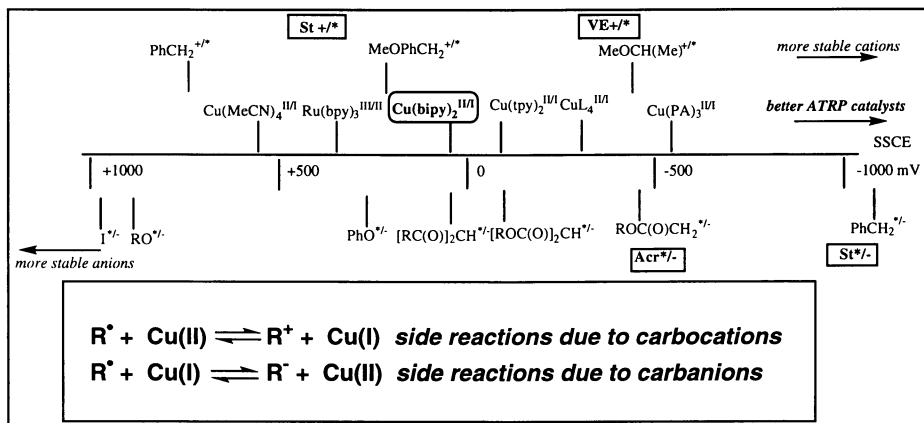
Scheme 7
Idealized Tetrahedral Cu(I) and Trigonal Bipyramidal Cu(II) Species
Involved in ATRP



There are several requirements for an effective ATRP catalyst. First, the metal complex must have an accessible one-electron redox couple to promote atom transfer, but this requirement alone is not sufficient. A second requirement is that upon one-electron oxidation, the coordination number of the metal center must be able to increase by one in order to accommodate a new ligand, X, via atom transfer. Another common feature to each of these systems is that the lower oxidation state complex has an even number of d-electrons which are all paired, providing a stable electronic configuration for the metal center. The higher oxidation state complex has an odd number of electrons, and can be thought of as a metalloradical. A third requirement for an effective ATRP catalyst is that it must show selectivity for atom transfer and therefore possess a low affinity for alkyl radicals and hydrogen atoms on alkyl groups. If not, then transfer reactions, such as β -H elimination and the formation of organometallic derivatives, may be observed. These reactions would reduce the selectivity of the propagation step and the livingness of the polymerization. The fourth requirement is that the metal center must not be a strong Lewis acid, otherwise the ionization of certain initiators or endgroups to carbocations may occur. These species most certainly would be short-lived under the polymerization conditions and therefore result in chain termination. Finally, the metal center should not participate in outer-sphere electron transfer processes. Scheme 8 presents some values for redox processes for the metal centers, together with the estimated potentials for the oxidation and reduction of organic radicals.(59-63) Some of these values were determined in various

solvents and some only estimated, however, they provide a general picture of some potential electron transfer processes.

Scheme 8
Redox Potential for Various Organometallic Complexes and Various Organic Radicals



There are several important conclusions from the inspection of Scheme 8. It appears that poor ATRP catalysts may additionally participate in an electron transfer process to oxidize many organic radicals, including styryl radicals. The $\text{Cu}(\text{MeCN})_4$ complex leads to cationic styrene polymerization.⁽⁶⁴⁾ As mentioned before, p-methoxystyrene also forms carbocations when $\text{Cu}(\text{bipy})_2$ is used⁽⁴⁵⁾ and the radical homopolymerization of vinyl ethers has been unsuccessful for the same reason. Thus, it may be predicted that using more powerful catalysts which better stabilize higher oxidation states (like CuX with aliphatic polyamines) the radical polymerization of some of these monomers can be accomplished.

On the other hand, a better catalyst may reduce the electrophilic radicals such as those in the polymerization of acrylates or acrylonitrile. $\text{Cu}(\text{bipy})_2$ can already reduce malonate, acetylacetonate and trichloromethyl radicals under the appropriate conditions. More powerful catalysts may increase the proportion of side reactions for electrophilic monomers. It seems that $\text{Cu}(\text{bipy})_2$ is a relatively universal catalyst which may be used for many but not all monomers. Further development of new ATRP catalysts may require specific design for each group of monomers.

The most important system variables in designing selective ATRP catalysts are the position of the atom transfer equilibrium and the dynamics of exchange between the dormant and active species. As mentioned above, adjusting the structure of the metal

catalyst will serve to achieve this aim. The equilibrium constant values required for the successful polymerization of methacrylates, styrenes, acrylates, and acrylonitrile range from 10^{-6} to 10^{-10} . Achieving the controlled / living radical polymerization of monomers possessing weaker stabilizing substituents, such as vinyl chloride, vinyl acetate, and potentially ethylene, will require a much more active catalyst (the equilibrium constant for benzyl bromide is in the range of 10^{-4} to 10^{-6}). The deactivation step, or the reaction of the polymeric radical with the copper(II) complex, must be very fast, ($k_d \approx 10^{7 \pm 1} \text{ M}^{-1} \text{ s}^{-1}$), otherwise the polymerization will display high polydispersities and poor control over molecular weights. In the limiting case in which the deactivation step is exceedingly slow, ATRP simply becomes a conventional free-radical polymerization. This is, for example, the case for the $\text{XCu}^{\text{I}}(\text{tpy})$ catalyst which may form a relatively stable $\text{X}_2\text{Cu}(\text{tpy})$ trigonal bipyramidal species which slowly deactivates growing radicals, resulting in a redox-type conventional radical polymerization of styrene.

An important factor that influences the position and dynamics of this equilibrium is the relative bond strengths of the corresponding carbon-halogen and copper-halogen bonds. Much lower polydispersities are observed in ATRP using an organobromine initiator with 2 dNbipy / CuBr than an organochlorine initiator with 2 dNbipy / CuCl. The difference in bond strengths between the carbon-bromine and copper(II)-bromine bonds is smaller relative to the carbon-chlorine and copper(II)-chlorine bonds. The free energy of equilibrium is slightly smaller for bromine-mediated ATRP ($\Delta G^\circ = 13 \text{ kcal mol}^{-1}$) versus chloride-mediated ATRP ($\Delta G^\circ = 14 \text{ kcal mol}^{-1}$). This difference allows bromine-mediated ATRP to be conducted at lower temperatures at which any potential side reactions and thermal self-initiation, in the case of styrene, are slower. Also, the copper(II)-bromine bond strength is smaller than the copper(II)-chloride bond strength, so the former bond should be weaker, resulting in a faster deactivation reaction. These facts are also consistent with earlier studies on the efficiency of free-radical polymerization inhibition using various metal salts. In these studies it was shown that for the polymerization of methyl methacrylate, CuBr_2 in DMF was approximately two times more efficient of an inhibitor than CuCl_2 in DMF.(49)

The key to tailoring the chemistry of the metal catalysts to achieve the desired atom transfer equilibrium constant and dynamics of exchange is the appropriate choice of ligands. The electronic, steric, and solubility characteristics of each ligand system will determine the effectiveness of the metal catalyst. Ligands that are good σ -donors and π -acceptors will stabilize the lower oxidation state of the metal center. This factor serves to shift the atom transfer equilibrium towards the side of the dormant species. When 2,2'-bipyridyl ligands with electron-withdrawing substituents, such as carbomethoxy groups,

at the 4,4'-positions are used in copper-catalyzed ATRP, the polymerization rate is >10 times slower relative to polymerizations using unsubstituted 2,2'-bipyridine. Apparently, the carbomethoxy groups make the ligands better π -acceptors and further stabilize the +1 oxidation state and destabilize the +2 oxidation state of copper. Such effects would reduce the corresponding atom transfer equilibrium constant.

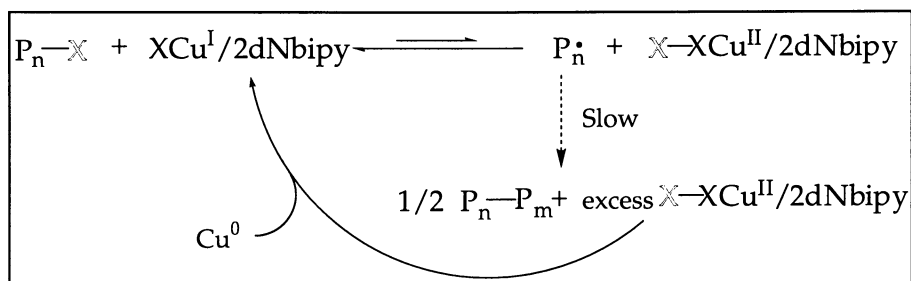
Ligands that sterically crowd the metal center prevent the approach of the alkyl halide initiator or endgroup and therefore are poor ligands for ATRP. Thus, the use of 6,6'-dialkylsubstituted-2,2'-dipyridyl ligand for copper-catalyzed ATRP results in no observable polymerization.

Ligands that possess long alkyl chains increase the solubility of the ATRP copper catalysts in nonpolar polymerization media. When 2,2'-bipyridine (bipy) is used, the copper halide is sparingly soluble in the polymerization medium and the polymerization is heterogeneous, whereas bipyridyl ligands with long alkyl chains at the 4,4'-positions (such as = 4,4'-di(5-nonyl)-2,2'-bipyridyl, dNbipy) completely solubilize the copper halide. Qualitatively, ATRP behaves in a similar manner whether or not the catalyst is highly soluble in the polymerization medium, because the catalyst is not bound to the growing chain. Somewhat higher polydispersities are observed in the heterogeneous systems due to the lower concentration of the Cu(II) complex (deactivator) and consequently a slower deactivation process; however, the overall difference is not too dramatic. For instance, in the bulk polymerization of styrene (at 100 °C with 0.5 mole % of 1-phenylethyl bromide, 1-PEBr, initiator) the polydispersity, M_w / M_n , averages around 1.1 when CuBr / 2dNbipy is the catalyst, versus 1.3 when CuBr / 2 bipy is the catalyst.(14,20)

The last, nearly trivial parameter which can affect ATRP is the solubility of both the Cu(I) and Cu(II) species. Sometimes, for synthesis of short chains with low polydispersities, a high concentration of XCu(II) species is necessary, however, this slows down polymerization. Thus, for the synthesis of longer chains, a lower solubility may be beneficial. Adjustment of the solubility of the catalyst by the ligand structure is very important in the synthesis of hyperbranched polymers, with a very high concentration of active halogen atoms.(65) For homogeneous systems, no polymerization of 2-(2-bromopropionyloxy)ethyl acrylate was observed because all Cu(I) species were very rapidly converted to XCu(II) species. However, in a heterogeneous system a lower stationary concentration of both Cu(I) and XCu(II) allowed controlled polymerization.(65) During the process, Cu(I) was progressively dissolving and converting to XCu(II) which was precipitating because of its low solubility; both species maintained their low stationary concentrations.

Another approach to reduce concentration of Cu(II) species involves its reaction with Cu(0) and regeneration of Cu(I). The addition of the zero valent metal, copper powder, allows for the slow removal of excess Cu(II) plausibly by a simple oxidation/reduction process (Scheme 9). In this case, the Cu(0) is oxidized to Cu(I) while the Cu(II) is reduced to Cu(I). Removal of small amounts of Cu(II) enhances the rate, while still maintaining control of the polymerization. For example, in bulk polymerization of MA at 90 °C initiated by 1 mol% of methyl 2-bromopropionate and catalyzed by 0.1% of CuBr/2dNbipy reaction rate increases 10 fold in the presence of 2 mol% of Cu(0) powder (no extra ligand is added) while molecular weights are well controlled and polydispersities increase only slightly.(66) Apparently, the position of the equilibrium in the disproportionation ($\text{CuX}_2 + \text{Cu}(0) = 2 \text{CuX}$) depends very strongly on ligands and it is as low as 10^{-6}M for water (67) but 10^5M for ethylene (68) and presumably has a similar large value for bipy as ligand.

Scheme 9

Plausible Mechanism for the Regeneration of CuX_2 by Cu(0)

4. Solvents and Additives: Typically, ATRP is conducted in bulk, but solvents may be used and are sometimes necessary when a polymer is insoluble in its monomer. Solution polymerizations are slower relative to bulk polymerizations using the same amounts of reagents due to the reaction orders of each component. When solvents are used they are usually very non-polar, such as benzene, *p*-dimethoxybenzene, and diphenyl ether, but some polar solvents, such as ethylene carbonate and propylene carbonate, have been used successfully.(31,37) Solvent choice should be dictated by several factors. First, with some solvents there is the potential for chain transfer, depending upon the corresponding transfer constant, C_s . This factor usually only limits the maximum molecular weight attainable in that particular solvent. Thus, when low molar mass polymer is targeted (i.e., $M_n < 20,000$) toluene and xylene can be used as ATRP solvents. Second, solvent interactions with the catalyst system should be considered. Specific interactions with the catalyst, such as solvolysis of the halogen ligand or displacement of

the bipyridyl ligands, should be avoided. For example, bromine-mediated ATRP of styrene in DMF and acetonitrile is much slower and exhibits less molecular weight control than the corresponding ATRP in nonpolar solvents or in bulk. Third, certain polymer endgroups, such as polystyryl halides, can undergo solvolysis or elimination of HX at 110 to 130 °C in many polar solvents.(13)

ATRP also can be conducted with additives to identify specific functional group compatibilities and incompatibilities. Additives that are good ligands for Cu(I) and (II) significantly reduce the rate of polymerization. The addition of five volume percent pyridine to the ATRP of styrene greatly slows down the rate of polymerization, and the addition of two mole equivalents of triphenylphosphine per copper center entirely deactivates the catalyst.(31) The polymerization is rather sensitive to oxygen. ATRP will proceed when a small amount of oxygen is added, because this amount of oxygen can be scavenged by the catalyst which is present at much higher concentration than the polymeric radicals. However, the reaction of oxygen with the catalyst reduces the concentration of the copper(I) complex and may form an excess of the copper(II) species. This reaction would also have the effect of reducing the rate of polymerization.

In a very recent paper it was proposed that propagation in Cu-based ATRP of MMA did not take place via a carbon-centered free radical, since no effect on rates and molecular weights was observed in the presence of phenols.(69) However, several earlier studies clearly demonstrated that although phenols do affect polymerization of styrene, their action on radical polymerization of (meth)acrylates is very weak. For example, less than 1% retardation was observed for MMA with 0.2 M of hydroquinone and 4-methoxyphenol even increased polymerization rate initiated by AIBN at 45 °C. In the latter case transfer coefficient is $k_{tr}/k_p < 0.0005$.(70) A similar observation was made for methyl acrylate, where inhibition was again insignificant at 50°C, $k_s/k_p < 0.0002$.(71) Thus, weak retardation/transfer effect of phenols on polymerization of (meth)acrylates does not contradict the radical mechanism. On the other hand, phenols may even accelerate polymerization by exchanging ligands at Cu center. Similar effect was noticed for Cu carboxylates and Cu PF₆.(55,72)

6. Temperature and Reaction Time: In ATRP, the observed rate of polymerization is enhanced by increasing temperature due to increases in both the rate constant for radical propagation and the atom transfer equilibrium constant. The atom transfer enthalpies for styrene ATRP are $\Delta H^\circ = 4.8 \text{ kcal mol}^{-1}$ ($\Delta S^\circ = -22 \text{ kcal mol}^{-1}$) for the bromine-mediated process and $\Delta H^\circ = 6.3 \text{ kcal mol}^{-1}$ ($\Delta S^\circ = -20 \text{ kcal mol}^{-1}$) for the chlorine-mediated process.(31) In the bromine-mediated ATRP of methyl acrylate, $\Delta H^\circ \approx 12 \text{ kcal mol}^{-1}$

which indicates that the formation of radicals is more endothermic in comparison to the styrene system. This result correlates well with the higher reactivity of the acrylate radical with respect to the styryl radical.

The energy of activation for radical propagation is appreciably higher than that for termination by radical combination and disproportionation. Consequently, the ratio k_p / k_t is higher and therefore better polymerization control (livingness) is observed at higher temperatures. If only the ratio of termination-to-propagation is considered, the best control will be observed for slower reactions at higher temperatures, but at elevated temperatures the rate of chain transfer and other side reactions also become faster. Therefore, an optimum temperature for each type of ATRP must be found. This temperature will depend upon the monomer, catalyst system (catalyst structure and activity may change with temperature), targeted molecular weight, and the chemist's patience.

The effect of reaction time is also important. At high polymerization conversions the rate of propagation is very slow, because of the dependence upon monomer concentration. The rate of most side reactions does not depend upon monomer concentration, so such processes may still proceed at their observed rate. Even though the rate of such side reactions may be perceived as slow, they can have a significant effect upon the structure of the final polymer. In such situations significant loss of endgroup functionality can occur. The fact that the final polydispersities may be very low and the polymer may appear to be well-defined could be misleading. Therefore, when conducting ATRP in which maintaining the endgroup functionality is a concern (i.e., in the preparation of block copolymers), the polymerization conversion should not exceed 95% in order to avoid potential endgroup loss.

Conclusions

Atom transfer radical polymerization is a new versatile method to control the radical polymerization of styrenes, various (meth)acrylates, acrylonitrile and other monomers. It can be used to prepare polymers with controlled architectures, compositions and functionalities. Although very often the same catalyst and initiator can be used for the synthesis of many polymers, particular reaction conditions, ratios of reagents and even the mode of addition of all the reaction components may affect control. Thus, it is important to understand the role of each component and the effect of its structure and concentration on ATRP. This paper only attempts to describe this complex system and more detailed kinetic and spectroscopic studies are necessary to determine the precise structure and reactivities of the Cu(I) and Cu(II) species, as well as the propagating species. It is possible that many of these species coexist and depending on monomer, metal, ligand,

protecting group, temperature, solvent and concentrations one species may dominate but others may be major contributors to the propagation and exchange reactions.

Acknowledgments

This research was supported by the industrial members of the ATRP Consortium at Carnegie Mellon University as well as by the National Science Foundation, Office of Naval Research, Petroleum Research Foundation and U. S. Army Research Office. I would like to acknowledge contribution of all past and current members of our research group whose efforts helped to better understand the complexed nature of ATRP: S. V. Arehart, P. Balchandani, K. L. Beers, S. Coca, V. Coessens, K. A. Davis, S. Gaynor, D. Greszta, T. Grimaud, C. B. Jasieczek, S. M. Jo, A. Kajiwara, P. J. Miller, Y. Nakagawa, H.-J. Paik, T. Patten, J. Qiu, J.-L. Wang, J.-S. Wang, M. Wei, B. E. Woodworth, and J. Xia.

References

- (1) Curran, D. P. *Synthesis* **1988**, 489.
- (2) Fischer, H. *J. Am. Chem. Soc.* **1986**, *108*, 3925.
- (3) Minisci, F.; Pallini, U. *Gazz. Chim. Ital.* **1961**, *91*, 1030.
- (4) Asscher, M.; Vofsi, D. *J. Chem. Soc.* **1963**, *1963*, 1887.
- (5) Bellus, D. *Pure Appl. Chem.* **1985**, *57*, 1827.
- (6) Iqbal, J.; Bhatia, B.; Nayyar, N. K. *Chem. Rev.* **1994**, *94*, 519.
- (7) Udding, J. H.; Tuij, K. J. M.; van Zanden, M. N. A.; Hiemstra, H.; Meyerstein, D. *J. Org. Chem.* **1994**, *59*, 1993.
- (8) Nagashima, H.; Ozaki, N.; Ishii, M.; Seki, K.; Washiyama, M.; Itoh, K. *J. Org. Chem.* **1993**, *58*, 464.
- (9) Lee, G. M.; Weinreb, S. M. *J. Org. Chem.* **1990**, *55*, 1281.
- (10) Grove, D. M.; van Koten, G.; Verschuuren, A. H. M. *J. Mol. Catal.* **1988**, *45*, 169.
- (11) Tsuji, J.; Sato, K.; Nagashima, H. *Chem. Lett.* **1981**, 1169.
- (12) Kamigata, N.; Sawada, H.; Kobayashi, M. *Tetrahedron Lett.* **1979**, 159.
- (13) Wei, M.; Matyjaszewski, K.; Patten, T. *Polym. Prepr. (Am. Chem. Soc., Div. Polym. Chem.)* **1997**, *38(1)*, 683.
- (14) Wang, J. S.; Matyjaszewski, K. *Macromolecules* **1995**, *28*, 7901.
- (15) Nishikawa, T.; Ando, T.; Kamigaito, M.; Sawamoto, M. *Macromolecules* **1997**, *30*, 2244.
- (16) Greszta, D.; K. Matyjaszewski *Polym. Prepr. (Am. Chem. Soc., Div. Polym. Chem.)* **1996**, *37(1)*, 569.

- (17) Haddleton, D.; Crossman, M. C.; Hunt, K. H.; Topping, C.; Waterson, C.; Suddaby, K. S. *Macromolecules* **1997**, *30*, 3992.
- (18) Wang, J. S.; Matyjaszewski, K. *Macromolecules* **1995**, *8*, 7572.
- (19) Wang, J. S.; Matyjaszewski, K. *J. Am. Chem. Soc.* **1995**, *117*, 5614.
- (20) Patten, T. E.; Xia, J.; Abernathy, T.; Matyjaszewski, K. *Science* **1996**, *272*, 866.
- (21) Percec, V.; Barboiu, B. *Macromolecules* **1995**, *28*, 7970.
- (22) Haddleton, D.; Jasieczek, C. B.; Hannon, M. J.; Shooter, A. J. *Macromolecules* **1997**, *30*, 2190.
- (23) Granel, C.; Dubois, P.; Jerome, R.; Teyssie, P. *Macromolecules* **1996**, *29*, 8576.
- (24) Uegaki, H.; Kotani, Y.; Kamigaito, M.; Sawamoto, M. *Macromolecules* **1997**, *30*, 2249.
- (25) Kato, M.; Kamigaito, M.; Sawamoto, M.; Higashimura, T. *Macromolecules* **1995**, *28*, 1721.
- (26) Matyjaszewski, K.; Wang, J. S. *WO 96/30421* **1996**
- (27) Wei, M.; Xia, J.; Matyjaszewski, K. *Polym. Prepr. (Am. Chem. Soc., Div. Polym. Chem.)* **1997**, *38(2)*, 233.
- (28) Wei, M.; Xia, J.; McDermott, N. E.; Matyjaszewski, K. *Polym. Prepr. (Am. Chem. Soc., Div. Polym. Chem.)* **1997**, *38(2)*, 231.
- (29) Xia, J.; Matyjaszewski, K. *Macromolecules* **1997**, *in press*,
- (30) Percec, V.; Barboiu, B.; Neumann, A.; Ronda, J. C.; Zhao, M. *Macromolecules* **1996**, *29*, 3665.
- (31) Matyjaszewski, K.; Patten, T.; Xia, J. *J. Am. Chem. Soc.* **1997**, *119*, 674.
- (32) Greszta, D.; Matyjaszewski, K. *Macromolecules* **1996**, *29*, 7661.
- (33) Fukuda, T.; Terauchi, T. *Chem. Lett.* **1996**, 293.
- (34) Matyjaszewski, K.; Lin, C.-H. *Makromol. Chem. Macromol. Symp.* **1991**, *47*, 221.
- (35) Litvinienko, G.; Müller, A. H. E. *Macromolecules* **1997**, *30*, 1253.
- (36) Bamford, C. H. In *Comprehensive Polymer Science*; G. Allen, S. L. Aggarwal and S. Russo, Eds.; Pergamon: Oxford, 1989; Vol. 3; pp 123.
- (37) Jo, S. M.; Gaynor, S. G.; Matyjaszewski, K. *Polym. Prepr. (Am. Chem. Soc., Div. Polym. Chem.)* **1996**, *37(2)*, 272.
- (38) Buback, M.; Gilbert, R. G.; Hutchinson, R. A.; Klumperman, B.; Kuchta, F.-D.; Manders, B. G.; O'Driscoll, K. F.; Russell, G. T.; Schweer, J. *Macromol. Chem. Phys.* **1995**, *196*, 3267.
- (39) Hutchinson, R. A.; Jr., D. A. P.; McMinn, J. H.; Fuller, R. E. *Macromolecules* **1995**, *28*, 4023.

- (40) Hutchinson, R. A.; Richards, J. R.; Aronson, M. T. *Macromolecules* **1994**, *27*, 4530.
- (41) Lyons, R. A.; Hutovic, J.; Piton, M. C.; Christie, D. I.; Clay, P. A.; Manders, B. G.; Kable, S. H.; Gilbert, R. G.; Shipp, D. A. *Macromolecules* **1996**, *29*, 1918.
- (42) Fischer, H. In *Free Radicals in Biology and Environment*; F. Minisci, Ed.; Kluwer Acad. Publ.: Dordrecht, 1997.
- (43) Walbiner, M.; Wu, J. Q.; Fischer, H. *Helv. Chim. Acta* **1995**, *78*, 910.
- (44) Nakagawa, Y.; Gaynor, S. G.; Matyjaszewski, K. *Polym. Prepr. (Am. Chem. Soc., Div. Polym. Chem.)* **1996**, *37(1)*, 577.
- (45) Qiu, J.; Matyjaszewski, K. *Polym. Prepr. (Am. Chem. Soc., Div. Polym. Chem.)* **1997**, *38(1)*, 711.
- (46) Heberger, K.; Walbiner, M.; Fischer, H. *Ang. Chem., Int. Ed. Engl.* **1992**, *31*, 635.
- (47) Wayner, D. D. M.; A., S. B.; Dannenberg, J. J. *J. Org. Chem.* **1991**, *56*, 4853.
- (48) Grimaud, T.; Matyjaszewski, K. *Macromolecules* **1997**, *30*, 2216.
- (49) Bengough, W. I.; O'Neill, T. *Trans. Faraday Soc.* **1968**, *1968*, 2415.
- (50) Paik, H.; Matyjaszewski, K. *Polym. Prepr. (Am. Chem. Soc., Div. Polym. Chem.)* **1996**, *37(2)*, 274.
- (51) Coca, S.; Davis, K.; Miller, P.; Matyjaszewski, K. *Polym. Prepr. (Am. Chem. Soc., Div. Polym. Chem.)* **1997**, *38(1)*, 689.
- (52) Coca, S.; Matyjaszewski, K. *Polym. Prepr. (Am. Chem. Soc., Div. Polym. Chem.)* **1997**, *38(1)*, 691.
- (53) Jo, S.; Paik, H.-J.; Matyjaszewski, K. *Polym. Prepr. (Am. Chem. Soc., Div. Polym. Chem.)* **1997**, *38(1)*, 697.
- (54) Greszta, D.; Matyjaszewski, K.; Pakula, T. *Polym. Prepr. (Am. Chem. Soc., Div. Polym. Chem.)* **1997**, *38(1)*, 709.
- (55) Davis, K.; O'Malley, J.; Paik, H. J.; Matyjaszewski, K. *Polym. Prepr. (Am. Chem. Soc., Div. Polym. Chem.)* **1997**, *38(1)*, 687.
- (56) Brown, H. C.; Fletcher, R. S. *J. Am. Chem. Soc.* **1949**, *71*, 1845.
- (57) Munakata, M.; Kitagawa, S.; Asahara, A.; Masuda, H. *Bull. Chem. Soc. Jpn.* **1987**, *60*, 1927.
- (58) Tyagi, S.; Hathaway, B.; Kremer, S.; Stratemeier, H.; Reinen, D. *J. Chem. Soc., Dalton Trans.* **1984**, 2087.
- (59) Wayner, D. D. M.; McPhee, D. J.; Griller, D. *J. Am. Chem. Soc.* **1988**, *110*, 132.
- (60) Bordwell, F. G.; Zhang, X. M. *J. Am. Chem. Soc.* **1994**, *116*, 973.
- (61) Sawyer, D. T.; Sobkowiak, A.; Roberts, J. L. *Electrochemistry for Chemists*; Wiley: New York, 1995.

- (62) Hapiot, P.; Pinson, J.; Yousfi, N. *New J. Chem.* **1992**, *16*, 877.
- (63) Saveant, J. M. *Tetrahedron* **1994**, *50*, 10117.
- (64) Haddleton, D. M.; Shooter, A. J.; Hannon, M. J.; Barker, J. A. *Polym. Prepr. (Am. Chem. Soc., Div. Polym. Chem.)* **1997**, *38(1)*, 679.
- (65) Gaynor, S.; Balchandani, P.; Kulfan, A.; Podwika, M.; Matyjaszewski, K. *Polym. Prepr. (Am. Chem. Soc., Div. Polym. Chem.)* **1997**, *38(1)*, 496.
- (66) Matyjaszewski, K. *unpublished results*
- (67) Endicott, J. F.; Taube, H. *Inorg. Chem.* **1965**, *4*, 473.
- (68) Ogura, T. *Inorg. Chem.* **1976**, *15*, 2301.
- (69) Haddleton, D. M.; Clark, A. J.; Crossman, M. C.; Duncalf, D. J.; Heming, A. M.; Morsley, S. R.; Shooter, A. J. *J. Chem. Soc., Chem. Commun.* **1997**, 1173.
- (70) Barton, S. C.; Bird, R. A.; Russell, K. E. *Can J. Chem.* **1963**, *41*, 2737.
- (71) Bagdasarian, K., S.; Sinitsina, Z. A. *J. Polym. Sci.* **1961**, *52*, 31.
- (72) Wei, M.; Xia, J.; Gaynor, S. G.; Matyjaszewski, K. *Polym. Prepr. (Am. Chem. Soc., Div. Polym. Chem.)* **1997**, *38(1)*, 685.

Atom Transfer Radical Polymerization of Methyl Methacrylate: Effect of Phenols

D. M. Haddleton, A. J. Shooter, A. M. Heming, M. C. Crossman,
D. J. Duncalf, and S. R. Morsley

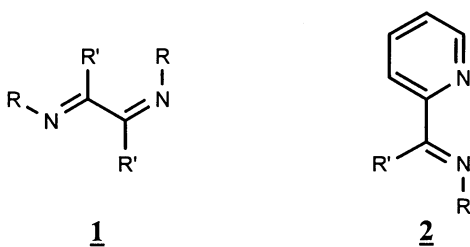
Department of Chemistry, University of Warwick, Coventry, CV4 7AL,
United Kingdom

Atom transfer radical polymerization of methyl methacrylate initiated by ethyl-2-bromoisobutyrate and catalyzed by 2-pyridinal-alkylimine copper(I) complexes has been demonstrated to be effective in the presence of large excesses of phenolic radical inhibitors. In the absence of phenol an induction period is observed which is reduced on addition of phenol, topanol, 4-methoxy phenol and 2,6-diisopropylphenol. Single crystal x-ray diffraction studies and variable temperature NMR experiments suggest that this is due to the formation of a bridged copper(II) species. The results indicate that propagation in this type of ATRP system does not proceed via a free radical but via a complexed bridging halide atom species.

Atom transfer radical polymerization (ATRP) is emerging as an efficacious method for the controlled polymerization of styrene, acrylates, methacrylates and other vinylic monomers (1 - 7). The reaction has been developed from the Kharash reaction used for carbon-carbon bond formation in organic synthesis. Two groups, independently, reported this chemistry for living polymerization of vinyl monomers. Sawamoto described the use of $\text{Ru}(\text{PPh}_3)_3\text{Br}_2$ in conjunction with an alkyl chloride and an aluminum phenoxide/alkoxide activator for the *living* polymerization of methyl methacrylate in toluene at 60 °C (5-6). Matyjaszewski utilized copper(I) halides in conjunction with 2,2'-bipyridine as a complexing ligand for the controlled radical polymerization of styrene, methyl and butyl acrylate and methyl methacrylate in a range of solvents at between 80 °C and 130 °C (1 - 4). The role of the 2,2'-bipyridine was originally described as increasing the solubility of the inorganic salt although with 2,2'-bipyridine a heterogeneous polymerization ensues. This work has been extended for styrene by use of a 4,4'-dialkyl substituted 2,2'-bipyridine e.g. 4,4'-di-n-heptyl-2,2'-bipyridine, which increases the solubility of the catalyst system in hydrocarbon such that living polymerization is observed with Mn up to 10,000 and PDI < 1.10 (3). It is noted that even with this soluble copper(I) species the reaction is approximately first order

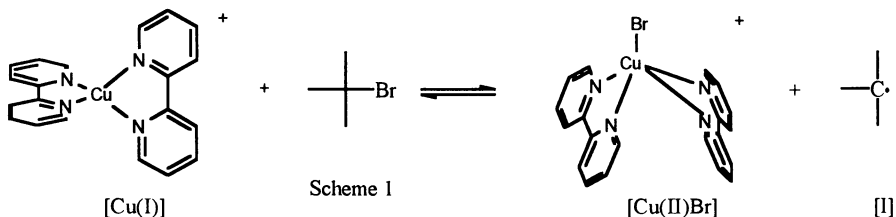
with respect to copper for both 1-phenylethyl bromide and 1-phenylethyl chloride initiated polymerization of styrene. Subsequently, Percec has reported that the alkyl halide initiator may be replaced with an arenesulfonyl chloride. Teyssie and Granel have extended the catalyst set to nickel(II) with Ni(II)[C₆H₃(CH₂NMe₂)₂-2,2,6]Br (8), although this was previously reported by Percec to decompose under the appropriate reaction conditions (7). Ni(II)[C₆H₃(CH₂NMe₂)₂-2,2,6]Br leads to living polymerization of methyl methacrylate with Mn up to 65,000 and PDI = 1.2 in toluene at 80 °C.

The role of the 2,2'-bipyridine (bpy) when used in conjunction with copper(I) halides is not only to solubilize the active species but to stabilize copper(I) relative to copper(II) by accepting electron density into a π^* orbital (9). We have reported that bipyridines may be replaced with other α -diimines with the N=C-C=N skeleton e.g. 1 and 2 where R, R' = alkyl, aryl, etc. (10). Both 1 and 2 also have the capability of accepting electron density into a π^* orbital and have been found to be superior to bpy in stabilizing metals in low oxidation states. Ligands such as 1 have recently been used coordinated to Ni as very effective ethene polymerization catalysts (11).



Both 1 and 2 type ligands are very facile to synthesize involving the reaction of the appropriate aldehyde, or ketone, with a primary amine. The wide range of R groups available, from primary amines and carbonyl compounds, as well as the possibility of substitution on the aromatic ring in the case of 2 gives control over the position of the Cu(I)/Cu(II) redox couple. Electron donating and withdrawing groups on the ligand stabilize Cu(II) and Cu(I) respectively, as well as allowing control over catalyst solubility. The availability of catalysts with a range of solubilities is important in determining the amount of active species present in solution as well as in the subsequent application of this chemistry to heterogeneous polymerization, e.g. mini-emulsion.

Both ourselves (10) and Matyjaszewski (4) have proposed the mechanism shown in scheme 1 as an integral part of this chemistry, where [I] initiates polymerization via free radical attack on a vinyl monomer. Propagation proceeds as in normal free radical polymerization. The reverse reaction, end-capping the polymer with a bromide atom and regenerating a [Cu(I)] complex, reduces the free radical concentration, and hence the rate of conventional bimolecular termination.



This mechanism allows for propagation to occur via a free radical process. Indeed, all three metal based ATRP catalysts Cu(I), Ru(II) and Ni(II) have been described as proceeding via a radical process. Sawamoto uses two tests to demonstrate the involvement of free radicals in the ATRP of MMA mediated by Ru(II): (A) the addition of radical inhibitors such as galvinoxyl or DPPH immediately stops or prevents polymerization from occurring and (B) ^{13}C NMR indicates the stereochemistry of the PMMA product to be consistent with a Bernoullian process with stereochemistry similar to PMMA prepared from AIBN in toluene at 60 °C (5, 12). Matyjaszewski also reports that the stereochemistry of PMMA as prepared with a [Cu(I)] catalyst is similar to that from classical free radical initiators and that galvinoxyl acts as an efficient inhibitor (2). Again these two pieces of evidence are used as proof for a free radical process. Teyssie also reports inhibition by galvinoxyl and a persistence ratio of close to unity with Ni(II) which are used as an argument for free radical propagation. It is noted that only in the case of Ni(II) are the radicals discussed as *being temporarily confined within the coordination sphere of the metal*. (8)

One of the potential advantages of a radical type living polymerization over an anionic polymerization is robustness towards various functional groups in monomers, solvents and impurities present in the reaction (13). As such we have been interested in examining the effect of various functionality's on ATRP. Surprisingly, we have found that certain phenolic compounds enhance ATRP as opposed to inhibiting polymerization as might have been expected. This paper discusses preliminary results from this study.

Experimental

General: Methyl methacrylate (MMA, Aldrich) and xylene (AR grade, Fischer Scientific) were purged with nitrogen for 2 hours prior to use. The initiator, ethyl-2-bromoisobutyrate (98%, Aldrich), and CuBr (99.999%, Aldrich) were used as received. The phenols used, phenol (99%, Pronalys AR), 4-methylphenol (99%, Aldrich), 2,6-diisopropylphenol (97%, Aldrich) and Topanol (2,6-di-*tert*-butyl-4-methylphenol, 99%, Aldrich) were all used as received.

Monomer conversion was measured by gravimetry. Molecular weights and molecular weight distributions were found by size exclusion chromatography using THF as eluent with one 5 μm guard and one mixed-E (3000 x 7.5mm) column (Polymer Laboratories), calibration was against poly(methyl methacrylate) standards.

Preparation of 2-pyridinal-pentylimine (1): n -Pentylamine (24.4 mL, 0.21 mol, 99%, Aldrich) was added dropwise to Pyridine-2-carboxaldehyde (20.0 mL, 0.21 mol, 99%, Aldrich) with stirring in an ice bath. After complete addition of the amine approximately 5 g of dried magnesium sulfate was added and the reaction left for a further 2 hours. The solution was filtered and distilled under reduced pressure. The product was collected at 60 °C, 0.4 mbar (14, 15). ^1H NMR (CDCl_3 , 250 MHz): δ = 8.60 (d, 1H), 8.33 (s, 1H), 7.94 (d, 1H), 7.69 (t, 1H), 7.27 (t, 1H), 3.63 (t, 2H), 1.69 (sextet, 2H), 1.31 (overlapping quintets, 2H each), 0.87 (t, 3H). 2-pyridinal-ethylimine (2), 2-pyridinal-propylimine (3), 2-pyridinal-butylimine (4) and 2-pyridinal-*tert*-butylimine (5)

were prepared in a similar manner replacing *n*-pentylamine with the appropriate primary amine.

Typical polymerization. In a typical reaction, CuBr (0.134 g; [Cu] : [Initiator] = 1 : 1) was placed in a predried Schlenk tube which was evacuated and then flushed with nitrogen three times. Methyl methacrylate (10 mL) followed by 2-pyridinal-pentylimine (0.17 mL, [ligand] : [Cu] = 2 : 1) was added with stirring and within a few seconds, a deep, brown solution formed. Xylene (20 mL) and , where appropriate, substituted phenol were then added and the flask heated in a constant temperature oil bath to 90 °C. When the solution had equilibrated ethyl-2-bromoisobutyrate (0.14 mL, [Monomer] : [Initiator]=100 : 1) was added. Samples were taken 30, 60, 120, 180, and 240 minutes after initiator was added.

Crystals for single crystal x-ray diffraction study. [Cu(CH₃CN)₄][BF₄], (**7**), was added to a solution of **5** in degassed methanol under nitrogen. The solution was filtered and red crystals suitable for a single crystal x-ray diffraction study recovered at 5 °C. Copper (I) bromide was added to a solution of **5** (two fold excess) in degassed methanol under nitrogen. An equimolar amount phenol with respect to **5** was then added and the solution cooled to 5 °C. After 24 Hrs green crystals were isolated.

Results and Discussion

Polymerization of MMA by Cu(I)Br/2,2'-bipyridine/ethyl-2-bromoisobutyrate (6**) in the presence of phenol.** Polymerization of MMA in xylene solution at 70 °C with [MMA] : [Initiator] = 100:1 (i.e. $M_{n,theor} = 10,000$) in the presence of CuBr and bpy proceeds to approximately 50% conversion after 180 mins, with PDI narrowing over the course of the reaction (Table I). The addition of a 5 mole equivalent of phenol dramatically increases the rate of polymerization reaching 76% conversion over the same time period. Increasing the amount of phenol by a factor of two results in the rate of polymerization increasing such that greater than 97% conversion is achieved in 180 mins. The increase in rate is seen by the increase in the gradient of a semi first order plot (gradient = $k_p[Pol^*]$, where Pol* is the active chain end). Each reaction shows an induction period, where the number of active species increases, prior to a relatively linear region indicating that the active species is not destroyed in the reaction. A value for $k_p[Pol^*]$, i.e. $k_{p(apparent)}$, can be calculated and this is found to increase from $1.2 \times 10^{-3} \text{ s}^{-1}$ to $5.5 \times 10^{-3} \text{ s}^{-1}$ on addition of phenol. Thus phenol accelerates the rate of polymerization and does not inhibit the reaction as might have been expected for either a radical or anionic propagation step. It is noted that in this set of reactions the PDI is considerably greater than would be expected for a living polymerization.

¹H NMR study; role of phenol. Figure 1a shows the variable temperature ¹H NMR spectrum of Cu(I)Br/2,2'-bipyridine in d⁶-DMSO. At room temperature we see four peaks from pseudo-tetrahedral Cu(bpy)₂⁺. At higher temperature, corresponding to

Table I. Polymerization of MMA, with Cu(I)Br/2,2'-bipyridine/ethyl-2-bromoisobutyrate 100 [MMA] : 1 [In] : 1 [CuBr] : 3 [bpy] at 70 °C.

[Phenol] /[In]	t/ mins	Mn	Mw	PDI	%Conv.
0	30	4984	8816	1.77	2.4
0	60	6390	9630	1.51	10.1
0	120	9287	14402	1.55	30.4
0	180	12392	18240	1.47	52.7
5	30	4444	6974	1.57	12.3
5	60	6841	10523	1.53	23.4
5	120	9877	15426	1.56	58.4
5	180	12038	18527	1.54	76.1
10.	30	5754	9182	1.6	26.8
10	60	8978	13420	1.5	47.1
10	120	10587	17535	1.66	78.8
10	180	14173	23064	1.63	97.6

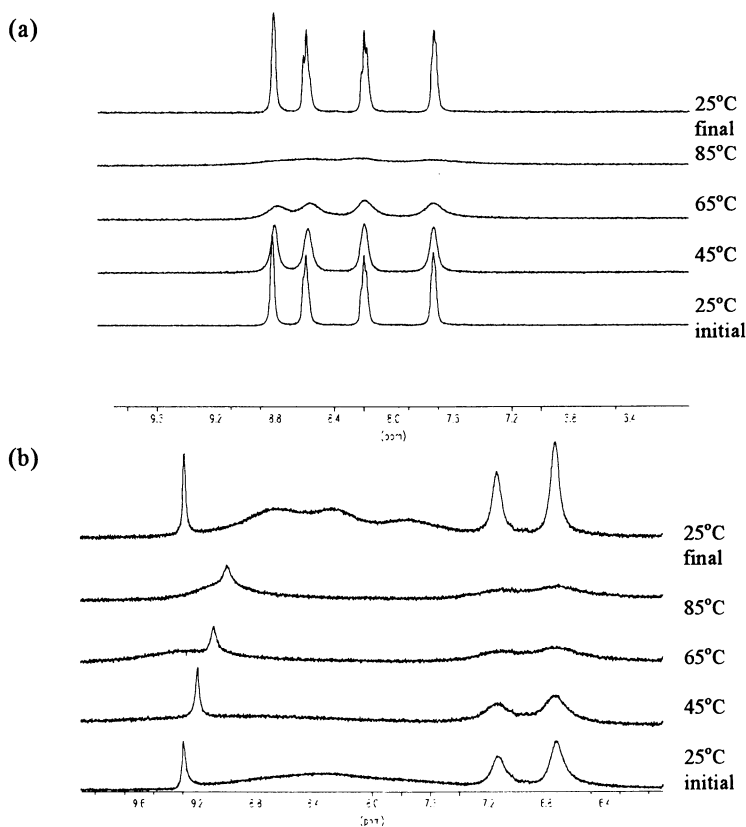


Figure 1. Partial 400 MHz ^1H NMR of (a) Cu(I)Br/2,2'-bipyridine and (b) Cu(I)Br/2,2'-bipyridine/phenol in $\text{d}^6\text{-DMSO}$

ATRP reaction temperature, exchange occurs on the NMR time scale indicated by the observed peak broadening. On cooling the original spectrum is regenerated. In the presence of phenol (Figure 1b), the bipyridine ligands exchange at 25 °C. Exchange of bipyridine with phenol occurs at the reaction temperature as evidenced by the broadening of the resonance's at approximately 6.7 and 7.1 ppm. This is good evidence for coordination of the phenol to copper at some point in the reaction.

Polymerization of MMA by Cu(I)Br/2-pyridinal-alkylimine /ethyl-2-bromoisobutyrate in the presence of phenol. Polymerization of MMA using copper complexes of 2-pyridinal-alkylimines **4** and **1** in conjunction with **1** as initiator in the presence of phenol leads to polymers of narrow PDI in high conversion (Table II). Increasing the amount of phenol relative to the amount of initiator and catalyst causes a slight increase in polymerization rate, as evidenced by a higher conversion after 240 mins, with no marked effect on the PDI. Figure 2 shows the *pseudo*-first order plots for reactions using **1** as the complexing ligand. There is a slight narrowing of

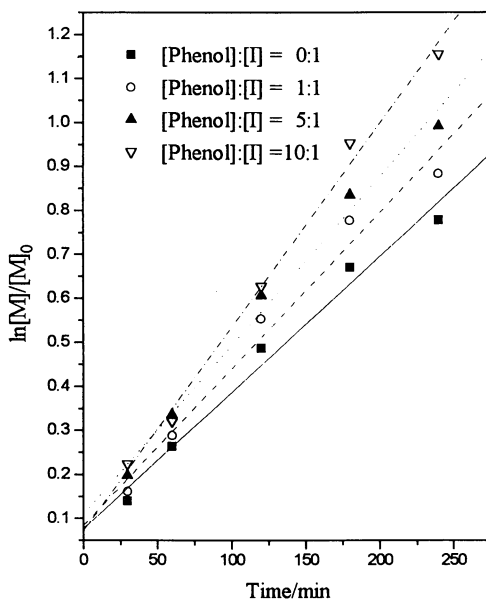


Figure 2. Kinetic plots for the polymerization of MMA, in the presence of different amounts of phenol, by Cu(I)Br/2-pyridinal-pentylimine 100 [MMA] : 1 [**6**] : 1 [CuBr] : at 90 °C in xylene solution .

PDI with **1** relative to **4**. This is ascribed to the solubility of the copper species derived from **1** being greater than that from **4**. This increase in solubility with an increase in alkyl chain length is similar to that observed by Matyjaszewski for various substituted 2,2'-bipyridine complexes.

Table II. Polymerization of MMA with Cu(I)Br/2-pyridinal-alkylimine /6 100 [MMA] : 1 [6] : 1 [CuBr] : at 90 °C in xylene solution, reaction stopped after 240 mins.

Ligand	[Phenol] : [6]	% Conv.	Mn	PDI
4	0	31	6530	1.30
4	1	40	6200	1.30
4	5	47	6190	1.29
4	10	56	6200	1.31
1	0	54	6790	1.21
1	1	59	7250	1.20
1	5	63	7610	1.22
1	10	68	8330	1.27

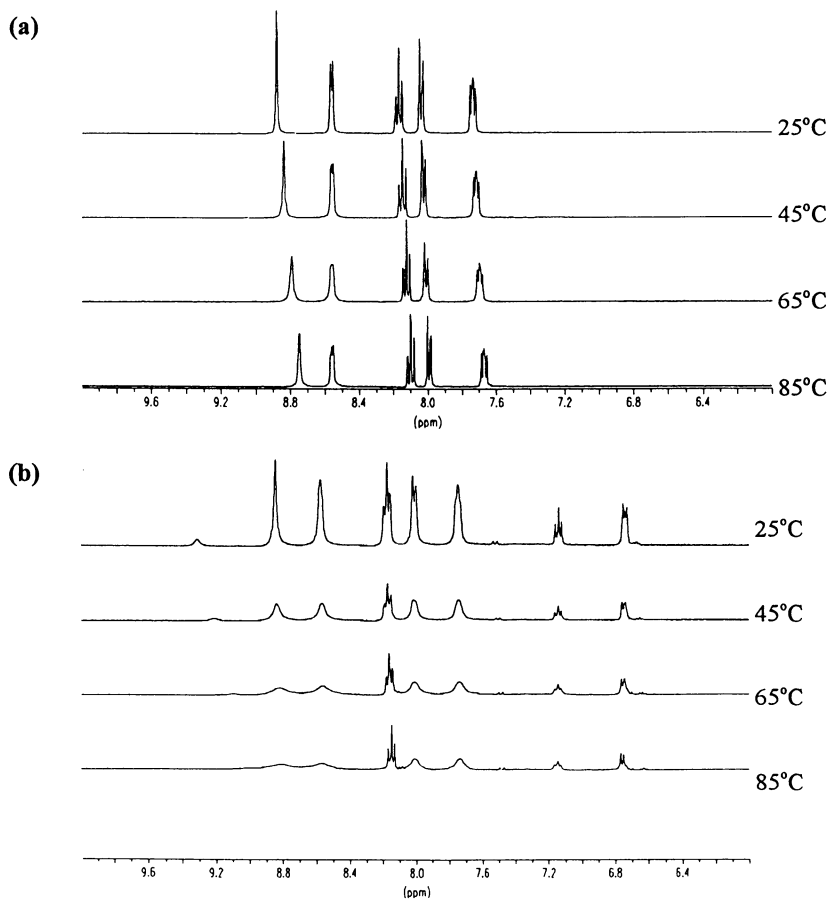


Figure 3. Partial 400 MHz ^1H NMR of (a) Cu(I)Br/ 2-pyridinal-butylimine and (b) Cu(I)Br/2-pyridinal-butylimine /phenol in d^6 -DMSO.

^1H NMR study; role of phenol. Figure 3a shows the partial 400 MHz ^1H NMR spectrum of $\text{Cu(I)Br}/\underline{3}$. Unlike 2,2'-bipyridine no exchange is observed even at elevated temperatures. Five resonances are observed at between 6 and 10 ppm, two doublets and two triplets from the ring protons and a singlet from the imine proton at approximately 8.8 ppm. When equimolar amounts of phenol, with respect to Cu(I)Br is added no exchange is observed at room temperature but exchange is seen at 85 $^\circ\text{C}$, which is similar to the reaction temperature.

Single crystal X-ray diffraction study: role of phenol. When $[\text{Cu}(\text{CH}_3\text{CN})_4][\text{BF}_4]$ is mixed with a two fold excess of $\underline{5}$ crystals of structure (Figure 4a) were isolated. $[\text{Cu}(\text{CH}_3\text{CN})_4][\text{BF}_4]$ was used as it is a source of soluble copper(I) and the large counter-ion gives good crystalline products. The structure shows the coordination of two equivalents of $\underline{5}$ to give a *pseudo*-tetrahedral copper(I) complex with BF_4 counter-ion (Figure 4a), as might have been expected (16). When the product from reaction of Cu(I)Br and $\underline{5}$ is isolated in the presence of phenol a dinuclear copper(II) complex is observed (Figure 4b). The two copper(II) centers are bridged with methoxy groups which presumably originate from the methanol solvent in addition to a coordinated bromide ligand. Full crystallographic details will be published elsewhere.

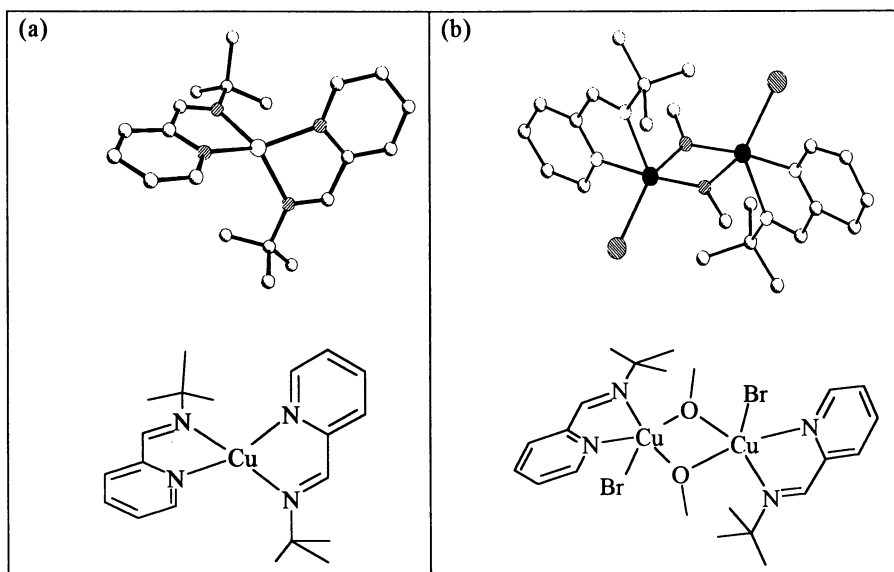


Figure 4. Single crystal X-ray diffraction structures.

Polymerization of MMA in the presence of substituted phenols. Substituted phenols are often used as free radical inhibitors during the storage and transport of methacrylates (17). However, polymerization of MMA by $\underline{6}$ in conjunction with a copper(I) Schiff base complex in the presence of a range of phenols occurs to high conversion in relatively short time periods (Table III) *polymerization is not inhibited*. Even with a ten

fold excess of substituted phenol, with respect to initiator, narrow molecular weight distribution polymer is observed. Figure 5 shows the SEC traces, normalized to conversion, for the polymerization in the presence of 4-methoxy phenol. The molecular weight and conversion both increase whilst PDI remains narrow. Little effect on rate is observed with equimolar amounts of substituted phenol. However, an increase in rate is observed with a ten fold excess. The presence of phenol also gives a slight narrowing of the PDI as compared to the control reactions

Figure 6 shows the effect of adding a stoichiometric amount of phenol on the rate of reaction. The results were obtained using automated dilatometry, collecting one data point every 20 s. The final rate of polymerization is similar in both the presence and absence of 4-methoxy phenol. Both are fairly linear between 60 and 180 minutes prior to showing a decrease in $k_p[\text{Pol}^*]$, the gradient of the graph. In control experiment an induction period is seen over the first 60 minutes, (observed as in an increase in $k_p[\text{Pol}^*]$). Induction periods have previously been observed in the ATRP of MMA using Ni(II) catalyst. The induction period is essentially removed by 4-methoxy phenol which suggests that the initiation reaction is not rate determining. This accounts for the narrowed PDI observed in the presence of phenol since all the chains begin growing at the same time

Table III. Polymerization of MMA with Cu(I)Br/2-pyridinal-alkylimine /6 100 [MMA] : 1 [6] : 1 [CuBr] : at 90 °C in xylene solution, reactions stopped at 240 mins.

Ligand	Phenol	[Phenol] :[6]	% Conv.	Mn	PDI
4	none	1	66.7	9260	1.22
4	phenol	1	66.1	9900	1.17
4	4-methoxy phenol	1	47.2	7280	1.21
4	2,6-diisopropyl phenol	1	64.0	8830	1.17
4	topanol	1	65.0	10090	1.14
1	none	1	57.8	7820	1.19
1	phenol	1	60.1	7810	1.21
1	4-methoxy phenol	1	54.4	7010	1.23
1	2,6-diisopropyl phenol	1	58.6	7820	1.19
1	topanol	1	56.8	7460	1.21
1	none	10	66.1	8110	1.21
1	phenol	10	70.5	9500	1.20
1	4-methoxy phenol	10	74.0	8970	1.25
1	2,6-diisopropyl phenol	10	64.9	7660	1.19
1	topanol	10	74.6	7970	1.21

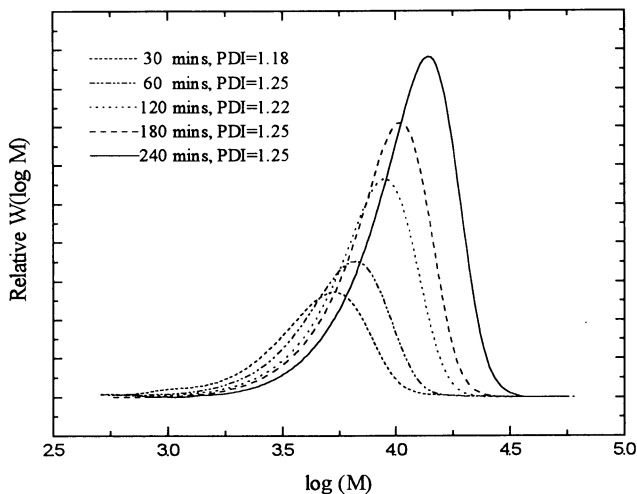


Figure 5. SEC overlay for the polymerization of MMA with Cu(I)Br/2-pyridinal-pentylimine 100 [MMA] : 1 [6] : 1 [CuBr] : at 90 °C in xylene solution in the presence of equimolar amounts of 4-methoxy phenol, areas normalized for conversion from gravimetry.

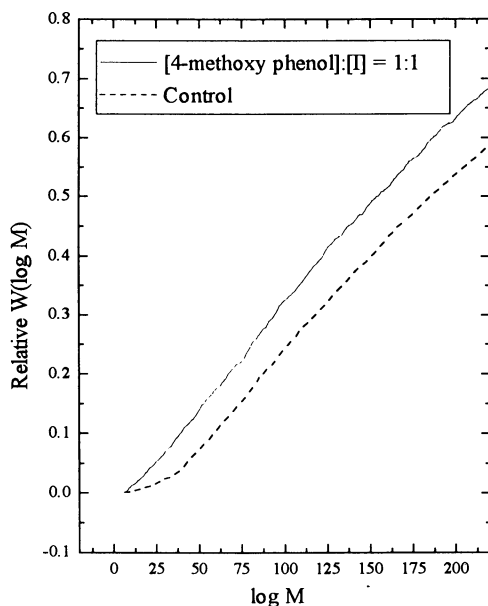
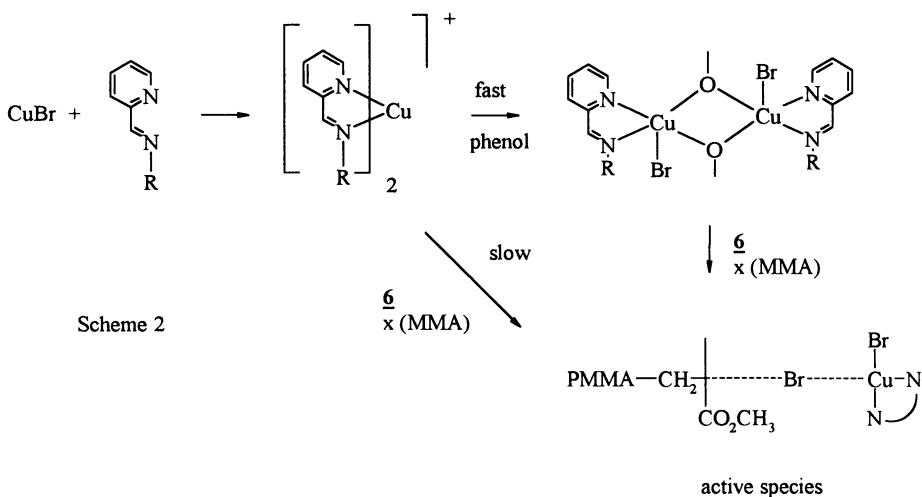


Figure 6. Dilatometry for the polymerization of MMA with Cu(I)Br/2-pyridinal-pentylimine 100 [MMA] : 1 [6] : 1 [CuBr] : at 90 °C in xylene solution in the presence and absence of 4-methoxy phenol. Conversion data obtained using dilatometry.

General Discussion. Atom transfer radical polymerization of MMA catalyzed by Cu(I)Br/2-pyridinal-alkylimine complexes is not inhibited by phenol or a range of substituted phenols, commonly used as free radical inhibitors. Indeed, phenols accelerate the overall polymerization rate. However, it is noted that phenolic inhibitors are usually more effective in the presence of oxygen (17). Inhibition and transfer constants for phenols are not readily available, nevertheless even if the rate of both transfer and inhibition is zero the acceleration of the rate of polymerization is indeed unexpected. This is due to the removal of an induction period which is observed in the absence of phenol. This induction period implies that the number of active polymerization sites increases over the initial stage of the reaction resulting in a broadening of the PDI. The single crystal x-ray diffraction study suggests that a possible role of the phenols is to accelerate the formation of dinuclear copper complexes which are intermediates in the polymerization mechanism. It seems likely that this also occurs in the absence of phenol but is accelerated by favorable bridging interactions. The exchange in solution, as observed by NMR supports this. The absence of inhibition of the rate of initiation in the presence of phenols suggests that propagation may not occur via a free radical process.

A combination of these results indicate that a copper(II) species maybe an active intermediate, with coordination to the bromine atom of the propagating polymer chain (scheme 2). It is likely that the second halide atom is also involved in a bridging species. At the onset of polymerization one of the bis coordinating ligands is displaced from the copper(I) center which is a relatively slow reaction in the absence the favorable phenolic bridging interaction. The coordinated polymer is most likely to also be in equilibrium with the free 2-pyridinal-alkylimine ligand in solution. The bromine atom is never fully displaced from the propagating polymer chain and hence propagation may occur via a concerted mechanism. We are currently undertaking experiments to investigate the mechanism of ATRP further which is undoubtedly more complex than at first thought.



Acknowledgments. We wish to thank the EPSRC (D. J. D and M. C. C. GR/K90364, GR/L10314, A. M. H. studentship, A. J. S. CASE award), Courtauld for funding and Dr. D. Kukulj for helpful discussions.

References

1. Wang, J.-S.; Matyjaszewski, K. *J. Am. Chem. Soc.* **1995**, *117*, 5614.
2. Matyjaszewski, K.; Wang, J.-S. *Macromolecules* **1995**, *28*, 7901.
3. Matyjaszewski, K.; Patten, T. E.; Xia, J. *J. Am. Chem. Soc.* **1997**, *119*, 674.
4. Matyjaszewski, K. *Curr. Opin. So. St. Mat. SCI.* **1996**, *1*, 769.
5. Kate, M.; Kamigaito, M.; Sawamoto, M.; Higashimura, T. *Macromolecules* **1995**, *28*, 1721.
6. Kotani, Y.; Kato, M.; Kamigaito, M.; Sawamoto M. *Macromolecules* **1996**, *29*, 6979.
7. Percec, V.; Barboiu, B.; Neumann, A.; Ronda, J. C.; Zhao, M. *Macromolecules* **1996**, *29*, 3665.
8. Granel, C.; Teyssie, P.; DuBois, P.; Jerome, P. *Macromolecules* **1996**, *29*, 8576.
9. Koten, G. van.; Vrieze, K. *Recl. Trav. Chim. Pays-Bays* **1981**, *100*, 129.
10. Haddleton, D. M.; Jasieczek, C. B.; Hannon, M. J.; Shooter, A. J. *Macromolecules* **1997**, in press.
11. Johnson, L. K.; Killian, C. M.; Brookhart, M. *J. Am. Chem. Soc.* **1995**, *117*, 6414.
12. Ando, T.; Kato, M.; Kamigaito, M.; Sawamoto, M. *Macromolecules* **1996**, *29*, 1070.
13. Davis, T. P.; Haddleton, D. M.; Richards, S. N.; *JMS -Rev. Macromol. Chem. Phys.*, **1994**, *C34*, 243
14. Bahr, V. G. *Z. Anorg. Allg. Chem.* **1957**, *292*, 119.
15. Jiang, Z.; Adams, S. E.; Sen, A. *Macromolecules* **1994**, *27*, 2694.
16. Dieck, H.; Stamp, L. *Z. Nat. B.* **1990**, *45*, 1369.
17. Moad, G.; Solomon, D. H. *The Chemistry of Free Radical Polymerisation*; Pergamon: Bath, 1995.

Chapter 18

Living Radical Polymerization Mediated by Transition Metals: Recent Advances

Mitsuo Sawamoto¹ and Masami Kamigaito

Department of Polymer Chemistry, Graduate School of Engineering,
Kyoto University, Kyoto 606-01, Japan

This paper discusses the current scope, mechanism, and some examples of living radical polymerizations mediated by transition metal-complexes. Combinations of alkyl and other halides (initiators; R-X) and metal complexes (MX_n) lead to living polymerizations of methacrylates, acrylates, and styrene at 60–100 °C; examples of the MX_n include homogeneous complexes of Ru(II), Ni(II), and Fe(II) such as $RuCl_2(PPh_3)_3$ and $NiBr_2(PnBu_3)_2$. In addition to controlled molecular weights and their very narrow distributions of the product polymers, these processes are characterized by (a) tolerance towards water and alcohols as solvents and occurrence of living polymerizations therein, (b) quantitative attachment of halogens at the ω -terminals that are able to re-initiate living polymerization in the presence of $RuCl_2(PPh_3)_3$, and (c) versatility towards various monomers as realized by modulating the structures of initiators and metal complexes. Some mechanistic aspects of the metal complex-mediated living radical polymerization are also discussed.

In the last few years, as vividly witnessed in several symposia attached to this ACS Meeting, many efforts have rapidly been devoted to development of living (or controlled) radical polymerization, and promising systems have begun to emerge (1,2). In 1994–96, for example (eq 1), we first reported living radical polymerization of methyl methacrylate (MMA) mediated by a ruthenium(II) complex in conjunction with carbon tetrachloride or related alkyl halides as initiators (R-X) (3–8). Similar living radical polymerizations via transition metal catalysis have recently been reported by Matyjaszewski (9), Percec (10), and Teyssié (11).

In the ruthenium-based systems the initiators R-X are mostly alkyl halides and their derivatives (e.g., haloketones) (4,5) whose carbon-halogen bonds are homolytically or radically cleaved by $RuCl_2(PPh_3)_3$ and other metal complexes to induce living and most likely radical propagation. As we proposed (2,3), a key to the fine reaction control is the Ru(II)-assisted *reversible and homolytic* cleavage of the carbon-halogen bond, which will reduce the instantaneous concentration of the active radicals and thereby suppress bimolecular termination reactions (radical recombination and disproportionation), which have been considered to be inherently unavoidable in conventional "free radical" polymerizations. Another important aspect is the rapid interconversion between the dormant/covalent alkyl halide terminals and the

¹Corresponding author

growth-active radical ends generated via the assistance of the ruthenium and other metal complexes (eq 1), which is crucial to achieve controlled molecular weights and narrow molecular weight distributions (MWDs).

Since these findings have been reported, the use of transition metal complexes as a component of initiating systems has rapidly been expanded and, more important, generalized, to achieve hitherto difficult well-defined, living radical polymerizations of methacrylates, acrylates, and styrene derivatives (1–3; also see below).

This paper discusses our recent results in this area, particularly directed to the scope and design of metal complexes and initiating systems, understanding of the mechanism of the living radical polymerizations, and the development of novel living processes such as those operable in alcohols and even in water.

Transition Metal-Mediated Living Radical Polymerization: Scope

Figure 1 summarizes the current scope of our living radical processes that have been extended on the basis of the original ruthenium-based system (2,3).

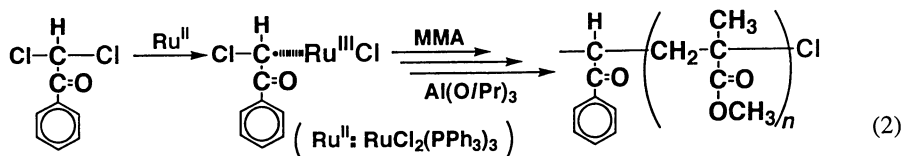
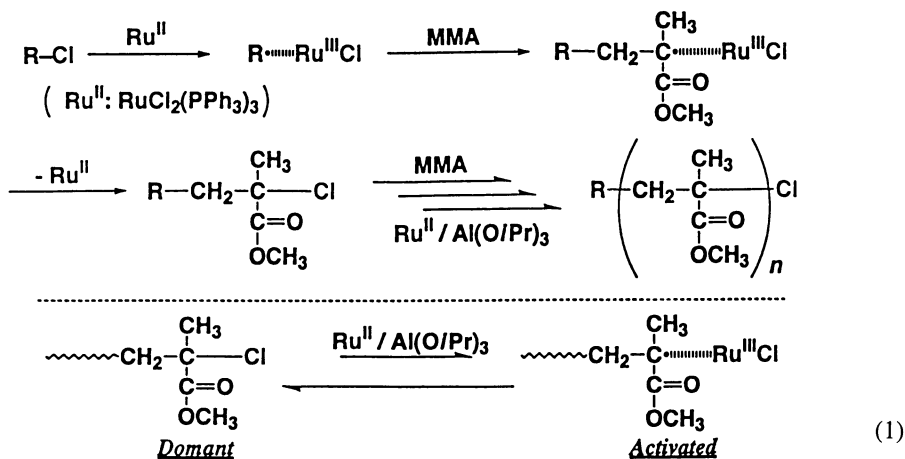
Initiators. The initiators for the metal-mediated living radical polymerizations are mostly alkyl halides (R–X; X = Cl, Br, I) and related compounds that have carbon–halogen bonds to be homolytically cleaved via the assistance of transition metal complexes (2,3,7). As summarized in Figure 1, reported examples include haloalkanes, haloketones, halonitriles, haloesters, and haloalkylbenzenes; note that the latter two groups bear "alkyl" moieties mimicking the structures of the growing ends to be generated from respective monomers. For example, esters of halogenated carboxylic acids are suited for (meth)acrylates and haloalkylbenzenes are preferentially employed for styrene and its derivatives. In addition, as shown below, haloketones are particularly suitable for MMA and related methacrylates to give polymers of controlled molecular weights and very narrow MWDs.

Metal Complexes. A feature of the metal-mediated living radical polymerizations is of course the use of transition metal complexes that induce reversible and homolytic cleavage of the initiator's carbon–halogen bond to give the initiating radical, along with the similar radical-forming processes in the propagation step. In this aspect, the metal complexes should be such that carry suitable metals, mostly group 8–10 transition metals, that can undergo one-electron oxidation to receive the halogen from the initiator in the radical forming (forward) step. Equally important, they should be able to regenerate the dormant covalent species by releasing the once-captured halogen via a one-electron reduction; there should be no oxidative addition reactions.

Thus, reported examples of these metal complexes include those of Ru(II) (4–6,8), Cu(I) (9,10a), Ni(II) (11,12), Fe(II) (13), and Rh (10b). They are almost invariably halides with suitable ligands, the latter including triaryl and trialkyl phosphines (4,8), amines (11), and related nitrogen bases (9). In our work, therefore, RuCl₂(PPh₃)₃ (4–8), FeCl₂(PPh₃)₃ (13), NiBr₂(PPh₃)₂ (12), and NiBr₂(P*n*Bu₃)₂ (12) are employed. As well known in transition metal chemistry, the roles of ligands are very important in determining their effectiveness in inducing suitable radical propagation processes, and these roles are not only for facilitating solubility of the halide salts but also to modify the electric and steric nature of the complexes as a whole. These points are now under investigation in our laboratories.

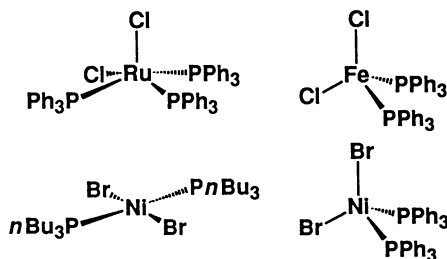
Living Radical Polymerization of MMA with Ru(II) Complex: Examples

In typical examples, living radical polymerization of MMA is initiated with RuCl₂(PPh₃)₃ coupled with dichloroacetophenone (**1**; initiator) and Al(O*i*Pr)₃ in toluene at 80 °C (eq 2 and Figure 2) (5). Under these relatively mild conditions, the polymerization proceeds quantitatively, though rather slow (requiring 5–30 hr in



● Transition Metal Complexes

(ML_n)



● Initiators (R-X)

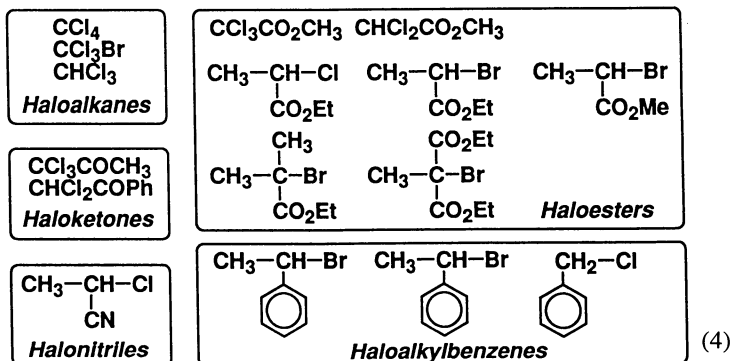
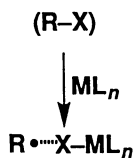


Figure 1. The status quo of transition metal-mediated living radical polymerizations: typical transition metal complexes (MX_n) and initiators (R-X) for suitable initiating systems (2,3).

completion) to give polymers of controlled molecular weights and very narrow MWDs ($M_w/M_n = 1.05\text{--}1.2$). The number-average molecular weights (M_n ; by SEC and $^1\text{H NMR}$) increases in direct proportion to MMA conversion and in excellent agreement with the calculated values based on the assumption that one polymer chain forms from one initiator molecule. The MWDs progressively shift toward higher molecular weights, while retaining their narrowness. All these aspects conform with the occurrence of living polymerizations. Addition of a fresh MMA feed to the completely polymerized solution further induced polymer growth that is also judged to be living, as seen from the linear extension of the molecular weight–conversion profile and the generation of very narrow MWDs.

Mechanistic Features

Some detailed studies have been carried out on this system to uncover the mechanism and other features.

Polymer End Groups. As suggested in eq 2, the poly(MMA) from the $1/\text{RuCl}_2(\text{PPh}_3)_3$ system carries an aromatic ketone residue of the initiator at the α -end and a tertiary chloride at the ω -end. This structure and the quantitative attachment of both end groups has been verified by 500 MHz $^1\text{H NMR}$ analysis (Figure 3; in cooperation with Professor Tatsuki Kitayama and his associates, Osaka University) (7).

For example, in addition to the large signals ($a1\text{--}c1$) of the poly(MMA) main chains, the spectrum exhibits sharp resonances ($a2\text{--}c2$) of the terminal MMA unit that carries ω -end chlorine originating from the initiator **1**. In particular, the terminal ester methyl group gives a sharp singlet ($c2$) next to the large peak of the corresponding pendent methyl. Because of the use of aromatic ketone as an initiator, the polymer shows a typical signals ($e\text{--}g$) assignable to the benzene ring attached to the polymer main chain; a small peak (d) due to the methine unit from **1** is also detected.

Integration of these terminal and main-chain resonances in turn gives the number-average molecular weight or the degree of polymerization of the sample, which turned out to be in excellent agreement with the calculated value, or confirming that one initiator fragment and the halogen are attached to the α - and ω -end groups, respectively.

Re-initiation of Living Radical Polymerization from Recovered Polymers. Equally important, the recovered polymers, even after work-up with acid and water, retain the chloride terminals from which they re-initiate similar living polymerization in the presence of $\text{RuCl}_2(\text{PPh}_3)_3$ and $\text{Al}(\text{O}i\text{Pr})_3$ (eq 3) (8). Figure 4 presents a typical result. Thus, polymer samples of molecular weights around 3,000–30,000 are isolated and purified from the living polymerization systems with $1/\text{RuCl}_2(\text{PPh}_3)_3$, and they are used as a macroinitiator for polymerization of MMA in toluene at 80 °C. The second-phase polymerization proceeds at nearly the same rate as in the first phase with **1**, and the produced polymers give clearly increased molecular weights and even narrowed MWDs. The M_n increased in proportion with MMA conversion from the molecular weight of the preformed polymeric initiator.

These results demonstrate the complete survival of the terminal chlorine groups and their ability to re-initiate living radical polymerization in the presence of $\text{RuCl}_2(\text{PPh}_3)_3$ and $\text{Al}(\text{O}i\text{Pr})_3$.

Effects of Additives. For understanding the polymerization mechanism with the transition metal complexes, a series of additives or potential terminating agents were added to the polymerization system initiated with $1/\text{RuCl}_2(\text{PPh}_3)_3/\text{Al}(\text{O}i\text{Pr})_3$ (8). The reaction was instantaneously quenched with stable radicals (nitroxides, etc.), whereas it remained intact and proceeded smoothly in the presence of methanol and water; namely:

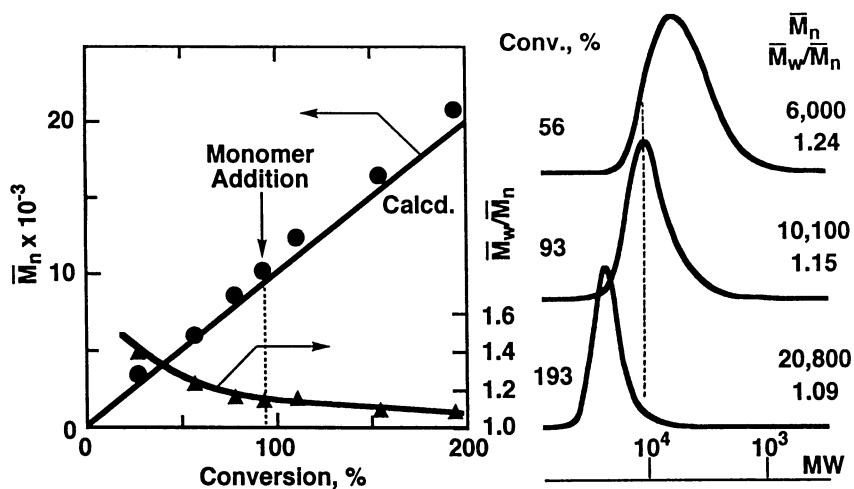
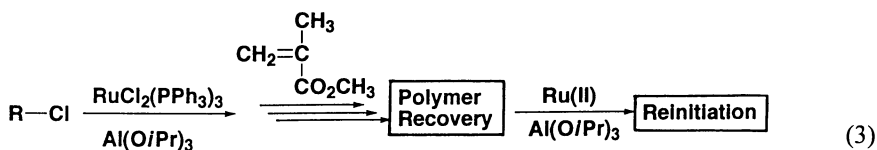


Figure 2. Living radical polymerization of MMA (2.0 M) with $1/\text{RuCl}_2(\text{PPh}_3)_3/\text{Al}(\text{O}i\text{Pr})_3$ (20/10/40 mM) in toluene at 80°C (5).



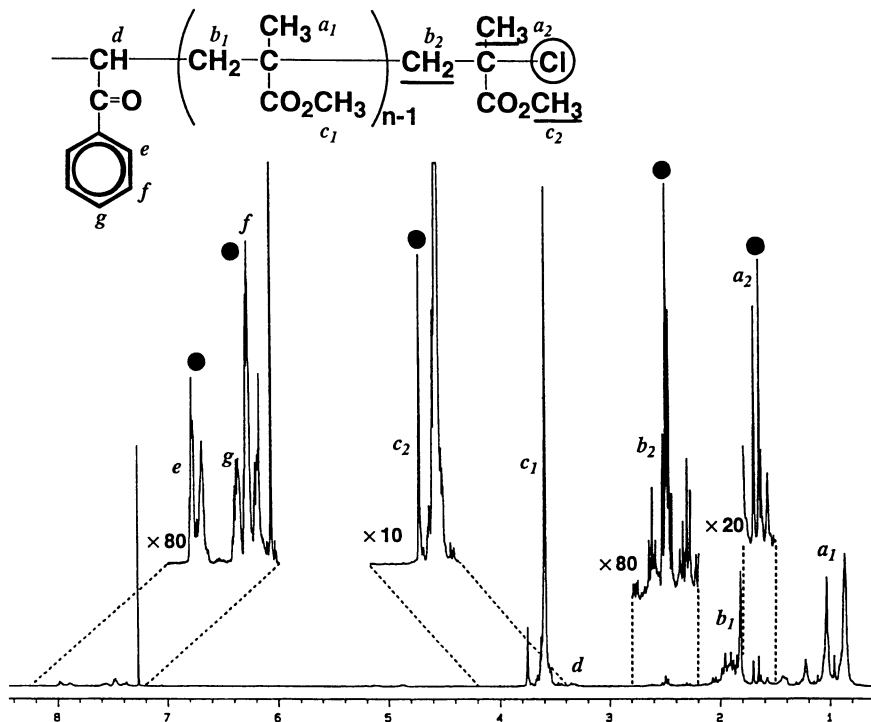


Figure 3. 500 MHz ^1H NMR spectrum of poly(MMA) obtained in the living radical polymerization with $1/\text{RuCl}_2(\text{PPh}_3)_3/\text{Al}(\text{O}i\text{Pr})_3$; $M_n = 2,500$; $M_w/M_n = 1.31$ (7).

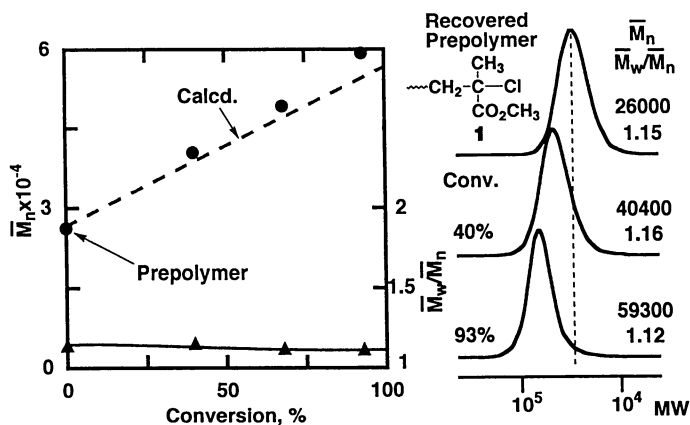


Figure 4. Living radical polymerization of MMA from a prepolymer with a carbon-chlorine terminal, obtained with the $1/\text{RuCl}_2(\text{PPh}_3)_3/\text{Al}(\text{O}i\text{Pr})_3$ (20/10/40 mM) and fully recovered from the reaction mixture (8). Polymerization conditions: MMA, 3.0 M; prepolymer (initiator)/ $\text{RuCl}_2(\text{PPh}_3)_3/\text{Al}(\text{O}i\text{Pr})_3 = 10/10/40$ mM; in toluene at 80 °C.

- *Radical quenchers* (galvinoxyl and TEMPO): *termination*
- *Anion quenchers* (methanol and water): *no effects*

In the former, the polymer molecular weights remained unchanged even after a prolonged time, whereas those with methanol and water smoothly increased just as in the system without any additive. The polymers quenched with TEMPO turned out to carry an *exo* methylene terminal that is most likely originated from the TEMPO-assisted hydrogen abstraction from the transient radical end.

These results strongly support a *radical* propagation mechanism.

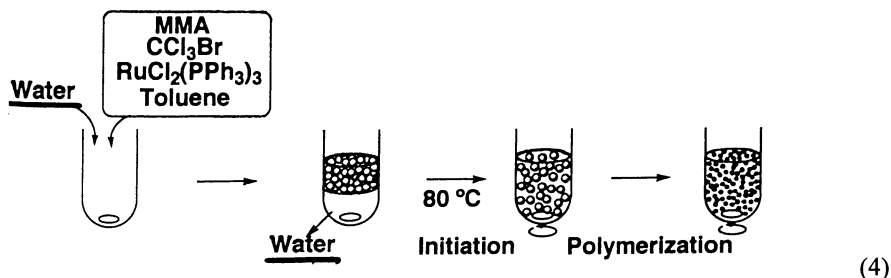
Living Radical Polymerization in Alcohols and Water

Living Polymerization in Alcohols. The absence of adverse effects of alcohols prompted us to examine their use as solvents for the ruthenium-mediated MMA polymerization (Figure 5) (8). Even in the presence of a large amount of methanol, 2-butanol, and 2-methyl-2-butanol (MMA/alcohol = 1/4 v/v) at 80 °C, living polymerization in fact proceeded, in which polymer molecular weights are directly proportional to conversion and narrow MWDs result. The reactions are faster than in toluene, suggesting an accelerating effect of polar solvents. Under our reaction conditions, the reaction mixtures with methanol are slightly hazy but without polymer precipitation, though the alcohol is a non-solvent for poly(MMA) with high molecular weights. With the other two alcohols the solutions are homogeneous and almost transparent.

Living Polymerization in Water. Importantly, the ruthenium-mediated polymerization can also be feasible in water (9,14). Thus, a deep brown solution of MMA and the $\text{CCl}_3\text{Br}/\text{RuCl}_2(\text{PPh}_3)_3/\text{Al}(\text{O}i\text{Pr})_3$ system was added to a large amount of water (MMA/ water = 1/4 v/v) at room temperature, and with vigorous stirring the heterogeneous mixture was placed in a water bath kept at 80 °C (eq 4). An efficient polymerization ensued, and the mixture became more difficult to phase-separate as conversion increased. The recovered polymers had relatively narrow MWDs ($M_w/M_n = 1.1\text{--}1.3$) and molecular weights proportional to conversion, indicating the occurrence of living polymerization in water. An important reason for this unique process is obviously the low oxophilicity of the ruthenium complexes, which permits them effective in water (and alcohol). Further research along with this line is in progress in our laboratories.

Living Polymerizations with Fe(II) and Ni(II) Complexes

Recently we have expanded the scope of transition metals for our living radical polymerization to Fe(II) and Ni(II) complexes in place of the Ru(II) counterparts. For example, living MMA polymerization proceeds with a combination of $\text{CH}_3\text{CBr}(\text{CO}_2\text{C}_2\text{H}_5)_2$ (initiator) and $\text{FeCl}_2(\text{PPh}_3)_2$ in toluene at 80 °C (Figure 6) (13). An



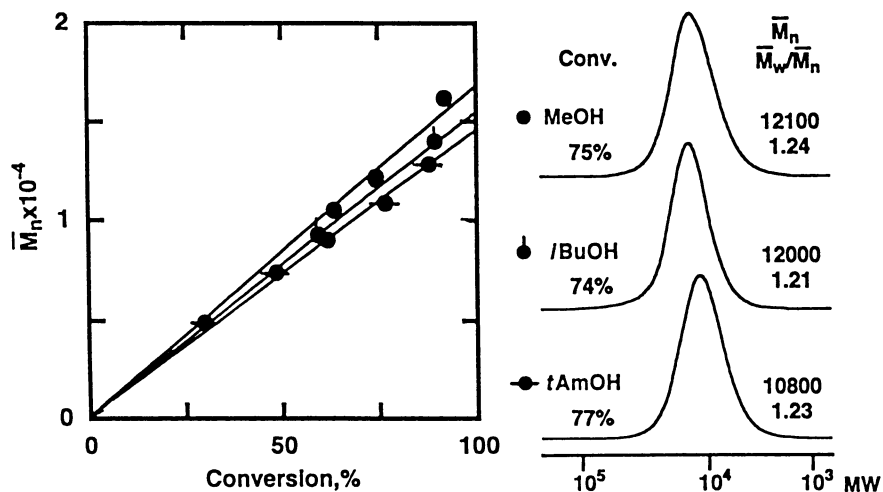


Figure 5. Living radical polymerization of MMA (2.0 M) with $1/\text{RuCl}_2(\text{PPh}_3)_3/\text{Al}(\text{O}i\text{Pr})_3$ (20/10/40 mM) in three alcohols at 80°C (8).

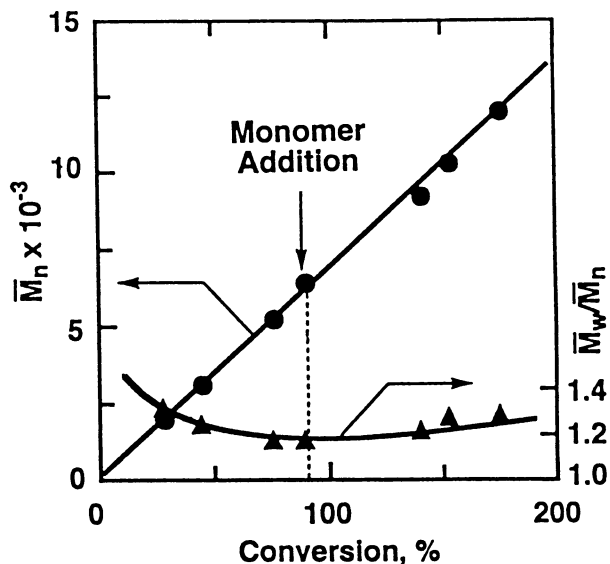
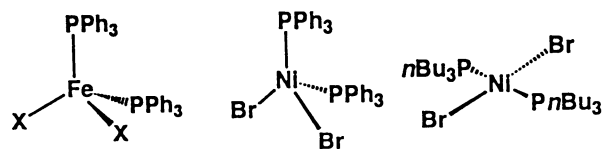


Figure 6. Living radical polymerization of MMA (2.0 M) with $\text{CH}_3\text{CBr}(\text{CO}_2\text{-C}_2\text{H}_5)_2/\text{FeCl}_2(\text{PPh}_3)_2$ (40/10 mM) in toluene at 80°C (10).

important aspect of this system is that it does *not* need such an aluminum compound as $\text{Al}(\text{O}i\text{Pr})_3$, which is required for the Ru(II)-based systems in organic media. Similarly, $\text{NiBr}_2(\text{PPh}_3)_2$ and $\text{NiBr}_2(\text{P}n\text{Bu}_3)_2$ induce living MMA polymerization with CCl_3Br as an initiator; for this $\text{Al}(\text{O}i\text{Pr})_3$ is either employed or not needed (12). Teyssié and his group also reported initiating systems based on Ni(II) complexes (11). The $\text{P}n\text{Bu}_3$ -complex is of interest because of its high solubility in organic solvents and higher thermal stability relative to the corresponding PPh_3 -complex.

Acknowledgments

With appreciation M.S. acknowledges the support from the New Energy and Industrial Technology Development Organization (NEDO), under the Ministry of International Trade and Industry, Japan (MITI), which provided the grant of the "Technology for Novel High-Functional Materials" Program for the "Precision Catalytic Polymerization" Project (1996–2000).

Literature Cited

- (a) Georges, M. K.; Veregin, R. P. N.; Kazmaier, P. M.; Hamer, G. K. *Trends Polym. Sci.* **1994**, *2*, 66. (b) Georges, M. K.; Veregin, R. P. N.; Kazmaier, P. M.; Hamer, G. K. *Macromolecules*, **1993**, *26*, 5316.
- Sawamoto, M.; Kamigaito, M. *Polymer Synthesis (Materials Science and Technology Series)*, Schlüter, A.-D., ed.; John Wiley: New York, NY, 1997; in press.
- Sawamoto, M.; Kamigaito, M. *Trends Polym. Sci.* **1996**, *4*, 371.
- Kato, M.; Kamigaito, M.; Sawamoto, M.; Higashimura, T. *Macromolecules* **1995**, *28*, 1721.
- Ando, T.; Kato, M.; Kamigaito, M.; Sawamoto, M. *Macromolecules* **1996**, *29*, 1070.
- Kotani, Y.; Kato, M.; Kamigaito, M.; Sawamoto, M. *Macromolecules* **1996**, *29*, 6979.
- Ando, T.; Kamigaito, M.; Sawamoto, M. *Tetrahedron* **1997**, in press.
- Nishikawa, T.; Ando, T.; Kamigaito, M.; Sawamoto, M. *Macromolecules* **1997**, *30*, 3244.
- (a) Wang, J. S.; Matyjaszewski, K. *J. Am. Chem. Soc.* **1995**, *117*, 5614. (b) Wang, J. S.; Matyjaszewski, K. *Macromolecules* **1995**, *28*, 7901. (c) Patten, T.; Xia, J.-H.; Abernathy, K.; Matyjaszewski, K. *Science* **1996**, *27*, 866. (d) Grimaud, Th.; Matyjaszewski, K. *Macromolecules*, **1997**, *30*, 2216. (e) Matyjaszewski, K.; Patten, T.; Xia, J.-H. *J. Am. Chem. Soc.* **1997**, *119*, 674.
- (a) Percec, V.; Barboiu, B. *Macromolecules*, **1995**, *28*, 7970. (b) Percec, V.; Barboiu, B.; Neumann, J.; Ronda, J. C.; Zhao, M. *Macromolecules*, **1996**, *29*, 3665.
- (a) Granel, C.; Dubois, Ph.; Jérôme, R.; Teyssié, Ph. *Macromolecules*, **1996**, *29*, 8576. (b) Granel, C.; Moineau, G.; Lecomte, Ph.; Dubois, Ph.; Jérôme, R.; Teyssié, Ph. *Polym. Prepr., Div. Polym. Chem., Am. Chem. Soc.* **1997**, *38* (1), 450.
- Uegaki, H.; Kotani, Y.; Kamigaito, M.; Sawamoto, M. *Macromolecules* **1997**, *30*, 3249.
- Ando, T.; Kamigaito, M.; Sawamoto, M. *Macromolecules* **1997**, *30*, in press; *Polym. Prepr., Jpn.* **1996**, *45*, 1141.
- Nishikawa, T.; Kamigaito, M.; Sawamoto, M. *Macromolecules*, submitted; *Polym. Prepr., Jpn.* **1996**, *45*, 1137; *Polym. Prepr., Div. Polym. Chem., Am. Chem. Soc.* **1997**, *38*(1), 740.

Chapter 19

Control of Radical Polymerizations by Metalloradicals

B. B. Wayland¹, S. Mukerjee¹, G. Poszmik¹, D. C. Woska¹, L. Basicke¹,
A. A. Gridnev², M. Fryd², and S. D. Ittel³

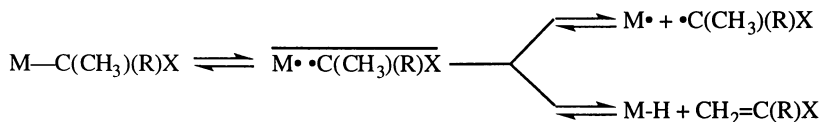
¹Department of Chemistry, University of Pennsylvania,
Philadelphia, PA 104-6323

²DuPont Marshall Laboratory, Philadelphia, PA 19146

³Central Research and Development, DuPont Experimental Station,
Wilmington, DE 19880-0328

Cobalt(II) porphyrin complexes ((por)Co^{II}) are used to illustrate how metalloradicals (M•) can function to control radical polymerization through both chain transfer catalysis and living polymerization. Chain transfer catalysis (CTC) is best achieved when there are minimal steric demands. This allows β -hydrogen abstraction from oligomer radicals by M•, as illustrated by the radical polymerization of methyl methacrylate in the presence of tetraanisylporphyrinato cobalt(II). When β -H abstraction from the oligomer radical is precluded by sterics, then a metalloradical mediated living radical polymerization (LRP) can occur. Radical polymerization initiated and mediated by organo-cobalt tetramesitylporphyrin complexes manifest high living character as shown by the linear increase in \bar{M}_n with conversion, formation of block copolymers and relatively low polydispersity homo and block copolymers. Kinetic studies provide rate and activation parameters for the living radical polymerization process.

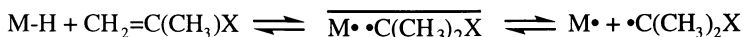
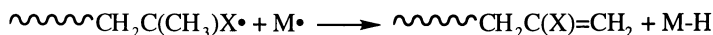
Bond homolysis of an organometallic complex (M-C(CH₃)(R)X) in solution proceeds through the intermediacy of a caged radical pair (M••C(CH₃)(R)X) that can recombine, separate into freely diffusing radicals, or react by M• abstracting a β -H from the organic radical to form a metal hydride (M-H) and an olefin (J).



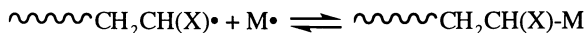
In the absence of events that irreversibly terminate radicals and metal hydride, the homolytic dissociation of an organo-metal complex can potentially provide a constant equilibrium source of both an organic radical and a metal hydride. The broad objectives of this program are to evaluate the kinetic and thermodynamic factors that

govern the bond homolysis and subsequent radical and metal hydride reactions, and to apply this information in exercising control over the radical polymerization of olefins. Chain transfer catalysis (CTC) and quasi-living radical polymerization (LRP) are two important processes that can be mediated and controlled by metalloradicals.

Chain transfer catalysis occurs when the metalloradical abstracts a β -H from the growing polymer radical to form a metal hydride that reinitiates polymerization by reaction with the olefin monomer (2–5). CTC is useful for controlling the polymer molecular weight and introducing terminal alkene functionality (6).



Metalloradical mediated LRP requires that the only reaction of the metalloradical is to bind reversibly with the growing polymer radical to produce a constant equilibrium concentration of propagating polymer radicals (7).



When a fixed initial quantity of radical source is used to initiate polymerization, neither CTC nor LRP can continue indefinitely because of inherent termination reactions of organic radicals and metal hydrides (*e.g.* $2 \text{R}\cdot \longrightarrow \text{R-R}$, $2 \text{M-H} \longrightarrow 2 \text{M}\cdot + \text{H}_2$, $\text{M-H} + \text{R}\cdot \longrightarrow \text{M}\cdot + \text{RH}$). Kinetic suppression of these termination reactions relative to polymer propagation is required in order to attain LRP. Formation of a dormant organometallic derivative (M-R) by reaction of M \cdot with R \cdot and M-H with olefin can be used, in principal, to control the concentrations of the active R \cdot and M-H species at levels where irreversible termination is improbable compared to monomer conversion. The general challenge is to design systems that minimize termination of active species, provide adequate organic radical concentrations for useful rates of polymerization, and selectively direct the radical polymerization to CTC or LRP. The specific challenges in using metalloradicals is to identify M \cdot species that bind and control the polymer radical concentration in the range for a useful rate of polymerization in a particular temperature range, and either facilitate or prohibit β -H abstraction from the polymer radical to attain effective CTC or LRP respectively.

Chain Transfer Catalysis by Cobalt(II) Porphyrins.

Four and five coordinate low spin ($s=1/2$) cobalt(II) complexes constitute a class of metalloradicals that are known to be effective chain transfer catalysts in radical polymerizations (2–6). Table I illustrates the inverse dependence of polymer chain length on the concentration of tetraanisylporphyrinato cobalt (II) ((TAP)Co) in the bulk radical polymerization of methylmethacrylate (MMA).

When perdeuterated MMA is substituted for MMA using the conditions in Table I, the average polymer chain length increases by a factor of 4.4 ± 0.4 (8). Both the deuterium isotope effect and the (TAP)Co^{II} concentration dependence for PMMA chain length indicate that the rate determining step for terminating polymer radical chain growth is β -H abstraction by (TAP)Co^{II}.

Studies of ¹H NMR line broadening for (TAP)Co-C(CH₃)₂CO₂CH₃ provide rate constants and activation parameters for a Co-R bond homolysis that models the (TAP)Co-PMMA oligomer complex (Figure 1) (9). Very rapid Co-R bond homolysis ($k_{\text{dis}}(333 \text{ }^\circ\text{K}) = 3,300 \text{ s}^{-1}$; $\Delta H^\ddagger = 18.2 \pm 0.5 \text{ kcal mol}^{-1}$; $\Delta S^\ddagger = 12 \pm 2 \text{ cal }^\circ\text{K}^{-1} \text{ mol}^{-1}$) results from a relatively small Co-R bond dissociation enthalpy ($\Delta H^\circ = 15 \text{ kcal mol}^{-1}$).

Table I: Effect of (TAP)Co^{II} Concentration on Oligomer Chain Length in Radical Polymerization of Bulk Methylmethacrylate.

[(TAP)Co ^{II}]	\bar{M}_n	\bar{M}_n'	\bar{M}_w/\bar{M}_n
4.0×10^{-4}	630	430	1.79
2.0×10^{-4}	1010	810	1.83
1.0×10^{-4}	1900	1700	2.06

[VAZO-52]_i = 0.04 M, reaction time 3 hours at T = 40 °C. Monomer conversion equals 20±1%, polystyrene standards used for GPC analysis.
 $\bar{M}_n = \bar{M}_n' - 2(\text{monomer molecular weight})$

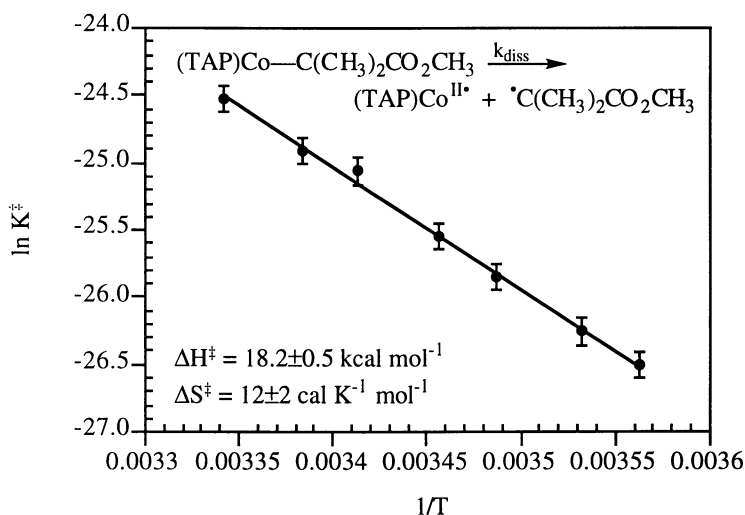


Figure 1. Determination of activation parameters for the homolytic dissociation of (TAP)Co—C(CH₃)₂CO₂CH₃ in CDCl₃ by NMR line width measurements. $K^\ddagger = k_{\text{diss}}(h/kT)$, $k_{\text{diss}} = \pi\Delta\nu_{1/2}$.

A series of kinetic-mechanistic and thermodynamic factors are favorable for effective CTC by cobalt(II) porphyrins in the radical polymerization of methyl methacrylate. Relatively small bond dissociation enthalpies and fast dissociation of the dormant intermediate organo-cobalt complexes ((por)Co-PMMA) provide favorable concentrations of PMMA• and (por)Co^{II}• to attain both fast monomer conversion and rapid termination of polymer chain growth by β-H abstraction from PMMA•. Exceptionally fast β-H abstraction by (por)Co^{II}• and re-addition of (por)Co-H to MMA that produces effective CTC result primarily from the small energy change in forming the radical pair (Co••R) intermediate from addition of (por)Co-H to MMA (Figure 2). Markovnikov regioselectivity for the addition of (por)Co-H with MMA that forms the more weakly bonded tertiary alkyl complex ((por)Co-C(CH₃)₂CO₂CH₃) is another important consequence of the hydrogen atom transfer mechanism (10).

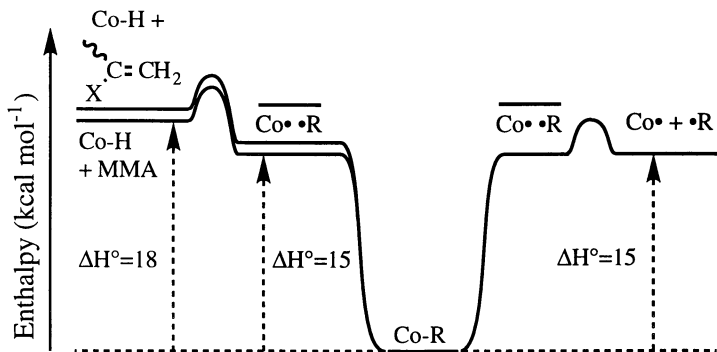


Figure 2. Illustration of the near thermally neutral reaction of (por)Co-H with MMA to produce a radical pair and the relatively small (por)Co-C(CH₃)₂CO₂CH₃ bond dissociation enthalpy (≈ 15 kcal mol⁻¹) that are favorable for chain transfer catalysis.

Living Radical Polymerization of Acrylates Controlled by Organo-Cobalt Porphyrins.

Substantial progress in attaining effective living radical polymerization of olefins has been achieved by controlling the propagating radical concentrations through equilibria with several different types of dormant species (11–27). Tetramesitylporphyrinato cobalt neopentyl ((TMP)Co-CH₂C(CH₃)₃) is observed to initiate and control the living radical polymerization of acrylates (22, 27). A combination of porphyrin ligand and oligomer radical steric demands provide a kinetic barrier that blocks β -H abstraction from the growing polymer radical by (TMP)Co• which shuts down the chain transfer pathway (Figure 3).

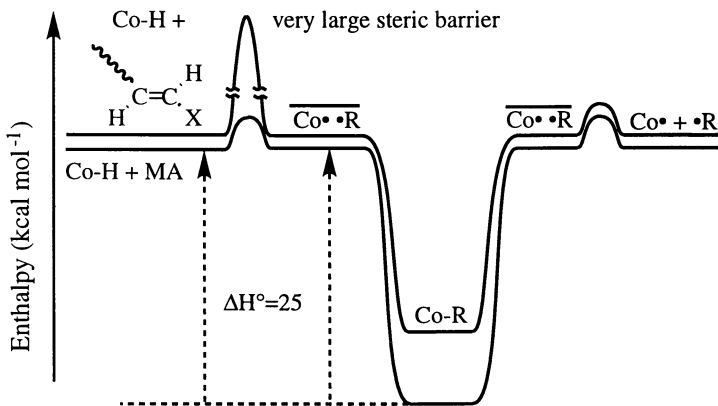


Figure 3. Illustration of the high activation barrier for β -H abstraction from MA polymer radical by (TMP)Co• that results from the large steric demands of the TMP is favorable for living radical polymerization.

The changes in degree of living character in radical polymerization of methyl acrylate (MA) with changes in porphyrin steric demands are illustrated by the use of a series of organo-cobalt porphyrin complexes to initiate and mediate the polymerization process. In the case of the tetraphenylporphyrin cobalt ((TPP)Co) system the polydispersity increases from 1.1 to 1.9 as the degree of polymerization increases from 80 to a maximum of ~200 which then remains approximately constant as the monomer conversion continues. This behavior for the (TPP)Co-MA system is a clear signature of CTC (Table II). The maximum degree of MA polymerization for a series of (porphyrin)Co-MA systems was observed to increase as the porphyrin steric demands increased which is consistent with polymer chain growth being limited through β -H abstraction by the (por)Co^{II} metalloradical.

Table II: Bulk Polymerization of MA by (TPP)Co-CH₂C(CH₃)₃

Time (hrs.)	% Conversion	\bar{M}_n	\bar{M}_w/\bar{M}_n
4	5	6,900	1.10
24	14	19,700	1.66
48	17	17,400	1.90
120	25	18,200	1.86

[(TPP)Co-CH₂C(CH₃)₃]_i = 1.0×10^{-3} M; [MA]_i = 2.5 M; [(TPP)Co^{II}]_i = 2.5×10^{-4} M; solvent = C₆D₆; T = 60 °C.

For a series of porphyrin derivatives, the maximum degree of MA polymerization increases as the steric demands of the porphyrin ligand increases. This is consistent with MA polymer chain length growth being limited through β -H abstraction by (por)Co^{II}• species. The ligand steric requirements of tetramesityl porphyrin (TMP) effectively prohibit β -H abstraction by (TMP)Co• such that the radical polymerization of MA initiated by (TMP)Co-CH₂C(CH₃)₃ manifests high living character (Table III) (22). (TMP)Co-CH(CH₃)CO₂CH₃ was substituted for the neopentyl derivative in the polymerization of MA in order to initiate the process with a species that more nearly emulates the oligomer-Co(TMP) complex that produces growing polymer chains. Reaction with MA at 60 °C in benzene results in the formation of PMA with relatively small polydispersities (1.1–1.2) and a linear increase in \bar{M}_n (6×10^3 to 1.6×10^5) with MA conversions of 3–85% (DP = 65–1850) (Table IV, Figure 4). Relatively large molecular weights ($\bar{M}_n > 5 \times 10^5$) and low polydispersities ($\bar{M}_w/\bar{M}_n < 1.15$) of acrylate polymers have been prepared using this approach (Table V) (22, 27).

Table III: Polymerization of MA using (TMP)Co-CH₂C(CH₃)₃

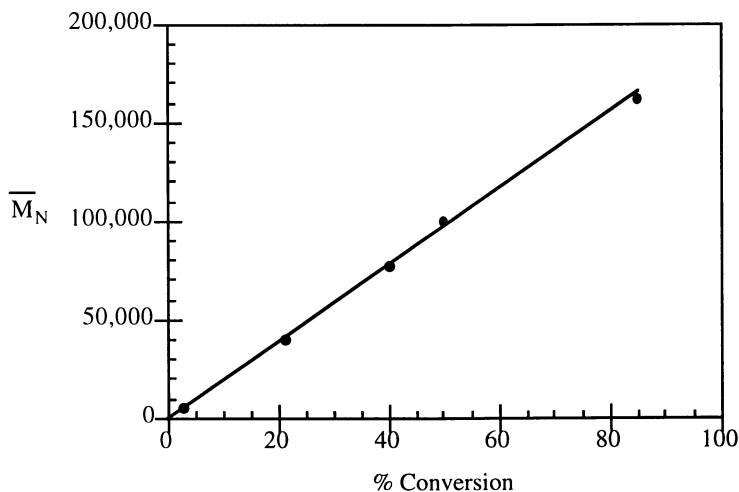
Time (hours)	% Conversion	\bar{M}_n	\bar{M}_w/\bar{M}_n
0.5	5.5	7,856	1.10
1.5	11.5	18,930	1.16
5	20	38,120	1.21
15	42	91,930	1.17
38	66	143,600	1.21

[(TMP)Co-CH₂C(CH₃)₃]_i = 1.0×10^{-3} M; [MA]_i = 2.5 M; [(TMP)Co^{II}]_i = 2.0×10^{-4} M; solvent = C₆D₆; T = 60 °C.

Table IV: Polymerization of MA using (TMP)Co-CH(CH₃)CO₂CH₃

Time (hours)	% Conversion	\bar{M}_n	\bar{M}_w/\bar{M}_n
0.5	3	5,900	1.12
6	21	40,300	1.17
12	40	76,500	1.21
20	50	99,000	1.21
96	85	163,000	1.10

$[(\text{TMP})\text{Co-CH}(\text{CH}_3)\text{CO}_2\text{CH}_3]_i = 1.15 \times 10^{-3} \text{ M}$; $[\text{MA}]_i = 2.5 \text{ M}$;
 $[(\text{TMP})\text{Co}^{\text{II}}]_i = 2.5 \times 10^{-4} \text{ M}$; solvent = C₆D₆; T = 60 °C.

Figure 4. Polymerization of MA in C₆D₆ at 60 °C using (TMP)Co-CH(CH₃)CO₂CH₃.Table V: Bulk Polymerization of MA by (TMP)Co-CH(CO₂CH₃)CH₃

Time (hrs.)	% Conversion	M_n	M_w/M_n
0.75	3.5	176,800	1.15
2.0	10.5	554,300	1.13

$[(\text{TMP})\text{Co-CH}(\text{CO}_2\text{CH}_3)\text{CH}_3]_i = 1.75 \times 10^{-4} \text{ M}$; $[\text{CH}_2=\text{CH}(\text{CO}_2\text{CH}_3)]_i = 10.5 \text{ M}$;
 $[(\text{TMP})\text{Co}^{\text{II}}]_i = 3.1 \times 10^{-5} \text{ M}$; solvent = MA; T = 60 °C.

The living nature of the MA polymerization induced by (TMP)Co organo complexes is also illustrated by formation of acrylate block copolymers. Reaction of (TMP)Co-CH(CH₃)CO₂CH₃ with MA ($[\text{MA}]/[(\text{TMP})\text{Co-CH}(\text{CH}_3)\text{CO}_2\text{CH}_3] = 2,174$) in benzene at 60 °C is used to form a block of PMA attached to (TMP)Co ($M_n = 39,500$, $M_w/M_n = 1.15$) (Figure 5a). Removal of unreacted MA followed by addition of butyl acrylate (BA) and benzene to the preformed PMA-Co(TMP) complex and heating at 60 °C results in BA polymerization (Figure 5b) to form an (MA)_n(BA)_m block copolymer ($M_n = (82-272) \times 10^3$, $M_w/M_n = 1.15-1.23$).

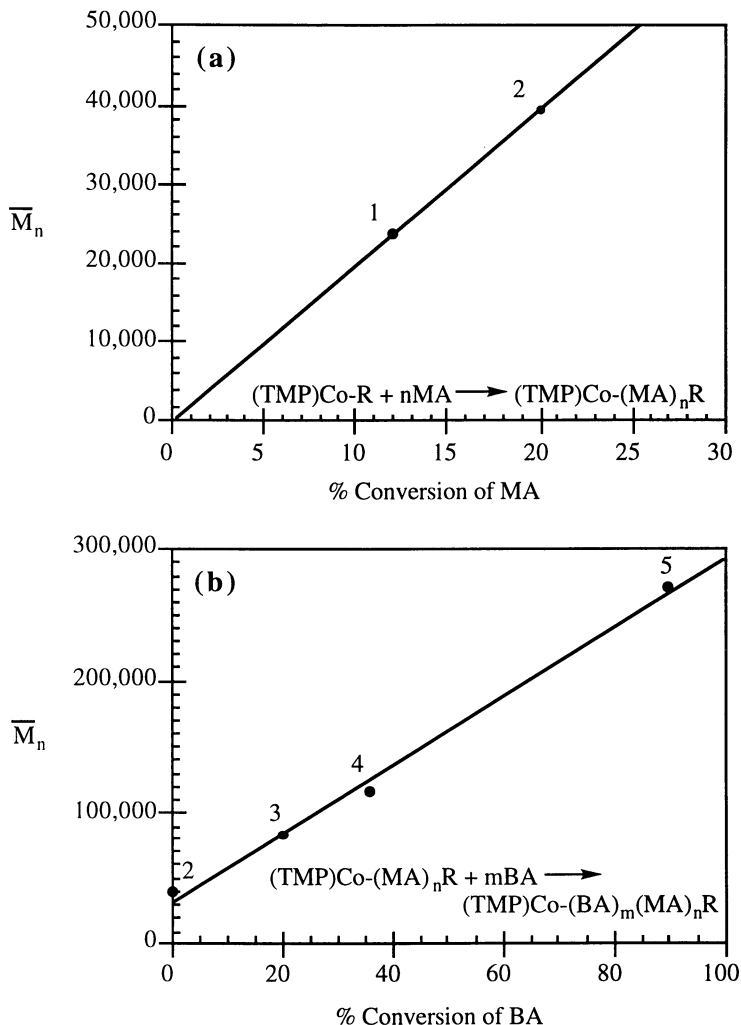
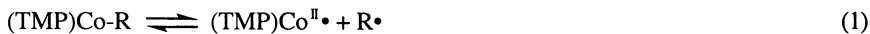


Figure 5. Block copolymerization of MA and BA by $(\text{TMP})\text{Co}-\text{CH}(\text{CH}_3)\text{CO}_2\text{CH}_3$ in C_6D_6 at 60°C . $[(\text{TMP})\text{Co}-\text{CH}(\text{CH}_3)\text{CO}_2\text{CH}_3]_i = 1.15 \times 10^{-3} \text{ M}$. a) $(\text{TMP})\text{Co}-\text{PMA}$ block $[\text{MA}]_i = 2.5 \text{ M}$; M_w/M_n 1) 1.14 2) 1.15; b) $(\text{TMP})\text{Co}-\text{PMA}-\text{PBA}$ block copolymer $[\text{BA}]_i = 2.5 \text{ M}$; M_w/M_n 3) 1.15 4) 1.17 5) 1.23.

Polymerization of acrylates induced by $(\text{TMP})\text{Co-R}$ complexes is envisioned to occur by the reaction sequence given by equations 1–5 ($X = \text{CO}_2\text{R}'$, $\text{R}' = \text{CH}_3$, $(\text{CH}_2)_3\text{CH}_3$). Bond homolysis of $(\text{TMP})\text{Co-R}$ produces a carbon centered radical (R^\bullet) (equation 1) that initiates polymerization by reacting with an acrylate monomer to form $\text{RCH}_2\text{CHX}^\bullet$ (equation 2) which either combines reversibly with $(\text{TMP})\text{Co}^{\text{II}}\bullet$ (equation 3) or reacts with additional acrylate monomers to form an oligomer radical (equation 4) that subsequently combines reversibly with $(\text{TMP})\text{Co}^{\text{II}}\bullet$ (equation 5).



Repetition of these events without radical termination or chain transfer would result in a fully living radical polymerization process. The real polymerization process cannot be fully living because of inherent bimolecular radical termination processes (equations 6 and 7) and $\text{H}\cdot$ transfer reactions with monomer, polymer, solvent (equation 8) and $(\text{TMP})\text{Co}^{\text{II}}\cdot$ (equation 9) which result in non-living polymer chains.



In spite of the processes that can limit polymer growth (equations 6–9), observation of linear increases in \bar{M}_n with conversion, formation of block copolymers, and relatively small polydispersities clearly demonstrate that $(\text{TMP})\text{Co-R}$ complexes initiate and control effective living radical polymerization of acrylates.

Representative results from rate studies for the polymerization of MA that is initiated and controlled by $(\text{TMP})\text{Co-R}$ complexes are illustrated in Figures 6, 7, and 8. In a radical polymerization, the rate of conversion of monomer (M) is first order in both the radical and monomer concentrations with the radical propagation constant (k_p) as the rate constant ($-d[M]/dt = k_p[\text{R}\cdot][M]$). In a living radical process, the concentration of radicals is maintained constant at a value determined by an equilibrium with a dormant species. In the organometallic mediated polymerization of MA, the radical concentration is determined by the equilibrium constant for the homolytic dissociation of $(\text{TMP})\text{Co-R}$ ($K_{\text{eq}} = [(\text{TMP})\text{Co}] [\text{R}\cdot] / [(\text{TMP})\text{Co-R}]$; $[\text{R}\cdot] = K_{\text{eq}} [(\text{TMP})\text{Co-R}] / [(\text{TMP})\text{Co}\cdot]$). The rate of MA polymerization is thus given by the expression such that the slope of the plot of

$$\frac{-d[\text{MA}]}{[\text{MA}]dt} = k_p K_{\text{eq}} \frac{[(\text{TMP})\text{Co-R}]}{[(\text{TMP})\text{Co}\cdot]}$$

$\ln([\text{MA}]_0/[\text{MA}]_t)$ versus time (t) gives the product of the propagation constant, k_p , and the equilibrium constant (K_{eq}) at temperature, T . Temperature dependence of the rate of MA polymerization gives the overall activation parameters (ΔH^\ddagger , ΔS^\ddagger) which are composed of activation parameters for the radical propagation (ΔH_p^\ddagger , ΔS_p^\ddagger) and the thermodynamic parameters (ΔH° , ΔS°) for the dissociation of $(\text{TMP})\text{Co-PMA}$. Kinetic analysis of the $(\text{TMP})\text{Co-R}$ controlled living polymerization of MA gives effective activation parameters of $\Delta H^\ddagger = \Delta H_p^\ddagger + \Delta H^\circ = 28 \text{ kcal mol}^{-1}$ and $\Delta S^\ddagger = \Delta S_p^\ddagger + \Delta S^\circ = 4.4 \text{ cal K}^{-1} \text{ mol}^{-1}$. Thermodynamic values for the homolytic dissociation of

(TMP)Co-PMA ($\Delta H^\circ = 24 \text{ kcal mol}^{-1}$, $\Delta S^\circ = 29 \text{ cal }^\circ\text{K}^{-1} \text{ mol}^{-1}$) are estimated by assuming that the activation parameters for radical propagation of MA are comparable to those determined for butylacrylate ($\Delta H_p^\ddagger \approx 4 \text{ kcal mol}^{-1}$; $\Delta S_p^\ddagger \approx -25 \text{ cal }^\circ\text{K}^{-1} \text{ mol}^{-1}$) (15, 18). The thermodynamic values obtained for dissociation of (TMP)Co-PMA ($\Delta H^\circ = 24 \text{ kcal mol}^{-1}$, $\Delta S^\circ = 29 \text{ cal }^\circ\text{K}^{-1} \text{ mol}^{-1}$) compare favorably with those determined for (TAP)Co-CH(CH₃)CO₂CH₃ ($\Delta H^\circ = 25.0 \pm 0.4 \text{ kcal mol}^{-1}$, $\Delta S^\circ = 34 \pm 1 \text{ cal }^\circ\text{K}^{-1} \text{ mol}^{-1}$) (9).

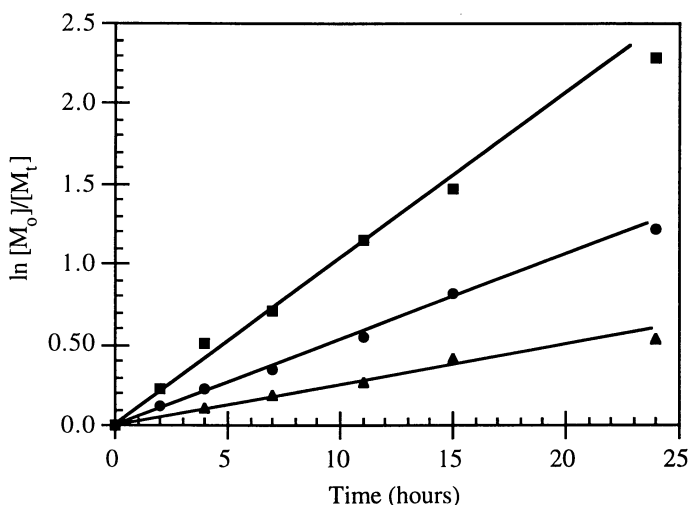


Figure 6. First order rate plots for polymerization of a 2.50 M solution of MA in C₆D₆ at 60 °C using $1.15 \times 10^{-3} \text{ M}$ (TMP)Co-CH(CH₃)CO₂CH₃ and varying initial concentrations of (TMP)Co• (■) $[(\text{TMP})\text{Co}\cdot]_i = 5.8 \times 10^{-3} \text{ M}$ (●) $[(\text{TMP})\text{Co}\cdot]_i = 1.38 \times 10^{-4} \text{ M}$ (▲) $[(\text{TMP})\text{Co}\cdot]_i = 2.53 \times 10^{-4} \text{ M}$.

Conclusions.

Cobalt(II) porphyrins are prototype metalloradicals that illustrate the control of radical polymerizations through both chain transfer catalysis (CTC) and living radical polymerization (LRP). Major challenges for the continued development of this area are to expand the range of both metalloradicals and monomers that can be incorporated into systems that accomplish CTC and LRP.

Acknowledgments

This research was supported by DuPont research fellowships and the National Science Foundation through NSF-CHE-95-27782.

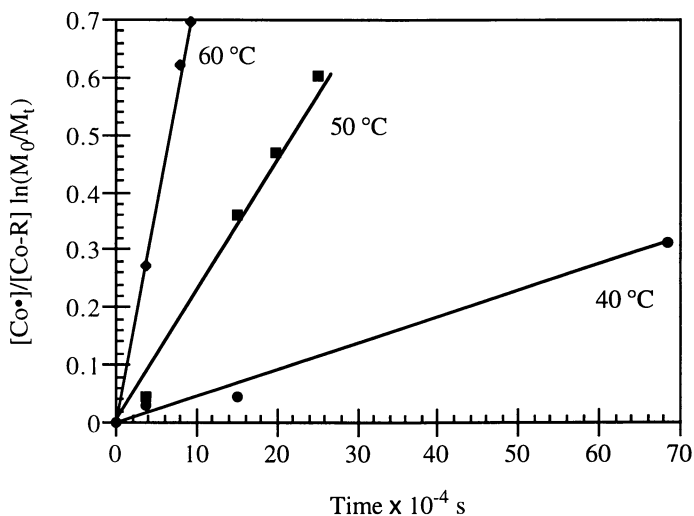


Figure 7. Kinetics for radical polymerization of (TMP)Co-PMA at various temperatures. Slope equals $k_p K_{\text{eq}}$ ($([\text{Co}\cdot]/[\text{Co-R}]) \ln(M_0/M_t) = k_p K_{\text{eq}} t$).

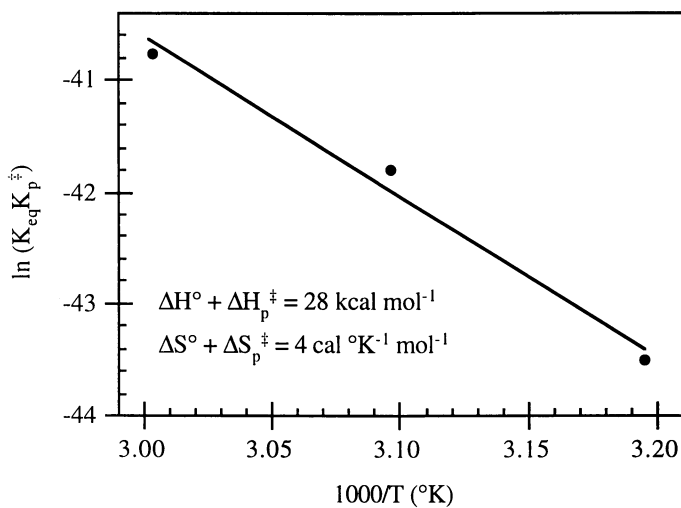


Figure 8. The plot of $\ln(K_{\text{eq}} K_p^\ddagger)$ versus $1/T$ yields the effective activation parameters for the polymerization of MA by (TMP)Co-PMA ($K_p^\ddagger = k_p/(h/kT)$).

References

1. Ng, F. T. T.; Rempel, G. L.; Mancuso, C.; Halpern, J. *Organometallics* **1990**, *9*, 2762.
2. Morozova, I. S.; Mairanovskii, V. G.; Smirnov, B. R.; Pushchaeva, L. M.; Enikolopyan, N. S. *Dokl. Akad. Nauk SSSR* **1981**, 258, 895.
3. Gridnev, A. A.; Bel'govskii, I. M.; Enikolopyan, N. S. *Dokl. Akad. Nauk SSSR* **1986**, 289, 616.
4. Davis, T. P.; Haddleton, D. M.; Richards, S. N. *J. Macromol. Sci., Rev. Macromol. Chem. Phys.* **1994**, *C34*, 243.
5. Gridnev, A. A.; Ittel, S. D. *Macromolecules* **1996**, *29*, 5864.
6. Parshall, G. W.; Ittel, S. D. *Homogeneous Catalysis*; Wiley: New York, NY, 1992; p. 85.
7. Otsu, T.; Yoshida, M.; Tazaki, T. *Makromol. Chem., Rapid Commun.* **1982**, *3*, 133.
8. Gridnev, A. A.; Ittel, S. D.; Wayland, B. B.; Fryd, M. *Organometallics* **1996**, *15*, 5116.
9. Woska, D. C.; Wayland, B. B. *Inorg. Chim. Acta*, in press.
10. Gridnev, A. A.; Ittel, S. D.; Fryd, M.; Wayland, B. B. *Organometallics* **1993**, *12*, 4871.
11. Georges, M. K.; Vergin, R. P. N.; Kazmaier, P. M.; Hamer, C. K.; Saban, M. *Macromolecules* **1994**, *27*, 7228.
12. Fukuda, T.; Terauchi, T.; Goto, A.; Ohno, K.; Tsujii, Y.; Miyamoto, T.; Kobatake, S.; Yamada, B. *Macromolecules* **1996**, *29*, 6393.
13. Yamada, B.; Miura, Y.; Nobukane, Y.; Aota, M. *ACS Polymer Preprints*, **1997**, *38*, 725.
14. Hawker, C. J.; Hedrick, J. L. *Macromolecules* **1995**, *28*, 2993.
15. Benoit, D.; Grimaldi, S.; Finet, J.; Tordo, P.; Fontanille, M.; Gnanou, Y.; *ACS Polymer Preprints*, **1997**, *38*, 729.
16. Puts, R.; Sogah, D. Y. *Macromolecules* **1996**, *29*, 3323.
17. Percec, V.; Barboiu, B.; Newmann, A.; Ronda, J. C.; Zhao, M. *Macromolecules*, **1996**, *29*, 3665.
18. Matyjaszewski, K.; Wang, J. S. *Macromolecules* **1995**, *28*, 7901.
19. Patten, T.; Xia, J.; Abernathy, T.; Matyjaszewski, K. *Science* **1996**, *272*, 866.
20. Haddleton, D. M.; Shooter, A. J. *ACS Polymer Preprints*, **1997**, *38*, 738.
21. Sawamoto, M.; Kato, M.; Kamigaito, M.; Higashimura, T. *Macromolecules* **1995**, *28*, 1721.
22. Wayland, B. B.; Poszmik, G.; Mukerjee, S.; Fryd, M. *J. Amer. Chem. Soc.* **1994**, *116*, 7943.
23. Arvanitopoulos, L. D.; King, B. M.; Huang, C.; Harwood, H. J. *ACS Polymer Preprints*, **1997**, *38*, 752.
24. Frechet, J. M. J.; Leduc, M. R.; Weimer, M.; Grubbs, R. B.; Liu, M.; Hawker, C. J. *ACS Polymer Preprints*, **1997**, *38*, 756.
25. Gaynor, S. G.; Edelman, S. Z.; Matyjaszewski, K. *Macromolecules* **1996**, *29*, 1079.
26. Nakano, T.; Okamoto, Y.; Sogah, D. Y.; Zheng, S. *Macromolecules* **1995**, *28*, 8705.
27. Wayland B. B.; Mukerjee, S.; Poszmik, G.; Woska, D. C.; Fryd, M. *ACS Polymer Preprints* **1997** 742.

Chapter 20

Photochemical Polymerizations Initiated and Mediated by Soluble Organocobalt Compounds

Labros D. Arvanitopoulos¹, Michael P. Greuel², Brian M. King¹,
Anne K. Shim¹, and H. James Harwood^{1,3}

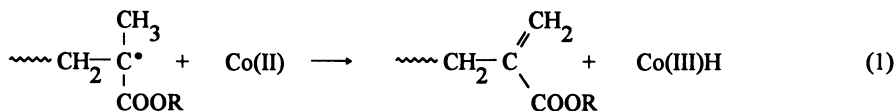
¹Maurice Morton Institute of Polymer Science, University of Akron,
Akron, OH 44325-3909

²3M Corporation, 3M Center, Building 236-GC-01, St. Paul, MN 55144-1000

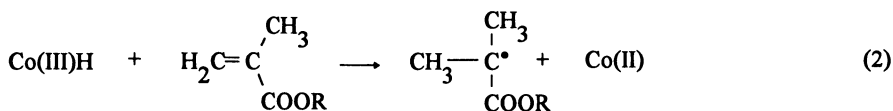
The use of organocobaloximes as photoinitiator/mediators for the controlled polymerization of acrylate esters is discussed. Polymer molecular weights increase with conversion for polymerizations conducted in the presence of chloroform, suggesting pseudo-living polymerization behavior, but catalytic chain transfer reactions compete with polymer chain growth at high conversions. However, block copolymers can be prepared by polymerizing monomers sequentially if conversions are kept below about 70 percent. Organocobaloximes bearing hydroxyl, carboxylic acid, ester, and nitrile groups can be used to prepare polymers bearing these functions at chain ends. Compounds bearing two or more cobaloxime moieties can be used for the preparation of triblock copolymers and polymers with star or radial-block architectures. The cobaloxime ends of the polymers can be functionalized by reaction with aromatic disulfides or methacrylate esters. Macromonomers with methacrylate functionality result, in addition, from the latter reactions.

Free radical initiated polymerizations that are mediated by organocobalt compounds can take two principal courses, catalytic chain transfer and pseudo-living polymerization. Of these, catalytic chain transfer has been the most studied and has become important industrially for the synthesis of oligomers of methacrylic acid and its esters. (1-5) This process involves the transfer of hydrogen atoms from a propagating polymer to a low spin cobalt compound. This yields an unsaturated polymer chain and a hydrocobalt intermediate, *viz.*

³Corresponding author



The hydrocobalt intermediate can then transfer a hydrogen atom to a monomer molecule and thereby initiate the growth of a new polymer chain, *viz.*



Reaction 1, being a radical-radical reaction, is extremely rapid and occurs at diffusion controlled rates. Overall, the catalytic chain transfer process is very efficient, turnover numbers for the termination/re-initiation sequences being in the thousands. Catalytic chain transfer works well with methacrylates, less well with styrenes, and not at all with acrylates. (1,2)

During efforts to polymerize and copolymerize acrylate esters in the presence of cobaloxime, an easily synthesized low spin Co(II) compound, we discovered that low molecular oligomers containing acrylate-cobalt bonds were produced. (6) This was indicated by chromatographic and spectroscopic evidence. It seemed reasonable to conclude that the growth of polyacrylate radicals had been terminated by combination with cobaloxime. A literature search revealed that free radicals react readily with cobaloxime and other low spin Co(II) compounds to form relatively stable Co(III) compounds.

Furthermore, the search revealed that the organocobalt compounds that result from these and other reactions are valuable models for vitamin B₁₂, a compound that is a source of free radicals in living systems. This led us to realize that the carbon-cobalt bonds present at the ends of the polyacrylates we had isolated could be reversibly broken, photochemically or thermally, and that cobaloxime and related Co(II) compounds could serve as mediators for the controlled free radical polymerization of acrylates and perhaps other monomers as well. In this paper, we provide information about our studies on this possibility, some of which have already appeared in preprint (6,7) and patent (8) formats. Another group has simultaneously been using cobalt porphyrins to mediate acrylate polymerizations with considerable success. (9-11)

Experimental

Acrylate and Methacrylate Esters. These were washed three times with 5 percent NaOH and then three times with distilled water to remove inhibitors. They were then dried with CaCl₂ for 2 hr and with CaH₂ overnight. Following vacuum fractional distillation over CaH₂, the center cuts were stored over 3Å Molecular Sieves under argon at -20°C until used.

Organo(pyridinato)cobaloximes. These were prepared according to published general procedures (12-16) via reactions of the bis(dimethylglyoximate)(pyridinato)-cobalt(I) anion with alkyl halides (benzyl bromide, 2-bromopropane, 1,6-dibromo-

hexane, xylidene dibromide, p-nitrobenzyl chloride) or oxiranes (1,2-epoxybutane) in methanol or by introducing hydrogen into a suspension of $\text{Co(DMG)}_2\cdot\text{H}_2\text{O}$ in methanol that contained a slight excess of pyridine and a stoichiometric amount of olefin (acrylic acid, ethyl acrylate, acrylonitrile, trimethylolpropane triacrylate and pentaerythritol tetraacrylate). The bright orange products were isolated (generally in about 65 percent yield) by pouring the reaction mixtures into water containing a little pyridine. They were purified by washing with distilled water until the washings were colorless. If the alkyl(pyridinato)cobaloxime was soluble in water, it was extracted with ether or methylene chloride and then recovered by evaporation of the solvent. The materials exhibited single spots when analyzed by TLC on silica gel. The products exhibited the expected relative areas when analyzed by $^1\text{H-NMR}$. They were dried at 40–60°C at 1 mm Hg and stored under argon in the dark. All reactions and manipulations were conducted under an atmosphere of argon and as much as possible in the dark.

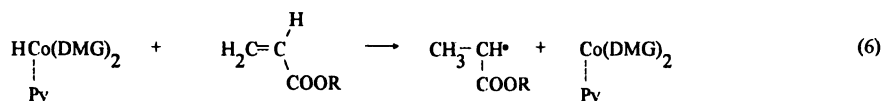
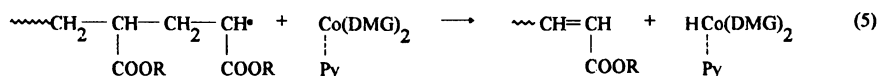
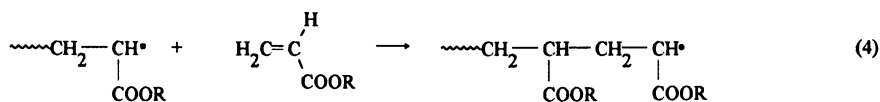
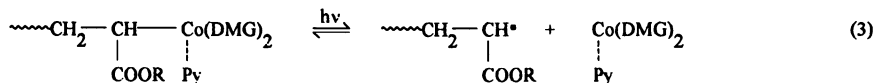
Polymerizations. These were conducted by exposing solutions containing monomer (20 mL), solvent (0, 20, 33 or 50 percent by volume) and organocobaloxime (0.125–0.5 mole percent based on monomer) to illumination by a 500W tungsten lamp. The reaction mixtures were flushed with dry argon prior to the reaction. Samples were periodically removed from the mixtures by syringe for analysis by NMR and GPC to determine conversions and molecular weights. Polymers were isolated by evaporating solvent and excess monomer at 40°C (1 mm Hg). When block copolymerizations were performed, polymerization of the first monomer was terminated, often after about 60 percent conversion, by turning off the tungsten lamp. Residual monomer and solvent were then removed in the dark using a rotary evaporator. Subsequently, fresh solvent and the second monomer were added to the system and illumination of the system was resumed.

$^1\text{H-NMR}$ measurements. These were made using a Varian Gemini 200 MHz instrument and CDCl_3 as the solvent. Conversions were calculated from the relative resonance areas of olefinic proton resonance due to unreacted monomer (5.7–6.8 ppm) and the relative resonance area due to methyleneoxy protons (4.1–4.3 ppm) of ethyl or butyl groups present on both monomer and polymer. The average numbers of monomers present per cobaloxime unit in the polymers and copolymers were calculated from the relative resonance areas of (pyridinato)cobaloxime group resonances and the relative area of methyleneoxy proton resonances of monomer units (4.1–4.3 ppm).

GPC measurements. These were obtained using a Waters Model 150-C ALC/GPC instrument equipped with a differential refractometer and a 6-column set with pore sizes of 10^6 , 10^5 , 10^4 , 10^3 , 500 and 100Å. THF flowing at 1 mL/min was the carrier liquid. A calibration based on standard poly(methyl methacrylate) samples was used.

Results and Discussion

Polymerization of acrylate esters in the presence of cobaloxime have been conducted photochemically using a 500W tungsten lamp source as a means to generate polymer radicals from alkylcobaloximes and cobaloxime-terminated polyacrylates. The process is believed to involve the following steps:



Reaction (3) represents the reversible initiation-termination process that is the heart of the cobaloxime mediated process. This is indicated here as a photochemical process, but the acrylate-cobalt bond can also be broken thermally. Reaction (4) is a conventional free radical propagation reaction, while reactions (5) and (6) are reactions that can terminate the growth of propagating radicals and reinitiate the growth of others. They are analogous to reactions (1) and (2) which predominate in the catalytic chain transfer polymerization of methacrylates. Reactions (5) and (6), if they occur to a significant extent, can limit the control that is possible in an alkylcobaloxime-initiated-cobaloxime-mediated acrylate monomer polymerization. Our studies have shown (a) that reaction (3), can be induced photochemically, thus enabling the polymerization to be mediated by cobaloxime, and (b) that propagation reactions predominate sufficiently over chain transfer reactions that this chemistry merits investigation as a route to polymers with controlled end group functionality, block copolymers and star polymers, etc.

Figure 1 provides conversion-time plots for polymerizations of an 80 percent solution of ethyl acrylate in chloroform containing 0.125 mole percent isopropyl(pyridinato)cobaloxime. The plot at the extreme left indicates that the reaction proceeds rapidly to nearly complete conversion in about 5 hours. There is no evidence of a Trommsdorff effect, even though the amount of solvent present was very small. The central plot shows the conversion-time curve that resulted after a second portion of monomer was added and polymerization was continued and the plot at the extreme right is the conversion-time curve that resulted after a third portion of monomer was added. It can be seen that the second and third portions of monomer polymerized at nearly the same rates as the first portion. This indicates that the activity of cobaloxime derived species present in the system was not lost appreciably during the course of the reaction. This and the fact that a Trommsdorff effect was not evident in any of the curves indicates that the polymerization is distinctly different from conventional acrylate polymerizations.

Figure 2 shows the molecular weight-conversion relationship obtained when a 66 percent solution of ethyl acrylate was polymerized in chloroform using 0.125 mole percent isopropyl(pyridinato)cobaloxime as the photoinitiator/mediator. The molecu-

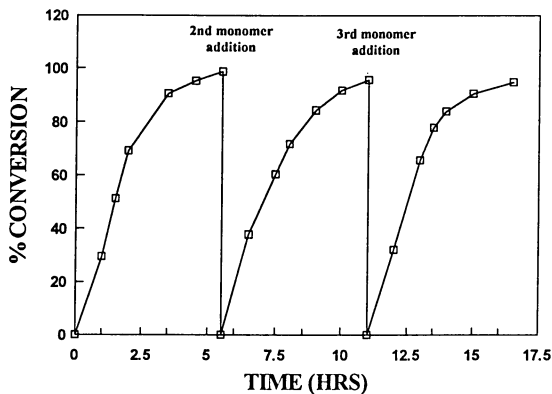


Figure 1. Conversion versus time for isopropyl(pyridinato)cobaloxime (0.125 mole percent) initiated polymerization of an 80 percent solution of ethyl acrylate in chloroform.

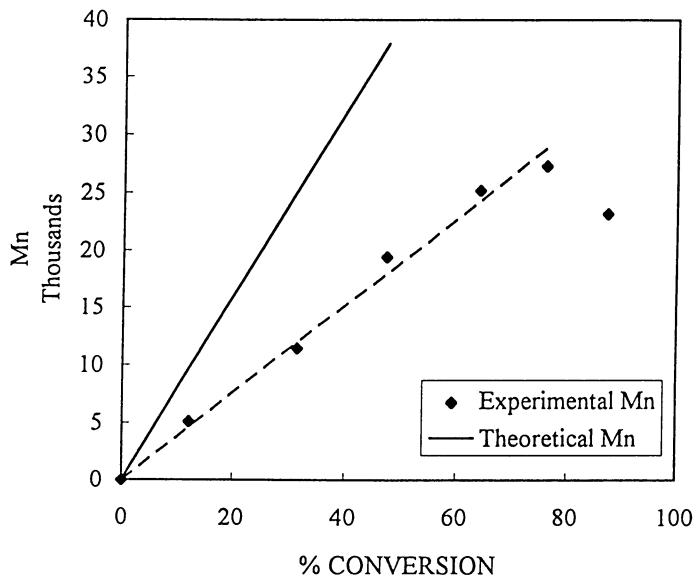


Figure 2. Number average molecular weight versus conversion for isopropyl(pyridinato)cobaloxime (0.125 mole percent) initiated polymerization of a 66 percent solution of ethyl acrylate in chloroform.

lar weight increases linearly up to approximately 70 percent conversion and then falls, perhaps due to chain transfer processes becoming significant as the monomer concentration decreases. Although the molecular weight-conversion curves are approximately linear at moderate conversions, the molecular weights are less than those calculated from conversions and initial alkylcobaloxime-monomer ratios, assuming chain transfer reactions or other means of limiting molecular weight do not operate.

The departure of observed molecular weights from theoretically expected values increases with conversion, becoming as much as 40 percent at high conversions, in some cases. Despite this, the molecular weights of the polymers can be controlled in chloroform solution by varying initial alkylcobaloxime/monomer (I/M) ratios. This is illustrated by Table I which compares the molecular weights of poly(ethyl acrylates) obtained after 60 percent conversion for various initial I/M ratios.

Table I. Number average molecular weight with respect to initiator/monomer ratio for isopropyl(pyridinato)cobaloxime initiated polymerization of a 50 percent solution of ethyl acrylate in chloroform.

Mole percent Initiator/Monomer	Number Average Molecular Weight		MWD	% Conversion
	GPC	Theoretical		
0.125	24400	51200	2.40	64
0.25	15000	24400	2.14	61
0.5	8500	12400	2.30	62

Mw/Mn values (MWD) for polyacrylates formed in these polymerizations are generally between 1.4 and 1.9, even at conversions above 90 percent. The values may reach 2.5 when large amounts of chloroform (e.g., 50 volume percent) are present, and they tend to increase with the amount of chloroform present. There are indications that they increase slightly with conversion.

Although some termination/transfer seems to occur in cobaloxime-mediated polymerizations of acrylates, block copolymers can be prepared by adding monomers sequentially to the polymerization mixture. Figure 3 shows GPC curves observed for a poly(ethyl acrylate) (Mn 7400, MWD 1.6) prepared in 60 percent conversion from a 66 percent solution of ethyl acrylate in chloroform and for a poly[(ethyl acrylate)-*b*-(butyl acrylate)] block copolymer prepared by using the poly(ethyl acrylate) sample as a macroinitiator for the polymerization of butyl acrylate. Although the curves are not completely resolved, the shape of the block copolymer curve is nearly the same as that of the parent copolymer, with only a slight indication of a low molecular weight tail. This indicates that blocking occurs efficiently if the conversion obtained in preparing the first block is not too high (i.e. < 60 percent).

Scope of the Reaction

These polymerizations are most conveniently conducted using chloroform as a diluent in amounts as low as 10 volume percent. Polymerizations conducted with bulk mono-

mer or using benzene, methylene chloride, or DMSO as diluents occur more slowly (Figure 4) and yield polymers whose molecular weights are low (1200-6000) and do not increase with conversion. Apparently chain transfer or termination competes effectively with propagation when diluents other than chloroform are present or are absent altogether. The almost unique behavior of chloroform as a necessary diluent may be related to its ability to react with cobaloxime and form the dichloromethyl radical and chlorocobaloxime, *viz.*



Control experiments have established that chlorocobaloxime is inert in these polymerization systems. Reaction 7 thus provides a means for the system to remove excess cobaloxime. If present in excess, cobaloxime would reduce polymerization rate and the number of monomer units incorporated in a polymer chain during the interval between a reinitiation and a termination step in the mediated process. Although we do not have at this time a good understanding of the role played by chloroform in this system, it does seem that it may be similar to that played by thermal styrene polymerization in TEMPO-mediated polymerizations.

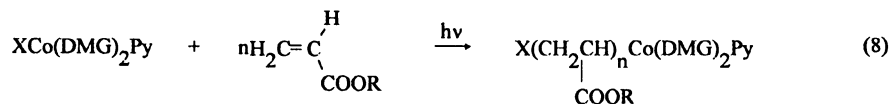
These polymerizations work well with acrylate esters but not with styrene or vinyl acetate. Copolymerization of a nearly equimolar mixture of acrylonitrile and ethyl acrylate occurred very slowly, affording a 15 percent yield of copolymer ($M_n = 7500$) in 4 days.

Polymerizations of acrylates conducted using most organo(pyridinato)cobaloximes as the initiator/mediator performed similarly, as will be discussed subsequently, except for benzyl(pyridinato)cobaloxime. This compound is not very soluble and slow polymerization rates are often obtained when it is used. In addition, it has been reported to undergo a side reaction that may interfere with its performance as an initiator/mediator.⁽¹⁷⁾ Organo(triphenylphosphinato)cobaloximes did not work well as initiator/mediators. Chain transfer seems to be very significant when these materials are used.

Since the best results that have been obtained thus far have been obtained in acrylate polymerizations conducted photochemically using organo(pyridinato)cobaloximes as initiator/mediators, we have explored ways to use this chemistry for controlling the end functionality and architecture of polyacrylates. Results of these approaches are summarized in the remainder of this paper.

Initiator Synthesis

Organocobaloximes can be synthesized by a variety of methods,⁽¹²⁻¹⁶⁾ and it is possible to prepare materials with useful functional groups, such as hydroxyl, carboxyl, ester, halogen and nitrile. When these are used as photoinitiators for acrylate polymerizations, polymers with useful functionality (X) can be prepared, *viz.*



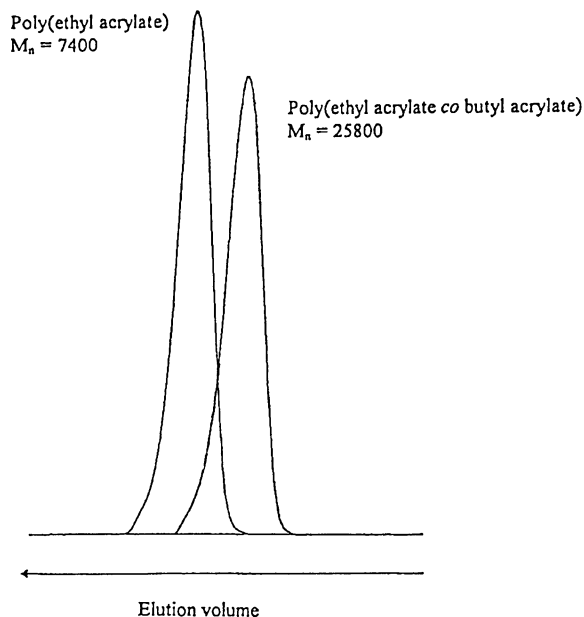


Figure 3. GPC curves of poly(ethyl acrylate) and of poly[(ethyl acrylate)-*b*-(butyl acrylate)] derived from it.

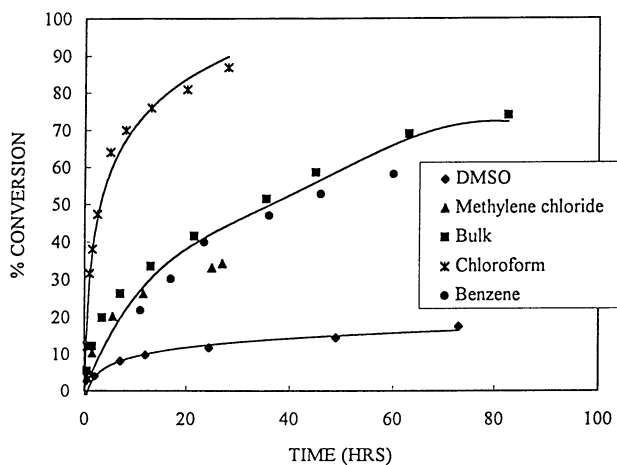


Figure 4. Conversion versus time curves for ethyl acrylate polymerizations conducted in bulk and various solvents using 0.125 mole percent isopropyl(pyridinato)cobaloxime (bulk, 50 percent in benzene, 66 percent in chloroform and 66 percent in DMSO) and 0.125 mole percent 1-carboethoxyethyl(pyridinato)cobaloxime (66 percent in methylene chloride).

The compounds that have been prepared and used as photoinitiator/moderators for acrylate polymerizations are listed in Table II, along with the yields obtained in their preparation.

Table II. Photoinitiator/Moderators Investigated and Yields Obtained in Their Preparation

Photoinitiator/Moderator	Yield, %
$C_6H_5CH_2Co(DMG)_2Py$	76
$p-NO_2C_6H_5CH_2Co(DMG)_2Py$	74
$Br(CH_2)_6Co(DMG)_2Py$	67
$CH_3CH_2CH(OH)CH_2Co(DMG)_2Py$	65
$(CH_3)_2CHCo(DMG)_2Py$	60
$CH_3CH(COOH)Co(DMG)_2Py$	54
$CH_3CH(COOCH_3)Co(DMG)_2Py$	75
$CH_3CH(CN)Co(DMG)_2Py$	93
$Py(DMG)_2CoCH_2C_6H_4CH_2Co(DMG)_2Py$	33
$Py(DMG)_2Co(CH_2)_6Co(DMG)_2Py$	(HERCO) 99
$CH_3CH_2C[CH_2CO_2C(CH_3)Co(DMG)_2Py]_3$	(TTPCO) 67
$C[CH_2CO_2C(CH_3)Co(DMG)_2Py]_4$	(PEPCO) 41
$C_6H_5CH_2Co(DMG)_2P(C_6H_5)_3$	70
$(CH_3)_2CHCo(DMG)_2P(C_6H_5)_3$	75

We have used the functionality X as a tag to investigate the efficiency of alkylcobaloximes as initiators and the extent that chain transfer and other processes are involved in the polymerizations. For example, when 6-bromohexyl(pyridinato)cobaloxime was used in large amount for ethyl acrylate polymerization, an oligomer having a Mn of 4600, as measured by GPC, was obtained. By comparing the relative area of resonance at $\delta = 3.3$ ppm ($-CH_2Br$, triplet) to that of methyleneoxy proton resonance at ≈ 4 ppm ($-OCH_2CH_3$) in the NMR spectrum of the polymer, an Mn of 4100 was calculated for the polymer. This indicated that about 90 percent of the polymer chains contained 6-bromohexyl end groups.

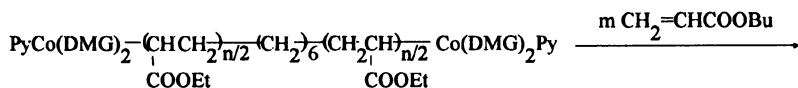
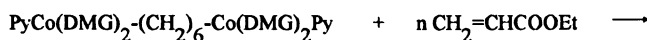
Similarly, GPC and NMR techniques were used to estimate Mn values for poly(ethyl acrylate)s prepared using isopropyl(pyridinato)cobaloxime. These studies were done because of the ease of preparing and handling this initiator and because the six methyl protons of isopropyl end groups in the polymers were easily measured by NMR. The resonance areas of the methyl protons of the isopropyl end groups and of the methyleneoxy protons on the ethyl acrylate groups were used to estimate Mn's by NMR. Table III compares Mn values determined by GPC and NMR with values calculated from initial monomer/cobaloxime ratios and conversions, assuming that chain transfer and termination reactions did not occur. The fractions of polymer chains with isopropyl ends, as calculated from the GPC and NMR results, are also provided. It can be seen that the percentage of functionalized chains decreases as conversion increases and that the difference between measured and calculated Mn's increases with conversion. Similar results were obtained when other organocobaloximes were used although extensive studies were not conducted with other initiators. It is clear

that some of the polymer chains are not initiated by the organocobaloximes. Chain transfer reactions are probably responsible for their formation.

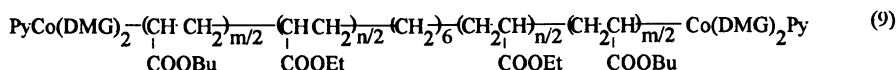
Table III. Number average molecular weight values determined by GPC and NMR and percentages of functionalized chains in poly(ethyl acrylate) prepared by polymerizing a 66 percent solution of ethyl acrylate in chloroform using isopropyl(pyridinato)cobaloxime (0.5 mole percent) as the photoinitiator/moderator.

% Conversion	Number Average Molecular Weight			% Functionalized Chains
	GPC	¹ H-NMR	Theoretical	
10	1930	1840	2020	95
35	5860	5360	7040	92
46	8190	7000	9120	86
60	9560	7850	12000	82
74	9750	7640	14800	78

Initiators containing several cobaloxime moieties were also synthesized and investigated. They are of interest for the synthesis of triblock copolymers and polymers with star (multi-arm) and radial-block architectures. For example, HEPCO was used for the synthesis of poly[(butyl acrylate)-*b*-(ethyl acrylate)-*b*-(butyl acrylate)], a triblock copolymer as shown below.



$$\text{Mn(GPC)}=19,000 ; \text{Mw/Mn}=2.4$$

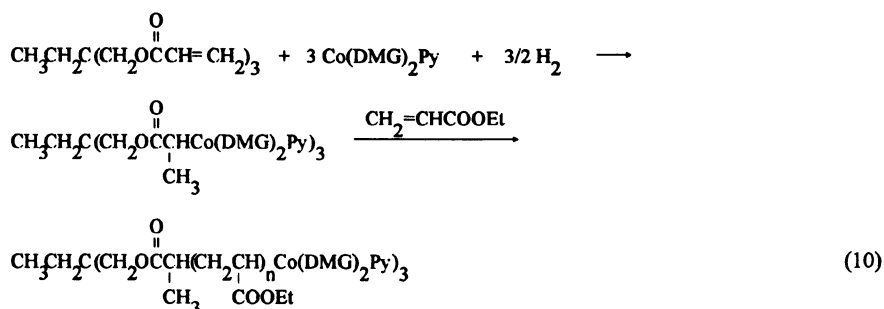


$$\text{Mn(GPC)}=33,500 ; \text{Mw/Mn}=2.7$$

This particular synthesis was made difficult by the poor solubility of HEPCO but the Mn's of the poly(ethyl acrylate) macroinitiator and the triblock copolymer derived from it were approximately 75 percent of those expected theoretically.

Similarly, photoinitiator/mediators containing three (TTPCO) and four (PEPCO) cobaloxime moieties per molecule were synthesized by adding hydrogen to a mixture of Co(DMG)₂Py and polyacrylate esters derived from tris(hydroxymethyl)-ethane and pentaerythritol. Figure 5 shows a Mn-conversion plot for the polymerization of ethyl acrylate using TTPCO. Mn increases linearly with conversion as expected for a mediated polymerization but the Mn values are approximately 80 percent of

the expected values. While this may be in part due to uncertainty in the GPC determinations, it seems that chain transfer reactions may also be responsible.



By comparing the resonance areas of the methyleneoxy protons of the acrylate groups in the polymers to the ortho proton resonances of the pyridines coordinated to the cobaloxime moiety it was established that the ratio of acrylate units to cobaloxime ends was approximately 80 percent of that expected based on the M_n 's determined by GPC, assuming each polymer molecule contained three cobaloxime groups. It seems reasonable to assume that all three arms of this star polymer grew uniformly but additional experiments need to be done to prove this. Table IV compares M_n values determined by NMR and GPC with theoretical values for several samples.

Table IV. Number average molecular weight values determined by GPC and NMR and calculated from monomer/initiator ratios and conversions for several star polymers prepared from ethyl acrylate and TTPCO.

	Number Average Molecular Weight		
	GPC	¹ H-NMR	Theoretical
	3200	2600	4300
	5100	4200	6800

Figure 6 shows that the conversion-time plots for ethyl acrylate polymerizations initiated by TTPCO and PEPCO (0.0625 mole percent Co) are similar. This indicates that a 4-arm star probably formed when PEPCO was the initiator/mediator.

Chain End Functionalization Studies. Provided that the cobaloxime units at the ends of growing polyacrylate chains are not lost by chain transfer or conventional termination reactions, they will be present at the end of the polymerization reactions and can be used to functionalize the ends of the polymer chains. Typical reactions of alkylcobaloximes (16,18) can be used for this. For example, photolysis of an ethyl acrylate sample having a terminal (pyridinato)cobaloxime group in the presence of bis(p-aminophenyl) disulfide yielded a polyacrylate with an aminophenylthioether group, as shown below.

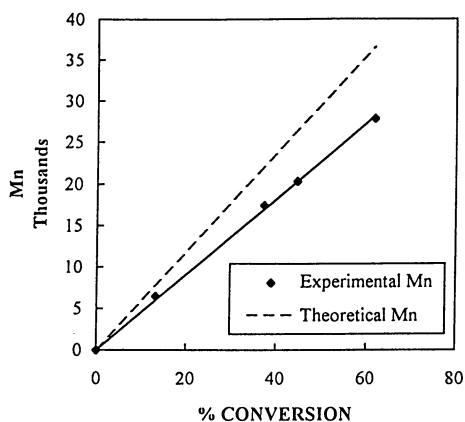


Figure 5. Number average molecular weight versus conversion for a TTPCO initiated polymerization of a 66 percent solution of ethyl acrylate in chloroform.

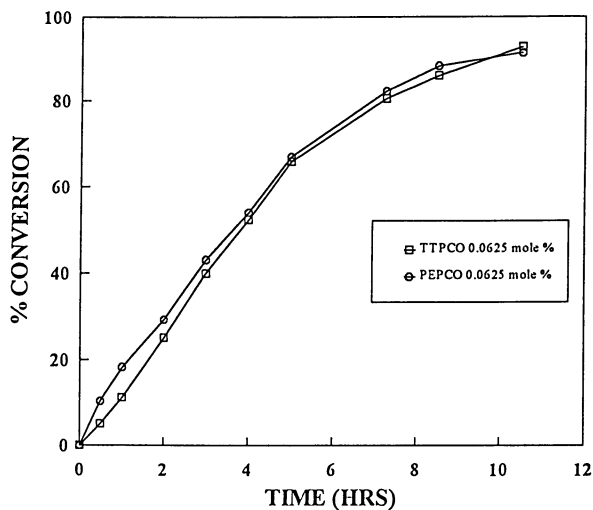
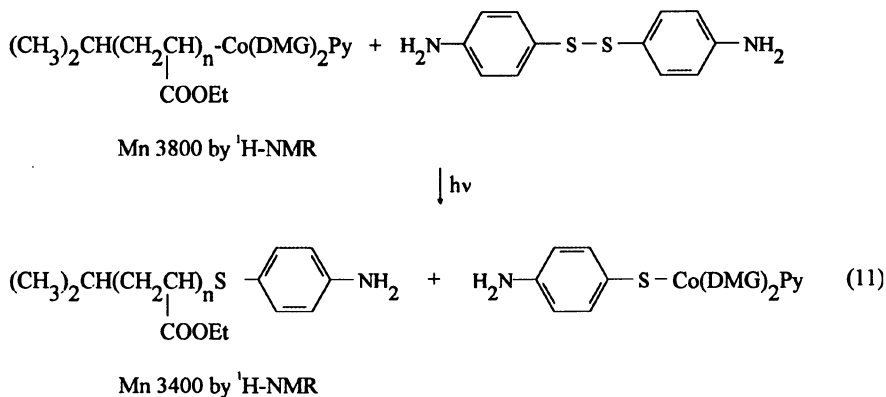
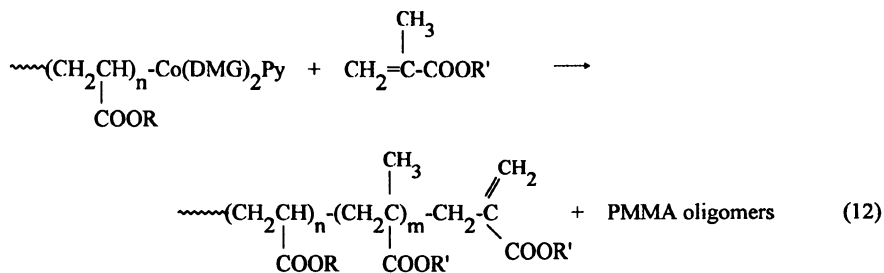


Figure 6. Conversion versus time relationships for polymerizations of ethyl acrylate initiated by TTPCO and PEPCO (0.0625 mole percent Co) in chloroform solution (66 volume percent monomer).

The *p*-aminophenylthioether end groups present in the polymer were identified by $^1\text{H-NMR}$ resonances at 3.8, 6.55 (doublet), 7.25 (doublet) ppm. The relative areas of these resonances, and those due to the methyleneoxy proton resonances of the ethyl acrylate units in the product were in excellent agreement with those expected based on the molecular weight of the original polymer, as estimated by GPC and NMR measurements, assuming complete conversion of cobaloxime ends to *p*-aminophenylthioether ends.



A very convenient way to functionalize the ends of the polymers that are attached to cobaloxime groups is to add a methacrylate ester. Such monomers undergo catalytic chain transfer reactions after having added to the polymer. This leads to polymers with only one or, at most, a few methacrylate units at the chain end, *viz.*



This approach can be used to introduce hydroxyl, carboxyl and oxirane units at the ends of the polymer. The products that result are, in addition, methacrylate-functional macromonomers. As a specific illustration of this approach, a cobaloxime terminated poly(ethyl acrylate) having a molecular weight of about 8000 was prepared. An amount of methyl methacrylate equal to ten times the amount of isopropyl(pyridinato)cobaloxime used to prepare the polymer was added to the polymerization mixture and the system was irradiated. This yielded a poly(ethyl acrylate) that was devoid of cobaloxime ends as indicated by its behavior on column chromatography. Figure 7 shows the $^1\text{H-NMR}$ spectrum of the polymer. It contains resonances of terminal methyl methacrylate units at 5.5, 6.2 and 3.7 ppm as well as methoxy proton resonance of methyl methacrylate units near chain ends at 3.5-3.6 ppm.

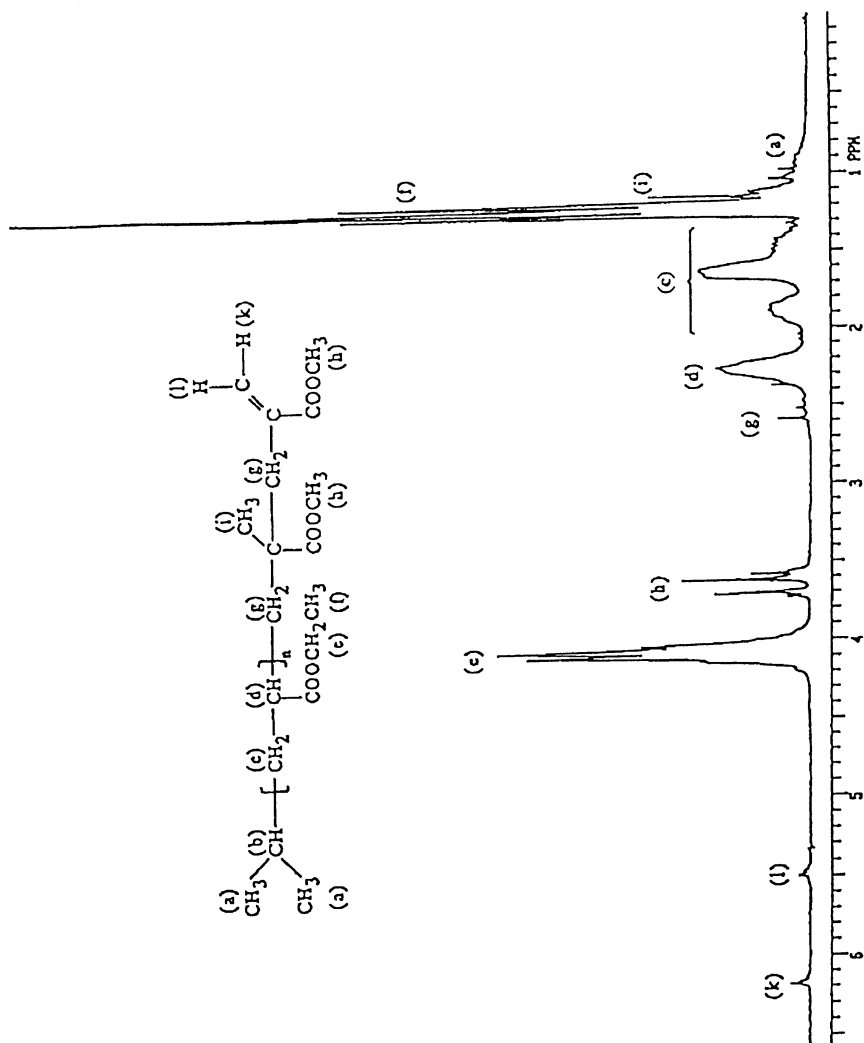


Figure 7. $^1\text{H-NMR}$ spectrum of a poly(ethyl acrylate) macromonomer.

After purification by column chromatography over silica, using chloroform as the eluent, the molecular weight of the polymer was 7600 as measured by GPC and 7100 as calculated for the relative areas of the olefinic proton resonance and the methyleneoxy proton resonances. It seems that chain end functionalization by this process is very efficient.

Conclusions

We thus conclude that pseudo-living polymerization behavior is obtained when acrylates are polymerized photochemically using organo(pyridinato)cobaloxime compounds as photoinitiator/mediators and that such polymerizations can be used for the synthesis of polymers with controlled end group functionality, block copolymers and polymers with star architectures. The polymerizations work best when chloroform is present and chloroform may even be necessary for pseudo-living behavior to be obtained. This feature of the polymerizations is not understood and requires further investigation.

Chain transfer accompanies these reactions and is especially significant at low monomer/organocobalt ratios. This behavior stands in marked contrast to the results obtained when cobalt porphyrins are used as mediators for thermal polymerizations of acrylates and chain transfer is insignificant. (9-11) This suggests that it may be possible to diminish the amount of chain transfer by changing the equatorial ligand present in the organocobalt compound.

Acknowledgments

The authors are grateful to PPG Industries, Inc., The B.F. Goodrich Company, and The Edison Polymer Innovation Corporation for supporting this study. The Rubber Division of the American Chemical Society awarded Labros D. Arvanitopoulos the Paul J. Flory Graduate Fellowship for 1995. We are thankful for this support and honor.

Literature Cited

1. Enikolopyan, N. S.; Smirnov, B. R.; Ponomarev, G. V.; Belgovskii, I. M. *J. Polym. Sci.: Polym. Chem. Ed.* **1981**, *19*, pp. 879.
2. Smirnov, B. R.; Plotnikov, V. D.; Ozerkovskii, B. V.; Roshchupkin, V. P.; Yenikolopyan, N. S. *Polymer Science U.S.S.R.* **1981**, *23(11)*, pp. 2807.
3. Burczyk, A. F.; O'Driscoll, K. F.; Rempel, G. L. *J. Polym. Sci.: Polym. Chem. Ed.* **1984**, *22*, pp. 3255.
4. Abbey, K. J.; Carlson, G. M.; Masola, M. J.; Trumbo, D. L. *Polymeric Materials, Science and Engineering Proceedings* **1986**, *55*, pp. 235.
5. Davis, T. P.; Haddleton, D. M.; Richards, S. N. *J. Macromol. Sci., Rev. Macromol. Physics* **1994**, *C3*, pp. 243.
6. Arvanitopoulos, L. D.; Greuel, M. P.; Harwood, H. J. *Amer. Chem. Soc., Div. Polym. Chem., Preprints* **1994**, *35(2)*, pp. 549.
7. Arvanitopoulos, L. D.; King, B. M.; Huang, C.-Y.; Harwood, H. J. *Amer. Chem. Soc., Div. Polym. Chem., Preprints* **1997**, *38(1)*, pp. 752.
8. Greuel, M. P.; Arvanitopoulos, L. D.; Harwood, H. J. *U.S. Patent* **5,468,785** Nov. 21, 1995.
9. Fryd, M.; Wayland, B. B.; Poszmik, G.; Mukerjee, S. L. *J. Amer. Chem. Soc.* **1994**, *116*, pp. 7343.

10. Wei, M.; Wayland, B. B.; Fryd, M. *Amer. Chem. Soc., Div. Polym. Chem., Preprints* **1997**, *38(1)*, pp. 681.
11. Wayland, B. B.; Mukerjee, S. L.; Poszmik, G.; Woska, D. C. *Amer. Chem. Soc., Div. Polym. Chem., Preprints* **1997**, *38(1)*, pp. 742.
12. Schrauzer, G. N.; Kohnle, J. *Chem. Ber.* **1964**, *97*, pp. 3056.
13. Schrauzer, G. N.; Sibert, J. W.; Windgassen, R. J. *J. Amer. Chem. Soc.* **1966**, *88*, pp. 3738.
14. Giannotti, G.; Merle, G.; Bolton, J. R. *J. Organomet. Chem.* **1975**, *99*, pp. 145.
15. Schrauzer, G. N. *Acc. Chem. Res.* **1968**, *1*, pp. 97 and references listed therein.
16. Dodd, D.; Johnson, M. D. *Organomet. Chem. Rev.* **1973**, *52*, 1.
17. Daikh, B. E.; Finke, R. G. *J. Amer. Chem. Soc.* **1992**, *114*, 2938.
18. Patel, U.F.; Pattenden, G. *J. Chem. Soc., Perkin Trans.* **1990**, *1*, 2703.

Controlled-Growth Free-Radical Polymerization of Methacrylate Esters: Reversible Chain Transfer versus Reversible Termination

Graeme Moad^{1,3}, Albert G. Anderson², Frances Ercole¹, Charles H. J. Johnson¹,
Julia Krstina¹, Catherine L. Moad¹, Ezio Rizzardo¹,
Thomas H. Spurling¹, and San H. Thang¹

¹Commonwealth Scientific and Industrial Research Organization, Molecular Science, Private Bag 10, Clayton South MDC, Victoria 3169, Australia

²Central Research and Development, Dupont Experimental Station, Wilmington, DE 19880-0101

Several processes for controlled growth free radical polymerization are contrasted with respect to reaction mechanism and their particular advantages and limitations. Kinetic simulation is used to examine relationships between reaction conditions, the significance of various side reactions, and the evolution of molecular weight distribution. Expressions used to calculate molecular weights and polydispersities for the various mechanisms are reported

Alkoxyamine-initiated polymerizations of methacrylate esters give only low conversions (10-40%, dependent on particular nitroxide and reaction conditions). Polymerization ceases due to a build up in the nitroxide concentration and the initially formed alkoxyamine is ultimately converted to an unsaturated macromonomer. The conversion, molecular weight and polydispersity are determined by the rate and equilibrium constants and combination:disproportionation ratio associated with the nitroxide - propagating radical reaction.

Polymerization of methacrylate monomers in the presence of methacrylate macromonomers provides a viable method for controlled growth polymerization to high conversions. However, narrow polydispersities are difficult to achieve by solution polymerization due to a slow rate of exchange between dormant and active propagating species.

A perusal of the recent literature in the field of polymer chemistry will bear witness to a marked resurgence of activity in the study of free-radical polymerization processes. This resurgence can be traced back to several major advances in our ability to control and predict the outcome of free radical polymerizations (1). Syntheses of narrow polydispersity polymers, block copolymers, gradient copolymers and other products of controlled-growth polymerization, once thought to be at odds with the nature of free-radical polymerization mechanisms, are now possible (1-8). Furthermore, as

³Corresponding author

techniques continue to be refined we can easily envisage how free-radical polymerization may soon become the preferred route to such structures.

In this paper we contrast several processes that have been developed for controlled-growth free radical polymerization and discuss their application to the synthesis of narrow polydispersity polymers based on methacrylic monomers pointing out their particular advantages and limitations. Kinetic simulation has been used to explore the relationships between reaction conditions, the extent and significance of various side reactions, and the evolution of the molecular weight distribution and to gain further understanding of the polymerization mechanisms.

Controlled-growth polymerization is usually considered synonymous with living polymerization (9). The keys to the development of processes for radical polymerization with living characteristics are methods which reduce the significance of processes which irreversibly terminate polymer chains with respect to that observed in conventional free radical polymerization. Two processes most important in this context are: termination by the bimolecular reactions of radical species (*i.e.* combination, disproportionation); and termination by chain transfer (to monomer, solvent, *etc.*). Three strategies (not mutually independent) should be considered in this regard.

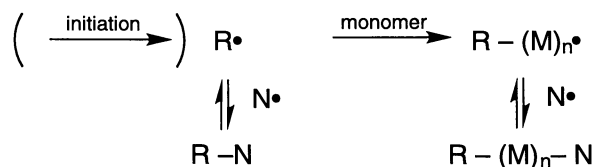
The first strategy is to limit the concentration of radical species so as to reduce the importance of radical-radical reactions. This involves providing a mechanism whereby some of the chains are held in a dormant state and providing an effective means for equilibration between active and dormant chains. Three mechanisms for achieving this will be considered in the following discussion: (a) reversible termination; (b) reversible atom or group transfer; and (c) reversible chain transfer

A second strategy is to modify the inherent reactivity of the propagating radicals such that propagation is preferred over the above-mentioned chain termination reactions (1). It has been suggested that some of the reagents currently used in controlled-growth radical polymerization may achieve this sought after goal by complexation of the propagating radical. However, there are currently no unequivocal examples of this behavior. The literature on template polymerization can also be consulted in this context (10). However, these methods do not have general application. We have previously been pointed out that the chain length distribution of the propagating radicals in controlled-growth free radical polymerizations is quite different to that in conventional radical polymerization. (11) In particular, depending on the particular mechanism (see below) there are no or relatively few short chain radicals. This should mean that the rate of radical-radical termination in controlled-growth free radical polymerization is lower than it is in the conventional process.

A third strategy is to choose reaction conditions such that the kinetic chain length, imposed by irreversible termination processes, is substantially higher than the chain length required for the polymeric product (11).

Mechanisms

(a) Reversible Termination. The first process we wish to consider is controlled radical polymerization based on a reversible termination step (Scheme 1) (1, 3-5).



Scheme 1

The first examples of this methodology appeared more than fifteen years ago (12) and a wide variety of reagents have now been utilized in this context. The process relies on the use of a reagent (N^\bullet) which reversibly caps the propagating species ($R-(M)_n^\bullet$) by radical-radical combination. Reagents that have been employed include various stable radicals, for example:

N^\bullet = nitroxides (5, 13-22)
 di- or triarylmethyl radicals (23-27)
 dithiocarbamyl radicals (12, 28-35)
 borinate radicals (36)
 verdazyl radicals (37)
 triazolanyl radicals (38)
 inorganic radicals (39)

and organometallic reagents, for example:

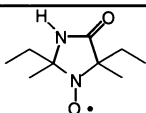
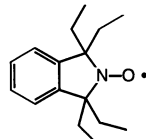
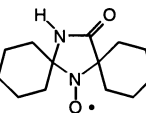
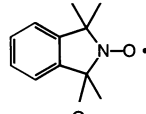
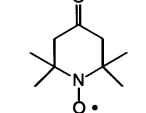
N^\bullet = square planar cobalt complexes (40-42)
 organo aluminum complexes (43, 44)

One of the most widely studied processes is alkoxyamine-initiated polymerization (in this case N^\bullet is a nitroxide) (13). However, while many papers have now appeared on the synthesis of narrow polydispersity polystyrene and derivatives (5, 16-22), relatively little has appeared on the synthesis of other polymers. In earlier reports (14, 15), we have shown that a major factor in the success of alkoxyamine-initiated polymerizations is the magnitude of the rate constants for alkoxyamine homolysis. Rate constants for the coupling of nitroxides with carbon centered radicals are high and may lie close to the diffusion controlled limit (19, 45-47). Thus, it is mainly the homolysis rate constant that determines the position of the equilibria and the rate of exchange between active and dormant propagating species. It is also important that the lifetime of the 'initiator' alkoxyamine is not substantially longer than those of the alkoxyamines formed during polymerization. We have also shown how the structure of the particular nitroxide and radical fragments determine the rate constant for alkoxyamine homolysis (15).

Ideally, the reaction between the propagating species and N^\bullet should occur exclusively by combination as shown in Scheme 1. A side reaction that can lead to chain death is disproportionation of the propagating species with N^\bullet (Scheme 2). This side reaction will limit conversion and block purity and lead to an increase in polydispersity. It has also been proposed (19, 48) that phenylethyl alkoxyamines may react by unimolecular elimination of hydroxylamine to yield the same products as would be produced by disproportionation. Although there is no literature precedent for the elimination process, based on the current experimental data, it is not possible to rigorously distinguish between these two mechanisms. It is also possible that both mechanisms operate simultaneously as appears to be the case in cobalt mediated polymerization (49, 50). For alkoxyamine-initiated polymerizations of styrene, the successful synthesis of narrow polydispersity and block copolymers indicates that, while formation of hydroxylamine is observed in some circumstances (51, 52), disproportionation (or elimination) is only a very minor pathway (19).

In the case of methacrylate polymerization, the importance of disproportionation is such that the alkoxyamines are converted after a relatively short polymerization time to the corresponding macromonomer and hydroxylamine (refer Scheme 2).

Table I. Molecular Weight/Conversion Data for Polymerizations (90°C, bulk) of Methyl Methacrylate in the Presence of Various Nitroxides.^a

Nitroxide (N•)	\bar{M}_n^b	\bar{M}_w/\bar{M}_n	Conv. %	[nitroxide]	[initiator] ^c	calc. \bar{M}_n^d
				M	M	
	35700	1.57	38.2	0.0077	0.0054	36800
	33800	1.65	35.8	0.0069	0.0054	34500
	20400 ^e	1.70	19.2	0.0077	0.0054	18500
	18300	1.71	18.4	0.0079	0.0054	17400
	5600	1.68	6.9	0.0115	0.0054	5900
	6500	1.44	6.4	0.0077	0.0049	6100
	10500	2.24	11.2	0.0076	0.0054	10800
	17000	3.30	17.5	0.0077	0.0054	16900
	22100	3.11	14.3	0.0076	0.0054	13800
	19200	4.10	17.9	0.0076	0.0054	17200

^a Reaction mixtures were placed in an ampoule, degassed with three freeze-thaw-evacuate cycles, and the ampoule sealed and heated in a constant temperature bath at the prescribed temperature. In each case a series of experiments was performed with reaction times between 0.5 and 6 hours

^b Molecular weights were determined by GPC and are given in polystyrene equivalents.

^c Initiator = azobis(2,4-dimethyl-2-pentanitrile).

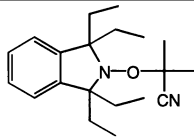
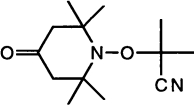
^d Calculated molecular weight based on an initiator efficiency of 90%. Values shown have been rounded to nearest hundred.

^e Reaction temperature = 100°C.

After less than 1 hour at 90°C, the reaction product is a MMA macromonomer (identified by ¹H NMR analysis in the case of lower molecular weight products) and the nitroxide moiety is largely converted into the corresponding hydroxylamine (indicated by a rapid formation of nitroxide on exposure of the reaction mixture to air). No further polymerization is observed for longer reaction times. Generally similar observations

(rapid polymerization followed by chain death) were made for experiments initiated by preformed alkoxyamines (see Table II).

Table II. Molecular Weight/Conversion Data for Polymerizations of Methyl Methacrylate in the Presence of Various Alkoxyamines.

Alkoxyamine	\bar{M}_n^a	\bar{M}_w/\bar{M}_n	Conv. %	[nitroxide] M	[alkoxyamine] M	Temp. °C
	13300	1.55	12.3	0	0.0108	80
	11100	1.66	14.4	0	0.0108	120
	13400	1.60	15.5	0.0001	0.0108	80
	11100	1.76	14.4	0.0001	0.0108	120
	5900	1.60	5.4	0	0.0108	120

^a Molecular weights were determined by GPC and are given in polystyrene equivalents.

Conversions, molecular weights and polydispersities depend on the particular nitroxide employed and its concentration. Even though the product is a “dead” polymer, the molecular weights obtained in these experiments are close to those expected based on the monomer conversion (see Figure 1).

A linear relationship between molecular weight and conversion is often quoted as an indication of living behavior. However, this observation only indicates that there are some living chains present in the system. As long as some living chains remain in the system and there are no other side reactions (*e.g.* transfer to monomer, solvent, *etc.*), the number average molecular weight is expected to vary in a linear way with conversion irrespective of the number of dead chains formed by radical-radical reactions. What this result does show is that the majority of chains are formed from the alkoxyamine and that there is no significant termination by chain transfer under the reaction conditions.

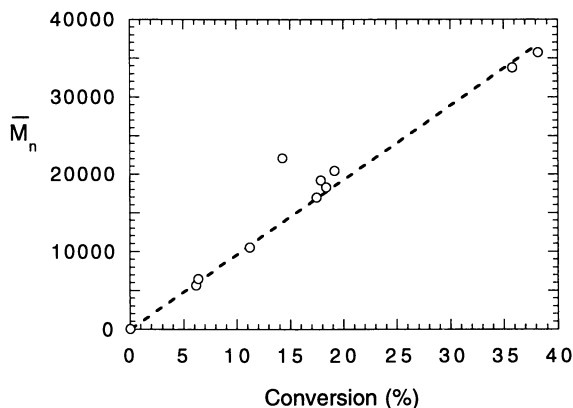
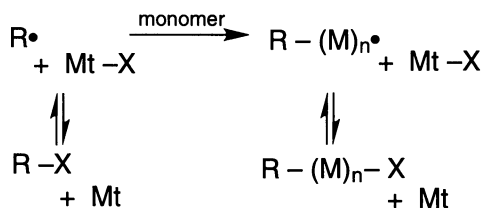


Figure 1. Molecular weights obtained in MMA polymerizations as a function of conversion. Data are from Table I. The dashed line indicates the molecular weight expected if the initiator efficiency is 90% (based on computer simulation).

We attribute the dependence of molecular weight, polydispersity and conversion on nitroxide structure to variations in the combination:disproportionation ratio and the association/dissociation equilibrium constant for the reaction between the MMA propagating species and the nitroxide. It is likely that the same factors which lead to enhanced alkoxyamine homolysis rates also lead to an increase in the extent of disproportionation. This effect is explored in more detail below.

It should be noted that the product of alkoxyamine-initiated polymerization of MMA is a macromonomer which will be reactive under the polymerization conditions (see section on reversible chain transfer below).

(b) Reversible Atom or Group Transfer. A second mechanism for controlled growth polymerization involves a reversible termination of the initiating or propagating species by transfer of an atom or group (X) from a metal complex (Mt-X) (2, 53-60). Examples of X include halogen and thiocyanate. The use of metal complexes based on ruthenium (2, 57-59), copper (53-56), and nickel (60) has been reported. Reaction mechanisms have not been fully elucidated. However, according to the most widely accepted mechanism (Scheme 3) this process can be considered analogous to that described above except that the propagating radical is converted to a dormant species by atom or group transfer rather than by radical-radical coupling. A further difference is that reactivation is a bimolecular process. In principle, only a very small concentration of the metal complex is required (equal to that of the propagating radical concentration). However, it has been found that much larger amounts are required. Typically concentrations of metal complex are of the same order of magnitude as the 'initiator' (R-X).



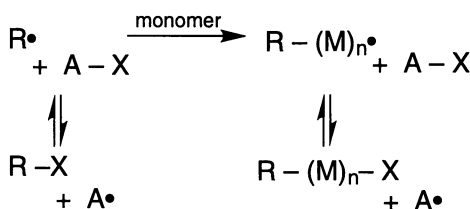
Scheme 3

According to this mechanism, since the chain equilibration process does not involve a radical-radical reaction, the complication of irreversible disproportionation competing with reversible termination is avoided. However, other side reactions (elimination of X from R-(M)_n-X, reaction with the metal complex by electron rather than ligand transfer) may be possible but have not been reported as complications. Requirements for the minimization of chain transfer and the self reaction of propagating species would still apply.

The process has been successfully applied to the synthesis of narrow polydispersity methacrylate polymers and block copolymers based on these as precursor materials (56, 58).

(c) Reversible (degenerative) chain transfer. A third method for achieving controlled-growth radical polymerization is based on reversible chain transfer (refer Scheme 4). The species A-X is a transfer agent which reacts with initiating (R•) or

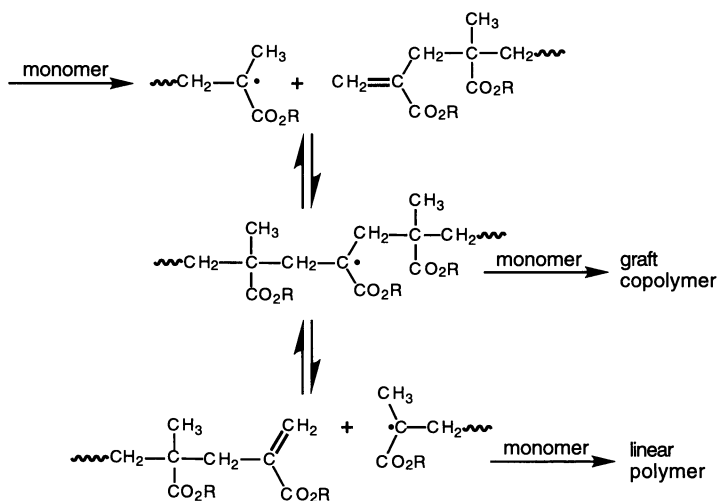
propagating radicals ($R-(M)_n^\bullet$) to give another transfer agent ($R-X$, $R-(M)_n-X$) and a species capable of initiating polymerization (A^\bullet). The rate of exchange between active (A^\bullet , R^\bullet , $R-(M)_n^\bullet$) and dormant species ($R-X$, $R-(M)_n-X$, $A-X$) is determined by the transfer constants of the species $A-X$ (and $R-X$, $R-(M)_n-X$) and the relative concentrations of these species vs monomer. This process has been termed degenerative chain transfer (61-63).



Scheme 4

In the processes (a) and (b) described above no external source of free radicals is required; even though such may in some circumstances control the rate of polymerization (21, 55). In controlled-growth radical polymerization based on reversible chain transfer, polymerization must, like conventional free-radical polymerizations, be continuously initiated by a source of free radicals.

The mechanism of chain transfer may be homolytic substitution. Certain alkyl iodides ($X=I$) have been shown to give this form of reversible chain transfer (62). Alternatively, chain transfer may occur by an addition-fragmentation sequence (64) as is observed for macromonomers of general structure $CH_2=C(Z)CH_2(A)_n$ [where $(A)_n$ is a free-radical leaving group and Z is usually an activating group, *e.g.* CO_2R or Ph] (11, 65, 66). The mechanism of the chain transfer step is shown in Scheme 5. The transferred group (X) is then the $CH_2=C(Z)CH_2-$ moiety.



Scheme 5

It is important that the lifetime of the adduct radical formed by addition to the macromonomer is short with respect to the life time of propagating species (otherwise there will be retardation) and that it does not react with monomer (to form a graft copolymer) or other radical species (to give inhibition).

In the case of polymerizations involving only methacrylate esters, there is little if any retardation and graft copolymer formation is generally not observed. Even so, attention must be paid to reaction conditions. Since the transfer constants of methacrylate macromonomers are <0.5 (67), the [macromonomer]:[monomer] ratio needs to be maintained as high as possible so as to maximize transfer events. This can be achieved through the use of starved feed conditions (11).

Initiation rates should be maintained as low as practicable consistent with obtaining an acceptable rate of polymerization since radical-radical reaction produces non-macromonomer (dead) chains (*i.e.* long kinetic chain lengths are essential).

Bearing these constraints in mind, the conditions that lead to narrow polydispersity polymers are most readily achieved by emulsion polymerization. Emulsion polymerizations can be performed at much lower [monomer]:[macromonomer] ratios than is possible in conventional bulk or solution polymerizations. The process is illustrated in Figure 2 for the synthesis of poly(2-ethyl hexyl methacrylate-*block*-methyl methacrylate) (11). The emulsion polymerization of 2-ethylhexyl methacrylate in the presence of a MMA macromonomer (\bar{M}_n 2040 and \bar{M}_w/\bar{M}_n 1.68) was carried out under feed conditions with the 2-ethylhexyl methacrylate added over 3.9 hours at a rate such that the instantaneous conversion was $> 95\%$. Polydispersities were observed to decrease with conversion while molecular weights increase linearly with conversion.

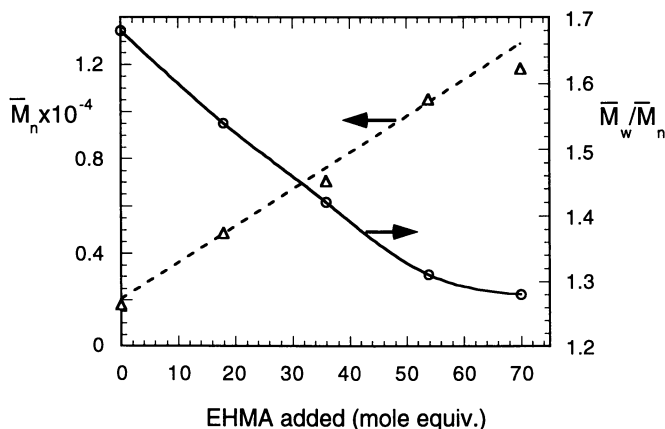


Figure 2. Evolution of molecular weight (—, ○) and polydispersity (---, △) with monomer addition for the emulsion polymerization of 2-ethylhexyl methacrylate in the presence of a MMA macromonomer. The dashed line is the expected molecular weight calculated from the monomer and macromonomer concentrations (11).

Notwithstanding these comments, controlled growth polymerizations, including the synthesis of block copolymers, can and has been successfully carried out by solution to yield block copolymers (11, 66). However, it is generally not possible to achieve the very narrow polydispersities or the high molecular weights that can be achieved by

emulsion polymerization. A typical GPC trace for a solution polymer is shown in Figure 3. The example is for MMA block copolymer based on a hydroxyethyl methacrylate macromonomer. The synthesis of this material has been detailed elsewhere (11). The factors that determine polydispersity and block/macromonomer purity in solution polymerizations are discussed in greater detail below.

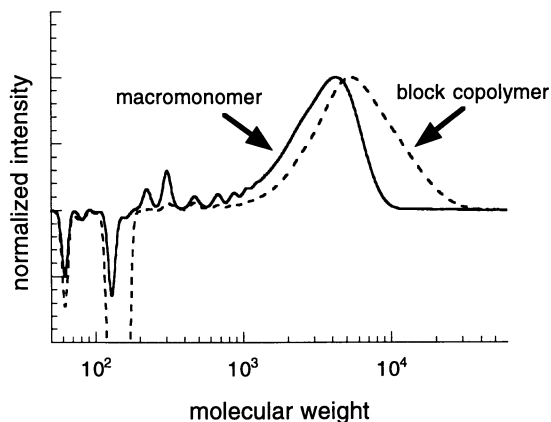


Figure 3. GPC Traces of hydroxethyl methacrylate macromonomer (\bar{M}_n 1230, \bar{M}_w/\bar{M}_n 2.5) (—) and poly(hydroxyethyl methacrylate-block-MMA) (\bar{M}_n 3620, \bar{M}_w/\bar{M}_n 1.83) (- - -) prepared by solution polymerization.

Kinetic Simulation of Controlled-Growth Free-Radical Polymerization

There have been a number of studies on kinetic simulation of living radical polymerization processes (14, 19, 68, 69). In 1990 we (14) reported a study of the alkoxyamine-initiated polymerization which demonstrated the potential of this chemistry (13) for the production of narrow polydispersity polymers. The simulation method involved the use of numerical integration to solve the complete set of differential equations which result from analysis of the reaction mechanism. This approach offers significant advantages. It is rigorous in being able to provide the time evolution for all species and processes involved in the polymerization process and it is simple to implement. Limitations arise because it is necessary, due to the way that the simulation time increases rapidly with the number of species included, to treat all those with chain length above some cut-off value as composite species. This cut off is in the range 200-1000 monomer units depending on the number and type of polymeric species included in the simulation. For example, the simulation can be speeded up by leaving out termination by combination and assuming that all radical-radical termination is by disproportionation. Such approximations which limit the accuracy of the simulation should be avoided. Another method for improving calculation efficiency is to treat all 'dead' species (from combination, disproportionation, transfer) together as a single distribution. This does not limit the accuracy of the simulation but does reduce the information content.

The original simulations (14) were carried out with use of a supercomputer. Advances in machine speed and programming efficiency mean that simulations of a

similar size can now be carried out on a workstation or one of the more powerful personal computers and somewhat larger calculations can be carried out on supercomputers. Nonetheless, the limitations still apply.

Very recently, Greszta and Matyjaszewski (19) reported the application of the PREDECI program (70) to study alkoxyamine-initiated polymerization of styrene. The PREDECI program overcomes the problem of having to treat high molecular weight species as a composite species by application of a Galerkin method to model molecular weight distributions (70). Work published to date indicates that this method is well suited to these simulations. However, the programming task associated with implementing the method is relatively complex and the commercial package is currently priced out of the reach of many users.

Application of the Method of Moments. Veregin *et al.* (68) and Yan *et al.* (69) have reported on modeling 'living' free-radical polymerization by adapting a method developed by Mueller *et al.* (61, 63, 71) for the study of living group transfer and cationic polymerizations. In these works, polydispersities were evaluated using a method of moments and Veregin *et al.* (68) have indicated that they can predict those observed in alkoxyamine-initiated polymerization of styrene. However, their approach is based on a simplified reaction mechanism which neglects *all* side reactions (including radical-radical termination or propagating species, chain transfer, *etc.*). Thus, while, the method appears useful in predicting polydispersities for some systems and may be valuable as a method for preliminary parameter estimation, it is limited in its application. The effects of the various side reactions cannot be readily assessed and no information on the time scale of the polymerization process is obtained.

In this work we show that, given the full mechanism and the associated kinetic parameters, the time-evolution of the molecular weights and polydispersities of polymers formed by polymerization processes can be accurately modeled by applying the method of moments. Expressions for moments of the molecular weight distribution for the polymeric species involved in conventional radical polymerization involving initiation, propagation, termination by (irreversible) combination or disproportionation, and (irreversible) chain transfer have appeared in the literature. The contributions to the moment expressions for the polymeric species involved in the various pathways associated with controlled growth free-radical polymerization can be simply derived and are reported below for the three mechanisms described above. It should be noted that the contributions due to the various reaction pathways associated with a polymerization are additive and thus can simply be summed as follows:

$$\begin{aligned} \frac{d\mu_x(P_n^\bullet)}{dt} &= \left(\Delta \frac{d\mu_x(P_n^\bullet)}{dt} \right)_{\text{initiation}} + \left(\Delta \frac{d\mu_x(P_n^\bullet)}{dt} \right)_{\text{propagation}} \\ &+ \left(\Delta \frac{d\mu_x(P_n^\bullet)}{dt} \right)_{\text{transfer}} + \left(\Delta \frac{d\mu_x(P_n^\bullet)}{dt} \right)_{\text{termination}} \\ &+ \left(\Delta \frac{d\mu_x(P_n^\bullet)}{dt} \right)_{\text{reversible termination}} + \dots \end{aligned}$$

These differential equations are readily solved by numerical integration.

In this preliminary study, we have assumed that all steps are chain length independent. This does not mean the chain length dependence of radical-radical termination and other steps is considered unimportant (*vide infra*). The full derivation

of these expressions and the derivation of expressions for the case where the rate constants are dependent on chain length will be reported elsewhere (72).

Moment expressions (a) Reversible Termination. In the case of alkoxyamine-initiated polymerization N^\bullet is a nitroxide.

Reaction		Rate constant
$P_n^\bullet + N^\bullet$	$\rightarrow P_nN$	k_{Nc}
P_nN	$\rightarrow P_n^\bullet + N^\bullet$	k_{-Nc}

Contributions to moments:

$$\Delta \frac{d\mu_x(P_n^\bullet)}{dt} = -k_{Nc} [N^\bullet] \mu_x(P_n^\bullet) + k_{-Nc} \mu_x(P_nN)$$

$$\Delta \frac{d\mu_x(P_nN)}{dt} = k_{Nc} [N^\bullet] \mu_x(P_n^\bullet) - k_{-Nc} \mu_x(P_nN)$$

The molecular weight of the group N is assumed to be negligible.

We also need to consider two side reactions. Namely, disproportionation between P_n^\bullet and N^\bullet and the reaction of the product of disproportionation (NH) with P_n^\bullet . In the case of alkoxyamine-initiated polymerization NH is a hydroxylamine.

Reaction		Rate constant
$P_n^\bullet + N^\bullet$	$\rightarrow P_n^d + NH$	k_{Nd}
$P_n^\bullet + NH$	$\rightarrow P_n^d + N^\bullet$	k_{NH}

Contributions to moments:

$$\Delta \frac{d\mu_x(P_n^\bullet)}{dt} = -k_{Nd} [N^\bullet] \mu_x(P_n^\bullet) - k_{NH} [NH] \mu_x(P_n^\bullet)$$

$$\Delta \frac{d\mu_x(P_n^d)}{dt} = k_{Nd} [N^\bullet] \mu_x(P_n^\bullet) + k_{NH} [NH] \mu_x(P_n^\bullet)$$

Another side reaction that has been postulated to complicate some systems is the unimolecular elimination of NH to give dead polymer.

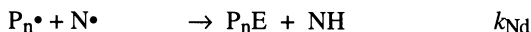
Reaction		Rate constant
P_nN	$\rightarrow P_n^d + NH$	k_{-Ne}

Contributions to moments:

$$\Delta \frac{d\mu_x(P_nN)}{dt} = -k_{-Ne} \mu_x(P_nN)$$

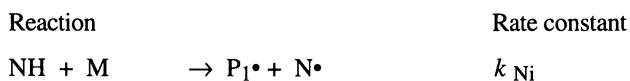
$$\Delta \frac{d\mu_x(P_n^d)}{dt} = k_{-Nc}\mu_x(P_nN)$$

In the case of polymerizations involving methacrylic monomers the product formed by disproportionation with N^\bullet is a macromonomer which may react further (see (d) below). The disproportionation reaction should therefore be written as follows:



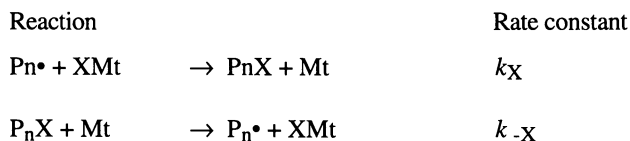
This pathway has not been included in the current simulations. For low conversion polymerizations, the consumption P_nE should be small.

A further reaction that may be considered is the donation of a hydrogen by NH to monomer to initiate a new chain. This reaction is of importance when N is a cobaloxime.



$$\Delta \frac{d\mu_x(P_n^\bullet)}{dt} = k_{Ni}[NH][M]$$

(b) Reversible Atom Transfer. An example is atom transfer polymerization (X=halogen, Mt=metal complex).



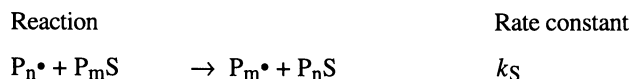
Contributions to moments:

$$\Delta \frac{d\mu_x(P_n^\bullet)}{dt} = -k_X [XMt]\mu_x(P_n^\bullet) + k_{-X} \mu_x(P_nX) [Mt]$$

$$\Delta \frac{d\mu_x(P_nX)}{dt} = k_X [XMt]\mu_x(P_n^\bullet) - k_{-X} \mu_x(P_nX) [Mt]$$

The molecular weight of the group X is assumed to be negligible.

(c) Reversible Chain Transfer. An example is transfer to iodo-compounds (S=iodine).



Contributions to moments:

$$\Delta \frac{d\mu_x(P_n^\bullet)}{dt} = k_S \{ \mu_x(P_n S) \mu_0(P_n^\bullet) - \mu_0(P_n S) \mu_x(P_n^\bullet) \}$$

$$\Delta \frac{d\mu_x(P_n S)}{dt} = -k_S \{ -\mu_x(P_n S) \mu_0(P_n^\bullet) + \mu_0(P_n S) \mu_x(P_n^\bullet) \}$$

The molecular weight of the group S is assumed to be negligible.

(d) Reversible Chain Transfer by Addition-Fragmentation. An example is transfer to methacrylate macromonomers (E=methacrylate unit).

Reactions		Rate constant
$P_n^\bullet + P_m E$	$\rightarrow A_{(n,m)}^\bullet$	k_E
$A_{(n,m)}^\bullet$	$\rightarrow P_m^\bullet + P_n E$	k_{-E1}
$A_{(n,m)}^\bullet$	$\rightarrow P_n^\bullet + P_m E$	k_{-E2}

The molecular weight of the group E is assumed to be negligible in deriving the moment equations. In this treatment, two independent moment expressions are associated with the adduct A. Experimental data suggest that, while the rate constants k_E show some chain length dependence for $n, m < 4$ (67), for chain lengths $n, m \geq 4$, $k_{-E1} = k_{-E2} = \text{constant} (= k_{-E})$. The moment expressions become somewhat more complex if the rate constant k_E is chain length dependent (72).

Contributions to moments:

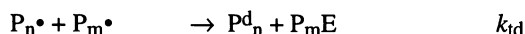
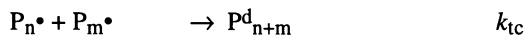
$$\frac{d\mu_x(P_n^\bullet)}{dt} = 0.5k_{-E}\mu_x(A_{(n,i)}^\bullet) + 0.5k_{-E}\mu_x(A_{(i,n)}^\bullet) - k_E \mu_0(P_n E)\mu_x(P_n^\bullet)$$

$$\frac{d\mu_x(P_m E)}{dt} = 0.5k_{-E}\mu_x(A_{(n,i)}^\bullet) + 0.5k_{-E}\mu_x(A_{(i,n)}^\bullet) - k_E \mu_x(P_n E)\mu_0(P_n^\bullet)$$

$$\frac{d\mu_x(A_{(n,i)}^\bullet)}{dt} = -k_{-E} \mu_x(A_{(n,i)}^\bullet) + k_E \mu_0(P_n E)\mu_x(P_n^\bullet)$$

$$\frac{d\mu_x(A_{(i,n)}^\bullet)}{dt} = -k_{-E}\mu_x(A_{(i,n)}^\bullet) + k_E \mu_x(P_n E)\mu_0(P_n^\bullet)$$

It should also be noted that methacrylate macromonomers have an identical structure to the unsaturated product from termination by disproportionation. Ideally, this should be taken into account when defining the products of the latter reaction. Thus:



Computation Procedure. The moment calculations were performed within a few minutes computation time on a Macintosh LC630 computer. The program to solve the differential equations was written in Language Systems Fortran version 1.2 (Fortner Research) and the NAG library subroutine D02EBE was used to perform numerical integration. Simulations of full molecular weight distributions were performed on a Cray YMP4e computer.

Kinetic Simulations of Methyl Methacrylate Polymerizations

The value of kinetic simulation will be illustrated by its application to two systems:

- The polymerizations of MMA in the presence of 1,1,3,3-tetraethylisindolin-N-oxyl for which the experimental data are shown in Tables I and II. The aims are to estimate the magnitude of the equilibrium constant (k_{-N}/k_{Nc}) associated with the reaction between the nitroxide and the MMA propagating radical and the relative importance of combination and disproportionation associated with this process (k_{Nc}/k_{Nd}).
- The polymerization of MMA in the presence of a transfer agent which gives reversible chain transfer. The aim is to establish the relationship between the magnitude of the transfer constant and the time-evolution of the polydispersity.

The main problem associated with any kinetic simulation is in choosing reasonable values of the rate constants. This is particularly a problem in the case of alkoxyamine initiated polymerization where few of the necessary rate constants have been measured directly.

Alkoxyamine-Initiated Polymerization. The following rate constants (Table III) taken from the literature have been used to describe MMA polymerization at 90°C with azobis(2,4-dimethyl-2-pentanitrile) as initiator.

Table III. Kinetic Parameters Used in Simulations

Reaction	Rate Constant	Value	Ref.
propagation	k_p	$1.16 \times 10^3 \text{ M}^{-1} \text{ s}^{-1}$	(73, 74)
termination	k_t	$3.70 \times 10^8 \text{ M}^{-1} \text{ s}^{-1}$	(74)
	k_{tc}/k_{td}	0.3	
initiator decomposition	k_d	$2.92 \times 10^{-2} \text{ s}^{-1}$	(75)
initiator efficiency	f	0.9	

No initiator efficiency data for azobis(2,4-dimethyl-2-pentanitrile) has been reported. The value of 0.9 at 90°C was chosen so as to provide agreement between expected and found molecular weights. The current simulations do not include such processes as transfer to monomer, macromonomer, etc.

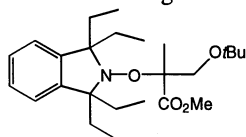
In order to choose appropriate values for the other kinetic parameters associated with alkoxyamine initiated polymerization, the effect of these rate constants on

molecular weight, polydispersity and polymerization rate was explored by kinetic simulation.

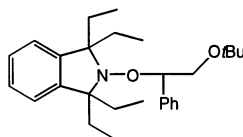
(a) Combination of Nitroxide and Propagating Radical (k_{NC}). Known rate constants for the reaction between simple alkyl radicals and nitroxides approach the diffusion controlled limit $ca\ 10^9\ \text{M}^{-1}\ \text{s}^{-1}$ at $18\ ^\circ\text{C}$ (45-47) while that for benzyl radicals is an order of magnitude lower at $ca\ 10^8\ \text{M}^{-1}\ \text{s}^{-1}$ at $18\ ^\circ\text{C}$ (47). The activation energy is reported to be small though non-zero (46). Rate constants also vary with the nature of the nitroxide and have some dependence on solvent (46). The rate constant for coupling of 2,2,6,6-tetramethylpiperidin-N-oxyl with polystyryl radicals has been estimated to be $ca\ 10^8\ \text{M}^{-1}\ \text{s}^{-1}$ at 120°C (19).

On this basis, k_{NC} at $90\ ^\circ\text{C}$ is likely to have a value in the range 10^7 to $10^8\ \text{M}^{-1}\ \text{s}^{-1}$.

(b) Alkoxyamine homolysis ($k_{\text{-N}}$). Few values of rate constants for alkoxyamine dissociation have been reported (15). For polystyryl radicals the dissociation rate is thought to be $ca\ 10^{-4}\ \text{s}^{-1}$ at 120°C (19). On the basis of the known dissociation rate for simple models (15), $k_{\text{-N}}$ for the MMA propagating species is likely to be several orders of magnitude higher (15).



$k_{\text{-N}}\ ca\ 2 \times 10^{-4}\ \text{s}^{-1}$ at 60°C



$k_{\text{-N}}\ < 2 \times 10^{-5}\ \text{s}^{-1}$ at 80°C

On this basis, values for $k_{\text{-N}}$ at $90\ ^\circ\text{C}$ in the range 10^{-2} to $10^0\ \text{s}^{-1}$ seem reasonable.

(c) Equilibrium Constant ($K = k_{\text{-N}}/k_{\text{NC}}$). The simulations show that the equilibrium constant $k_{\text{-N}}/k_{\text{NC}}$ rather than the absolute value of the rate constants will determine the polymerization kinetics over the timescale of interest. An example of how the molecular weight decreases and polydispersity increases as K increases is shown in Figure 4. Similar data are obtained from simulations where $k_{\text{-N}}$ is in the range 10^{-1} - $10^1\ \text{s}^{-1}$. Other rate constants used in the simulation are as shown in Table III and [monomer] = 8.68 M, [initiator] = 0.0055 M, [nitroxide] = 0.0115 M and a reaction time of 6 hours.

(d) Disproportionation Combination Ratio ($k_{\text{Nd}}/k_{\text{NC}}$). Early work carried out with TEMPO derivatives at lower temperatures (60°C) under conditions where trapping is essentially irreversible suggest that the extent of disproportionation with nitroxides (2,2,6,6-tetramethylpiperidin-N-oxyl, 1,1,3,3-tetramethylisodolin-N-oxyl) should be small ($\ll 2\%$) since these products are not observed (76). The predicted dependence of the degree of polymerization and polydispersity on $k_{\text{Nd}}/k_{\text{NC}}$ for a given reaction time (1 hour) and K (10^{-8}) is shown in Figure 5. As the extent of disproportionation ($k_{\text{Nd}}/k_{\text{NC}}$) increases, the molecular weight decreases and the polydispersity increases. Note that the value of k_{Nd} that gives rise to a particular molecular weight and polydispersity is constant for a given value of K (for $k_{\text{-N}}\ 10^{-2}$). Thus, the following rate constant combinations (Table IV) all give rise to a similar polymerization rate and product with similar polydispersity and degree of polymerization (the same within $<1\%$; other rate constants as shown in Table III;

[monomer] = 8.68 M, [initiator] = 0.0055 M, [nitroxide] = 0.0115 M and a reaction time of 6 hours).

Table IV. Rate Constant Combinations Giving Similar Polymerization Kinetics.

K M	k_{Nc} $M^{-1} s^{-1}$	k_{-N} s^{-1}	k_{Nd}/k_{Nc}	k_{Nd} $M^{-1} s^{-1}$
10^{-8}	10^7	0.1	0.006	6×10^4
10^{-8}	10^8	1	0.0006	6×10^4
10^{-8}	10^9	10	0.00006	6×10^4

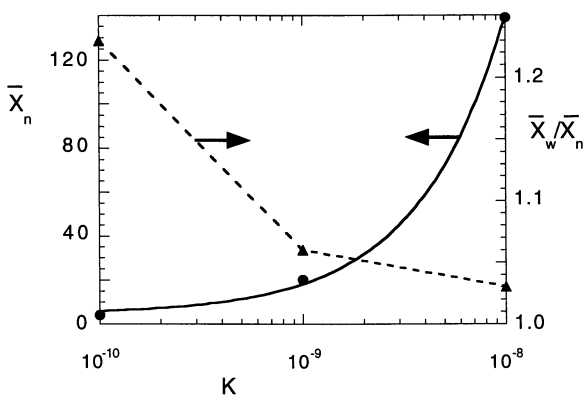


Figure 4. Results of simulations showing the dependence of the degree of polymerization (—) and polydispersity (---) on the equilibrium constant K . Reaction parameters given in text.

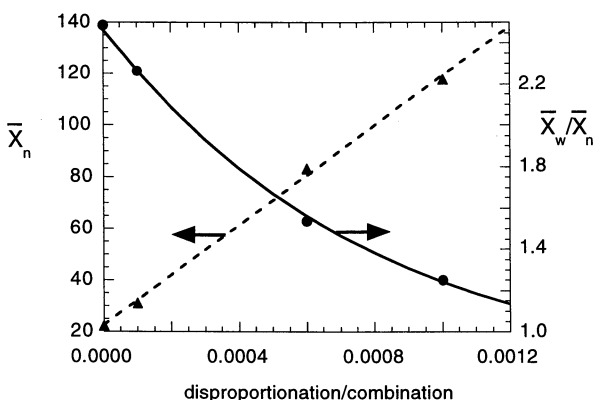


Figure 5. Results of simulations showing the dependence of the degree of polymerization (—) and polydispersity (---) on the disproportionation combination ratio k_{Nd}/k_{Nc} . Reaction parameters given in text.

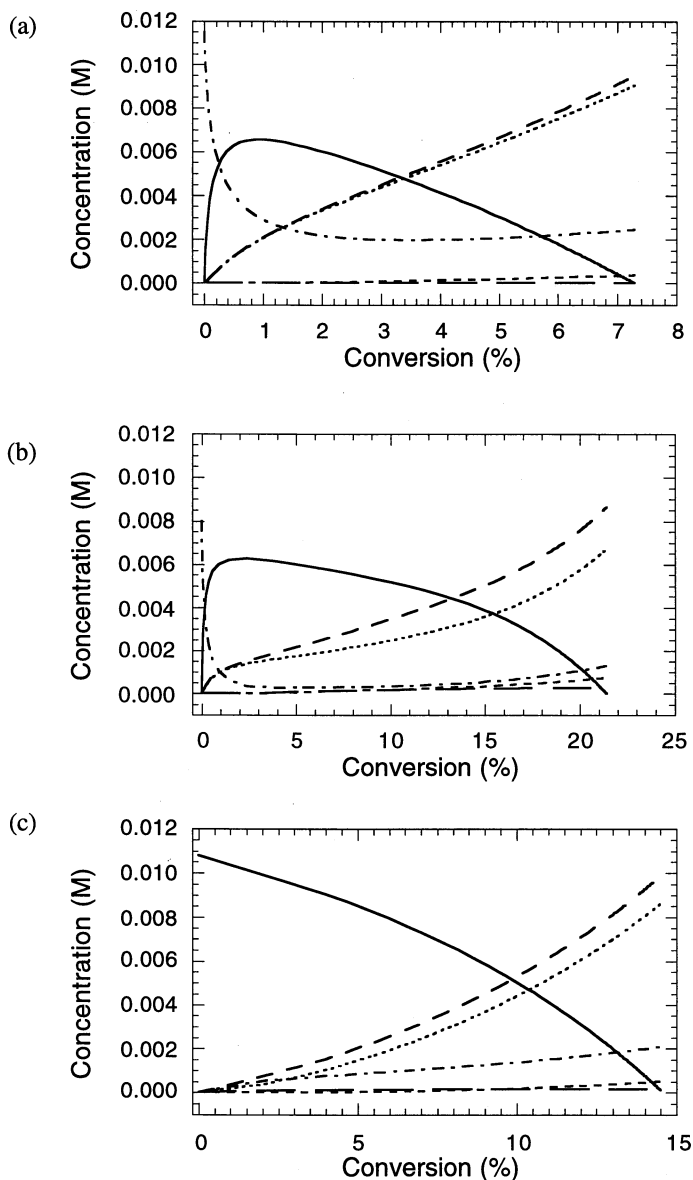


Figure 6. Variation in concentrations with conversion for alkoxyamine - P_nN (—), dead polymer formed by combination or disproportionation (— —), dead polymer formed by chain transfer to hydroxylamine (— — —), macromonomer from disproportionation with nitroxide (— · —), nitroxide (· · ·) and hydroxylamine (- - - -) for systems (a) 1, (b) 2 and (c) 3 described in Table V.

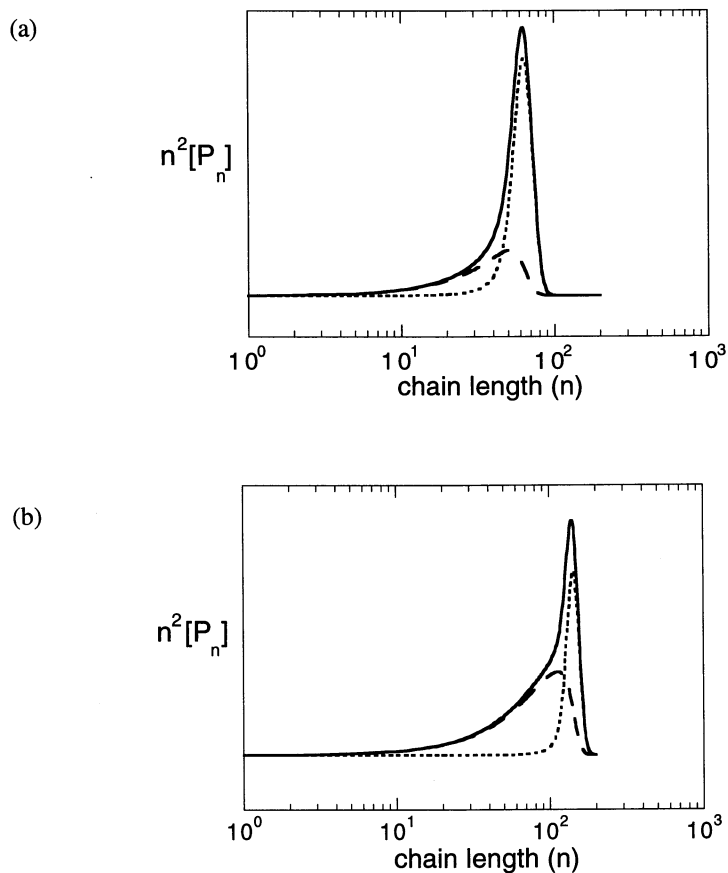


Figure 7. Calculated 'GPC traces' for polymerization system 1 (refer Table V) for (a) 0.5 and (b) 1 hour reaction time. Overall (—), alkoxyamine (- - -), dead polymer (- · - ·). Y axis in arbitrary concentration units.

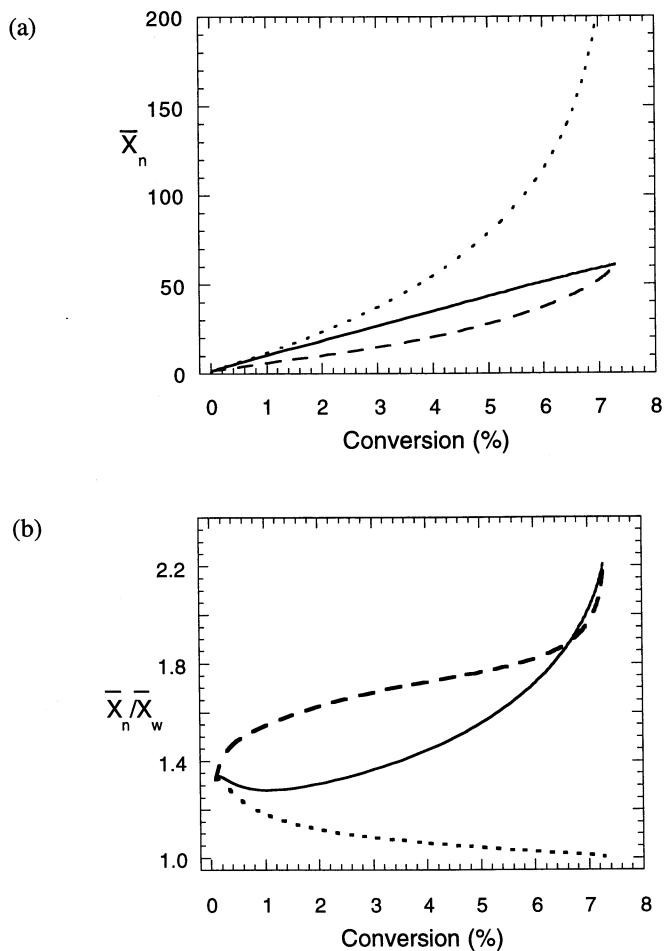


Figure 8 Evolution of (a) molecular weight and (b) polydispersity with conversion for polymerization system 1 (refer Table V). Total polymer (—), alkoxyamine (- - -), dead polymer (— — —).

Conclusions. Alkoxyamine initiated polymerizations of MMA, whether initiated by a mixture of nitroxide and initiator or by a preformed alkoxyamine, give low to moderate conversions of monomer (10–40%). The rate of polymerization slows due to the increase in the nitroxide concentration. This favors the propagating radical reacting with nitroxide at the expense of propagation. The alkoxyamine is ultimately converted to a MMA macromonomer and a hydroxylamine.

Even though the kinetic parameters found to fit the experimental data are possibly not unique, it is possible to reach some general conclusions on the factors controlling the nature of the product. For polymerizations involving 1,1,3,3-tetraethylisindolin-N-oxyl, the data are consistent with an equilibrium constant K of $ca\ 10^8\ M$. This compares with a value of $ca\ 10^{11}\ M$ estimated for styrene polymerization in the presence of 2,2,6,6-tetramethylpiperidin-N-oxyl (19). The higher K is most likely due to a faster rate of alkoxyamine homolysis for the MMA system. Chain death can be attributed to a disproportionation reaction between nitroxide and propagating radical. The extent of disproportionation relative to combination is estimated significantly less than 0.1%. At higher conversions, because of the higher nitroxide concentration, there is an increased probability of that propagating species will react with the nitroxide (reversibly by combination or irreversibly by disproportionation) rather than monomer.

It is found experimentally that the conversion, and molecular weight and polydispersity of the product strongly depend on the structure of the nitroxide involved. The narrowest polydispersities ($ca\ 1.5$) and highest conversions (approaching 40%) result from the use of 5-membered ring nitroxides. It is proposed that increased steric congestion about the C-O bond undergoing scission, which is an important factor in causing an increased rate of alkoxyamine homolysis, also results in an increase in the disproportionation:combination ratio for the reaction between nitroxide and propagating radical.

Lower combination:disproportionation ratios and lower values of K both result in increased polydispersities, reduced molecular weights, and lower conversions at chain death. A combination of these factors can rationalize the observed dependence of the polymerization kinetics on nitroxide structure (Table I). Further refinement of the kinetic parameters will follow from additional experimental data. In particular, measurements of concentrations of nitroxide and hydroxylamine during the experiment and a study of the short time behavior (prior to chain death) would be desirable.

Polymerization with Reversible Chain Transfer. The following rate constants (Table VII) taken from the literature have been used to describe MMA polymerization at 60°C.

Table VII. Kinetic Parameters Used in Simulations

Reaction	Rate constant	Value	Ref.
propagation	k_p	$0.67 \times 10^3\ M^{-1}\ s^{-1}$	(73, 74)
termination	k_t	$3.40 \times 10^8\ M^{-1}\ s^{-1}$	(74)
	k_{tc}/k_{td}	0.3	
initiator decomposition	k_d	$8.4 \times 10^{-6}\ s^{-1}$	(1)
initiator efficiency	f	0.7	
[macromonomer]		0.1 M	
[monomer]		8.91 M	
[initiator]		0.03 M	

Rate Constants associated with Reversible Chain Transfer. Recently, we have determined Arrhenius parameters for the various steps (*cf.* Scheme 4) associated with addition-fragmentation chain transfer involving MMA macromonomers in MMA polymerization (67). The value of k_E was found to be independent of chain length for chain lengths greater than 3 units and at 80°C should have a value of $2.7 \times 10^3 \text{ M}^{-1} \text{ s}^{-1}$. The value of k_{-E} could not be estimated precisely. However, the observation that these polymerizations showed no retardation with respect to polymerizations carried out in the absence of macromonomer suggests a value greater than 10^2 s^{-1} . As long as k_{-E} is above this value, it has no influence on molecular weights or on the polymerization kinetics.

Results of Simulations. The value of k_E/k_p determines the shape of the molecular weight distribution and the viability of narrow polydispersity polymer synthesis. In Figures 9-11 we indicate how the values of k_E/k_p determines the way in which the molecular weight, polydispersity and macromonomer purity evolve with conversion. The simulations are for a series of polymerizations described by the rate constants given in Table VII and with various values of k_E/k_p .

In order to obtain a linear molecular weight conversion profile and narrow polydispersities characteristic of living polymerization in a bulk polymerization of MMA, it is necessary that the value of k_E/k_p must be greater than 10 and approach 100. However, the overall molecular weight and the macromonomer purity at >95% conversion is the same for polymerizations with k_E/k_p greater 3. Thus, even though the products formed in polymerizations with relatively low k_E/k_p have a relatively broad polydispersities, the fraction of dead chains is small. This observation is of critical importance since it means that it is possible to prepare block copolymers and telechelics of reasonable purity using reagents with relative low k_E/k_p .

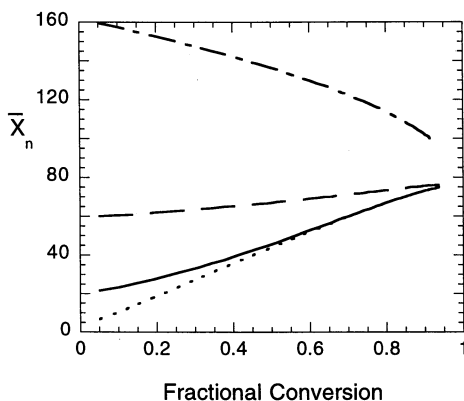


Figure 9. Dependence of degree of polymerization of polymer formed on conversion for system described by the rate constants shown in Table VII and with $k_E/k_p = 100$ (-----), $k_E/k_p = 10$ (—), $k_E/k_p = 3$ (— · —), $k_E/k_p = 1$ (· · · · ·).

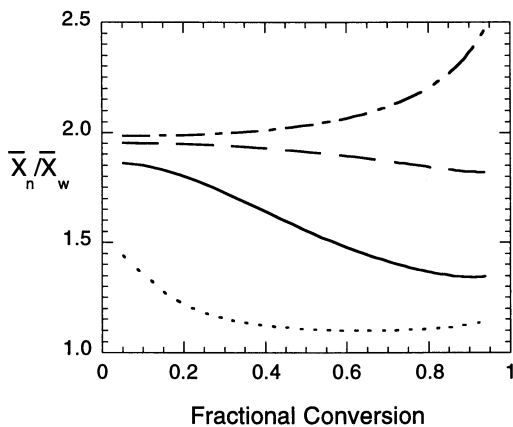


Figure 10. Dependence of polydispersity of polymer formed on conversion for system described by the rate constants shown in Table VII and with $k_E/k_p = 100$ (- - - -), $k_E/k_p = 10$ (—), $k_E/k_p = 3$ (— — —), $k_E/k_p = 1$ (— - —).

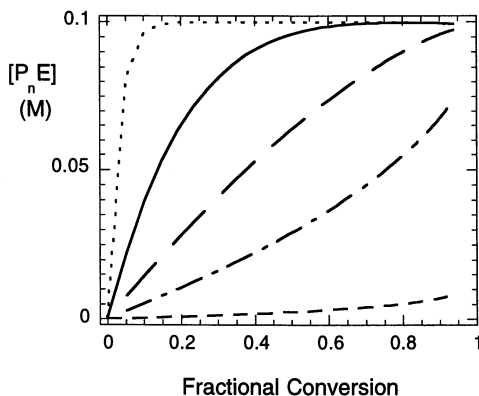


Figure 11. Dependence of concentration of the product macromonomer $[P_n E]$ on conversion for system described by the rate constants shown in Table VII and with $k_E/k_p = 100$ (- - - -), $k_E/k_p = 10$ (—), $k_E/k_p = 3$ (— — —), $k_E/k_p = 1$ (— - —). The concentration of dead polymer (- - - -) is independent of k_E/k_p .

The methacrylate macromonomers are characterized by having a value of k_E/k_P of < 1.0 (transfer constant < 0.5) (67). The resultant low rate of equilibration between active and dormant chains means that these reagents are not suited for use in batch polymerization processes. To use these reagents it is necessary to manipulate the reaction conditions so as to increase the rate of exchange between dormant and living polymer chains. The rate of exchange can be increased simply by reducing the monomer concentration relative to that of the macromonomer. It is then necessary to feed the monomer so as to obtain the desired molecular weight. It may also be necessary to use a reduced initiator concentration to keep the number of dead chains below at an acceptable level.

The predicted conversion dependence of the molecular weight and polydispersity for a polymer prepared in the presence of a macromonomer with $k_E/k_P = 0.8$ (other rate constants as summarized in Table VII) is shown in Figure 12. The following initial conditions were used in the polymerization: $[\text{monomer}]_0$ 0.891 M; $[\text{initiator}]_0$ 0.016 M; $[\text{macromonomer}]_0$ 0.1 M. The monomer and initiator were fed at a rate such that their concentrations were maintained at a near constant level. Even though the overall polydispersity remains broad throughout the polymerization (at *ca* 2.0), a linear molecular weight conversion profile is obtained (see Figure 12) and final macromonomer purity (fraction of 'living chains' = $[\text{total macromonomer}]/[\text{total polymeric species}]$) is $>70\%$ at 80% monomer conversion (see Figure 13). Conversion of the precursor macromonomer is predicted to be $>70\%$.

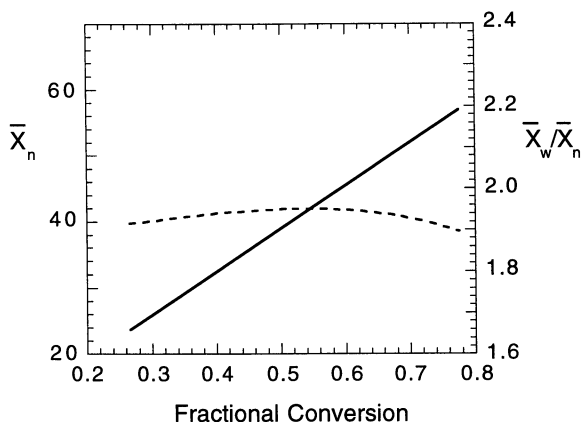


Figure 12. Predicted evolution of molecular weight (—) and polydispersity (---) as a function of monomer conversion during feed polymerization process. Reaction conditions given in text.

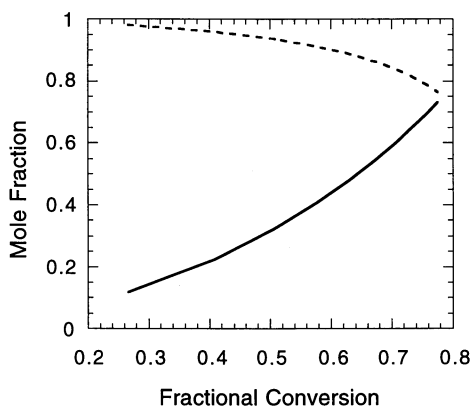


Figure 13. Predicted evolution of the conversion of macromonomer (—) and fraction of 'living' chains (- - - -) as a function of monomer conversion during feed polymerization process. Reaction conditions given in text.

Conclusions. Even though narrow polydispersities are difficult to achieve by solution polymerization due to a slow rate of exchange between dormant and active propagating species, polymerization of methacrylate monomers in the presence of methacrylate macromonomers provides a viable method for the synthesis of block copolymers. Success depends on the use of feed conditions to maximize the rate of exchange between dormant and active propagating species. That much narrower polydispersities can be achieved by emulsion polymerization can be attributed to the fact that it is possible to utilize much lower instantaneous monomer concentrations during feed processes whilst maintaining a long kinetic chain length.

Macromonomer purities and polydispersities predicted for solution feed polymerizations by simulation appear worse than those observed experimentally. One possible explanation is that the effects of chain length dependent termination (to increase the kinetic chain length) have not been allowed for. This will be examined in future work.

Abbreviations

I•	initiator derived radical
M	monomer
MMA	methyl methacrylate
N•	stable free radical
P _n •	propagating species of chain length <i>n</i>
P _n ^d	'dead' species formed by disproportionation or combination of chain length <i>n</i>
P _n N	species formed by reversible termination process of chain length <i>n</i>
P _n E	macromonomer of chain length <i>n</i> , species formed by reversible addition-fragmentation chain transfer
k _E	rate constant for addition to macromonomer

k_i	rate constant for initiator decomposition
f	efficiency of initiator decomposition
k_p	rate constant for propagation
k_t	rate constant for termination
k_{tc}/k_{td}	combination:disproportionation ratio
\bar{M}_n	number average molecular weight
\bar{M}_w	weight average molecular weight
\bar{M}_w/\bar{M}_n	polydispersity
\bar{X}_n	number average degree of polymerization
\bar{X}_w	weight average degree of polymerization
\bar{X}_w/\bar{X}_n	polydispersity
$\mu_x(P_n) = n^x[P_n]$	xth moment of molecular weight distribution for species P_n

Other kinetic parameters and species are defined in the text.

Acknowledgments

The support of Drs Chuck Berge and Michael Fryd (DuPont Marshall Laboratories, Philadelphia) is gratefully acknowledged. We also thank Dr Alexei Gridnev (DuPont, Experimental Station, Wilmington) for providing a preprint of his forthcoming publication (52).

Literature Cited.

- (1) G. Moad and D. H. Solomon *The Chemistry of Free Radical Polymerization* Pergamon: Oxford, 1995.
- (2) M. Sawamoto and M. Kamigaito *Trends Polym. Sci.*, **1996**, 4, 371-7.
- (3) G. Moad, E. Rizzardo and D. H. Solomon In *Comprehensive Polymer Science*; G. C. Eastmond, A. Ledwith, S. Russo and P. Sigwalt Eds.; Pergamon: London, 1989; vol 3, p 141.
- (4) D. Greszta, D. Mardare and K. Matyjaszewski *Macromolecules*, **1994**, 27, 638-44.
- (5) M. K. Georges, R. P. N. Veregin, P. M. Kazmaier and G. K. Hamer *Trends Polym. Sci.*, **1994**, 2, 66-72.
- (6) B. Ameduri, B. Boutevin and P. Gramain *Adv. Polym. Sci.*, **1997**, 127, 87-142.
- (7) E. Rizzardo and G. Moad In *The Polymeric Materials Encyclopaedia: Synthesis, Properties and Applications*; J. C. Salamone Ed.; CRC Press: Boca Raton, Florida, 1996; vol 5, p 3834-40.
- (8) S. Gaynor, D. Greszta, D. Mardare, M. Teodorescu and K. Matyjaszewski *J. Macromol. Sci., Chem.*, **1994**, A31, 1561-78.
- (9) R. P. Quirk and B. Lee *Polym. Int.*, **1992**, 27, 359-67.
- (10) Y. Y. Tan In *Comprehensive Polymer Science*; G. C. Eastmond, A. Ledwith, S. Russo and P. Sigwalt Eds.; Pergamon: London, 1989; vol 3, p 245-59.
- (11) J. Krstina, C. L. Moad, G. Moad, E. Rizzardo, C. T. Berge and M. Fryd *Macromol. Symp.*, **1996**, 111, 13-23.
- (12) T. Otsu and M. Yoshida *Makromol. Chem., Rapid Commun.*, **1982**, 3, 133-40.

- (13) D. H. Solomon, E. Rizzardo and P. Cacioli US 4,581,429 (*Chem. Abstr.* (1985) 102: 221335q)
- (14) C. H. J. Johnson, G. Moad, D. H. Solomon, T. H. Spurling and D. J. Vearing *Aust. J. Chem.*, **1990**, *43*, 1215-30.
- (15) G. Moad and E. Rizzardo *Macromolecules*, **1995**, *28*, 8722-8.
- (16) C. J. Hawker *Macromolecules*, **1996**, *29*, 2686-8.
- (17) T. Fukuda and T. Terauchi *Chem. Lett.*, **1996**, 293-4.
- (18) E. Yoshida *J. Polym. Sci., Part A: Polym. Chem.*, **1996**, *34*, 2937-43.
- (19) D. Greszta and K. Matyjaszewski *Macromolecules*, **1996**, *29*, 7661-7670.
- (20) D. Bertin and B. Boutevin *Polym. Bull. (Berlin)*, **1996**, *37*, 337-44.
- (21) T. Fukuda, T. Terauchi, A. Goto, K. Ohno, Y. Tsujii, T. Miyamoto, S. Kobatake and B. Yamada *Macromolecules*, **1996**, *29*, 6393-8.
- (22) S. A. F. Bon, M. Bosveld, B. Klumperman and A. L. German *Macromolecules*, **1997**, *30*, 324-6.
- (23) A. Bledzki, D. Braun and K. Titzschkau *Makromol. Chem.*, **1983**, *184*, 745-54.
- (24) A. Bledzki, D. Braun, W. Menzel and K. Titzschkau *Makromol. Chem.*, **1983**, *184*, 287-94.
- (25) T. Otsu and T. Tazaki *Polym. Bull. (Berlin)*, **1986**, *16*, 277-84.
- (26) T. Otsu, A. Matsumoto and T. Tazaki *Polym. Bull. (Berlin)*, **1987**, *17*, 323-30.
- (27) T. Tazaki and T. Otsu *Polym. Bull. (Berlin)*, **1987**, *17*, 127-34.
- (28) T. Doi, A. Matsumoto and T. Otsu *J. Polym. Sci., Part A: Polym. Chem.*, **1994**, *32*, 2911-8.
- (29) T. Doi, A. Matsumoto and T. Otsu *J. Polym. Sci., Part A: Polym. Chem.*, **1994**, *32*, 2241-9.
- (30) T. Otsu, T. Matsunaga, T. Doi and A. Matsumoto *Eur. Polym. J.*, **1995**, *31*, 67-78.
- (31) P. Lambrinos, M. Tardi, A. Polton and P. Sigwalt *Eur. Polym. J.*, **1990**, *26*, 1125-35.
- (32) A. R. Kannurpatti, S. Lu, G. M. Bunker and C. N. Bowman *Macromolecules*, **1996**, *29*, 7310-5.
- (33) V. B. Golubev, M. Y. Zaremskii, S. M. Mel'nikov, A. V. Olenin and V. A. Kabanov *Polymer Science*, **1994**, *36*, 264-9.
- (34) S. R. Turner and R. W. Blevina *Macromolecules*, **1990**, *23*, 1856-9.
- (35) M. Roha, H.-T. wang, J. H. Harwood and A. Sebenik *Macromol. Symp.*, **1995**, *91*, 81-92.
- (36) T. C. Chung, W. Janvikul and H. L. Lu *Macromolecules*, **1996**, *118*, 705-6.
- (37) B. Yamada, H. Tanaka, K. Konishi and T. Otsu *J. Macromol. Sci., Chem.*, **1994**, *A31*, 351-66.
- (38) D. Colombani, M. Steenbock, M. Klapper and K. Müllen *Macromol. Rapid Commun.*, **1997**, *18*, 243-51.
- (39) J. D. Druliner *Macromolecules*, **1991**, *24*, 6079-82.
- (40) B. B. Wayland, G. Poszmik, S. L. Mukerjee and M. Fryd *J. Am. Chem. Soc.*, **1994**, *116*, 7943-4.
- (41) I. S. Morozova, A. G. Oganova, V. S. Nosova, D. D. Novikov and B. R. Smirnov *Bull. Acad. Sci. USSR*, **1987**, 2628-30.
- (42) L. D. Arvanitopoulos, M. P. Gruel and H. J. Harwood *Polym. Prepr. (Am. Chem. Soc., Div. Polym. Chem.)*, **1994**, *35*(2), 549-50.
- (43) D. Mardare, K. Matyjaszewski and S. Coca *Macromol. Rapid Commun.*, **1994**, *15*, 37-44.

- (44) M. Dimonie, D. Mardare, K. Matyjaszewski, S. Coca, V. Dragutan and J. Ghiviriga *Macromol. Rapid Commun.*, **1992**, *13*, 283-8.
- (45) A. L. J. Beckwith, V. W. Bowry and G. Moad *J. Org. Chem.*, **1988**, *53*, 1632-41.
- (46) A. L. J. Beckwith, V. W. Bowry and K. U. Ingold *J. Am. Chem. Soc.*, **1992**, *114*, 4983-92.
- (47) V. W. Bowry and K. U. Ingold *J. Am. Chem. Soc.*, **1992**, *114*, 4992-6.
- (48) B. Howell, D. B. Priddy, I. Q. Li, P. B. Smith and P. E. Kastl *Polym. Bull. (Berlin)*, **1996**, *37*, 451-6.
- (49) F. T. T. Ng, G. L. Rempel and J. Halpern *J. Am. Chem. Soc.*, **1982**, *104*, 621-3.
- (50) F. T. T. Ng, G. L. Rempel, C. Mancuso and J. Halpern *Organometallics*, **1990**, *9*, 2762-72.
- (51) I. Li, B. Howell, K. Matyjaszewski, T. Shigemoto, P. B. Smith and D. B. Priddy *Macromolecules*, **1995**, *28*, 6692-3.
- (52) A. A. Gridnev *Macromolecules*, **1997**, submitted.
- (53) J.-S. Wang and K. Matyjaszewski *Macromolecules*, **1995**, *28*, 7901-10.
- (54) J.-S. Wang, S. Gaynor and K. Matyjaszewski *Macromolecules*, **1995**, *28*, 7572-3.
- (55) K. Matyjaszewski, T. E. Patten and J. Xia *J. Amer. Chem. Soc.*, **1997**, *119*, 674-80.
- (56) T. Grimaud and K. Matyjaszewski *Macromolecules*, **1997**, *30*, 2216-8.
- (57) M. Kato, M. Kamigaito, M. Sawamoto and T. Higashimura *Macromolecules*, **1995**, *28*, 1721-3.
- (58) Y. Kotani, M. Kato, M. Kamigaito and M. Sawamoto *Macromolecules*, **1996**, *29*, 6979-82.
- (59) T. Nishikawa, T. Ando, M. Kamigaito and M. Sawamoto *Macromolecules*, **1997**, *30*, 2244-2248.
- (60) H. Uegaki, Y. Kotani, M. Kamigaito and M. Sawamoto *Macromolecules*, **1997**, *30*, 2249-53.
- (61) A. H. E. Müller, R. Zhuang, D. Yan and G. Litvenko *Macromolecules*, **1995**, *28*, 4326-33.
- (62) S. Gaynor, J.-S. Wang and K. Matyjaszewski *Macromolecules*, **1995**, *28*, 8051-6.
- (63) A. H. E. Müller, R. Zhuang, D. Yan and G. Litvenko *Macromolecules*, **1995**, *28*, 7335-8.
- (64) E. Rizzardo, G. F. Meijs and S. H. Thang *Macromol. Symp.*, **1995**, *98*, 101-23.
- (65) J. Krstina, G. Moad, E. Rizzardo, C. L. Winzor, C. T. Berge and M. Fryd *Macromolecules*, **1995**, *28*, 5381-5.
- (66) G. Moad, C. L. Moad, J. Krstina, E. Rizzardo, C. T. Berge and T. R. Darling PCT Int. Appl. WO 9615157 (*Chem. Abstr.* (1996) 125: 115512)
- (67) G. Moad, C. L. Moad, E. Rizzardo and S. H. Thang *Macromolecules*, **1996**, *29*, 7717-26.
- (68) R. P. N. Veregin, P. G. Odell, L. M. Michalak and M. K. Georges *Macromolecules*, **1996**, *29*, 3346-52.
- (69) D. Yan, H. Jiang and X. Fan *Macromol. Theory Simul.*, **1996**, *6*, 333-45.
- (70) M. Wulkow *Macromol. Theory Simul.*, **1996**, *5*, 393-416.
- (71) A. H. E. Müller, R. Zhuang, D. Yan and G. Litvenko *Macromolecules*, **1996**, *29*, 5065-71.
- (72) C. H. J. Johnson, G. Moad and T. H. Spurling **1997**, to be submitted.

- (73) M. Buback, L. H. Garcia-Rubio, R. G. Gilbert, D. H. Napper, J. Guillot, A. E. Hamielec, D. Hill, K. F. O'Driscoll, O. F. Olaj, J. Shen, D. Solomon, G. Moad, M. Stickler, M. Tirrell and M. A. Winnik *J. Polym. Sci., Part C: Polym. Lett.*, **1988**, *26*, 293-7.
- (74) H. K. Mahabadi and K. F. O'Driscoll *J. Macromol. Sci., Chem.*, **1977**, *A11*, 967-76.
- (75) C. G. Overberger and M. B. Berenbaum *J. Am. Chem. Soc.*, **1951**, *73*, 2618-2621.
- (76) D. Bednarek, G. Moad, E. Rizzardo and D. H. Solomon *Macromolecules*, **1988**, *21*, 1522-8.

Free-Radical Synthesis of Functional Polymers Involving Addition-Fragmentation Reactions

P. Chaumont¹, D. Colombani², L. Boiteau², J. P. Lamps², M.-O. Zink²,
C. P. R. Nair³, and D. Charmot⁴

¹Université Claude Bernard, LEMPB, Bât. 305, 43 Boulevard du 11
Novembre 1918, 69622 Villeurbanne, France

²Institut Charles Sadron, 6 rue Boussingault, 67083 Strasbourg, France

³Polymer & Special Chemical Division, Vikram Sarabhai Space Center,
Trivendrum 69022, India

⁴Centre de Recherches Rhône-Poulenc, 52 rue de la Haie Coq, 93308,
Aubervilliers, France

The synthesis of functionalized polymers by means of addition-fragmentation agents in free radical polymerization has been studied in order to determine the efficiency of the method. In such systems, a strong decrease of the rate of polymerization, that can be attributed to some retardation or degradative chain transfer, is generally observed. A study of the kinetics of these systems has been initiated in order to investigate the cause of such retardation and its influence on the functionality of the polymers formed.

Chain transfer reactions have been extensively used in free radical polymerization in order to both control the molar mass and to functionalize polymers. The conventional chain transfer agents such as mercaptans act by hydrogen abstraction. This radical transfer is a one step process, *i.e.* the thiyl radical and the terminated polymer are formed simultaneously.

Reactions other than hydrogen abstractions may be used in order to achieve the same goals. This is the case of the so-called addition-fragmentation reactions, which are two step processes. A recent review (*1*) has been published, giving a list of such addition-fragmentation chain transfer agents (AFCTA). As the overall process is the same as in the classical chain transfer reactions, *i.e.* the termination of the polymer chain and the re-initiation of a new one, the activity of AFCTAs is generally analysed in the same way, by determining the chain transfer constants. However, the two step reactions of such systems implies some differences. This article deals with the calculation of the kinetics of such systems, and the prediction of the functionality of the polymers formed, whatever the AFCTA used.

In order to compare the mathematical predictions with some experimental data, the results obtained in the study of pentadiene-like AFCTA have been used. Since the

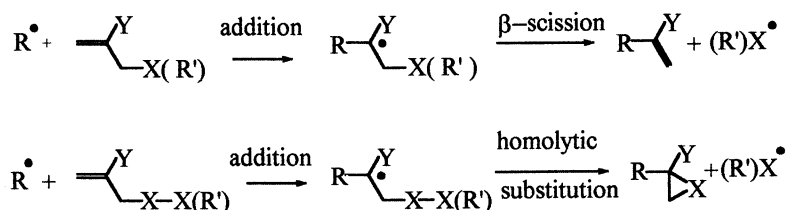
main objective of this paper is not to describe such systems, these latter studies have been published (2a) or will be published elsewhere (2b). However, some information needed for the comprehensiveness of the text are reported below.

Experimental

Polymerizations were carried out in the bulk, excepted an experiment devoted to the study of the influence of the concentration of the overall polymerization medium, and at low conversion, *i.e.* below 10%, in order to maintain the ratio [AFCTA]/[Monomer] constant. All reactants were purified as previously described (2a). The polymerizations were carried out in sealed ampoules, the polymerization medium being degassed by freeze-*vacuum*-thaw cycles. The instruments used for macromolecular and chemical characterizations are described in reference 2a.

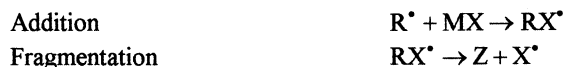
Mechanism and Kinetics of Addition-Fragmentation Reactions

Addition-fragmentation reactions will now be considered in detail. Such reactions may be described as the result of (a) the addition of some radical species, the "primary radicals", to the addition site of the AFCTA, which is generally an alkene structure, giving rise to the formation of a new "intermediate radical" and (b) the subsequent intramolecular evolution of this latter intermediate radical, the so-called fragmentation reaction, *i.e.* the breaking of some "weak" bonds located elsewhere inside the molecule. This latter reaction may be (a) a β -scission or (b) an homolytic substitution (Cf. Scheme 1).



Scheme 1. Addition-fragmentation Reaction

If R° represents the primary radical, MX the AFCTA, RX° the intermediate radical, Z the product and X° the radical expelled in the reaction medium after the fragmentation reaction respectively, such processes can be written as:



If k_a is the rate constant of the addition reaction, k_f is the rate constant of the fragmentation process, and if $[\text{R}^\bullet]$ represents the concentration of the primary radical and $[\text{RX}^\bullet]$ the concentration of the intermediate radical respectively, then the rates of these two reactions can be written as:

$$\begin{array}{ll}
 \text{Addition} & \text{R}_a = k_a [\text{R}^\bullet] [\text{MX}] \quad (1) \\
 \text{Fragmentation} & \text{R}_f = k_f [\text{RX}^\bullet] \quad (2)
 \end{array}$$

However, these equations do not take into account the origin and the rate of formation of the primary radicals R° . Whatever the value of this constant and whatever the evolution of the expelled radical X° , due to the steady state hypothesis regarding the radical $[RX^\circ]$ it can be considered that R_s is equal to R_f , if side reactions are ignored.

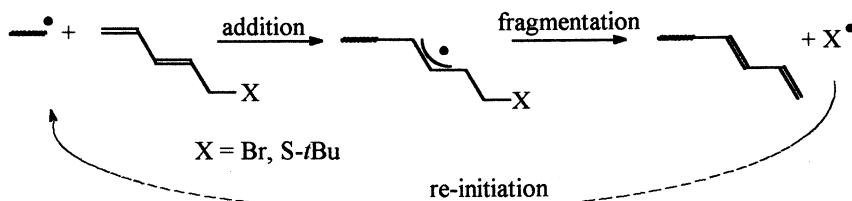
Thus, the ratio of the two radical concentrations can be written as:

$$\frac{[RX^\circ]}{[R^\circ]} = \frac{k_a[MX]}{k_f} \quad (3)$$

Hence, at low values of k_f compared to k_a , a high concentration of the intermediate radical RX° is expected. Due to this high value of $[RX^\circ]$, the rate of side reactions involving the intermediate radical may be increased. The same behavior is expected by increasing the concentration of the AFCTA.

Addition-Fragmentation Reactions in Free Radical Polymerisation Processes

When the AFCTA is added to a free radical polymerization medium, the growing macroradicals (P°) replace the primary radical R° described in the preceding paragraph, but the reaction sequence remains the same (Cf. Scheme 2). As a result of the addition-fragmentation chain transfer reaction, a functionalized polymer is formed, and the expelled X° radical re-initiates a new polymer chain.



Scheme 2. Addition-fragmentation chain transfer reaction

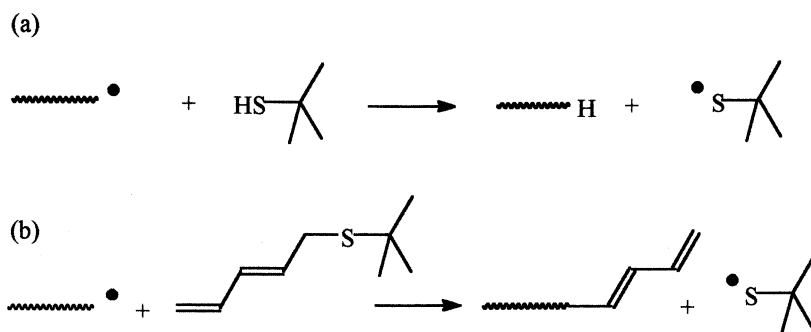
In such experiments, the concentration of the AFCTA is generally much lower than the concentration of the monomer (M). However, in many cases (*1*), even low concentrations of AFCTA may provoke a strong decrease of the molar mass of the formed polymer, this is expected for a chain transfer agent, but also a strong decrease of the overall rate of polymerization (R_p). In conventional chain transfer studies, such behavior is generally described as the consequence of a low rate of re-initiation.

Two cases are observed (*3*): (a) If the rate constant of the chain transfer reaction k_{tr} is of the same order of magnitude as the rate constant of propagation k_p , the behavior is described as "retardation". (b) If k_{tr} is much greater than k_p a "degradative chain transfer" is obtained.

Thus, a conventional explanation for the decrease of the rate of polymerization in the presence of AFCTA is the primary radical termination (*2a*). However, in many studies of AFCTAs, such retardations or degradative chain transfers may be observed,

even though the rate of re-initiation is not expected to be particularly slow, such an example is the case of the polymerization of methyl methacrylate (MMA) in the presence of 5-*t*-butylthiopentadiene (TBTP) as AFCTA (Cf. Figure 1).

In fact, the radical expelled in the polymerization medium after the addition fragmentation process, X° , is a *t*-butylthiyl radical, which does not provoke considerable retardation of the polymerization of MMA, as is observed when the classical 2-methyl-2-propanethiol is used instead of the pentadienic AFCTA (Cf. Scheme 3 and Figure 1).



Scheme 3. Chain transfer reactions using
(a) a conventional mercaptan and (b) pentadienic AFCTA

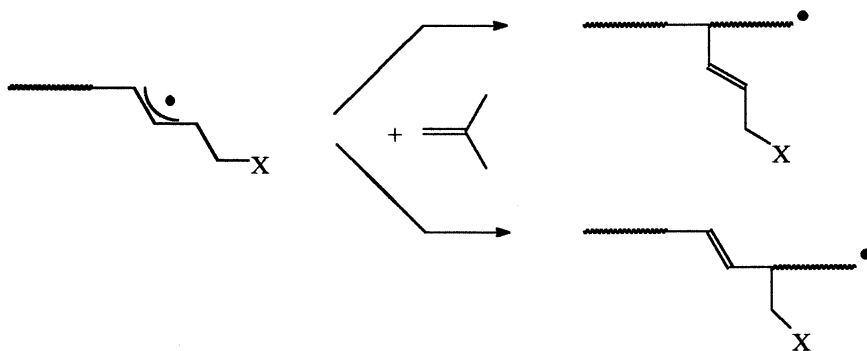
Thus, the decrease of the overall rate of polymerization by primary radical termination which is invoked in the reference 2a seems to be not sufficient to explain the magnitude of this decrease, in contrast to other systems like thiuramdisulfide iniferters (4). Therefore, the kinetics of such systems have been re-examined.

In order to find other reactions which might causes decrease of R_p , it must be first remarked that the sulfur content of the poly(methyl methacrylate) obtained by using TBTP is higher than expected. According to the scheme of addition-fragmentation chain transfer reactions (Cf. Scheme 2), the number of sulfur atoms per polymer chain (n_s) must be less than unity. This expected value < 1 comes from the fact that the polymer chains may be initiated both by the radical formed by the thermolysis of the initiator and by the radical X° expelled in the medium after the fragmentation reaction.

Generally, due to multiple transfer reaction steps during the lifetime of each radical generated by the initiator, the number of chains initiated by X° , *i.e.* the thiyl radical, is much higher than the number of chains initiated by the initiator. Thus, the number of sulfur atoms per chain, due to the presence of the thiyl fragment at the "beginning" of the chain, must be close to, but less than, one.

Nevertheless, in the case of the polymerization of MMA with TBTP as chain transfer agent in bulk conditions, the experimental value is close to 2.5 (2). This abnormal value can be explained by the occurrence of some side reactions, namely the cross propagation of the intermediate radical (Cf. Scheme 4). This latter hypothesis is difficult to prove directly but some experimental facts are compatible only by this explanation, such as the decrease of n_s when the overall concentration of the polymerization medium is decreased (see paragraph dealing with the interconversion).

One very important consequence of the occurrence of this cross-propagation reaction, is the fact that the lifetime of the intermediate radicals, *i.e.* the macroradical species present in the polymerization medium between the addition and the fragmentation reactions, appears to be high enough to allow side reactions, which are in competition with the fragmentation process. This "long" lifetime may be interpreted as the consequence of a slow fragmentation process because of the stability of the intermediate radical and/or the stability of the weak carbon-sulfur bond. For example, by using bromo-pentadiene instead of TBTP, n_s becomes equal to 0.9 (2b).



Scheme 4. Cross-propagation of the intermediate macroradical.

Whatever may be the explanation of the long lifetime of the intermediate radicals, it affords more opportunities for other side reactions involving these macroradical species to occur, including an increase in occurrence of termination processes. Such termination processes, like polymer radical homo- and cross-terminations, are generally invoked in conventional free radical copolymerizations involving two different monomers, to explain the decrease of the rate of polymerization, especially the cross-termination reaction. Thus, two questions arise from this analysis: (a) Is it possible to explain the decrease of the rate of polymerization by the occurrence of polymer radical terminations? (b) What is the consequence of such termination processes on the functionality of the polymers formed?

Kinetic Studies

In order to answer these two preceding questions, an equation for the rate of polymerization must first be established. The chemical reactions taken into account are listed in Table I.

According to the proposed hypothesis, *i.e.* the absence of retardation and/or degradative chain transfer reactions, the only termination reactions considered are the reactions involving macroradical species. Due to the low relative concentration of the AFCTA with respect to the concentration of the monomer, the influence of the penultimate effect can be neglected. Lastly, it can be assumed that if experiments are carried out at low conversions of the monomer the following are avoided: (a) the effect of the viscosity of the polymerization medium on the kinetics of the

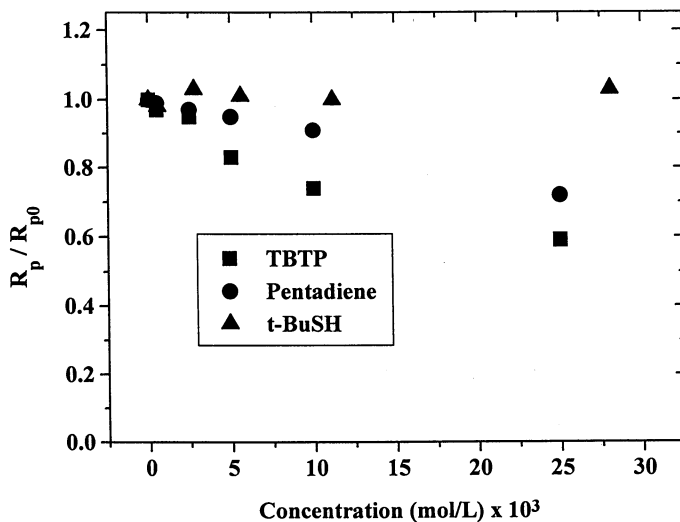


Figure 1. Variation of the relative rate of polymerization of MMA in the presence of TBTP, Pentadiene and t-Butyl-mercaptan.

Table I. Reactions Involved in the Free Radical Polymerization of Vinyllic Monomers in the Presence of Addition-Fragmentation Chain Transfer Agents

	<i>Constants</i>	<i>Products</i>	<i>Notations</i>	<i>Rate</i>	<i>Remarks</i>
<i>Initiator</i>					
I ₂	k _d	I°		R _d	
<i>Initiations</i>					
I° + M	k _i	IM°	P°	R _i	Initiation
I° + MX	k _{xi}	IX°	PX°	R _{xi}	
X° + M	k' _i	XM°	P°	R' _i	Re-initiation
X° + MX	k' _{xi}	XX°	PX°	R' _{xi}	
<i>Macroradicals</i>					
<i>Reactions</i>					
P° + M	k _h	P°		R _h	
P° + MX	k _a	PX°		R _a	Addition
PX° + M	k _x	P°		R _x	Cross propag.
PX° + MX	k' _h	PX°		R' _h	
PX°	k _f	Pf + X°		R _f	Fragmentation
<i>Terminations</i>					
2 P°	k _t	P		R _t	
P° + PX°	k _{et}	P		R _{et}	Cross termin.
PX°	k _{tx}	P		R _{tx}	

macroradical reactions and (b) the change of the relative concentration of the AFCTA versus the concentration of the monomer expected if the chain transfer constant is not equal to one.

Applying the steady state conditions to all radical species, four equations are obtained:

$$[I^\circ] \Rightarrow R_i + R_{xi} = R_d \quad (5)$$

$$[X^\circ] \Rightarrow R'_i + R'_{xi} = R_f \quad (6)$$

$$[P^\circ] \Rightarrow R_i + R'_i + R_h + R_x = R_a + R_h + R_t + R_{ct} \quad (7)$$

$$[PX^\circ] \Rightarrow R_{xi} + R'_{xi} + R_a = R_x + R_f + R_{ct} + R_{tx} \quad (8)$$

Adding equation 7 and 8 and subtracting equation 6 gives:

$$R_i + R_{xi} = R_t + 2 R_{ct} + R_{tx} \quad (9)$$

Equation 9 reflects the fact that, in absence of some degradative processes, the overall rate of initiation is equal to the overall rate of termination of the macroradical species. As the rate of initiation (equation 5) is equal to R_d , *i.e.* the rate of thermolysis of the initiator moderated by the efficiency factor, it can be assumed that, if the only parameter modified in these experiments is the concentration of AFCTA, then the overall rate of termination remains constant.

In particular, the overall rate of termination is equal to the rate of termination of the experiment carried out in absence of AFCTA, R_{t0} ; such a condition can be written as:

$$R_{t0} = R_t + 2R_{ct} + R_{tx} \quad (= R_d) \quad (10)$$

Equation 10 may be developed as:

$$k_t [P^\bullet]_0^2 = k_t [P^\bullet]^2 + 2k_{ct} [P^\bullet] [PX^\bullet] + k_{tx} [PX^\bullet]^2 \quad (11)$$

Introducing α as the ratio of the two macroradical species ($\alpha = [PX^\bullet]/[P^\bullet]$), the above equation may be written as:

$$\frac{[P^\bullet]}{[P^\bullet]_0} = \left(1 + 2 \frac{k_{ct}}{k_t} \alpha + \frac{k_{tx}}{k_t} \alpha^2 \right)^{-1/2} \quad (12)$$

The overall rate of polymerization is calculated as the sum of all the reactions giving rise to the increase of any macroradical species:

$$R_p = R_h + R'_h + R_a + R_x \quad (13)$$

The fact to consider the addition step of the addition-fragmentation process as a propagation step is not conventional. In the case of mercaptans, such consideration is

not founded because of the termination of the chain through hydrogen abstraction. However, in the case of addition-fragmentation, the addition step provokes the increase of the degree of conversion value by one. Such influence may be neglected in conventional experimental conditions, *i.e.* low concentration of AFCTA, as discussed in the paragraph dealing with the study of the chain transfer constant.

Equation 13 can be written as:

$$R_p = k_h[P^*][M] + k'_h[PX^*][MX] + k_a[P^*][MX] + k_x[PX^*][M] \quad (14)$$

In absence of AFCTA, the rate of polymerization becomes:

$$R_{p0} = k_h[P^*]_0[M] \quad (15)$$

Dividing equation 14 by equation 15 expresses the relative rate of polymerization:

$$\frac{R_p}{R_{p0}} = \frac{[P^*]}{[P^*]_0} \left[1 + \frac{k_x}{k_h} \alpha + \left(\frac{k'_h}{k_h} \alpha + \frac{k_a}{k_h} \right) \frac{[MX]}{[M]} \right] \quad (16)$$

Finally, replacing the ratio $[P^*]/[P^*]_0$ in the equation 16 by the value written in equation 12, the equation of the relative rate of polymerization is obtained:

$$\frac{R_p}{R_{p0}} = \frac{1 + \frac{k_x}{k_h} \alpha + \left(\frac{k'_h}{k_h} \alpha + \frac{k_a}{k_h} \right) \frac{[MX]}{[M]}}{\left(1 + 2 \frac{k_{ct}}{k_t} \alpha + \frac{k_{tx}}{k_t} \alpha^2 \right)^{1/2}} \quad (17)$$

Generally, few values of the rate constants used in the above equation are known. Five parameters ($k_x, k'_h, k_a, k_{ct}, k_{tx}$) in equation 17 are to be determined. However, it can be remarked that this equation is compatible with both the increase and decrease of the relative rate of polymerization, depending upon the values of α and of the rate constants.

Interconversion

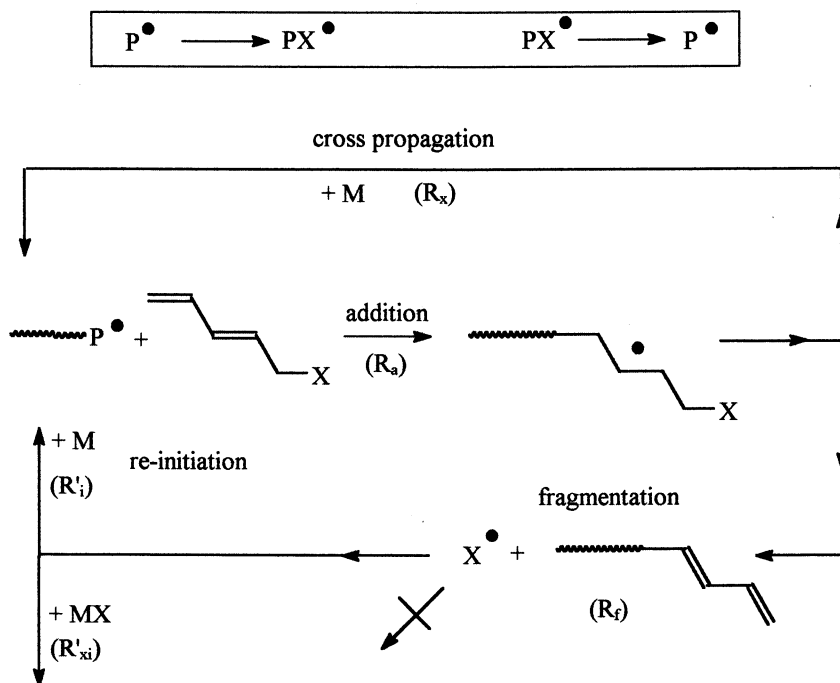
In order to determine α , an attempt to apply the same type of calculations as in the case of classical free radical copolymerizations has been made, *i.e.* the fact that the rate of interconversion of the two macroradical species must be equal.

The reactions involved in the interconversion of P° and PX° are shown in the Scheme 5. It can be seen that, according to our hypothesis of the absence of side reactions involving the radical X° , the conversion of P° into PX° is achieved by the first step of the addition-fragmentation process, and the conversion of PX° into P° is achieved by both (a) the cross-propagation and (b) the fragmentation of the PX°

radical. In fact, this latter reaction does not directly provoke the formation of a P^\bullet radical, but a X^\bullet radical.

However, as it is shown in the Scheme 5, the only evolution of this radical is (a) the re-initiation of a new polymer chain, *i.e.* the formation of a new P^\bullet radical, and (b) the addition onto the AFCTA. This latter reaction (a) gives rise to the formation of a new X^\bullet radical and/or (b) is slower than the re-initiation because of the greater concentration of the monomer compared to the concentration of the AFCTA.

Thus, it can be assumed that the rate of fragmentation of the macroradical PX^\bullet is actually approximately the same as that of the rate of reinitiation of P^\bullet . The fragmentation process appears to act as an interconversion process of PX^\bullet into P^\bullet .



Scheme 5. Reactions involved in the interconversion process.

Commenting on this conclusion, it should be remarked that the expression "slow rate of re-initiation" seems to be inappropriate to explain the behavior of retardation. In fact, the rate of any chemical reaction results from (a) the value of the rate constant, (b) the concentrations of the reagents and (c) the order of the reaction for each reagents. In the case of the re-initiation process involving the X^\bullet radical, the rate constant may be low, *i.e.* the reactivity of the radical may be low. However, as the rate of formation of this radical species is governed by the fragmentation process, the only direct consequence of a low value of the re-initiation constant is the increase of the concentration of the X^\bullet radical into the polymerization medium. In the absence of any

side reaction, $[X^\circ]$ increases rapidly until the rate of re-initiation becomes equal to the rate of fragmentation, which is generally expected if the steady state hypothesis is verified. A consequence of this increase of $[X^\circ]$ may be the simultaneous increase of any side reaction involving this radical, such as termination reactions. However, if the rate constant of re-initiation is not equal to zero, *i.e.* the radical X° is able to react with the monomer, the low value of the rate constant of re-initiation does not affect directly the overall rate of polymerization.

As a consequence of the above discussion, it can be assumed that:

$$R_a = R_x + R_f \quad (18)$$

The above equation may be developed as:

$$k_a[P^\bullet][MX] = k_x[PX^\bullet][M] + k_f[PX^\bullet] \quad (19)$$

The parameter α may be calculated as:

$$\alpha = \frac{k_a[MX]}{k_x[M] + k_f} \quad (20)$$

Actually, this expression represents both (a) free radical copolymerization if $k_x[M] \gg k_f$ and (b) the addition-fragmentation processes, if $k_x[M] \ll k_f$. In this latter case, the expression is identical to the equation 3. In intermediate cases, such as the polymerization of MMA in the presence of TBTP, a decrease of the concentration of the monomer must also decrease the yield of the copolymerization compared to the yield of fragmentation. This conclusion has been confirmed. Thus, if n_s is equal to 2.3 in bulk conditions, this value becomes equal to 1.2 when the system, *i.e.* with the same relative concentrations of the reagents, is polymerized at 20% in toluene(2b).

Replacing α in equation 17 gives the final expression of the relative rate of polymerization as:

$$R_p = \frac{1 + \frac{k_x}{k_h} \frac{k_a[MX]}{k_x[M] + k_f} + \left(\frac{k'_h}{k_h} \frac{k_a[MX]}{k_x[M] + k_f} + \frac{k_a}{k_h} \right) \frac{[MX]}{[M]}}{\left(1 + 2 \frac{k_{ct}}{k_t} \frac{k_a[MX]}{k_x[M] + k_f} + \frac{k_{tx}}{k_t} \left(\frac{k_a[MX]}{k_x[M] + k_f} \right)^2 \right)^{1/2}} \quad (21)$$

The usefulness of such equation is very limited, due to the large number of unknown parameters. However, it appears that it is not necessary to invoke degradative behavior of the chain transfer reaction to explain the strong decrease of the rate of polymerization. Thus, as suggested by equation 21, such decrease could be due to high values of the cross-termination constant between the two macroradicals, k_{ct} , and/or of the homo-termination constant of the intermediate radical, k_{tx} .

Since such high values do not depend upon the fragmentation process, they can be checked easily by the comparison of the decrease of the relative rate of polymerization

determined for two systems: (a) monomer A / AFCTA and (b) monomer A / monomer B, since the monomer B presents a chemical structure analogue to that of AFCTA, *i.e.* the same structure of the addition site. Such a comparison is shown in Figure 1 (see also Table II) for the systems (a) MMA/TBTP and (b) MMA/pentadiene. It can be seen that the decrease of the relative rate of polymerization is of the same order of magnitude, the slight difference between the two curves being easily explained by the difference of the reactivity of the pentadiene group in the case of AFCTA compared to the case of pentadiene.

Chain transfer constant

The chain transfer constant of any AFCTA may be calculated in the same way as a conventional chain transfer reaction, *i.e.* through the determination of the kinetic chain length (ν) of the polymer⁵ formed. This kinetic chain length represents the average number of steps of growth per effective radical and is given by the ratio of the propagation rate to the rates of all processes involving the termination of the chain.

Thus, if R_T stands for the rate of macroradical terminations, ν can be written as:

$$\nu = \frac{R_p}{R_T + R_f} \Leftrightarrow \frac{1}{\nu} = \frac{R_T}{R_p} + \frac{R_f}{R_p} \quad (22)$$

In the absence of AFCTA, the kinetic chain length becomes:

$$\nu_0 = \frac{R_{p0}}{R_T} \quad (23)$$

Since the overall rate of macroradical termination is the same, the variation of the relative rate of polymerization can be taken into account and written as follows:

$$\frac{1}{\nu} = \frac{1}{\nu_0} \frac{R_{p0}}{R_p} + \frac{R_f}{R_p} \quad (24)$$

Replacing R_f and R_p by their values, the above equation can be written as:

$$\frac{1}{\nu} = \frac{1}{\nu_0} \frac{R_{p0}}{R_p} + \frac{k_f \alpha}{(k_h + k_x \alpha)[M] + (k_s + k_t' \alpha)[MX]} \quad (25)$$

In order to simplify this equation, it can be assumed that (a) the cross propagation and (b) the homo-propagation of the intermediate radical may be neglected. In other words, the chain transfer process is a "pure" addition-fragmentation reaction. In this case, the α parameter can be written as:

$$\alpha = \frac{k_s [MX]}{k_f} \quad (26)$$

Table II. Bulk Polymerization^a of MMA in the Presence of Additives MX

<i>Additive MX</i>	<i>Concentration of MX (mol/L × 10⁴)</i>	<i>Relative Rate of Polymerization^b</i>
TBTP	0.0	1.00
	0.5	0.97
	2.5	0.95
	5.0	0.83
	10	0.74
	25	0.59
	Pentadiene	0.0
0.5		0.99
2.5		0.97
5.0		0.95
10		0.91
25		0.72
t-BuSH		0.0
	0.6	0.98
	2.8	1.03
	5.6	1.01
	11	1.00
	28	1.03

^aExperimental Conditions: [AIBN] = 3.05×10^3 mol/L, temperature 60°C, polymerization time 1 hour.

^bRatio of rates of polymerization with and without AFCTA, determined from SEC data.

Therefore, the kinetic chain length becomes:

$$\frac{1}{\nu} = \frac{1}{\nu_0} \frac{R_{p0}}{R_p} + \frac{k_a}{k_h + k_a} \frac{[MX]}{[M]} \quad (27)$$

Thus, the conventional chain transfer constant, as determined by Mayo's equation, can be written as:

$$C_{tr} = \frac{k_a}{k_h + k_a} \frac{[MX]}{[M]} \quad (28a)$$

In the above equation 28, the expression $k_a \frac{[MX]}{[M]}$ comes from the fact that the addition has been considered as a propagation step. This equation may be written as :

$$\frac{1}{C_{tr}} = \frac{k_h}{k_a} + \frac{[MX]}{[M]} \quad (28b)$$

Thus, the dependency of C_{tr} to the ratio $[MX]/[M]$ remains low if $[MX]/[M] \ll k_h/k_a$, that is generally the case for experiments carried out in the presence of low concentrations of the transfer agent. However, the chain transfer constant is expected to decrease with the increase of the concentration of the AFCTA and the decrease of the concentration of the monomer. Furthermore, the calculation is much more complicated if the cross-propagation interferes with the fragmentation process.

However, in all cases, a constant may be found by the extrapolation of the C_{tr} value to a null concentration of AFCTA: $C_{tr0} = k_a/k_h$. For systems exhibiting low values of C_{tr0} , this extrapolated constant may be used in order to calculate the kinetic chain length.

Functionality

By using the chain transfer constant C_{tr0} , the functionality (f) of the formed polymer may be derived as the ratio of the number of functionalized chains versus the overall number of polymer chains formed during the lifetime of an effective radical. In order to calculate this number, the decrease of the kinetic chain length due to the decrease of the relative rate of polymerization must be considered. Therefore, the functionality can be written as:

$$f = \frac{\frac{\nu_0 R_p}{R_{p0}} - 1}{\frac{\nu_0 R_p}{R_{p0}}} \quad (29)$$

By replacing v by its value, it becomes:

$$f = \frac{\frac{R_p}{R_{p0}} C_{tr0} v_0 \frac{[MX]}{[M]}}{1 + \frac{R_p}{R_{p0}} C_{tr0} v_0 \frac{[MX]}{[M]}} \quad (30)$$

From this last equation, a decrease of the functionality can be expected with (a) a decrease of the relative rate of polymerisation, (b) a decrease of the chain transfer constant, (c) a decrease of the kinetic chain length of the homopolymer and (d) a decrease of the ratio $[AFCTA]/[\text{monomer}]$. In order to check the dependency of the functionality to the relative rate of polymerization, both C_{tr0} and v_0 values have been taken from the study of the system MMA/TBTP (2), *i.e.* $C_{tr0} = 2.4$, $v_0 = 4000$. For each value of the ratio $[TBTP]/[MMA]$, the experimental decrease of the relative rate of polymerization has been measured.

As shown in Figure 2, with 1% of TBTP, the relative rate of polymerization is roughly 0.3, whereas the functionality of the formed polymer remains greater than 0.95.

Conclusion

The main results of this study are: (a) The decrease of the relative rate of polymerization observed in many chain transfer reaction involving addition-fragmentation processes can be explained by the termination reaction involving the

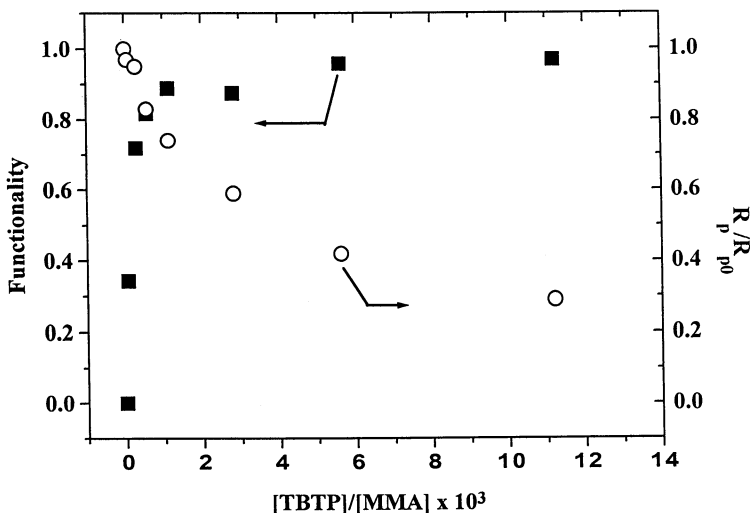


Figure 2. Theoretical functionality (equation 30) of polymer formed. Bulk polymerization of MMA in the presence of TBTP as chain transfer agent.

macroradical species. The occurrence of some degradative side reactions, like primary radical termination, is not necessary to observe a strong decrease of the rate of polymerization, even if such degradative side reactions cannot be *a priori* excluded. (b) For such systems, the chain transfer constant shows some dependency upon the concentration of the AFCTA that can be neglected in conventional experimental conditions. (c) The influence of the decrease of the relative rate of polymerization on the functionality may be neglected, since the chain transfer activity of the AFCTA and its concentration remain sufficiently high.

Acknowledgments

The authors thank the referees for suggestions and remarks. This work was kindly supported by Rhône-Poulenc Chimie.

Literature Cited

1. Colombani, D.; Chaumont, P. *Prog. Polym. Sci.* **1996**, *21*, 439.
2. (a) Nair, C. P. R.; Chaumont, P.; Charmot, D. *J. Polym. Sci., Polym. Chem.*, **1995**, *33*, 2773. (b) Chaumont, P.; Colombani, D.; Zink, M.O.; Charmot, D. (to be published).
3. Odian, G. *Principles of Polymerization*, 2nd Edition, Wiley : **1981**, p.227.
4. Nair, C.P.R.; Chaumont, P.; Clouet G. *Macromolecular Design, Concept and Practice*, Mishra, N.M. Ed.; Polymer Frontier International : **1994**, p.431.
5. Rempp, P.; Merrill E.W. *Polymer Synthesis*, Hüthig & Wepf : **1986**, p.79.

Chapter 23

Applications of Barton Esters in Polymer Synthesis and Modification via Free-Radical Processes

W. H. Daly and T. S. Evenson

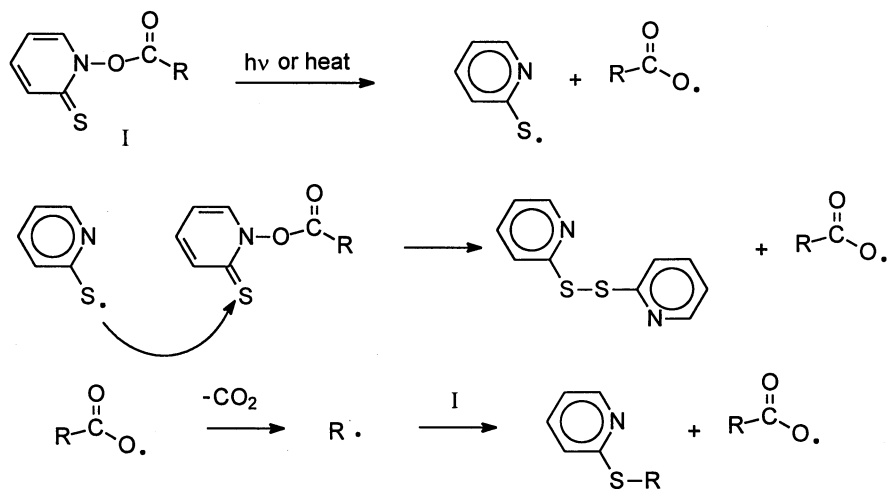
Macromolecular Studies Group, Department of Chemistry, Louisiana State University, Baton Rouge, LA 70803-1804

Esters of N-hydroxypyridine-2-thione (Barton esters) dissociate homolytically upon exposure to heat or visible light generating initiating alkyl or benzoyloxy radicals and non-initiating 2,2'-dipyridyl disulfide. Kinetics of free radical styrene polymerization are independent of phenyl Barton ester concentration; the molecular weight is controlled by chain transfer to initiator. Incorporation of Barton esters into the side groups of polymer chains facilitates synthesis of graft copolymers with minimal concomitant homopolymerization. Copoly(4-vinylbenzoyl chloride-*r*-styrene), carboxylated poly(arylene ether sulfones) and carboxymethyl cellulose have been converted to the corresponding poly(Barton esters) and utilized to prepare graft copolymers with styrene and methyl methacrylate.

Thiohydroxamic esters, including esters of N-hydroxypyridine-2-thione, were first used as free-radical precursors by Derek Barton (1), and have come to be known as Barton esters. N-hydroxypyridine-2-thione esters are most easily synthesized by reacting the sodium salt of N-hydroxypyridine-2-thione and an acid chloride (2). Carboxylic acids may also be converted to Barton esters using coupling reagents such as chloroformates or dicyclohexylcarbodiimide (3). Through the use of different carboxylic acid substrates and thiohydroximes, a wide variety of Barton esters can be synthesized (4-6).

The decomposition of Barton esters by heat or visible light initially yields acyloxy radicals and pyridine thiol radicals (Scheme 1). Laser flash photolysis studies have shown that the pyridine thiol radical is consumed by attacking the pyridine thione ring of the starting Barton ester producing 2,2'-dipyridyl disulfide and a second acyloxy radical (7). The aliphatic acyloxy radicals lose carbon dioxide rapidly to form carbon centered radicals. If no trapping reagents are present, the radical intermediate can induce the cleavage of another molecule of Barton ester to produce a thioether.

If an appropriate trapping reagent (X-Y) captures the alkyl radicals, a more useful organic transformation can be achieved. Barton has used these free radicals in several organic syntheses in the presence of many common functional groups (1-6). For example, reductive decarboxylation occurs when X-Y is RS-H and decarboxylative chlorination is accomplished in 95% yield (4) when X-Y is Cl-CCl₃. Formation of an acid chloride by treatment with thionyl chloride followed by reaction with sodium N-oxypyridine-2-thione produced a Barton ester intermediate. Irradiation of this intermediate in carbon tetrachloride induces a homolysis to an acyloxy radical, which decarboxylates to an alkyl radical. Attack by the alkyl radical on one of the carbon-chlorine bonds of carbon tetrachloride yields a chlorinated product and a trichloromethyl radical which propagates a chain reaction by attacking the thiocarbonyl of a second Barton ester and regenerating an acyloxy radical. Judicious selection of X-Y allows elaboration of reactive acid derivatives under rather mild conditions.

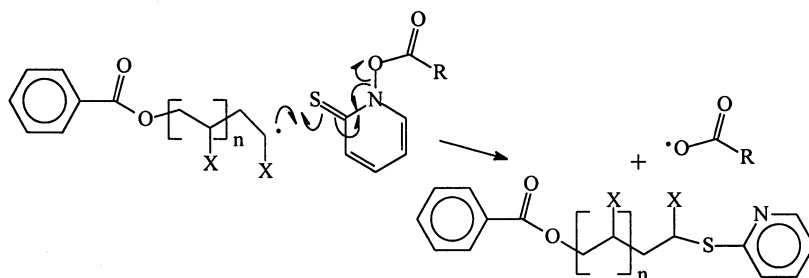


Scheme 1. Barton Ester Decomposition

Barton esters (BE) have been used as chain transfer agents to control free-radical polymerizations (8). Polymerizations of styrene, methyl methacrylate, methyl acrylate and vinyl acetate initiated by either benzoyl peroxide (BPO) or azobisisobutyronitrile (AIBN) were conducted in the presence of Barton ester. The chain transfer constants (C_x) for the various Barton esters ($R=C_{15}H_{31}$, Bz, or Ph) were then calculated by the Mayo method (9) from the molecular weight data obtained by size exclusion chromatography (SEC). The chain transfer mechanism involves induced decomposition of the BE by propagating radical attack on the thiocarbonyl of the BE as shown in Scheme 2. Chain transfer constants for several Barton esters in the monomers used are summarized in Table I.

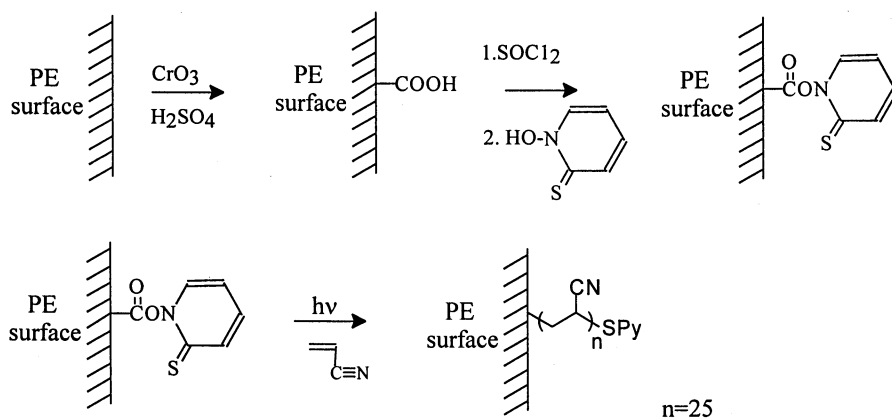
Table I. Chain Transfer Constant, C_x , for Barton Esters (8)

R	Methyl methacrylate	Styrene	Methyl acrylate	Vinyl acetate
$C_{15}H_{31}$	4.0	3.8	20	36
Benzyl	4.3	3.9		80
Phenyl	2.8			



Scheme 2. Chain Transfer to Barton Ester

Barton esters have been used to modify polymer film surfaces by grafting (10). Generation of carboxyl groups of the surface of polyethylene by oxidation followed by esterification with N-hydroxypyridine-2-thione introduced Barton ester sites on the film (Scheme 3). These esters were then decomposed by visible light in the presence of acrylonitrile to form polyacrylonitrile grafts on the film surface. The average graft length was estimated by infrared (IR) spectroscopy to be 25 monomer units. This is the first reported application of Barton esters as initiators.



Scheme 3. Barton Esters Applied to Grafting on Polyethylene

It is the goal of this research to show the versatility of Barton esters as initiators in the radical polymerization of vinyl monomers. Further, the unique

properties of Barton esters as initiators and chain transfer agents present several opportunities for controlling molecular architecture, particularly in preparing graft copolymers.

Experimental

Materials. All materials were obtained from Aldrich unless noted otherwise. Styrene was dried over sodium sulfate, passed through a short alumina column, then vacuum distilled before use. Methyl methacrylate was purified by vacuum distillation before use. All monomers were purged with argon before polymerization. Dichloromethane (DCM) and tetrahydrofuran (THF) were obtained from Mallinckrodt, and the DCM was distilled from CaH_2 before use. Sodium N-oxypyridine-2-thione was obtained from Olin and purified by previously published procedure (2). Carboxylated poly(aryl ether sulfone) samples were obtained from National Research Council-Canada. All polymer samples were dried under vacuum at 25°C for 24 hours.

Characterization. Molecular weights were determined with a size exclusion chromatograph equipped with a Waters differential refractometer and a Dawn multiangle light scattering detector. The dried polymers were dissolved in THF and eluted at a flow rate of 0.9 mL/min through Phenogel columns from Phenomenex. SEC calibration was performed using polystyrene standards. Molecular weights of linear copolymers were calculated using light scattering data assuming that the dn/dc of the corresponding homopolymer in THF could be applied. The cellulose copolymers were analyzed in toluene.

Matrix assisted laser desorption/ionization (MALDI) time of flight (TOF) mass spectrometry (MS) was performed on low molecular weight polymers on a PerSeptive Biosystems Voyager linear MALDI-TOF MS equipped with a nitrogen laser (337 nm) and a dual micro-channel plate detector. Samples were ionized from an indoleacrylic acid (IAA) matrix.

Proton nuclear magnetic resonance (NMR) was performed on a Bruker 250 MHz instrument. Fourier transform (FT) IR was performed on a Perkin-Elmer 1760 FTIR spectrometer, utilizing KBr pellets of polymer samples.

Initiation of Homopolymerization. Phenyl and *tert*-butyl Barton esters were prepared by a previously published procedure (2). Initial polymerizations were performed in bulk with 0.05 mol methyl methacrylate or styrene. Initiation was accomplished using 0.5 mmol Barton ester (*tert*-butyl for MMA and phenyl for styrene) and temperatures of 95° (MMA) or 100°C (styrene). Dissolution of the polymers in THF and reprecipitation in methanol facilitated in the removal of any yellow color from pyridine disulfides and remaining Barton ester. Low molecular weight samples of polystyrene were synthesized using 2 mole % (0.18M) solutions of phenyl Barton ester in styrene. Initiation was effected by either heating a 10 mL aliquot to 80°C in the absence of light, or subjecting a 10 mL aliquot to the light of a 125 W tungsten lamp at a distance of 30 cm at 25°C. The low molecular weight samples were examined by IR, SEC, and MS.

Rates of polymerization were measured with a dilatometer using solutions of phenyl Barton ester in styrene, and initiating polymerization by either heating the solutions to 80°C in the absence of light or subjecting the solutions to the light of a tungsten lamp as described above. Solutions were prepared with concentrations from 8mM-80mM. Polymerizations were limited to approximately 15% conversion. The polymer samples were dissolved in THF, reprecipitated in methanol, filtered, and dried.

Polymerizations of styrene by benzoyl peroxide in the presence of phenyl Barton ester were also performed. A stock solution of benzoyl peroxide (0.01M) in styrene was prepared, and 10 mL aliquots were used to make solutions with phenyl Barton ester with concentrations ranging from 0.02M-0.1M. The polymerizations were performed by heating the solutions to 60°C in the absence of light. The polymers were reprecipitated in methanol, filtered, and dried.

N-Hydroxypyridine-2-thione, Methacryloyl Ester Copolymers. The copolymers were synthesized by heating to 70°C solutions of benzoyl peroxide (0.12 g, 0.5 mmol), methacryloyl chloride (0.26 g, 2.5 mmol), and methyl methacrylate (5.0 g, 0.05 mol) in 5.0 mL of benzene. Similar experiments yielded copolymers with 5 mole % acryloyl chloride and styrene. A 0.5 mL aliquot of polymer solution was precipitated in methanol and isolated for SEC analysis. To the remaining solution, sodium N-oxypyridine-2-thione, 0.37 g (2.5 mmol) was added and stirred in the absence of light at room temperature for 2 hours. A 5 mL aliquot of this solution was mixed with 5.0 mL dodecanethiol and heated to 75°C for 24 hours. The polymer was dissolved in THF and reprecipitated in methanol twice. The dried polymer was then examined by SEC. Another 5 mL aliquot of copolymer solution was mixed with 2.5 g (0.025 mol) of styrene and heated to 75°C for 24 hours. The resulting polymer was isolated by precipitation in methanol and analyzed by NMR and SEC.

N-Hydroxypyridine-2-thione, Vinylbenzoate Copolymers. 4-Vinylbenzoyl chloride was synthesized by heating 0.5 g (3.4 mmol) 4-vinylbenzoic acid and 1.0 g oxalyl chloride in 2.0 mL benzene. The benzene and excess oxalyl chloride were removed by vacuum. The residual yellow oil was obtained in 96% yield, examined by proton nuclear magnetic resonance {NMR, CDCl₃, δ=8.05 (d, 2H), 7.50 (d, 2H), 6.75 (dd, 1H), 5.90 (d, 1H), 5.45 (d, 1H)}, and used without further purification. 4-Vinylbenzoyl chloride, 0.41 g (2.5 mol), was copolymerized at 60 °C with 5.0 g (0.05 mol) styrene by 0.12 g (0.5 mmol) benzoyl peroxide in 5.0 mL benzene. A 0.5 mL aliquot of this solution was precipitated in methanol and stirred for 1 hour to assure complete conversion of the acid chloride to the methyl ester, the polymer was then isolated and dried. The acid chloride groups in the remaining polymer solution were reacted with 0.37 g (2.5 mmol) sodium N-oxypyridine-2-thione for 2 hours in the absence of light at room temperature. A 5.0 mL aliquot of modified copolymer solution, was heated to 75°C in the presence of 5.0 g (0.05 mol) of styrene for 24 hours. The polymer solution was precipitated in methanol, filtered, then dried; 6.2g of graft copolymer was obtained (61% conversion). The graft copolymer and the backbone copolymer (isolated from methanol) were then analyzed by NMR and SEC.

A second 5.0 mL aliquot was heated at 75°C for 24 hr in the presence of 5.0 mL of dodecanethiol before isolating the polymer as described above.

A polystyrene-*g*-poly(methyl methacrylate) was also synthesized. The backbone was synthesized as described above. The BE copolymer was precipitated in methanol, filtered, and dried to remove remaining monomer. Linear copolymer yield was 2.42 g (conversion = 45%). After dissolving 0.5 g of the BE copolymer in 5.0 g (0.05 mol) methyl methacrylate, exposure to visible light at 25°C effected copolymerization. The copolymer was precipitated in methanol and dried, yield = 2.02 g (MMA conversion = 31%). The copolymer was analyzed by NMR and SEC. Extractions on 0.1 g samples of the copolymer were performed using either 10 mL ethanol or cyclohexane. The extracts were evaporated to dryness, dissolved in CDCl₃, and analyzed by NMR.

Poly(aryl ether sulfone) Graft Copolymers. Graft copolymerization experiments have also been performed by grafting styrene or 4-vinylpyridine to a poly(aryl ether sulfone) backbone. The carboxylated poly(aryl ether sulfone) (DS=1.0, 0.5 g) was dissolved in 15 g thionyl chloride and refluxed until evolution of HCl ceased. The excess thionyl chloride was evaporated, the acid chloride derivative was vacuum dried, and then dissolved in dry dichloromethane. Sodium N-oxypyridine-2-thione (0.5 g, 3.4 mmol) was added and stirred for 4 hours in the absence of light at room temperature. The resultant BE modified poly(aryl ether sulfone) was purified by precipitation in methanol, filtered, and dried. Quantitative yield of Barton ester was confirmed by UV-Visible spectroscopy of CHCl₃ solutions of the modified polymers using a previously reported extinction coefficient (5). Grafting was accomplished by adding 0.2 g poly(aryl ether sulfone-Barton ester) to a mixture of 10 g (0.096 mol) vinyl monomer and 2.3 g of dimethylformamide (DMF), followed by exposing the solution to visible light at 25°C for 12 hours. The poly(aryl ether sulfone)-*g*-polystyrene was isolated by precipitation in methanol and analyzed by SEC, ¹H NMR (in CDCl₃), and IR. A corresponding poly(aryl ether sulfone)-*g*-polyvinylpyridine was prepared using similar conditions and precipitated in methanol, filtered, and dried by vacuum.

Introduction of Barton ester groups was achieved on carboxylated poly(aryl ether sulfones) with degrees of substitution equal to 0.15, 0.54, and 1.0. A stock solution of styrene (75mole% in DMF) was prepared. Samples of Barton ester-substituted polysulfones (D.S. = 1) were dissolved in the styrene/DMF mixture so that the concentration of Barton ester was 1-100 mM. The solutions were exposed to visible light as before. The polymers were precipitated in methanol, filtered, and dried. The copolymers were then analyzed by NMR and SEC.

Carboxymethyl Cellulose Graft Copolymers. Carboxymethyl cellulose, CMC, samples (M_w ca. 250,000, Aldrich) with DS= 0.7, 0.9, 1.2 were used (1.07-1.56 g, 5 mmol carboxylic acid). The polymers were slurried in pyridine in 1% w/v concentration. The mixtures were cooled to -15°C. Isobutyl chloroformate, 0.69 g (5 mmol), was added and stirred for 20 minutes under nitrogen atmosphere. Sodium N-oxypyridine-2-thione, 0.75 g (5 mmol), was then added and the mixture was stirred in the dark for 1 hour under nitrogen at -15°C. The modified cellulose was dried by

evaporation using nitrogen at room temperature. Quantitative conversion of Barton ester was confirmed by UV-Visible spectroscopy of CHCl_3 solution. The BE-cellulose was slurried in 55 mL styrene and the mixture was irradiated with visible light. The resulting copolymer was diluted with THF, precipitated in methanol, filtered, and dried. The graft copolymers were weighed, then analyzed by NMR, IR, and SEC. Copolymer solutions (10 wt% in toluene) were filtered through a fritted funnel to remove any insoluble fraction. The mass of the insoluble portion was measured. Extractions of the copolymers were performed using cyclohexane at 34°C. The extraction mixture was filtered through a 0.2 micron filter (Whatman) and analyzed by UV-Vis spectroscopy.

Results and Discussion

Initiation of Homopolymerization. *tert*-Butyl Barton ester was used to initiate the bulk polymerization of methyl methacrylate and acrylonitrile. Solution polymerizations were conducted in benzene and dimethylformamide respectively. The poly(methyl methacrylate)s isolated exhibited molecular weights between 60-80K and polydispersities of 1.9 - 2.5. Phenyl Barton ester was used to initiate styrene and 4-vinylpyridine polymerizations either in bulk or after diluting the monomers with 25 mole % DMF. Polystyrene molecular weights were 50-70K, with polydispersities of 1.9-2.4 and conversions of 70-80% were easily achieved. These results encouraged further studies; the styrene/phenyl Barton ester system was chosen as a model system.

The mechanism for polymerization is shown in Scheme 4. For the phenyl Barton ester, initiation is shown occurring with the benzyloxy radical. While most alkyl acyloxy radicals lose carbon dioxide readily (11), aromatic acyloxy radicals lose carbon dioxide 10^5 times slower (12). The benzyloxy radical is therefore expected to initiate polymerization before decarboxylation occurs. After initiation, propagation occurs via normal radical polymerization means. Polymer chains are terminated predominately by a chain transfer reaction with the initiator, which results in a pyridinesulfide end-group. Based upon the independence of polymerization rate on BE concentration, termination by coupling of growing chains or coupling between growing chains and pyridine thiol radicals are minor contributors to the process. As discussed above, the pyridine sulfide radical promotes a molecularly induced homolysis of BE and does not appear to initiate polymerization. The chain transfer constants for 2-pyridine thiol (13) and 2,2'-bipyridyl disulfide (14) are orders of magnitude less than those reported for the Barton ester so it is unlikely that either of these potential intermediates contribute significantly to the polymerization kinetics. Thus, the kinetics of polymerization can be described by the following equations:

$$\begin{aligned}
 R_i &= k_i [\Phi\text{COO}\cdot][\text{M}] = f k_d [\text{I}] \\
 R_p &= k_p [\text{M}][\text{M}\cdot] \\
 R_{tr} &= k_{tr} [\text{I}][\text{M}\cdot] \\
 R_t &= 2k_{t(pp)} [\text{M}\cdot]^2 + k_{t(ps)} [\text{M}\cdot][\text{PyS}\cdot] \\
 -d[\text{M}\cdot]/dt &= -k_i [\Phi\text{COO}\cdot][\text{M}] - k_{si} [\text{PyS}\cdot][\text{M}] + k_{tr} [\text{I}][\text{M}\cdot] + 2k_{t(pp)} [\text{M}\cdot]^2 \\
 &\quad + k_{t(ps)} [\text{M}\cdot][\text{PyS}\cdot] + k_{tr2} [\text{M}\cdot][\text{PySSPy}\cdot]
 \end{aligned}$$

If $k_{tr} [I][M] \gg 2k_{(pp)} [M]^2 + k_{(ps)} [M][PyS] + k_{tr2} [M][PySSPy]$ and $k_i [\Phi COO][M] \gg k_{si} [PyS][M]$, then:

$$-d[M]/dt = -k_i [\Phi COO][M] + k_{tr} [I][M].$$

Assuming a steady-state, i.e., $-d[M]/dt = 0$, $f k_d [I] = k_{tr} [I][M]$ and $[M] = f k_d / k_{tr}$,

$$R_p = k_p [M] f k_d / k_{tr}.$$

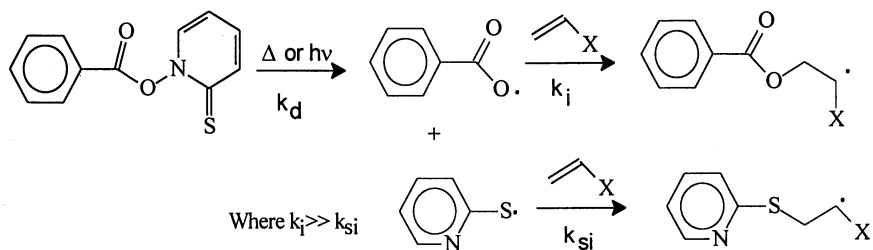
Indeed, the rates of polymerization measured by dilatometry are independent of initiator concentration. Based upon an average kinetic chain length, $n_{av} = R_p / (R_{tr} + R_t)$, and assuming that $R_{tr} \gg R_t$, the $Dp_{av} = n_{av} = k_p [M] / k_{tr} [I]$ which shows that the molecular weight is controlled by the monomer to initiator ratio. The chain transfer constant for the initiator, $C_1 = k_{tr}/k_p$, is calculated from the slope of $1/Dp_{av}$ vs $([I]/[M])$.

The structure of the end-groups was confirmed by MALDI-TOF mass spectrometry. Low molecular weight polystyrenes were prepared by polymerizing solutions of phenyl Barton ester (2 mol %) in styrene by heat or light. The polymers were characterized first by SEC; the M_n 's for the samples were 5300 and 6900 for thermal initiated and for light initiated samples respectively. The samples were then analyzed by MALDI-TOF-MS. By subtracting the appropriate number of monomer units for each oligomer, the remaining mass is the mass of the end-groups. Average end-group mass was calculated to be 229.3 for the heat initiated PS, and 230.3 for the light initiated PS, each with a measurement error of +/- 3. The total mass of the benzoyloxy and pyridine sulfide units is 231. The mass spectra support the mechanism where the initiating fragment is the benzoyloxy group, and the terminal fragment is the pyridine sulfide group as would be expected when the molecular weight is controlled by chain transfer to the initiator. The presence of the benzoyloxy end group was confirmed by infrared spectroscopy. Along with the characteristic C-C, C-H, and aromatic stretches, a sharp peak at 1726 cm^{-1} was present. This peak is indicative of an ester carbonyl stretch.

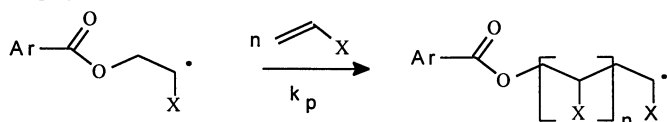
In a series of kinetic experiments, initiations were carried out either by heating solutions in a dilatometer to 80°C in the absence of light, or by subjecting solutions to the visible light of a tungsten lamp at 25°C . The rates of polymerization for the various concentrations and initiation methods are given in Table II. The rates are dependent upon temperature or light intensity, but the rates measured are the same order of magnitude as those found with conventional initiators at the lower initiator concentrations. The rate of polymerization was found to be independent of initiator concentration, supporting the assumptions made in the polymerization mechanism.

The molecular weights of the polymers isolated from the dilatometry experiments were measured by SEC. The molecular weight data is also shown in Table II. Figure 1 shows the linear relationship between $1/Dp$ and $[I]/[M]$. From the molecular weight data, C_1 was calculated to be 0.95-0.96; these results were consistent with those of Meijs (8) for C_x in similar systems. The polymerizations were repeated at 60°C with added benzoyl peroxide initiator. The resulting value for C_x , calculated by the Mayo method (9), was 1.4.

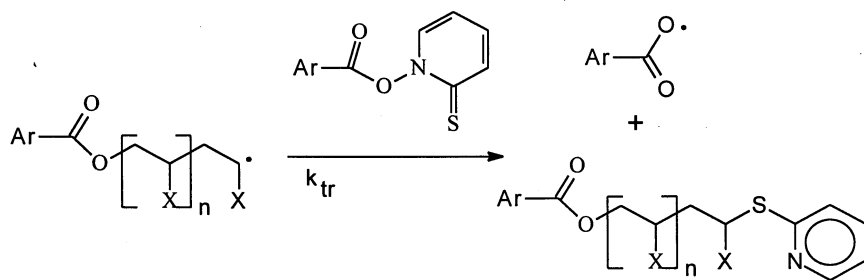
Initiation



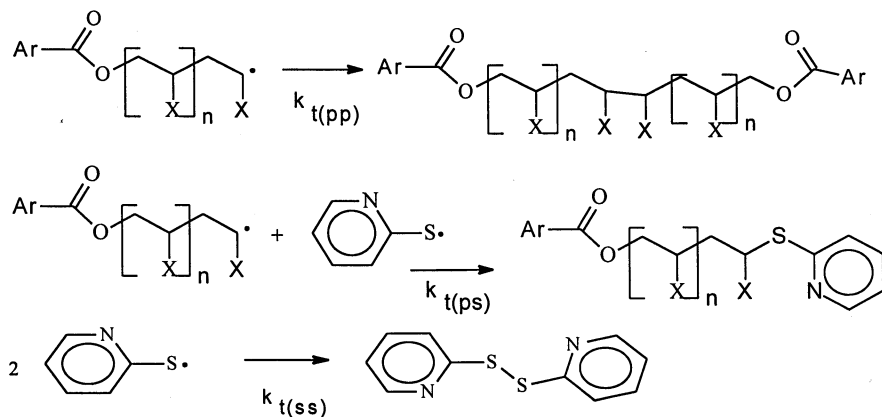
Propagation



Chain transfer to initiator



Termination by coupling



Scheme 4. Mechanism of Polymerization

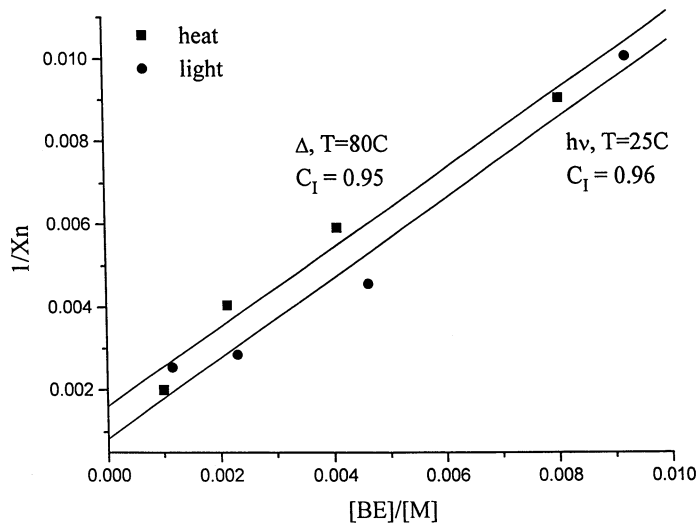


Figure 1. Influence of initiator to monomer ratio on the reciprocal degree of polymerization. No cointiator added.

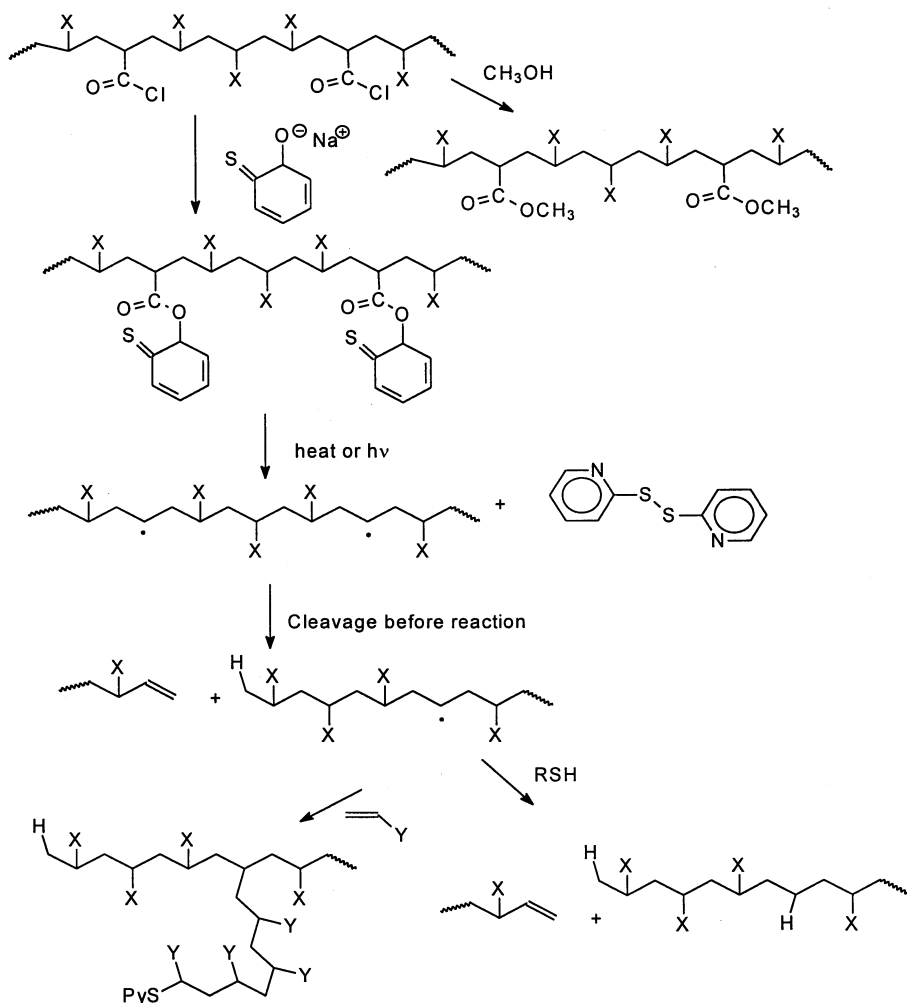
Backbone Stability. Because Barton esters are easily synthesized from reactive carboxylic acid derivatives, initial graft copolymerizations were attempted from backbone polymers containing acid chloride units. Barton esters are especially useful in the synthesis of graft copolymers because they decompose into an initiating alkyl radical and a relatively unreactive pyridine sulfide radical with a propensity to attack BE residues. Thus, two radicals are formed on the polymer backbone along with a relatively inert 2,2'-dipyridyl disulfide by-product. This favors grafting to the substrate polymer with a minimal amount of concomitant homopolymerization. Only one other previously published procedure for graft copolymerization describes asymmetric initiator substituents; it involves a Friedel-Crafts alkylation and subsequent oxidation to form hydroperoxides (15).

Table II. Influence of BE Concentration on Polystyrene Rp and Mol. Wt.

[I] (mM)	Rp (min ⁻¹)	Mw	Mn
Thermal Initiation, T=80°C			
8.7	7.2e-4	88,000	52,000
18.6	8.0e-4	40,000	26,000
35.6	7.2e-4	25,000	18,000
70.1	7.7e-4	23,000	11,000
Photo Initiation, T=25°C			
10.0	3.6e-4	74,000	41,000
20.0	3.7e-4	64,000	37,000
40.0	3.6e-4	39,000	23,000
80.0	3.6e-4	20,000	10,000

Our planned synthesis for forming polymeric Barton esters is shown in Scheme 5. In the initial syntheses, the vinyl-X repeat units in the backbone were either methyl methacrylate or styrene; and the vinyl-Y repeat units for grafting was styrene. In the synthesis of the backbone, methyl methacrylate was copolymerized with methacryloyl chloride (19:1 MMA:acid chloride) in benzene solution, initiated by BPO. In similar experiments, styrene was copolymerized with acryloyl chloride (19:1 sty:acid chloride). Analysis of the linear copolymers by SEC assumes that the dn/dc's for homopolymer were appropriate. Barton esters were then formed on the backbone copolymers. To these modified backbone copolymers, more monomer was added. The solutions containing esterified backbone and additional monomer were heated to effect the decomposition of the Barton esters. The resulting polymers were isolated and analyzed by SEC. The molecular weights of the expected graft polymers were actually slightly less than those of the original backbone polymers. The explanation for these unexpected results is a chain cleavage reaction. The proposed mechanism for chain cleavage is also shown in Scheme 5. When the decomposition of a Barton ester on a backbone polymer chain results in the formation of a free radical directly on the carbon chain of the polymer, chain cleavage can result.

This theory was tested by decomposing the Barton esters of the modified polymer backbones in the presence of dodecanethiol. If the decomposition of a Barton ester resulted in a free radical that abstracted hydrogen from thiol, the polymer molecular weight would be unchanged. However, if the decomposition of Barton ester results in chain cleavage before interaction with thiol, a reduction in molecular weight would be observed. The molecular weights of the polymers after decomposition of the Barton esters were approximately half of the molecular weights of the unreacted polymers. These results confirm that the chain breaking mechanism is competitive with hydrogen abstraction. Due to the chain cleavage side reaction, no further characterizations were performed on these polymers.



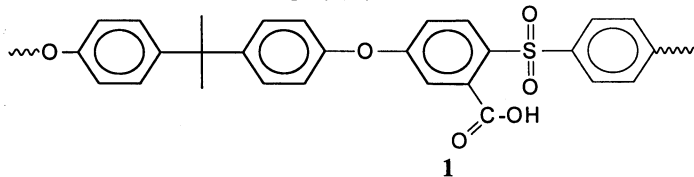
Scheme 5. Graft Copolymerization with Acryloyl Copolymers

Graft Copolymerization to Styrene Benzoate Derivatives. To further test the feasibility of using Barton esters for graft copolymerization, and to avoid the formation of free radicals directly on a polymer backbone, the acid chloride monomer, 4-vinylbenzoyl chloride (4-VBC) was synthesized from 4-vinylbenzoic acid. The 4-VBC was copolymerized with styrene (19:1 sty:acid chloride) in the presence of benzoyl peroxide (99:1 sty:BPO) to give a polymer chain suitable for grafting. A portion of the polymer with the acid chloride pendant groups was then reacted to form Barton esters. Aliquots of this polymer were then heated either in the presence of dodecanethiol to test for backbone stability, or styrene to initiate grafting. The polymers were analyzed by SEC. The polymer heated in the presence of dodecanethiol showed no change in molecular weight.

Styrene was grafted to the 4-VBBE copolymer and the graft copolymer was analyzed by SEC. The SEC-LS curves are shown in Figure 2. The shift towards lower elution volume and increased light scattering intensity of the SEC curves indicate that grafting occurred. Assuming that the 4-VBC copolymerizes randomly with styrene, the degree of substitution on the backbone was 5%. Then, assuming quantitative synthesis of Barton ester, the number of Barton ester moieties per chain (and grafts per chain) is calculated to be 8. Based on the difference in M_n of the two polymers, the average graft length for the branched polymer is then estimated to be 12 monomer units.

A graft copolymer polystyrene-*g*-poly(methyl methacrylate) was synthesized. As before, the backbone was synthesized from styrene and 4-VBC. Barton esters were synthesized, and this backbone copolymer was isolated to insure the purity of the backbone by removing remaining monomer. The backbone polymer was dissolved in methyl methacrylate, and the Barton ester pendant groups were decomposed by light to effect copolymerization, a 300% weight increase was observed. Analysis of the copolymer by NMR indicated the presence of both polystyrene and poly(methyl methacrylate). To insure that the sample was not merely a mixture of homopolymers, and was in fact a graft copolymer, extractions were performed on samples by ethanol or cyclohexane. Analysis of the extracts by NMR did not indicate the presence of pure homopolymer.

Grafting to Poly(aryl ether sulfone) Backbone. Graft copolymerization experiments have also been performed by grafting styrene or 4-vinylpyridine to a well characterized carboxylated poly(aryl ether sulfone) (1) backbone. The substrate



polymer was converted to an acid chloride, and then to a Barton ester. The grafting was accomplished by adding the poly(aryl ether sulfone-BE) to a mixture of vinyl monomer and DMF (3:1 proportion), and exposing the solution to visible light. The weight gain of the copolymer was 311%. The poly(aryl ether sulfone)-*g*-polystyrene

was analyzed by SEC and ^1H NMR (CDCl_3). The SEC curves and molecular weight data are shown in Figure 3. The results of the SEC and NMR experiments show that polystyrene was successfully grafted to the polysulfone. The mass increase of the poly(aryl ether sulfone)-*g*-polyvinylpyridine copolymer was 93%.

The effects of degree of substitution and polymer concentration on grafting efficiency and graft length was explored using carboxylated poly(aryl ether sulfone)s with degree of substitution equal to 0.15, 0.54, 1.0. Samples of these Barton ester-substituted polysulfones were dissolved in a 75% styrene in DMF mixture so that the Barton ester concentration was 10 - 100 mM, then polymerization was effected by light. The resulting copolymers were purified, weighed, and analyzed by NMR and SEC. The results in Table III clearly show an additional effect of degree of substitution on graft length. The calculated length is based upon the mean concentration of Barton ester in solution does not accurately reflect the observed graft length. If the chain transfer constant is recalculated using the data obtained on polymers at the lowest concentration and/or lowest DS, an apparent C_x is obtained that considers the effect of chain transfer to intramolecular Barton ester groups. Using the "polymer" C_x , a reasonable prediction of the graft length formed based upon mean Barton ester and styrene concentrations is feasible. Graft length measured is an average of graft lengths measured by mass increase, NMR, and SEC.

Table III. Polysulfone-*g*-polystyrene Synthesis

Substrate mass (g)	[BE](mM) ^a	%weight gain	graft ^b length	calc. ^c length	calc. ^d length
DS=0.15					
0.04	1.4	1050	162	5290	290
0.22	7.5	114	43	980	55
0.44	15.0	32	25	490	28
DS=0.54					
0.05	5.3	860	54	1390	78
0.27	28.5	200	12	260	15
0.51	53.8	104	11	130	8
DS=1.0					
0.06	10	867	36	750	41
0.30	50	200	10	150	8
0.60	100	92	8	75	4

^aIn 10 mL 75 mole% styrene in DMF

^bAverage of values from mass increase, NMR, and SEC

^cCalculated from $[\text{BE}]/[\text{M}]$ and $C_x=0.96$

^dCalculated from $[\text{BE}]/[\text{M}]$ and $C_x=17.2$

Grafting to Carboxymethyl Cellulose Backbone. Further graft copolymers were synthesized from carboxymethylcellulose (CMC) as shown in Scheme 6. Barton esters were synthesized on the cellulose by using a mixed anhydride intermediate (16,17). The carboxylate groups were first reacted with isobutyl chloroformate to

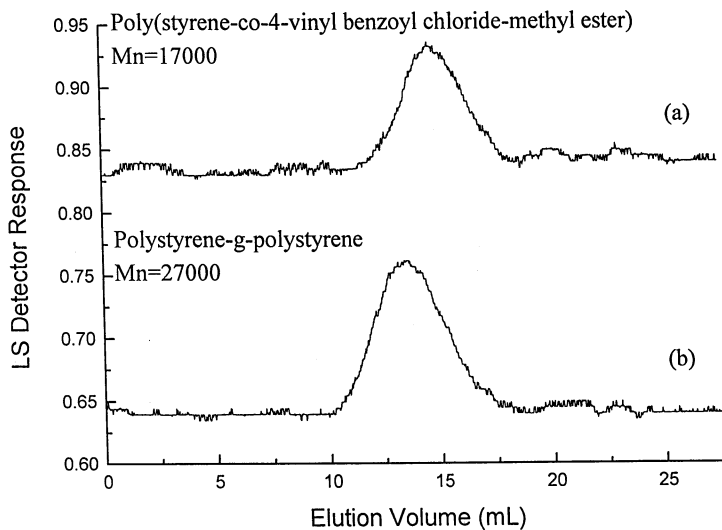


Figure 2. SEC-LS (THF eluent, 0.9ml/min flow rate) of copolymers before (a) and after (b) grafting.

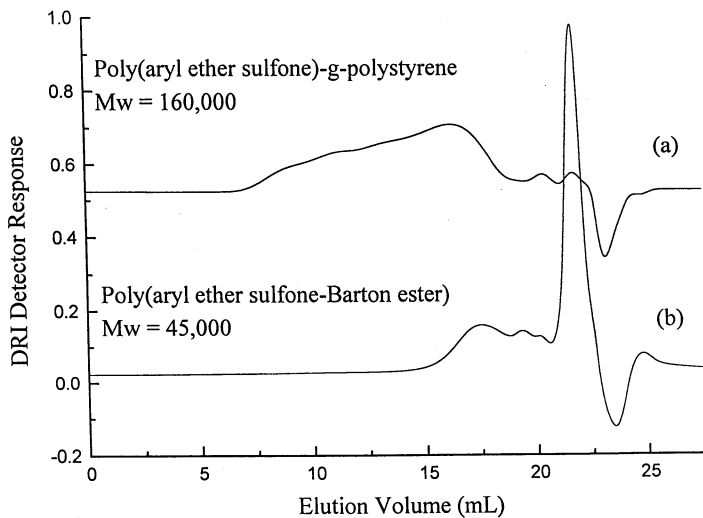


Figure 3. SEC curves of (a) graft copolymer and (b) backbone.

form the mixed anhydride, then sodium 2-pyridinethiol-1-oxide was added to form the Barton esters. The modified cellulose samples were then dissolved in styrene and subjected to visible light to form graft copolymers. Three grades of CMC were used in the grafting experiments. All were molecular weight ca. 250,000, but had DS=0.7, 0.9, 1.2. The graft copolymers formed were weighed, then analyzed by NMR, IR, and SEC. The results are compiled in Table IV.

Table IV. Carboxymethylcellulose-g-Polystyrene Copolymers

DS ^a	Substrate Mass (g)	% Weight Gain	Graft Length ^b	% Soluble in	
				Toluene	Cyclohexane
0.7	1.56	319	13	90	6.6
0.9	1.3	422	13	93	6.7
1.2	1.07	635	13	95	6.8

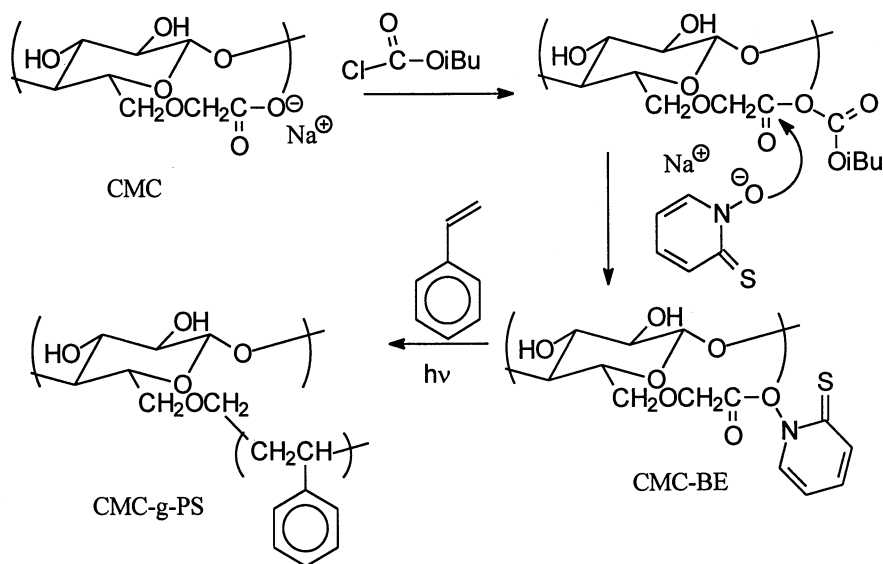
^a [BE](mM) = 91, in styrene

^b Average of values from mass increase and NMR

The graft lengths calculated from NMR and mass increase were in agreement and the averages are shown in Table IV. The percent soluble in cyclohexane was calculated from UV-Vis data using the previously reported extinction coefficient for polystyrene (18). Absorption due to residual styrene monomer is also possible. In any case, the amount of homopolymer formed is low. The amount insoluble in toluene is also low, and may be due to variations in the CMC itself. SEC-LS experiments assume that the dn/dc for homopolystyrene is applicable. Molecular weights (M_w) for the copolymers ranged from 170,000 to 200,000. These low values make graft length calculations impossible, and indicate that chain-breaking reactions are occurring to some extent along with grafting. The IR spectra do not show carbonyl peaks, indicating that decarboxylation occurs before any reactions with styrene.

Conclusions

The results show that Barton esters serve as initiators in the polymerization of vinyl monomers. Further, chain transfer to Barton ester allows for control of molecular weight and end-group composition. Polymeric initiators can be produced by converting carboxyl substituents on backbone polymers to Barton esters using either the corresponding acid chloride or isobutyl formyl anhydride to promote reaction with sodium 2-pyridinethiol-1-oxide. Decomposition of the Barton ester substituted backbone polymers in the presence of vinyl monomer results in the formation of graft copolymers with minimal homopolymerization. The length of the graft formed depends upon the extent of Barton ester substitution on the backbone as well as the monomer to initiator ratio employed in copolymerization. Grafting may be accompanied by backbone chain cleavage, particularly when initiating radicals reside directly on the backbone.



Scheme 6. Formation of Carboxymethylcellulose-g-polystyrene

Acknowledgments. We would like to thank Michael Guiver of the National Research Council of Canada for the polysulfone samples. We would also like to thank Tracy McCarley of the Louisiana State University Chemistry Department Mass Spectrometry Facility for the mass spectra. Also, we would like to thank Tommy Menuet for his work with the polysulfone copolymers as part of the Howard Hughes undergraduate research program. Additional work on the poly(aryl ether sulfone) copolymers was completed by Laura Wolf as part of the Louisiana State University Chemistry Department undergraduate research program.

Literature Cited.

1. Barton, D.H.R. and Kretzschmar, G., *Tetrahedron Letters*, **1983**, 24 (52), 5889-5892.
2. Barton, D.H.R.; Bridon, D.; Fernandez-Picot, I.; Zard, S., *Tetrahedron*, **1987**, 43, 12, 2733-2740.
3. Barton, D.H.R. and Samadi, M., *Tetrahedron*, **1992**, 48 (35), 7083-7090.
4. Barton, D.H.R. and Motherwell, W.B., *Heterocycles*, **1984**, 21, 1-19.
5. Barton, D.; Crich, D.; Motherwell, W., *Tetrahedron*, **1985**, 41 (19), 3901-3924.
6. Crich, D., Quintero, L., *Chem. Rev.*, **1989**, 89, 1413-1432.
7. Aveline, B. M., Kochevar, I. E., Redmond, R. W., *J. Am. Chem. Soc.*, **1995**, 117, 9699-9708.
8. Meijs, G.F. and Rizzardo, E., *Polymer Bulletin*, **1991**, 26, 291-295.
9. Gregg, R.A. and Mayo, F.R., *Discuss. Faraday Soc.*, **1947**, 2, 328.
10. Bergbreiter, D.E., and Zhou, J., *J. Polym. Sci.: Part A: Polym. Chem.*, **1992**, 30, 2049-2053.

11. Martin, J.; Taylor, J.; Drew, E., *J. Am. Chem. Soc.*, **1967**, *89*, 129-130.
12. DeTar, D.F., *J. Am. Chem. Soc.*, **1967**, *89*, 4058.
13. Nair, C.P.; Richou, M.C.; Chaumont, P.; Clouet, G., *Eur. Polym. Journal*, **1990**, *26*, *7*, 811-815.
14. Costanza, A.J.; Coleman, R.J.; Pierson, R.M.; Marvel, C.S.; King, C., *J. Polym. Sci.*, **1955**, *17*, 319-340.
15. Metz, D.J., and Mesrobian, R.B., *J. Polym. Sci.*, **1955**, *16*, 345-355.
15. Barton, D.H.R., Herve, Y., Potier, P., Thierry, J., *J. Chem. Soc. Chem. Commun.*, **1984**, 1298-1299.
17. Barton, D.H.R., Gero, S.D., Quiclet-Sire, B., Samadi, M., *Tetrahedron: Asymmetry*, **1994**, *5*, *11*, 2123-2136.
18. Klopfer, W., *European Polymer Journal*, **1975**, *11*, 203-208.

Chapter 24

How to Make Polymer Chains of Various Shapes, Compositions, and Functionalities by Atom Transfer Radical Polymerization

Scott G. Gaynor and Krzysztof Matyjaszewski¹

Department of Chemistry, Carnegie Mellon University, 4400 Fifth Avenue, Pittsburgh, PA 15213

Atom transfer radical polymerization, ATRP, is a controlled / “living” radical polymerization system which has been developed in our laboratories. The use of ATRP to prepare well-defined polymers with novel compositions (statistical, alternating, block), topologies (linear, graft, branched, hyperbranched), and functionalities (telechelic polymers, functional monomers, etc.) is reviewed.

Polymer chemistry is largely driven by the motivation to make new materials that are better than those that currently exist. Whether it be a rheologist studying the effects of polymer additives, a synthetic chemist synthesizing new materials or studying the mechanism of existing polymerization systems, the goal of making better materials remains the same. To make better materials, two approaches can be taken: make new formulations of existing polymers or prepare completely new polymers. Although formulation is widely used, it is not the focus of this chapter.

To prepare new polymers, two routes can be taken. The first involves the synthesis and polymerization of new monomers, and the second is to use existing monomers to prepare polymers with novel compositions, topologies, and/or functionalities. Since it is economically more feasible to use existing monomers, there has been a strong desire to optimize/control existing polymerization systems. The ultimate control of a polymerization system is the attainment of a living polymerization.

Living polymerizations are polymerizations with no chain breaking reactions such as transfer and termination.^(1,2) The polymers prepared by these systems are generally characterized with degrees of polymerization defined by $DP_n = \Delta[M]/[I]_0$ ($\Delta[M]$ and $[I]_0$ are the concentration of reacted monomer and added initiator, which should be consumed at low conversion, respectively) and narrow molecular weight distributions, $M_w/M_n < 1.1$. Living polymerizations also allow for the preparation of polymers with novel compositions and topologies, i.e., block copolymers or graft copolymers, respectively.⁽³⁾ Unfortunately, most living polymerizations have been confined to ionic polymerization systems,⁽³⁾ which are limited to only a small number of monomers and have rarely been

¹Corresponding author

used for the random/statistical copolymerization of two or more monomers. Also, as the reaction conditions require the complete absence of water, the extension of living polymerizations into commercial applications has been limited.

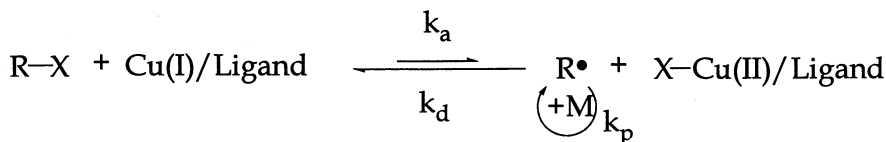
To overcome the drawbacks presented by ionic polymerization systems, it has been desirable to develop a living polymerization system based on radical polymerization. Radical polymerization has three benefits: the number of monomers that can be (co)polymerized radically is quite extensive, a wide variety of monomers can be copolymerized and the polymerizations are tolerant of water and, in some cases, can be conducted in water. However, obtaining a living radical polymerization was thought to be nearly impossible due to the unavoidable bimolecular termination of two propagating radicals.

To reduce the contribution of bimolecular termination, it has been proposed that an equilibrium between active and dormant species be established with the equilibrium shifted towards the dormant species, thus keeping the instantaneous concentration of the active radicals low.⁽⁴⁾ By keeping the radical concentration low, the contribution of termination can be suppressed to low levels. Since termination is present, such systems which do provide control of molecular weight and molecular weight distributions similar to the living ionic polymerizations should be called controlled or "living" polymerizations.⁽⁵⁾

Many systems have been proposed to provide controlled / "living" radical polymerization systems,⁽⁶⁻¹⁴⁾ but these have generally provided poor control of molecular weights ^(6,10,13,14) or were successful for only one class of monomers, i.e., only styrenes,⁽⁸⁾ acrylates,^(9,12) or methacrylates.⁽¹¹⁾ In our laboratories, we have pioneered the development of copper based atom transfer radical polymerization, ATRP, as a general controlled / "living" radical polymerization system.⁽¹⁵⁻¹⁷⁾ The polymerization system based on copper and other transition metals has been shown to be especially robust, as it has been used to obtain well-defined polymers of styrene(s),⁽¹⁵⁻²²⁾ acrylates,^(16,23,24) methacrylates,^(16,25-32) and acrylonitrile.⁽³³⁻³⁵⁾

ATRP involves the reversible activation and deactivation of alkyl halides by transition metal complexes, Scheme 1. Activation of the organic halide (R-X) occurs via an inner sphere electron transfer reaction between the transition metal (e.g., Cu(I)/ligand) and the organic halide (rate constant k_a), resulting in the formation of a radical and the transition metal whose oxidation state has increased by one and now has the halide covalently bound to it (X-Cu(II)/ligand). The resulting radical then initiates the polymerization of the monomer(s). As the polymer chain propagates (rate constant k_p), it reacts with the metal halide, which should be a good deactivator of radical polymerizations (rate constant k_d), to reform the lower oxidation state metal complex and an oligomer/polymer chain with a halogen end group. This reaction repeats itself, now using the oligomer/polymer as the organic halide to reinitiate the polymerization. As long as deactivation of the propagating radical is sufficiently fast, well-defined polymers with $DP_n = \Delta[M]/[I]_0$ and $M_w/M_n < 1.5$ are obtained. It should be noted that in

Scheme 1



conventional radical polymerizations, the minimum polydispersity that can be obtained is $M_w/M_n = 1.5$, assuming termination by coupling and low conversion.

By using ATRP, we have been able to exploit the potential that controlled / "living" radical polymerizations provide the synthetic polymer chemist. This chapter outlines the work that has been done in our laboratories to prepare polymers with well-defined molecular weights, compositions, topologies, and/or functionalities.

Composition

Homopolymers

As stated above, ATRP has been shown to successfully polymerize a wide variety of monomers. The first examples of ATRP used a heterogeneous catalyst system, copper(I)-X complexed with 2, 2'-bipyridyl (bipy). Although the catalyst was largely heterogeneous, sufficient amounts of copper (I) were soluble to allow for activation of the organic halides, and thus catalyze the polymerization. Monomers that were successfully polymerized were styrene, acrylates, and methyl methacrylate.^(15,16) These polymers had molecular weights that were proportional to $\Delta[M]/[I]_0$ and had polydispersities that were much lower than conventional radical polymerizations, $1.1 < M_w/M_n < 1.5$.

The development of homogeneous catalysts (4, 4'-alkyl substituted bipyridines), first reported by our group,⁽¹⁷⁾ allowed for the synthesis of polymers with very narrow molecular weight distributions, $M_w/M_n \leq 1.1$.^(17,18,20,25) The enhancement of the control of the polymerization by using homogeneous catalysts was ascribed to the increase in the solubility of the copper (II)-X species. Since the molecular weight distribution is dependent on the chain length and the rate of exchange between active and dormant species,^(36,37) $M_w/M_n = 1 + [(k_p[R-X]/k_d[Cu(II)-X])]$, it can be seen that by increasing the concentration of deactivator, the polydispersity will be lower.

This effect was also demonstrated by using copper (I)/bipy in a highly polar solvent which would render the catalyst completely soluble. An example is the ATRP of acrylonitrile ^(34,35) in ethylene carbonate. In these polymerizations, the molecular weights increased linearly with conversion and the resulting polymers had very narrow molecular weight distributions, $M_w/M_n < 1.05$. Figure 1 shows a representative MALDI-TOF spectrum of the obtained polyacrylonitrile. This represents the first example of such well-defined polyacrylonitrile.

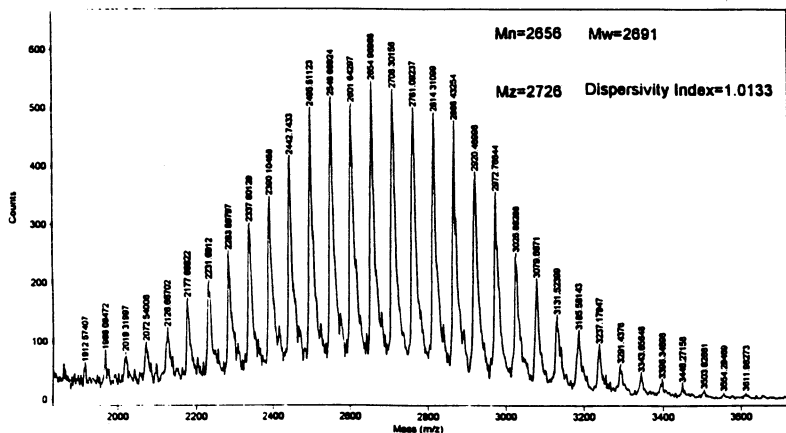


Figure 1. MALDI-TOF spectrum of polyacrylonitrile prepared by ATRP.

Statistical and Gradient Copolymers

To extend the usefulness of ATRP, copolymerizations of two different monomers were undertaken. Table 1 lists some of the copolymers that have been successfully prepared. The first entry, a Sty/MMA copolymer, was polymerized using the heterogeneous copper(I)/bipy catalyst. Although the molecular weights of these polymers were relatively well controlled, the polydispersities were somewhat high. Much narrower molecular weight distributions, $M_w/M_n < 1.2$, were obtained for the Sty/BA copolymers when a homogeneous catalyst was used, copper(I)/dNbipy (dNbipy = 4, 4'-di(5-nonyl)-2, 2'-bipyridyl). It should be noted that the control of the polymerization was maintained regardless of the relative amounts of comonomer. This is in contrast to other reports of the copolymerization of styrene and acrylates using nitroxide based "living"/radical polymerizations.(38-40)

ATRP has also been used to copolymerize radically polymerizable monomers with monomers that can not be homopolymerized radically. Examples of this are the copolymerizations of isobutene with acrylates or acrylonitrile using Cu (I)/bipy. When an excess of isobutene was in the monomer mixture, alternating copolymers were obtained.

Although vinyl acetate has not yet been homopolymerized by ATRP, copolymers of vinyl acetate and methyl acrylate have been successfully prepared, possibly due to a faster cross-propagation step in comparison with homopropagation for vinyl acetate.

Table 1. Copolymers Prepared by ATRP^a

A	B	% A		M_n	M_w / M_n	T_g (°C)
		Feed	Polymer			
Sty	MMA	49	47	11,700	1.4	
Sty	BA	13	13	13,800	1.18	-38
		23	25	11,200	1.18	-24
		51	55	11,200	1.12	-17
		75	69	12,000	1.11	-48
		87	83	12,300	1.13	-72
Isobutene	MA	50	26	6,500	1.5	-24
	AN	78	50	3,500	1.5	48
	BA	78	49	3,180	1.4	-48
AN	Sty	47	61	14,150	1.05	
MA	VAc	50	83 (36% Conv.)	1,840	1.3	

a) All conversions are >90% unless indicated. Sty = styrene; BA = butyl acrylate; MA = methyl acrylate; MMA = methyl methacrylate; AN = acrylonitrile; VAc = vinyl acetate.

Based on the reactivity ratios of the monomers, one monomer is often consumed at a faster rate than its comonomer. In conventional free radical polymerizations, this results in a distribution of comonomer compositions among the polymer chains unless under azeotropic conditions. That is, the polymer chains have varying amounts of comonomer; some contain more monomer A, while others, less monomer A. The distribution of compositions arises from the continually changing monomer feed in the polymerization system as one monomer is consumed faster than another. In controlled / "living" radical polymerizations all of the polymer chains grow at nearly the same rate

with very little termination. Therefore, the change in monomer feed composition is recorded in the *individual* polymer chains. Since the change in monomer concentration along the polymer chain is formed spontaneously, these types of polymers have been termed *spontaneous gradient copolymers*. Examples of these gradient copolymers are the Sty/BA copolymers listed in Table 1.(41) Other examples include Sty/MMA, MA/MMA, and Sty/MA.(42,43)

If the reactivity ratios of the monomers are similar and gradient copolymers can not be readily prepared spontaneously, *forced (or controlled) gradient copolymers* can be prepared by addition of one (or more) monomer(s) during the polymerization. An example of the preparation of a gradient copolymer by the forced gradient approach is the synthesis of Sty/AN (44) or Sty/MA (45) gradient copolymers.

Block Copolymers

Block copolymers are polymers which consist of two or more monomers that are segregated into separate regions of the polymer chain, but are covalently bound to each other. The simplest method to prepare block copolymers is by sequential addition of monomer B to a "living" polymer comprised of monomer A. The classic example is the synthesis of polystyrene/polybutadiene block copolymers by anionic polymerization.(2) ATRP has been used in a similar manner to prepare block copolymers of radically polymerizable monomers.(15,46)

Since activated halogen functional groups, such as benzyl halides, 2-halopropionate, or sulfonyl halides, can be used to initiate ATRP, block copolymers of non-radically polymerized monomers and radically polymerizable vinyl monomers can be prepared by using macroinitiators containing these halogen groups. The synthesis of such copolymers have been described as transformation polymerizations. Such transformations from cationic, ring opening metathesis polymerization (ROMP) or step-growth polymerizations to controlled / "living" radical polymerizations have been performed successfully in our laboratories.

Transformation from "Living" Carbocationic to Controlled/Living" Radical Polymerization

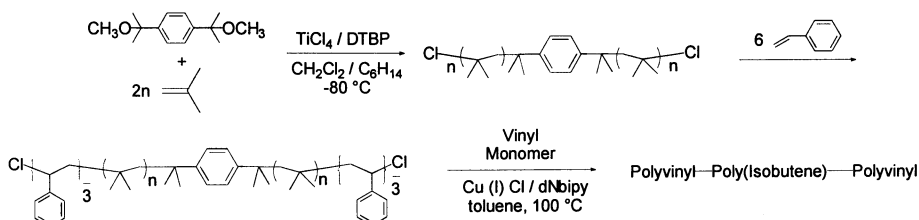
Several controlled / "living" carbocationic polymerizations are mechanistically similar to ATRP, with the exception that the carbon-halogen bond is heterolytically cleaved, not homolytically. Therefore, it was proposed that polymers prepared by controlled / "living" carbocationic polymerization could be used as macroinitiators for ATRP. This was first demonstrated by the cationic polymerization of styrene using 1-phenylethyl chloride in the presence of $\text{SnCl}_4/n\text{-Bu}_4\text{NCl}$.(47) AB block copolymers were successfully prepared by using the obtained polymers as macroinitiators for the polymerization of styrene, methyl acrylate and methyl methacrylate.

As styrene can be polymerized by ATRP, such block copolymers need not be prepared using cationic techniques. Therefore, to demonstrate that this transformation chemistry is useful, the formation of ABA block copolymers of isobutene (B) with radically polymerizable monomers (A) was undertaken.(48,49) Polyisobutene was polymerized using a difunctional initiator, *p*-dicumylmethyl ether, with a $\text{SnCl}_4/2$, 6-di-*t*-butyl pyridine catalyst, Scheme 2. Before quenching of the polymerization, a small amount of styrene was added to the reaction to cap the polyisobutene chains with a few units of styrene. This was done to prevent the elimination of HCl from the

polyisobutene ends, avoid heterolytic cleavage of the carbon halogen bond in the presence of copper (I) catalysts, and facilitate homolytic cleavage using styryl-halogen chain ends.

After the polymer was isolated ($M_n = 7,500$; $M_w/M_n = 1.3$), it was dissolved in a radically polymerizable monomer and used as a macroinitiator for ATRP, Scheme 2. Monomers that were successfully polymerized include: styrene ($M_n = 13,400$; $M_w/M_n = 1.2$), methyl acrylate ($M_n = 11,800$; $M_w/M_n = 1.4$), methyl methacrylate ($M_n = 23,100$; $M_w/M_n = 1.5$) and isobornyl acrylate ($M_n = 17,300$; $M_w/M_n = 1.4$). The copolymers prepared with styrene, methyl methacrylate or isobornyl acrylate were thermoplastic elastomers.

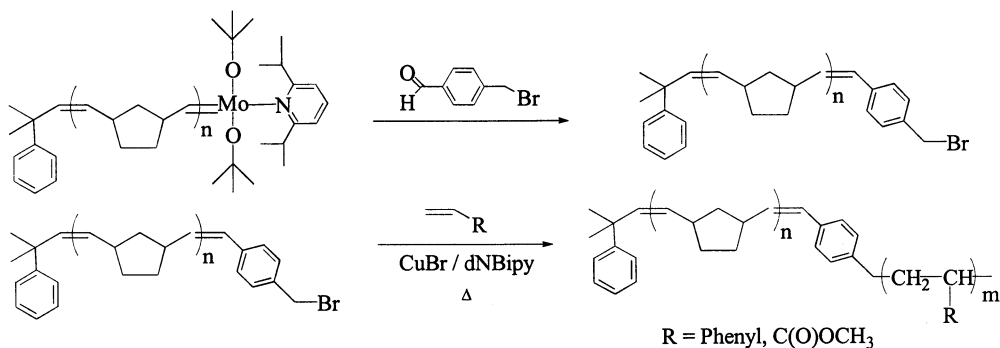
Scheme 2



Transformation from Living ROMP to "Living" Radical Polymerization

AB block copolymers of vinyl polymers with either polynorbornene or polydicyclopentadiene were synthesized by first conducting the living ROMP using a molybdenum catalyst, Scheme 3. The molybdenum catalyst was removed from the chain ends by quenching with *p*-bromomethylbenzaldehyde to yield the polynorbornene, $M_n = 59,000$; $M_w/M_n = 1.06$ (or polydicyclopentadiene, $M_n = 11,300$; $M_w/M_n = 1.5$) macroinitiator. These macroinitiators were successfully used to prepare block copolymers with either styrene or methyl acrylate. Figures 2 and 3 show SEC chromatograms of the macroinitiators and the resulting block copolymers. As can be seen, there was a clean formation of the block copolymers using the ROMP prepared macroinitiators.⁽⁵⁰⁾

Scheme 3



Transformation from Polycondensation to "Living" Radical Polymerization

Macroinitiators were prepared from poly(dimethyl siloxane), PDMS, and polysulfone. Commercially prepared PDMS, with either Si-H or vinyl end groups, was used in a hydrosilation reaction using a Karstedt's catalyst, Scheme 4. These bifunctional macroinitiators were then used to polymerize vinyl monomers such as styrene, butyl acrylate, methyl acrylate and isobornyl acrylate. The resulting polymers were ABA block copolymers, Table 2, and those prepared with styrene or isobornyl acrylate were thermoplastic elastomers.(51)

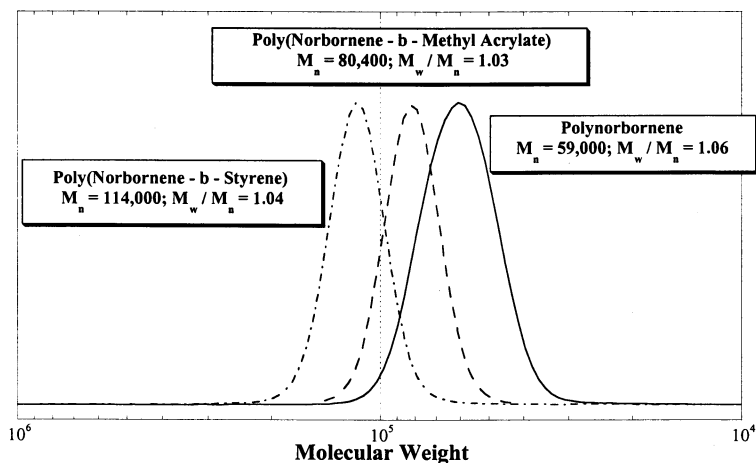


Figure 2. SEC chromatograms of polynorbornene/vinyl AB block copolymers.

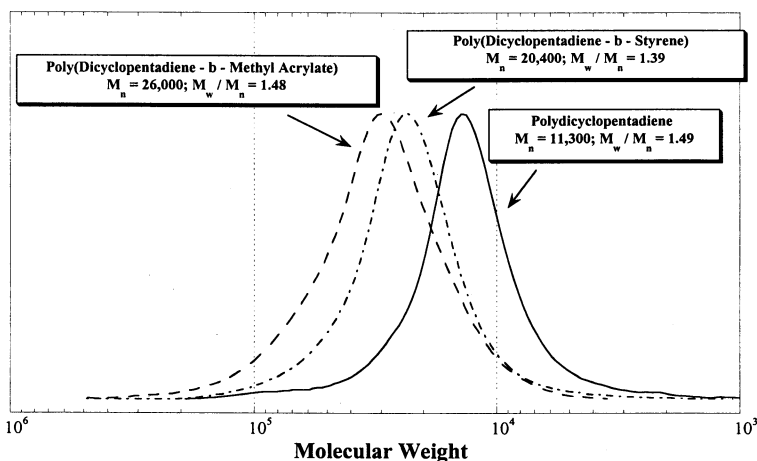


Figure 3. SEC chromatograms of polydicyclopentadiene/vinyl AB block copolymers.

Scheme 4

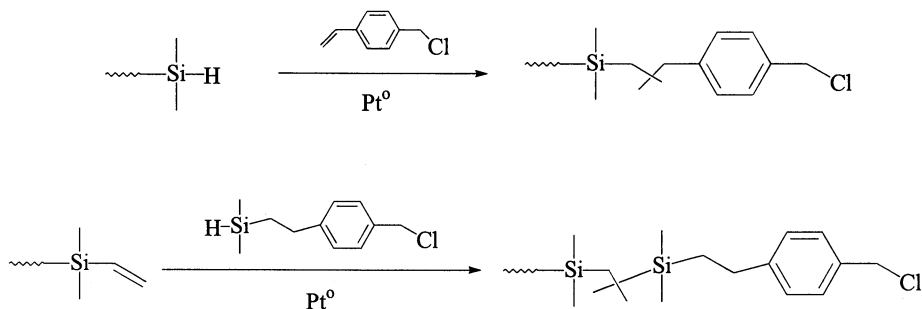
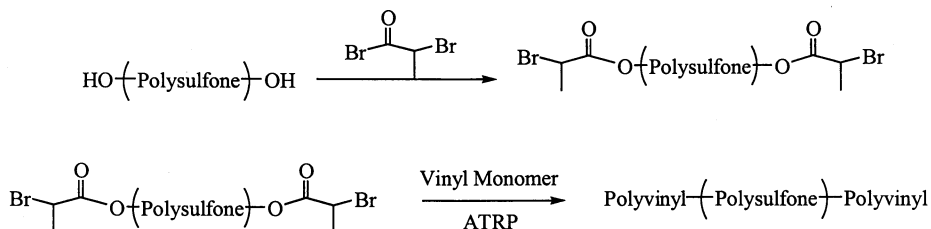


Table 2. ABA Block Copolymers of PDMS with Vinyl Monomers

PDMS M_n	M_w/M_n	Monomer	M_n	M_w/M_n
4,500	1.2	Styrene	9,800	1.2
9,800	2.4	Styrene	20,700	1.6
2,600	1.2	Methyl Acrylate	4,600	1.3
4,500	1.2	Isobornyl Acrylate	13,700	1.6
9,800	2.4	Butyl Acrylate	24,000	1.6

Polysulfone ($M_n = 4,480$; $M_w/M_n = 1.5$) was prepared by condensation of bis(4-fluorophenyl) sulfone and an excess of bisphenol A. This was then reacted with 2-bromopropionyl bromide to prepare the α,ω -bis(2-bromopropionyloxy)polysulfone, Scheme 5. This macroinitiator successfully initiated the polymerization of both styrene and butyl acrylate, Figure 4.(52) Both of these materials were soluble in common solvents and were cast as transparent films.

Scheme 5



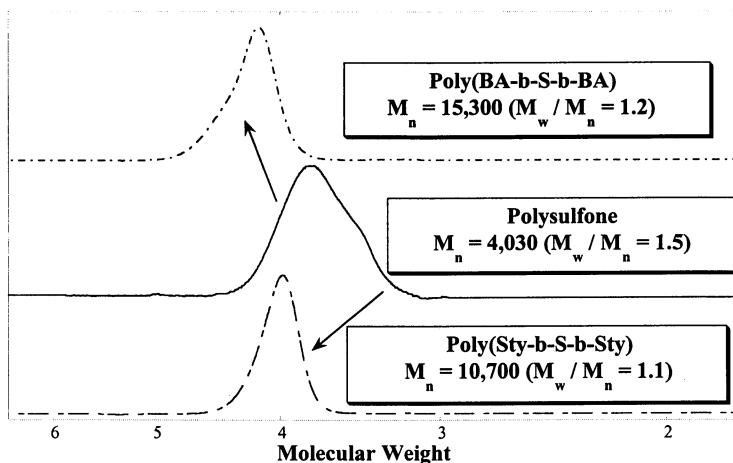


Figure 4. SEC chromatograms of polysulfone macroinitiator and ABA block copolymers of polysulfone (S) with polystyrene (Sty) or poly(butyl acrylate) (BA).

Polymer Architecture

Graft Copolymers

There are three methods to prepare graft copolymers: grafting-through, grafting-onto and grafting-from. Grafting-through involves the copolymerization of a monomer with a macromonomer, while the grafting-onto or -from methods either attach growing polymer chains onto a polymer backbone or grow them off of it. We have used ATRP to prepare graft copolymers by the grafting-through and grafting-from methods.

For grafting-through, we were able to prepare macromonomers (MM) of polystyrene with a vinyl acetate end group by using vinyl chloroacetate to initiate the ATRP of styrene, Scheme 6. Since the reactivity ratios of styrene and vinyl acetate are not favorable for cross propagation between the two monomers, only styrene was polymerized while the vinyl acetate end groups remained unreacted. This resulted in the formation of well-defined polystyrene with a vinyl acetate end group. The functionality of the polymers was > 90% as molecular weights determined by ^1H NMR and SEC were in agreement with each other.^(53,54)

The macromonomers were then copolymerized with N-vinyl pyrrolidinone, NVP, by conventional radical polymerization in DMF. DMF was used since it was a good solvent for both the polystyrene and poly(NVP) chains. After the graft copolymer was precipitated and isolated, it had swelled in solvents that were selective for either the poly(NVP) backbone (water) or the polystyrene side chains (benzene). The polymers were also found to be highly water absorbent. Table 3 lists the results of the copolymerizations using macromonomers of various size and weight percents. The equilibrium water content was determined by soaking a dry polymer sample in water for a week and determining the amount of water that was present in the sample (by weight).

Scheme 6

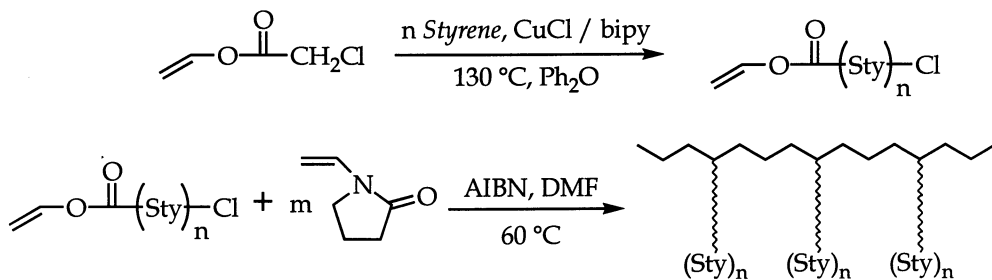


Table 3. Physically Crosslinked Hydrogels Prepared Using ATRP

MM M_n	MM wt% ^a	Copolymer M_n	M_w/M_n	Grafts/Chain	% Water
5,800	34 (40)	316,000	5.9	18.6	85
	13 (20)	219,000	2.5	4.9	92
	7.7 (10)	185,000	1.8	2.5	97
11,900	40 (50)	65,700	1.6	2.2	82
	30 (30)	83,300	1.8	2.1	93
	24 (20)	114,200	1.8	2.3	92

a) Wt% of graft copolymer as determined by ^1H NMR. Values in parenthesis are amounts of macromonomer added to polymerization reaction.

Thermoplastic elastomers were synthesized using ATRP to graft from commercially available isobutene copolymers, Scheme 7. Poly(isobutene) copolymers with *p*-methylstyrene (PIB-BMS) or isoprene (PIB-PIP(Br)), which had been brominated to provide initiating sites for ATRP, are the commercial Exxpro™ elastomers. Upon dissolving these macroinitiators in the respective monomer, a copper (I) catalyst was added and the reaction mixture heated. The molecular weight of the polymers increased with conversion and with increasing graft chain length, i.e., wt% grafts, Table 4.

Scheme 7

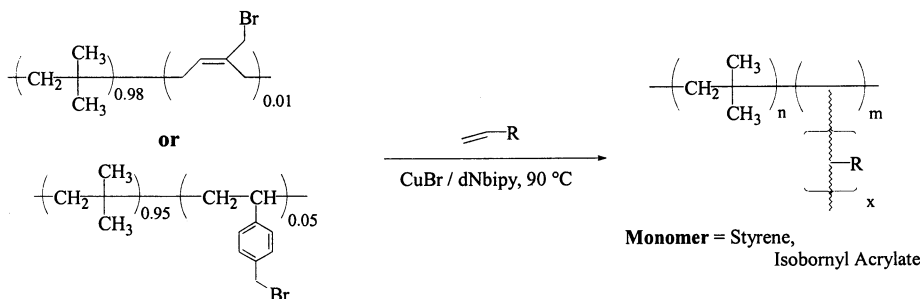


Table 4. Graft Copolymers with Isobutene Backbones Prepared by ATRP

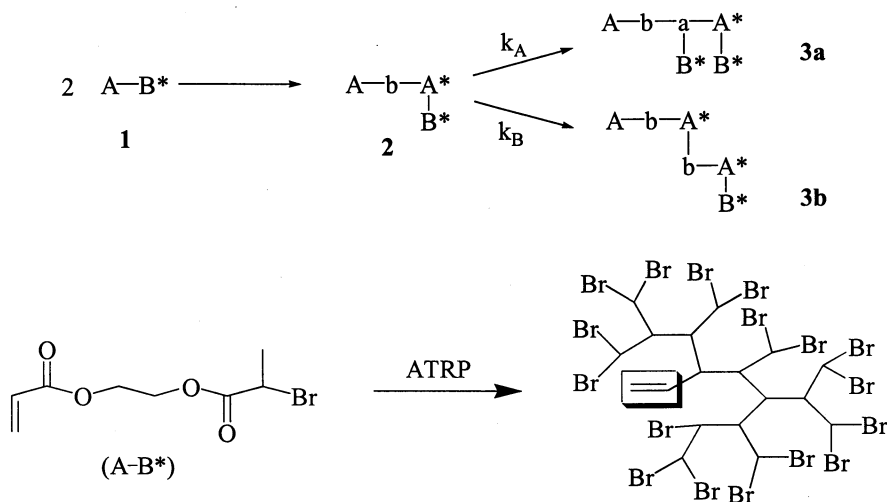
Backbone	M_n^a	Graft	M_n^a	Wt % Grafts	T_g (°C)
PIB - BMS	108,000(2.3)	Styrene	139,000(2.5)	14	-52
			193,000(2.6)	33	5
			250,000(2.4)	69	-60, 98
		Isobornyl Acrylate	181,000(2.5)	21	-10
PIB-PIP(Br)	273,000(1.8)	Styrene	359,000(1.7)	14	-51
			387,000(1.7)	18	-52
		Isobornyl Acrylate			

a) Values in parenthesis are polydispersities, M_w/M_n .

Branched and Hyperbranched Polymers

The preparation of highly branched polymers by polycondensation reactions was first proposed by Flory (55) and put to synthetic use by Webster and Kim.(56,57) However, not until Frechet demonstrated that functionalized vinyl monomers could be used (58) was it possible to prepare hyperbranched polymers by chain growth processes such as ionic or radical polymerization. This polymerization has been termed, "Self Condensing Vinyl Polymerization (SCVP)." Frechet cationically polymerized *m*-(1-chloroethyl)styrene to obtain hyperbranched polystyrene. Subsequently, it was extended to radical polymerization using TEMPO based systems (59) and ATRP.(60)

Scheme 8



The mechanism of chain growth to obtain hyperbranched polymers has been discussed elsewhere,⁽⁵⁸⁻⁶³⁾ and is only briefly outlined in Scheme 8. The monomer is described by AB*. The A represents the double bond and the B* is a functional group which can be activated to initiate the polymerization of the double bonds. A* is a newly formed active (or potentially active) site, whereas a and b represent the corresponding inactive parts of the macromolecule. The scheme shows that, after activation of the B* group and addition of monomer there are now two sites in the dimer **2** which can be activated (A* and B*) to initiate polymerization, i.e., formation of **3a** and **3b**. Subsequent activation at any of the sites results in a branched polymer, so long as the relative rate constants of polymerization at A* (k_A) and B* (k_B) are similar.^(62,63) It should be noted that each macromolecule has one double bond which can also participate in the polymerization and be incorporated into other growing polymer chains.

To expand the scope of hyperbranched polymers that could be prepared by SCVP using ATRP, we prepared several acrylic AB* monomers.⁽⁶¹⁾ For example, 2-(2-bromopropionyloxy)ethyl acrylate (BPEA) was prepared by reacting 2-bromopropionyl bromide with 2-hydroxyethyl acrylate. The acrylic double bond is A, and the 2-bromopropionyloxy group is B*. This monomer was polymerized in bulk using 1 mol% of copper (I) bromide and 2 mol% 4, 4-di-(*t*-butyl)-2, 2-bipyridine (dTbipy).

The polymerization was monitored by ¹H NMR, Figure 5, and SEC, Figure 6. In the ¹H NMR spectra, the signals from the double bonds are observed from 6.5 to 5.8 ppm. The signal at 4.4 ppm is assigned to the ethylene linkage and the protons geminal to bromine in A* and B*. The doublet at 1.8 ppm is the signal from the methyl protons in the 2-bromopropionyloxy group. The signals at 3.8 and 1.5 ppm are from *p*-dimethoxybenzene (internal GC standard) and dTbipy, respectively. As the polymerization progressed, two new sets of signals appeared: the broad set of signals (2.8-1.5 ppm) and the multiplet at 1.2 ppm. The broad set of signals was assigned to the formation of the CH₂-CH polymer backbone by polymerization of the double bonds. The signal at 1.2 ppm was assigned to the methyl protons in **b** (The bromine in B* was homolytically cleaved to form the radical which then reacted with a double bond to initiate polymerization.). By comparison of the intensity of signal (**b**), 1.2 ppm, to that of the methyl group geminal to bromine (B*), 1.8 ppm, the proportion of **b** and B* could be calculated in the polymer. From these proportions, the degree of branching (DB) ⁽⁶⁴⁾ in the macromolecule was calculated, DB ≈ 0.49.⁽⁶³⁾

In the SEC chromatograms, Figure 6, the lower molecular weight species, i.e., monomer, dimer, trimer, etc., can be seen in the early stages of the polymerization. As the polymerization progressed, these species were consumed and incorporated into other polymer chains to form the higher molecular weight polymer. It should be noted that the molecular weights listed were determined against linear polystyrene standards, and are not indicative of the true molecular weight of the macromolecule due to branching. After precipitation into methanol, the low molecular weight species were easily fractionated, leading to a polymer with a higher molecular weight ($M_n = 6,510$) and lower polydispersity ($M_w/M_n = 3.3$).

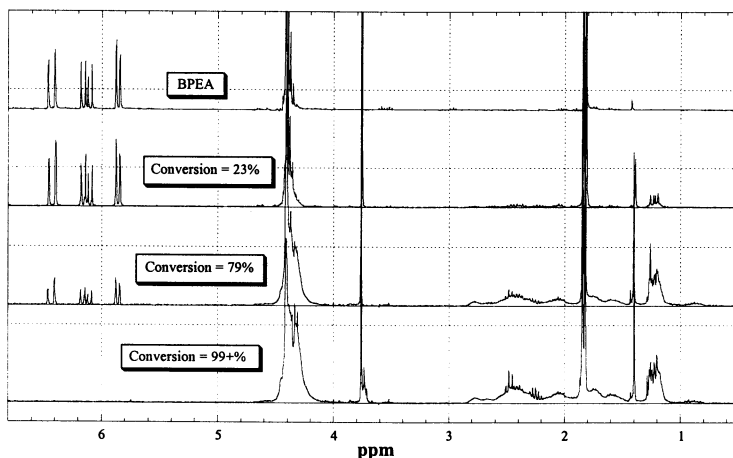


Figure 5. ^1H NMR spectra of BPEA and polymer samples at various conversions.

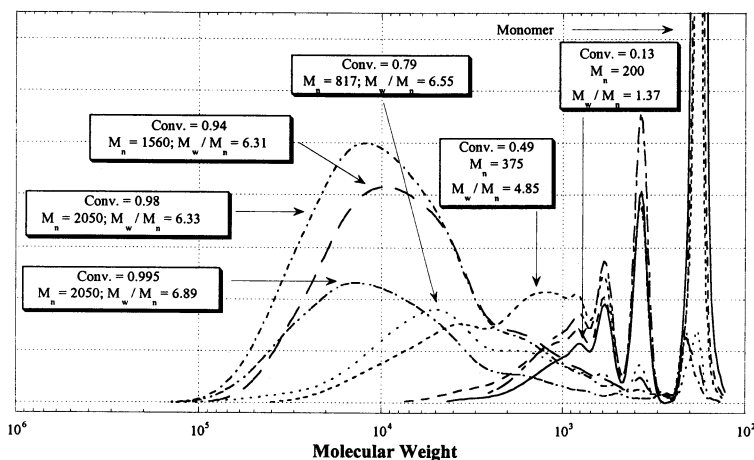


Figure 6. Overlay of SEC chromatograms of the ATRP of BPEA at various conversion. Molecular weights were obtained against linear polystyrene standards.

The density of branching in the polymer can be attenuated by copolymerization of the AB^* monomer with a conventional vinyl monomer. This has been demonstrated for the copolymerization of *p*-chloromethylstyrene (CMS) with styrene. The first order kinetics of the polymerization were linear, as in the ATRP of linear polymers. However, a plot of M_n versus conversion, Figure 7, shows a deviation from the expected behavior, assuming only linear polymer chains. This deviation was ascribed to the incorporation of the double bonds on the polymer chain ends as a result of being initiated by CMS.

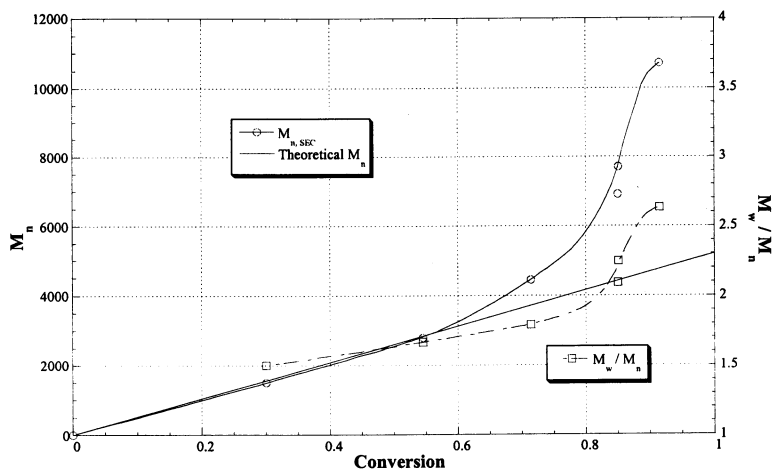


Figure 7. Plot of M_n and M_w/M_n versus conversion for the copolymerization of CMS (2 mol%) with styrene by ATRP.

It has also been possible to prepare star and/or multi-armed polymers. This is accomplished by using a multifunctional initiator. The initiator can be a small molecule, i.e., hexakis(bromomethyl)benzene,(46) or a macromolecule, i.e., the hyperbranched poly(2-(2-bromopropionyloxy)ethyl acrylate).(65)

Functionalized Polymers by ATRP

Polymerization of Functional Monomers

Since radical reactions are tolerant of functional groups, such as hydroxyl and amine, it is possible to polymerize monomers which contain various functional groups. We have demonstrated that ATRP can also be extended to polymerize various functional monomers such as styrenes and acrylates.

A study of the Hammett relationship of ring substituted styrenes was undertaken.(66) A linear relationship was observed in the Hammett plot, Figure 8, with the styrenes containing electron withdrawing substituents having faster rates of polymerization. It was subsequently determined that this rate enhancement was not due to the substituent's effect on the propagating radical but on the destabilization of the dormant polymer chain end, P-X. This required lower activation energies to cleave the carbon-halogen bond and form the radical; the result was a shift in the equilibrium increasing the concentration of the propagating radicals.

Acrylates with functional groups were also successfully polymerized. These acrylates included glycidyl acrylate (GA), 2-hydroxyethyl acrylate (HEA), vinyl acrylate (VA) and allyl acrylate (AA).(23) All were successfully polymerized with the exception of allyl acrylate, Table 5. Polymerization of the allyl acrylate by ATRP resulted in the formation of a gel. Presumably, this was due to the polymerization of both the acrylate and allyl functional groups. Such a side reaction was not observed in the polymerization of vinyl acrylate. The higher observed molecular weights as compared to the theoretical values for the polymerization of HEA was attributed to the differences obtained by SEC

when comparing the poly(HEA) to linear polystyrene standards since good agreement between $M_{n,th}$ and values measured by NMR and MALDI was observed for lower molecular weight polymer.

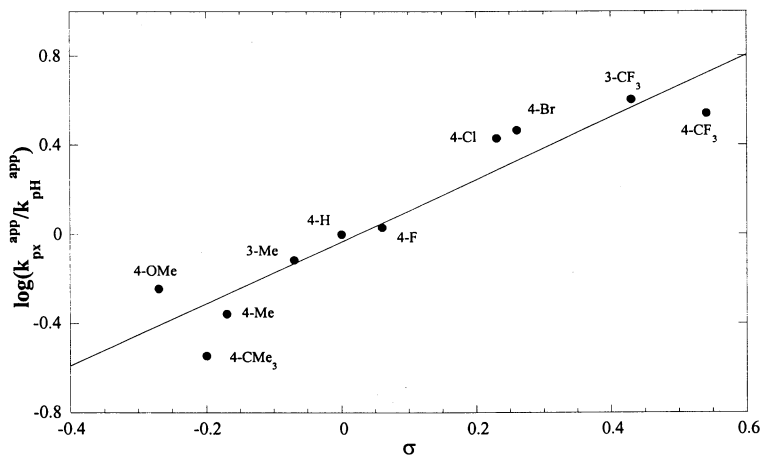


Figure 8. Hammett plot of the polymerization of substituted styrenes by ATRP.

It has not been possible to directly polymerize monomers that contain carboxylic acid functionalities such as acrylic acid. However, the polymerization of *t*-butyl acrylate or isobornyl acrylate by ATRP has been successful.⁽²⁴⁾ This polymer was then treated with acid in the presence of water to yield poly(acrylic acid).

Table 5 Polymerization of Functional Acrylates by ATRP

Monomer	Conv. (%)	$M_{n,th}$	$M_{n,SEC}$	M_w/M_n
GA	95	3,440	4,320	1.23
	98	25,000	27,500	1.21
	98	50,000	52,800	1.20
HEA	92	3,130	6,170	1.19
	91	15,000	30,000	1.19
	90	18,000	36,000	1.17
VA	89	2,940	2,810	1.21
AA	99		Insoluble	

Polymers with Functional End Groups

The simplest way to obtain end functionalized polymers by ATRP is to use an initiator that contains the desired functional group. For example, if allyl terminated polymers were desired, allyl halides could be used as initiators for ATRP.⁽⁶⁷⁾ Since such initiators are simple molecules, many are commercially available. Tables 6 and 7 list the results obtained for a variety of functional initiators in the polymerization of styrene and methyl acrylate.

Table 6. Preparation of Functional Polystyrene Prepared by ATRP

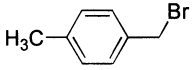
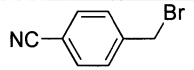
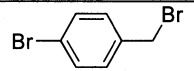
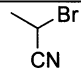
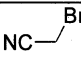
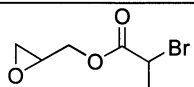
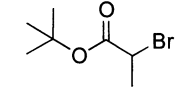
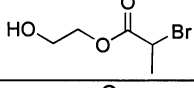
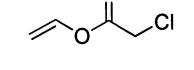
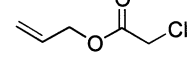
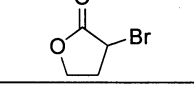
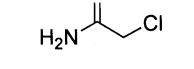
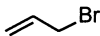
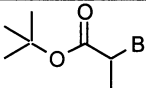
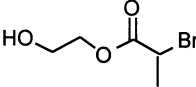
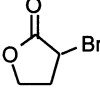

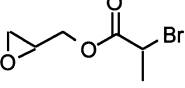
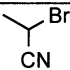
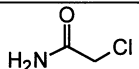
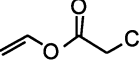
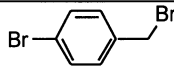
Initiator Structure	Initiator Name	% Conv.	M_n, SEC	M_w/M_n
	4-Methylbenzyl bromide	51	4,400	1.17
	4-Cyanobenzyl bromide	48	5,500	1.10
	4-Bromo-benzyl bromide	48	4,500	1.16
	2-Bromopropionitrile	48	5,100	1.09
	Bromoacetonitrile	48	4,500	1.10
	Glycidol 2-bromopropionate	62	6,800	1.12
	tert-Butyl 2-bromopropionate	41	4,000	1.17
	Hydroxyethyl 2-bromopropionate	48	7,500	1.10
	Vinyl chloroacetate	94	5,800	1.12
	Allyl chloroacetate	14	2,600	1.77
	α -Bromobutyrolactone	41	4,000	1.17
	2-Chloroacetamide	12	4,000	1.51

Table 7. Preparation of Functional Poly(Methyl Acrylate) Prepared by ATRP

Initiator Structure	Initiator Name	%Conv	$M_{n, SEC}$	M_w/M_n
	Allyl bromide	89	6220	1.34
	2-Bromopropionic acid tert-butyl ester	94	3980	1.22
	Hydroxyethyl 2-bromopropionate	97	4560	1.30
	α -Bromo-n-butyrolactone	83	4120	1.13
	4-Cyanobenzyl bromide	93	4110	1.13
	Glycidyl 2-bromopropionate	93	4020	1.23
	2-Bromopropionitrile	82	3550	1.10
	2-Chloroacetamide	32	7220	1.22
	Vinyl chloroacetate	70	3260	1.34
	4-Bromo-benzyl bromide	95	4010	1.22

ATRP is not limited to just using functional initiators to introduce functional groups to the polymer chain ends. Because all chains have halogen end groups, these can be converted to other functional groups by nucleophilic/electrophilic substitution and addition reactions.⁽⁶⁸⁾ This has been demonstrated by conversion of α,ω -dibromopolystyrene to α,ω -diaminopolystyrene⁽⁶⁹⁾ The difunctional polystyrene was prepared by using *p*-bromoxylene as an initiator for the ATRP of styrene. The resulting α,ω -dibromopolystyrene was then treated with trimethylsilyl azide in the presence of

tetrabutyl ammonium fluoride. Further, the α,ω -diazidopolystyrene was reacted with lithium aluminum hydride to afford the α,ω -diaminopolystyrene.

The transformation of halogen groups to azido groups was used to prepare crosslinkable materials. The hyperbranched polymer obtained by the ATRP of BPEA, as described in the previous section, was treated with trimethylsilyl azide to afford a hyperbranched polymer with azido functional groups, Scheme 9. Upon heating or irradiation, this fluid material became brittle and insoluble in solvents. In the DSC of the polymer sample, Figure 9, a large exotherm occurred at 180 °C when the azido groups decomposed and crosslinking ensued. This was confirmed by qualitative DMTA, Figure 10. At 200 °C, the shear modulus of the polymer sample increased dramatically. (The observed upper limit of the shear modulus of the sample was the upper limit of the DMTA instrument in the shear mode.)

Scheme 9

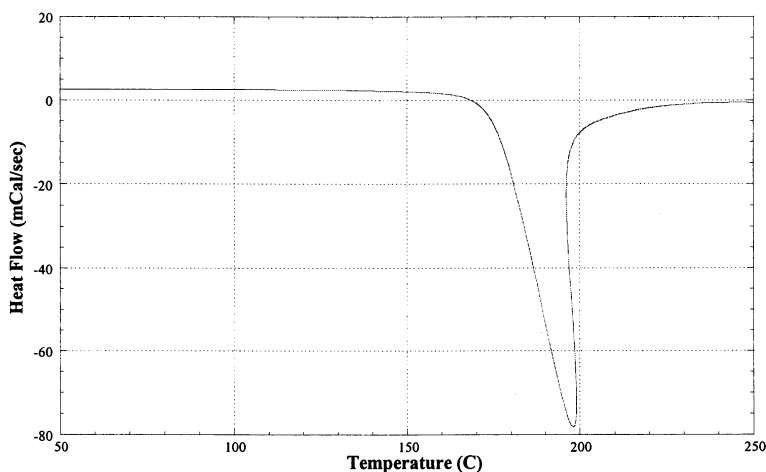
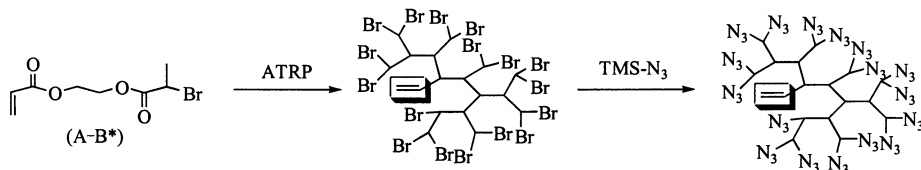


Figure 9. DSC of azido functionalized hyperbranched BPEA.

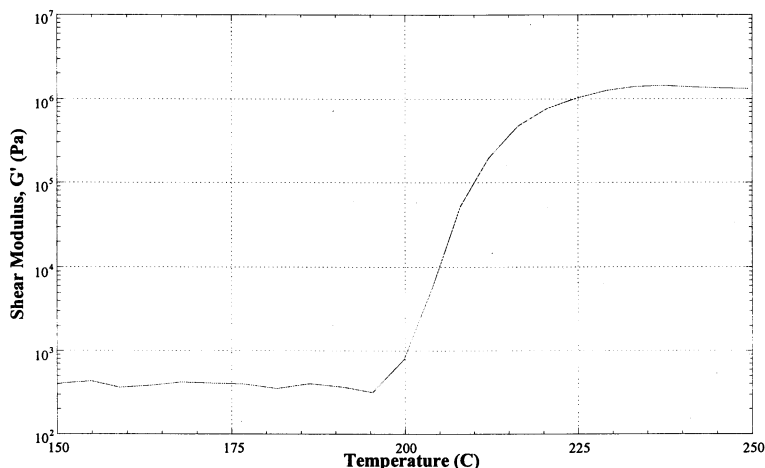


Figure 10. DMTA of azido functionalized hyperbranched BPEA.

Conclusions

Atom transfer radical polymerization, ATRP, is a controlled / “living” radical polymerization system which uses an equilibrium between active radicals and dormant alkyl halide chain ends to maintain a low concentration of radicals while obtaining well-defined polymers with $DP_n = \Delta[M]/[I]_0$ and $M_w/M_n < 1.5$. This system has been demonstrated to be successful for the polymerization of a wide variety of monomers including substituted styrenes, functional acrylates, methacrylates, and acrylonitrile.

ATRP has also been successfully used to copolymerize the above monomers, as well as others that can not be homopolymerized by ATRP. These monomers include isobutene, and vinyl acetate. The composition of the polymers has been extended beyond simple random/statistical copolymers to include block copolymers. Block copolymers have also been prepared by transformation polymerizations from carbocationic, ROMP and step-growth polymerizations.

ATRP has allowed for the preparation of polymeric materials with novel architectures by radical polymerization. Examples include graft, branched and hyperbranched (co)polymers.

ATRP allows for the synthesis of functionalized polymers by simply using a functional initiator. The halogen end groups at the polymer chain end(s) can also be converted into more useful functional groups by simple organic chemistry reactions.

In summary, ATRP has been shown to be a versatile and robust polymerization system which allows for the preparation of a wide variety of polymeric materials by radical polymerization.

Acknowledgments

This research was supported by the industrial members of the ATRP Consortium at Carnegie Mellon University (Akzo-Nobel, Asahi Chemical Industry Co., Bayer, BF Goodrich, Ciba, DSM Research, Elf Atochem, Geon, Kaneka, Japan Synthetic Rubber Co., PPG, and Rohm & Haas) as well as by National Science Foundation, Office of

Naval Research, Petroleum Research Foundation, and U. S. Army Research Office. We acknowledge contribution of all past and current members of our research group who have synthesized many new materials by ATRP covered in this review: S. V. Arehart, P. Balchandani, K. L. Beers, S. Coca, V. Coessens, K. A. Davis, D. Greszta, T. Grimaud, C. B. Jasieczek, S. M. Jo, A. Kajiwara, P. J. Miller, Y. Nakagawa, H.-J. Paik, T. Patten, J. Qiu, J.-L. Wang, J.-S. Wang, M. Wei, B. E. Woodworth, and J. Xia.

References

- (1) Szwarc, M. *Nature* **1956**, *178*, 1168.
- (2) Szwarc, M. *Carbanions, Living Polymers and Electron Transfer Processes*; Interscience: New York, 1968.
- (3) Webster, O. *Science* **1991**, *251*, 887.
- (4) Greszta, D.; Mardare, D.; Matyjaszewski, K. *Macromolecules* **1994**, *27*, 638.
- (5) Matyjaszewski, K.; Müller, A. H. E. *Amer. Chem. Soc., Polym. Preprints* **1997**, *38(1)*, 6.
- (6) Otsu, T.; Yoshida, M. *Makromol. Chem. Rapid Commun* **1982**, *3*, 127.
- (7) Solomon, D. H.; Rizzardo, E.; Cacioli, P. *US 4,581,429* **1985**
- (8) Georges, M. K.; Veregin, R. P. N.; Kazmaier, P. M.; Hamer, G. K. *Macromolecules* **1993**, *26*, 2987.
- (9) Wayland, B. B.; Pszmik, G.; Mukerjee, S. L.; Fryd, M. *J. Amer. Chem. Soc.* **1994**, *116*, 7943.
- (10) Gaynor, S. G.; Wang, J. S.; Matyjaszewski, K. *Macromolecules* **1995**, *28*, 8051.
- (11) Rizzardo, E.; Meija, G. F.; Thang, S. H. *Macromol. Symp.* **1995**, *98*, 101.
- (12) Arvanopoulos, L. D.; Greuel, M. P.; Harwood, H. J. *Amer. Chem. Soc., Polym. Preprints* **1994**, *35(2)*, 549.
- (13) Harwood, H. J.; Christov, L.; Guo, M.; Holland, T. V.; Huckstep, A. Y.; Jones, D. H.; Medsker, R. E.; Rinaldi, P. L.; Saito, T.; Tung, D. S. *Macromol. Symp* **1996**, *111*, 25.
- (14) Wunderlich, W.; Benfaremo, N.; Klapper, M.; Müllen, K. *Macromol. Rapid Commun.* **1996**, *17*, 433.
- (15) Wang, J.-S.; Matyjaszewski, K. *J. Amer. Chem. Soc.* **1995**, *117*, 5614.
- (16) Matyjaszewski, K.; Wang, J.-S. *Macromolecules* **1995**, *28*, 7901.
- (17) Matyjaszewski, K.; Patten, T.; Xia, J.; Abernathy, T. *Science* **1996**, *272*, 866.
- (18) Matyjaszewski, K.; Patten, T. E.; Xia, J. *J. Amer. Chem. Soc* **1997**, *119*, 674.
- (19) Percec, V.; Barboiu, B. *Macromolecules* **1995**, *28*, 7970.
- (20) Percec, V.; Barboiu, B.; Newmann, A.; Ronda, J. C.; Zhao, H. *Macromolecules* **1996**, *29*, 3665.
- (21) Qiu, J.; Matyjaszewski, K. *Macromolecules* **1997**, *in press*.
- (22) Wei, M.; Xia, J.; McDermott, N. E.; Matyjaszewski, K. *Polym. Prepr. (Am. Chem. Soc., Div. Polym. Chem.)* **1997**, *38(2)*, 231-232.
- (23) Coca, S.; Matyjaszewski, K. *Amer. Chem. Soc., Polym. Preprints* **1997**, *38(1)*, 691.
- (24) Coca, S.; Davis, K.; Miller, P.; Matyjaszewski, K. *Amer. Chem. Soc., Polym. Preprints* **1997**, *38(1)*, 689.
- (25) Grimaud, T.; Matyjaszewski, K. *Macromolecules* **1997**, *30*, 2216.
- (26) Kato, M.; Kamigaito, M.; Sawamoto, M.; Higashimura, T. *Macromolecules* **1995**, *28*, 1721.

- (27) Nishikawa, T.; Ando, T.; Kamigaito, M.; Sawamoto, M. *Macromolecules* **1997**, *30*, 2244.
- (28) Uegaki, H.; Kotani, Y.; Kamigaito, M.; Sawamoto, M. *Macromolecules* **1997**, *30*, 2249.
- (29) Granel, C.; Dubois, P.; Jerome, R.; Teyssie, P. *Macromolecules* **1996**, *29*, 8576.
- (30) Haddleton, D. M.; Jasieczek, C. B.; Hannon, M. J.; Shooter, A. J. *Macromolecules* **1997**, *30*, 2190.
- (31) Ando, T.; Kamigaito, M.; Sawamoto, M. *Macromolecules* **1997**, *30*, 4507.
- (32) Wei, M.; Xia, J.; Matyjaszewski, K. *Polym. Prepr. (Am. Chem. Soc., Div. Polym. Chem.)* **1997**, *38(2)*, 233-234.
- (33) Jo, S. M.; Gaynor, S. G.; Matyjaszewski, K. *Amer. Chem. Soc., Polym. Preprints* **1996**, *37(2)*, 272.
- (34) Jo, S. M.; Paik, H.-j.; Matyjaszewski, K. *Amer. Chem. Soc., Polym. Prep.* **1997**, *38*, 697.
- (35) Matyjaszewski, K.; Jo, S. M.; Paik, H.-j.; Gaynor, S. G. *Macromolecules* **1997**, in press.
- (36) Matyjaszewski, K.; Lin, C.-H. *Makromol. Chem. Macromol. Symp.* **1991**, *47*, 221.
- (37) Müller, A. H. E.; Litvinenko, G.; Yan, D. *Macromolecules* **1996**, *29*, 2346.
- (38) Fukuda, T.; Terauchi, T.; Goto, A.; Tsujii, Y.; Miyamoto, T. *Macromolecules* **1996**, *29*, 3050.
- (39) Hawker, C. J.; Elce, E.; Dao, J.; Volksen, W.; Russell, T. P.; Barclay, G. G. *Macromolecules* **1996**, *29*, 2686.
- (40) Mansky, P.; Liu, Y.; Huang, E.; Russell, T. P.; Hawker, C. J. *Science* **1997**, *275*, 1458.
- (41) Arehart, S. V.; Greszta, D.; Matyjaszewski, K. *Amer. Chem. Soc., Polym. Preprints* **1997**, *38(1)*, 705.
- (42) Greszta, D.; Matyjaszewski, K. *Amer. Chem. Soc., Polym. Preprints* **1996**, *37(1)*, 569.
- (43) Pakula, T.; Matyjaszewski, K. *Macromol. Theory & Simulat.* **1996**, *5*, 987.
- (44) Greszta, D.; Matyjaszewski, K.; Pakula, T. *Amer. Chem. Soc., Polym. Preprints* **1997**, *38(1)*, 709.
- (45) Greszta, D.; Matyjaszewski, K.; Pakula, T. *Polym. Prepr. (Am. Chem. Soc., Div. Polym. Chem.)* **1997**, *38*, 709.
- (46) Wang, J. S.; Greszta, D.; Matyjaszewski, K. *Amer. Chem. Soc., PMSE* **1995**, *73*, 416.
- (47) Coca, S.; Matyjaszewski, K. *Macromolecules* **1997**, *30*, 2808.
- (48) Coca, S.; Matyjaszewski, K. *Amer. Chem. Soc., Polym. Preprints* **1997**, *38(1)*, 693.
- (49) Coca, S.; Matyjaszewski, K. *J. Poly. Sci., Polym. Chem.* **1997**, in press.
- (50) Coca, S.; Paik, H.-j.; Matyjaszewski, K. *Macromolecules* **1997**, in press.
- (51) Nakagawa, Y.; Miller, P.; Pacis, C.; Matyjaszewski, K. *Amer. Chem. Soc., Polym. Preprints* **1997**, *38(1)*, 701.
- (52) Gaynor, S. G.; Matyjaszewski, K. *Macromolecules* **1997**, *30*, 4247.
- (53) Beers, K.; Gaynor, S. G.; Matyjaszewski, K. *Amer. Chem. Soc., Polym. Preprints* **1996**, *37(1)*, 571.
- (54) Beers, K. L.; Kern, A.; Matyjaszewski, K. *Amer. Chem. Soc., Polym. Preprints* **1997**, *38(1)*, 695.
- (55) Flory, P. J. *J. Amer. Chem. Soc.* **1952**, *74*, 2718.

- (56) Webster, O. W.; Kim, Y. H. *Amer. Chem. Soc., Polymer Preprints* **1988**, *29*(2), 310.
- (57) Webster, O. W.; Kim, Y. H. *J. Amer. Chem. Soc.* **1990**, *112*, 4592.
- (58) Frechet, J. M. J.; Henmi, M.; Gitsov, I.; Aoshima, S.; Leduc, M.; Grubbs, R. B. *Science* **1995**, *269*, 1080.
- (59) Hawker, C. J.; Frechet, J. M. J.; Grubbs, R. B.; Dao, J. J. *Amer. Chem. Soc.* **1995**, *117*, 10763.
- (60) Gaynor, S. G.; Edelman, S. Z.; Matyjaszewski, K. *Macromolecules* **1996**, *29*, 1079.
- (61) Gaynor, S. G.; Kulfan, A.; Podwika, M.; Matyjaszewski, K. *Macromolecules* **1997**, *30*, 5192.
- (62) Gaynor, S. G.; Matyjaszewski, K. *Macromolecules* **1997**, *in press*.
- (63) Yan, D.; Muller, A. H. E.; Matyjaszewski, K. *Macromolecules* **1997**, *in press*.
- (64) A perfectly linear polymer is defined as having a degree of branching, $DB = 0$. A perfectly branched polymer, i.e., a dendrimer, $DB = 1$.
- (65) Gaynor, S. G.; Balchandani, P.; Kulfan, A.; Podwika, M.; Matyjaszewski, K. *Amer. Chem. Soc., Polym. Preprints* **1997**, *38*(1), 496.
- (66) Qiu, J.; Matyjaszewski, K. *Amer. Chem. Soc., Polym. Preprints* **1997**, *38*(1), 711.
- (67) Matyjaszewski, K.; Coca, S.; Nakagawa, Y.; Xia, J. *Amer. Chem. Soc., PMSE Preprints* **1997**, *76*, 147.
- (68) Nakagawa, Y.; Gaynor, S. G.; Matyjaszewski, K. *Amer. Chem. Soc., Polym. Preprints* **1996**, *37*(1), 577.
- (69) Matyjaszewski, K.; Nakagawa, Y.; Gaynor, S. G. *Makromol. Chem. Rapid Commun.* **1997**, *in press*.

Controlled Radical Polymerization Methods for the Synthesis of Nonionic Surfactants for CO₂

D E. Betts, T. Johnson, D. LeRoux, and J. M. DeSimone¹

Department of Chemistry, CB 3290, Venable and Kenan Laboratories,
University of North Carolina at Chapel Hill, Chapel Hill, NC 27599-3290

Several examples of fluorocarbon containing amphiphilic block copolymers have been synthesized using controlled free radical polymerization methods. These block copolymers contain a CO₂ soluble fluorocarbon acrylate or methacrylate block and a CO₂ insoluble block that is either lipophilic or hydrophilic. The synthesis of these block copolymers is well suited to the controlled free radical polymerization methods of iniferter and atom transfer radical polymerization (ATRP). Additionally, the synthesis of block copolymers containing a poly(dimethylsiloxane) (PDMS) block using a combined living anionic and iniferter synthetic technique is described. These block copolymers have been characterized by GPC, ¹H-NMR, and SANS, and their solubility in CO₂ has been examined. Potential uses for these block copolymers include surfactants for dispersion polymerizations in CO₂ and cleaning and surface treatment technologies.

Only a few classes of polymers show appreciable solubility in supercritical carbon dioxide under relatively "mild" conditions (T < 100 °C, P < 5000 psi): amorphous or low melting fluoropolymers and silicones (1-5). These CO₂ soluble materials have been termed "CO₂-philic" because they have high solubility at relatively low temperatures and pressures (6). Conventional hydrocarbon polymers, either hydrophilic or lipophilic, are relatively insoluble in CO₂ (7) and are therefore termed "CO₂-phobic." However, some block copolymers containing a CO₂-phobic hydrocarbon segment and a CO₂-philic fluorocarbon segment are soluble in CO₂ (2,3). These amphiphilic block copolymer materials are currently being studied for their use as surfactants in the dispersion polymerization of several different classes of monomers in CO₂ (8,9). In addition, they are also being used in cleaning and surface treatment technologies that take advantage of the enhanced emulsification capabilities afforded by surfactant modified CO₂ (10). Micelles may form when block copolymers are dissolved in a solvent that is selectively good for one of the blocks but is a nonsolvent for the other block (11-13). For AB diblock copolymers dissolved in CO₂, where the A block is a CO₂-philic block and the B block is CO₂-phobic, we have shown that the

¹Corresponding author

B blocks aggregate to form the core of a micelle which is surrounded by a corona of solvated A blocks. The CO₂-phobic block may be either lipophilic or hydrophilic. Within the CO₂-phobic core of the micelle, the solubilization of otherwise CO₂ insoluble materials is achieved (10).

Controlled free radical polymerization techniques provide the best route for the preparation of these amphiphilic block copolymers due to the relative ease of synthesis and the limited mechanisms by which the fluorocarbon monomers can be polymerized. In addition, since most fluoropolymers are insoluble in common organic solvents, the compatibility of controlled free radical polymerization techniques with a wide range of solvents makes these techniques the most versatile methods available (14,15). Specifically, iniferter (16) and atom transfer radical polymerization (ATRP) (17,18) are attractive routes to the synthesis of these block copolymers. We report the synthesis of both lipophilic and hydrophilic hydrocarbon-fluorocarbon block copolymers using both iniferter and ATRP polymerization techniques. We also report the synthesis of silicone block copolymers by crossover from a living anionic polymerization to iniferter (19).

The concept of iniferter was first demonstrated by T. Otsu in 1982 for the synthesis of polymers by a radical mechanism with a controlled structure and functionality (16,20). The technique was subsequently used for the synthesis of block copolymers (21,22). The term "iniferter" comes from the three-fold role of the compound: *initiator*, chain *transfer* agent, and reversible *terminating* agent. The reversible termination of the polymer chain allows for the synthesis of block copolymers. The iniferter technique makes use of a photoactive compound that upon photolysis yields an initiating fragment (R•) and a stable free radical species (S•), typically a thiuram, which serves as a reversible capping agent (Figure 1). The end capping agent does not initiate polymerization. Iniferter polymerizations typically give molecular weight polydispersity indices (PDIs) of 1.4 - 1.8. In contrast to iniferter, ATRP employs a haloalkane that serves as the initiator along with a copper(I) catalyst and a dipyridyl ligand that serves to help solubilize the copper catalyst. ATRP polymerizations are typically run at 80 - 130 °C. In ATRP, initiation occurs by the abstraction of the halogen atom from the haloalkane by the copper(I) catalyst giving a carbon-centered radical that initiates polymerization, and a copper(II) species. The radical polymerization is controlled by the reversible transfer of the halogen atom between the growing polymer chain and the copper species (Figure 1). Polymers synthesized by ATRP typically have PDIs less than 1.3, but values less than 1.1 have been reported (17,18,23). Both iniferter and ATRP give well defined polymers with controlled structure, functionality and polymer molecular weight.

The iniferter controlled free radical polymerization technique is effective for the synthesis of a wide range of hydrophilic, lipophilic and fluorocarbon polymers including poly(2-dimethylaminoethyl methacrylate) (PDMAEMA), poly(2-hydroxyethyl methacrylate) (HEMA), polystyrene (PS), poly(vinyl acetate) (PVAc), poly(1,1'-dihydroperfluorooctyl acrylate) (PFOA), and poly(1,1'-dihydroperfluorooctyl methacrylate) (PFOMA). While the types of monomers that can be used with ATRP are more limited than for iniferter (*e.g.* FOA and acetates do not work), ATRP gives much more controlled and well-defined polymers. ATRP has proven to be effective for the polymerization of a broad range of lipophilic hydrocarbon monomers including acrylates, methacrylates and styrenics as well as fluorocarbon monomers such as FOMA, 2-(N-ethylperfluorooctanesulfonamido)ethyl acrylate (FOSEA), 2-(N-ethylperfluorooctanesulfonamido)ethyl methacrylate (FOSEMA), 1,1',2,2'-tetrahydroperfluorooctyl methacrylate (TM), and 1,1',2,2'-tetrahydroperfluorooctyl acrylate (TA-N) (24). Although ATRP is quite useful for making lipophilic-fluorocarbon block copolymers, the synthesis of hydrophilic-fluorocarbon block copolymers must overcome the complexation of the copper catalyst species to the polar groups frequently encountered in hydrophilic monomers. One solution is the use of protected hydrophilic monomers such as 2-(trimethylsilyloxy)ethyl methacrylate (HEMA-TMS) and *tert*-

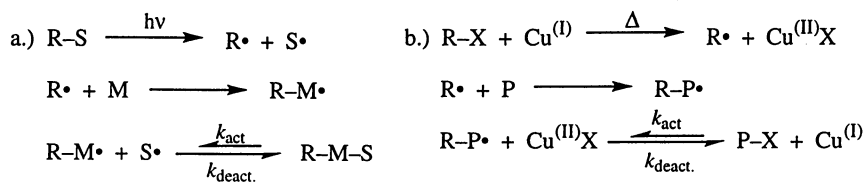
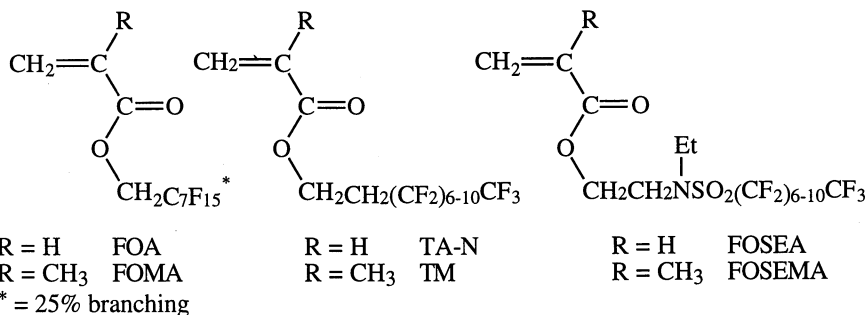


Figure 1. Mechanism of Polymerization a.) Iniferter b.) ATRP

butylacrylate (*t*-BuA) to yield PHEMA and poly(acrylic acid) respectively upon deprotective hydrolysis after polymerization.



Both the iniferter and ATRP controlled free radical polymerization techniques offer the same advantages as conventional free radical polymerizations: relative ease of synthesis and monomer compatibility. Additionally, they offer the ability to control the polymer structure and functionality thus affording polymers with narrow polydispersities, targeted molecular weights and complex architectures.

Experimental

Materials. Tetraethylthiuram disulfide (TD, Aldrich) was recrystallized twice from methanol and the purity was checked by ¹H-NMR. *sec*-Butyllithium (1.3 M in cyclohexane, Aldrich), copper(I) bromide (99.999%, Aldrich), 2,2'-dipyridyl (99+%, Aldrich), ethyl 2-bromoisobutyrate (98%, Aldrich) and diethyldithiocarbamate sodium salt (Aldrich) were used as received. Benzyl *N,N*-diethyldithiocarbamate (BDC) and xyllylene bis(*N,N*-diethyl dithiocarbamate) (XDC) were synthesized as described in the literature (15,21,22). Styrene (Aldrich), vinyl acetate (Aldrich), 1,1-dihydroperfluorooctyl acrylate (FOA, 3M), and 1,1-dihydroperfluorooctyl methacrylate (FOMA, 3M) were passed through an alumina column to remove the inhibitor and deoxygenated by purging with argon prior to use. Hexamethylcyclotrisiloxane (D₃, Acros) was kindly provided by Bayer and was purified by vacuum sublimation. 1-(dimethylchloro-silyl)-2-(*p,m* chloromethyl phenyl) ethane was synthesized as described in the literature (25). Cyclohexane (Fisher) was stirred over concentrated sulfuric acid for ca. 2 weeks, decanted, and distilled over sodium under an argon atmosphere prior to use. Tetrahydrofuran (THF, Mallinckrodt) was distilled from a sodium/benzophenone solution under argon atmosphere prior to use. Methanol (Mallinckrodt), heptane (Mallinckrodt), acetone (Mallinckrodt), and α,α,α -trifluorotoluene (TFT, Aldrich, 99+%) were used as received. 1,1,2-trichloro-2,2,1-trifluoroethane (F-113, DuPont) was used as received. Carbon dioxide (SFC/SFE Grade) was kindly provided by Air Products and was used as received.

Iniferter.

Synthesis of Polystyrene-Iniferter (TD-PS). Polystyrene was synthesized by the iniferter controlled free radical method using TD as the iniferter as reported earlier (15). The polymerizations were conducted in bulk and stopped at about 50% conversion. In a typical polymerization, 1.90 g of TD was dissolved in 15.0 g of deinhibited styrene monomer. The solution was then purged with argon and placed in a constant temperature bath at 70 °C for 15 hours. At the end of the reaction, the viscous

polymer solution was diluted with THF and then the polymer was recovered by precipitation into a ten fold excess of methanol and dried under vacuum. (Gravimetric yield = 7.9 g, 53.9%, $M_n = 3.2$ kg/mol, PDI = 1.9). The polymer was purified twice by dissolution in THF and precipitation into methanol (reprecipitation yield = 89%). The M_n and PDI of the purified polymer were determined to be 3.7 kg/mol and 1.7, respectively.

Synthesis of Poly(Vinyl Acetate)-Iniferter (BDC-PVAc). Poly(vinyl acetate) was synthesized using BDC as the iniferter. The polymerizations were conducted in bulk and stopped at about 20% conversion. In a typical polymerization, 40 g of deinhibited vinyl acetate monomer was added to a quartz flask equipped with a stir bar and then 1.0 g of BDC was added along with 2.2 mg of TD. (The TD added does not initiate polymerization of the vinyl acetate but serves to better control the polymerization of the reactive monomer by increasing the concentration of the end capping agent in solution through chain transfer (26).) The flask was then sealed with a septum and purged with argon. The solution was photolyzed at room temperature with stirring for 30 hours in a sixteen bulb Rayonet equipped with 350 nm wavelength bulbs. The polymer was then collected by precipitation into heptane and dried under vacuum giving a crude yield of 8.7 g, or 21.7% ($M_n = 4.7$ kg/mol, PDI = 1.5). The polymer was purified twice by dissolution in acetone and precipitation into heptane (reprecipitated yield = 8.3 g, 95.4%). The M_n and PDI of the purified polymer were 4.4 kg/mol and 1.6, respectively.

Block Copolymer Synthesis. The diblock copolymers were synthesized by the subsequent polymerization of a fluorocarbon monomer using either TD-PS, BDC-PVAc or XDC-PDMAEMA as the macroiniferter. The synthesis of XDC-PDMAEMA was conducted in a manner similar to the synthesis of BDC-PVAc but using XDC. Polymerizations were conducted in TFT as the solvent. While the polymerizations with BDC-PVAc were homogeneous throughout the reaction, the polymerizations with TD-PS were initially cloudy but became clear after a few hours of irradiation. As an illustration, the synthesis of PVAc-*b*-PFOA is described herein. In a typical experiment, 2.0 g BDC-PVAc ($M_n = 4.4$ kg/mol) was dissolved in 25 mL of TFT in a quartz flask equipped with a stir bar. FOA monomer (18.0 g) was then added and the flask was purged with argon. After purging, the solution was photolyzed at room temperature with stirring for 30 hours in a sixteen bulb Rayonet equipped with 350 nm bulbs. The polymer was then collected by precipitation into methanol and dried under vacuum (yield = 12.7 g, 61.9%). The block copolymer was purified by Soxhlet extraction using methanol for ca. 2 days to remove any unreacted PVAc homopolymer. The composition and relative molecular weights of the blocks in the block copolymer were determined by $^1\text{H-NMR}$ (M_n PVAc = 4.4 kg/mol, 34.9 mol %; PFOA $M_n = 43.1$ kg/mol, 65.1 mol %).

Silicone block copolymer synthesis.

Synthesis of PDMS-iniferter. The PDMS-iniferter was synthesized by the living anionic polymerization of D_3 according to procedures described in the literature. A 35% D_3 /cyclohexane solution (17.5 g, 50 mL) was added via syringe to a flame dried round bottom flask equipped with a stir bar and under argon atmosphere. *Sec*-butyllithium (0.45 mL, 5.85×10^{-4} mol) was then added via syringe to the flask to give a targeted molecular weight of 30 kg/mol. The solution was allowed to stir for about 2 h and then 20 v/v % (10 mL) of dry THF was added to start the chain propagation. The reaction was allowed to proceed for two days and then was terminated with a six fold molar excess (0.87 g, 3.51×10^{-3} mol) of 1-(dimethylchlorosilyl)-2-(*p,m* chloromethyl phenyl) ethane. Upon adding the terminating agent, the precipitation of lithium chloride was observed and the solution was left to stir for

several hours. The PDMS was then precipitated into methanol and isolated using a separatory funnel. The polymer was dried under vacuum and its weight and yield determined (yield = 14.8 g, 84.5%).

The PDMS was then functionalized to afford the PDMS-iniferter. The polymer was dissolved in ca. 30 mL THF and a three fold molar excess of diethylthiocarbamate sodium salt (0.40 g, 1.76×10^{-3} mol) was added. The yellow solution was stirred overnight at room temperature. The PDMS-iniferter was precipitated into ethanol and dried under vacuum. The PDMS-iniferter was then purified by dissolving in hexanes and washing with a 3:1 methanol:water mixture. After washing, it was collected and dried under vacuum (yield = 13.1 g, 95%). The M_n and PDI of the polymer were 26.8 kg/mol and 1.10, respectively.

PDMS Block Copolymer Synthesis. Block copolymers of PDMS with vinyl monomers such as FOA and VAc were synthesized. The synthesis of PDMS-*b*-PVAc is described as an example. Deinhibited vinyl acetate monomer (1.0 g), 5.0 g of the PDMS-iniferter ($M_n = 26.8$ kg/mol), and 15 mL of THF were added to a quartz flask equipped with a stir bar. The flask was then purged with argon and photolyzed for 30 h in a 16 bulb Rayonet equipped with 350 nm bulbs. At the end of the reaction, the polymer was precipitated into methanol, collected, and dried under vacuum (yield = 4.3 g, 70.5%). Molecular weight determination of the second block was determined by subtracting the molecular weight of the PDMS block synthesized from the total block copolymer molecular weight as determined by GPC (M_n block copolymer = 39.8 kg/mol, PDI = 1.4; M_n PVAc block = 13.0 kg/mol, 29.5 mol %).

ATRP.

Synthesis of Poly(methyl methacrylate) (PMMA). Into a round bottom flask equipped with a stir bar was added 20.0 g deinhibited methyl methacrylate monomer, 0.78 g (4×10^{-3} mol) ethyl 2-bromoisobutyrate, 0.58 g (4×10^{-3} mol) copper(I) bromide, 1.87 g (1.2×10^{-2} mol) dipyrldyl, and 20 mL ethyl acetate as solvent. The flask was then sealed with a septum and purged with argon. After purging, the flask was placed into a 100 °C oil bath for 5.5 hours. The reaction was heterogeneous due to the insolubility of the copper catalyst. At the end of the reaction, the reaction solution was diluted with ethyl acetate and passed through a short alumina column to remove the copper catalyst. The polymer was precipitated into methanol, collected, and dried under vacuum (yield = 14.9 g, 74.6%, $M_n = 8.1$ kg/mol, PDI = 1.3).

Block Copolymer Synthesis. The previously synthesized PMMA block (3.24 g, $M_n = 8.1$ kg/mol) was placed into a round bottom flask equipped with a stir bar. TFT (40 mL) was added as the solvent for the reaction and 5.7×10^{-2} g (4×10^{-4} mol) copper(I) bromide and 0.19 g (1.2×10^{-3} mol) dipyrldyl were added. Deinhibited FOMA monomer (20 g) was then added and the flask was sealed with a septum and purged with argon. After purging, the flask was placed in a 110 °C oil bath for 5.5 h. At the end of the polymerization, the flask was removed from the oil bath and the reaction solution was diluted and passed through a short alumina column to remove the insoluble copper catalyst. The polymer was then precipitated into heptane, collected, and dried under vacuum (yield = 5.9 g, 25.4%). The block copolymer was purified by Soxhlet extraction using THF and the relative block lengths were determined by $^1\text{H-NMR}$ (PMMA: $M_n = 8.1$ kg/mol, 26.7 mol %; PFOMA: $M_n = 104.0$ kg/mol, 73.3 mol%).

Characterization. The molecular weight data for the polymer samples were determined using a Waters 150-CV gel permeation chromatograph (GPC) with

UltraStyragel columns of 100, 500, 10^3 , and 10^4 Å porosities using THF as the eluent and PS standards (Showa Denko). The molecular weight data for the PDMS homopolymers and block copolymers were determined using a modular Waters 610 GPC instrument with two UltraStyragel columns of 10^3 and 10^4 Å porosities and a μ Styragel HT linear column, using dichloromethane as the eluent and PS standards (Showa Denko). $^1\text{H-NMR}$ spectra were obtained from a Bruker WM250 spectrometer. $^1\text{H-NMR}$ spectra of the hydrocarbon/fluorocarbon block copolymers were conducted in a mixed solvent of F-113 and either CDCl_3 or d_6 -acetone.

Results and Discussion

For the synthesis of diblock copolymers using the iniferter polymerization technique as developed by Otsu, the CO_2 -phobic block was synthesized first using either TD or BDC as the iniferter in conjunction with either heat or UV light, respectively. Additionally, for the formation of BAB triblock copolymers, the difunctional photoiniferter XDC was used. The polymer formed with terminal dithiocarbamate groups was then isolated, purified and characterized. The macroiniferter first block was then used, in the presence of UV light, to initiate the polymerization of the second monomer (CO_2 -philic fluorocarbon) to form the block copolymer. UV irradiation of the macroiniferter causes the reactive end groups to dissociate generating polymeric radicals which, in the presence of additional monomer, initiate the polymerization of the second monomer and lead to the formation of the second block of the block copolymer (Figure 2). Through the use of this technique, block copolymers such as PS-*b*-PFOA, PS-*b*-PFOMA, PVAc-*b*-PFOA, PVAc-*b*-PFOMA, PFOA-*b*-PVAc-*b*-PFOA, PDMAEMA-*b*-PFOMA and PTAN-*b*-PDMAEMA-*b*-PTAN have been successfully synthesized.

Listed in Tables I and II are several examples of PVAc-*b*-PFOA and PS-*b*-PFOA diblock copolymers synthesized using the iniferter technique and the description of their solubility in CO_2 at 65 °C and 5000 psi. These conditions correspond to a CO_2 density of 0.846 g/cc. As can be seen in comparison between the two materials, the PVAc block copolymers have a much higher solubility in CO_2 than the PS block copolymers. The PVAc block copolymers are soluble and form transparent solutions with a PVAc mole % of greater than 55%, compared to the PS block copolymers that are only soluble up to a PS mole % of around 30%. This is due to the much higher solubility of PVAc in CO_2 than PS: McHugh has shown that PS of molecular weight greater than 1000 g/mol is insoluble in CO_2 even at temperatures of 225 °C and 30,000 psi, while PVAc of a molecular weight of 125,000 g/mol is soluble in CO_2 at about 9000 psi and room temperature (7).

Table I. PVAc-*b*-PFOA Diblock Copolymers

M_n (kg/mol)	PVAc ^a		PFOA ^b M_n (kg/mol)	CO_2 Solubility ^c 65 °C, 5k psi
	PDI	Mole %		
4.4	1.6	34.9	43.1	clear
4.4	1.6	24.8	70.1	clear
10.3	1.5	55.8	43.1	clear
30.9	1.5	75.3	53.5	turbid

^aCharacterized by GPC. ^bCharacterized by $^1\text{H-NMR}$. ^c4% wt/vol; determined visually with a high pressure view cell.

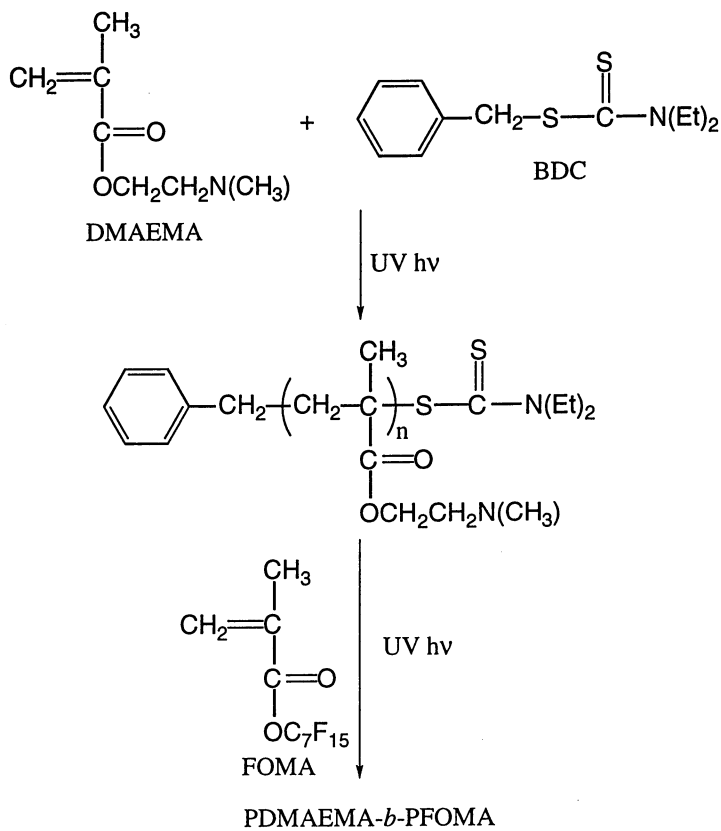


Figure 2. Synthesis of PDMAEMA-*b*-PFOMA Using the Iniferter Technique.

Table II. PS-*b*-PFOA Diblock Copolymers

M_n (kg/mol)	PS ^a		PFOA ^b M_n (kg/mol)	CO ₂ Solubility ^c 65 °C, 5k psi
	PDI	Mole %		
3.7	1.7	37.0	27.5	cloudy
3.7	1.7	28.9	39.8	clear
3.7	1.7	20.9	61.2	clear
4.5	1.8	44.5	24.5	turbid
6.6	1.6	45.1	34.9	translucent
6.6 ^d	1.6	41.2	42.3	clear

^aCharacterized by GPC. ^bCharacterized by ¹H-NMR. ^c4% wt/vol; determined visually with a high pressure view cell. ^d PS-*b*-PFOMA.

An adaptation of the synthesis scheme developed by Kumar for the crossover from a living anionic synthesis to controlled free radical iniferter synthesis (27) was used for the synthesis of several PDMS-*b*-PFOA and PDMS-*b*-PVAc block copolymers. In this synthesis technique, the siloxane block is synthesized first using established living anionic polymerization techniques. At the end of the polymerization the chain ends are terminated with 1-(dimethylchlorosilyl)-2-(*p,m*-chloromethyl phenyl)ethane to afford the benzyl chloride terminated poly(dimethyl siloxane). The terminal chloro group is then substituted with diethyldithiocarbamic acid to afford the diethyldithiocarbamate terminated PDMS. This macroiniferter-PDMS can then be used in conjunction with UV light to initiate the polymerization of a second monomer to yield a diblock copolymer (Figure 3). The results of the synthesis of a PDMS-*b*-PVAc diblock copolymer is given in Table III. The anionic polymerization of the first block (PDMS) gave a very narrow molecular weight distribution with a PDI of 1.1. The polymerization of the second block (PVAc) using the iniferter technique broadened the polydispersity of the block copolymer due to the less "living" nature of the iniferter polymerization. The PDMS-*b*-PVAc block copolymer synthesized by this technique was also employed as a stabilizer for the dispersion polymerization of vinyl acetate in CO₂ (28).

Table III. PDMS-*b*-PVAc

M_n (kg/mol)	PDMS block		Vinyl Acetate block		
	PDI	Mole %	M_n (kg/mol)	PDI ^a	Mole %
26.8	1.1	70.5	13.0	1.4	29.5

^a Polydispersity of the block copolymer.

Several hydrocarbon monomers, including acrylates, methacrylates, styrenics, and acetates, along with several fluorocarbon monomers have been successfully polymerized using the controlled free radical polymerization techniques (iniferter or ATRP). Of the block copolymers synthesized, the PS-*b*-PFOA, PS-*b*-PFOMA and

PVAc-*b*-PFOA block copolymers have been studied by small angle neutron scattering (SANS) in CO₂ and found to self assemble into micelles with a hydrocarbon core and a fluorocarbon corona (10). Furthermore, these block copolymers have been found to be effective stabilizers for dispersion polymerizations in CO₂ (9).

SANS studies of several examples of the PS-*b*-PFOA block copolymers synthesized using the iniferter technique have shown that these amphiphiles self associate in CO₂ to form spherical micelles with a PS hydrocarbon core stabilized by a PFOA fluorocarbon corona. It was also noted that the size and aggregation number of the micelles changed slightly based on the density of the CO₂ medium. These block copolymers were also shown to solubilize CO₂ insoluble 500 g/mol polystyrene oligomer into the CO₂ continuous phase (10). The SANS studies were complemented with high pressure, high-resolution NMR spectroscopy of these block copolymers in supercritical CO₂ (29). ¹H-NMR studies revealed that at low CO₂ densities only the resonances from the PFOA blocks are visible, indicative of the PS blocks being immobilized in micelle cores. But with increasing CO₂ density, the PFOA resonances shift upfield, and NMR signals from the PS blocks grow in and also shift upfield. The appearance of the PS resonances arises from the increased mobilization of the PS blocks in the micelle core as the core is plasticized and the PFOA solubility is increased by the denser CO₂.

These PS-*b*-PFOA block copolymers were also studied in the solid phase by X-ray photoelectron spectroscopy (XPS) (30). PFOA is a very low surface energy material (ca. 11 dyn/cm) while PS has a fairly high surface energy (40 dyn/cm); these materials therefore are expected to strongly phase separate. XPS studies confirmed that PFOA preferentially exists at the air/surface interface. The enhanced mole % of PFOA at the surface was also shown to increase upon annealing as this increased the polymer chain mobility, allowing the PFOA chains to move to the surface. For an unannealed PS-*b*-PFOA sample comprised of 50 mole % PS, less than 20 mole % PS was found at the surface. The mole % PS was observed to further decrease to less than 10% upon annealing.

Additionally, these block copolymers are effective stabilizers in the dispersion polymerization of styrene in CO₂. In using these block copolymers as stabilizers it was observed that the length of the anchoring block (PS) relative to the length of the solubilizing block (PFOA) is very important to the stability of the latex formed and the particle size obtained. The best results were obtained using the block copolymers with the longer anchoring blocks (Table IV) (9).

Table IV. Results of Styrene Polymerizations in CO₂^a

Stabilizer ^b (kg/mol)	Stabilizer conc. (w/v)	yield (%)	M _n (kg/mol)	Particle size (μm)
none	0	22.1	3.8	—
PS3.7- <i>b</i> -PFOA ^{17.0}	4	72.1	19.2	0.40
PS4.5- <i>b</i> -PFOA ^{24.5}	4	97.7	22.5	0.24
PS6.6- <i>b</i> -PFOA ^{34.9}	4	93.6	23.4	0.24

^a Polymerizations in CO₂ at 3000 psi and 65 °C in a 10 mL high pressure view cell with 2.0 g styrene and 2.4 x 10⁻² M AIBN. ^bFor simplicity, the block copolymer molecular weights are listed as PS<M_n>-*b*-PFOA<M_n>.

Based upon the results obtained from the SANS studies of the PS-*b*-PFOA block copolymers which showed that the size of the micelle changed slightly with pressure, the concept of a critical micelle density (CMD) was developed. Below the critical density, the surfactants are predominantly located in micelles. But, at higher densities, the block which was previously insoluble and in the core of the micelle is solubilized in the denser CO₂ medium and the surfactant exists as unimers in solution (Figure 4) (10,31). Due to the higher CO₂ solubility of PVAc compared to PS (7), PVAc-*b*-PFOA block copolymers were synthesized by the iniferter technique with the idea that these block copolymers would exhibit greater changes in solution aggregation behavior than the PS-*b*-PFOA block copolymers and thus clearly demonstrating the existence of a CMD. Indeed, the existence of a CMD was clearly seen by SANS for a PVAc-*b*-PFOA block copolymer. At lower densities the PVAc block is relatively insoluble leading to the formation of micelles in solution, but at higher densities the PVAc block is solubilized leading to a decrease in the aggregation number and the breakup of the micelles into unimers.

In PVAc dispersion polymerization studies in CO₂ with these PVAc-*b*-PFOA block copolymers these block copolymers proved to be effective stabilizers, affording stable latexes, high yield, and high molecular weight PVAc (28).

When using ATRP to make block copolymers, a haloalkane (*e.g.* (1-bromoethyl)benzene, ethyl 2-bromoisobutyrate) was used as the initiator in conjunction with either copper(I) chloride or bromide and 2,2'-dipyridyl as the catalyst. The initiator:copper halide:dipyridyl mole ratio typically used was 1:1:3. In the presence of sufficient heat, the halogen atom is believed to dissociate from the haloalkane initiator giving an initiating alkyl-radical which initiates polymerization of the first monomer to form the first block. After polymerization of the first block is complete, the halogen endcapped polymer is isolated, purified, and characterized. The formation of the second block is accomplished by sufficiently heating a solution of the redissolved first block, the second monomer, additional copper halide, and dipyridyl catalyst (Figure 5). Using ATRP, various block copolymers have been synthesized including poly(methyl methacrylate)-*b*-PFOMA, PHEMA-*b*-PFOMA, PS-*b*-PFOMA, poly(*t*-butylacrylate)-*b*-PFOMA, and poly(ethylhexyl acrylate)-*b*-PFOMA (Table V).

Table V. Hydrocarbon-fluorocarbon block copolymers synthesized by ATRP

Hydrocarbon block	M_n (kg/mol)	PDI	Fluorocarbon block	M_n (kg/mol)
PMMA	8.1	1.3	PFOMA	104.0
P(<i>t</i> -BuAc)	5.0	1.6	PFOMA	52.6
PHEMA	4.0	1.5	PFOMA	40.0

In the synthesis of these hydrocarbon-fluorocarbon block copolymers, the first block synthesized is typically the hydrocarbon block due to the relative ease of characterization (high solubility in common organic solvents) compared to the fluorocarbon block. The hydrocarbon block molecular weight was determined by GPC, and ¹H-NMR was used to determine conversion and polymer purity. Once the hydrocarbon-fluorocarbon block copolymer was made, it was purified by Soxhlet extraction with a good solvent for the hydrocarbon homopolymer block, and characterized by ¹H-NMR to determine the relative molecular weight of the second block in comparison to the first block.

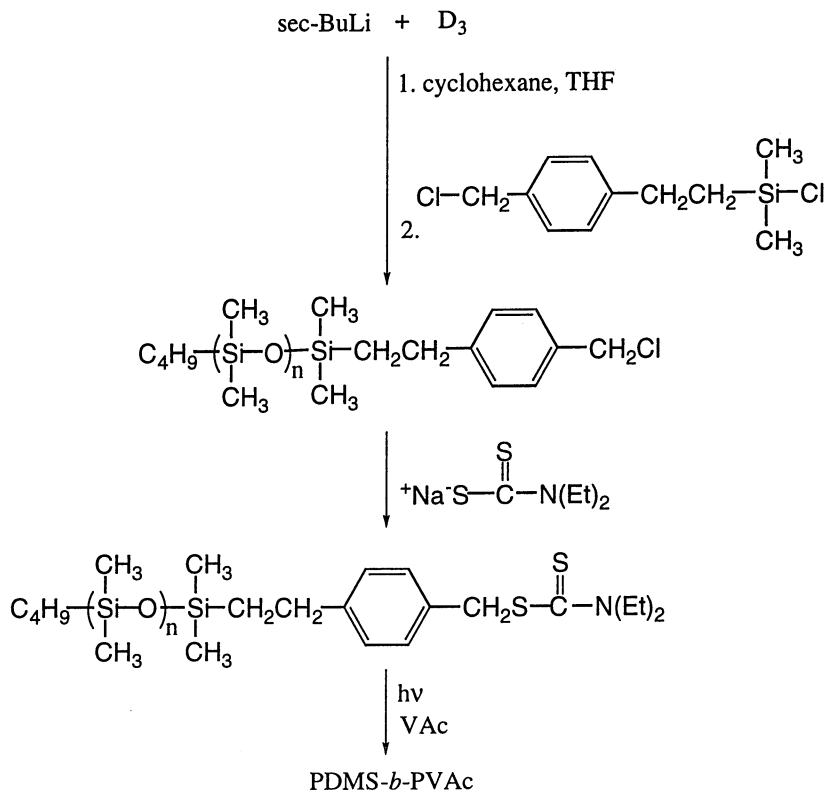


Figure 3. Synthesis of PDMS-*b*-PVAc Via the Combination of Anionic and Iniferter Polymerization Techniques

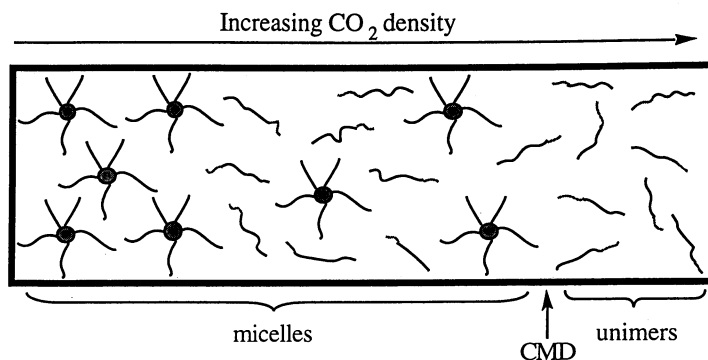
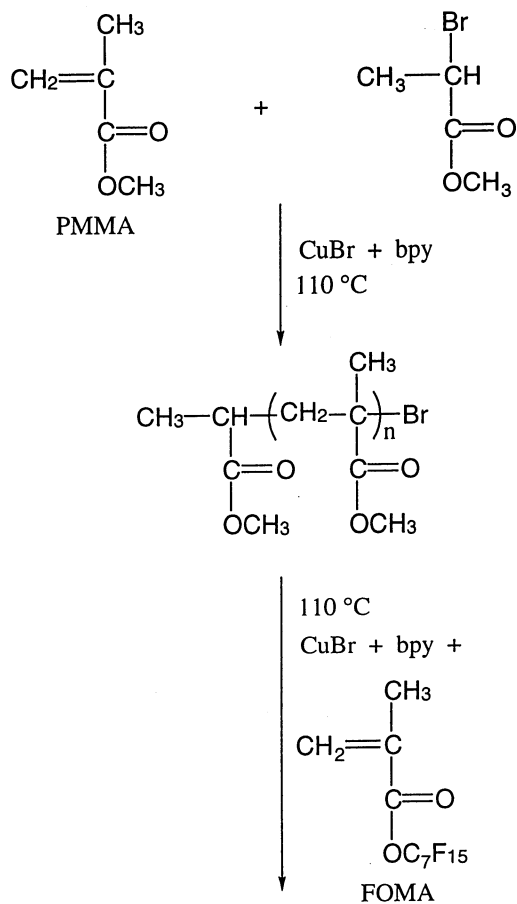


Figure 4. Illustration of Critical Micelle Density (CMD)



PMMA-*b*-PFOMA

Figure 5. Synthesis of PMMA-*b*-PFOMA Using ATRP

Conclusion.

ATRP and iniferter controlled free radical polymerization techniques have been found to be effective for the synthesis of various hydrocarbon-fluorocarbon block copolymers. Several of the hydrocarbon-fluorocarbon block copolymers synthesized have been shown to be effective stabilizers for dispersion polymerizations in CO₂. Additionally, these block copolymers have been studied using various analytical techniques including SANS, ¹H-NMR, and XPS. Many of the block copolymers synthesized are soluble in CO₂ under suitable conditions and have been observed to self assemble into micelles that display interesting solution behavior. These micelles have been observed to change in size based upon the density of the CO₂ phase, leading to the concept of a critical micelle density. XPS analysis showed these block copolymers to be strongly phase separated with the fluorocarbon block being dominant at the surface. Research is continuing to design and synthesize more effective and well defined stabilizers for dispersion polymerizations in CO₂ and the emulsification of CO₂-insoluble materials. The latter has implications for the use of CO₂ in surface treatment and cleaning technologies.

Acknowledgments.

The authors have greatly appreciated Scott Gaynor and Kris Matyjaszewski for their assistance with the initial ATRP polymerizations. We gratefully acknowledge financial support from the NSF through a Presidential Faculty Fellowship (JMD: 1993-1997), the *Environmentally Benign Chemical Synthesis and Processing Program* sponsored by the NSF and the EPA, and the *Consortium for Polymeric Materials Synthesis and Processing in Carbon Dioxide* sponsored by DuPont, Air Products and Chemicals, Hoechst-Celanese, Eastman Chemical, B. F. Goodrich, Xerox, and Bayer. In addition, we thank Isco for the donation of a syringe pump.

Literature Cited.

- (1) DeSimone, J. M.; Guan, Z.; Elsbernd, C. S. *Science* **1992**, 257, 945.
- (2) DeSimone, J. M.; Guan, Z.; Elsbernd, C. S. *Polym. Prep. (Am. Chem. Soc. Div. Polym. Chem.)* **1992**, 33, 329.
- (3) DeSimone, J. M.; Guan, Z.; Combes, J. R.; Elsbernd, C. S. *Polym. Prep. (Am. Chem. Soc. Div. Polym. Chem.)* **1993**, 34, 447.
- (4) Hoefling, T.; Stofesky, D.; Reid, M.; Beckman, E.; Enick, R. M. *J. Supercrit. Fluids* **1992**, 5, 237.
- (5) McHugh, M.; Krukoni, V. *Supercritical Fluid Extraction - Principles and Practice*; Butterworths: Boston, 1986.
- (6) DeSimone, J. M.; Maury, E. E.; Combes, J. R.; Mencologlu, Y. Z. *Polym. Prep. (Am. Chem. Soc. Div. Polym. Mater. Sci. Eng.)* **1993**, 68, 41.
- (7) Rindfleisch, F.; DiNoia, T. P.; McHugh, M. A. *J. Phys. Chem.* **1996**, 100, 15581.
- (8) DeSimone, J. M.; Maury, E. E.; Mencologlu, Y. Z.; McClain, J. B.; Romack, T. J.; Combes, J. R. *Science* **1994**, 265, 356.
- (9) Canelas, D. A.; Betts, D. E.; DeSimone, J. M. *Macromolecules* **1996**, 29, 2818.
- (10) McClain, J. B.; Betts, D. E.; Canelas, D. A.; Samulski, E. T.; DeSimone, J. M.; Londono, J. D.; Cochran, H. D.; Wignall, G. D.; Chillura-Martino, D.; Triolo, R. *Science* **1996**, 274, 2049.
- (11) Price, C. *Developments in Block Copolymers*; Elsevier Applied Science Publisher: London, U. K., 1982.

- (12) Vagberg, L. J. M.; Cogan, K. A.; Gast, A. P. *Macromolecules* **1991**, *24*, 1670.
- (13) Tuzar, Z.; Kratochvil, P. In *Surface and Colloid Science*; E. Matijevic, Ed.; Plenum Press.: New York, 1993; Vol. 15; pp 1-83.
- (14) DeSimone, J. M.; Guan, Z. *Polym. Prep. (Am. Chem. Soc. Div. Polym. Chem.)* **1993**, *34*, 614.
- (15) DeSimone, J. M.; Guan, Z. *Macromolecules* **1994**, *27*, 5527.
- (16) Otsu, T.; Yoshida, M. *Makromol. Chem., Rapid Commun.* **1982**, *3*, 127.
- (17) Patten, T. E.; Xia, J.; Abernathy, T.; Matyjaszewski, K. *Science* **1996**, *272*, 866.
- (18) Wang, J.-S.; Matyjaszewski, K. *Macromolecules* **1995**, *28*, 7901.
- (19) Kumar, R. C.; Andrus Jr., M. H.; Mazurek, M. H. US Patent 5 057 619, 1991.
- (20) Otsu, T.; Tazaki, T.; Yoshida, M. *Makromol. Chem., Rapid Commun.* **1982**, *3*, 133.
- (21) Otsu, T.; Kuriyama, A. *Polym. J.* **1985**, *17*, 97.
- (22) Otsu, T.; Kuriyamam, A. *Polym. Bull.* **1984**, *11*, 135.
- (23) Matyjaszewski, K.; Patten, T. E.; Xia, J. *J. Am. Chem. Soc.* **1997**, *119*, 674.
- (24) Romack, T.; DeSimone, J. M.; Gaynor, S.; Matyjaszewski, K. unpublished results.
- (25) Riffle, J. S.; Sinai-Zingde, G.; DeSimone, J. M.; Hellstern, A. M.; Chen, D. H.; Yilgor, I. *Polym. Prep. (Amer. Chem. Soc. Div. Polym. Chem.)* **1988**, *29*, 93.
- (26) Doi, T.; Matsumoto, A.; Otsu, T. *J. Polym. Sci., Polym. Chem. Ed.* **1994**, *32*, 2911.
- (27) Kumar, R. C.; Andrus Jr., M. H.; Dueltgen, R. R.; Mazurek, M. H. *Polym. Prep. (Am. Chem. Soc. Div. Polym. Chem.)* **1994**, *35*, 786.
- (28) Canelas, D. P.; Betts, D. E.; DeSimone, J. M. *Polym. Prep. (Am. Chem. Soc., Div. Polym. Chem.)* **1997**, *38(2)*, 628.
- (29) Dardin, A.; Cain, J. B.; DeSimone, J. M.; Johnson Jr., C. S.; Samulski, E. T. *Macromolecules* **1997**, *30*, 3593.
- (30) Kassis, C. M.; Steehler, J. K.; Betts, D. E.; Guan, Z.; Romack, T. J.; DeSimone, J. M.; Linton, R. W. *Macromolecules* **1996**, *29*, 3247.
- (31) Betts, D. E.; DeSimone, J. M. *Polym. Prep. (Am. Chem. Soc. Div. Polym. Mater. Sci. Eng.)* **1996**, *74*, 252.

Design Strategies for Branched and Highly Branched Macromolecular Architectures Using Nitroxide-Mediated Living Free-Radical Procedures

Craig J. Hawker¹, Eva E. Malmström¹, Jean M. J. Fréchet², Marc R. Leduc²,
R. Bernard Grubbs², and George G. Barclay³

¹IBM Almaden Research Center, 650 Harry Road, San Jose, CA 95120-6099

²Department of Chemistry, University of California, Berkeley, CA 94720-1460

³Shipley Company, 455 Forest Street, Marlborough, MA 01752-3092

Free radical procedures play a dominant role in the synthesis of a wide variety of commodity polymers due to the mild, non-demanding reaction conditions and compatibility with numerous functional groups. However, one of the major disadvantages of free radical polymerizations is the lack of control over macromolecular structure. For example, the polymers obtained are frequently polydisperse and the technique provides poor control over molecular weight, chain ends, and architecture. Many of these shortcomings have recently been overcome using nitroxide mediated 'living' free radical procedures, coupled with well defined unimolecular alkoxyamine initiators. In this report, various strategies for the control of polymeric structure and macromolecular architecture using novel 'living' free radical procedures will be discussed and compared with currently available techniques.

The control and manipulation of the physical and mechanical properties of polymeric materials is an ongoing challenge in polymer science.¹ One method which has recently gained prominence as a means to obtain this goal is the controlled incorporation of branching in linear polymer structures. Low levels of branching gives graft copolymers, while increasing the amount of branching leads to hyperbranched structures and eventually to dendritic macromolecules. These highly branched macromolecules, such as dendrimers and hyperbranched polymers, are a new class of macromolecular architecture which have received considerable attention recently.² One of the primary reasons for this explosion of interest in branched macromolecules is the belief that new and/or improved properties will be observed for these materials. In fact a number of unique properties, such as intrinsic viscosity,³

melt viscosity,⁴ molecular inclusion,⁵ etc. have already been observed for dendritic macromolecules and many more will not doubt be realized as other macromolecular architectures become available. For example, globular dendrimers are believed to be essentially free of chain entanglements, in direct contrast to most linear polymers where physical properties are dominated by chain entanglements. This leads to the observed differences in intrinsic and melt viscosity for dendrimers when compared to linear polymers. However one difficulty associated with dendritic and hyperbranched macromolecules is the limited range of reaction types that can be used for their construction. By their design, dendrimers and hyperbranched macromolecules are typically prepared by condensation chemistry. Since one of the most intriguing and potentially useful applications for branched macromolecules is in their blending with commodity linear polymers to improve the mechanical and physical properties of the linear material, the restriction to polymers based on polycondensation chemistry severely limits the study and exploitation of these materials. In a similar vein, well defined graft copolymers are typically prepared by living techniques, such as anionic polymerization, which are synthetically demanding and incompatible with a wide range of useful functional groups and monomer units.⁶ This results in a narrow range of possible structures with little opportunity for the incorporation of functional groups.

The development of an alternative approach to branched macromolecular architectures which relies on simple free radical chemistry is therefore highly desirable and would alleviate many of the above difficulties. Such an objective would, under traditional free radical polymerization conditions, be extremely problematic, if not impossible. This is due to the uncontrolled nature of normal free radical polymerizations coupled with numerous termination reactions which leads to polydisperse, poorly defined materials. Also the tendency to undergo termination by radical-radical recombination is a serious drawback for branched systems since coupling of the chain ends would soon result in crosslinking and gelation. The recent development of a "living" free radical polymerization process based on stable nitroxide radicals as reversible chain termination agents offers the possibility of reducing the influence of termination reactions and therefore overcoming many of the drawbacks traditionally associated with free radical chemistry. Nitroxide mediated 'living' free radical procedures may therefore have a number of advantages when compared to traditional techniques for the preparation of novel branched polymer systems.

The development of a polymerization process, based on free radical chemistry, which displays many of the characteristics of a living polymerization has long been a goal of polymer chemists.⁷ Early attempts to realize a "living" free radical procedure involved the concept of reversible termination of growing polymer chains by iniferters,^{8,9} however this concept was plagued by high polydispersities and poor control over the functional groups at the chain ends. Following this approach Moad and Rizzardo¹⁰ introduced the use of stable nitroxide free radicals, such as 2,2,6,6-tetramethylpiperidinyloxy (TEMPO), as reversible terminating agents to "cap" the growing polymer chain. The advantages of using nitroxide free radicals are their near diffusion controlled rate of reaction with carbon centered free radicals which leads to

efficient capping of the growing chain end and their inability to self-initiate vinyl polymerizations. Subsequently, Georges¹¹ refined the use of TEMPO in "living" free radical polymerizations and demonstrated that narrow molecular weight distribution polystyrene (PD. = 1.10-1.30) could be prepared using bulk polymerization conditions. Recently, it has been shown that nitroxide mediated "living" free radical polymerizations can also be used to control molecular weight¹² and chain end functional groups¹³ while maintaining low polydispersities and permitting the synthesis of block copolymers.¹⁴ These results, combined with the complementary work of Sawamoto,¹⁵ Matyjaszewski,¹⁵ Percec,¹⁶ and Jerome¹⁶ in the related area of metal assisted 'living' radical polymerization, have demonstrated that a free radical polymerization process having the characteristics of a living polymerization can be achieved.

We foresee that in addition to the intrinsic scientific interest possessed by both the "living" free radical procedure and these new branched macromolecules based on addition monomers, a large number of potential advanced technological applications exist. This is due to the greatly improved properties, such as rheology and compatibilization, that we anticipate for these novel materials when compared to their linear or even star analogs as well as the ability to tailor and control the number and, in some cases, location of reactive functionalities or catalytic sites. Such property enhancements and/or new properties may prove useful in a variety of advanced materials and technological applications such as compatibilizing agents, surface agents, polymeric additives, modifying agents for a variety of polymer properties (melt rheology, compressibility, modulus, etc.), macromolecular catalysts and carriers (i.e. dye or drug applications), high performance crosslinking agents, etc.

In this report, we detail the underlying features of nitroxide mediated 'living' free radical procedures which permit numerous strategies to be developed for the synthesis of branched polymers. These branched macromolecular architectures range from graft copolymers to hyperbranched macromolecules and hybrid dendritic-linear block copolymers. The advantages of 'living' free radical strategies will be compared and contrasted with traditional procedures used for the synthesis of complex macromolecular architectures. It should be noted that many of the strategies developed for nitroxide mediated systems can also be successfully applied to ATRP polymerizations.

Experimental Section

Nuclear magnetic resonance spectroscopy was performed on a Bruker AM 250 FT-NMR spectrometer using deuterated chloroform as solvent and tetramethylsilane as internal reference. Gel permeation chromatography was carried out on a Waters chromatograph connected to a Waters 410 differential refractometer with THF as the carrier solvent. Differential scanning calorimetry was performed on a Perkin Elmer DSC-7 calorimeter using a scanning rate of 10°C/minute under a nitrogen atmosphere. The glass transition temperature was defined as the half way point of transition heat flow. Analytical TLC was performed on commercial Merck plates coated with silica gel GF254 (0.25 mm thick). Silica gel for flash chromatography

was Merck Kieselgel 60 (230-400 mesh). All solvents used for synthesis were dried and distilled in the appropriate manner before use.

1-Phenyl-1-(2',2',6',6'-tetramethyl-1'-piperidinyloxy)ethane 1,

To ethylbenzene (100 ml) was added di-*t*-butyl peroxide (5.0 g, 33.0 mmol) followed by TEMPO (10.5 g, 66.0 mmol). The reaction mixture was then heated at reflux under argon for 16 hours and evaporated to dryness. The crude product was purified by flash chromatography eluting with hexane gradually increasing to 1:1 hexane/dichloromethane. This gave the TEMPO derivative, **1**, as a crystalline white solid which could be recrystallized from cold ethanol (-78°C), (7.20 g, 42%); m.p. 46-47°C; IR (neat) 2950, 1490, 1390, 1375, and 1040 cm⁻¹; ¹H NMR (CDCl₃) δ 0.64, 1.05, 1.16, 1.36 (each br s, 12H, CH₃), 1.23-1.58 (m, 6H, CH₂); 1.44 (d, *J* = 7 Hz, 3 H, CH(CH₃)), 4.76 (q, *J* = 7 Hz, 1 H, CH(CH₃)), and 7.25-7.35 (m, 5 H, ArH); ¹³C NMR (CDCl₃) δ 17.22, 20.34, 23.55, 31.59, 34.49, 40.37, 59.66, 83.10, 126.59, 126.74, 127.97, and 145.84; mass spectrum (EI) *m/z* 261.

1-Benzyloxy-2-phenyl-2-(2',2',6',6'-tetramethyl-1'-piperidinyloxy)ethane 13,

To a solution of benzoyl peroxide (4.0 g, 16.5 mmol) in distilled styrene (160 ml) was added 2,2,6,6-tetramethyl-1-piperidinyloxy (TEMPO) (5.68 g, 36.4 mmol) and the solution heated at 80 C under nitrogen for 20 hours. After cooling the solution was evaporated to dryness and purified by flash chromatography eluting with 1:1 hexane/dichloromethane, gradually increasing to 1:9 hexane/dichloromethane to give the modified TEMPO initiator, **13**, as a pale yellow oil (2.64 g, 42%); IR (neat) 3100-2850, 1720, and 1200 cm⁻¹; ¹H NMR (CDCl₃) δ 0.75, 1.07, 1.21, 1.37 (each br s, 12H, CH₃), 1.38-1.52 (m, 6H, CH₂); 4.53 (ABq, *J* = 6 Hz, 1 H, CHH), 4.83 (ABq, *J* = 6 Hz, 1 H, CHH), 5.06 (ABq, *J* = 3 Hz, 1 H, CH), 7.25-7.56 (m, 8 H, ArH) and 7.91 (B of ABq, *J* = 6 Hz, 2H, ArH); ¹³C NMR (CDCl₃) δ 17.09, 20.31, 34.00, 40.36, 60.01, 66.68, 83.90, 127.54, 127.97, 128.18, 129.48, 130.14, 132.72, 140.61, and 166.20; mass spectrum (EI) *m/z* 381; Anal. Calcd. for C₂₄H₃₁NO₃: C, 75.6; H, 8.19; N, 3.67. Found: C, 76.0; H, 7.97; N, 3.86.

1-Hydroxy-2-phenyl-2-(2',2',6',6'-tetramethyl-1'-piperidinyloxy)ethane 7,

To a solution of the benzyl ester, **13**, (3.2 g, 8.4 mmol) in ethanol (100 ml) was added aqueous sodium hydroxide (10 ml of a 1N solution, 10.0 mmol) and the solution heated at reflux under nitrogen for 2 hours. After cooling, the solution was evaporated to dryness, partitioned between water (200 ml) and dichloromethane (200 ml) and the aqueous layer extracted with dichloromethane (2 x 100 ml). The combined organic layers were dried with magnesium sulfate, evaporated to dryness and the crude product purified by flash chromatography eluting with 1:4 hexane/dichloromethane, gradually increasing to 1:9 hexane/dichloromethane to give the hydroxy derivative, **7**, as a pale yellow oil (2.01 g, 87%); ¹H NMR (CDCl₃) δ 1.14, 1.21, 1.33, 1.50 (each br s, 12H, CH₃), 1.38-1.72 (m, 6H, CH₂); 3.71 (br d, *J* =

9 Hz, 1 H, *CHH*), 4.21 (d of d, $J = 2$ and 6 Hz, 1 H, *CHH*), 5.29 (d of d, $J = 2$ and 3 Hz, 1 H, *CH*), 5.88 (br s, *OH*); and 7.25-7.56 (m, 5 H, *ArH*); ^{13}C NMR (CDCl_3) δ 17.15, 20.41, 20.73, 32.76, 34.61, 40.23, 40.41, 60.38, 61.69, 69.73, 83.59, 126.20, 127.89, 128.34, and 138.92; mass spectrum (EI) m/z 277; Anal. Calcd. for $\text{C}_{17}\text{H}_{27}\text{NO}_2$: C, 73.6; H, 9.81; N, 5.05. Found: C, 73.8; H, 10.05; N, 5.08.

2-Phenyl-2-(2',2',6',6'-tetramethyl-1-piperidinyloxy)-1-(4'-vinylbenzyloxy)ethane

4, To a solution of the alcohol, **7**, (1.0 g, 3.6 mmol) in dry tetrahydrofuran (20 ml) was added sodium hydride (200 mg, 5.0 mmol) and the mixture stirred at room temperature for 10 minutes. A solution of p-vinylbenzyl chloride (1.52 g, 10.0 mmol, 3.0 equiv.) was added and the mixture stirred at room temperature for 1 hour, then heated at reflux for 16 hours. The reaction mixture was then evaporated to dryness and partitioned between dichloromethane (50 ml) and water (50 ml) and the aqueous layer extracted with dichloromethane (2 x 50 ml). The combined organic layers were dried, evaporated to dryness and purified by flash chromatography eluting with 1:1 hexane/dichloromethane increasing to dichloromethane. This gave the styrene derivative, **4**, as a pale yellow oil. Yield 71%; ^1H NMR (CDCl_3) δ 0.63, 1.01 (each br s, 6H, CH_3), 1.15-1.55 (m, 12H, 3 x CH_2 and 2 x CH_3), 3.65 (ABq, $J = 6$ Hz, 1 H, *CHH*), 3.95 (ABq, $J = 6$ Hz, 1 H, *CHH*), 4.41 (s, 2H, CH_2), 4.84 (d of d, $J = 2$ and 6 Hz, 1 H, *CHH*), 5.20 (d of d, $J = 2$ and 7 Hz, 1 H, =*CHH*), 5.71 (d of d, $J = 2$ and 6 Hz, 1 H, =*CHH*), 6.66 (d of d, $J = 6$ and 7 Hz, 1 H, =*CH*), 7.08 (d, 2H, *ArH*) and 7.25-7.52 (m, 7 H, *ArH*); ^{13}C NMR (CDCl_3) δ 17.17, 20.56, 33.87, 40.48, 59.36, 72.74, 72.83, 85.41, 113.52, 126.04, 127.24, 127.53, 127.82, 127.88, 136.62, 138.14, and 141.79; mass spectrum (EI) m/z 393.

General Procedure for Synthesis of Dendritic Initiators, [G-4]-init, **11**,

To a solution of the alcohol, **7**, (392 mg, 1.50 mmol) in dry tetrahydrofuran (25 ml) was added sodium hydride (80 mg, 60% dispersion in oil, 2.0 mmol) and the reaction mixture was stirred under argon at room temperature for 15 minutes. The dendritic bromide, [G-3]-Br, **10**, (1.70 g, 0.51 mmol) dissolved in dry tetrahydrofuran (10 ml) was then added dropwise and the reaction mixture heated at reflux under argon for six hours. The reaction mixture was then cooled, evaporated to dryness, and partitioned between dichloromethane (100 ml) and water (100 ml). The aqueous layer was extracted with dichloromethane (2 x 50 ml) and the combined organics dried and evaporated to dryness. The crude product was purified by flash chromatography eluting with dichloromethane gradually increasing to 1:9 diethyl ether/dichloromethane to give the dendritic initiator, **11**, as a colorless foam (1.61 g, 86%); IR (neat) 2950, 1500, 1380, and 1030 cm^{-1} ; ^1H NMR (CDCl_3) δ 0.54 (br s, 3H, CH_3), 0.91-1.50 (br m, 15H, CH_2 and CH_3), 3.55 (ABq, 1H, *CHH*), 3.88 (ABq, 1H, *CHH*), 4.36 (s, 2 H, CH_2), 4.85, 4.92 and 5.00 (each s, 28H, ArCH_2O), 4.89 (ABq, 1H, *CH*), 6.35-6.60 (complex m, 21H, *ArH*), and 7.25-7.35 (m, 45 H, *ArH*); ^{13}C NMR (CDCl_3) δ 17.30, 20.49, 34.10, 39.76, 40.58, 60.06, 70.09, 70.18, 72.93,

85.51, 101.35, 101.71, 106.00, 106.50, 127.18, 128.05, 128.70, 136.90, 139.37, 139.50, 141.31, 142.10, 159.96, 160.17, and 160.28.

Copolymer of 4 with styrene, 5, A solution of the styrene-TEMPO monomer, **4**, (450 mg, 1.15 mmol), styrene (2.40 g, 23.0 mmol, 20 equiv.) and AIBN (40 mg, 0.23 mmol) in dry tetrahydrofuran (20 ml) was heated at reflux under argon for 24 hours. The reaction mixture was evaporated to dryness, redissolved in dichloromethane (10 ml) and precipitated into methanol (500 ml) followed by hexane (500 ml). The copolymer, **5**, was isolated as a white powder. Yield 72%; $M_n = 12\ 000$ and PD = 1.80; $^1\text{H NMR}$ (CDCl_3) δ 0.65, 0.90-1.70, 3.65, 3.95, 4.30, 4.82, and 6.40-7.25 (br m); $^{13}\text{C NMR}$ (CDCl_3) δ 17.25, 39.0-43.5, 125.3 (br), 127.5 (br), 128.30, and 144.7-145.8 (a number of resonances were too small to observe).

Preparation of graft polymers, 8, A solution of the polymeric initiator, **5**, (200 mg, 0.085 mmol equiv.) in styrene (1.82 g, 17.5 mmol, 200 equiv.) was heated at 130°C with stirring under argon for 72 hours. During this time the viscosity of the solution was observed to gradually increase and the clear reaction mixture eventually solidified. The reaction mixture was then dissolved in dichloromethane (25 ml) and precipitated into hexane (1 l) followed by re-precipitation into methanol (1 l). The graft polystyrene, **8**, was isolated as a white solid after drying. Yield 80%; $M_n = 86\ 000$ and PD = 2.01; $^1\text{H NMR}$ (CDCl_3) δ 0.90-1.70 (br m), and 6.40-7.25; $^{13}\text{C NMR}$ (CDCl_3) δ 39.0-44.5, 125.0 (br), 127.5 (br), and 144.5-146.0.8

General Procedure for Macromonomer Copolymerization

A mixture of the initiator, **1**, (65.0 mg, 0.25 mmol) and poly(caprolactone) macromonomer, **2**, ($M_n = 3\ 500$, PD. = 1.10) (2.00 g, 0.6 mmol) was dissolved in styrene (7.02 g, 67.5 mmol) and the reaction mixture heated at 125°C for 48 hours. During this time the polymerization mixture became progressively more viscous and eventually solidified. The reaction mixture was then cooled to room temperature and redissolved in tetrahydrofuran (25 ml) and precipitated (2x) into methanol (1 l) to give the graft copolymer, **13**, as a white solid; (8.24 g, 82 %); IR. 3200-3000, 2920, 2850, 1720, 1600, 1490, 1470 cm^{-1} ; $^1\text{H NMR}$ (CDCl_3) δ 1.28-2.05 (complex m), 2.30 (t, CH_2CO); 4.10 (t, CH_2OCO); and 6.40-7.22 (complex m); $^{13}\text{C NMR}$ (CDCl_3) δ 22.30, 40.20, 40.35-45.0 (broad multiplet), 53.20, 125.40, 127.62, 127.98, 144.50-145.5 (br), and 173.5.

Results and Discussion

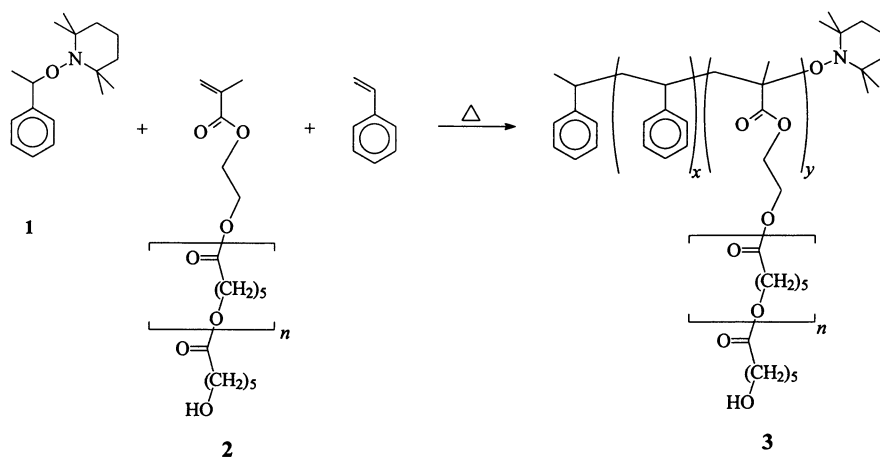
One of the unique features associated with 'living' free radical procedures which permit the synthesis of numerous complex macromolecular architectures is the compatibility of the alkoxyamine initiating center with a wide variety of reaction conditions.¹⁷ This allows functionalized unimolecular initiators to be readily prepared and then polymerized, or coupled with a preformed polymer, to give well

defined multifunctional or polymeric initiators. This feature, coupled with the low occurrence of radical-radical coupling reactions, allows a wide variety of complex macromolecular architectures to be prepared. Alternatively, the tolerance of nitroxide mediated 'living' free radical polymerizations to various functional groups permits well defined linear polymers with functionalized chain ends or backbone units to be prepared which can then be coupled to give unusual graft, star, and block polymers.

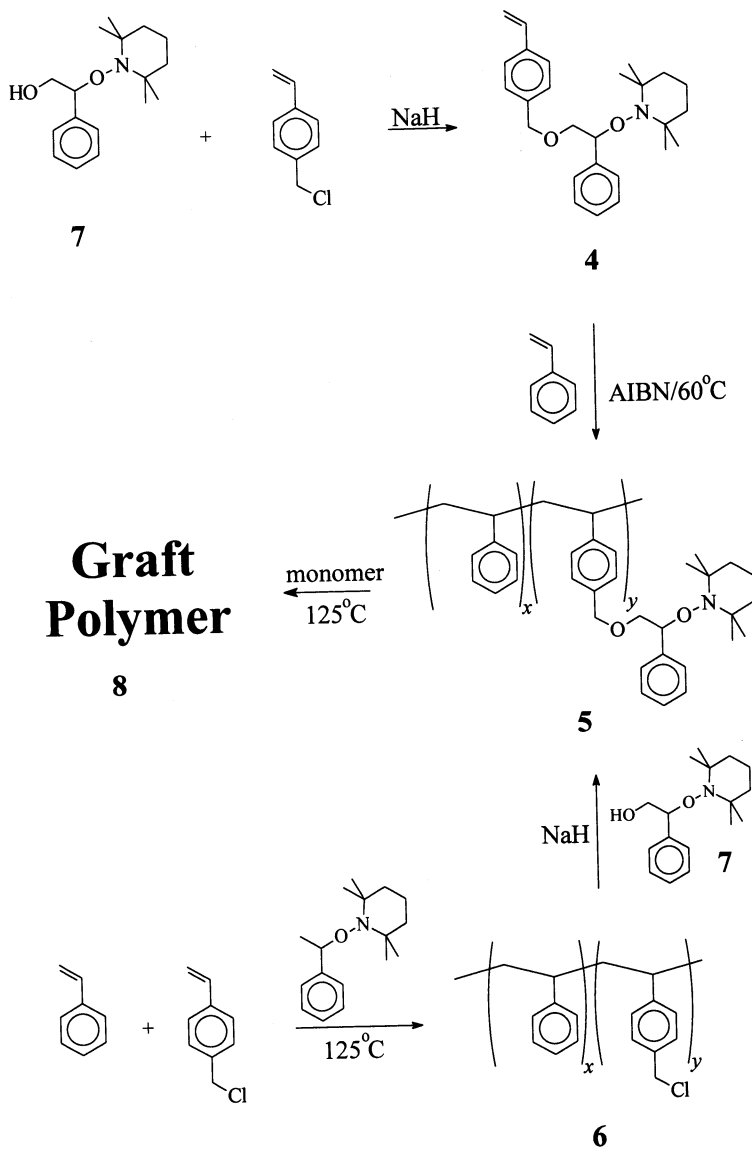
Graft Copolymers. The high degree of latitude available in the design of synthetic strategies for the preparation of complex macromolecular architectures is perhaps best appreciated by examining the synthesis of graft copolymers using 'living' free radical procedures. Essentially all possible strategies for the construction of graft copolymers can be, or have been, accomplished using 'living' free radical chemistry. For example, the polymerization of macromonomers has been demonstrated using the alkoxyamine, **1**, as unimolecular initiator.¹⁸ As shown in scheme 1, copolymerization of methacrylate terminated poly(caprolactone), **2**, with styrene using the unimolecular **1** gives the graft copolymer, **3**, which was shown to have the anticipated structure by a variety of spectroscopic and chromatographic techniques.¹⁹ Significantly, even under standard bulk polymerization conditions a variety of macromonomers could be readily incorporated with the weight percentage of macromonomer in the final graft copolymer being essentially the same as the feed percentage. The degree of control over the structure of the graft copolymers was also not affected by the bulk polymerization conditions and low polydispersity materials with controlled molecular weights were routinely obtained. It should be noted that the preparation of well defined graft copolymers of styrene and poly(caprolactone) by other techniques is not feasible due to the reactivity of the ester linkages in poly(caprolactone) and further demonstrates the versatility of 'living' free radical procedures.

Alternatively, a polymeric initiator containing numerous initiating sites along the backbone can be prepared and then arms grown from the backbone to give the desired graft copolymer. The versatility of 'living' free radical procedures is further exemplified in this instance since the two possible approaches to polymeric initiators can be realized using alkoxyamine derivatives. In the first example, a monomer unit, **4**, containing a single alkoxyamine group is polymerized under normal free radical conditions to give the desired linear polymeric initiator, **5** (Scheme 2).²⁰ This result is noteworthy since it demonstrates the stability of the initiating alkoxyamine group to standard free radical conditions and may indicate that the initiating center is stable to a variety of other polymerization conditions. If this is the case, new graft copolymers containing vinyl grafts and backbones formed from condensation, metathesis, or ring opening polymerizations may be easily prepared.

Polymeric initiators, such as **5**, can also be prepared by coupling of reactive polymers with a functionalized alkoxyamine. For example, a mixture of styrene and p-chloromethylstyrene can be polymerized using the unimolecular initiator, **1**, to give a well defined linear polymer, **6**, which contains numerous chloromethyl groups along the backbone. Reaction of **6** with the sodium salt of the hydroxy functionalized alkoxyamine, **7**, then gives the polymeric initiator, **5** (Scheme 2).²¹ The advantage of this route is that the molecular weight and polydispersity of the backbone polymer



Scheme 1

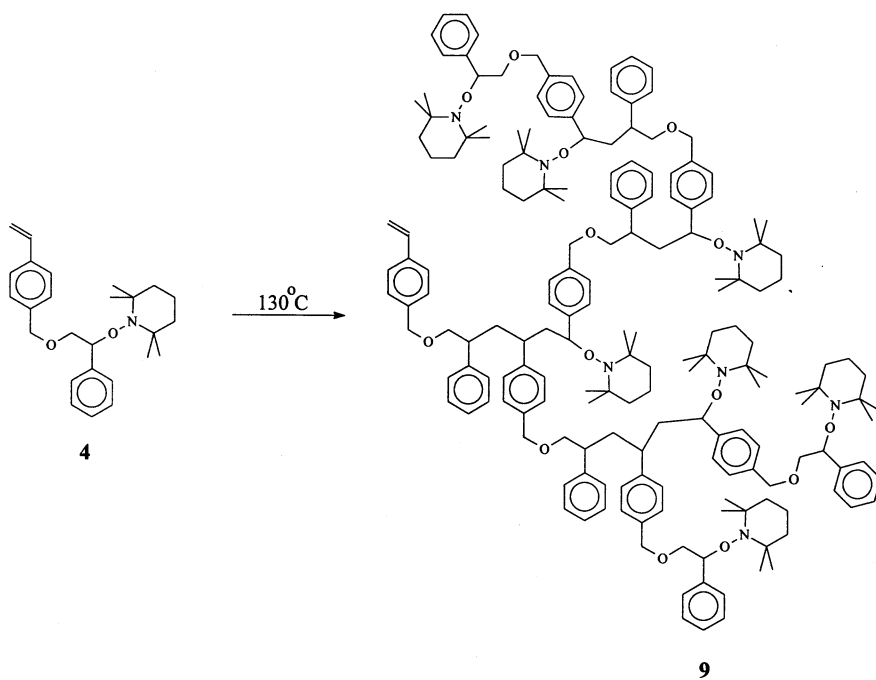


Scheme 2

can be readily controlled by the 'living' free radical procedure and also demonstrates the compatibility of nitroxide chemistry with reactive functional groups. In both cases a range of graft copolymers could be readily grown from the backbone and it was found that the individual grafts grow at approximately the same rate with little or no crosslinking due to radical coupling reactions.

Hyperbranched Macromolecules. The ability to introduce polymerizable groups into the alkoxyamine structure also raises the possibility of preparing hyperbranched macromolecules by nitroxide mediated 'living' free radical procedures. The success of this approach is based on the recent report by Fréchet of a novel self-condensing vinyl polymerization which, under cationic conditions, affords hyperbranched polymers.²² The important feature of this self-condensing strategy is a single monomer unit which contains a polymerizable double bond as well as an initiating center. Application to alkoxyamines then gives self-condensing monomers such as **4** which contain a polymerizable styrene group as well as an initiating/propagating alkoxyamine group. Therefore, polymerization of **4** at 130°C was found to give the hyperbranched macromolecule, **9**, whose structure was confirmed by a combination of nmr and infrared spectroscopy (Scheme 3).²³ Significantly, no insoluble or cross-linked material was observed, which provides further support for the low occurrence of termination by radical-radical coupling in nitroxide mediated systems. Interestingly, when the kinetics of the reaction are investigated it is apparent that the polymerization involves the step-wise coupling of vinyl monomers and oligomers, typical of condensation polymerizations, yet it proceeds by 'living' free radical vinyl chemistry. This can be better appreciated if the evolution of molecular weight is followed with time which clearly shows a gradual build up, and then disappearance, of dimers, trimers, and low molecular weight oligomers (Figure 1). It should be noted that this system is different from the Cu(I) assisted 'living' free radical polymerization of p-chloromethylstyrene as reported by Matyjaszewski.²⁴ In contrast to the above case, where propagation occurs from only secondary benzylic radical intermediates, the polymerization of p-chloromethylstyrene involves both primary and secondary radical intermediates. Since it has been recently shown that propagation from a primary radical is a much less efficient process than from a secondary radical,¹⁷ the structure of both hyperbranched systems should be different. In the alkoxyamine case, the polymerization is a true self-condensing vinyl polymerization leading to a hyperbranched macromolecule with a higher degree of branching than the branched macromolecule obtained from p-chloromethylstyrene.

The versatility of 'living' free radical systems can also be used to extend this concept of vinyl based hyperbranched macromolecules to hyper-star and randomly branched macromolecular architectures. The presence of bound alkoxyamine groups at the numerous chain ends of **9** permits further chain growth to be initiated and star branched polymers with a hyperbranched core to be obtained. Alternatively the self-condensing monomer, **4**, can be copolymerized with normal vinyl monomers to give novel randomly branched macromolecular architectures.²⁰ In this case, **4**, acts as both the initiating group for the formation of linear units as well as branch points for the assembling of these linear units into a randomly branched structure. The



Scheme 3

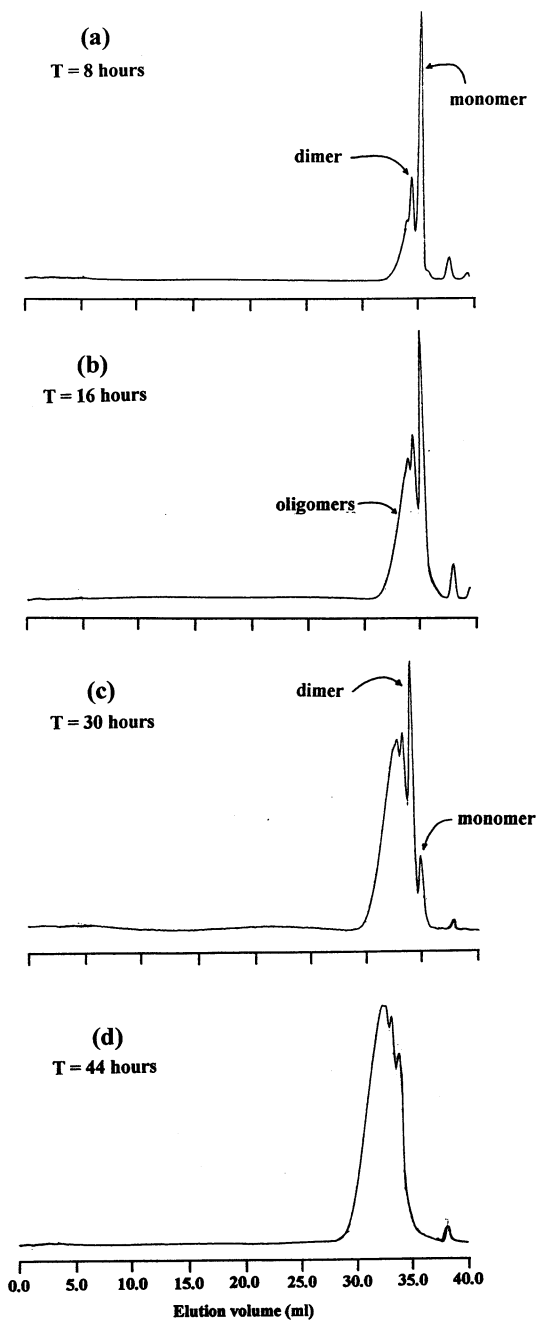


Figure 1. Gpc traces for the homopolymerization of the self-condensing monomer, **4**, at (a) 8 hours; (b) 16 hours; (c) 30 hours; and (d) 44 hours.

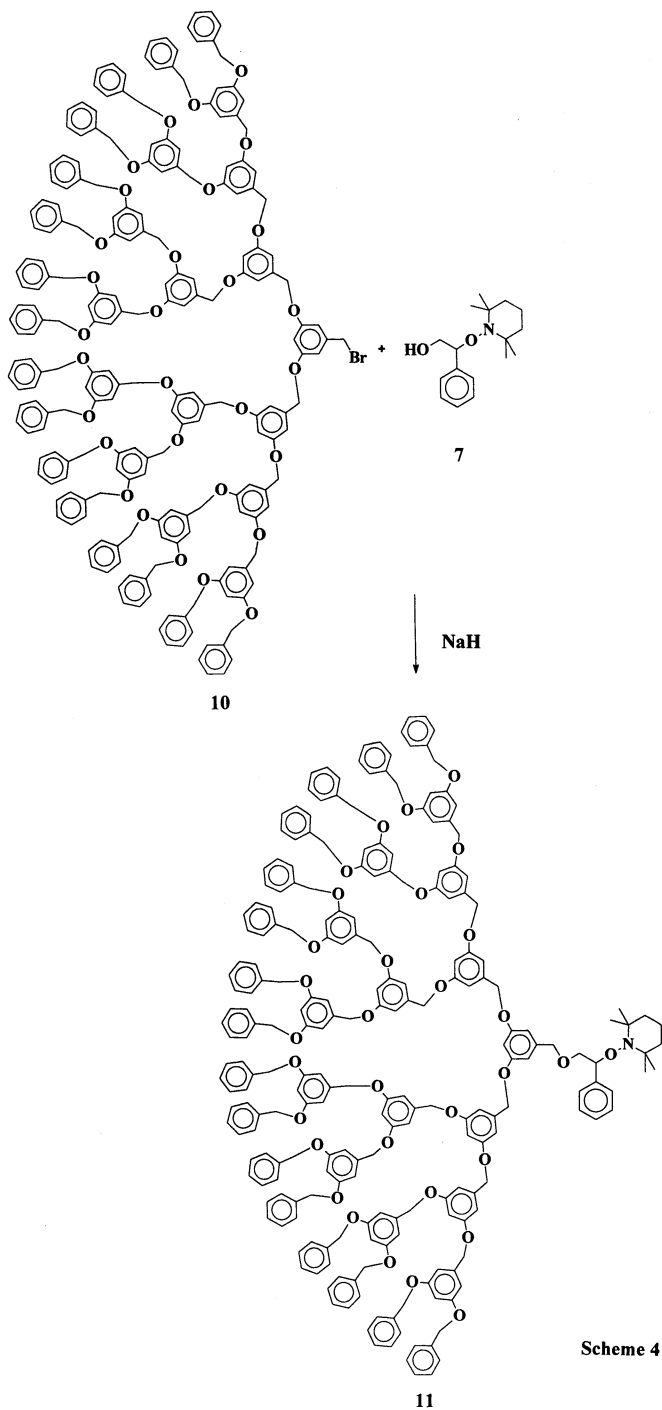
interesting feature of these novel macromolecular architectures is that the linear units have low polydispersities and controlled molecular weights which further reinforces the degree of control available in 'living' free radical polymerizations.

Hybrid Dendritic-Linear Macromolecules. The compatibility of the alkoxyamine functionality with a wide range of reaction conditions also allows their incorporation into a variety of macromolecular architectures at predetermined locations. One example of this modular approach to the preparation of complex structures is the synthesis of hybrid dendritic-linear block copolymers by 'living' free radical procedures.²⁵ In this case, dendritic polyether macromolecules containing a single bromomethyl group at the focal point are prepared by the convergent growth approach. The focal point group is then used as the attachment point for the functionalized alkoxyamine by reaction of **10** with **7** in the presence of sodium hydride. This gives the dendritic initiator, **11**, which has a single alkoxyamine initiating group at its focal point (Scheme 4). A variety of monomers and comonomer mixtures can then be polymerized under standard 'living' free radical conditions using **11** to give a series of novel hybrid dendritic-linear block copolymers, **12**, in which the molecular weight of the linear block could be accurately controlled by the ratio of **11** to monomer. For example, polymerization of a 4:1 mixture of styrene and methyl methacrylate (150 equivalents) with **11** gave the block copolymer, **12**, which was shown to have a M_n of 18 000 and a polydispersity of 1.10. This compares favorably with the theoretical molecular weight of 17 500 (Scheme 5). The structure of **12** was confirmed by ¹H and ¹³C nmr spectroscopy and GPC which showed the total absence of starting dendrimer in the final hybrid block copolymer (Figure 2). It should be noted that the synthesis of hybrid dendritic-linear block copolymers by other techniques is either difficult, or in the case of **12** not possible.

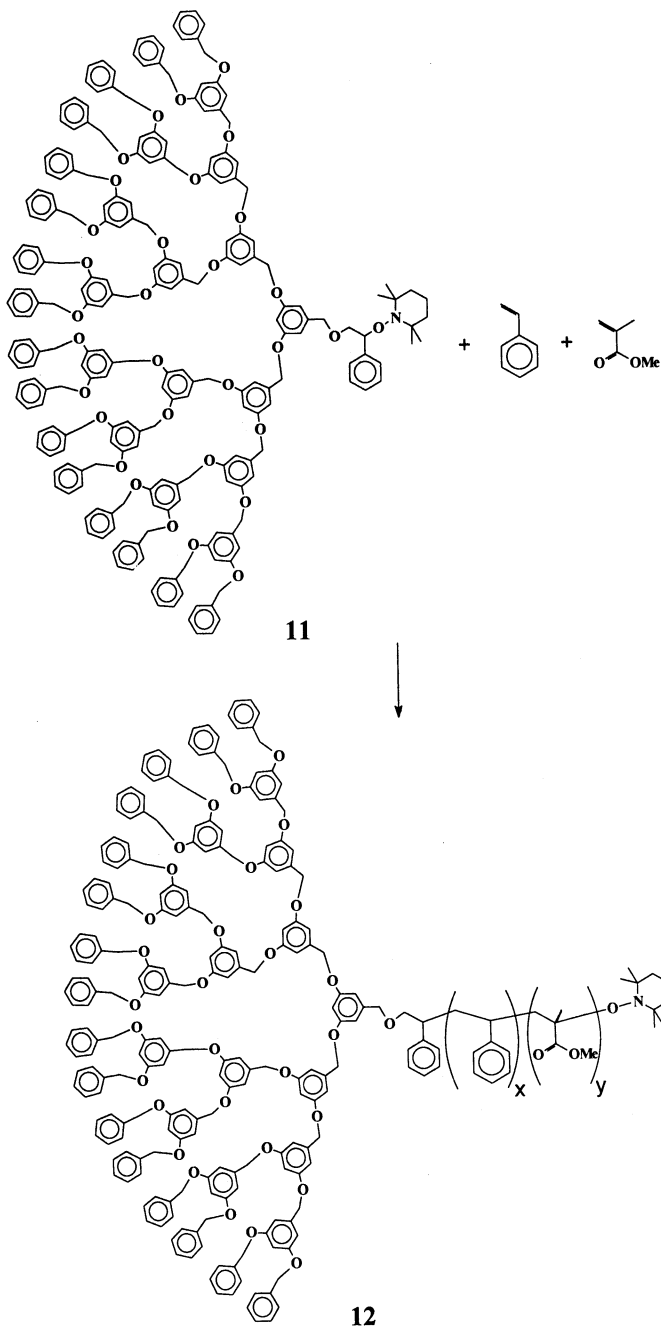
Conclusion

It is apparent from the above discussion that the versatility of 'living' free radical procedures, coupled with their synthetic ease, opens up a number of unique possibilities in polymer synthesis, especially in the preparation of complex macromolecular architectures. Unique polymeric architectures, such as hybrid dendritic-linear block copolymers, which are difficult, if not impossible, to prepare using known techniques can now be prepared readily. Also known macromolecular architectures such as graft copolymers can be prepared with significantly greater synthetic ease while permitting an improvement in structural control. It is envisaged that the increased availability of these complex macromolecular architectures, coupled with the ability to readily incorporate reactive functional groups, will lead to advanced materials for a variety of technological applications ranging from adhesives²⁶ to advanced coatings.²⁷

Acknowledgments. Financial support from the National Science Foundation under Grant No. DMR-9400354 which supports the Center for Polymeric Interfaces and



Scheme 4



Scheme 5

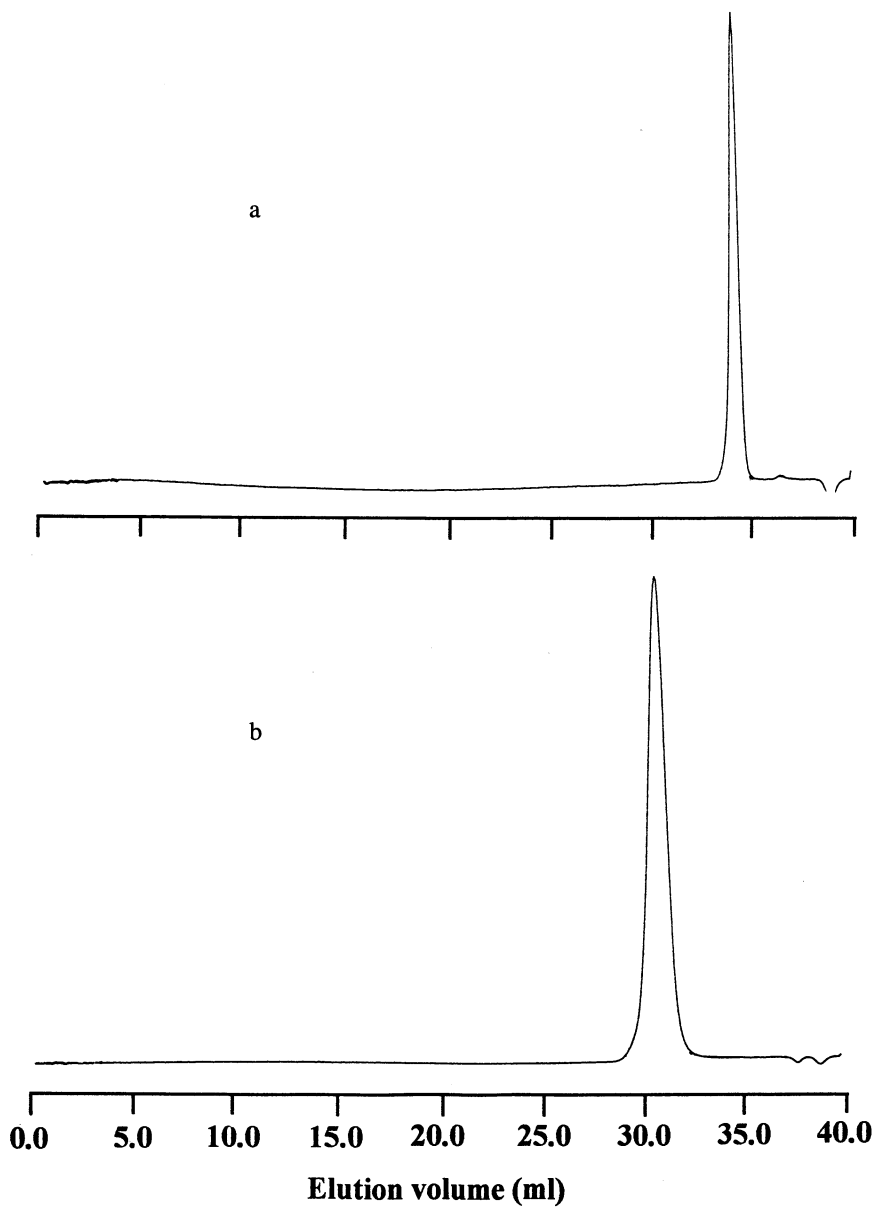


Figure 2. Comparison of the GPC traces for the starting (a) dendritic initiator, **11**, and (b) the final hybrid dendritic-linear block copolymer, **12**.

Macromolecular Assemblies, NSF grant DMR-9641291, and by the IBM Corporation is gratefully acknowledged.

References

- (1) Fréchet, J.M.J. *Science* **1994**, *263*, 1710.
- (2) Hawker, C. J.; Fréchet, J.M.J. *New Methods of Polymer Synthesis, Vol. 2*, J.R. Ebdon and G.C. Eastmond (eds.), Chapman and Hall Publishers, 1995, chap. 8, p. 290.
- (3) Mourey, T.H.; Turner, S.R.; Rubenstein, M.; Fréchet, J.M.J.; Hawker C.J.; Wooley, K.L. *Macromolecules*, **1992**, *25*, 2401.
- (4) Hawker, C.J.; Farrington, P.; Mackay, M.; Fréchet, J.M.J.; Wooley, K.L. *J. Am. Chem. Soc.*, **1995**, *117*, 6123.
- (5) Jansen, J.F.; de Brabander van den Berg, E.M.; Meijer, E.W. *Science*, **1994**, *266*, 1226.
- (6) Rempp, P.; Lutz, P.J., *Comprehensive Polymer Science*, vol. 6, Pergamon press, Oxford, **1989**, p. 403.
- (7) Webster, O. W. *Science* **1994**, *251*, 887.
- (8) Otsu, T.; Matsunaga, T.; Kuriyama, A.; Yoshida, M. *Eur. Polym. J.* **1989**, *25*, 643.
- (9) Turner, S. R.; Blevins, R. W. *Macromolecules* **1990**, *23*, 1856.
- (10) Moad, G.; Rizzardo, E.; Solomon, D. H. *Macromolecules* **1982**, *15*, 909; Solomon, D.H.; Rizzardo, E.; Cacioli, P., U.S. Patent 4,581,429, March 27, 1985.
- (11) Georges, M. K.; Veregin, R. P. N.; Kazmaier, P. M.; Hamer, G. K. *Macromolecules* **1993**, *26*, 2987.
- (12) Hawker, C.J. *J. Am. Chem. Soc.* **1994**, *116*, 11314; Hammouch, S. O.; Catala, J.M. *Macromol. Rapid Commun.* **1996**, *17*, 149; Li, I.Q.; Howell, B.A.; Koster, R.A.; Priddy, D.B. *Macromolecules* **1996**, *29*, 8554.
- (13) Frank, B.; Gast, A.P.; Russell, T.P.; Brown, H.R.; Hawker, C.J. *Macromolecules* **1996**, *29*, 6531; Hawker, C.J.; Hedrick, J.L. *Macromolecules*, **1995**, *28*, 2993.
- (14) Yoshida, E.; Ishizone, T.; Hirao, A.; Nakahama, S.; Takata, T.; Endo, T. *Macromolecules* **1994**, *27*, 3119.
- (15) Kato, M.; Kamigaito, M.; Sawamoto, M.; Higashimura, T. *Macromolecules* **1995**, *28*, 1721; Wang, J. S.; Matyjaszewski, K. *Macromolecules* **1995**, *28*, 7901; Wang, J. S.; Matyjaszewski, K. *J. Am. Chem. Soc.* **1995**, *117*, 5614.
- (16) Percec, V.; Barboiu, B. *Macromolecules* **1995**, *28*, 7970; Granel, C.; DuBois, P.; Jerome, R.; Teyssie, P. *Macromolecules* **1996**, *29*, 8576.
- (17) Hawker, C.J.; Barclay, G.G.; Orellana, A.; Dao, J.; Devonport, W. *Macromolecules* **1996**, *29*, 5245; Connolly, T.J.; Baldovi, M.V.; Mohtat, N.; Scaiano, J.C. *Tet. Letts.*, **1996**, *37*, 4919.
- (18) Li, I.; Howell, B.A.; Ellaboudy, A.; Kastl, P.E.; Priddy, D.B. *Polym. Prepr.*, **1995**, *36(1)*, 469; Li, I.; Howell, B.A.; Matyjaszewski, K.; Shigemoto, T.; Smith, P.B.; Priddy, D.B. *Macromolecules*, **1995**, *28*, 1841; Howell, B. A.; Priddy, D.B.; Li, I.Q.; Smith P.B.; Kastl, P.E. *Polym. Bull.*, **1996**, *37*, 451.

- (19) Hawker, C.J.; Mecerreyes, D.; Elce, E.; Dao, J.; Hedrick, J.L.; Barakat, I.; Dubois, P.; Jerome, R.; Volksen, W. *Macromol. Chem. Phys.*, **1997**, *198*, 155.
- (20) Hawker, C.J. *Angew Chem. Int. Ed. Engl.*, **1995**, *34*, 1456.
- (21) Grubbs, R.B.; Hawker, C.J.; Dao J.; Fréchet, J.M.J. *Angew. Chem. Int. Ed. Eng.* **1997**, *36*, 270.
- (22) Fréchet, J.M.J.; Henmi, M.; Gitsov, I.; Aoshima, S.; Leduc, M.; Grubbs, R.B. *Science* **1995**, *269*, 1080.
- (23) Hawker, C.J.; Fréchet, J.M.J.; Grubbs, R.B.; Dao J. *J. Am. Chem. Soc.* **1995**, *117*, 10763.
- (24) Gaynor, S.; Edelman, S.; Matyjaszewski, K. *Macromolecules*, **1995**, *28*, 6381.
- (25) Leduc, M.R.; Hawker, C.J.; Dao, J.; Fréchet, J.M.J. *J. Am. Chem. Soc.* **1996**, *118*, 11111.
- (26) Kulasekere, R.; Kaiser, H.; Ankner, J. F.; Russell, T. P.; Brown, H. R.; Hawker, C. J.; Mayes, A. M. *Macromolecules* **1996**, *29*, 5493; Kulasekere, R.; Kaiser, H.; Ankner, J. F.; Russell, T. P.; Brown, H. R.; Hawker, C. J.; Mayes, A. M. *Physica B* **1996**, *221*, 306.
- (27) Mansky, P.; Liu, Y.; Huang, E.; Russell, T. P.; Hawker, C. J. *Science* **1997**, *275*, 1458.

Stereochemical Control of Free-Radical Polymerization of Vinyl Monomers

Tamaki Nakano and Yoshio Okamoto

Department of Applied Chemistry, Graduate School of Engineering,
Nagoya University, Chikusa-ku, Nagoya 464-01, Japan

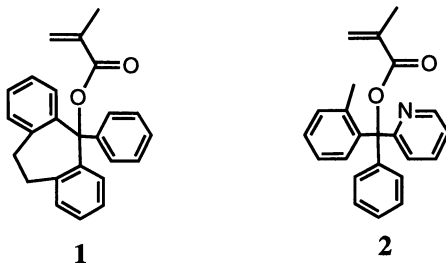
This chapter describes stereoregulation methods for free-radical polymerization based on (I) rationally designed monomers, (II) chiral initiators and chain-transfer agents, (III) reaction conditions (monomer concentration, temperature, solvent), and (IV) template molecules. Method I includes polymerization of bulky methacrylates giving highly isotactic polymers. Method II involves menthol-based peroxides and thiols that can control helicity in 1-phenyldibenzosuberyl methacrylate polymerization. Method III was effective for triphenylmethyl methacrylate polymerization where isotacticity content of resulting polymer was controllable in the range >99-64%. Method IV was realized for methacrylic acid polymerization in the presence of amine compounds.

Stereoregulation by free-radical polymerization has been achieved only in limited cases. On the other hand, stereochemical control of polymerization is an important topic in macromolecular chemistry because polymer properties are often significantly influenced by main-chain configuration and conformation, and various effective methods and catalysts for stereoregulation have been found for anionic, coordination, and related polymerizations (1,2). However, because free-radical polymerization is applicable to much wider range of monomers and generally less expensive compared with the other polymerizations (3), it will be a powerful and practical tool for producing various types of polymers having ordered structures once effective methods for stereocontrol are developed. This article describes our recent studies on configurational and conformational control of free-radical polymerization.

Control Based on Monomer Design

Monomer structure can affect propagation stereochemistry not only in free-radical but also in the other polymerizations. Although free-radical polymerization of vinyl monomers such as acrylic monomers, vinyl esters, and styrene generally results in atactic polymers or polymers that are moderately rich in syndiotacticity (4,5), use of rationally designed monomers can lead to more ordered structures including highly isotactic main-chain and also can induce configurational or conformational chirality in the main chain.

Bulky or Chiral Monomers. Several bulky, triarylmethyl methacrylates have been known to give isotactic polymers by free-radical polymerization as well as by asymmetric anionic polymerization (4-6). The isotactic specificity in the polymerization of the monomers is related to helix formation of growing radical chain and the degree of stereospecificity is dependent on the structure of ester group. Above all, 1-phenyldibenzosuberyl methacrylate (**1**) leads to an almost perfectly isotactic polymer by radical mechanism (7,8). The growing radical derived from **1** may have more complete, rigid helical structure compared with those derived from other monomers such as triphenylmethyl ester and its analogues that result in lower isotactic specificity. The higher rigidity of poly-**1**'s helix may be based on the rigidity of the ester group. Because the two phenyl groups of **1** are tied to each other with an ethylene group, the side group of **1** should have less freedom of internal rotation of bondings compared with triphenylmethyl group.



In the polymerization of chiral **2**, use of optically active monomer can lead to a helical polymer with excess right- or left-handed helicity although the isotacticity of poly-**2** is lower (~75%) compared with the poly-**1** obtained under similar conditions (9). **Table I** summarizes the conditions and results of polymerization of **2** having various enantiomeric excesses (e.e.'s). The e.e. values of the monomer had little effect on the tacticity of the obtained polymers, suggesting that the helix formation is mainly governed by the bulkiness of monomer but little by chirality of the monomer in this case. The obtained polymers showed optical activity which was opposite in sign to that of the starting monomer. This strongly suggests that the optical activity of the polymers is mainly based on excess helicity of the main chain. The optically pure (+)-**2** gave a polymer with large levorotation (run 7), but by anionic polymerization, the same monomer gave a highly isotactic polymer whose optical activity was about twice as large as that of the radically obtained polymer (10). The smaller optical activity of the radically obtained polymer seems to be based on the lower isotacticity which can mean that the polymer has shorter single-handed helical sequences compared with the anionically obtained polymer.

Table I. Radical Polymerization of **2** with (*i*-PrOCOO)₂ at 40°C in Toluene^a

Run	E.e. (%) of monomer in feed	Polymer ^b			E.e. (%) of remaining monomer ^e
		Yield (%)	$[\alpha]_{365}^{25}$ ^c (deg)	Tacticity (%) ^d mm / mr / rr	
1	0	90.4	0	74 / 19 / 7	0
2	-6.9	98.6	+76	73 / 19 / 8	-3.4
3	-15.9	88.4	+246	72 / 19 / 9	-9.0
4	-26.1	84.9	+313	72 / 21 / 7	-20.6
5	-53.4	95.5	+520	75 / 19 / 7	-50.3
6	-80.0	90.8	+608	75 / 19 / 7	-74.6
7	+100	93.7	-617	74 / 16 / 10	+100
8 ^f	+100		-1280	98 / 1 / 1	+100

^aConditions: $[2]/[(i\text{-PrOCOO})_2] = 13$, time 24 h. ^bHexane-insoluble part. Degree of polymerization and Mw/Mn of the polymer were in the range 32-35 and 1.52-1.77, respectively. ^cIn CHCl₃-2,2,2-trifluoroethanol (9/1). ^dDetermined by GPC of PMMA derived from poly-**2**. ^eDetermined by chiral HPLC analysis. ^fAnionic polymerization with *n*-BuLi in tetrahydrofuran at -78°C.

SOURCE: Adapted from ref. 9.

Figure 1 shows the relation between the e.e. of monomeric unit in the polymer and the optical activity (absolute value) of the polymer based on the data in **Table I**. The e.e. of monomeric unit was calculated from the polymer yield, the e.e. of the starting monomer, and the e.e. of the recovered monomer. The optical rotation of the polymer was in all cases larger than that expected based on the e.e. of monomeric unit which is indicated as a line connecting the optical activity values at 0% and 100% e.e.'s of monomeric unit. This observation can reasonably rule out the possibility that the optical activity of the polymer arises simply from the chiral side group of monomeric units. In addition, it can be concluded that an excess helical sense induced by the effect of successive, several (-)-monomeric units based on the major antipode of the starting monomer, can overcome the opposite chiral induction based on the incorporation of (+)-monomeric unit based on the minor antipode of the monomer. In the polymerization of **2** having different e.e.'s, low enantiomer selection was observed. The e.e. of the unreacted monomer was always lower than that of the starting monomer, meaning that the excess antipode was selectively incorporated into the polymer chain.

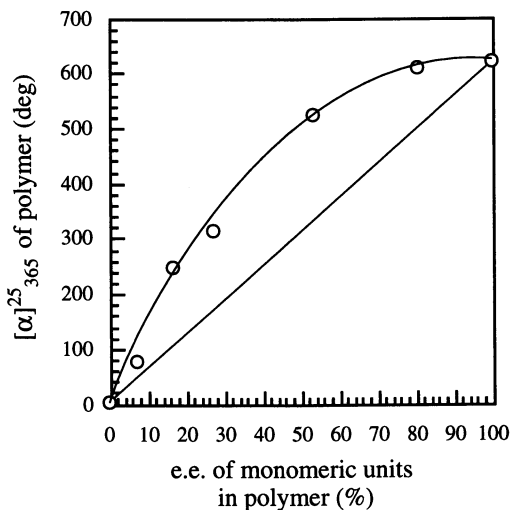
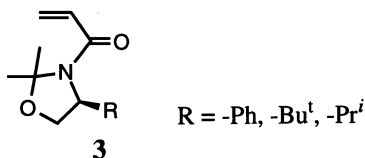


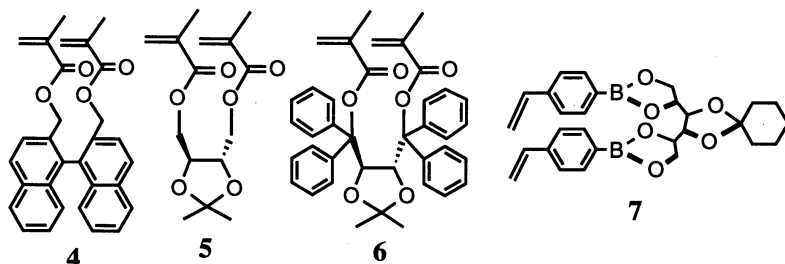
Figure 1. Relation between the absolute values of optical activity of the poly-2s and the e.e. of monomeric units in the polymers. (Reproduced from ref. 9. Copyright 1995 American Chemical Society).

Optically active acrylamides **3** also afford isotactic polymers (mm ~92%) (*11*). It has been shown that in the oligomerization of **3**, growing radical adds to the vinyl group of monomer selectively from one enantioface by the steric influence of the chiral side group.



Cyclopolymerization of Bifunctional Monomers. Design of bifunctional monomers that cyclopolymerize is another approach to stereoregulation. Cyclopolymerization of **4** and **5** gives polymers rich in heterotacticity (poly-**4**, mm/mr/rr = 14/51/33; poly-**5**, mm/mr/rr = 12/49/39) (*12,13*). In the cyclopolymerization of **6**, an isotactic polymer (mm 84%) is produced; probably a cyclization effect and helix formation of growing radical are both responsible for the result (*14,15*). The optically active monomer **7** having two styrene moieties gives polystyrene by copolymerization with styrene followed by removal of the chiral side group (*16*). In this polymerization, configurational chirality is induced to the main-chain asymmetric centers through cyclization of **7** that forms (*S,S*)-dyad units in a largely atactic polystyrene chain and the resulting polystyrene shows optical activity ($[\alpha]_{365}^{30}$ -0.5 to -3.5°).

PMMA derived from the heterotactic-rich poly-5 also shows optical activity ($[\alpha]_{405}^{20} -4.3^\circ$) and CD absorptions based on configurational chirality of main chain.



Control by Chiral Initiator and Chain-Transfer Agent

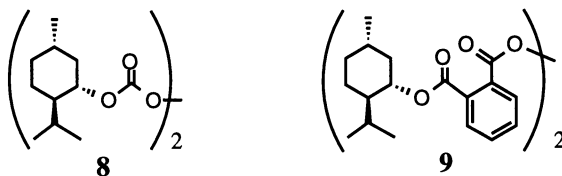
As described in the preceding section, **1** gives almost perfectly isotactic polymer (**7,8**). The poly-**1** prepared under achiral reaction conditions is considered to be an equimolar amount mixture of right- and left-handed helices. This assumption was supported by chiral HPLC analysis of the polymer in which the polymer was resolved into (+)- and (-)-fractions probably corresponding to single handed helical isomers. We carried out the polymerization of **1** under chiral reaction conditions in order to examine the possibility of production of single-handed helical poly-**1** via free-radical mechanism (*17*).

Polymerization of 1 with Chiral Initiator. The possibility of chiral induction through initiation and the following stages of propagation was tested using chiral initiators **8** and **9** that were synthesized from optically active menthol. **Table II** shows the conditions and results of polymerization. The polymerization products were mostly insoluble in common solvents but contained a THF-soluble, benzene-hexane (1:1) (B/H)-insoluble fraction. This fraction, which has a degree of polymerization of ca. 40-45 and is free from oligomeric products, was separated from the original products and used for chiroptical property analysis. The polymer obtained using **8** at $[1]/[8] = 1$ showed dextrorotation though the one obtained at $[1]/[8] = 50$ did not show significant optical activity (runs 1 and 2). The optically active polymer exhibited CD absorptions whose spectral pattern was similar to that of one-handed helical poly-**1** obtained by asymmetric anionic polymerization (*18*), indicating that the optical activity is based on excess right- or left-handed helicity. The production of the optically active polymer only at the higher $[1]/[8]$ ratio suggests that the helix-sense selection took place more effectively through primary radical termination rather than through initiation reaction. Because a polymer chain obtained from **1** is considered to have a complete helical structure probably without helix reversals or some defects, helix-sense selection through initiation reaction would give an optically active polymer regardless of the concentration of **8**. The conclusion was supported by GPC analysis of the polymer with polarimetric and UV detections. The GPC analysis of the polymer of run 2 indicated that the polymer consists of (+)-fraction with higher molecular weight and (-)-fraction with lower molecular weight. This can be explained in terms of unequal rates of primary radical termination for (+)- and (-)-helical growing radicals having opposite sense of helix.

Table II. Helix-Sense-Selective Free-Radical Polymerization of **1** with **8** and **9** as Initiator in Toluene

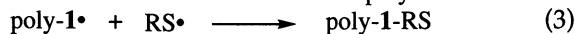
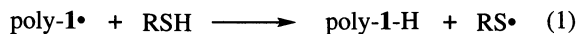
Run	Initiator	[1]/[8 or 9]	Temp. (°C)	Yield ^a (%)	THF-insol. part		THF-sol., B/H-insol. part	
					Yield (%)	Yield (%)	[α] ₃₆₅ ^b (deg)	DP ^c
1	8	50	40	75	69	1	~0	40
2	8	1	50	48	30	3	+40	44
3	9	1	50	59	41	12	+20	40

^aHexane-insoluble products. ^bMeasured in THF. ^cDetermined by GPC analysis of PMMA derived from poly-**1**.
SOURCE: Adapted from ref. 18.



The polymerization with **9** also gave optically active polymer (run 3) but the polymer showed a CD spectrum that is more similar to that of **9** itself rather than to that of helical poly-**1** obtained by anionic polymerization. The chiroptical properties of poly-**1** of run 3 may be principally ascribed to the chiral group attached to the chain terminals originating from the initiator.

Polymerization of 1 with Chiral Chain-Transfer Agent. Chiral thiols as chain-transfer agents can induce single-handed helix through the three possible mechanisms as shown as eqs. (1)-(3) where a dot (•) denotes a radical electron:



Reaction (1) is hydrogen transfer from a thiol to a helical growing radical, (2) initiation or polymerization by the thio radical formed through (2), and (3) coupling termination of a helical growing radical with the thio radical formed through (2).

The polymerization of **1** was carried out with (*i*-PrOCOO)₂ in the presence of (+)- and (-)-neomenthanethiol (**10**) and (-)-menthanethiol (**11**). The conditions and results are shown in **Table III**. Under all conditions, optically active polymers were obtained and optical activity of the polymers was larger than that of the polymers obtained using chiral initiators. The use of (+)- and (-)-**10** resulted in the polymers with opposite optical activity. Also, a higher concentration of **10** results in a lower overall yield of products and higher optical activity of the polymer. The polymers showed a similar CD spectral pattern to that of anionically obtained single-handed helical poly-

1, indicating the optical activity of the polymers obtained in the presence of the chiral thiols is based on excess single-handed helicity.

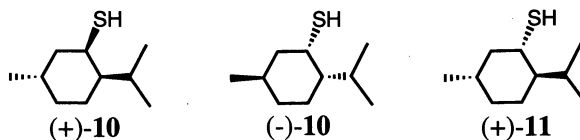
From GPC analysis of the polymer of run 3, it was found that the polymer consisted of (-)-fraction with higher molecular weight and (+)-fraction of lower molecular weight. The (+)- and (-)-fractions collected by GPC fractionation experiments exhibited CD spectral patterns which are symmetrical to each other. This strongly suggests that the opposite sign of optical rotation means opposite excess helicity in the fractions. These results indicated that chiral induction occurred through the reactions of eqs. (1) and/or (3) (termination reactions). However, detailed ¹H NMR studies of PMMA derived from the poly-**1** of run 3 showed that the polymer bears a hydrogen atom and no neomenthyl group at the ω-end of the main chain. This observation excludes the possibility of chiral induction through eq. (3). Therefore, it can be concluded that difference in the hydrogen transfer rate in eq. (1) for (+)- and (-)-growing radicals is responsible for the helix-selection.

The GPC fractionation of poly-**1** of run 3 gave a (-)-fraction whose optical activity was estimated to be ca. $[\alpha]_{365} -750^\circ$. This value corresponds to an enantiomeric excess of ca. 40% that means a mixture of (-)- and (+)-helices in a ratio of 7 to 3.

Table III. Helix-Sense-Selective Free-Radical Polymerization of **1** with (*i*-PrOCOO)₂ at 40°C in the Presence of **10** and **11** as Chain-Transfer Agent in Toluene

Run	Chain-Transfer Agent	[1]/[10 or 11]	Yield ^a	THF-insol. part ^b	THF-sol., B/H-insol. part		
				Yield (%)	Yield (%)	$[\alpha]_{365}^c$ (deg)	DP ^d
1	(+)- 10	0.05	82	73	2	-80	42
2	(+)- 10	0.1	80	70	3	-130	41
3	(+)- 10	0.2	71	54	5	-140	42
4	(+)- 10	0.4	18	~0	11	-140	40
5	(-)- 10	0.4	19	~0	10	+110	51
6	(+)- 11	0.05	86	82	2	+60	50

^aHexane-insoluble products. ^bDegree of polymerization was in the range 84-150 as determined by GPC analysis of PMMA derived from poly-**1**. ^cMeasured in THF. ^dDetermined by GPC analysis of PMMA derived from poly-**1**. SOURCE: Adapted from ref. 17.

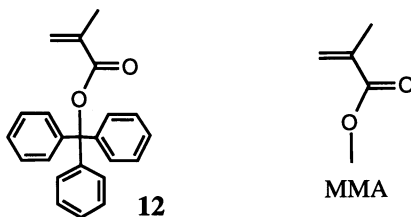


Polymerization of **1** in the presence of optically active menthol or neomenthol also gave optically active, helical polymers. The alcohols appeared to function as chain transfer agents similarly to the chiral thiols.

Control by Adjusting Reaction Conditions (Monomer Concentration, Temperature, and Solvent)

Free-radical stereochemistry is generally recognized to be almost independent on the reaction conditions such as substrate concentration, temperature, and solvent. However, we have found that the reaction conditions remarkably affect the stereochemistry of polymerization of triphenylmethyl methacrylate (**12**) and tacticity of the polymer can be controlled in a wide range by simply adjusting the three factors in reaction conditions (8).

Controlled Stereochemistry of Polymerization of 12. The conditions and results of polymerization of **12** are shown in Table IV along with those of **1** and MMA. In the polymerization of **12**, higher polymerization temperatures and lower $[M]_0$ gave higher isotacticity (runs 1-6). Tetrahydrofuran (THF) and chloroform as solvent were found to lead to higher isotacticity of the products than toluene. Polymerization in THF under the same conditions as those for run 3 gave a polymer with a triad tacticity of mm / mr / rr = 99.1 / 0.9 / ~0. The isotacticity of poly-**12** obtained by free-radical polymerization was previously reported to be 64% (19) but thus we have achieved nearly perfect isotacticity that is comparable to that of poly-**12** obtained by asymmetric anionic polymerization (20,21). In contrast, the effect of reaction conditions on the propagation stereochemistry was not seen for **1** and MMA polymerizations giving an almost perfectly isotactic polymer (runs 7-10) and a polymer rich in syndiotacticity (runs 11-13), respectively.



A proposed mechanism for the stereocontrol is based on postulated existence of at least two types of propagating radicals with different monomer addition stereochemistries that are interchangeable and of different thermodynamic stability. The propagating radical in TrMA polymerization has been assumed to take helical conformation (6,19). However, the helical conformation may have some flexibility in the chain terminals and the proposed two propagating radicals may have conformational differences in the vicinity of the active end of the chain. The stereochemical characteristics described above can be interpreted using these models as shown in Figure 2. On monomer addition, the thermodynamically less stable radical (conformation) having lower meso monomer addition probability is formed and this can stereomutate to the other radical having a higher meso monomer addition probability at a rate comparable to monomer addition. The stereomutation of growing radical can be faster than propagation at a lower $[M]_0$ and a higher reaction temperature can facilitate the stereomutation. Solvent may also affect the conformation of growing radical and its mutation.

Table IV. Free Radical Polymerization of Methacrylates in Toluene under Various Reaction Conditions^a

Run	Monomer	[M] ₀ (M)	Temp (°C)	Tacticity ^b
				mm / mr / rr
1	12	0.95	60	63.6 / 24.1 / 12.3
2	12	0.34	60	82.6 / 13.1 / 4.3
3	12	0.18	60	93.4 / 5.2 / 1.4
4	12	0.12	60	98.2 / 1.7 / 0.1
5	12	0.18	40	81.7 / 13.4 / 4.9
6	12	0.18	30	69.9 / 20.2 / 9.9
7	1	0.17	60	99.9 / 0.1 / ~0
8	1	0.17	40	99.8 / 0.2 / ~0
9	1	0.17	30	99.7 / 0.3 / ~0
10	1	0.40	60	99.5 / 0.3 / 0.2
11	MMA	6.3	40	2.5 / 30.8 / 66.7
12	MMA	0.82	40	2.5 / 31.3 / 66.2
13	MMA	0.23	40	2.6 / 31.0 / 66.4

^aInitiator: AIBN for the polymerizations at 60°C, (*i*-PrOCOO)₂ for the polymerizations at 30°C and 40°C. [Monomer]/[Initiator] = 50 or 25. ^bDetermined by ¹H NMR as PMMA.
SOURCE: Adapted from ref. 8.

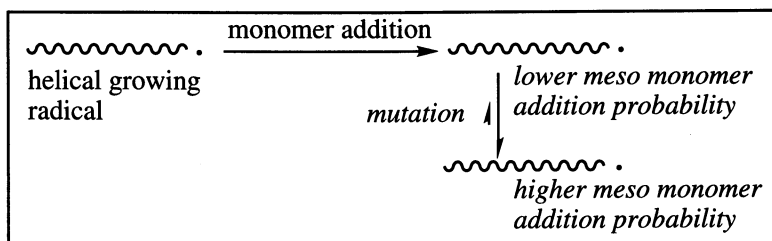


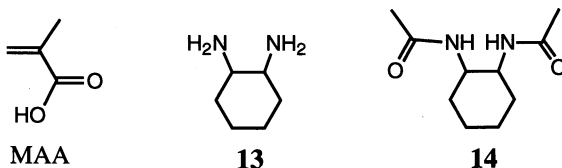
Figure 2. A proposed mechanism for the stereochemical characteristics in the polymerization of **12**.

The growing radical derived from **1** also takes helical conformation but the helix may be too rigid to allow the two types of propagating species assumed for the polymerization of **12**. The growing species in the MMA polymerization may have only the thermodynamically stable conformation because the conformational dynamics of MMA growing radical is reasonably assumed to be much faster than that of the growing radical of **12** under the reaction conditions shown in **Table IV**.

Control Based on Template Molecule

As described in the first section of this chapter, proper design of monomer can lead to controlled stereostructure of polymer by free-radical polymerization. In such type of polymerization, the side group of monomer can be considered as "template" that controls reaction stereochemistry of the vinyl moiety through steric repulsion. However, this technique has an inherent limitation that synthesizing polymers with various tacticities requires polymer reactions involving cleavage of the covalent bonding between the template moiety and polymer main chain as in the conversion from poly-1 to poly(methacrylic acid) by hydrolysis. In order to improve this method, we have searched for reaction systems involving a relatively weak interaction between monomer and template.

Methacrylic Acid Polymerization in the Presence of Amines. We found that stereochemistry of methacrylic acid (MAA) polymerization can be regulated in the presence of various amine compounds including racemic and optically active 1,2-diaminocyclohexane (**13**) (22). Table V summarizes the conditions and results of polymerization of MAA using α, α' -azobisisobutyronitrile (AIBN).



Degree of polymerization (DP), molecular weight distribution (Mw/Mn), and tacticity of the products were determined by the analysis of PMMA derived from the obtained poly(MAA). A simple procedure consisting of removal of polymerization solvent, addition of small amount of HCl-MeOH, methylation of diazomethane in benzene, and removal of benzene insoluble part (HCl salt of amine) readily gave the PMMA (benzene solution) from the polymerization mixture. The polymerizations in MeOH and CHCl₃ without using amines exhibited different stereochemical features which are consistent with the previous report (23). The presence of amines resulted in increased iso- and heterotacticity (mm and mr) at the expense of syndiotacticity (rr) in both MeOH and CHCl₃. The effect was more obvious for the polymerization in CHCl₃ than in MeOH, suggesting that polar interaction between the amines and MAA has a role in the stereoregulation. Also, higher Mn's and broader Mw/Mn's were observed in the presence of amines especially for the polymerization in CHCl₃. Among the amines examined in this study, **13** had the most significant stereoeffect although the effect of chirality of **13** ((±)-trans-, (R,R)-trans-, or cis-) was not clearly observed. The interaction between MAA and the added amine in CHCl₃ was suggested to be based on both H-bonding between **13** and MAA and ionic interaction between ammonium cation of **13** and MAA anion by IR analysis. The stoichiometry of the interaction in CDCl₃ was found to be [MAA]/[**13**] = ca. 3/2 by ¹H NMR analysis. In contrast to **13**, N-acetylated **13** (**14**) did not show clear effects on polymerization stereochemistry. Therefore, ionic interaction may be more important than H-bonding in inducing stereochemistry of the main chain although the acylation experiment cannot completely rule out H-bonding effects.

Table V. MAA Polymerization Using AIBN in the Presence and the Absence of Amine Compounds at 60°C^a

Run	Solvent	Amine	Tacticity ^b
			mm / mr / rr
1	MeOH	(<i>R,R</i>)- 13	4.0 / 34.6 / 61.4
2	MeOH	none	3.9 / 29.1 / 67.0
3	CHCl ₃	(<i>R,R</i>)- 13	16.3 / 48.8 / 34.9
4	CHCl ₃	CH ₃ (CH ₂) ₄ NH ₂	12.9 / 46.2 / 40.9
5	CHCl ₃	cyclohexyl-NH ₂	12.3 / 47.0 / 40.7
6	CHCl ₃	none	8.1 / 41.0 / 50.9

^a[MAA]₀ = 0.1 M, [-NH₂]₀ = 0.1 M, [AIBN]₀ = 0.004 M.

^bDetermined by ¹H NMR as PMMA.

Previously, several methods of stereoregulation for MAA polymerization were studied. Syndiotactic specificity of MAA polymerization in 2-propanol was reported to be enhanced up to rr = 95% by lowering reaction temperature to -78°C (24). Concerning increasing isotactic specificity, polymerization of MAA complexes affording optically active poly(MAA) is known though this method requires fairly complicated procedures of polymer synthesis and isolation (25,26). Thus, the use of amines provides a simpler way of enhancing isospecificity of MAA polymerization. Also, although stereochemistry of MAA polymerization can be affected by changing polymerization solvent (23), the method using amines is advantageous in that it is effective even at much lower concentration of amine (0.05M) compared with solvent concentration.

Literature Cited

- 1) *Macromolecular Design of Polymeric Materials*; Hatada, K.; Kitayama, T.; Vogl, O., Eds.; Plastic Engineering 40; Marcel Dekker: New York, NY, 1997.
- 2) *Catalysis in Precision Polymerization*; Kobayashi, S., Ed.; Wiley: Chichester, Sussex, 1997.
- 3) Moad, G.; Solomon, D. H. *The Chemistry of Free Radical Polymerization*; Elsevier: Oxford, 1995.
- 4) Hatada, K.; Kitayama, T.; Ute, K. *Prog. Polym. Sci.* **1988**, *13*, 189.
- 5) Yuki, H.; Hatada, K. *Adv. Polym. Sci.* **1979**, *31*, 1.
- 6) Okamoto, Y., Nakano, T. *Chem. Rev.* **1994**, *94*, 349.
- 7) Nakano, T.; Mori, M.; Okamoto, Y. *Macromolecules* **1993**, *26*, 867.
- 8) Nakano, T.; Matsuda, A.; Okamoto, Y. *Polym. J.* **1996**, *28*, 556.
- 9) Okamoto, Y.; Nishikawa, M.; Nakano, T.; Hatada, K. *Macromolecules* **1995**, *28*, 5135.
- 10) Okamoto, Y., Yashima, D.; Hatada, K. *J. Polym. Sci., Part C: Polym. Lett.* **1987**, *25*, 297.
- 11) Porter, N. A.; Allen, T. R.; Breyer, R. A. *J. Am. Chem. Soc.* **1992**, *114*, 7676.

- 12) Nakano, T.; Sogah, D. Y. *J. Am. Chem. Soc.* **1995**, *117*, 534.
- 13) Kakuchi, T.; Kawai, T.; Katoh, S.; Haba, O.; Yokota, K. *Macromolecules* **1992**, *25*, 5545.
- 14) Nakano, T.; Okamoto, Y.; Sogah, D. Y.; Zheng, S. *Macromolecules* **1995**, *28*, 8705.
- 15) Wulff, G.; Gladow, S.; Kühneweg, B.; Krieger, S. *Macromol. Symp.* **1996**, *101*, 355.
- 16) Wulff, G.; Dhal, P. K. *Angew. Chem., Int. Ed. Engl.* **1989**, *28*, 196.
- 17) Nakano, T.; Shikisai, Y.; Okamoto, Y. *Polym. J.* **1996**, *28*, 51.
- 18) Nakano, T.; Matsuda, A.; Mori, M.; Okamoto, Y. *Polym. J.* **1996**, *28*, 330.
- 19) Yuki, H.; Hatada, K.; Niinomi, T.; Kikuchi, Y. *Polym. J.* **1970**, *1*, 36.
- 20) Nakano, T.; Okamoto, Y.; Hatada, K. *J. Am. Chem. Soc.* **1992**, *114*, 1318.
- 21) Okamoto, Y.; Suzuki, K.; Ohta, K.; Hatada, K.; Yuki, H. *J. Am. Chem. Soc.* **1979**, *101*, 4763.
- 22) Nakano, T.; Ishigaki, Y.; Okamoto, Y. *Polym. Prepr. Japan* **1996**, *45*(2), 126.
- 23) Krakovayk, M. G.; Anufrieva, E. V.; Sycheva, E. A.; Sheveleva, T. V. *Macromolecules* **1993**, *26*, 7375.
- 24) Lando, J. B.; Semen, J.; Farmer, B. *Macromolecules* **1970**, *3*, 524.
- 25) Kataoka, S.; Ando, T. *Kobunshi Ronbunshu* **1980**, *37*, 185. (*Chem. Abstr.* **1980**, *92*, 198833q).
- 26) Kataoka, S.; Ando, T. *Polym. Commun.* **1984**, *25*, 24.

Author Index

- Anderson, Albert G., 332
Aota, M., 200
Arvanitopoulos, Labros D., 316
Barclay, George G., 433
Basickes, L., 305
Benoit, D., 225
Bergman, Frank A. C., 236
Betts, D. E., 417
Beuermann, Sabine, 84
Boiteau, L., 362
Bon, Stefan A. F., 236
Buback, Michael, 84
Charmot, D., 362
Chaumont, P., 362
Christie, David I., 104
Clay, Paul A., 104
Colombani, D., 362
Coote, Michelle L., 120
Crossman, M. C., 284
Curran, Dennis P., 62
Daimon, K., 170
Daly, W. H., 377
Davis, Thomas P., 120
DeSimone, J. M., 417
Duncalf, D. J., 284
Ercole, Frances, 332
Evenson, T. S., 377
Finet, J. P., 225
Fontanille, M., 225
Fréchet, Jean M. J., 433
Fryd, M., 305
Fukuda, Takeshi, 180
Gaynor, Scott G., 396
Georges, M. K., 170
German, Anton L., 236
Ghosez-Giese, Anne, 50
Giese, Bernd, 50
Gilbert, Robert G., 104
Gnanou, Y., 225
Gossage, Robert A., 72
Goto, Atsushi, 180
Greuel, Michael P., 316
Gridnev, A. A., 305
Grimaldi, S., 225
Grove, David M., 72
Grubbs, R. Bernard, 433
Haddleton, D. M., 284
Harwood, H. James, 316
Hawker, Craig J., 433
Heming, A. M., 284
Heuts, Johan P. A., 120
Howell, B. A., 214
Ittel, S. D., 305
Jastzebski, Johann T. B. H., 77
Johnson, Charles H. J., 332
Johnson, T., 417
Johnston, Lloyd P. M., 120
Kamachi, Mikiharu, 145
Kamigaito, Masami, 296
King, Brian M., 316
Klumperman, Bert, 236
Krstina, Julia, 332
Lamps, J. P., 362
Leduc, Marc R., 433
LeRoux, D., 417
Li, I. Q., 214
Malmström, Eva E., 433
Matyjaszewski, Krzysztof, 2, 258, 396
Miura, Y., 200
Moad, Catherine L., 332
Moad, Graeme, 332
Morsley, S. R., 284
Mukerjee, S., 305
Nair, C. P. R., 362
Nakano, Tamaki, 451
Nobukane, Y., 200

Ohno, Kohji, 180
Okamoto, Yoshio, 451
Poszmik, G., 305
Priddy, D. B., 214
Pross, Addy, 31
Radom, Leo, 31
Rizzardo, Ezio, 332
Sawamoto, Mitsuo, 296
Shim, Anne K., 316
Shooter, A. J., 284
Spurling, Thomas H., 332
Thang, San H., 332

Tordo, P., 225
Tsuji, Yoshinobu, 180
van Es, J. J. G. Steven, 236
van Koten, Gerard, 72
Veregin, R. P. N., 170
Wayland, B. B., 305
Wong, Ming Wah, 31
Woska, D. C., 305
Yamada, B., 200
Zhu, Yucheng, 214
Zink, M.-O., 362

Affiliation Index

Australian National University, 31
Ben Gurion University, 31
Carnegie Mellon University, 2, 258, 396
Central Michigan University, 214
Centre de Recherches Rhône-Poulenc,
362
Commonwealth Scientific and Industrial
Research Organisation, 332
Dow Polystyrene Research &
Development, 214
DuPont Experimental Station, 305, 332
DuPont Marshall Laboratory, 305
Eindhoven University of Technology, 236
IBM Almaden Research Center, 433
Institut Charles Sadron, 362
Institut für Physikalische Chemie der
Georg-August-Universität, 84
Kyoto University, 180, 296
Louisiana State University, 377
Nagoya University, 451
National University of Singapore, 31
Osaka City University, 200
Osaka University, 145
Shipley Company, 433
Sydney University, 104
3M Corporation, 316
Université Bordeaux I, 225
Université Claude Bernard, 362
Université de Provence, 225
University of Akron, 316
University of Basel, 50
University of California—Berkeley, 433
University of New South Wales, 120
University of North Carolina at Chapel
Hill, 417
University of Pennsylvania, 305
University of Pittsburgh, 62
University of Warwick, 284
Utrecht University, 72
Vikram Sarabhai Space Center, 362
The Xerox Research Centre of Canada,
170

Subject Index

- Ab initio* molecular orbital theory
ab initio theory range of levels in Pople diagram, 33*f*
accuracy vs. computational expense, 33
curve-crossing model, 34–36
energy profile schematic from calculations, 32*f*
Hartree–Fock procedures, 34
Moller–Plesset perturbation theory, 34
quadratic configuration interaction (QCI), 34
theoretical approach for radical addition to alkenes, 31–32
- Acrylate monomers
conversion studies by pulsed sequence PLP(PS–PLP) experiments, 99–100
conversion studies by single-pulse PLP experiments, 94–95
end-functionalization with cobaloxime photoinitiator/mediators, 326, 328–330
living radical polymerization by organo-cobalt porphyrins, 308–310
low monomer conversion by PLP–SEC experiments, 90–91
organo-cobalt porphyrin for block copolymers, 310–311
organo-cobalt porphyrin reaction sequences, 311–312
photochemical polymerization with cobaloximes, 318–322
representative rate study for cobalt(II) complex-controlled polymerization, 312–314
triblock copolymers, star and radial-block polymers, 325–327
- Acrylonitrile, peculiarities of ATRP, 268
- Addition-fragmentation reactions
chain transfer constant, 372, 374
chemical reactions in kinetic studies, 367*t*
contribution to controlled/living radical polymerization, 17
cross propagation of the intermediate radical, 365–366
degenerative chain transfer special case, 22
free radical polymerization processes, 364–366
functionality of polymer chains, 374–376
interconversion process, 369–372
kinetic studies, 366–369
mechanism and kinetics, 363–364
moment expression in simulation for alkoxyamine-initiated polymerization, 345–346
polymerization of MMA, 364–365, 367*f*
retardation behavior, 370–371
retardation or degradative chain transfer, 364–365
theoretical functionality of MMA polymerization, 375*f*
two-step processes, 362
- AIBN (2,2'-azobisisobutyronitrile)
initiator for nitroxide-mediated styrene polymerization, 227–230
- Alfrey–Price equation, polymerization by radical addition to alkenes, 59–60
- Alkene substituents, steric effects on radical additions, 55–56
- Alkoxyamine-mediated radical polymerization. *See* Nitroxide-mediated radical polymerization
- Alkyl halides
initiators for ATRP, 268–271

- initiators for transition metal-mediated living radical polymerization, 297, 298*f*
- Allyl stannanes, unimolecular chain transfer reagent, 68–69
- Atom transfer radical addition (ATRA), plausible mechanism from evidence, 258–259
- Atom transfer radical polymerization (ATRP)
 - acrylonitrile peculiarities, 268
 - block copolymer compositions, 400–404
 - block copolymer macroinitiators from living carbocationic polymerization, 400–401
 - block copolymer macroinitiators from living ring-opening metathesis polymerization (ROMP), 401–402
 - block copolymer macroinitiators from polycondensation, 402–404
 - branched and hyperbranched polymer architecture, 406–409
 - contribution to controlled/living radical polymerization, 17–18
 - controlled architectures, compositions, and functionalities, 279–280
 - electronics of ligand substituents controlling catalyst solubility, 285
 - examples of block copolymer formation, 428, 430*f*, 431
 - experimental MMA ATRP with copper(I) complexes and phenolic compounds, 286–287
 - functionalized polymers, 409–414
 - general mechanism schematic, 260*f*
 - graft copolymer architecture, 404–406
 - graft copolymer by graft from method, 405–406
 - graft copolymer by grafting-through method, 404–405
 - homopolymer compositions, 398
 - hydrocarbon-fluorocarbon block copolymers, 419–421, 428*t*
 - hyperbranched polymer with azido groups for crosslinking, 413–414
 - initiation improvement methods, 269–271
 - initiator structure resemblance to dormant macromolecule, 10–11
 - kinetics of catalytic process, 262–264
 - ligands common for copper-based ATRP, 261
 - mechanism adaptation from atom transfer radical addition, 258–260
 - methyl acrylate peculiarities, 267–268
 - methyl methacrylate peculiarities, 266–267
 - monomers in copper-based ATRP system, 261
 - MMA polymerization in presence of phenol, 287–290
 - MMA polymerization in presence of substituted phenols, 291–293
 - polyacrylonitrile in ethylene carbonate, 398
 - polydispersity decreasing with conversion for fast exchange, 263–264
 - polymerization initiator and catalyst concentration dependent, 12–13
 - polymerization of functional monomers, 409–410
 - polymers with functional end groups, 410–413
 - preparation of functional poly(methyl acrylate), 410, 412*t*
 - preparation of functional polystyrene, 410, 411*t*
 - proposed concerted mechanism for propagating PMMA chain, 294
 - proposed mechanism allowing propagation via free radical process, 285–286
 - rate law neglecting termination contribution, 262–263
 - reverse ATRP mechanism, 260

- reversible activation/deactivation of alkyl halides by transition metal complexes, 397
- reversible homolytic cleavage to covalent species, 20–21
- role of 2,2'-bipyridine ligand with copper(I) halides, 285
- role of catalysts, 271–277
- role of initiators, 268–271
- role of monomers, 264–268
- role of phenol in MMA polymerization, 287–291
- role of solvents and additives, 277–278
- role of temperature and reaction time, 278–279
- ruthenium-based complexes, 284–285
- sensitivity to oxygen, 278
- statistical and gradient copolymer compositions, 399–400
- styrene peculiarities, 265–266
- synthesis of poly(methyl methacrylate) and subsequent block copolymer, 423
- Atom transfer radical reactions
- cascade radical annulation reactions, 66–68
- contribution to controlled/living radical polymerization, 13
- moment expression in kinetic simulation for alkoxyamine-initiated polymerization, 344
- moment expression in kinetic simulation for MMA, 344
- ATRP. *See* Atom transfer radical polymerization (ATRP)
- 2,2'-Azobisisobutyronitrile (AIBN)
- initiator for nitroxide-mediated styrene polymerization, 227–230
- Bader analysis, extent of charge transfer, 32, 41
- Barton esters (BE)
- backbone stability, 387–388
- t*-butyl and phenyl BE initiators, 383
- carboxymethyl cellulose graft copolymer procedure, 382–383
- chain transfer agents, 378
- chain transfer mechanism and constants, 378–379
- decomposition by heat or visible light, 377–378
- free radicals in organic syntheses, 378
- graft copolymerization to styrene benzoate derivatives, 389, 391*f*
- grafting to carboxymethyl cellulose backbone, 390, 392–393
- grafting to poly(aryl ether sulfone) backbone, 389–390, 391*f*
- homopolymerization initiation results, 383–387
- influence of BE concentration on rate and molecular weight, 387*f*
- initiation of homopolymerization procedure, 380–381
- initiator for polyacrylonitrile grafts on polyethylene, 379–380
- kinetics of polymerization, 383–386, 387*f*
- mechanism of BE-initiated polymerization, 383, 385
- methacryloyl ester copolymer preparation, 381
- poly(aryl ether sulfone) graft copolymer preparation, 382
- structure of end groups, 384
- unexpected chain cleavage reaction, 387–388
- vinylbenzoate copolymer preparation, 381–382
- Benson-type additivity rules, reaction enthalpies for radical addition to alkenes, 39
- Block copolymers
- amphiphilic copolymers for use in carbon dioxide, 418–419
- ATRP examples, 428, 430*f*
- ATRP macroinitiators from living carbocationic polymerization, 400–401

- ATRP macroinitiators from living ring-opening metathesis polymerization, 401–402
- ATRP macroinitiators from polycondensation, 402–404
- crossover from living anionic to iniferter synthesis, 426, 429*f*
- examples of diblock copolymers by iniferter technique, 424–426
- iniferter copolymers as stabilizers for styrene polymerization in carbon dioxide, 427
- synthesis methods by ATRP, 423–424
- synthesis methods by iniferter controlled radical polymerization, 421–423
- Branched and hyperbranched polymers
- atom transfer radical polymerization, 406–409
- See also* Dendrimers; Hyperbranched macromolecules
- 1,3-Butadiene, propagation rate constants by ESR, 151–153
- n*-Butyl acrylate, controlled polymerization with nitroxide mediator, 231–234
- N-t*-Butyl-1-diethylphosphono-2,2-dimethylpropyl nitroxyl (DEPN)
- controlled *n*-butyl acrylate polymerization with AIBN, 231–234
- controlled styrene polymerization with AIBN, 227–232
- t*-Butyl hydroperoxide, effect on polymerization rate and *M_w/M_n* for living radical polymerization, 211–212
- Camptothecin family of anti-tumor agents, radical annulations, 67–68
- Carbocationic polymerization
- contribution to controlled/living radical polymerization, 15
- living polymerization system, 3
- Cascade radical reactions
- atom transfer method, 63
- Dowd-Beckwith ring expansion followed by cyclization, 64, 65*f*
- Giese reactions by unimolecular chain transfer reactions (UMCT), 68–69
- intermolecular reaction sequences, 68–69
- intramolecular cyclization, 64
- intramolecular 1,5-hydrogen transfer, 64
- intramolecular ring-opening, 64
- organic synthetic method, 62–63
- radical annulations, 66–68
- radical translocation-cyclization sequence, 65
- reagents tributyltin hydride and tris(trimethylsilyl)silicon hydride, 62–63
- sequences of intramolecular reactions, 64–65
- Catalysts for ATRP
- copper-catalyzed ATRP, 271–277
- copper powder Cu(0) for Cu(I) regeneration, 277
- idealized tetrahedral Cu(I) and trigonal bipyramidal Cu(II) species, 273
- ligand choice for tailoring catalysis, 275–276
- optimum ratio of ligand to copper, 271–272
- possible structures of Cu(I) with bidentate ligands, 272
- requirements for effective catalysis, 273–275
- Catalytic chain transfer, radical reactivity ratio determination, 137–139
- Chain end functionalization
- aminophenylthioether group on polyacrylate, 326, 328
- cobaloxime-mediated photochemical acrylate polymerization, 326, 328–330
- methacrylate units on macromonomer ends, 328
- Chain transfer agents, chiral thiols for stereochemical control, 456–457
- Chain transfer catalysis

- favorable kinetic, mechanistic, and thermodynamic factors, 307–308
 metalloradicals, 305–308
- Chain transfer constants
 addition-fragmentation reactions, 372, 374
 effect of radical reactivity ratios for styrene-MMA copolymerization, 140–141
- Chain transfer in copolymerization, radical reactivity ratio determination, 136–137
- Chain transfer reactions
 addition-fragmentation process, 363–366, 372, 374
 moment expression in kinetic simulation for alkoxyamine-initiated polymerization, 344–345
 moment expression in kinetic simulation for MMA, 344–345
 rate constants, 353
 simulation for MMA polymerization, 352–356
- Cobalt(II) porphyrins
 chain transfer catalysis in MMA polymerization, 306–308
 living radical polymerization of acrylate block copolymers, 310–311
 living radical polymerization of acrylates, 308–310
 reaction sequence for cobalt-induced acrylate polymerization, 311–312
 representative rate study for methyl acrylate polymerization, 312–314
- Controlled-growth free radical polymerization
 addition-fragmentation sequence of degenerative chain transfer, 339
 degenerative chain transfer mechanism, 338–341
 kinetic simulation, 341–346
 kinetic simulation of MMA polymerization, 346–352
 method of moments application in kinetic simulations, 342–346
 reversible atom or group transfer mechanism, 338
 reversible chain transfer mechanism, 338–341
 reversible termination mechanism, 333–338
- Controlled/"living" polymerization requirements
 chain transfer and termination effects, 4–6
 controlled system properties, 3–4
 fast initiation prerequisite, 8
 polydispersity effects from active and dormant species exchange, 6–8
 reversibility of propagation, 8
 terminology, 3
- Controlled/"living" radical polymerization
 amphiphilic block copolymers, 419–421
 atom transfer radical polymerization (ATRP), 226–227
 controlled/living nature of DEPN-mediated polystyrene, 230–232
 ESR measurements of nitroxyl radical and rotational correlation time in styrene, 245–246
 evolution of process development, 13–18
 fundamental controlled radical polymerization kinetics, 247–248
 future outlook, 23–25
 initial overall rate of styrene polymerization, 244–245
 MMA polymerized with $\text{Cu}^{\text{I}}\text{X}(\alpha\text{-diimine})$ compounds, 79
 nitroxyl stable radicals reversibly trapping growing polymeric radicals, 226
 organonickel complex catalysis, 76
 phosphonate-containing nitroxyl radical, 226–227, 228f
 stepwise growth presumable from styrene evaluation, 248–252

- Trommsdorff effect suppression in styrene, 246–247, 248*f*, 249*f*
See also Atom transfer radical polymerization (ATRP); Living free radical polymerization; Nitroxide-mediated radical polymerization
- Controlled/"living" radical polymerization approaches
 concepts and contributing groups, 18, 19*f*
 degenerative transfer process, 21–22
 reversible formation of persistent hypervalent radicals, 21
 reversible homolytic cleavage of covalent species, 19–21
- Controlled photochemical polymerization.
See Photochemical polymerization
- Controlled radical system peculiarities
 active and dormant species exchange, 9–10
 chain transfer and termination suppression, 8–9
 initiator structure resembling dormant macromolecular species, 10–11
 thermal self-initiation contribution, 11–13
- Copolymers, statistical and gradient by ATRP, 399–400
- Copper-based ATRP. *See* Atom transfer radical polymerization (ATRP)
- Cross propagation, addition-fragmentation reaction, 365–366, 370
- Curve-crossing model, *ab initio* molecular orbital theory, 34–36
- Cyclic nitroxides
 effect of *t*-butyl hydroperoxide on polymerization rate and Mw/Mn, 211–212
 five-membered cyclic nitroxide structures and synthesis, 202–204
 oxazolidinyloxy radical inactive in styrene polymerization, 209–210
 polymerization characteristics with cyclic nitroxides, 210–211
 polymerization efficiency estimation by dimethoxy-BPO/TEMPO, 204–205
 polymerization rate comparisons with TEMPO, 205–207
 polystyrene Mn comparisons with TEMPO, 207–209
 polystyrene MWD comparisons with TEMPO, 209
- Cyclization intramolecular cascade radical reaction, 64
- Cyclopenta-fused quinolines, radical annulations, 66–67
- Cyclopolymerization, stereochemical control for bifunctional monomers, 454–455
- Degenerative transfer process
 active and dormant species exchange, 10
 addition-fragmentation process, 22
 approach to controlled/living radical polymerization, 21–22
 contribution to controlled/living radical polymerization, 17
 mechanism, 338–341
- Dendrimers
 dendritic initiator, 437–438, 446
 hybrid dendritic-linear macromolecules, 445–447
 organonickel complex catalysis, 76–78
 starting dendrimer absence in block copolymer, 448*f*
- DEPN. *See* *N-t*-Butyl-1-diethylphosphono-2,2-dimethyl propyl nitroxyl (DEPN)
- Diene compounds, ESR studies of radical addition, 147, 150–151
- Dithiocarbamate. *See* Iniferter controlled free radical polymerization
- Dowd-Beckwith ring expansion-cyclization, cascade radical reaction, 64, 65*f*
- Electron acceptors, influence on ESR spectra of primary radicals, 157–159

- Electron spin resonance (ESR)
- block polymer of *p*-methoxystyrene and cyclohexene oxide by electron transfer, 160–162
 - equilibrium constant measurement for reversible dissociation of initiator adduct, 186, 187*f*
 - experimental procedure for nitroxyl radical in styrene polymerization, 253
 - highly resolved spectra for detection of propagating radicals, 146–150
 - hyperfine splitting constants for diene compounds, 147
 - influence of electron acceptors on primary radicals, 157–159
 - measurements of nitroxyl radical and rotational correlation time, 238–239, 245–246
 - photolysis of 2,4,6-trimethylbenzoyl diphenylphosphine oxide (TMDPO), 161, 163–166
 - polymer effect on propagation rate constant determination, 154–157
 - propagation rate constants compared with pulsed-laser polymerization (PLP) values, 151
 - propagation rate constants for radical polymerization, 151*t*
 - propagation rate constants of thermal vs. photo-initiated polymerization, 153, 154*t*, 155*f*
 - radical addition modes in unsymmetrical diene compounds, 147, 150*f*, 151
 - radical/cation transformation polymerization, 157–160
 - rate constant determinations for photopolymerization, 151–153
 - schematic of time-resolved ESR spectroscopy, 163*f*
 - studies of radical polymerization of vinyl and diene compounds, 145–146
 - time-resolved ESR study, 161, 163–166
- Electron transfer reaction of free radicals
- block polymer of *p*-methoxystyrene and cyclohexene oxide, 160–161
 - influence of electron acceptor on ESR spectra of primary radicals, 157–159
 - radical/cation transformation polymerization, 157, 160
- End-group analysis of nitroxide-mediated radical polymerization
- analysis of chromophore-tagged polystyrene, 219–223
 - high chain-end purity only for short chains, 223–224
 - initiator/mediator synthesis with chromophore, 216–218
 - nitroxyl end-group by NMR and nitrogen analysis, 215
- Entry rate coefficients, free radical emulsion polymerization, 111
- Free radical emulsion polymerization
- comparing theory and experiment, 114–116
 - distributions for zero-one and pseudo-bulk conditions, 109–112
 - entry rate coefficients, 111
 - obtaining rate coefficients from MWD data, 104–105, 107–108
 - seeded styrene polymerization procedure, 108–109
 - surface anchoring for MWD at higher conversions, 116–117
 - termination rate coefficient comparison with relaxation experiments, 113–114
 - termination rate coefficient theory, 105–106
 - theory for molecular weight distributions, 106–107
 - zero-one and pseudo-bulk kinetics, 105
- Free radical polymerization. *See* Stereochemical control of free radical polymerization
- Functionality of polymer chains
- addition-fragmentation reactions, 374–376

- ATRP of functional monomers, 409–410
 polymers with functional end groups by ATRP, 410–414
- Gel effect, termination rate coefficient in emulsion polymerization, 117
- Gel permeation chromatography–ultraviolet (GPC–UV)
 analysis of chromophore-tagged polystyrene, 219–223
 initiator/mediator synthesis with chromophore, 216–218
 nitroxyl end-group analysis with chromophore tags, 216
- Giese reactions, unimolecular cascade radical reactions, 68–69
- GPC–UV. *See* Gel permeation chromatography–ultraviolet (GPC–UV)
- Graft copolymers
 atom transfer radical polymerization, 404–406
 nitroxide-mediated polymerization of styrene and macromonomer, 439–440
 nitroxide synthesis, 436
 polymeric initiator synthesis, 438
 polymeric initiator with numerous initiating sites, 439, 441–442
 preparation from polymeric initiator, 438
 schematic of routes to polymeric initiator, 441
See also Dendrimers; Hyperbranched macromolecules; Barton esters (BE)
- Group transfer polymerization
 contribution to controlled/living radical polymerization, 15
 living polymerization system, 3
 mechanism for controlled-growth radical polymerization, 338
 mechanisms with organozinc radicals, 79–80
 organozinc with coordinated α -diimines, 78–80
- Hammett σ^- parameters, radical addition to monosubstituted alkenes, 52–53
- Hartree–Fock procedure, *ab initio* molecular orbital theory, 34
- Homolytic cleavage of covalent species
 approach to controlled/living radical polymerization, 19–21
 atom transfer radical polymerization, 20–21
 bulky arylalkyl radicals, 20
 dithiocarbamate iniferters, 20
 nitroxide moderators for styrene polymerization, 20
 weak direct bond of metalloradical and organic radical, 20
- N*-Hydroxypyridine-2-thione esters
 decomposition by heat or visible light, 377–378
- methacryloyl ester copolymers
 procedure, 381
 synthetic methods, 377
- vinylbenzoate copolymer procedure, 381–382
See also Barton esters (BE)
- Hyperbranched macromolecules
 evolution of molecular weight buildup, 444*f*
- Cu(I)-assisted living radical polymerization of *p*-chloromethylstyrene, 442
- nitroxide-mediated living free radical procedures, 442–445
- polymerization of monomer with both styrene and initiating/propagating alkoxyamine groups, 443
- Inhibitors, contribution to controlled/living radical polymerization, 15
- Iniferter controlled free radical polymerization
 block copolymer characterization in carbon dioxide, 427

- block copolymer stabilizers for styrene polymerization in carbon dioxide, 427
- block copolymer synthesis using macroiniferters, 422
- critical micelle density for block copolymers, 428, 429*f*
- crossover from living anionic to iniferter synthesis for block copolymers, 426, 429*f*
- dithiocarbamate contribution to controlled/living radical polymerization, 16, 20
- examples of diblock copolymer formation, 424–426
- hydrocarbon-fluorocarbon block copolymers, 419, 420*f*
- iniferter tetraethylthiuram disulfide, 421
- silicone block copolymer synthesis, 422–423
- synthesis of polystyrene-iniferter (TD-PS), 421–422
- synthesis of poly(vinyl acetate)-iniferter (BDC-PVAc), 422
- Initiation
- initiation improvement methods for ATRP, 269–271
- rate constants for phosphorus-centered radicals, 161, 163–166
- role of alkyl halides, 268–269
- Interconversion in addition-fragmentation reaction, 369–372
- Iron(II) complex, living radical polymerization of MMA, 297, 302–304
- Isoprene
- ESR spectra, 150*f*
- propagation rate constants by ESR, 151–153
- Isotacticity. *See* Stereochemical control in free radical polymerization
- IUPAC Working Party, pulsed laser polymerization–size exclusion chromatography (PLP–SEC)
- discussions, 87, 89, 101
- Kharasch addition reaction
- concentration effects on catalysis, 74–75
- mechanistic studies of nickel-catalyzed addition, 73–75
- organonickel complexes with diaminoaryl ligand, 72–73, 75
- organonickel ligand modification, 73–74
- spectroscopic studies during catalysis, 74
- Ligands for copper-based ATRP
- 2,2'-bipyridine derivatives, 261–262
- optimum ratio of ligand to copper, 271–272
- tailoring the chemistry of metal catalysts, 275–277
- Living anionic polymerization, contribution to controlled/living radical polymerization, 15
- Living free radical polymerization
- acrylate block copolymers by organo-cobalt porphyrins, 310–311
- acrylate polymerization by organo-cobalt porphyrins, 308–310
- activation-deactivation process, 180–181
- blocking agents, 181
- chain growth without chain breaking, 3
- overview of TEMPO-mediated polymerization, 200–202
- preparation of novel block and graft copolymers by ATRP, 396–398
- reaction sequence for organo-cobalt porphyrin-controlled polymerization, 311–312
- representative rate study for organo-cobalt complex polymerization, 312–314
- See also* Atom transfer radical polymerization (ATRP); Controlled/"living" radical polymerization; Nitroxide-mediated radical polymerization
- Macromonomers, MMA by controlled-growth polymerization, 335–338

- Mayo dimer, thermal self-initiation
contribution to controlled radical
polymerization, 11
- Mayo method, rate coefficient
determinations, 104–105, 107–108, 117
- Methacrylates
conversion studies by pulsed sequence
PLP (PS–PLP) experiments, 97–98
isotactic specificity of triarylmethyl
methacrylates polymers, 452–454
low monomer conversion by PLP–SEC
experiments, 89–91
polymer optical activity comparison with
enantiomeric excess of monomer, 452–
454
protecting groups (diaryl and triaryl)
contribution to controlled radical
polymerization, 16
reaction conditions for stereochemical
control in radical polymerization, 458–
459
See also 1-Phenyldibenzosuberyl
methacrylate
- Methacrylic acid, polymerization with
amines for stereochemical control, 460–
461
- Method of moments in kinetic simulations
atom transfer moment expression, 344
controlled-growth free radical
polymerization, 342–343
moment expression for chain transfer,
344–345
moment expression for chain transfer by
addition-fragmentation, 345–346
reversible termination moment
expression, 343–344
- Methyl acrylate
functionalized poly(methyl acrylate) by
ATRP, 410, 412*t*
living radical polymerization by organo-
cobalt porphyrins, 308–311
peculiarities of ATRP, 267–268
- Methyl methacrylate (MMA)
reaction conditions for stereochemical
control in radical polymerization, 458–
459
chain transfer catalysis by Co(II)
porphyrins, 306–308
kinetic simulation of alkoxyamine-
initiated polymerization, 346–352
nitroxide screening for living radical
polymerization, 335–338
peculiarities of ATRP, 266–267
phenol addition to ATRP, 287–293
polymerization rate with additives, 373*t*
propagation rate constants by ESR, 151–
153
rate variation with chain transfer agents,
367*f*
ruthenium(II) complex-mediated living
radical polymerization, 297, 299, 300*f*
theoretical functionality with chain
transfer agent, 375*f*
- Methyl radical addition to alkenes
alkene ionization energy and electron
affinity influences, 42–43
curve-crossing representation of
potential energy profile of reaction,
34–36
effect of level of theory on calculated
barriers, 36–37
polar effect examinations, 41, 42*t*
theoretical and experimental result
comparison for ethylene, 38–39, 40*t*
See also Radical addition to alkenes
MMA. *See* Methyl methacrylate (MMA)
- Molecular orbital theory, polar effects for
radical addition to alkenes, 54–55
- Molecular weight distributions (MWD)
instantaneous number for zero-one and
pseudo-bulk systems, 106–107
rate coefficient determination, 107–108,
117–118
surface anchoring at higher conversions,
116–117

- zero-one and pseudo-bulk conditions of styrene emulsion polymerization, 109–112
- Moller-Plesset perturbation, *ab initio* molecular orbital theory, 34
- Monomer conversion. *See* Pulsed laser polymerization (PLP)
- Monomer reactivity ratios, effect on radical reactivity ratios, 132–134
- Nickel(II) complex, living radical MMA polymerization, 297, 302–304
- Nitroxide-mediated radical polymerization
- activation mechanism of styrene/nitroxyl system, 186, 188–190
 - activation rate constant by GPC, 186, 188–190
 - activation rate constant for styrene/nitroxyl system, 186, 188–194
 - activation rate constant from polydispersity evolution, 191–193
- AIBN/nitroxide-mediated styrene polymerization, 227–232
- branched macromolecular structures, 433–435
- n*-butyl acrylate polymerization with DEPN, 231–234
- chromophore-tagged initiator/mediator synthesis, 216–218
- computer simulation of styrene/TEMPO system, 193–196
- controlled/living nature of nitroxide-mediated polystyrene, 230–232
- controlled polymerization of styrene, 244–252
- cyclic nitroxide mediators, 200–202
- diffusion coefficients for nitroxyl and polymeric radicals, 238–239
- elementary reactions, 181–182, 183*f*
- end-group analysis of chromophore-tagged polystyrene, 219–223
- equilibrium constant for initiation adduct, 186, 187*f*
- high chain-end purity only for short chains, 223–224
- impact of alkoxyamine homolysis on polymerization kinetics, 241–244
- initiator choice with DEPN-controlled styrene polymerization, 227–230
- kinetic simulations for MMA polymerization, 346–352
- overview of TEMPO-mediated polymerization, 200–202
- polymerization rates equivalent to nitroxide-free system, 182, 184–186
- quantitating polymer-bound chromophores by GPC–UV, 216
- rate of alkoxyamine C–O bond homolysis, 239–240
- relative inertness of nitroxides, 240
- reversible homolytic alkoxyamine dissociation, 236–237
- styrene polymerization with DEPN, 227–231
- temperature dependence on dissociation rate constant, 190–191
- terminal nitroxyl by NMR and nitrogen analyses, 215
- volume contraction correction for polymerization kinetics, 242–244
- See also* Cyclic nitroxides; Dendrimers; Graft copolymers; Hyperbranched macromolecules; Nitroxides; Stable free radical polymerization
- Nitroxides
- canonical structures, 239*f*
 - diffusion coefficients of radical species, 238–239
 - effect of excess TEMPO on styrene polymerization, 174–178
 - intrinsic chemical reaction between radicals in trapping reaction, 239
 - phosphonate-containing nitroxyl radical, 227, 228*f*
 - radical trapping rate, 237–238
 - reversible homolytic cleavage to covalent species, 20

- rotational correlation time of nitroxide
by ESR spectra, 238–239, 245–246
- synthesis of *N-t*-butyl-1-diethylphosphono-2,2-dimethylpropyl nitroxyl (DEPN), 227
- TEMPO concentration vs. time in styrene polymerization, 176–178
- See also* Cyclic nitroxides
- Organocobaloximes**
initiator/mediator for photochemical polymerization, 318–319
initiator synthesis, 322, 324
multifunctional initiator/mediator for star and radial-block architectures, 325–327
- Organometallic complexes**
living radical polymerization, 305–306, 313
See also Cobalt(II) porphyrins
- Organonickel complexes**
controlled radical polymerization, 76
dendrimer catalysts, 76–78
heterogeneous catalysis, 78
homogeneous catalysis, 72–73, 75
mechanistic studies of nickel-catalyzed Kharasch addition, 73–75
nickel ions incorporation in inorganic colloids, 78
potential mechanism, 74–76
- Organozinc radicals**
 α -diimine ligands, 78–80
group transfer reactions, 78–80
radical mechanisms in group transfer, 79–80
- N*-Oxypyridine-2-thione**
carboxymethyl cellulose graft copolymer procedure, 382–383
poly(aryl ether sulfone) graft copolymer procedure, 382
See also Barton esters (BE)
- Penultimate model, radical reactivity ratios, 121–122**
- Persistent hypervalent radicals, controlled/living radical polymerization, 21**
- Phenols**
acceleration of MMA polymerization rate by phenol in ATRP, 294
ATRP enhancement study, 286, 292*t*
MMA polymerization by ATRP with substituted phenols, 291–293
role of phenol in ATRP of MMA, 287–291
- Phenyl vinyl ether (PVE)**
initiation rate constants by ESR, 164*t*
time-resolved ESR study, 161, 164–166
1-Phenyldibenzosuberyl methacrylate isotactic polymer by radical mechanism, 452
polymerization with chiral chain transfer agent, 456–457
polymerization with chiral initiator, 455–456
- Phosphorus-centered radicals**
photoinitiators, 161
time profiles of ESR signal due to diphenylphosphonyl radicals, 165*f*
time-resolved ESR study, 161, 163–166
- Photochemical polymerization**
acrylate conversion and molecular weight vs. time, 319–321
actual molecular weight (M_n) vs. theoretical, 324–325
block acrylate copolymer preparation, 321, 323*f*
chain-end functionalization studies, 326, 328–330
chloroform necessary diluent with cobaloxime, 322, 323*f*
molecular weight control by initiator/monomer ratio, 321
organocobaloxime initiator synthesis, 322, 324
organocobaloxime as photoinitiator/mediator of acrylate esters, 316–317, 330

- polymerization method with
organo(pyridinato)cobaloximes, 317–318
- polymerization steps for acrylates, 318–319
- star and radial-block architectures from multifunctional
photoinitiator/mediators, 325–327
- subsequent polymerization at equivalent rates, 319
- Trommsdorff effect absent for acrylate polymerization, 319
- Poly(ethylene oxide) macromonomers, propagation rate determination, 154–157
- PREDICI simulation program
controlled-growth radical polymerization, 341–342
- pulsed laser polymerization–size exclusion chromatography (PLP–SEC) procedure discussions, 87–88, 92–93
- Propagation rate coefficients
comparison of thermal and photo-initiated radical polymerization, 153–155
- effect of radical reactivity ratios for styrene–MMA copolymerization, 139–140
- effect of uncertainty on radical reactivity ratios, 131–132
- ESR determination of
photopolymerization, 151–153
- polymer effect by ESR with
poly(ethylene oxide) macromonomers, 154–157
- See also* Pulsed laser polymerization (PLP)
- Pseudo-bulk class of emulsion polymerization
instantaneous MWD number, $P(M)$, 106–107
- kinetic theory, 105
- obtaining rate coefficients from MWD data, 107–108
- styrene emulsion polymerization procedure, 108–110
- Pulsed laser polymerization (PLP)
principal types of PLP experiments, 85f
- propagation rate constant comparisons with ESR, 151
- PS–PLP with spectroscopic analysis of monomer conversion, 95–101
- pulse sequence (PS–PLP) experiments, 85–86
- radical reactivity ratios from PLP–derived propagation rate coefficients, 126–131
- single pulse (SP–PLP) experiments, 85–86
- size exclusion chromatography (PLP–SEC) technique, 84–85, 87–93
- SP–PLP with spectroscopic analysis of monomer conversion, 94–95, 100–101
- Pulse sequence–pulsed laser polymerization (PS–PLP)
conversion studies of slow propagating monomers, 85–86
- monomer conversion experiments with spectroscopic analysis, 95–99, 101
- Pyridine, slowing rate of styrene ATRP, 278
- Quadratic configuration interaction (QCI), *ab initio* molecular orbital theory, 34
- Quinolines, cyclopenta-fused, radical annulations, 66–67
- Radial-block polymer architectures, multifunctional cobaloxime initiator/mediator, 325–327
- Radical addition reactions, contribution to controlled/living radical polymerization, 13
- Radical addition to alkenes
ab initio molecular orbital theory, 31–32
- addition of methyl radical to alkenes, 39–44

- addition of other radicals to alkenes, 44–47
- assessment of theoretical procedures, 36–39
- t*-butyl radical comparisons, 46–47
- charge-transfer states for radicals, 44, 45
- enthalpy dependence of barriers for radical addition reaction, 44–47
- experimental measurements by mercury method, 50–51
- influence of alkene electron affinity, 43
- influence of alkene ionization energy, 43
- molecular orbital theory for polar effects, 54–55
- polar and stability effects, 52–55
- polar effects in the addition reactions, 44–46
- propagation step in radical polymerization, 50
- radical polymerization, 59–60
- regioselectivity, 56–58
- shielding substituents on olefins, 57
- stereochemistry, 58–59
- steric effects, 55–56
- theoretical considerations, 32–36
- See also* Methyl radical addition to alkenes
- Radical annulations, cascade reactions, 66–68
- Radical reactions. *See* Cascade radical reactions
- Radical reactivity ratios (*s*)
- alternative measuring methods, 135–136
- assumptions in statistical analysis, 124–131
- catalytic chain transfer viable alternative, 137–139
- chain transfer in copolymerization as alternative, 136–137
- implications of reported values, 134–135
- increasing *s* effect on calculated fraction of unsaturated end-groups, 140–142
- increasing *s* effect on chain transfer constant, 140–141
- increasing *s* effect on propagation rate coefficient, 139–140
- limited physical meaning, 120
- penultimate model, 121–122
- problems with current determination, 122–124
- terminal model as basis, 121–122
- uncertainty of homopropagation rate coefficients, 131–132
- uncertainty of monomer reactivity ratios, 132–134
- See also* Statistical analysis of radical reactivity ratios
- γ -Radiolysis relaxation experiments
- average termination rate coefficients, 117
- termination rate coefficient comparison, 113–114
- Reactivity ratios. *See* Monomer reactivity ratios; Radical reactivity ratios (*s*)
- Retarders, contribution to controlled/living radical polymerization, 15
- Ring-opening intramolecular radical reaction, 64
- Ring-opening metathesis polymerization, 3, 401–402
- Rotating sector, radical reactivity ratio determination, 126–129
- Ruthenium(II) complex, living radical polymerization of MMA, 297, 299, 300
- Self condensing vinyl polymerization (SCVP), hyperbranched polymers, 406
- Sequential radical reactions. *See* Cascade radical reactions
- Shielding substituents, radical additions to alkenes, 57
- Single pulse–pulsed laser polymerization (SP–PLP)
- conversion studies of monomers with high propagation rates, 85–86

- monomer conversion with online spectroscopic analysis, 94–95, 100–101
- Size exclusion chromatography–pulsed laser polymerization (PLP–SEC)
- low monomer conversion restriction, 84–85
- PLP–SEC experiments, 87–93
- PREDICI simulation program, 87–88, 92–93
- Smoluchowski model
- diffusion rate coefficient of trapping, 239
- termination rate coefficient, 105, 116
- Spatially intermittent polymerization, radical reactivity ratios, 126–129
- Stable free radical polymerization
- living free radical polymerization, 170–173
- nitroxide concentration vs. time for styrene polymerization, 176–178
- polymerization sample properties, 174, 178*t*
- preparation of initiator–nitroxide complex, 175–176
- role of excess nitroxide (TEMPO), 170, 174–178
- schematic of styrene with benzoyl peroxide/TEMPO, 171
- styrene polymerization methods, 174
- See also* Nitroxide-mediated radical polymerization; TEMPO-mediated styrene polymerization
- Star polymer, multifunctional cobaloxime initiator/mediator, 325–327
- Statistical analysis of radical reactivity ratios
- error in independent variable, 125–126
- independent normally distributed error variance, 126–129
- weighted non-linear least squares, 124–125
- weighting of residuals, 129–131
- Stereochemical control of free radical polymerization
- bulky or chiral monomers, 452–454
- chiral initiator, 455–456
- chiral menthol or neomenthol chain transfer agents, 457
- chiral thiol chain transfer agents, 456–457
- cyclopolymerization of bifunctional monomers, 454–455
- methacrylic acid polymerization in the presence of amines, 460–461
- model for characteristics of triphenylmethyl methacrylate, 458, 459*f*
- monomer design, 452–455
- reaction conditions, 458–459
- Stokes–Einstein–Debye equation, isotropic rotational diffusion of nitroxide, 238–239
- Stokes–Einstein equation, nitroxide diffusion coefficient, 238
- Styrene emulsion polymerization. *See* Free radical emulsion polymerization
- Styrene monomer
- controlled polymerization with AIBN and DEPN mediator, 227–232
- conversion studies by pulse sequence PLP(PS–PLP) experiments, 96–97, 99, 101
- end–functionalized polystyrene by ATRP, 410, 411*t*
- low monomer conversion by PLP–SEC experiments, 87–90, 93
- peculiarities of atom transfer radical polymerization, 265–266
- propagation rate constants by electron spin resonance, 151–153
- See also* Cyclic nitroxides; Nitroxide-mediated radical polymerization; Stable free radical polymerization
- Tandem radical reactions. *See* Cascade radical reactions
- TEMPO-mediated styrene polymerization

- effect of camphorsulfonic acid-type additives, 172–173
- initiator structure resemblance to dormant macromolecular species, 10–11
- stable free radical polymerization, 170–173
- TEMPO concentration vs. time, 176–178
- thermal self-initiation contribution, 11–13
- See also* Nitroxide-mediated radical polymerization; Stable free radical polymerization
- Termination
- mechanism in controlled-growth radical polymerization, 333–338
 - moment expression in kinetic simulation for alkoxyamine-initiated polymerization, 343–344
- Termination rate coefficients
- comparing theory and experiment, 114–116
 - comparison with relaxation experiments, 113–114
 - determination from MWD, 107–108
 - gel effect contribution in free radical polymerization, 117
 - pulsed laser polymerization experiments, 92–93, 96–101
 - Smoluchowski model, 105, 116
 - styrene emulsion polymerization procedure, 108–112
 - theory in free radical polymerization, 105–106
- 2,2,6,6-Tetramethylpiperidinyl-1-oxyl (TEMPO). *See* Nitroxides; TEMPO-mediated styrene polymerization
- Transfer rate coefficients, pulsed laser polymerization experiments, 91
- Transition metal-mediated living radical polymerization
- additive effects, 299, 302
 - alkyl halides as initiators, 297
 - examples of MMA polymerization with Ru(II) complex, 297
 - living radical polymerization in alcohols and water, 302–303
 - living radical polymerization of MMA with Fe(II) and Ni(II) complexes, 302–304
 - mechanistic features, 299–302
 - polymer end groups, 299, 301*f*
 - re-initiating polymerization in recovered polymers, 299–301
 - ruthenium-based systems with alkyl halide initiators, 296–297
 - typical transition metal complexes and initiators, 297, 298*f*
- Triblock copolymers, multifunctional cobaloxime initiator/mediator, 325
- 2,4,6-Trimethylbenzoyl diphenylphosphine oxide (TMDPO)
- initiator rate constants for vinyl monomer polymerization, 164
 - photolysis to phosphorus-centered radicals, 161
 - time-resolved ESR study, 161, 163–166
- Triphenylphosphine, copper catalyst deactivator in ATRP, 278
- Trommsdorff effect suppression, controlled/living styrene polymerization, 246–247, 248*f*, 249*f*
- Unimolecular chain transfer, radical annulation reactions, 66
- Unsaturated end-groups, effect of radical reactivity ratios on styrene-MMA copolymerization, 140–143
- Vinyl acetate
- ESR spectra of photo-initiated polymerization, 147, 149*f*
 - propagation rate constants by ESR, 151–153
- Vinyl chloride
- ESR spectra of photo-initiated polymerization, 147, 149*f*

propagation rate constants by ESR, 151–153

N-Vinylpyrrolidinone, peculiarities in ATRP, 268

Zero-one class of emulsion

polymerization

instantaneous MWD number, $P(M)$, 106

kinetic theory, 105

obtaining rate coefficients from MWD data, 107

styrene emulsion polymerization

procedure, 108–110, 111*f*, 112*f*